

rec'd with letter
dtd. 9/30/91

PRELIMINARY

**EVALUATION OF THE GEOLOGIC
RELATIONS AND
SEISMOTECTONIC STABILITY
OF THE YUCCA MOUNTAIN AREA
NEVADA NUCLEAR WASTE
SITE INVESTIGATION (NNWSI)**

TETA

**PROGRESS REPORT
30 SEPTEMBER 1991**

*Sam
Please enter
into system
Thanks
Bill Beuke
9/29/91*

**CENTER FOR NEOTECTONIC STUDIES
MACKAY SCHOOL OF MINES
UNIVERSITY OF NEVADA, RENO**

9210020067 910930
PDR WASTE PDR
WM-11

*102.8
WM-11
NH23
%*

INDEX TO YUCCA MOUNTAIN PROGRESS REPORT
1 OCTOBER 1990 - 30 SEPTEMBER 1991

- I. General Task
Introduction and Summary of activities conducted during the contract period.
- II. Task 1, Quaternary Tectonics
Summary of activities conducted during the contract period.
Results of research for the contract period.
Appendix A
Final report on Varnish Samples collected from the Monte Cristo Area.
Appendix B
The maximum background earthquake for the Basin and Range province, western North America.
Appendix C
Historical surface faulting in the Basin and Range province, western North America: implications for fault segmentation.
Appendix D
An explanation to accompany the geologic map of Crater Flat, Nevada (First Draft).
Appendix E
Late Quaternary faulting at Crater Flat, Yucca Mountain, southern Nevada.
- III. Task 3, Mineral Deposits, Volcanic Geology
Introduction and summary of activities conducted during the contract period.
Appendix A
Magmatic and Hydrothermal Activity, Caldera Geology, and Regional Extension in the Western Part of the Southwestern Nevada Volcanic Field.
Appendix B
Abstract. Geologic and tectonic setting and Miocene volcanic stratigraphy of the Gold Mountain - Slate Ridge area, Southwestern Nevada.
Appendix C
Abstract. Structural geology and Neogene extensional tectonics of the Gold Mountain-Slate Ridge area, southwestern Nevada.
Appendix D
Abstract. Multiple Episodes of Au-Ag mineralization in the Bullfrog Hills, SW Nevada, and their relation to coeval extension and volcanism.
Appendix E
Contrasting styles of epithermal precious-metal mineralization in the southwestern Nevada volcanic field.

Appendix F

Compositional controls on the gold contents of silicic volcanic rocks: 15th International Geochemical Exploration Symposium Program with Abstracts.

Appendix G

Ash-Flow Volcanism of Ammonia Tanks Age in the Oasis Valley Area, SW Nevada: Bearing on the Evolution of the Timber Mountain Calderas and the Timing of Formation of the Timber Mountain II Resurgent Dome.

IV. Task 4, Seismology

Summary of activities conducted during the contract period.

Appendix A

Real-Time Analogue and Digital Data Acquisition through CUSP.

V. Task 5, Tectonics, Neotectonics

Highlights of major research accomplishments and brief summaries of research results.

Appendix A

Structure of the western Pahranagat Shear System.

Appendix B

Structural analysis of Bare Mountain, southern Nevada.

Appendix C

Mesozoic and Cenozoic structural geology of the CP Hills, Nevada Test Site, Nye County, Nevada; and regional implications.

Appendix D

Neotectonics of the southern Amargosa Desert, Nye County, Nevada and Inyo County, California.

Appendix E

Quaternary tectonics and basin history of Pahrump and Stewart Valley, Nevada and California.

Appendix F

Mesozoic deformation in the Nevada Test Site and vicinity: A new perspective from the CP Hills, Nye County, Nevada.

Appendix G

The origin of large local uplift in extensional regions.

VI. Task 8, Basinal Studies

Executive Summary of activities conducted during the contract period.

Appendix A

The Mississippian Antler Foreland and Continental Margin in southern Nevada: the Eleana Formation Reinterpreted.

Appendix B

Mississippian Stratigraphy and Tectonics of East-Central Nevada: Post-Antler Orogenesis.

Appendix C

Mississippian through Permian Orogenesis in eastern Nevada: Post-Antler, Pre-Sonoma tectonics of the western Cordillera.

YEARLY REPORT
YUCCA MOUNTAIN PROJECT

TASK 4

October 1, 1990 to Sept 30, 1991

James N. Brune

SUMMARY OF PROPOSED ACTIVITIES: We proposed to (1) Develop our data logging and analysis equipment and techniques for analyzing seismic data from the Southern Great Basin Seismic Network (SGBSN), assuming eventual access to the data by satellite (2) Investigate the SGBSN data for evidence of seismicity patterns, depth distribution patterns, and correlations with geologic features (3) Repair and maintain our three broad band downhole digital seismograph stations at Nelson, Nevada, Troy Canyon, Nevada, and Deep Springs, California (4) Install, operate, and log data from a super sensitive microearthquake array at Yucca Mountain (5) Continue to seek funding and plan for installation of an underground laser strainmeter-tiltmeter facility at Yucca Mountain.

SUMMARY OF ACTIVITIES

- (1) Continued activities to upgrade the CUSP data logging for eventual use on Yucca Mountain data (see attached preprint).
- (2) Shipped our Guralp seismometers back to the manufacturer for alteration of a design error. This design error caused the instruments to go non-linear on high frequency local earthquakes.
- (3) Continued to operate the 4-station microearthquake array at Yucca Mountain. After discussions with USGS personnel we improved our ability to distinguish local mine blasts from microearthquakes.
- (4) Continued analysis of the Szymansky report.
- (5) Continued analysis of site effects at Mammoth Lakes and Anza, California, for possible application of techniques to Yucca Mountain area.
- (6) Attended workshop on engineering lessons from the Mexico and Chile earthquakes, San Diego.
- (7) Began work on a system to estimate magnitudes from microearthquake data.
- (8) Began analysis of a preprint by Gomberg on the strain pattern in southern Nevada.
- (9) Began investigation of attenuation of 20 hz energy in the Basin and Range. Investigated techniques for measuring attenuation

at Anza, California, for possible use at Yucca Mountain.

(10) By invitation visited Baba Atomic Research Center, Bombay, India, for conference and seminar on atomic waste disposal.

(11) Visited Univ. of California, San Diego, to discuss use of digital seismic arrays for seismic hazard and seismic source mechanism studies. Consulted with colleagues about future of proposed strain meter installation at Yucca Mountain.

(12) Studied techniques for determining source characteristics from digitally recorded microearthquakes.

(13) Improvised microearthquake recording system to record microearthquakes from the Mammoth Lakes region for comparison with Yucca Mountain microearthquake results.

(14) Investigated techniques for extrapolating microearthquake occurrence rates to estimate occurrence rates for larger earthquakes.

(15) Began comparison of microearthquakes recorded at the Mammoth microearthquake stations with those recorded at Yucca Mountain.

(15) Reviewed preprint by Gomberg on seismicity level at Yucca Mountain.

(16) Developed technique for estimating magnitudes for microearthquakes recorded at Yucca Mountain. Made preliminary estimates of attenuation Q for 20 hz energy at Yucca Mountain.

(16) Attended meetings of Seismological Society of America, San Francisco. Presented paper on Yucca Mountain microearthquake study.

(16) Drafted manuscript on microearthquakes at Yucca Mountain, Nevada.

(17) Received repaired Guralp instruments. Installed repaired instruments at Nelson, Nevada. Repaired vandalized facility at Nelson.

(18) Finalized curve for defining magnitudes of microearthquakes at Yucca Mountain.

(19) Completed testing on remaining Guralp instruments returned from England. Found one horizontal for Troy Canyon defective.

(20) Compared magnitude between Northern Nevada Network and SGBSN. Found unexplained bias of 1/2 magnitude unit ($UNRSL > SGBSN$).

(21) Filtered selected Northern Nevada Network station to duplicate Yucca Mtn. microearthquake response in order to revise attenuation profile for Mammoth area to Yucca Mtn.

**Annual Progress Report—General Task
Prepared by C. H. Jones**

1 October 1990 to 30 September 1991

Introduction

This report provides a summary of progress for the project "Evaluation of the Geologic Relations and Seismotectonic Stability of the Yucca Mountain Area, Nevada Nuclear Waste Site Investigation (NNWSI)." This progress report was preceded by the progress report for the year from 1 October 1989 to 30 September 1990. Initially the report will cover progress of the General Task, followed by sections describing progress of the other ongoing Tasks which are listed below.

- Task 1 — Quaternary Tectonics
- Task 3 — Mineral Deposits, Volcanic Geology
- Task 4 — Seismology
- Task 5 — Tectonics, Neotectonics
- Task 8 — Basinal Studies

**General Task
Staff**

Steven G. Wesnousky, Project Director, Peizhen Zhang (until 1 Nov. 1990), Postdoctoral Fellow, Craig H. Jones (since 1 January 1991), Postdoctoral Fellow, Ingrid Ramos, Secretary.

Administrative Activities

The General task continued to coordinate and oversee activities of the research tasks. Administrative activities are principally oversight of budgets and preparation of monthly reports, and coordination and collation of research reports and reviews required by the contract in a timely manner. Dr. Wesnousky has also represented NWPO at a number of meetings with the NRC and other federal agencies during the last year.

Technical Activities

Research activities conducted by the general task have focused on the tectonics of the Yucca Mountain region. Dr. Peizhen Zhang continued neotectonic studies of the Panamint Valley. Research conducted by Dr. Jones has focussed more on the seismological and tectonic framework of the entire lithosphere. Because Yucca Mountain lies near the boundary between two very different extensional regimes, general tectonic study of both regions will improve understanding of the Yucca Mountain site. In addition to the research projects actually conducted over this period, preparations have been made for using earthquakes in the NTS/Yucca Mountain area to construct three-dimensional velocity structures; these structures will also improve the confidence in the location of earthquakes in the area. Field investigations in the region suggest the possibility of conducting in the next year neotectonic investigations along faults to the west of Yucca Mountain that will improve understanding of the overall distribution of deformation in the Basin and Range.

The first project represents the completion of a project initiated by Dr. Jones. In this experiment, seismometers were deployed in the high Sierra Nevada of southern California in 1988. Teleseisms and regional earthquake arrival times recorded by this network were used to examine the crustal and upper mantle structure beneath the southern Sierra. The results, presently in a manuscript in review, have proven quite controversial: While extension in the upper crust has accommodated over 250 km of motion in the Basin and Range, it appears from this work (when placed in context for the entire region) that the downward continuation of that deformation actually lies under the Sierra Nevada to the west. This deformation is inferred to have warmed and thinned the anti-buoyant mantle lithosphere, thus causing the Sierra Nevada to rise. Such a model has important implications in the Yucca Mountain area, because Death Valley's deformation lies only a few miles to the southwest. Understanding the lithosphere-scale tectonics of the region should improve the framework for systematically examining the Yucca Mountain site; this work complements the earlier study of Dr. Zhang (see last year's report), who described, without providing a tectonic explanation, the evolution of faulting in the Death Valley area through time. A continuation of the seismological investigation into the Basin and Range toward Yucca Mountain is planned.

The second project is something of an outgrowth of the first; Dr. Jones, because of the above described work, was invited to participate in an international conference on the tectonics of rifting held in early November, 1990. The authors of presentations were invited to write papers for a proceedings volume; the four workers who represented the Basin and Range (Wernicke, Farmer, Walker, and Jones) combined to write a single paper that attempts to integrate geological, geochemical, and geophysical observation. Dr. Jones has been responsible for the geophysical study and the overall compilation and preparation of the manuscript. Although the paper contains considerable review, the geophysical section explores the variation in the style of deformation through the Basin and Range by taking seismic velocity profiles of the crust that have been obtained in the past few years and converting them into density structures. Armed with the density of the crust, one can infer how much of the variation in elevation seen through the Basin and Range is due to variations in density in the crust; what remains is probably due to variations in the mantle. Results of this study that bear on Yucca Mountain directly are that to the north, extensional deformation in the mantle probably lies under the central part of the Basin and Range, while to the south, deformation in the upper mantle lies under the western flank of the Basin and Range. This implies that a major lithospheric boundary lies near the Yucca Mountain area; this boundary might be responsible for the diffuse band of seismicity that crosses the Basin and Range at this latitude.

A third project is a continuation of work undertaken with Drs. Leslie Sonder (Dartmouth College) and Steven Salyards (New Mexico State University), which in turn was inspired by earlier work of Nelson and Jones (1987). Paleomagnetic samples have been gathered in Miocene sediments near Lake Mead in order to understand the mechanics that accompany the creation of "oroflexes," which are great bends in the earth's crust adjacent to large strike-slip faults. These bends are best understood through paleomagnetic work, which can constrain the exact amount of bending. Earlier work by Nelson and Jones documented the presence of an oroflex in the Las Vegas Range northwest of Las Vegas; that study lacked the spatial resolution to understand the mechanical underpinnings of the deformation and also could not constrain the age of deformation. The present study should solve both problems, for the young sediments in the Lake Mead area are well exposed and have not been as deformed as the sedimentary rocks in the Las Vegas Range. Although the study is still proceeding, data to date clearly show that the oroflex does extend to the southeast and formed within the past 15-20 m.y.. This same structure or one

analogous to it might extend into Yucca Mountain, where similar paleomagnetic rotations have been observed by USGS scientists over the past few years. Completion of this work should provide insight into structures that might be present in Yucca Mountain itself, including, possibly, the presence of large, subhorizontal decollements.

A fourth project initiated by Dr. Wesnousky and conducted with Dr. Jones investigates the physical parameters that control the partitioning of slip between a vertical fault and an adjacent dipping fault through the use of a simple model. The model was improved and expanded for use on fault systems within continents from models originally developed to understand analogous phenomena observed at plate boundaries. This model was initially applied to the San Andreas fault and it indicates that the slip rate along the San Andreas should vary as a function of the geometry of the adjacent dipping faults. It also provides some insights into the variation of physical characteristics of the faults that control the strength of the fault. A manuscript was prepared and submitted to *Science*. Within the Basin and Range, several faults exhibit similar behavior: one large, vertical fault will tend to be strike-slip, while an adjacent fault might have oblique-slip on its dipping surface. Such fault systems include the Death Valley and Owens Valley fault systems. We are now beginning to investigate the possible implications of these results with respect to the Yucca Mountain site are now being investigated.

PROGRESS REPORT

Task 1 Quaternary Tectonics

1 October 1990 to 30 September 1991

**John W. Bell
Principal Investigator**

**Alan R. Ramelli
Co-investigator**

**Craig M. dePolo
Co-Investigator**

SUMMARY OF ACTIVITIES CONDUCTED DURING THE CONTRACT PERIOD

During the contract period, the following activities were conducted by Task 1:

- * J.W. Bell made a presentation on Quaternary faulting at and near Yucca Mountain to the National Academy of Sciences Panel on Coupled Processes, and a three-page paper titled "Evidence for late Quaternary faulting in Crater Flat" was included in the DOE field trip guidebook prepared for the Academy panel.
- * C.M. dePolo and J.W. Bell organized and led a two-day field trip to the 1932 Cedar Mountain earthquake area for the Nuclear Waste Technical Review Board.
- * J.W. Bell and A.R. Ramelli reviewed the DOE Study Plan 8.3.1.17.4.6 "Quaternary Faulting Within the Site area" and submitted a 5 page report to the Nevada Nuclear Waste Project Office.
- * J.W. Bell and C.M. dePolo re-reviewed the NRC Staff Technical Position on "Investigations to Identify Fault Displacement and Seismic Hazard at a Geologic Repository" and submitted a two-page report to the Nuclear Waste Project Office.
- * J.W. Bell attended a Geological Society of America Penrose Conference on surface-dating techniques at which Yucca Mountain data were presented.
- * J.W. Bell presented the paper "Late Quaternary Surficial Geology in Crater Flat, Yucca Mountain, Nevada" at the 1991 Geological Society of America Cordilleran Section meeting in San Francisco.
- * J.W. Bell presented the paper "Tephtras and Late Holocene Alluvial-fan Deposition in West-central Nevada: Is There a Connection?" at the Annual Meeting of the Geological Society of America in San Diego.
- * The manuscript "Late Quaternary Geomorphology and Soils in Crater Flat, Next to Yucca Mountain, Southern Nevada" was completed by F.F. Peterson, J.W. Bell, R.I. Dorn, and A.R. Ramelli and submitted to *Quaternary Research* (copy attached).
- * A.R. Ramelli and J.W. Bell contributed the surficial geology and Quaternary faults to the Geologic Map of the Crater Flat 7½-minute quadrangle completed by J. Faulds and D. Feuerbach (copy attached). The map will be published by the Nevada Bureau of Mines and Geology.
- * C.M. dePolo completed the manuscript "The Maximum Background Earthquake for the Basin and Range Province, Western North America" and submitted it to *Seismological Society of America Bulletin* (copy attached).

- * A.R. Ramelli and J.W. Bell completed the manuscript "Late Quaternary Faulting at Crater Flat, Yucca Mountain, Southern Nevada" and submitted it to *Geology* (copy attached).
- * J.W. Bell completed compilation of the surficial geology of the Mina 7½-minute quadrangle. The map will be co-authored with J. Oldow (Rice University) and published by the Nevada Bureau of Mines and Geology.
- * J.W. Bell submitted and received results for four ¹⁴C samples from faulted deposits along the 1932 Cedar Mountain fault.
- * J.W. Bell submitted 13 tephra samples from the 1932 Cedar Mountain earthquake region to Andre Sarna-Wojcicki of the U.S. Geological Survey for chemical identification. A total of 10 ¹⁴C samples was collected from the tephra sequence and submitted to Geochron Laboratories for dating.
- * A total of thirty-nine tephras has been collected for the Cedar Mountain study, of which J.W. Bell has petrographically analyzed thirty-two of these to date.
- * R.I. Dorn completed analyses and dating of rock varnish samples from the 1932 Cedar Mountain area and submitted a final consultants report (copy attached).
- * Low-sun-angle aerial photography (1:12,000-scale) was flown of three areas containing historical and Holocene surface faulting: the 1954 Fallon-Stillwater earthquake area; the 1934 Excelsior Mountain earthquake area; and the Benton Springs fault zone which lies within the 1932 Cedar Mountain area.

RESULTS OF RESEARCH FOR THE CONTRACT PERIOD

Areas of research for the contract period included the following:

- * A.R. Ramelli and J.W. Bell completed compilation of allostratigraphic relations for Crater Flat.
- * J.W. Bell continued allostratigraphic studies in the 1932 Cedar Mountain earthquake area.
- * C.M. dePolo continued detailed mapping of faulting associated with the 1932 Cedar Mountain earthquake.

Crater Flat Allostratigraphy

A final synthesis of allostratigraphic relations in Crater Flat was completed with the results contained within two manuscripts. Soils and geomorphic data are presented in a paper titled "Late Quaternary Geomorphology and Soils in Crater Flat, Next to Yucca Mountain, Southern Nevada" which is submitted to *Quaternary Research*. Large-scale mapping of these relations is contained on the 1:24,000-scale "Geologic Map of the Crater Flat 7½-minute Quadrangle" produced jointly with the Center for Volcanic and Tectonic Studies at the University of Nevada, Las Vegas.

As described in previous reports (e.g., Bell et al., 1990), six principal allostratigraphic units are defined for Crater Flat, and these units can be used to constrain recency and recurrence of Quaternary fault movement. Based on rock varnish cation-ratio and ¹⁴C AMS dating at twenty-two sites, the six Crater Flat allostratigraphic units have the following approximate ages:

Crater Flat <<6.6 ka
Little Cones 6.6-11.1 ka
Late Black Cone 17.3-30.3 ka
Early Black Cone 130-190 ka
Yucca 360-370 ka
Solitario 450 to >740 ka

Although the accuracy and precision of rock varnish dating has recently been questioned by several investigators (Bierman and Gillespie, 1991; Bierman et al., 1991; Reneau and Raymond, 1991), the Crater Flat rock varnish dates are regarded as being accurate age approximations for several reasons. Bierman and Gillespie challenge the analytical procedures used by Crocker Nuclear Laboratory at UC Davis which performed the cation ratio analyses for Dorn. They contend that the UC Davis data are flawed based on the

laboratory's inability to differentiate barium from titanium. In a rebuttal, Cahill (in press) demonstrates that Bierman and Gillespie have misinterpreted raw data values from his laboratory and lack an acceptable protocol for conducting interlaboratory comparisons. In addition, all Crater Flat data were cross-checked for this project by R.I. Dorn who performed additional cation-ratio determinations using microprobe and ICP analyses which are not sensitive to the barium problem.

Reneau and Raymond (1991) take issue with the entire concept of cation-ratio dating and suggest that no systematic changes in cation ratios actually occur. They speculate that the apparent trend in cation ratios with increasing is merely an artifact of analytical procedural error. The procedure has been verified by numerous other researchers, however, (e.g., Loendorf, 1991), and the lack of correlation between varnish age and cation ratios may be related to variations in cation-leaching sites on sample surfaces. Dorn and Krinsley (1991) illustrate that only varnishes with continuous layering should be used for paleoenvironmental study because other varnish textures may show either increases or decreases in cation ratios depending on postdepositional modifications.

The cation-leaching curve previously constructed and the derived cation-ratio ages for Crater Flat units (Fig. 1) are consistent with other independent stratigraphic data. Uranium-series analyses of pedogenic carbonate from a Late Black Cone age soil exposed in U.S. Geological Survey trench CF-3 (Ku, 1989; Luo and Ku, 1991) yielded uranium-thorium ages consistent with a rock varnish age from the same location and with other ^{14}C data from Crater Flat. Figure 2 shows the relationship between uranium-series ages and the cation-leaching curve. Twelve of the Crater Flat samples used to define this curve were dated by ^{14}C AMS analysis. The presence of Bishop ash (~730 ka) in the Solitario unit (Marith Reheis, 1991, written communication) is further verification of the rock varnish age relations.

Cedar Mountain Allostratigraphy

Allostratigraphic studies in the 1932 Cedar Mountain region consisted of several separate elements all of which were directed toward providing better stratigraphic and age control relative to defining recurrent movement on the 1932 rupture zone.

Four samples of buried vesicular A (Av) horizon were collected from trench 3 (Fig. 3). Although no megascopic organic material was visible in any of the samples, these buried soils horizons contained enough minute organic material to be dated by accelerator mass spectrometry. The dates are determined on bulk organic carbon content, and thus are mean residence time (MRT) dates:

Sample	CM-3-1	12,840 ± 110 yrs
	CM-3-2	9,226 ± 93
	CM-3-3	3,878 ± 99
	CM-3-4	13,160 ± 190

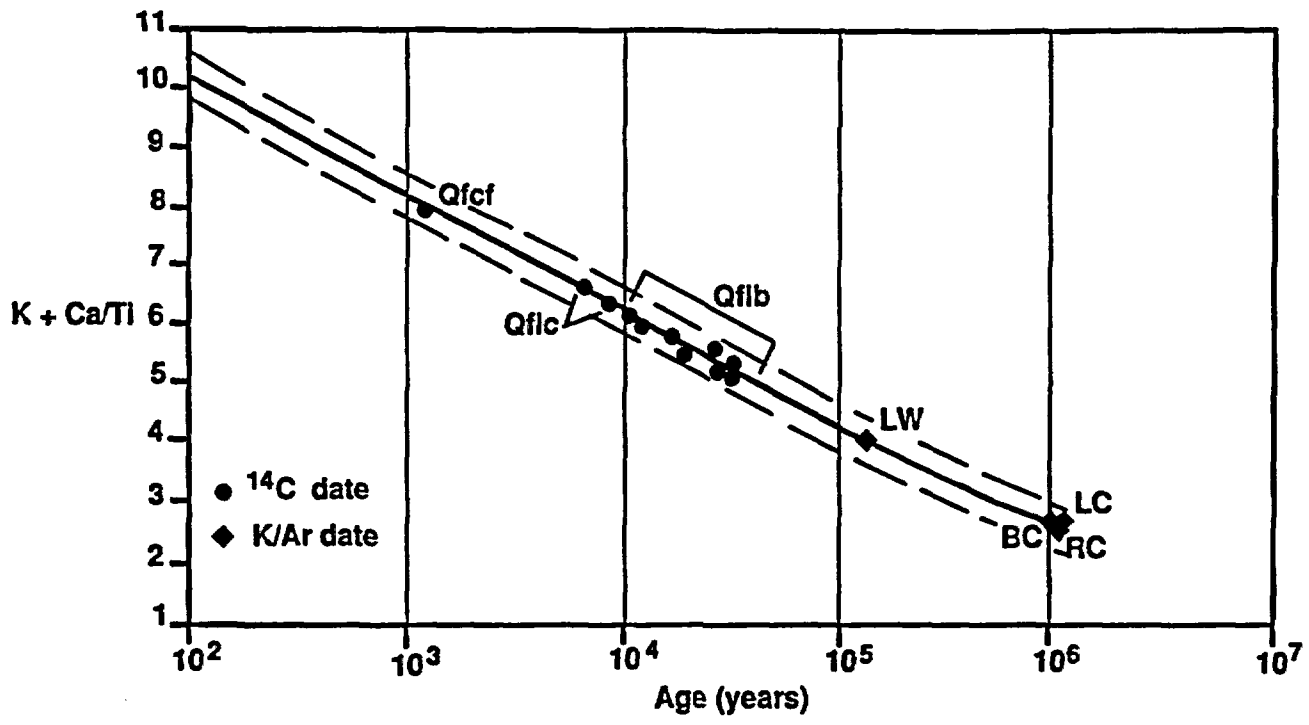


Figure 1. Crater Flat cation-ratio leaching curve. Units: Qfcf, Crater Flat; Qflc, Little Cones; Qflb, Late Black Cone; LW, Lathrop Wells; BC, Black Cone; RC, Red Cone; LC, Little Cones basalt.

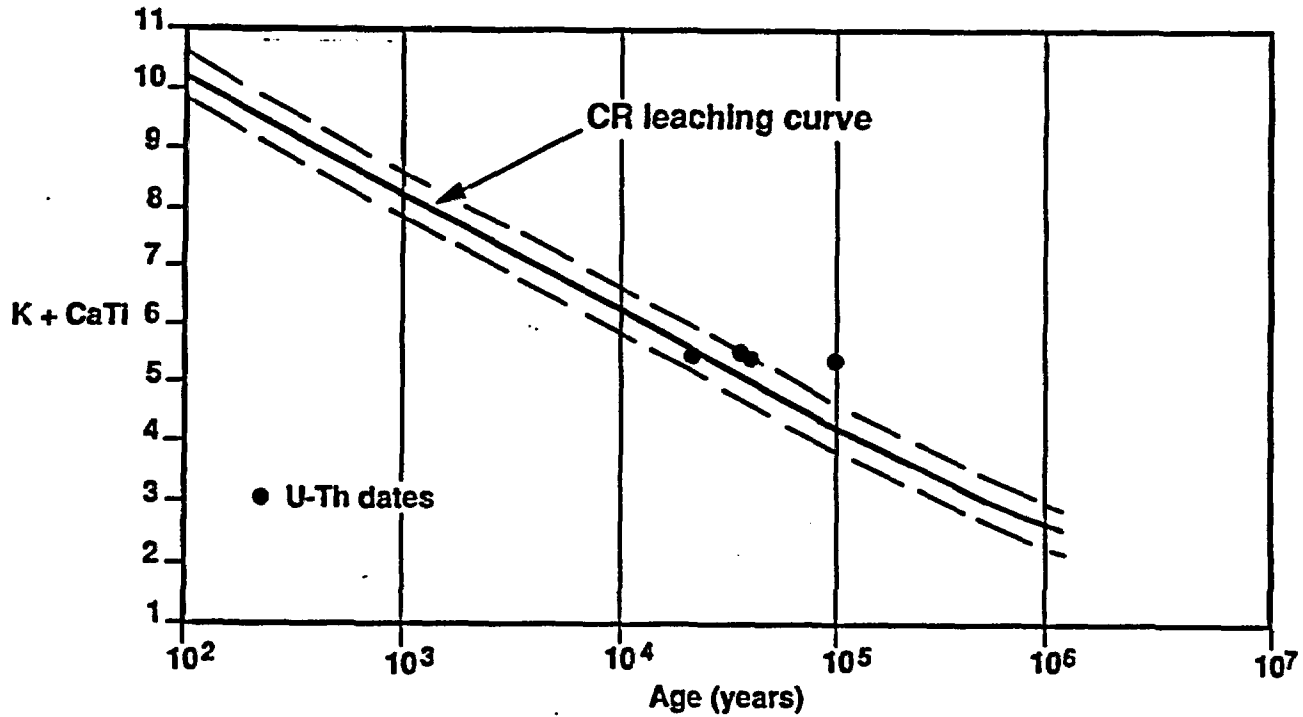


Figure 2. Relation of U-series dates to CR curve, as shown in Figure 1.

Samples CM-3-1,-2, and -4 were collected from the same stratigraphic horizon in trenches 3A and 3B. The horizon consists of a strongly vesicular Av that caps the lowermost ponded silt horizon in both trenches. Sample CM-3-3 was collected from the uppermost "platy" silt in trench 3A which lies immediately beneath the modern Av horizon. This horizon is a buried soil formed on the uppermost ponded silt in the trench exposure.

The age date results indicate that the stack of ponded silts buttressed and faulted against the 1932 fault trace are likely of latest Pleistocene to Holocene age. Although the MRT dates may only be average estimates, they strongly suggest, when taken together with the degree of soil development, that the stack is on the order of 10,000-20,000 years in age. Samples CM-3-1, -2, and -4 are likely close to the true numerical age of the soil, and they probably date the time of burial by the overlying silt unit fairly closely.

Tephrochronology

Petrographic analysis of the thirty-nine volcanic ashes collected in the Cedar Mountain area indicates that the tephra of Holocene age may be differentiated on the basis of refractive index (Table 1). In particular, the Turupah Flat ash is ubiquitous in the study area and serves as a principal late Holocene stratigraphic datum. It is bracketed by ¹⁴C dates of 1455 ± 140 and 1590 ± 130 yrs obtained during this study, and it has a consistent refractive index of about 1.494. The other tephra lie both stratigraphically above and below the Turupah Flat ash, and they can similarly be tentatively identified on the basis of refractive indices. The ashes have also been submitted to Andre Sarna-Wojcicki of the U.S. Geological Survey for positive chemical identification, and the results of his microprobe analyses are pending.

Table 1. Refractive indices of tephra samples from the Cedar Mountain region.

<u>1.492</u>	<u>1.494</u>	<u>>1.496 <1.498</u>	<u>1.498</u>
BS14	BS1	BS2	BS7
	BS4	BS12	BS18
	BS5	BS20	BS24
	BS11	BS21	BS26
	BS13	BS22	CM4
	BS15	BS25	CM5
	BS16	BS27	CM6
	BS19		
	BS23		
	WR1		
	WR2		
	WR4		
	WA1		
	Turupah 1		
	11 Mile 1		
	E. Job 1		

TRENCHES 3A, 3B, 3C

ISOMETRIC FENCE DIAGRAM

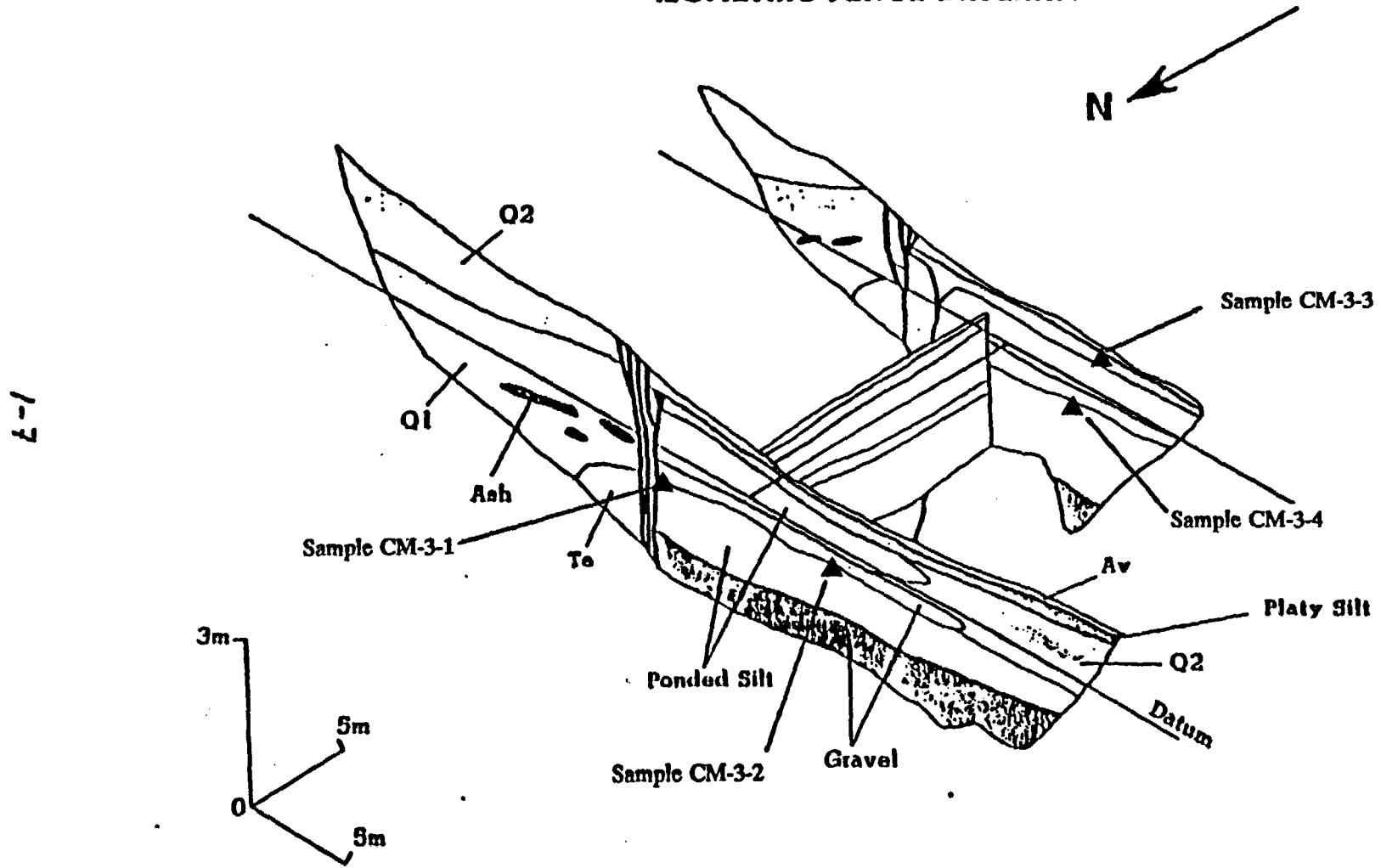


Figure 3. Location of radiocarbon samples in Monte Cristo Valley trench 3.

Rock Varnish Analyses

A total of fourteen rock varnish samples were collected and analyzed by Ronald I. Dorn for both ^{14}C age and cation ratio. The final consultants report containing all analytical data is attached to this report. Eight of the rock varnish samples were dated by AMS ^{14}C and provide approximate ages for the Qf2 and Qf3 allostratigraphic units. All rock varnish ages are consistent with pre-mapped surficial relations as well as with the tephrochronology.

The most recent synthesis of allostratigraphic relations and rock varnish ages is shown on Figure 4.

Mapping of 1932 Ruptures

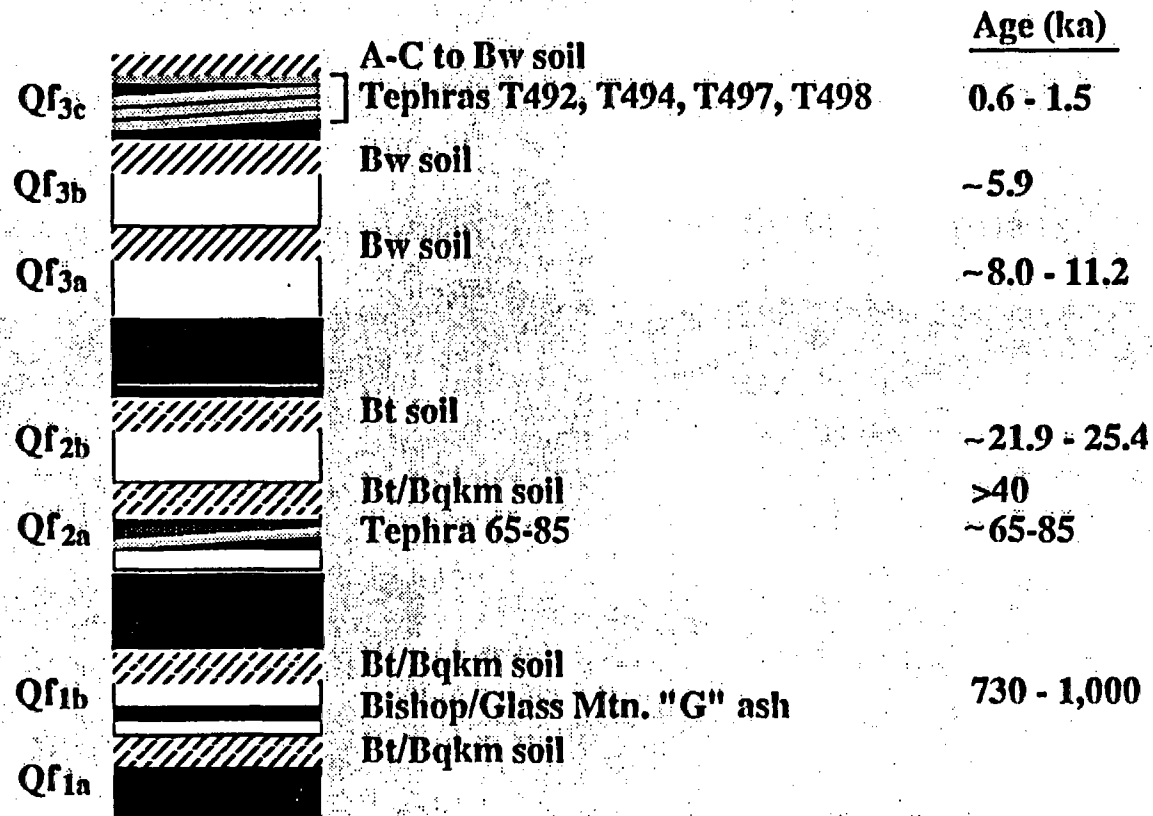
Work by C.M. dePolo continued on transferring the 1932 Cedar Mountain earthquake ruptures to 1:24,000-scale base maps. This will eventually allow better small scale maps representing the surface ruptures to be made, with more accurate surface break locations, lengths, orientations, and spacings between ruptures. These maps will become some of the core data for our manuscript on the earthquake to be submitted to the Journal of Geophysical Research. These maps will also be annotated in the future to make tectonic strip maps documenting the surface breaks from the 1932 earthquake. These strip maps are intended to be published through the NBMG.

Some field work was conducted on the 1932 surface breaks. In particular, ruptures in Gabbs Valley, near "earthquake hill," and near the Paradise Peak Mine were inspected. "Earthquake hill," as it was referred to by Gianella and Callaghan (1934) is peculiar because the surface break virtually surrounds a small hill. This hill is made up of tuffaceous sediments, warped into a gentle syncline, plunging 5° to the northwest. After inspection of aerial photographs and in the field, it seems that this rupture may be more due to shaking and gravitational sliding of this block downslope, and not to tectonic faulting. This location is an outlier of the mapped surface ruptures, so the width of tectonic faulting associated with this event may be slightly less than previously measured.

A field visit was conducted with University of California, Berkeley paleontologist Dr. Howard Schorn and California Academy of Sciences Entomologist Dr. Harvey Scudder to better understand the faulted sediments in Stewart Valley. In the center of these sediments in Stewart Valley there is an absence of mapped surface faulting from the 1932 Cedar Mountain earthquake. The gap in surface faulting may be tectonic but it may also be the result of sediments absorbing the rupture, or the rupture may have been subtle and was never mapped.

Eugene Callaghan's notes for the 1932 Cedar Mountain earthquake were obtained from the USGS, so all original notes from the 1932-1933 field work are now in hand. These will greatly aid in understanding the information presented in Gianella and Callaghan (1934) as

Cedar Mountain Area Allostratigraphy



b-1

Figure 4. Generalized section illustrating Cedar Mountain stratigraphy and ages.

well as reveal some subtle observations that were not published.

Maps and reports from surrounding mines were gathered to give a better perspective on the regional geologic framework of the 1932 earthquake area. These data reveal more clearly the nature and history of local detachment surfaces and their present day positions and orientations. Such information is vital in evaluating the potential contribution of detachment surfaces to the distribution of surface faulting during the 1932 earthquake.

REFERENCES

- Bell, J.W., Ramelli, A.R., and dePolo, C.M., 1990, Progress report for the period 1 October 1989 to 30 September 1990, Task 1 Quaternary tectonics: Final project report submitted to the Nevada Nuclear Waste Project Office, 15 p.
- Bierman, P.R., and Gillespie, A.R., 1991, Accuracy of rock-varnish chemical analyses: implications for cation-ratio dating: *Geology*, v. 19, p. 196-199.
- Bierman, P.R., Gillespie, A.R., Kuehner, S., 1991, Precision of rock-varnish chemical analyses and cation-ratio ages: *Geology*, v. 19, p.135-138.
- Cahill, T.A., in press, Comment on "Accuracy of rock-varnish chemical analyses: implications for cation-ratio dating: *Geology*.
- Dorn, R.I., and Krinsley, D.H., 1991, Cation-leaching sites in rock varnish: *Geology*, v. 19, p. 1077-1080.
- Gianella, V.P. and Callaghan, E., 1934, The Cedar Mountain, Nevada, earthquake of December 20, 1932: *Seismological Society of America Bulletin*, v. 24, p. 345-377.
- Ku, T.L., 1989, Uranium-series age dating of pedogenic calcium carbonate samples from the Yucca Mountain area, in Bell and others, Progress report for the period 1 July 1988 to 30 September 1989, Task 1 Quaternary tectonics: Final report submitted to Nevada Nuclear Waste Project Office, Carson City, Nevada.
- Luo, S., and Ku, T.L., 1991, U-series isochron dating: a generalized method employing total-sample dissolution: *Geochimica et Cosmochimica Acta*, v. 25, p. 555-564.
- Loendorf, L.L., 1991, Cation-ratio varnish dating and petroglyph chronology in southeastern Colorado: *Antiquity*, v. 65, p. 246-255.
- Reneau, S.L., and Raymond, R., 1991, Cation-ratio dating of rock varnish: why does it work?: *Geology*, v. 19, p. 937-940.

APPENDIX A

**FINAL REPORT ON
VARNISH SAMPLES COLLECTED FROM
MONTE CRISTO AREA**

for

**YUCCA MOUNTAIN PROJECT
(Purchase Order No. 126,398)**

as part of the

Investigation of J.W. Bell

by

**Ronald I. Dorn, Ph.D.
2031 S. Sierra Vista Dr.
Tempe, AZ 85282
(602) 966-4245**

October 25, 1990

INTRODUCTION

The purpose of this investigation is to provide rock varnish dates on geomorphic surfaces in the Monte Cristo Valley area, in particular surfaces associated with the Benton Springs and Cedar Mountain faults.

The investigation has four phases. The first phase of the investigation was the sampling of rock varnish with J. W. Bell in May of 1990. The second phase was the preparation of samples for chemical analysis. The third phase was the chemical measurement of samples. The fourth phase is the analysis of these data.

The samples were collected from fourteen different sites:

1-JWB-1-CM-18
 1-JWB-1-CM-22
 1-JWB-1-CM-33
 1-JWB-1-CM-34
 1-JWB-1-CM-35
 1-JWB-1-BS-9
 1-JWB-1-BS-27
 1-JWB-1-BS-28
 1-JWB-1-BS-34
 1-JWB-1-BS-35
 1-JWB-1-BS-37
 1-JWB-1-BS-39
 1-JWB-1-BS-41
 1-JWB-1-BS-42

Samples were collected for three types of rock varnish dating. (1) Rock varnish cation ratios were measured on samples from all sites. (2) Accelerator radiocarbon dates were submitted for analysis from 8 sites. (3) Uranium-series analyses will be conducted on samples from sites 1-JWB-1-BS-35 and 1-JWB-1-BS-41. The rock varnish has been removed from the rock surface, but the uranium-series dating must wait for experiments to be conducted on proper sample extraction procedures. In addition, samples were collected from 1-JWB-1-CM-21 for experimental dating by *in situ* carbon-14 measurements on soil cobbles buried by ponded sediments. These samples have not been processed for *in situ* carbon-14, but I hope to get collaborative scientists working on this dating technique interested in analyzing the sample.

Results are reported here for rock varnish cation-ratios and rock varnish radiocarbon analyses.

METHODS

Rock varnish samples were collected in the field and assessed in the laboratory according to criteria outlined elsewhere (Dorn, 1989, table 2; Dorn et al., 1990; Krinsley et al., 1990).

Samples for cation-ratio dating were prepared according to the methods outlined in Dorn (1989) and Dorn et al. (1990). However, a new cleaning technique was also instituted for particularly 'dirty' samples. Varnish scrapings were ground up into a fine powder (less than 2 microns), suspended in deionized water, and let settle for a few minutes. The rock contaminants settled out first, leaving the rock varnish behind. The sample contamination assessment procedures in Dorn (1989) were used to assess

contamination after cleaning by this new technique. I estimate the greatest contamination to be about 4% by volume and less than 2% by chemistry in BS 9 and BS 34 since the underlying rocks that were sampled had minimal amounts of Ca, K, and Ti. The other sites are estimated to have less than 2% contamination by volume and less than 2% contamination by chemistry.

Samples for radiocarbon dating were prepared by the technique similar to Dorn et al. (1989), but with a significant advance. When the varnish was scraped, organic mats were removed from the varnish/rock interface rather than bulk samples of the lowest layer in the varnish. These subvarnish organic samples were identified as coming from the varnish/rock interface by pieces of the underlying rock being attached to the organic mats. These samples were then pretreated as in Dorn et al. (1989), with HF and HCl to remove loose organics attached to clays and carbonates. The organics were analyzed by accelerator mass spectrometry at the Institute of Nuclear Science in New Zealand (Lowe et al., 1988).

RESULTS

Table 1 presents a summary of cation ratio measurements from each of the sites. Table 2 presents radiocarbon dates from 8 sites and their corresponding cation-ratios used in the development of a cation-leaching curve. Table 3 presents raw cation ratio measurements, reasons why certain analyses were rejected, and cation-ratio age-estimates for sites not radiocarbon dated.

Table 1. Cation-ratio analyses from each site. Results are reported with a 1 sigma error. The sites are ordered from oldest (top) to youngest (bottom).

Site	(K+Ca)/Ti
1-JWB-1-BS-41	Range 3.79 - 4.06, where 3.79 best reflects minimum age of site
1-JWB-1-BS-35	4.40 ± 0.14
1-JWB-1-BS-27	5.42 ± 0.09
1-JWB-1-BS-28	5.48 ± 0.12
1-JWB-1-CM-22	5.50 ± 0.11
1-JWB-1-BS-37	5.50 ± 0.11
1-JWB-1-BS-39	5.52 ± 0.16
1-JWB-1-CM-18	5.56 ± 0.23
1-JWB-1-CM-33	6.59 ± 0.10
1-JWB-1-BS-42	6.82 ± 0.15
1-JWB-1-CM-35	7.03 ± 0.10
1-JWB-1-CM-34	7.13 ± 0.15
1-JWB-1-BS-34	9.07 ± 0.20
1-JWB-1-BS-9	9.27 ± 0.60

Table 2. Cation-ratio and radiocarbon data used in the construction of a cation-leaching curve for the Monte Cristo area.

Site	Age	Cation Ratio (K+Ca)/Ti	Lab No. of Radiocarbon Date
Initial Ratio	100	10.65 ± 0.53	
JWB BS34	625 ± 75	9.07 ± 0.20	NZA 1382
JWB CM35	5900 ± 90	7.03 ± 0.10	NZA 1380
JWB BS42	8000 ± 100	6.82 ± 0.15	NZA 1368
JWB CM33	11,250 ± 120	6.59 ± 0.10	NZA 1381
JWB CM18	21,940 ± 360	5.56 ± 0.23	NZA 1377
JWB BS37	22,170 ± 370	5.5 ± 0.11	NZA 1360
JWB CM22	22,740 ± 360	5.50 ± 0.11	NZA 1417
JWB BS27	25,430 ± 480	5.42 ± 0.09	NZA 1379

Figure 1 presents my best estimate for the cation-leaching curve in the Monte Cristo Valley. The cation-ratios and radiocarbon dates align up nicely for the last ~ 11ka. However, the four radiocarbon dates and corresponding cation ratios in the 21-26 ka range do not align up with the other points. The most reasonable perspective to take is that the curve breaks at about 11 ka and leaching rates were more intense in the latest Pleistocene.

Figure 1. Cation-leaching curve for the Monte Cristo Valley and vicinity. The least-squares regressions can be described by the following equations:

Equation #1: $CR = 14.67 - 2.01 (\text{Log}_{10} \text{Age})$; where age is ≤ 11 ka

Equation #2: $CR = 20.89 - 3.56 (\text{Log}_{10} \text{Age})$; where age is ≥ 11 ka

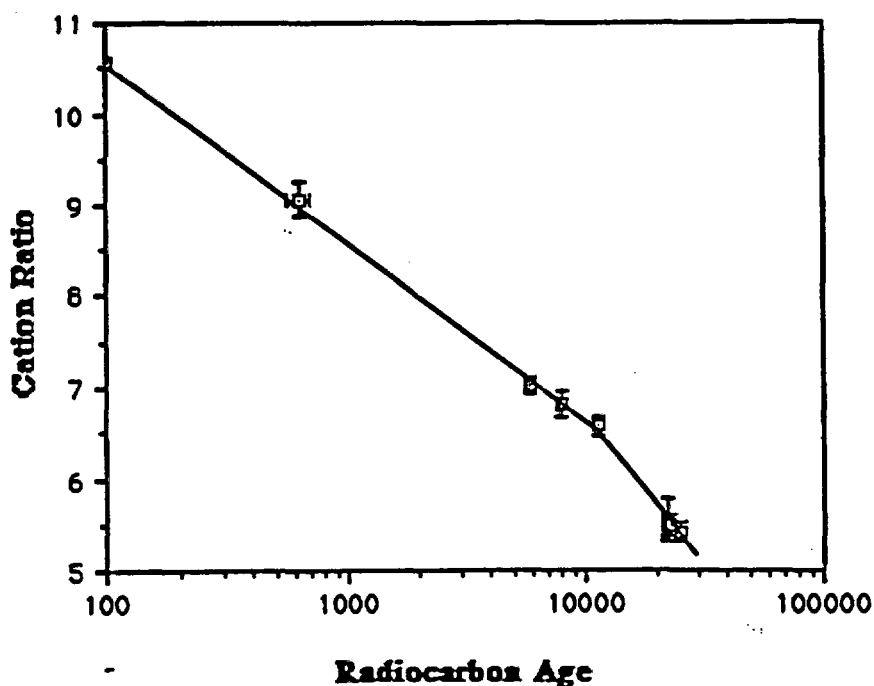


Table 3. Cation-ratio dates and raw chemical data.

Sites Using Equation #1: CR= 14.67 - 2.01 (Log10 Age); where age is \leq 11 ka																
Sample	Age	CR	Ave \pm 1 sigma	Na	Mg	Al	Si	P	K	Ca	Ti	Mn	Fe	Cu	Zn	Ba
8 I-JWB-1-BS9-probe-a	336	9.595	598	0.04	* nm	22.77	35.02	nm	2.16	1.87	0.42	2.03	7.18	0.08	0.00	0.03
I-JWB-1-BS9-probe-b	498	9.25	361	2.13	nm	19.73	39.59	nm	2.14	1.56	0.40	2.20	11.82	0.00	0.07	0.00
I-JWB-1-BS9-probe-c	188	10.1		1.08	nm	20.52	38.80	nm	2.24	1.70	0.39	2.05	9.00	0.16	0.05	0.02
I-JWB-1-BS9-probe-d	743	8.902		0.00	nm	23.05	36.78	nm	2.00	1.65	0.41	1.90	9.75	0.00	0.00	0.03
I-JWB-1-BS9-probe-e	878	8.756		0.00	nm	19.76	40.31	nm	2.01	1.58	0.41	1.87	14.14	0.00	0.00	0.00
I-JWB-1-BS9-probe-f	1,368	8.37		1.98	nm	21.18	30.94	nm	2.07	1.78	0.46	1.85	9.71	0.08	0.00	0.00
I-JWB-1-BS9-probe-g	528	9.2		0.07	nm	27.91	43.54	nm	2.37	1.77	0.45	2.01	1.22	0.00	0.00	0.04
I-JWB-1-BS9-probe-h	878	8.757		0.68	nm	16.10	31.81	nm	1.79	1.45	0.37	2.23	2.15	0.15	0.09	0.00
I-JWB-1-BS9-probe-i	184	10.12		0.03	nm	21.22	36.33	nm	2.28	1.97	0.42	2.53	13.42	0.00	0.00	0.00
I-JWB-1-BS9-probe-j	921	8.714		0.01	nm	20.19	39.17	nm	2.01	1.65	0.42	2.00	11.83	0.00	0.00	0.00
I-JWB-1-BS9-probe-k	845	8.789		0.16	nm	22.00	38.59	nm	1.54	1.80	0.38	2.05	11.86	0.00	0.05	0.00
I-JWB-1-BS9-probe-l	872	8.762		0.08	nm	19.00	32.13	nm	2.02	1.66	0.42	1.97	8.11	0.00	0.10	0.60
I-JWB-1-BS9-probe-m	194	10.07		0.04	nm	23.41	38.19	nm	1.01	1.71	0.27	1.74	7.82	0.00	0.00	0.00
I-JWB-1-BS9-probe-n	319	9.639		1.01	nm	20.04	37.55	nm	1.97	1.50	0.36	3.04	4.15	0.02	0.06	0.10
I-JWB-1-BS9-probe-o	211	10		0.55	nm	19.11	36.20	nm	1.88	1.62	0.35	1.90	6.88	0.27	0.00	0.40
* I-JWB-1-CM34-ICP-a	5,533	7.15	5,719	0.34	1.56	18.35	21.30	1.02	2.34	1.45	0.53	12.06	17.77	nm	nm	0.65
I-JWB-1-CM34-ICP-b	5,056	7.23	953	0.36	1.82	15.76	18.13	1.16	2.81	2.25	0.70	12.30	13.42	nm	nm	0.19
I-JWB-1-CM34-ICP-c	4,104	7.41		0.26	1.04	12.04	46.06	1.03	1.38	1.51	0.39	8.20	7.37	nm	nm	0.14
I-JWB-1-CM34-ICP-d	6,130	7.06		0.46	0.98	6.85	29.71	1.09	2.42	0.48	0.41	14.35	5.17	nm	nm	0.11
I-JWB-1-CM34-ICP-e	7,110	6.93		0.25	2.17	9.48	20.91	0.69	2.50	1.59	0.59	15.74	14.42	nm	nm	0.12
I-JWB-1-CM34-ICP-f	6,192	7.05		0.35	1.70	12.44	27.72	1.01	2.44	0.64	0.44	10.95	10.60	nm	nm	0.09
I-JWB-1-CM34-ICP-g	5,908	7.09		0.39	1.82	11.89	19.31	1.19	2.40	1.00	0.48	13.22	17.10	nm	nm	0.11
I-JWB-1-CM34-ICP-H-Ca-reject		15.49		0.39	2.36	9.22	17.75	0.90	2.94	7.92	0.70	4.27	12.78	nm	nm	0.13
Sites Using Equation #2: CR= 20.89 - 3.56 (Log10 Age); where age is \geq 11 ka																
Sample	Age	CR	Ave \pm 1 sigma	Na	Mg	Al	Si	P	K	Ca	Ti	Mn	Fe	Cu	Zn	Ba
I-JWB-1-BS39-ICP-a	21,175	5.47	20,651	1.60	1.09	14.65	25.21	1.32	2.03	1.58	0.66	12.50	19.76	nm	nm	0.14
I-JWB-1-BS39-ICP-b	19,449	5.60	2,153	0.59	7.44	6.55	28.86	0.82	1.14	2.89	0.72	11.28	10.30	nm	nm	0.67
I-JWB-1-BS39-ICP-c	23,012	5.34		0.59	0.87	16.82	20.30	1.24	1.20	1.15	0.44	9.66	8.07	nm	nm	0.11
I-JWB-1-BS39-ICP-d	23,171	5.33		0.46	1.15	9.53	9.03	1.55	2.04	1.69	0.70	14.11	21.72	nm	nm	0.15
I-JWB-1-BS39-ICP-e	19,150	5.63		0.56	2.02	22.94	25.02	1.42	1.98	1.40	0.60	5.05	5.18	nm	nm	0.16
I-JWB-1-BS39-ICP-f	17,952	5.73		0.55	1.12	22.56	25.23	1.21	1.62	2.20	0.67	5.12	6.16	nm	nm	0.58
I-JWB-1-BS39-ICP-g-MCF reject		2.25		0.78	1.75	21.49	32.44	1.01	0.97	0.72	0.75	13.04	10.36	nm	nm	0.14
I-JWB-1-BS39-ICP-h-Ti reject		1.48		0.57	1.20	28.84	4.90	0.71	0.99	1.60	1.75	5.79	14.13	nm	nm	0.16
Sample	Age	CR	Ave \pm 1 sigma	Na	Mg	Al	Si	P	K	Ca	Ti	Mn	Fe	Cu	Zn	Ba
I-JWB-1-BS28-ICP-a	22,528	5.37	21,121	2.50	0.95	21.92	30.13	1.84	2.74	1.02	0.70	9.81	6.25	nm	nm	0.00
I-JWB-1-BS28-ICP-b	20,063	5.55	1,579	0.49	0.77	21.84	23.49	0.92	1.80	1.20	0.54	5.01	5.47	nm	nm	0.15
I-JWB-1-BS28-ICP-c	18,711	5.66		1.20	1.20	18.40	39.25	0.78	2.25	1.13	0.60	6.34	7.61	nm	nm	0.13
I-JWB-1-BS28-ICP-d	21,495	5.45		0.47	0.90	35.85	17.06	1.63	0.99	1.25	0.41	2.56	4.19	nm	nm	0.10
I-JWB-1-BS28-ICP-e	22,962	5.34		5.00	1.10	15.22	12.10	1.66	1.80	1.46	0.61	13.55	8.25	nm	nm	0.12

1-15

91-1

1-JWB-1-BS28-ICP-f	20,963	5.49		0.46	1.54	19.66	41.26	0.62	1.96	1.77	0.68	6.99	2.81	nm	nm	0.13
1-JWB-1-BS28-ICP-q-Ca reject		18.44		0.34	1.49	5.08	16.09	1.05	2.64	8.06	0.58	2.07	14.42	nm	nm	0.10
Sites Too Old For Calibration																
Sample	Age (Eq. 1)	CR	Age (Eq. 2)	Na	Mg	Al	Si	P	K	Ca	Tl	Mn	Fe	Cu	Zn	Ba
1-JWB-1-BS41-ICP-a	261,260	3.79	62,720	0.28	1.30	17.30	43.15	0.65	1.90	1.16	0.81	7.53	7.15	nm	nm	0.13
1-JWB-1-BS41-ICP-c	249,319	3.83	61,080	0.41	1.46	15.39	24.49	0.77	1.20	1.40	0.68	7.07	6.09	nm	nm	0.12
1-JWB-1-BS41-ICP-d	240,295	3.86	59,832	0.22	2.07	31.83	9.65	0.52	1.30	0.41	0.44	1.59	8.09	nm	nm	0.14
1-JWB-1-BS41-ICP-e	226,690	3.91	57,899	0.29	1.93	18.78	29.97	0.77	1.48	2.04	0.90	7.64	7.66	nm	nm	0.18
1-JWB-1-BS41-ICP-f	221,636	3.93	57,168	0.44	2.43	18.97	30.91	0.86	1.54	2.00	0.90	7.72	8.20	nm	nm	0.13
1-JWB-1-BS41-ICP-q	199,025	4.03	53,805	0.47	1.87	16.80	25.95	1.03	1.45	1.66	0.77	8.18	6.29	nm	nm	0.15
1-JWB-1-BS41-ICP-h	197,117	4.03	53,514	0.33	1.96	22.43	18.16	0.88	2.23	0.68	0.72	3.44	9.29	nm	nm	0.10
1-JWB-1-BS41-ICP-i	191,670	4.06	52,675	0.46	1.85	18.37	30.85	1.20	1.55	2.23	0.93	8.14	9.12	nm	nm	0.15
Sample	Age (Eq. 1)	CR	Age (Eq. 2)	Na	Mg	Al	Si	P	K	Ca	Tl	Mn	Fe	Cu	Zn	Ba
1-JWB-1-BS35-ICP-a	158,720	4.22	47,364	0.34	1.98	8.31	32.19	0.77	1.21	3.43	1.10	6.85	10.77	nm	nm	0.13
1-JWB-1-BS35-ICP-b	158,131	4.23	47,265	0.36	1.66	17.20	26.27	1.34	1.31	1.52	0.67	7.60	5.54	nm	nm	0.15
1-JWB-1-BS35-ICP-c	125,877	4.43	41,564	0.39	1.37	18.03	31.58	1.11	2.57	2.25	1.09	12.81	12.70	nm	nm	0.13
1-JWB-1-BS35-ICP-d	118,114	4.48	40,099	0.25	2.00	31.32	13.03	0.88	1.44	1.02	0.55	2.24	10.08	nm	nm	0.18
1-JWB-1-BS35-ICP-e	116,739	4.49	39,835	0.32	2.18	10.15	29.39	0.75	1.14	3.73	1.08	6.63	7.85	nm	nm	0.71
1-JWB-1-BS35-ICP-f	108,291	4.56	38,184	0.53	1.25	12.12	36.69	1.56	1.54	0.54	0.46	5.84	5.10	nm	nm	0.50
1-JWB-1-BS35-ICP-q-Tl reject		0.97		0.31	2.19	24.75	27.14	0.67	1.96	0.51	2.55	14.97	3.69	nm	nm	0.13
Sites Used in Calibration																
Sample		CR	Ave \pm 1 sigma	Na	Mg	Al	Si	P	K	Ca	Tl	Mn	Fe	Cu	Zn	Ba
1-JWB-1-BS42-ICP-a		6.87	6.82	0.56	1.25	12.12	18.51	1.41	2.50	1.69	0.61	15.02	16.08	nm	nm	0.11
1-JWB-1-BS42-ICP-b		6.63	0.15	0.19	2.85	10.08	19.40	0.57	1.77	1.08	0.43	11.34	18.24	nm	nm	0.17
1-JWB-1-BS42-ICP-c		7.07		0.45	1.54	25.02	31.80	1.69	2.77	0.98	0.53	7.97	8.25	nm	nm	0.15
1-JWB-1-BS42-ICP-d		6.81		0.23	0.89	15.73	21.36	0.40	3.62	2.37	0.88	7.36	17.78	nm	nm	0.00
1-JWB-1-BS42-ICP-e		6.72		0.38	1.51	7.93	44.21	1.06	1.60	1.08	0.40	5.37	6.58	nm	nm	0.12
1-JWB-1-BS42-ICP-f		6.81		0.19	1.59	17.89	27.69	0.59	1.60	1.94	0.52	6.39	7.68	nm	nm	0.12
1-JWB-1-BS42-ICP-q-Ca reject		18.62		0.68	0.85	5.89	36.01	1.28	2.08	6.39	0.45	9.10	4.96	nm	nm	0.11
Sample		CR	Ave \pm 1 sigma	Na	Mg	Al	Si	P	K	Ca	Tl	Mn	Fe	Cu	Zn	Ba
1-JWB-1-BS34-ICP-a		8.73	9.07	0.32	2.05	14.07	21.34	1.06	3.57	2.20	0.66	7.64	21.70	nm	nm	0.09
1-JWB-1-BS34-ICP-b		8.82	0.20	0.23	2.29	7.75	24.06	0.90	3.91	2.26	0.70	7.89	21.92	nm	nm	0.16
1-JWB-1-BS34-ICP-c		8.99		0.36	2.48	12.45	15.05	0.72	6.64	2.34	1.00	17.46	14.16	nm	nm	0.20
1-JWB-1-BS34-ICP-d		9.06		0.27	2.07	15.23	16.97	1.00	2.89	6.10	0.99	4.62	8.35	nm	nm	0.12
1-JWB-1-BS34-ICP-e		9.08		0.33	2.00	22.20	27.65	0.92	1.82	1.72	0.39	5.75	5.89	nm	nm	0.15
1-JWB-1-BS34-ICP-f		9.19		0.36	1.40	16.97	18.08	0.94	2.75	2.03	0.52	13.89	13.93	nm	nm	0.16
1-JWB-1-BS34-ICP-g		9.23		0.29	2.09	7.14	15.14	0.91	1.50	2.56	0.44	7.99	11.78	nm	nm	0.13
1-JWB-1-BS34-ICP-h		9.24		0.31	1.96	21.81	8.65	0.93	3.30	1.33	0.50	9.83	8.62	nm	nm	0.17
1-JWB-1-BS34-ICP-i		9.31		0.38	1.39	6.08	20.42	0.94	2.97	1.50	0.48	11.80	11.43	nm	nm	0.13
1-JWB-1-BS34-ICP-j-Ca reject		18.95		0.62	1.43	9.42	24.65	1.87	1.94	4.47	0.34	11.04	5.03	nm	nm	0.10
1-JWB-1-BS34-ICP-k-Tl reject		1.14		0.42	1.58	24.29	30.12	0.67	1.76	0.20	1.72	10.46	7.06	nm	nm	0.14

1-1

Sample	Age	CR	Ave ± 1 sigma	Na	Mg	Al	Si	P	K	Ca	Ti	Mn	Fe	Cu	Zn	Ba
I-JWB-1-BS37-ICP-a		5.46	5.50	0.58	1.26	16.73	17.83	1.31	1.10	1.52	0.48	13.70	15.04	nm	nm	0.00
I-JWB-1-BS37-ICP-b		5.64	0.11	2.03	0.98	11.31	26.05	0.34	0.93	5.87	1.20	5.75	6.60	nm	nm	0.20
I-JWB-1-BS37-ICP-c		5.36		1.34	1.85	16.32	39.83	0.89	1.66	1.34	0.56	11.15	13.14	nm	nm	0.12
I-JWB-1-BS37-ICP-d		5.54		0.76	1.65	9.34	25.44	1.03	1.33	2.42	0.68	12.33	8.88	nm	nm	0.14
I-JWB-1-BS37-ICP-e		5.51		1.70	1.04	9.24	33.18	1.64	2.24	1.49	0.68	4.16	6.62	nm	nm	0.00
I-JWB-1-BS37-ICP-f		5.58		0.63	2.02	7.33	36.59	0.86	1.54	1.42	0.53	4.44	9.14	nm	nm	0.10
I-JWB-1-BS37-ICP-g		5.38		0.62	0.89	22.24	23.12	1.50	1.59	1.21	0.52	5.04	6.21	nm	nm	0.11
I-JWB-1-BS37-ICP-h-Ca reject		18.49		0.46	1.90	4.19	14.72	1.01	2.84	6.52	0.51	4.28	12.75	nm	nm	0.15
I-JWB-1-BS37-ICP-i-Ti reject		1.77		0.34	2.77	20.74	32.86	0.60	2.54	0.61	1.78	8.78	7.64	nm	nm	0.00
Sample		CR	Ave ± 1 sigma	Na	Mg	Al	Si	P	K	Ca	Ti	Mn	Fe	Cu	Zn	Ba
I-JWB-1-BS27-ICP-a		5.49	5.42	0.44	1.87	7.46	29.57	1.11	1.65	4.20	1.07	7.37	10.19	nm	nm	0.10
I-JWB-1-BS27-ICP-b		5.53	0.09	0.90	1.03	26.63	31.05	1.14	1.95	0.38	0.42	3.86	5.36	nm	nm	0.13
I-JWB-1-BS27-ICP-c		5.25		0.42	1.04	24.77	25.78	1.56	1.80	1.30	0.59	4.09	4.96	nm	nm	0.10
I-JWB-1-BS27-ICP-d		5.40		0.20	0.95	13.51	41.03	0.93	0.81	2.27	0.57	7.48	9.03	nm	nm	0.12
I-JWB-1-BS27-ICP-e		5.42		0.39	2.11	5.65	8.29	1.25	1.84	3.20	0.93	4.78	29.96	nm	nm	0.11
I-JWB-1-BS27-ICP-f		5.44		0.85	1.99	12.89	17.32	1.11	1.56	0.67	0.41	14.48	8.84	nm	nm	0.19
I-JWB-1-BS27-ICP-g-K reject		10.28		0.09	0.85	6.75	19.58	0.47	7.53	2.92	1.02	11.89	10.01	nm	nm	0.13
Sample		CR	Ave ± 1 sigma	Na	Mg	Al	Si	P	K	Ca	Ti	Mn	Fe	Cu	Zn	Ba
I-JWB-1-CM22-ICP-a		5.45	5.50	1.20	1.10	8.41	27.87	1.30	1.19	2.08	0.60	10.24	11.33	nm	nm	0.14
I-JWB-1-CM22-ICP-b		5.60	0.11	0.35	1.01	4.47	6.67	0.91	2.04	2.61	0.83	9.00	30.03	nm	nm	0.13
I-JWB-1-CM22-ICP-c		5.64		0.87	1.88	15.77	19.31	1.01	1.25	0.92	0.38	14.33	11.11	nm	nm	0.00
I-JWB-1-CM22-ICP-d		5.52		0.32	0.95	34.10	10.64	0.90	1.72	0.99	0.49	2.25	5.90	nm	nm	0.11
I-JWB-1-CM22-ICP-e		5.37		0.15	1.89	17.51	32.53	0.76	1.45	1.50	0.55	11.98	13.27	nm	nm	0.11
I-JWB-1-CM22-ICP-f		5.41		0.32	1.92	19.29	22.77	0.85	1.78	1.03	0.52	6.80	7.16	nm	nm	0.13
I-JWB-1-CM22-ICP-g-Ca-reject		17.26		0.32	1.31	4.68	38.92	2.49	1.77	7.15	0.52	9.55	5.57	nm	nm	0.08
Sample		CR	Ave ± 1 sigma	Na	Mg	Al	Si	P	K	Ca	Ti	Mn	Fe	Cu	Zn	Ba
I-JWB-1-CM18-ICP-a		5.41	5.56	0.26	1.28	20.18	20.39	1.09	2.00	1.35	0.62	6.33	6.03	nm	nm	0.12
I-JWB-1-CM18-ICP-b		5.87	0.23	0.48	1.63	18.63	26.52	1.07	1.20	0.66	0.32	5.87	13.09	nm	nm	0.15
I-JWB-1-CM18-ICP-c		5.52		0.66	0.94	17.30	19.53	0.97	1.30	1.24	0.46	10.01	9.15	nm	nm	0.11
I-JWB-1-CM18-ICP-d		5.78		0.29	1.98	17.80	25.95	1.22	0.91	0.75	0.29	10.25	12.15	nm	nm	0.14
I-JWB-1-CM18-ICP-e		5.37		0.71	1.26	14.22	26.35	0.97	1.70	0.70	0.45	15.72	6.56	nm	nm	0.00
I-JWB-1-CM18-ICP-f		5.24		0.25	0.65	14.48	25.74	1.92	3.68	1.56	1.00	13.67	14.50	nm	nm	0.00
I-JWB-1-CM18-ICP-g		5.71		0.56	0.91	13.62	15.27	2.44	1.86	0.99	0.50	6.90	11.02	nm	nm	0.16
Sample		CR	Ave ± 1 Sigma	Na	Mg	Al	Si	P	K	Ca	Ti	Mn	Fe	Cu	Zn	Ba
I-JWB-1-CM33-ICP-a		6.78	6.59	0.55	1.34	14.68	13.96	2.24	1.13	1.24	0.35	12.19	10.28	nm	nm	0.11
I-JWB-1-CM33-ICP-b		6.55	0.10	0.38	1.81	31.72	29.13	0.97	1.81	0.81	0.40	3.58	5.20	nm	nm	0.15
I-JWB-1-CM33-ICP-c		6.60		0.62	0.83	4.54	16.64	1.41	2.45	1.71	0.63	13.80	12.72	nm	nm	0.12
I-JWB-1-CM33-ICP-d		6.51		0.25	2.15	10.70	23.62	1.02	1.22	1.64	0.44	13.26	7.62	nm	nm	0.15
I-JWB-1-CM33-ICP-e		6.51		0.38	1.13	14.24	27.85	1.60	1.83	3.53	0.82	3.67	13.81	nm	nm	0.08
I-JWB-1-CM33-ICP-f		6.61		0.48	0.14	11.33	22.21	0.10	3.54	2.41	0.90	16.26	12.04	nm	nm	0.14
I-JWB-1-CM33-ICP-g-K-reject		11.01		0.21	0.37	18.77	18.45	0.42	6.64	2.30	0.81	12.35	14.36	nm	nm	0.00

Sample	CR	Ave ± 1 Sigma	Na	Mg	Al	Si	P	K	Ca	Ti	Mn	Fe	Cu	Zn	Ba
I-JWB-I-CM35-ICP-a	7.13	7.03	0.36	1.56	17.35	19.13	1.12	2.02	1.46	0.49	7.41	7.38	nm	nm	0.13
I-JWB-I-CM35-ICP-b	7.18	0.10	0.49	1.13	19.74	22.35	1.23	1.23	1.64	0.40	7.00	19.22	nm	nm	0.15
I-JWB-I-CM35-ICP-c	6.87		0.48	1.24	11.44	31.41	1.41	2.08	2.59	0.68	5.37	9.92	nm	nm	0.11
I-JWB-I-CM35-ICP-d	6.95		0.55	0.97	10.79	30.79	1.26	2.35	3.42	0.83	5.35	11.97	nm	nm	0.13
I-JWB-I-CM35-ICP-e	7.01		0.43	1.57	28.64	25.68	1.27	2.34	1.02	0.48	4.95	5.21	nm	nm	0.11
I-JWB-I-CM35-ICP-f	7.05		0.28	1.53	13.83	16.48	0.65	1.66	1.37	0.43	8.23	9.24	nm	nm	0.10
I-JWB-I-CM35-ICP-g	7.05		0.45	1.84	12.72	17.01	1.14	2.96	1.97	0.70	11.58	16.74	nm	nm	0.15
I-JWB-I-CM35-ICP-h-MCF-reject	3.22		0.43	2.07	23.97	26.08	0.74	0.97	1.32	0.71	4.99	4.85	nm	nm	0.08
Footnotes:															
* nm means not measured															
• ICP refers to inductively coupled plasma															
& probe refers to analysis by wavelength dispersive electron microprobe															
§ ICP and probe analyses from the same site are not on the same material															
'MCF reject' means the sample was rejected due to anomalous concentrations of microcolonial fungi that reduced the cation ratio															
'K reject' means the sample was rejected due to anomalous concentrations of potassium															
'Ca reject' means the sample was rejected due to anomalous concentrations of calcium															
'Ti reject' means the sample was rejected due to anomalous concentrations of titanium															

(1) Perhaps the 50-150 ka ash was deposited in an older alluvial unit, and the younger alluvial unit dated with varnish represents a relatively thin wedge of sediment. If so, this is significant, because it provides a rare opportunity to obtain volume of aggradational units in the latest-Pleistocene. If this interpretation is followed, the depth of the ash provides a maximum depth of accumulation for the unit dated by varnish.

(2) It is conceivable that all the varnishes from these sites eroded by enhanced acidity during the latest-Pleistocene. If the sites were occupied by Bristlecone and Limber Pines, for example, the secretion of acids from the decay of the litter would tend to dissolve the manganese and erode the varnish.

I do not prefer this hypothesis, because the varnish that was dated is nicely layered. Even if such biogeochemical erosion was intense, I would expect to see remnants of varnish preserved, but heavily pitted and eroded. I did observe pitted and eroded varnishes from all sites, but there were avoided in the dating work. Another reason why I do not favor this possibility is that I also get nicely layered varnishes from the older sites (BS35, BS41). This suggests it is possible to preserve layered varnishes throughout the latePleistocene.

(3) Perhaps the 50-150 ka age of the ash needs to be reexamined.

Interpretation of Cation-Ratio Age Estimates

Table 3 is broken down into four categories. The first category provides cation-ratio ages for BS9 and CM 34 that were not radiocarbon dated. The average and error for the age estimates are based on chemical measurements by inductively coupled plasma (ICP) and wavelength dispersive microprobe (probe) on varnishes on individual boulders. The ages for BS9 and CM34 are based on equation #1, that defines the curve during the Holocene.

The second category provides cation ratio ages for BS39 and BS28, based on equation #2, that defines the curve for the latest Pleistocene. Even if an individual wanted to argue that there was little justification for breaking the cation-leaching curve at about 11 ka, I would treat the cation-ratios as relative age information. I would point out that the radiocarbon dates from -21 to -25 ka have a narrow range of cation ratios from 5.42 to 5.56. And the cation-ratios of BS28 (5.48 ± 0.12) and BS39 (5.52 ± 0.16) rest in this range and should be placed in this time range.

The third category provides cation ratios for Sites BS35 and BS41. These low ratios are beyond the range of the radiocarbon calibration. I hope that is useful information. I have provided cation-ratio ages for the cation ratios from these sites, based on equation 1 and equation 2. These 'ages' have no basis in reality, since there is little justification for extending either of these curves. I just thought that you might be interested in this data. I hope that the sample processing methods for uranium-series dating of rock varnish are developed in the near future, since I have already prepared the samples.

The fourth category of data in table 3 are the cation ratios used in the construction of the cation-leaching curve.

SUMMARY

Cation-ratios from all sites collected in May of 1990 are reported. They provide a relative sequence of ages at present. Accelerator radiocarbon dates provide minimum ages for eight sites. These radiocarbon dates are used to provide cation-age ages for sites not radiocarbon dated, except for two sites beyond the range of radiocarbon dating.

REFERENCES

- Dorn, R.I. 1989. Cation-ratio dating: a geographic perspective. Progress in Physical Geography, v. 13, p. 559-596.
- Dorn, R.I., Jull, A.J.T., Donahue, D.J., Linick, T.W., and Toolin, L.T. 1989. Accelerator mass spectrometry radiocarbon dating of rock varnish. Bulletin, Geological Society of America, v. 101, p. 1363-1372.
- Dorn, R.I., Cahill, T.A., Eldred, R.A., Gill, T.E., Kusko, B.H., Bach, A.J., and Elliott-Fisk, D.L. 1990. International Journal of PIXE, v. 1, 157-195.
- Krinsley, D.H., Dorn, R.I., and Anderson, S.W. 1990. Factors that interfere with the age determination of rock varnish. Physical Geography, v. 11, p. 97-119.
- Lowe, D.C., Brenninkmeijer, C.A.M., Manning, M.R., Sparks, R., and Wallace, G. 1988. Radiocarbon determination of atmospheric methane at Baring Head, New Zealand. Nature, v. 332, p. 522-525.

APPENDIX B

**THE MAXIMUM BACKGROUND EARTHQUAKE
FOR THE BASIN AND RANGE PROVINCE,
WESTERN NORTH AMERICA**

Craig M. dePolo

**Nevada Bureau of Mines and Geology &
Center for Neotectonic Studies
Mackay School of Mines
University of Nevada, Reno**

July 1991

1-21

Introduction

The western United States is a region where many faults can easily be identified as seismogenic sources, allowing a straightforward estimation of seismic hazard. Less apparent is the significant hazard posed by background seismicity not directly linked to obvious sources. The aspect of background seismicity considered here is the size of the largest background earthquakes, sometimes called floating or random earthquakes. This study compiles historical earthquakes from magnitude 6 to 7 in the Basin and Range province to constrain the largest magnitude of the background activity.

The Basin and Range province of the western United States and northern Mexico is an actively deforming Cenozoic extension province (fig. 1). Spatial and temporal variations in rates of activity and in the style of faulting have occurred within this province throughout the Cenozoic. Contemporary rates of tectonic activity are higher in the northern part of the province and along its eastern and western margins. Historical seismicity in the province is concentrated in three major belts: 1) the western margin of the province, 2) the Central Nevada - Eastern California seismic belt, within the western part of the province, and 3) the Intermountain seismic belt, along the eastern margin of the province.

Twenty-two historical earthquakes from the Basin and Range province (fig. 1) were considered in this study (Tables 1, 2, 3). Due to variation in reported magnitudes, three types of magnitudes are used: surface-wave (M_s), local (M_L), and moment (M_w) magnitudes. Over the magnitude range being considered, M 6 to 7, these different magnitude scales yield similar values (Kanamori, 1983), and the values considered here are taken together in a single data set. For some of the earlier events, magnitudes are reported without reference to magnitude type; these are left undifferentiated (M) in Table 1. Although no systematic

study has been undertaken to evaluate errors and variability in the magnitude values used in this paper, they are estimated to be accurate within about 0.3 magnitude units.

Three main types of surface rupture are considered in this paper following Slemmons and dePolo (1986): primary, secondary, and sympathetic surface rupture. Primary surface rupture is fault displacement that is believed to be directly connected to subsurface seismogenic displacement, whereas secondary surface rupture has a branching or secondary relation to the main seismogenic fault. Primary surface rupture can be further subdivided into "minor" and "significant;" these relate to very incompletely expressed and representative of subsurface rupture, respectively. Sympathetic surface displacement is triggered slip along a fault that is "isolated" from the main seismogenic fault.

Maximum Background Earthquake (MBE)

Floating and random earthquakes are terms used to describe scattered seismicity, not usually attributed to a specific fault. Use of the term "floating earthquake" is somewhat confusing, however, because it implies a lack of understanding of, or relationship to, seismotectonics. Seismologist colleagues have mused that a floating earthquake must be a bad location iteration with a negative depth or a sonic boom. The term "random earthquake" suggests a statistical behavior that may not necessarily apply to these events, especially during swarming or clustering activity. The term "background seismicity" is also commonly used, but it implies a broader range of earthquake sizes (especially lower magnitudes) than considered here. The latter term is modified slightly to reflect the interest in the largest events, and the term "maximum background earthquake" (MBE) is used to describe these events (dePolo and others, 1990).

A maximum background earthquake is the largest event that occurs without significant primary surface rupture. This includes non-surface rupture events, as well as, those associated with small secondary and sympathetic surface breaks. These events may occur proximal to, or in areas that lack, late Quaternary faults. Because most of these events are associated with no or minor surface breaks, and are poorly preserved in the surficial geologic record, they can be difficult or impossible to characterize directly.

Background Earthquakes from the Basin and Range Province

An earthquake data set limited to the Basin and Range province was used for two principal reasons. First, the Basin and Range province exhibits an extensional tectonic style throughout its extent, although it has places, such as the west-central area, where contemporary translation may dominate. Second, the choice of events from a crustal area having relatively consistent seismic attenuation properties which can affect the consistency of magnitudes (Bonilla and others, 1984; Everndon and others, 1981). Previous studies in the eastern Basin and Range province have noted several earthquakes with magnitudes up to $6\frac{3}{4}$ which apparently occurred on structures having no surface expression (Doser, 1985; U. S. Bureau of Reclamation, 1986).

In this paper, two types of background earthquakes ($M \geq 6$) are compiled: those lacking surface rupture (Table 1), and those having secondary or sympathetic surface rupture with no or minor primary, tectonic surface rupture (Table 2). Also compiled are earthquakes with significant primary rupture that have magnitudes that are ≤ 7 (Table 3). Twenty three background events have occurred since 1920 that had magnitudes ≥ 6 . Five additional earthquakes were immediate aftershocks of primary-surface-rupture earthquakes;

four of these events were associated with the 1959 Hebgen Lake, Montana earthquake (M 6.5, 6, 6.5, 6) and one with the July 6 1954 Rainbow Mountain, Nevada earthquake (M 6). These aftershocks are not considered further here. Earthquakes occurring prior to 1920 are poorly documented and hence were not used, although many earthquakes of magnitude 6 or greater with no reported surface rupture occurred within the Basin and Range province.

Fourteen earthquakes ($M \geq 6$) lacking reported surface rupture have occurred in the Basin and Range province since 1920. Most of these earthquakes are in the magnitude range of 6 to 6.3. The largest event had a magnitude of M_w 6.6 (M 6 3/4), and is considered a reliable event to include because it was well studied for evidence of surface deformation and earthquake size (Pardee, 1926).

Eight earthquakes ranging in magnitude from 6 to 6.6 had secondary or minor primary surface rupture. Surface breaks associated with these events were commonly distributed and exaggerated in size. Only two events may have had some minor primary surface rupture: The 1934 Hansel Valley and the Chalfant Valley earthquakes. Displacements were on the order of 11 cm or less for the Chalfant Valley event; the Hansel Valley earthquake had 50 cm of displacement, but most if not all of this was probably due to liquefaction (McCalpin, 1989, pers. comm.). Most of the surface ruptures associated with the events in Table 2 were so minor (mostly less than 5 cm) that they were quickly obscured or eroded, and are not generally preserved in the geologic record.

Theoretical Considerations

Another consideration in the assessment of the MBE is to check that the simple physics of an earthquake that does not rupture the surface in the Basin and Range province is consistent with the maximum magnitude estimated from historical earthquakes. This argument is not definitive because there are several variables which cannot be rigorously constrained, but the range of magnitude values for reasonable estimates of these variables can be examined for a simple model. A circular rupture that is tangent with the surface and the base of the seismogenic zone is considered. Since most of the faults in the Basin and Range province appear to have a dip somewhat shallower than vertical, a commonly-encountered, 60° dip is used. Perhaps the most uncertain parameter in this model is the stress drop, however, a stress drop of at least 1 bar and as high as 100 bars seems to be a reasonable range (Kanamori and Anderson, 1975; Hanks, 1977). Using the relation developed by Brune (1970, 1971) for circular ruptures,

$$M_0 = (16/7)(r^3)(sd)$$

seismic moments (M_0 , dyne-cm) were estimated. In this relation r is radius (in centimeters) and sd is average stress drop (in dyne/cm²). These moments were converted to moment magnitudes for comparison to the historical earthquakes using Hanks and Kanamori's (1979) relation:

$$M_w = (2/3 \log M_0) - 10.7.$$

Values from these relations are presented in Table 4 for several different values of stress drop and two different estimates of seismogenic depth, 12 and 15 km. Magnitude values of these hypothetical earthquake ruptures are equivalent or larger than the historical MBE for average stress drops of 100 and 40 bars or higher for seismogenic depths of 12 and 15 km,

respectively. Since these are reasonable values for Basin and Range province earthquakes, it is concluded that the historical MBE is consistent with this simple physical model of earthquakes.

Discussion

The tabulation of historical earthquakes without surface rupture (Table 1) suggests that the MBE for the Basin and Range province is at least magnitude 6.3 and may be as high as magnitude 6.6. Only two events \leq magnitude 6.6 had significant primary surface rupture: the 1950 Fort Sage earthquake (M_s 5.6) and the July 1954 Rainbow Mountain earthquake (M_s 6.3). Contrasting this with the occurrence of 14 events without reported surface rupture and eight events with only minor surface rupture, suggests that most earthquakes of magnitude 6.6 and less in the Basin and Range province generally do not rupture the surface. Although minor primary surface faulting has occurred in some events (Table 2), it is unlikely to be preserved in the surficial geologic record.

Figure 2 is a histogram showing the number of non-surface rupture, secondary and other breaks, and primary surface rupture events that have occurred since 1920 over the magnitude range of 6 to 7. This figure shows the overlap between non-surface rupture and primary surface rupture events ($\sim M$ 6.3 - M 6.6).

Figure 3 shows this relationship with respect to maximum surface displacement. This figure shows the non-surface rupture and other minor ruptures all \leq to 20 cm displacement except for the 1934 Hansel Valley earthquake, which was probably enhanced by liquefaction. Further these events show no real trend of size increase with magnitude. In contrast, the primary surface rupture events do show a trend of increasing in maximum

surface displacement with magnitude. It is thought that these primary displacements are representative of the slip at depth, and are appropriate for developing regression equations for estimating potential earthquake sizes. It is also interesting to note that the intersection of this trend with the 0 displacement axis is around magnitude 6.5 to 6.6.

Even though different tectonic rates characterize the Basin and Range province, tectonic rate is not considered to be a determining factor in identifying earthquakes lacking surface rupture or in establishing the size of the MBE. Although the distribution of tectonic rates in the Basin and Range province is not well known, based on tectonic geomorphology and seismicity, areas with relatively higher strains exist (Eddington and others, 1987). Most earthquakes in this study have occurred in areas with apparent high strain rates. Because the timeframe of this study is so short, (70 years) it seems that this is only the effect of more earthquakes occurring in higher strain-rate areas since more are likely to occur, or occur more often. Significant earthquakes, such as the 1925 Clarkston, Montana (M_w 6.6) and 1935 Helena, Montana (M 6 & 6.3) were in areas that appear geomorphically to have relatively moderate strain rates. The MBE developed here is thought to be valid for the entire Basin and Range seismotectonic province, but, the frequency of this event likely varies with changes in regional strain rates.

The MBE can be considered the upper bound for background seismicity studies. Such a magnitude distribution or single event are commonly used in probabilistic studies as having a random occurrence over an area, using the number of historical background earthquakes from the area over various magnitude ranges. A deterministic way to input the MBE is to consider it occurring a set, or statistically determined, distance away from the site being analyzed. Because of the lack of precision involved in the magnitudes, it may be

more desirable and/or convenient to use magnitude 6.5 as the MBE value.

The MBE can also be considered the lower-bound magnitude for various magnitude-fault parameter regression equations developed or used in the Basin and Range province. Such regressions are commonly used for scaling the size of potential earthquakes that can occur along a fault. Estimations below the MBE magnitude are likely based on incompletely expressed or secondary ruptures.

Conclusions

The term "maximum background earthquake" appears to be a descriptive and an adequate term for referring to the largest background earthquake, or those without significant primary surface rupture.

In the Basin and Range province, earthquakes in the magnitude range of 6 to 6.6 without significant surface rupture far outnumber the number of earthquakes below magnitude 6.6 that have significant primary surface rupture. The maximum background earthquake for the Basin and Range province is magnitude 6.6, based on the historical earthquake record. This is consistent with a simple physics model of earthquake faulting without surface rupture.

Acknowledgements

I would like to thank James Brune and Diane dePolo for reviews and comments on this paper. This study was supported by a grant from the Nevada Nuclear Waste Projects Office.

References

- Beck, Paul Joseph, 1970, The southern Nevada-Utah border earthquakes, August to December, 1966: University of Utah. Masters Thesis, 61 p.
- Bell, John W., 1984, Quaternary fault map of Nevada, Reno Sheet: Nevada Bureau of Mines and Geology, Map 79.
- Bolt, Bruce A. and Miller, Roy D., 1975, Catalogue of earthquakes in northern California and adjoining areas: Seismograph Stations, University of California, Berkeley, California, 567 p.
- Bonilla, M. G., Mark, R. K., and Lienkaemper, J. J., 1984, Statistical relations among earthquake magnitude, surface rupture length, and surface fault displacement: Bull. of the Seismological Society of America, v. 74, p. 2379-2422.
- Brune, James N., 1970, Tectonic stress and the spectra of seismic shear waves from earthquakes: Journal of Geophysical Research, v. 75, p. 4997-5009.
- Brune, James N., 1971, Correction [Tectonic stress and the spectra of seismic shear waves from earthquakes]: Journal of Geophysical Research, v. 76, p. 5002.
- Callaghan, Eugene and Gianella, Vincent P., 1935, The earthquake of January 30, 1934, at Excelsior Mountains, Nevada: Bull. of the Seismological Soc. of America, v. 25, p. 161-168.
- Clark, M. M., Yount, J. C., Vaughan, P. R., and Zepeda, R. L., 1982, Map showing surface ruptures associated with the Mammoth Lakes, California, earthquakes of May 1980: U. S. Geological Survey, Miscellaneous Field Studies Map MF-1396.
- dePolo, Craig M. and Ramelli, Alan R., 1987, Preliminary report on surface fractures along the White Mountains fault zone associated with the July 1986 Chalfant Valley earthquake sequence: Bulletin of the Seismological Society of America, v. 77, p. 290-296.
- dePolo, C. M., Bell, J. W., and Ramelli, A. R., 1990, Estimating earthquake sizes in the Basin and Range province, western North America: perspectives gained from historical earthquakes, in Proceedings from High level radioactive waste management: American Nuclear Society, v. 1, p. 117-123.
- dePolo, Craig M., Clark, Douglas G., Slemmons, D. Burton, and Aymard, William H., 1989, Historical Basin and Range province surface faulting and fault segmentation, in Fault segmentation and controls of rupture initiation and termination, Schwartz, David P. and Sibson, Richard H., eds.: United States Geological Survey, Proceedings of Conference XLV, Open-File Report 89-315, p. 131-162.

- dePolo, Craig M., Clark, Douglas G., Slemmons, D. Burton, and Ramelli, Alan R., 1991, Historical surface faulting in the Basin and Range Province, western North America: implications for fault segmentation: *Journal of Structural Geology*, v. 13, p. 123-136.
- Doser, Diane I., 1985, The 1983 Borah Peak, Idaho and 1959 Hebgen Lake, Montana earthquakes: models for normal fault earthquakes in the Intermountain seismic belt, in *Proceedings of workshop XXVIII on the Borah Peak, Idaho, earthquake*, Stein, Ross S. and Bucknam, Robert C., eds.: United States Geological Survey, Open-File Report 85-290, p. 368-384.
- Doser, Diane I., 1988, Source parameters of earthquakes in the Nevada seismic zone (1915-1943): *Journal of Geophysical Research*, v. 93, p. 15,001-15,016.
- Doser, Diane I., 1989a, Source parameters of Montana earthquakes (1925-1964) and tectonic deformation in the northern Intermountain seismic belt: *Bulletin of the Seismological Society of America*, v. 79, p. 31-51.
- Doser, Diane I., 1989b, Extensional tectonics in northern Utah-southern Idaho, U.S.A., and the 1934 Hansel Valley sequence: *Physics of Earth and Planetary Interiors*, v. 48, p. 64-72.
- Doser, Diane I. and Smith, Robert B., 1989, An assessment of source parameters of earthquakes in the Cordillera of the western United States: *Bulletin of the Seismological Society of America*, v. 79, p. 1383-1409.
- Eddington, P. K., Smith, R. B., and Renggli, C., 1987, Kinematics of Basin and Range intraplate extension, in *Continental extensional tectonics*, Coward, M. P., Dewey, J. F., and Hancock, P. L., eds.: Geological Society Special Publication, No. 28, p. 371-392.
- Everndon, J. F., Kohler, W. M., and Clow, G. D., 1981, Seismic intensities of earthquakes of the conterminous United States - their prediction and interpretation: *United States Geological Survey Professional Paper 1223*, 56 p.
- Gianella, Vincent P., 1957, Earthquake and faulting, Fort Sage Mountains, California, December 1950: *Bulletin of the Seismological Society of America*, v. 47, p. 173-177.
- Hanks, Thomas C., 1977, Earthquake stress drops, ambient tectonic stresses and stresses that drive plate motions: *Pure and Applied Geophysics*: v. 115, p. 441-458.
- Hanks, T. C., and Kanamori, H., 1979, A moment-magnitude scale: *Journal of Geophysical Research*, v. 84, p. 2348-2350.
- Kachadoorian, Reuben, Yerkes, R. F., and Waananen, A. O., 1967, Effects of the Truckee California, Earthquake of September 12, 1966: *United States Geological Survey, Circular 537*, 14 p.

- Kanamori, H., 1983, Magnitude scale and quantification of earthquakes: *Tectonophysics*, v. 93, p. 185-199.
- Kanamori, Hiroo and Anderson, Don L., 1975, Theoretical basis of some empirical relations in seismology: *Bulletin of the Seismological Society of America*, v. 65, p. 1073-1095.
- Gawthrop, W. H. and Carr, W. J., 1988, Location refinement of earthquakes in the southwestern Great Basin, 1934-1974, and seismotectonic characteristics of some important events: *United States Geological Survey, Open-File Report 88-560*, 64 p.
- Gianella, Vincent P., 1951, Fort Sage Mountain, California, earthquake of December 14, 1950: *Geological Society of America, Bulletin*, v. 62, p. 1502.
- Lienkaemper, J. J., Pezzopane, S. K., Clark, M. M., and Rymer, M. J., 1987, Fault fractures formed in association with the 1986 Chalfant Valley, California, earthquake sequence: preliminary report: *Bull. Seismological Society of America*, v. 77, p. 297-305.
- Pardee, J. T., 1926, The Montana earthquake of June 27, 1925: *United States Geological Survey, Professional Paper 147-B*, 17 p.
- Pitt, A. M., Weaver, Craig S., and Spence, William, 1979, The Yellowstone Park Earthquake of June 30, 1975: *Bulletin of the Seismological Society of America*, v. 69, p. 187-205.
- Richins, William D., 1979, Earthquake data for the Utah region, in *Earthquake studies in Utah, 1850 to 1978*, Arabasz, Walter J., Smith, Robert B., Richins, William D., eds.: *University of Utah Seismograph Stations, Department of Geology and Geophysics, University of Utah, Special Publication*, p. 57-251.
- Shenon, P. J., 1936, The Utah earthquake of March 12, 1934, in Neumann, F., *United States earthquakes, 1934: United States Department of Commerce, Serial No. 593*, p. 43-48.
- Slemmons, D. B., 1957, Geological effects of the Dixie Valley-Fairview Peak, Nevada, earthquakes of December 16, 1954: *Bull. of the Seismological Society of America*, v. 47, p. 353-375
- Slemmons, David B., Jones, Austin E., and Gimlett, James I., 1965, *Catalog of Nevada earthquakes, 1852-1960: Bulletin of the Seismological Society of America*, v. 55, p. 537-583.
- Slemmons, D. Burton and dePolo, Craig M., 1986, Evaluation of active faulting and associated hazards, in *Active tectonics*, Wallace, R. E., ed.: *National Academy Press*, p. 45-62.
- Tocher, D., 1956, Movement on the Rainbow Mountain fault: *Seismological Society of America Bulletin*, v. 55, p. 519-565.

United States Bureau of Reclamation, 1986, Seismotectonic study for Palisades Dam and reservoir, Palisades project: United States Bureau of Reclamation, Seismotectonic Report 86-3, 198 p.

Table 1 Earthquakes $M > 6$ in the Basin and Range province since 1920 without surface rupture. Numbers in location column correspond with locations in Figure 1.

<u>Date</u>	<u>Location</u>		<u>Magnitude</u>	<u>References</u>
Sep. 29, 1921	Elsinore, UT	(1)	6 M_L	1
Oct. 1, 1921	Elsinore, UT	(1)	6 M_L	1
June 28, 1925	Clarkston, MT	(2)	6.6 M_w	2
June 25, 1933	Wabuska, NV	(3)	6 M_L	3
Oct. 19, 1935	Helena, MT	(4)	6.3 M	4
Oct. 31, 1935	Helena, MT	(4)	6 M	4
Nov. 23, 1947	Virginia City, MT	(5)	6.3 M	4
Dec. 29, 1948	Verdi, NV	(6)	6 M_L	3
May 23, 1959	Dixie Valley, NV	(7)	6.3 M_L	5
June 23, 1959	Schurz, NV	(8)	6.3 M_L	3
Sep. 22, 1966	Clover Mtn., NV	(9)	6.1 M	6
Mar. 27, 1975	Pocatello, ID	(10)	6.0 M_L	1
June 30, 1975	Yellowstone, MT	(11)	6.1 M_L	7
Nov. 23, 1984	Round Valley, CA	(12)	6.1 M_L	8

Table 2 Earthquakes $M > 6$ in the Basin and Range province since 1920 with associated secondary surface ruptures, but no or only minor primary rupture. Numbers in location column correspond to locations in Figure 1.

<u>Date</u>	<u>Location</u>		<u>D_{max} (cm)</u>	<u>Magnitude</u>	<u>References</u>
Jan. 30, 1934	Excelsior Mtn., NV	(13)	13	6.3 M_L	9
Mar. 14, 1934	Hansel Valley, UT*	(14)	50	6.6 M_s	10
Sept. 12, 1966	Boca Valley, CA	(15)	5	6.0 M_L	11
May 25, 1980	Mammoth Lakes, CA	(16)	20	6.1 M_L	12
May 25, 1980	Mammoth Lakes, CA	(16)	20	6.0 M_L	12
May 25, 1980	Mammoth Lakes, CA	(16)	20	6.1 M_L	12
May 27, 1980	Mammoth Lakes, CA	(16)	20	6.2 M_L	12
July 21, 1986	Chalfant Valley, CA*	(17)	11	6.5 M_L	13

* = possible minor primary surface rupture

Table 3 Earthquakes $M \leq 7$ in the Basin and Range province since 1920 with significant primary surface rupture. Numbers located in location column correspond to locations in Figure 1.

<u>Date</u>	<u>Location</u>	<u>Magnitude</u>	<u>D_{max}</u> <u>(cm)</u>	<u>References</u>
Dec. 14, 1950	Fort Sage, CA (18)	M 5.6	60	14
July 6, 1954	Rainbow Mtn., NV (19)	M _s 6.3	30	15
Aug. 24, 1954	Stillwater, NV (20)	M _s 7	76	16
Dec. 16, 1954	Dixie Valley, NV (21)	M _s 6.8+	270	17

Table 4 Theoretical Moment Magnitudes for Earthquakes that do not Rupture the Surface

<u>Stress</u> <u>Drop</u> <u>(Bars)</u>	<u>M_v</u> <u>(r=6.9 km)</u>	<u>M_v</u> <u>(r=8.7 km)</u>
1	5.2	5.4
10	5.9	6.1
20	6.1	6.3
30	6.2	6.4
40	6.4	6.6
50	6.4	6.6
60	6.4	6.6
70	6.5	6.7
80	6.5	6.7
90	6.5	6.7
100	6.6	6.8

References

- 1 Richins (1979)
- 2 Doser (1989a); Pardee (1926)
- 3 Slemmons and others (1965)
- 4 Doser and Smith (1989)
- 5 Gawthrop and Carr (1988)
- 6 Beck (1970);
- 7 Pitt and others (1979)
- 8 U.C. Berkeley Cat.

- 9 Callaghan and Gianella (1935), Doser (1988), dePolo and others (1989)
- 10 Shenon (1936), Doser (1989b)
- 11 Kachadoorian and others (1967), Bolt and Miller (1975)
- 12 U.C. Berkeley Cat., Clark and others (1982)
- 13 U.C. Berkeley Cat., dePolo and Ramelli (1987), Lienkaemper and others (1987)

- 14 Gianella (1957), Bonilla and others (1984)
- 15 Tocher (1956), Bonilla and others (1984)
- 16 Tocher (1956), Bonilla and others (1984), Bell (1984)
- 17 Slemmons (1957), Bonilla and others (1984)

- Figure 1** The Basin and Range province of western North America and the locations of earthquakes considered in this study. The numbers correspond to those listed in the location column of Tables 1, 2, and 3.
- Figure 2** Histogram showing the number of non-surface rupture, secondary and other minor surface breaks, and primary surface ruptures occurring over the magnitude range 6 to 7.
- Figure 3** Graph showing magnitude versus maximum surface displacement for non-surface rupture, secondary and other minor surface breaks, and primary surface displacements. Note the break in the maximum displacement scale. The additional data used for the larger primary surface rupture events is compiled in dePolo and others (1991). Uncertainties in the magnitude values are estimated to be on the order of a third of a magnitude unit. Uncertainties in surface displacement measurements scale with displacement, from a few to ten centimeters for the smaller displacements and up to perhaps a half a meter or so for the larger displacements.

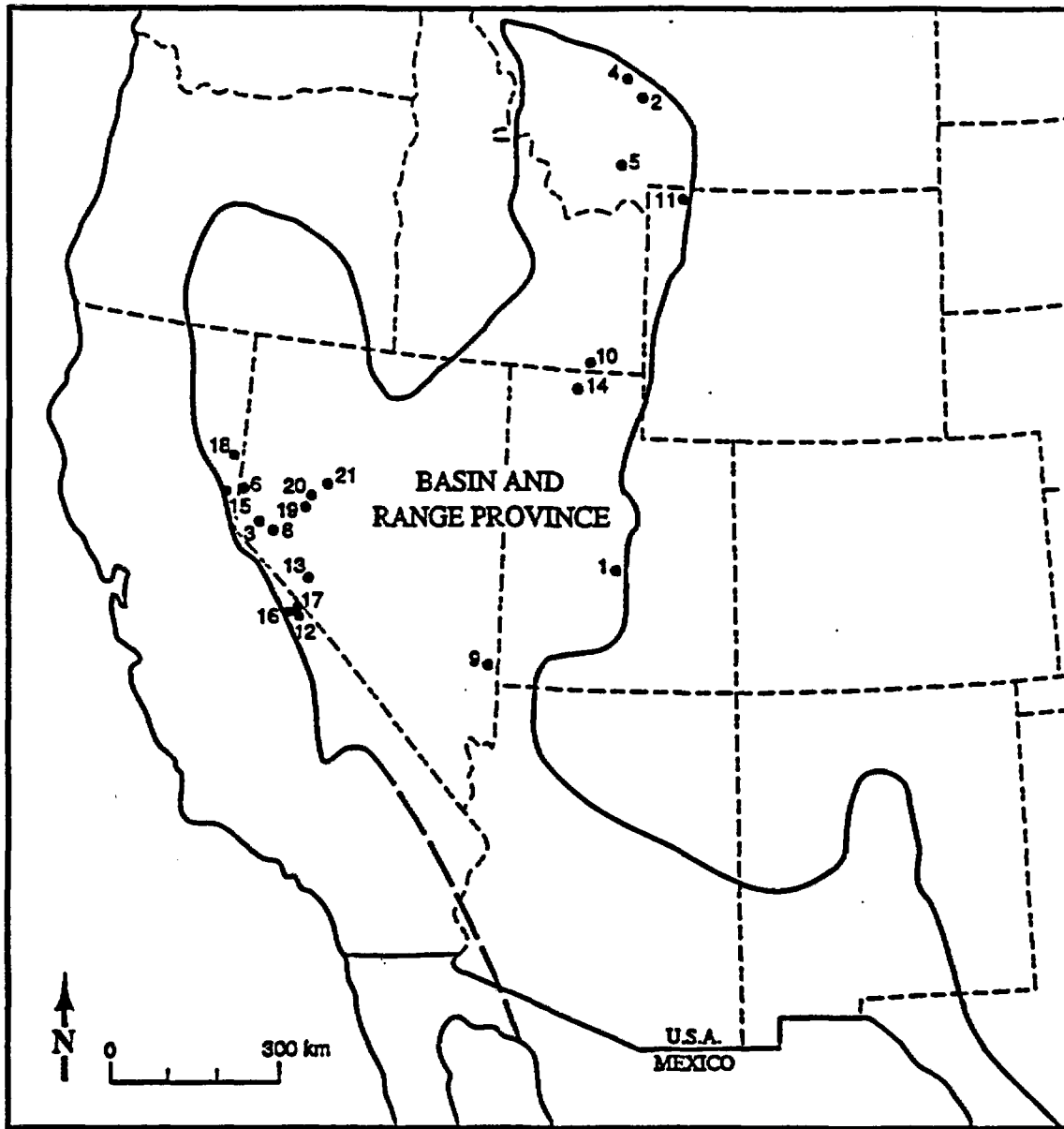


Fig 1

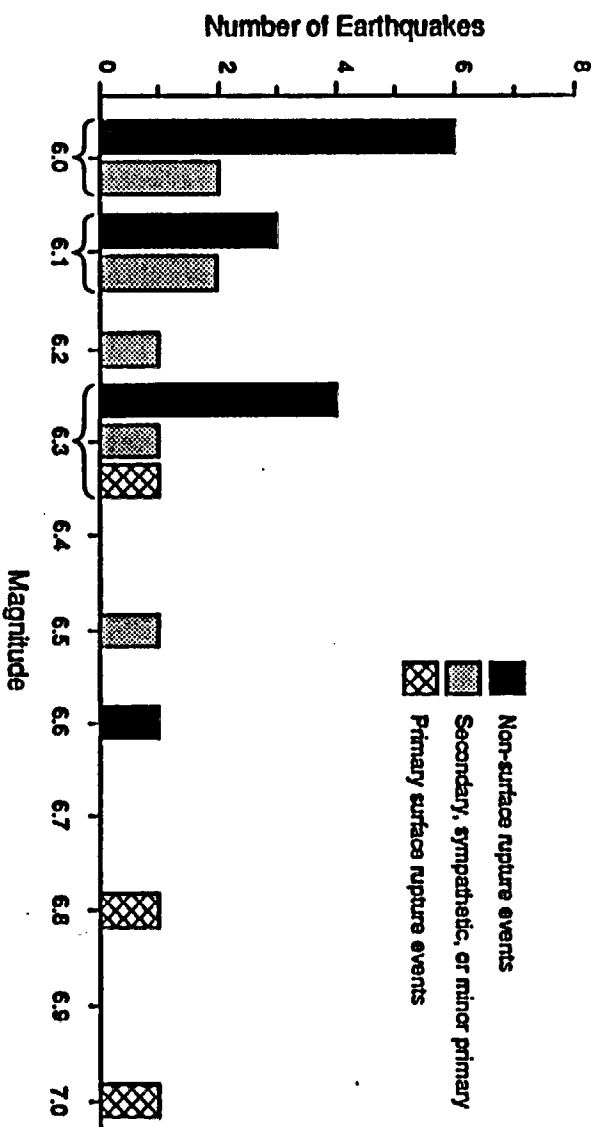


Fig 2

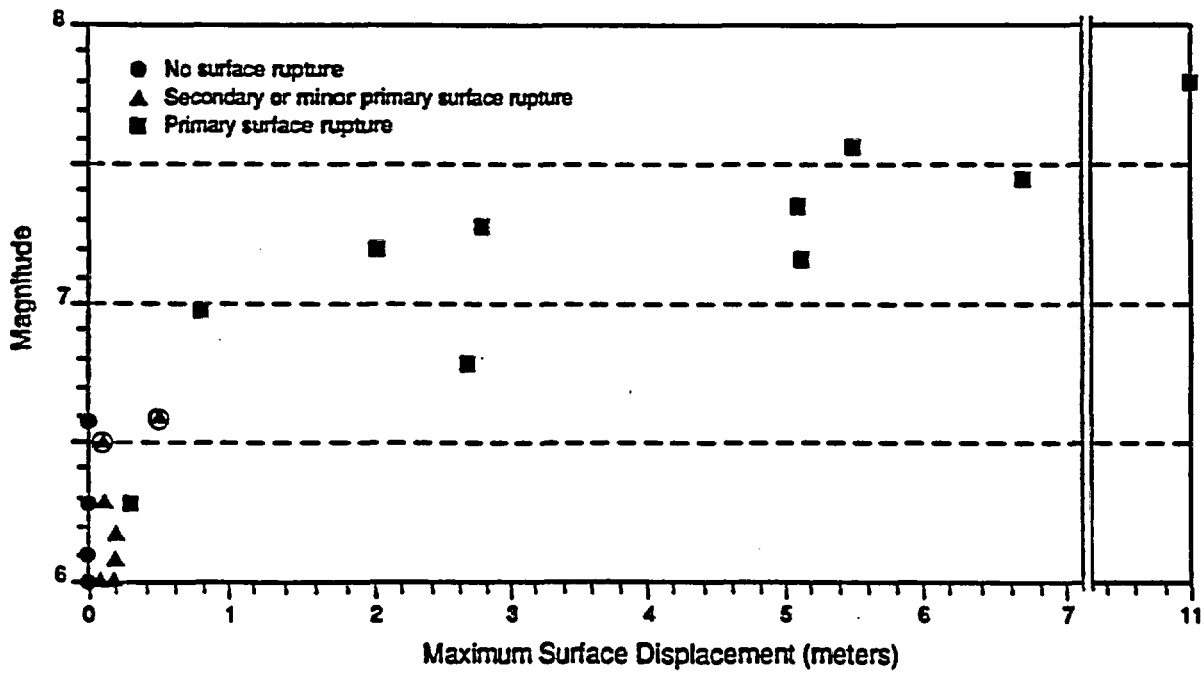


Fig 3

APPENDIX C

Historical surface faulting in the Basin and Range province, western North America: implications for fault segmentation

CRAIG M. DEPOLO

Nevada Bureau of Mines and Geology, Mackay School of Mines, University of Nevada, Reno, NV 89557, U.S.A.

DOUGLAS G. CLARK and D. BURTON SLEMMONS

Center for Neotectonic Studies, Mackay School of Mines, University of Nevada, Reno, NV 89557, U.S.A.

and

ALAN R. RAMELLI

Nevada Bureau of Mines and Geology, Mackay School of Mines, University of Nevada, Reno, NV 89557, U.S.A.

(Received 21 December 1989; accepted in revised form 20 June 1990)

Abstract—The distribution of surface ruptures caused by 11 historical earthquakes in the Basin and Range province of western North America provides a basis for evaluating earthquake segmentation behavior of faults in extensional tectonic settings. Two of the three moderate magnitude ($5.5 < M < 7$) events appear to be confined to individual geometric or structural segments. The remaining nine events, eight of which had large magnitudes ($M \geq 7$), ruptured multiple geometric or structural segments. Several of these events had widely distributed surface-rupture patterns, ruptured in complex manners, and extended beyond distinct fault-zone discontinuities. Some of the surface ruptures associated with these events may have resulted from sympathetic or secondary surface faulting. Approximately one-half of the surface rupture end points coincided with distinct fault-zone discontinuities.

This study indicates that earthquake ruptures in extensional tectonic settings may not be confined to individual geometric or structural segments. Some rupture-controlling discontinuities may be difficult to identify and significant faulting may occur beyond postulated rupture end points. Rupture of multiple geometric or structural segments should be considered in the evaluation of large earthquakes. Several lines of evidence, particularly timing information, are needed to delineate potential earthquake segments in the Basin and Range province.

INTRODUCTION

INDIVIDUAL historical earthquakes rarely rupture entire fault zones (Albee & Smith 1966). Seismic hazard analyses, therefore, require an estimate of how much of a given fault zone will rupture during future earthquakes to characterize earthquake sizes. Several techniques have been developed to estimate potential earthquake-rupture lengths, including half-length, fractional fault length and fault segmentation techniques (dePolo & Slemmons in press). Of these, the fault segmentation technique is the most appealing, principally because it incorporates more physical and paleoseismic information than other techniques. Fault segmentation modeling involves the division of fault zones into discrete segments separated by rupture-controlling discontinuities.

This paper summarizes 11 historical earthquakes from the Basin and Range extensional province (Fig. 1). These events exhibit a wide range of variability in their surface rupture patterns, from simple to very complex. The goal of this study was to explore the features that may have controlled or influenced the ends of these

earthquake ruptures and to characterize the ruptures with respect to fault segments. Surface ruptures with normal, normal-oblique and strike-slip senses of displacement are represented.

Three types of surface rupture are considered in this paper: primary, secondary and sympathetic. Primary surface rupture is fault displacement that is believed to be directly connected to subsurface seismogenic displacement, whereas secondary surface rupture has a branching or secondary relation to the main seismogenic fault. Sympathetic surface rupture is triggered slip along a fault that is 'isolated' from the main seismogenic fault.

FAULT SEGMENTATION

Fault segmentation has been described at a wide range of scales and with varying criteria. This has led to different definitions of the term "segment", making it important to understand a specific author's definition of the word and to clearly define the term when using it. This study examines historical "earthquake segments", or those parts of a fault zone or fault zones that have

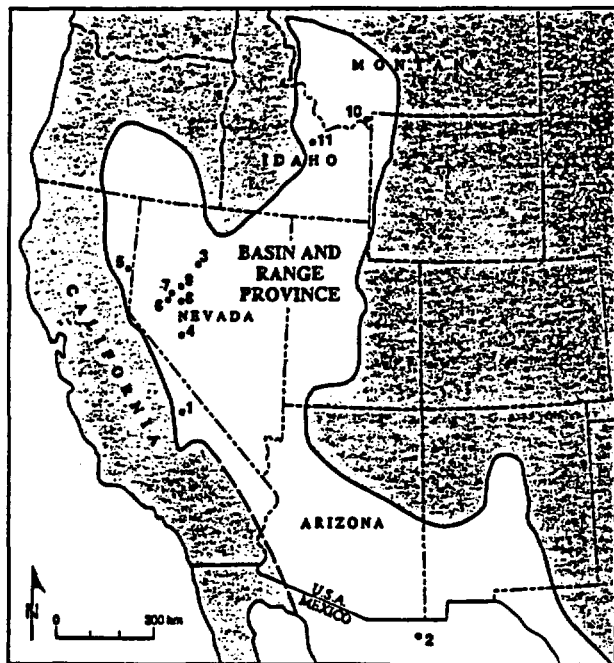


Fig. 1. Location map of primary surface faulting earthquakes in the Basin and Range province, western North America. 1, 1872 Owens Valley; 2, 1887 Sonora, Mexico; 3, 1915 Pleasant Valley; 4, 1932 Cedar Mountain; 5, 1950 Fort Sage Mountain; 6, 1954 Rainbow Mountain; 7, 1954 Stillwater; 8, 1954 Fairview Peak; 9, 1954 Dixie Valley; 10, 1959 Hebgen Lake; 11, 1983 Borah Peak. Boundary of the Basin and Range province modified from Stewart (1983).

ruptured during individual earthquakes. Large earthquake segments may comprise one or more fault segments as defined in other ways, such as by fault geometry or fault structure (geometric and structural segments, respectively).

Earthquake segmentation involves the identification and characterization of discontinuities along fault zones which may potentially act as barriers to earthquake ruptures. Many compilations of the characteristics of fault-zone discontinuities have been presented (e.g. Schwartz & Coppersmith 1984, 1986, Slemmons & dePolo 1986, Knuepfer *et al.* 1987, Barka & Kadinsky-Cade 1988, Wheeler & Krystinik 1988, dePolo *et al.* 1989, Knuepfer 1989, Crone & Haller 1991). Indicators of fault-zone discontinuities include: geometric, structural, behavioral, paleoseismic, geomorphic, geological, geophysical and rheological data (dePolo *et al.* 1989). Several lines of evidence are needed to identify a potential earthquake discontinuity and to evaluate its persistence through time. An important consideration for earthquake discontinuities is scale; in general, only the larger features (scales on the order of hundreds of meters to kilometers) appear capable of arresting propagating earthquake ruptures (Sibson 1989, Crone & Haller 1991).

The most common fault-zone discontinuities can be grouped into three major categories: geometric, structural and behavioral. These distinctions are used for descriptive purposes; there are 'gray areas' between categories and some discontinuities may fit into more

than one category. Geometric discontinuities include changes in fault orientation (bends), step overs, and separations or gaps in a fault zone (see Crone & Haller 1991). Wheeler (1987) pointed out that geometric discontinuities in plan view may not have a significant effect on earthquake ruptures with a normal sense of displacement. An abrupt bend in plan view of a normal fault, for example, can accommodate a vertical-slip vector, and would not necessarily inhibit a propagating rupture. Thus, the sense of displacement is an important factor to consider in the evaluation of geometric data. Structural discontinuities include fault branches, intersections with other faults and folds, and terminations at cross structures. Since the ends of fault zones can be considered structural discontinuities, distinct or individual faults can be classified as structural segments. Behavioral discontinuities include changes in slip rates, interseismic intervals, senses of displacement or creeping vs locked behavior.

Paleoseismic data can clarify the rupture histories of earthquake segments and the long-term behavior of discontinuities. In this paper, paleoseismicity refers specifically to prehistoric earthquakes. Determining the history and lateral extent of paleoearthquake segments along a fault zone can provide direct temporal and spatial evidence of previous segmented behavior. Unfortunately, paleoseismic data are limited for most of the events presented in this paper.

BASIN AND RANGE PROVINCE

The Basin and Range province of the western United States and northern Mexico is an actively deforming Cenozoic extensional province (Fig. 1). Spatial and temporal variations in the rates of activity and in the style of faulting have occurred within this province throughout the Cenozoic. Contemporary rates of tectonic activity are higher in the northern part of the province and along its eastern and western margins. Regions of active extension are marked by high heat flow, thin crust, sparsely distributed bimodal volcanism and earthquakes with focal depths generally limited to 10–15 km or less. Geologic, geomorphic and geophysical data indicate that extensional tectonism has resulted in widespread domains of tilted fault blocks, horst and graben development, and a heterogeneous upper crust, both structurally and lithologically (Stewart 1980). Historical seismicity in the province is concentrated in three major belts: (1) the western margin of the province, (2) the central Nevada–eastern California seismic belt, within the western part of the province; and (3) the northern part of the Intermountain seismic belt, along the eastern margin of the province.

HISTORICAL SURFACE-FAULTING EVENTS

Eleven earthquakes that have been associated with primary tectonic surface rupture in the Basin and Range

Table 1. Historical primary, tectonic surface faulting events in the Basin and Range province. Number corresponds to those in Fig. 1. M = moment or intensity magnitude, undifferentiated, M_w = moment magnitude, M_s = surface-wave magnitude, M_L = local magnitude

No.	Date	Magnitude	Earthquake or fault	Main style of surface faulting
1	26 March 1872	$M = 7.7-8.0+$	Owens Valley, California	Strike-slip
2	03 May 1887	$M_w = 7.2-7.4$	Sonora, Mexico	Normal
3	03 October 1915	$M_s = 7.6$	Pleasant Valley, Nevada	Normal
4	21 December 1932	$M_s = 7.2$	Cedar Mtn. Nevada	Strike-slip
5	14 December 1950	$M_L = 5.6$	Fort Sage Mtn. California	Normal
6	06 July 1954	$M_s = 6.3$	Rainbow Mtn. Nevada	Normal
7	24 August 1954	$M_s = 7$	Stillwater, Nevada	Normal
8	16 December 1954	$M_s = 7.2$	Fairview Peak, Nevada	Normal-oblique
9	16 December 1954	$M_s = 6.8$	Dixie Valley, Nevada	Normal
10	17 August 1959	$M_s = 7.5$	Hebgen Lake, Montana	Normal
11	29 October 1983	$M_s = 7.3$	Borah Peak, Idaho	Normal

province are reviewed in this paper (Table 1 and Fig. 1). These events are not uniformly distributed throughout the Basin and Range province, but occur in discrete spatial and temporal groupings (Wallace 1987). Seven of the 11 events occurred in the NNE-trending central Nevada–eastern California seismic belt (Wallace 1984a); the 1959 Hebgen Lake and 1983 Borah Peak earthquakes are located in the Intermountain seismic belt.

Due to variations in the types of magnitude reported for different events, different magnitude scales are used here. These events, however, lie within a magnitude range over which these different scales are reasonably comparable (see Kanamori 1983). The following acronyms are used in this paper to distinguish the different scales: (M_s) surface-wave magnitude, (M_L) local magnitude, (M_w) moment magnitude and (M) undifferentiated moment or intensity magnitudes.

1872 Owens Valley, California, earthquake

The 26 March 1872 Owens Valley earthquake is the largest historical event in the Basin and Range province, in terms of estimated magnitude, maximum displacement and rupture length. It had an estimated magnitude of $M7.7-8+$, and was felt strongly over an area of 324,000 km² (Oakeshott *et al.* 1972, Coffman & von Hake 1973, Hanks & Kanamori 1979, Beanland & Clark in press). The earthquake caused about 90–110 km of surface faulting along the Owens Valley fault zone (OVFZ) (Fig. 2). Surface displacements were dominantly right-lateral strike-slip, with a single-trace maximum lateral offset of 7 m, an average lateral offset of 6 m, a maximum vertical offset of 4.4 m and an average vertical offset of 1 m (Beanland & Clark in press). A maximum surface displacement of 11 m (normal-right oblique) is derived by adding displacement from two parallel fault traces in the Lone Pine area (Lubetkin & Clark 1988, Beanland & Clark in press). The surface rupture consisted of a relatively straight central section located in the middle of a large graben (Owens Valley) and more distributed, non-linear northern and southern sections (Fig. 2).

The north and south ends of the 1872 rupture are at or

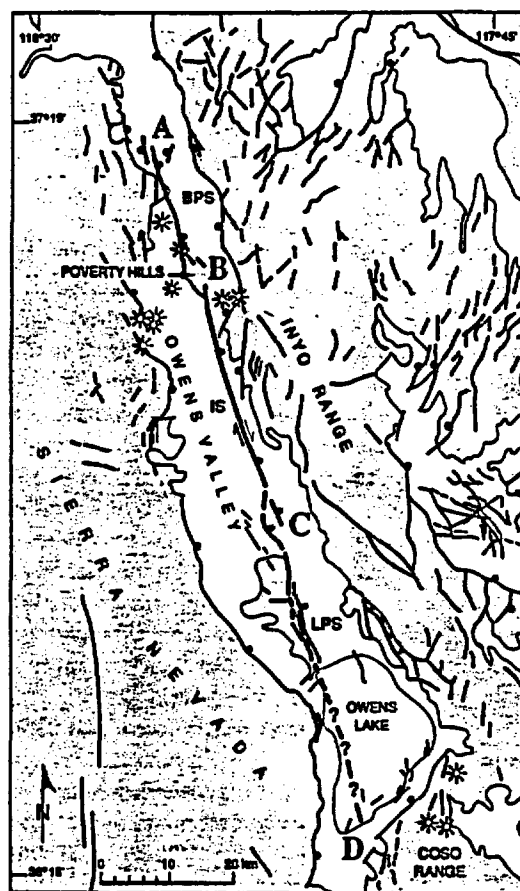


Fig. 2. Surface ruptures from the 1872 Owens Valley earthquake (from Beanland & Clark in press). BPS = Big Pine segment, IS = Independence segment, LPS = Lone Pine segment. Stars are Quaternary volcanic centers. Bedrock from Matthews & Burnett (1965), Strand (1967). Streitz & Stinson (1974) and Dunne *et al.* (1978). Bold lines denote the surface ruptures. Medium weight lines denote other selected faults. Balls are shown on the downthrown side of faults with normal components. Thrust faults are shown with barbs. Patterned areas are bedrock. White areas are alluviated valleys and basins. The large letters on figures are end points or discontinuities discussed in text.

near extensional basins. The north end of the rupture zone steps and distributes slip into the northern Owens Valley, creating small closed depressions (Fig. 2, point A). The exact position of the southern end of the 1872 surface rupture is less certain. The 1872 rupture clearly

offsets shorelines at the northern edge of Owens Lake, whereas near the southern edge, the amount of tectonic displacement is less clear due to extensive liquefaction. The southern end of the 1872 rupture is probably terminated where the southern Owens Lake basin is bounded by NE-trending faults and the Coso Range (Fig. 2, point D).

Beanland & Clark (in press) divide the OVFZ into seven segments on the basis of fault continuity, strike and style. We apply a more generalized segmentation criteria than Beanland & Clark, although we adopt some of their segment names. From south to north, the OVFZ can be divided into at least three geometric segments (Fig. 2): the Lone Pine segment, the Independence segment and the Big Pine segment. These segments are defined primarily on the basis of geometric discontinuities. The exact location of the southern end of the Lone Pine segment is uncertain, but it appears to terminate near intersecting cross faults (Fig. 2, point D). Because of the presence of young lacustrine sediments and liquefaction features, the OVFZ is difficult to delineate along the southern 18 km of this segment. Based on a 1-km-wide right step and a slightly more westerly strike of lineaments and faults mapped by Carver (1969) in the dried Owens Lake bottom, the distinction of this southern part as a fourth geometric segment may be warranted. The Lone Pine segment is distinct from near the northern part of Owens Lake northward for about 32 km to a 1.5-km-wide right step (approximate cross-strike distance) between the Lone Pine and Independence segments (Fig. 2, point C). The Lone Pine segment is as much as 2.5 km wide, and has a greater surface trace complexity and a larger normal component than the Independence segment. The Independence segment (35 km long) is a remarkably linear, narrow fault zone (as much as 0.5 km wide), with small sag ponds and other minor structural complexities, such as small steps in the fault trace. At the northern end of the Independence segment, the Poverty Hills form a prominent discontinuity in the OVFZ (Fig. 2, point B). The presence of this discontinuity is interpreted based on several factors: (1) change in fault geometry and distribution; (2) intersections with other faults; (3) a postulated left step in the fault zone (Martel 1984); (4) a bedrock high between the Owens Lake and Bishop basins and associated geophysical anomalies; and (5) Quaternary volcanism. The 1872 surface rupture was deflected across Poverty Hills, but the discontinuity did not terminate the rupture. The Big Pine segment extends for 23 km northward from the Poverty Hills. This segment trends slightly more westerly than the rest of the OVFZ and exhibits a complex pattern with several fault strands.

The 1872 event is interpreted to have ruptured at least three geometric segments along the OVFZ. Differences in surface complexity and in the amount of vertical slip component between the Lone Pine and Independence segments further distinguishes these as behavioral segments. The OVFZ shows evidence of at least two prior Holocene events which may have ruptured the same segments as in 1872 (Beanland & Clark 1987).

1887 Sonora, Mexico, earthquake

The 3 May 1887 Sonora earthquake, in the southern Basin and Range province, had an estimated magnitude of M_w 7.2–7.4 and an estimated felt area of nearly 2,000,000 km² (Dubois & Smith 1980, Dubois & Sbar 1981, Herd & McMasters 1982). Dominantly normal-slip surface faulting occurred along approximately 75 km of the Pitaycachi fault (Bull & Pearthree 1988), making this the longest normal-slip surface rupture in the worldwide historical record. Fault scarps produced during this event ranged in height from 0.5 to 4+ m (Bull & Pearthree 1988, Pearthree *et al.* 1990). Herd & McMasters (1982) measured a maximum normal-slip displacement of 5.1 m.

Surface faulting during the 1887 earthquake occurred along a mountain front–alluvium contact for much of the rupture length (Goodfellow 1888, Bull & Pearthree 1988). The surface rupture can be divided into three geometric segments (P. A. Pearthree personal communication 1988). The southern segment is about 22 km long and had less than 1 m vertical displacement, significantly less displacement than that to the north. It dies out in bedrock at its southern end, and is separated from the main rupture by a 2.5-km-wide right step (Fig. 3, points D and C). The central segment follows the mountain front of the Sierra de San Luis for much of its overall length of 39 km and includes the largest surface displacements. Near its southern end, the central segment departs from a 60° bend in the range front, has a right step of about 0.5 km, and extends 10 km to the south across a large valley, where it dies out just south of a bedrock hill within the valley. The northern 14 km of the surface rupture splays from the range front, follows an alluvium–pediment contact for several kilometers, and extends 5 km into the San Bernardino Valley (Bull & Pearthree 1988). This northern part of the rupture is considered a third segment based on a bend of approximately 30°, bifurcation into several parallel fault traces, and divergence from the range front (Fig. 3, point B). Surface ruptures and cumulative displacement are essentially continuous through this discontinuity.

The Sonora earthquake was associated with a relatively simple, narrow surface rupture, mainly along a range front. The surface rupture can be divided into three geometric segments. Bull & Pearthree (1988) estimated that about 200,000 years had elapsed since the event prior to 1887, and that the prehistoric surface rupture appears to be similar in length and amount of displacement to the historical earthquake.

1915 Pleasant Valley, Nevada, earthquake

The 3 October 1915 Pleasant Valley earthquake had a magnitude of M_w 7.6 (Bonilla *et al.* 1984), and was felt from southern Washington to northern Mexico, and from western Colorado to the Pacific coast. Four major fault scarps formed a right-stepping en échelon pattern (Fig. 4) for a combined, end-to-end rupture length of 60 km (Wallace 1984b). From northeast to southwest,

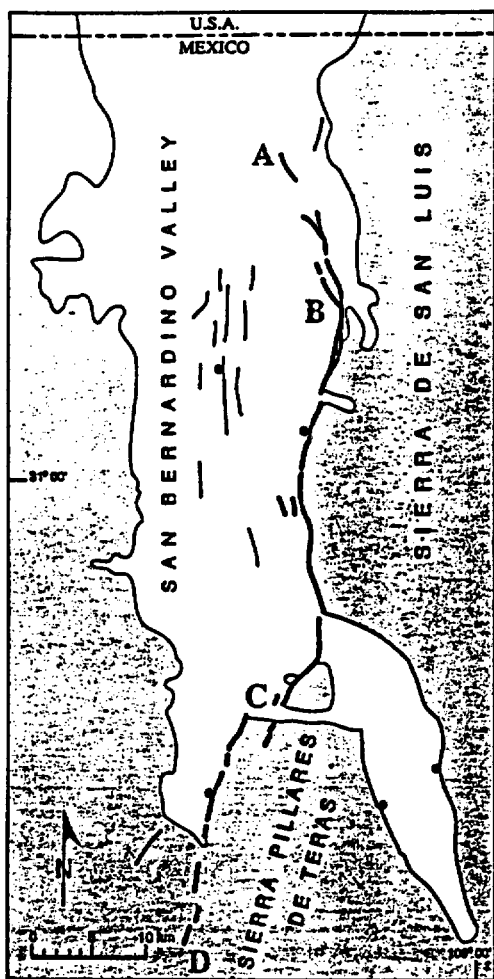


Fig. 3. Surface ruptures from the 1887 Sonora, Mexico, earthquake (from Bull & Fearthree 1988). Bedrock from Direccion General de Geografia del Territorio Nacional (1981) and Sumner (1977). Annotation as Fig. 2.

the major 1915 earthquake scarps are: China Mountain (length (L) = 10 km; maximum displacement (D_{max}) = 1.5 m), Tobin (L = 8.5 km; D_{max} = 4.7 m), Pearce (L = 30 km; D_{max} = 5.8 m) and Sou Hills (L = 10.5 km; D_{max} = 2.7 m). The cross-strike distances between the en échelon steps range from 3.5 to 6 km. A fifth scarp near the crest of the Stillwater Range (L = 1.5 km; D_{max} = 1.2? m) has been attributed to gravitational spreading (Wallace 1984b), but its position as a potential fifth right-step within a zone of faulting with a similar spacing, orientation and west-side-down character is consistent with a tectonic origin. If this scarp is tectonic, the total rupture-zone length is 74 km, and the southern step and gap in faulting is 10.4 km (Fig. 4, point E).

The four principal surface ruptures from the 1915 earthquake occurred near the base of W-facing range blocks and mainly followed pre-existing late Quaternary fault scarps. Faulting was predominately dip-slip, with a maximum vertical displacement of 5.8 m on the Pearce scarp, and an overall average vertical displacement of 2 m (Wallace 1984b). Up to 2 m of right-lateral offset occurred locally.

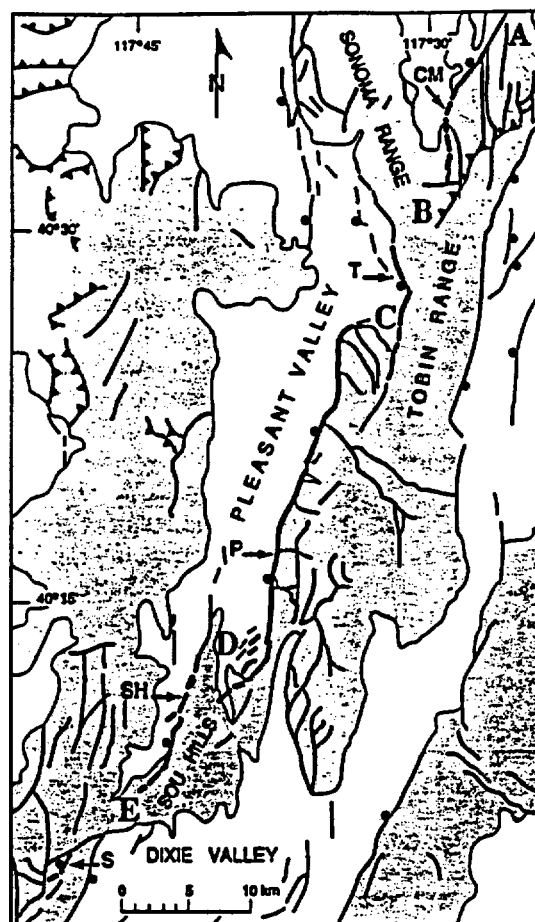


Fig. 4. Surface ruptures from the 1915 Pleasant Valley earthquake (from Wallace 1984b). CM = China Mountain segment, T = Tobin segment, P = Pearce segment, SH = Sou Hills segment, S = Stillwater segment. Bedrock from Stewart & Carlson (1978) and Wallace (1984a). Annotation as Fig. 2.

Surface rupture produced by the 1915 earthquake occurred along four or five structural or geometric segments, based on the continuity of horst blocks, the pattern of late Quaternary fault scarps, and large steps in the fault zone. The largest surface displacements were along the Pearce and Tobin segments (Page 1934). These two segments bound the west side of the Tobin Range and are separated by a 3.5-km-wide right step (Fig. 4, point C). This step distinguishes these as geometric segments. The China Mountain and Sou Hills ruptures bound different range blocks (separate from the Tobin Block), and are therefore considered structural segments.

The southern end of 1915 surface faulting (excluding the 1.5-km-long failure at the crest of the Stillwater Range) coincides with the Sou Hills transverse bedrock zone (Fonseca 1988) (Fig. 4, point E). Fonseca (1988) used geologic, geomorphic and paleoseismic data to show that the Sou Hills have acted as a profound barrier to propagating surface ruptures throughout the Quaternary. The southern end of surface faulting also coincides with aeromagnetic and gravity cross-structures, and a pronounced change in the tilt directions of range blocks north and south of the approximate latitude of

the Sou Hills (Stewart 1980, Thenhaus & Barnhard 1989).

The northern part of the 1915 surface rupture crossed the Tobin Range with a 6-km-wide step (cross-strike distance) in surface faulting between the Tobin and China Mountain scarps (Wallace 1984b) (Fig. 4, point B). The north end of the Tobin scarp is aligned with conspicuous late Quaternary fault scarps that continue tens of kilometers to the northwest along the west flank of the Tobin and Sonoma Ranges, which did not rupture in 1915 (Wallace 1984b).

The 1915 earthquake segment consisted of four and possibly five structural or geometric segments, which form an en échelon pattern with surface offsets separated by right steps as large as 6 km (cross-strike distances). Wallace (1989) suggested that the distributed surface-faulting pattern may be the result of displacement along a fault at depth that trends oblique to the surface faults, and only ruptured those portions of the surface faults located above the source zone.

1932 Cedar Mountain, Nevada, earthquake

The 21 December 1932 Cedar Mountain earthquake was a complex right-lateral strike-slip event that produced a widely distributed surface-rupture pattern (Gianella & Callaghan 1934). This event had a magnitude of $M_s 7.2$ and a felt area of 850,000 km² (Coffman & von Hake 1973, Abe 1981). The epicenter of the 1932 earthquake was located in or near Gabbs Valley, near the north end of the rupture zone (Gianella & Callaghan 1934) (Fig. 5). The zone of surface ruptures is approximately 60 km in length (end-to-end measurement), 6–14 km wide, and generally trends southeast from the epicentral area. Surface ruptures were not confined to a mountain front or a single topographic feature, but rather were distributed broadly across three valleys and short parts of adjacent mountain fronts. Parts of several faults were ruptured (Fig. 5), including the Stewart–Monte Cristo Valley fault zone (SMCFZ), and several shorter, unnamed faults in the Stewart and Gabbs Valleys (Molinari 1984a,b, dePolo *et al.* 1987b). Modeling of body waveforms from regional and teleseismic seismograms indicates that the main event consisted of two subevents that are spatially related to the northern and southern halves of the rupture zone (Doser 1988).

The northern termination of 1932 surface faulting is indistinct and consisted of several widely-spaced, small ruptures in Gabbs Valley that generally had displacements less than a few decimeters (Gianella & Callaghan 1934) (Fig. 5, point A). One of the northernmost ruptures occurred on the southern end of a fault that had small displacements during the 1954 Fairview Peak earthquake. The southern part of the 1932 rupture zone had longer and more narrowly confined surface breaks and larger displacements than the northern end, but also involved several, distributed fault traces. The longest and most continuous surface faulting occurred for about 17 km along the SMCFZ in northern Monte Cristo Valley, with maximum lateral displacements of 1–2 m

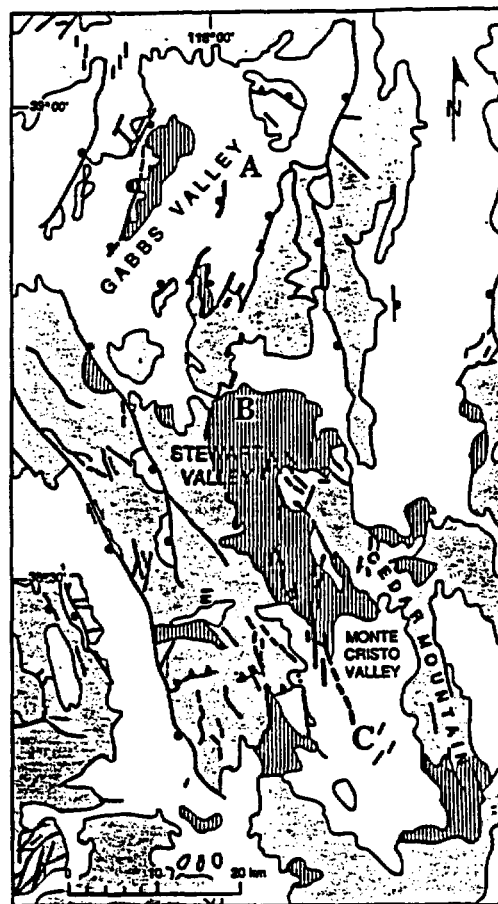


Fig. 5. Surface ruptures from the 1932 Cedar Mountain earthquake (from Gianella & Callaghan 1934, Molinari 1984a). Areas with vertical patterns are Tertiary sediments. Bedrock and Tertiary sediments from Stewart & Carlson (1978). Ruptures along the Stewart–Monte Cristo fault zone trend NNW from point C. Annotation as Fig. 2.

and normal-slip displacements of as much as 0.5 m (Molinari 1984a, dePolo *et al.* 1987a). The southern end of surface faulting is in the vicinity of cross-faults and an extensional basin (Fig. 5, point C).

The northern and southern areas of surface faulting (Fig. 5, point B) are separated by a 9-km gap in coseismic faulting. Within this gap in surface faulting, many folds are present in surficial and Miocene sedimentary deposits, but not in older volcanic and basement rocks (Molinari 1984a). Molinari (1984a) suggests that shallow detachment may be responsible for these folds and that such deformation may account for the lack of discrete surface ruptures. Surface ruptures trend more northeasterly north of this gap in surface faulting than to the south.

The extent of surface rupture associated with the 1932 earthquake would have been difficult or impossible to predict due to the widespread distribution of many small surface ruptures. The distributed nature of surface faulting complicates application of fault segmentation modeling. The Cedar Mountain earthquake can be interpreted as being the result of multiple faults (structural segments) failing in sequence, potentially adding to the complexity of surface faulting and the event's magnitude.

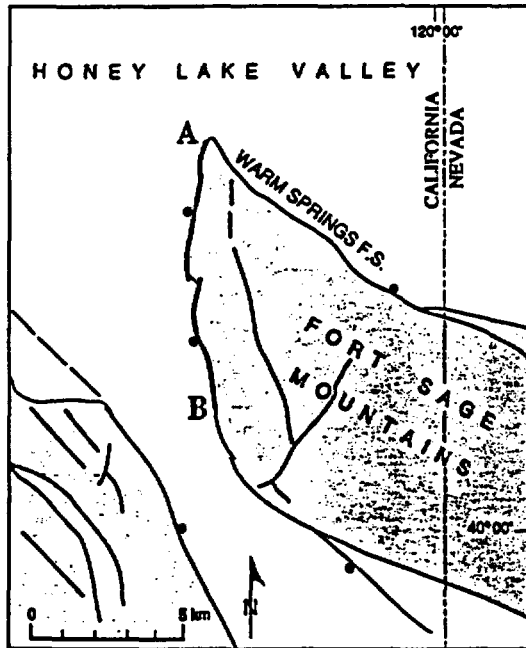


Fig. 6. Surface ruptures from the 1950 Fort Sage Mountain earthquake (from Gianella 1957). Bedrock from Lydon *et al.* (1960), Burnett & Jennings (1962) and Bonham (1969). Annotation as Fig. 2.

1950 Fort Sage Mountains, California, earthquake

The Fort Sage Mountains earthquake of 14 December 1950 had a magnitude of $M_L 5.6$ and was felt over an area of $52,000 \text{ km}^2$ (Coffman & von Hake 1973, Bonilla *et al.* 1984). A 9.5-km-long scarp formed at the western base of the Fort Sage Mountains along the Fort Sage Mountains fault (Gianella 1951, 1957). The rupture was composed of two distinct, continuous breaks, separated by a 320-m left-step (Fig. 6). Although the maximum discrete offset at the surface was 20 cm, the surface displacement may have been as much as 60 cm if folding of alluvium is considered (Gianella 1957). The sense of displacement at the surface was normal slip with no evidence of lateral offset (Gianella 1957).

The Fort Sage Mountains, the Fort Sage Mountains fault, and the 1950 surface ruptures are ostensibly terminated at their northern end by the Warm Springs fault system (Fig. 6, point A), which bounds the northeastern side of the Fort Sage Mountains (Lydon *et al.* 1960, Bonham 1969, Grose 1984). The southern end of surface faulting is 2 km short of a 38° bend in the fault (Fig. 6, point B) and in the mountain front (broad salient). Surface ruptures from the 1950 earthquake appear to be confined to a single geometric segment.

1954 Rainbow Mountain and Stillwater, Nevada, earthquakes

The Rainbow Mountain and Stillwater earthquakes of 6 July and 24 August 1954 ($M_L 6.3$ and 7, respectively) (Bonilla *et al.* 1984) were the first two of four closely spaced surface-rupturing earthquakes in west-central Nevada during a 6-month period.

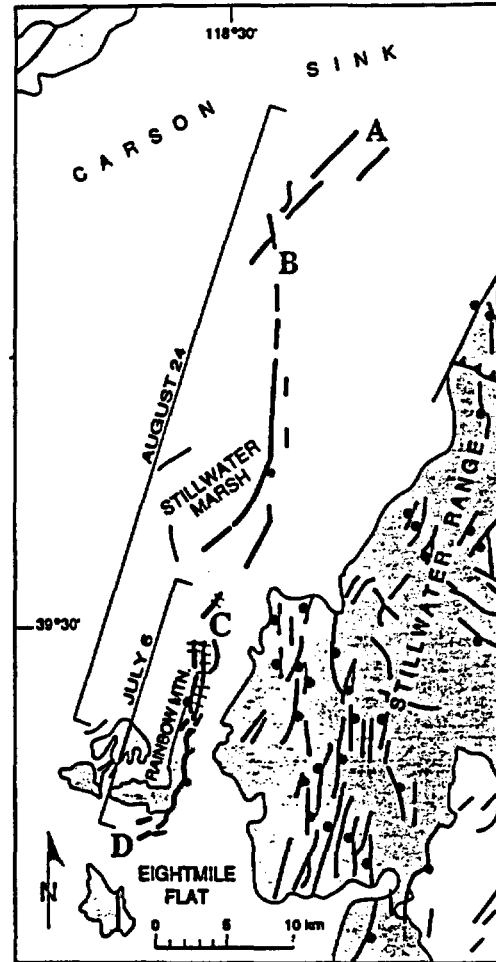


Fig. 7. Surface ruptures from the 1954 Rainbow Mountain and Stillwater earthquake (from Tocher 1956, Bell 1984). Hachured lines designate extent that ruptured during the 6 July and the 23 August earthquakes. The extent of surface rupturing from each of these earthquakes is shown in brackets. Bedrock from Morrison (1964) and Page (1965). Annotation as Fig. 2.

The 6 July event produced 18 km of surface faulting along a single structural segment (Fig. 7). Most of this rupture ($\sim 10 \text{ km}$) lies at the base of Rainbow Mountain. Extensive fractures and small E-facing scarps as much as 30 cm high formed along a NNW-trending zone along the eastern base of Rainbow Mountain and into adjacent Quaternary basins (Tocher 1956). Both ends of this rupture are somewhat diffuse, with surface ruptures distributing and dying out in young basin fill (Fig. 7, points C and D).

The 24 August Stillwater earthquake reactivated and increased the heights of fault scarps at the northern end of the 6 July rupture (Fig. 7) and also ruptured 34 km northward across the Stillwater Marsh to the Carson Sink (Tocher 1956, Bell 1984). The Stillwater earthquake produced scarps as much as 76 cm high. The location of the northern end of this rupture is somewhat uncertain, but surface faulting appears to die out near point A on Fig. 7. The southern end of surface faulting died out within the surface rupture produced by the Rainbow Mountain earthquake. Coseismic displacement from both events apparently occurred along at

least three fault traces (Fig. 7, hachured symbol). The August event is interpreted as consisting of two structural segments, based primarily on an intersecting relationship (Fig. 7, point B). A difference in strike of 40° also exists between these two segments.

Neither the July nor August earthquakes produced measurable lateral offsets at the surface (Tocher 1956). Focal mechanisms, however, indicate significant strike-slip components, particularly for the July event (Doser 1986). Doser (1986) modeled the July earthquake as a double event. The first subevent is believed to have produced the bulk of the seismic moment release and was dominated by strike-slip displacement, whereas the second subevent was shallower and had a larger normal-slip component. Doser suggested that the surface rupture may be more directly related to the second event, partially explaining the lack of lateral offset at the surface.

The July and August surface ruptures broke along faults that had little or no tectonic surface deformation since the deposition of $\sim 12,000$ year Lake Lahonton sediments (Bell 1981, Bell *et al.* 1984). Surface rupture from the July event occurred along a single structural segment, whereas surface rupture from the August event occurred along two structural segments and overlapped for about 12 km with the July surface ruptures.

1954 Fairview Peak–Dixie Valley, Nevada, earthquakes

The Fairview Peak and Dixie Valley earthquakes of 16 December 1954 ($M_s 7.2$ and 6.8 , respectively; Bonilla *et al.* 1984, Doser 1986) produced a complex pattern of surface ruptures in a 102 km by 32 km N-trending belt in west-central Nevada (Fig. 1). The Fairview Peak earthquake produced a 67-km-long N-trending zone of normal-right oblique-slip on three primary traces (Fig. 8): the Fairview Peak, Westgate and Gold King faults. The focal-plane solution of Doser (1986) has a preferred nodal plane that strikes $N10^\circ W$, dips $60^\circ NE$, and has a significant right-lateral component. The Dixie Valley earthquake followed the Fairview Peak event by about $4\frac{1}{2}$ min and caused dominantly normal-slip surface rupture along the eastern flank of the Stillwater Range (Fig. 9).

The northern end of surface faulting attributed to the Fairview Peak earthquake is near a small salient in Louderback Mountain and where the Dixie Valley widens considerably (Fig. 8, point D). The southern end of surface faulting splits into multiple discontinuous ruptures south of Bell Flat, and extends south of Mount Anna.

Three structural segments are interpreted for the Fairview Peak event based on surface rupture along three different faults, the Fairview, Gold King and Westgate faults. The Fairview segment ruptured approximately 32 km along the eastern base of Slate Mountain, Fairview Peak, and Chalk Mountain. Normal-right oblique-slip dominated, with maximum displacements of 3.7 m right-lateral, and 3.1 m normal-slip (Slemmons 1957). The Fairview segment rupture

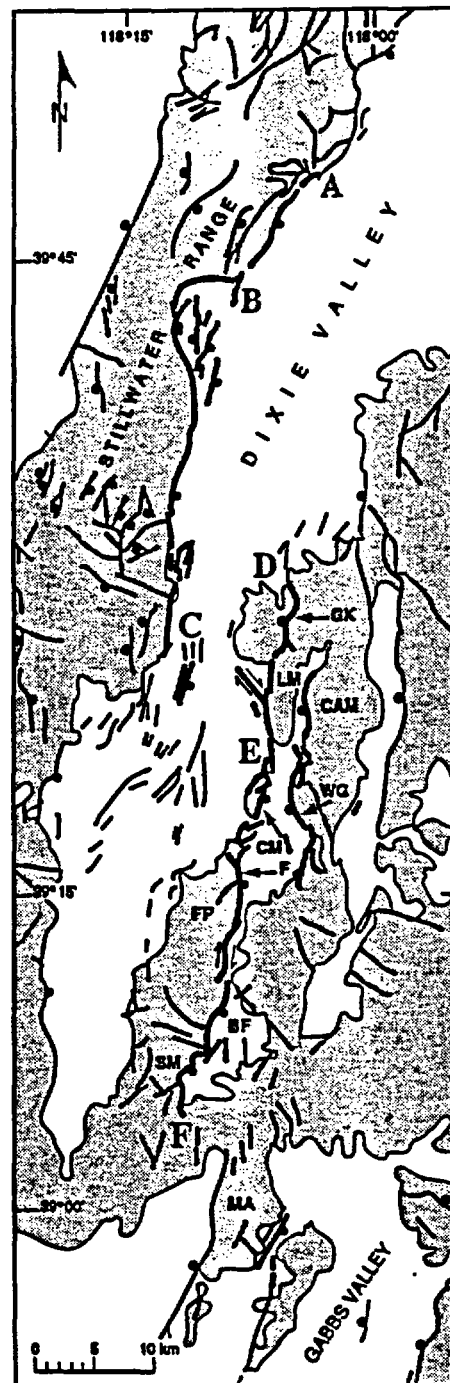


Fig. 8. Surface ruptures from the 1954 Fairview Peak and Dixie Valley earthquakes (from Slemmons 1957, Bell 1984, P. Zhang, personal communication 1990). GK = Gold King segment, LM = Louderback Mountain, CAM = Clan Alpine Mountains, WG = West Gate segment, CM = Chalk Mountain, MA = Mount Anna. Bedrock from Page (1965), Willden & Speed (1974) and Stewart & Carlson (1978). Annotation as Fig. 2.

follows the Fairview Peak range front north to where it branches into a series of NE-trending en échelon breaks, then continues as a range-front fault along Chalk Mountain and across an alluviated gap south of Louderback Mountain (Fig. 8, point E). Surface rupture continued for a distance of ~ 16 km to the north on the W-dipping Gold King segment, partly along the western edge of Louderback Mountain and partly in bedrock

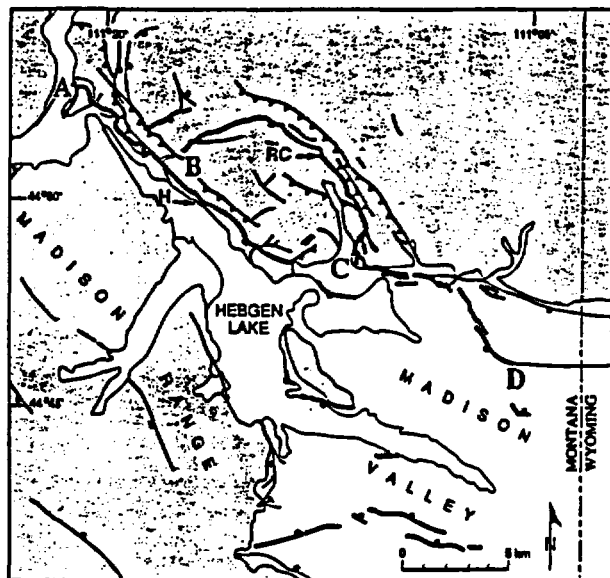


Fig. 9. Surface ruptures from the 1959 Hebgen Lake earthquake (surface ruptures and bedrock from U.S. Geological Survey 1964). H = Hebgen segment, RC = Red Canyon segment. Red Canyon is the alluvial valley just north of point C. Annotation as Fig. 2.

within the range. The Fairview and Gold King segments can be distinguished both structurally, because they occurred on faults that bound opposite sides of mountain blocks and have opposite dips, and behaviorally, based on differences in the amount of lateral slip and downthrown sides. Normal-slip displacements on the Gold King segment of as much as 60 cm may have been similar to surface displacement on this segment during the 1903(?) Wonder earthquake (Slemmons *et al.* 1959). This is one of the few cases of recurrent historical surface faulting in the United States. Recent field work indicates a significant component of right-lateral slip along a fault trace that splays away from the Gold King segment, northwestward into Dixie Valley (P. Zhang, personal communication 1990). The Westgate segment is a west-side-down range-front fault that parallels and is 2–4 km east of the Fairview and Gold King segments. Eighteen kilometers of surface rupture occurred along the Westgate segment, with maximum displacements of approximately 1 m normal slip and 0.5 m right-lateral slip.

Waveform inversion modeling by Doser (1986) indicates that the Fairview Peak event was a double and possibly triple event. However, this can not be clearly related to the segmentation model presented here. It is unclear how the seismic moment was distributed between these segments and how much of this faulting was secondary or sympathetic. For example, the Westgate and Gold King segments may be secondary or sympathetic ruptures in relation to the primary rupture of the Fairview segment.

The Dixie Valley earthquake ruptured a zone 43–47 km long on the west side of Dixie Valley. Rupture during this event probably did not cross a 10-km-wide left-step across Dixie Valley to the Fairview Peak rupture, although the distinctions of surface faulting produced by the two closely spaced earthquakes is con-

tural. Normal displacements of more than 2 m were measured along the Dixie Valley rupture (Slemmons 1957). The southern end of surface faulting coincides approximately with the southeastern end of the Stillwater Range, and had a complex, distributed rupture pattern (Fig. 8, point C).

The Dixie Valley earthquake ruptured through a large range-front re-entrant, called “the bend”, and surface faulting continued for about 12 km north of a $\sim 40^\circ$ change in the strike of the range-front fault (Fig. 8, point B). The portion of the fault north of the bend is considered a second geometric segment based on these changes. Displacement along this segment was generally about 0.5 m or less. The northern end of the surface rupture (Fig. 8, point A) coincides with a 0.8 km right step in the fault zone and a cross fault in the range (P. Zhang personal communication 1989). This cross fault may be part of a N-trending fault zone within the Stillwater Range that intersects, and may disrupt, a NE-trending fault pattern to the southwest. A magnetic anomaly associated with the Humboldt lopolith crosses the Dixie Valley fault in the general vicinity of the northern end of the 1954 rupture. Speed (1976) estimated the thickness (depth) of the lopolith as just over 1 km from the surface, using gravity and geologic data. Such a shallow feature in the crust probably would not have affected the rupture at depth, but may have influenced the near-surface rupture pattern.

The range front and late Quaternary fault scarps are essentially continuous beyond the northern limit of the Dixie Valley rupture. Bell & Katzer (1990) postulated that the northern part of the Dixie Valley earthquake rupture overlapped with the adjacent earthquake segment to the north, possibly by as much as 25 km. This is an important example of how significant overlap of earthquake segments can occur, and can potentially be identified.

In summary, surface faulting during the 1954 Fairview Peak–Dixie Valley earthquakes occurred mainly at or near the alluvium–bedrock range-front boundary and nearly always followed prehistoric fault scarps (Slemmons 1957). At least three complex structural segments failed during the Fairview Peak earthquake: the Fairview segment, the Gold King segment and the Westgate segment. The Dixie Valley earthquake appears to have ruptured two geometric segments along the Dixie Valley fault zone.

1959 Hebgen Lake, Montana, earthquake

The 18 August 1959 Hebgen Lake earthquake ($M_s 7.5$) (Doser 1985) produced a complex, 28-km-long (end-to-end distance, including secondary, antithetic ruptures), surface-rupture pattern near the southern end of the Madison Range in southwestern Montana. The event was felt over 870,000 km² (Stover 1985) and produced dramatic fault scarps, landslides and large-scale basin subsidence. The main shock is the largest earthquake recorded in the Intermountain seismic belt. Seismologic data suggest that the event was composed

of two principal subevents about 5 s apart on one or more WNW-trending fault planes dipping 45–60°S, with pure dip-slip motion (Doser 1985).

Pronounced normal-slip displacement occurred on the Red Canyon and Hebgen faults (structural segments) (Fig. 9), with secondary and minor displacement on several additional faults. The Red Canyon and Hebgen faults strike chiefly W to NW, discordant to the NNW trend of the prominent Madison Range. The Red Canyon fault ruptured for 23 km in a complex, curving trace that closely paralleled Laramide-age (late Cretaceous to early Cenozoic) fold axes and thrust fault surfaces (Witkind *et al.* 1962). The maximum vertical displacement ($D_{\max} = 4.6$ m) occurred where bedding and pre-existing fault planes were favorably oriented for S- to SW-dipping normal slip (Myers & Hamilton 1964). The 12-km-long Hebgen fault rupture ($D_{\max} = 5.5$ m) similarly appears to have been controlled by Laramide structures (Witkind *et al.* 1962). The end-to-end length of the ruptures along the Hebgen and Red Canyon faults is about 24 km.

Several faults antithetic to the Hebgen and Red Canyon faults also ruptured during this event, forming a large graben which was downdropped at the time of the earthquake (Myers & Hamilton 1964). These breaks were generally along small faults and monoclines, and are secondary in origin. There was also a 2.4-km-long sympathetic surface rupture along the west side of the Madison Range (not shown in Fig. 9). These breaks were about 11 km from the nearest primary surface rupture (Hebgen fault) and had as much as 1 m of vertical offset (Myers & Hamilton 1964).

At least two discrete structural segments failed during the 1959 Hebgen Lake earthquake, the Red Canyon and Hebgen faults. The Red Canyon rupture can be subdivided into two smaller geometric segments. At the mouth of Red Canyon, the Red Canyon rupture had a pronounced change in scarp continuity, height and complexity. At this point (Fig. 9, point C), the rupture played into numerous traces, made a bend of about 60°, and occupied the same geomorphic position as the Hebgen fault, potentially merging with the Hebgen fault at depth. The southeastern end of the rupture is at a 55° bend in the fault zone within alluvium in Madison Valley (Fig. 9, point D). The northwestern end of the Hebgen fault rupture is at a cross fault (Fig. 9, point A). The Red Canyon and Hebgen fault segments could have been delineated on the basis of pre-existing fault scarps along much of their lengths, despite their relatively subdued geomorphic expression and the Red Canyon fault's location within the range (Witkind *et al.* 1962, Hall & Sablock 1985).

1983 Borah Peak, Idaho, earthquake

The $M_s 7.3$ Borah Peak earthquake of 28 October 1983 produced about 36 km of surface rupture at the western base of the Lost River Range in east-central Idaho (Crone & Machette 1984). The event was felt over 670,000 km² of the United States and a large part of

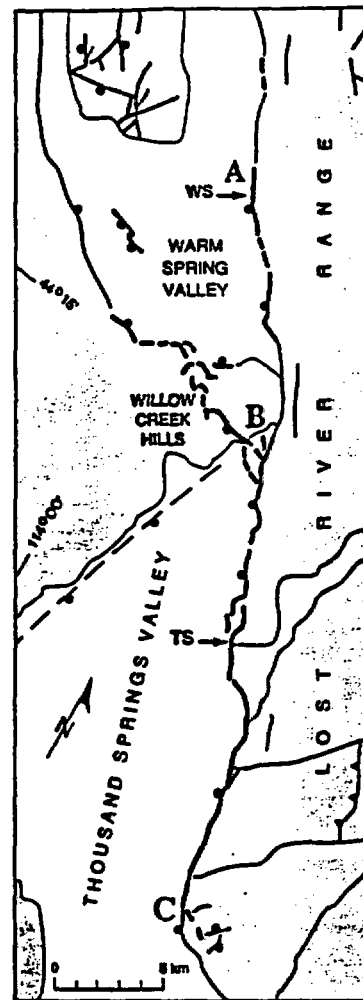


Fig. 10. Surface ruptures from the 1983 Borah Peak earthquake (from Crone & Machette 1984, Susong *et al.* 1990). Bedrock from Bond (1978) and Rember & Bennett (1979a, b). WS = Warm Springs segment, TS = Thousand Springs segment. Annotation as Fig. 2.

western Canada (Stover 1985). It produced surface faulting on two well-defined segments of the 140-km-long Lost River fault and a branch fault (Scott *et al.* 1985). Doser & Smith's (1985) preferred fault-plane solution of N48°W, 45°W, with approximately 5:1 normal to left-lateral displacement, agrees closely with measurements of surface slip. Rupture is believed to have propagated unilaterally to the northwest from a nucleation point 15–16 km deep near the southern end of surface faulting (Doser & Smith 1985).

Surface rupture (Fig. 10) occurred on three main traces: from south to north, a 21-km-long section of the Lost River fault that constitutes the main rupture and includes the maximum vertical displacement of 2.7 m and a maximum left-lateral offset of 0.7 m; a 14-km-long WNW-trending branching rupture across a series of bedrock hills (Willow Creek Hills) and out onto Antelope Flat ($D_{\max} = 1.6$ m); and a 8-km-long northern rupture ($D_{\max} = 1$ m) that also coincides with the Lost River fault (Crone & Machette 1984, Crone *et al.* 1987). The Lost River fault has been divided into six or seven discrete fault segments based on differing geomorphic expression, structural relief and ages of most recent

surface faulting (Scott *et al.* 1985). The southern and northern sections of the 1983 ruptures correspond to the Thousand Springs segment and the central portion of the Warm Spring segment of the Lost River fault, respectively. A gap in surface faulting at Willow Creek Hills separates these two segments (Fig. 10, point B); these two segments are considered geometric segments based on this gap in surface faulting.

The southern end of the Thousand Springs segment is marked by transverse faults in bedrock and an abrupt change in the strike of the range-front forming a salient (Fig. 10, point C). Susong *et al.* (1990) mapped NE- and NW-trending sets of faults within the bedrock; some of the NW-trending faults had minor surface displacement in 1983 (Vincent & Bull 1989). Susong *et al.* (1990) suggested that these networks of faults mark the nucleation point of the rupture and acted to arrest the spread of the rupture to the south. The rupture appears to have propagated northwestward from near this point some 20 km along the Lost River fault to a transverse bedrock ridge (Willow Creek Hills) between Thousand Springs and Warm Spring Valleys (Fig. 10, point B), where it was partially deflected west-northwest (Crone *et al.* 1985). Faulting on the range front continued for about 8 km to the northwest on the Warm Spring segment, after a gap of 4.8 km, and died out along the range-front fault (Fig. 10, point A) (Crone & Machette 1984). Surface cracks with little or no displacement are locally present for another 5 km to the north (Crone *et al.* 1985). If these cracks are included, the total length would increase to >39 km.

Crone & Haller (1991) point out that although the total length of surface faulting is 36 km, most of the seismic moment release from the main shock was associated with rupture of the Thousands Springs segment, and that surface rupture along the Warm Spring segment is secondary or sympathetic in nature. The boundary between these two segments is described as "leaky" by Crone & Haller, essentially terminating the rupture, but allowing minor displacement at depth and/or strong ground motion to trigger slip on the Warm Spring segment. Likewise, the branching rupture through Willow Creek Hills is thought to be secondary. Because of the branching structural discontinuity, this is considered a separate structural segment.

The style and amount of displacement in 1983 was similar to a mid-Holocene (Hanks & Schwartz 1987, Cluer 1988) event documented on the Thousand Springs segment (Hait & Scott 1978, Schwartz & Crone 1985). Similarities between the two most recent events on this segment support the earthquake segmentation and characteristic earthquake model (Schwartz & Copper-smith 1984). The most recent paleoseismic event along the Warm Spring segment occurred just prior to 5.5–6.2 ka (Schwartz & Crone 1988), about the same time as the mid-Holocene event on the Thousand Springs segment. However, surface displacements along the Warm Spring segment from this paleoearthquake were at least twice as much as those from the 1983 event, and surface ruptures were much more extensive (D. P. Schwartz

Table 2. Summary of segmentation of historical Basin and Range province surface-faulting events. Number of fault segments interpreted in this study and types of discontinuities represented are listed. G = geometric discontinuity, S = structural discontinuity, B = behavioral discontinuity

Date/Event	Magnitude	Fault segments
1872 Owens Valley	7.7–8+	3 G, B
1887 Sonora	7.2–7.4	2–3 G
1915 Pleasant Valley	7.6	4–5 G, S
1932 Cedar Mountain	7.2	>3 G, S
1950 Fort Sage	5.6	1 G
1954 Rainbow Mountain	6.3	1 S
1954 Stillwater	7	2 S
1954 Fairview Peak	7.2	3–4+ S, B
1954 Dixie Valley	6.8	2 G
1959 Hebgen Lake	7.5	2–3 G, S
1983 Borah Peak	7.3	2–3 S

personal communication 1988). A single mid-Holocene event may have ruptured both the Thousand Springs and Warm Spring segments, but with larger displacements along the Warm Spring segment than occurred in 1983. Alternatively, a second earthquake may have occurred along the Warm Spring segment relatively close in time to the mid-Holocene event on the Thousand Springs segment or following a prior "1983-type" event (D. P. Schwartz personal communication 1988).

DISCUSSION

The 11 historical events associated with surface faulting in the Basin and Range province exhibit a large degree of variability in the amount and style of surface rupture. Some surface ruptures are concentrated along range fronts in relatively narrow zones (e.g. 1954 Dixie Valley and 1983 Borah Peak earthquakes), whereas other ruptures are complex and widely distributed (e.g. 1932 Cedar Mountain and 1954 Fairview Peak earthquakes). Moderate and strong earthquakes (magnitude 5–7) tended to cause simpler surface ruptures than the larger events. The eight earthquakes with magnitude ≥ 7 ruptured multiple geometric or structural segments (Table 2); these include the 1872 Owens Valley earthquake (three geometric segments) and the 1915 Pleasant Valley earthquake (four or five structural or geometric segments). Failure of these multiple segments may be responsible for some of the multiple ruptures observed by seismologists for large events in the Basin and Range province (Doser & Smith 1989, Jackson & White 1989).

Many of the largest events (magnitude ≥ 7.2) involved complex, widely distributed rupture patterns (e.g. 1915 Pleasant Valley, 1932 Cedar Mountain and 1954 Fairview Peak earthquakes). These events ruptured consecutive and parallel structural segments along range fronts and across ranges and valleys and produced complicated patterns of surface faulting involving primary, secondary and sympathetic displacements. Some possible underlying causes for the complex and widely distributed surface ruptures in the Basin and Range province include: (1) decoupling and detachment faulting in

the mid to upper crust (Burchfiel 1965, Hardyman 1978, 1984, Wallace 1979, 1989, Molinari 1984a); (2) occurrence in heterogeneous, highly tectonized crust with pre-existing structures and fabrics, and varying lithologies; (3) triggering of multiple ruptures either by exceedence of seismic failure thresholds of adjacent faults or through sympathetic displacement; and (4) significant or dominant strike-slip displacement components that cut across pre-existing structural grains or splay upwards (flower structures).

Additional detailed paleoseismic studies will be important for determining to what extent the complex patterns of historical ruptures are the result of characteristic earthquakes that ruptured similar multiple geometric and structural segments during past events (Schwartz & Coppersmith 1984, 1986, Schwartz 1988). In cases where paleoearthquakes are clustered spatially and temporally, it may be difficult to delineate individual earthquake segments from paleoseismic data alone. For example, at some future time, using only paleoseismic techniques, it would be difficult to distinguish between the 1954 Rainbow Mountain and Stillwater earthquakes, or to temporally differentiate the historical ruptures in the Central Nevada seismic belt.

Approximately half of the 11 historical surface ruptures ended at discontinuities that could have been identified as indicators of fault-zone discontinuities based on such characteristics as cross faults, branch faults, extensional basins, ends of mountain ranges, transverse-bedrock ridges and salients. The other half were either widely distributed with indistinct end points, or ended at locations at the surface that did not coincide with clear indicators of fault zone discontinuities.

The structural and geometric segment lengths from these earthquakes fall in three groupings: (1) 8.5–12 km; (2) 17–23 km; and (3) 30–39 km. The middle grouping clusters near a proposed general maximum segment length of 20 km for normal faults (Jackson & White 1989). However, two of the segments considered here from dominantly normal-slip displacement earthquakes had significantly longer lengths: the 1887 Sonora earthquake (central segment—39+ km) and the 1915 Pleasant Valley earthquake (Pearce segment—30 km).

Recent studies of well-recorded historical events have concluded that seismic moment release may be concentrated along portions of a fault or earthquake segment, or dominated by an individual segment (e.g. 1983 Borah Peak earthquake). Unfortunately, with the exception of the 1983 Borah Peak earthquake, it is difficult to clearly discern which segments may have dominated the moment release, although some speculations can be made based on multiple-event interpretations from analysis of seismograms, variations in the amount of surface rupture, and fault geometry relative to the main rupture.

As is the case for most of the 11 events, the magnitude of the 1983 Borah Peak earthquake ($M_s 7.3$) was considerably larger than what would be estimated for individual segments of the Lost River fault zone (Freeman *et al.* 1986). Rupture of the 22-km-long Thousand Springs segment alone yields an estimated magnitude $M_s 6.7-6.8$

event, using magnitude vs fault-length relations from Slemmons (1982) and Bonilla *et al.* (1984). A 36 km rupture length yields an estimated magnitude of $M_s 6.9-7.1$. This underscores the importance of considering uncertainties in estimated magnitudes, as well as potential multiple segment failures. Further, the use of other fault parameters, such as maximum surface displacement, for determining magnitude values can help cross-check individual estimates of earthquake size.

CONCLUSIONS

Surface ruptures from historical earthquakes in the Basin and Range province have exhibited a wide variety of faulting patterns, from simple to complex. Moderate and strong earthquakes have tended to cause simpler surface ruptures, whereas, surface ruptures from events of magnitude 7 and greater have involved the failure of multiple geometric or structural segments. Many of the events larger than magnitude 7.2 had complex, widespread surface-rupture patterns.

Approximately half of the endpoints of historical Basin and Range province surface ruptures coincided with distinct fault-zone discontinuities. The other half ended in either widely distributed breaks and/or did not coincide with clear indicators of discontinuities. In several cases, historical surface faulting has ruptured through or occurred on both sides of pronounced geometric and structural discontinuities. Thus, some earthquake discontinuities may be difficult to identify and significant faulting may occur beyond postulated discontinuities. Several lines of evidence are required to evaluate earthquake discontinuities, one of the most important of which is timing information for past earthquakes.

These observations indicate that simple earthquake segmentation models may be inadequate for evaluating larger earthquakes in the Basin and Range province. Seismic hazard assessments in the province should consider ruptures of multiple geometric or structural segments, and should rely on different types of data and large uncertainties in earthquake segment lengths and earthquake-size estimations. Further studies of historical earthquakes and fault zone behavior, and the development of new information, such as geophysical and paleoseismic data, will increase our understanding of the complexities of earthquake ruptures in extensional provinces. With additional data, behavioral models can be developed for fault zones (e.g. Machette *et al.* 1989) and a more accurate understanding and delineation of earthquake segments may be possible.

Acknowledgements—We would like to thank Sarah Beanland, John Bell, Diane dePolo, Dick Meeuwig, Phil Pearthree and, especially, Tony Crone for useful discussions, comments and reviews which improved the manuscript. Special thanks also to Kris Pizarro of the Nevada Bureau of Mines and Geology for preparing the figures. This study was supported in part by a grant from the Nevada Nuclear Waste Project Office.

REFERENCES

- Abe, K. 1981. Magnitudes of large shallow earthquakes from 1904 to 1980. *Phys. Earth. & Planet. Interiors* 27, 72-80.
- Albee, A. L. & Smith, J. L. 1966. Earthquake characteristics and fault activity in southern California. In: *Engineering Geology in Southern California* (edited by Lung, R. & Proctor, R.). Ass. Engng Geol., Los Angeles Section, 9-34.
- Barka, A. A. & Kadinsky-Cade, K. 1988. Strike-slip fault geometry in Turkey and its influence on earthquake activity. *Tectonics* 7, 663-684.
- Beanland, S. & Clark, M. 1987. The Owens Valley fault zone, and surface rupture associated with the 1872 earthquake (Abs.). *Seism. Res. Lett.* 58, 32.
- Beanland, S. & Clark, M. C. In press. The Owens Valley fault zone, eastern California, and surface rupture associated with the 1872 earthquake. *Bull. U.S. Geol. Surv.*
- Bell, J. W. 1981. Quaternary fault map of the Reno 1° by 2° quadrangle. *U.S. Geol. Surv. Open-file Rep.* 81-982.
- Bell, J. W. 1984. Quaternary fault map of Nevada-Reno sheet. 1/250,000 scale map. *Nevada Bur. Mines & Geol. Map* 79.
- Bell, J. W. & Katzer, T. 1990. Timing of late Quaternary faulting in the 1954 Dixie Valley earthquake area, central Nevada. *Geology* 18, 622-625.
- Bell, J. W., Slemmons, D. B. & Wallace, R. E. 1984. Roadlog: Reno to Dixie Valley-Fairview Peak earthquake areas. In: 1984 *Geol. Soc. Am. Ann. Meet., West. Geol. Excurs. Guidebook 4* (edited by Lintz, J.), 425-472.
- Bond, J. G. 1978. Geologic map of Idaho. 1/500,000 scale map. Idaho Bur. Mines & Geol.
- Bonham, H. F. 1969. Geology and mineral deposits of Washoe and Storey Counties, Nevada. *Bull. Nevada Bur. Mines & Geol.* 70.
- Bonilla, M. G., Mark, R. K. & Lienkaemper, J. J. 1984. Statistical relations among earthquake magnitude, surface rupture length, and surface fault displacement. *Bull. seism. Soc. Am.* 74, 2379-2411.
- Bull, W. B. & Pearthree, P. A. 1988. Frequency and size of Quaternary surface ruptures of the Pitaycachi fault, northeastern Sonora, Mexico. *Bull. seism. Soc. Am.* 78, 956-978.
- Burchfiel, B. C. 1965. Structural geology of the Specter Range quadrangle, Nevada, and its regional significance. *Bull. geol. Soc. Am.* 76, 175-192.
- Burnett, J. L. & Jennings, C. W. 1962. Geologic map of California, Chico Sheet. 1/250,000 scale map. Calif. Div. Mines & Geol.
- Carver, G. A. 1969. Quaternary tectonism and surface faulting in the Owens Lake Basin, California. Unpublished M.S. thesis, University of Nevada, Reno.
- Ciur, J. K. 1988. Quaternary geology of Willow Creek and some age constraints on prehistoric faulting, Lost River Range, east-central Idaho. *Bull. seism. Soc. Am.* 78, 946-955.
- Coffman, J. L. & von Hake, C. A. 1973. Earthquake history of the United States, revised edition (through 1970). *U.S. Dept Commerce Publ.* 41-1.
- Crone, A. J. & Haller, K. M. 1991. Segmentation and the coseismic behavior of Basin and Range normal faults: examples from east-central Idaho and southwestern Montana, U.S.A. *J. Struct. Geol.* 13, 151-164.
- Crone, A. J. & Machette, M. N. 1984. Surface faulting associated with the Borah Peak earthquake, central Idaho. *Geology* 12, 664-667.
- Crone, A. J., Machette, M. N., Bonilla, M. G., Lienkaemper, J. J., Pierce, K. L., Scott, W. E. & Bucknam, R. C. 1985. Characteristics of surface faulting accompanying the Borah Peak earthquake, central Idaho. *U.S. Geol. Surv. Open-file Rep.* 85-290, 43-58.
- Crone, A. J., Machette, M. N., Bonilla, M. G., Lienkaemper, J. J., Pierce, K. L., Scott, W. E. & Bucknam, R. C. 1987. Surface faulting accompanying the Borah Peak earthquake and segmentation of the Lost River fault, central Idaho. *Bull. seism. Soc. Am.* 77, 739-770.
- dePolo, C. M., Bell, J. W. & Ramelli, A. R. 1987a. Geometry of strike-slip faulting related to the 1932 Cedar Mountain earthquake, central Nevada. *Geol. Soc. Am. Abs. w. Prog.* 19, 371.
- dePolo, C. M., Clark, D. G., Slemmons, D. B. & Aymard, W. H. 1989. Historical Basin and Range province surface faulting and fault segmentation. *U.S. Geol. Surv. Open-file Rep.* 89-315, 131-163.
- dePolo, C. M., Ramelli, A. R. & Bell, J. W. 1987b. Visit to trenches along the southern part of the 1932 Cedar Mountain earthquake ruptures, Monte Cristo Valley, Nevada. Unpublished field guide, Nevada Bur. Mines & Geol.
- dePolo, C. M. & Slemmons, D. B. In press. Estimation of earthquake size for seismic hazards. *Geol. Soc. Am. Rev. Engng. Geol.* 3.
- Dirección General de Geografía del Territorio Nacional. 1981. Carta Geológica, Tijuana Sheet. 1/1,000,000 scale map. Secretaría de Programación y Presupuesto, Estados Unidos Mexicanos.
- Doser, D. I. 1985. Source parameters and faulting processes of the 1959 Hebgen Lake, Montana, earthquake sequence. *J. geophys. Res.* 90, 4537-4555.
- Doser, D. I. 1986. Earthquake processes in the Rainbow Mountain-Fairview Peak-Dixie Valley, Nevada, region 1954-1959. *J. geophys. Res.* 91, 12,572-12,586.
- Doser, D. I. 1988. Source parameters of earthquakes in the Nevada seismic zone, 1915-1943. *J. geophys. Res.* 93, 15,001-15,015.
- Doser, D. I. & Smith, R. B. 1985. Source parameters of the 28 October 1983 Borah Peak, Idaho, earthquake from body wave analysis. *Bull. seism. Soc. Am.* 75, 1041-1051.
- Doser, D. I. & Smith, R. B. 1989. An assessment of source parameters of earthquakes in the Cordillera of the Western United States. *Bull. seism. Soc. Am.* 79, 1383-1409.
- Dubois, S. M. & Sbar, M. L. 1981. The 1887 earthquake in Sonora: Analysis of regional ground shaking and ground failure. *U.S. Geol. Surv. Open-file Rep.* 81-437.
- Dubois, S. M. & Smith, A. W. 1980. The 1887 earthquake in San Bernardino Valley, Sonora: Historical accounts and intensity patterns in Arizona. *Spec. Tech. Pap. Arizona Bur. Geol. & Min.* 3.
- Dunne, G. C., Rachel, M. G. & Sylvester, A. G. 1978. Mesozoic evolution of rocks of the White, Inyo, Argus and Slate Ranges, eastern California. In: *Mesozoic Paleogeography of the Western United States, Pacific Coast Paleogeography Symposium 2. Soc. econ. Paleont. Miner.*, 189-207.
- Fonseca, J. 1988. The Sou Hills: a barrier to faulting in the central Nevada seismic belt. *J. geophys. Res.* 93, 475-489.
- Freeman, K. J., Fuller, S. & Schell, B. A. 1986. The use of surface faults for estimating design earthquakes; implications of the 28 October 1983, Idaho earthquake. *Ass. Engng. Geol.* 23, 325-332.
- Gianella, V. P. 1951. Fort Sage Mountain, California, earthquake of December 14, 1950. *Bull. geol. Soc. Am.* 62, 1502.
- Gianella, V. P. 1957. Earthquake and faulting, Fort Sage Mountains, California, December, 1950. *Bull. seism. Soc. Am.* 47, 173-177.
- Gianella, V. P. & Callaghan, E. The Cedar Mountain, Nevada, earthquake of December 20, 1932. *Bull. seism. Soc. Am.* 24, 345-377.
- Goodfellow, G. E. 1888. The Sonora earthquake. *Science* 11, 162-166.
- Grose, T. L. T. 1984. Geologic map of the State Line Peak Quadrangle, Nevada-California. *Nevada Bur. Mines Geol. Map* 82.
- Hait, M. H., Jr. & Scott, W. E. 1978. Holocene faulting, Lost River Range, Idaho. *Geol. Soc. Am. Abs. w. Prog.* 10, 217.
- Hall, W. B. & Sablock, P. E. 1985. Comparison of the geomorphic and surficial fracturing effects of the 1983 Borah Peak, Idaho earthquake with those of the 1959 Hebgen Lake, Montana earthquake. *U.S. Geol. Surv. Open-file Rep.* 85-290, 141-152.
- Hanks, T. C. & Kanamori, H. 1979. A moment magnitude scale. *J. geophys. Res.* 84, 2348-2350.
- Hanks, T. C. & Schwartz, D. P. 1987. Morphologic dating of the pre-1983 fault scarp on the Lost River fault at Doublespring Pass Road, Custer County, Idaho. *Bull. seism. Soc. Am.* 77, 837-846.
- Hardyman, R. F. 1978. Volcanic stratigraphy and structural geology of the Gillis Canyon quadrangle, northern Gillis Range, Mineral County, Nevada. Unpublished Ph.D. thesis, University of Nevada, Reno.
- Hardyman, R. F. 1984. Strike-slip, normal, and detachment faults in the northern Gillis Range, Walker Lane of west central Nevada. In: 1984 *Geol. Soc. Am. Ann. Meet., West. Geol. Excurs. Guidebook 4* (edited by Lintz, J.), 184-199.
- Herd, D. G. & McMasters, C. R. 1982. Surface faulting in the Sonora, Mexico, earthquake of 1887. *Geol. Soc. Am. Abs. w. Prog.* 14, 172.
- Jackson, J. A. & White, N. J. 1989. Normal faults in the upper continental crust: observations from regions of active extension. *J. Struct. Geol.* 11, 15-36.
- Kanamori, H. 1983. Magnitude scale and quantification of earthquakes. *Tectonophysics* 93, 185-199.
- Knuepfer, P. L. K. 1989. Implications of the characteristics of end-points of historical surface fault ruptures for the nature of fault segmentation. *U.S. Geol. Surv. Open-file Rep.* 89-315, 193-228.
- Knuepfer, P. L. K., Bamberger, M. J., Turko, J. M. & Coppersmith, K. J. 1987. Characteristics of the boundaries of historical surface fault ruptures. *Seism. Res. Lett.* 58, 31.
- Lebetkin, L. K. C. & Clark, M. C. 1988. Late Quaternary activity along the Lone Pine fault, eastern California. *Bull. geol. Soc. Am.* 100, 755-766.
- Lydon, P. A., Gay, T. E., Jr. & Jennings, C. W. 1960. Geologic map of California, Westwood Sheet. *Calif. Div. Mines & Geol.*

- Machette, M. N., Personius, S. F., Nelson, A. R., Schwartz, D. P. & Lund, W. R. 1989. Segmentation models and Holocene movement history of the Wasatch fault zone, Utah. *U.S. geol. Surv. Open-file Rep.* 89-315, 229-245.
- Martel, S. J. 1984. Structure of the Owens Valley fault zone near Poverty Hills, Owens Valley, California. *Geol. Soc. Am. Abs. w. Prog.* 16, 585.
- Matthews, R. A. & Burnett, J. L. 1965. Geologic map of California, Fresno Sheet. 1/250,000 scale map. *Calif. Div. Mines & Geol.*
- Molinari, M. P. 1984a. Late Cenozoic geology and tectonics of Stewart and Monte Cristo Valleys, west-central Nevada. Unpublished M.S. thesis, University of Nevada, Reno.
- Molinari, M. P. 1984b. Late Cenozoic structural geology of Stewart and Monte Cristo Valleys, Walker Lane of west-central Nevada. In: 1984 *Geol. Soc. Am. Ann. Meet., West. Geol. Excurs. Guidebook 4* (edited by Lintz, J.), 219-231.
- Morrison, R. B. 1964. Lake Lahontan: Geology of southern Carson Desert, Nevada. *Prof. Pap. U.S. geol. Surv.* 401.
- Myers, W. B. & Hamilton, W. 1964. Deformation accompanying the Hebgen Lake earthquake of August 17, 1959. *Prof. Pap. U.S. geol. Surv.* 435-1, 55-98.
- Oakeshott, G. B., Greensfelder, R. W. & Kahle, J. E. 1972. 1872-1972. . . one hundred years later. *Calif. Div. Mines. Geol. Calif. Geol.* 25, 55-61.
- Page, B. M. 1934. Basin-range faulting of 1915 in Pleasant Valley, Nevada. *J. Geol.* 43, 690-707.
- Page, B. M. 1965. Preliminary geologic map of a part of the Stillwater Range, Churchill County, Nevada. 1/125,000 scale map. *Nevada. Bur. Mines & Geol. Map 28*.
- Pearthree, P. A., Bull, W. B. & Wallace, T. C. 1990. Geomorphology and Quaternary geology of the Pitaycachi fault, northeastern Sonora, Mexico. *Spec. Pap. Arizona geol. Surv.* 7, 124-135.
- Rember, W. C. & Bennett, E. H. 1979a. Geologic map of the Challis quadrangle, Idaho. 1/250,000 scale map. *Idaho Bur. Mines & Geol.*
- Rember, W. C. & Bennett, E. H. 1979b. Geologic map of the Dubois quadrangle, Idaho. 1/250,000 scale map. *Idaho Bur. Mines & Geol.*
- Schwartz, D. P. 1988. Geologic characterization of seismic sources: moving into the 1990s. In: *Earthquake Engineering and Soil Dynamics II—Recent Advances in Ground Motion Evaluation* (edited by Von Thun, J. L.). *Geotech. Spec. Publs Am. Soc. Civil Engrs* 20, 1-42.
- Schwartz, D. P. & Coppersmith, K. J. 1984. Fault behavior and characteristic earthquakes: examples from the Wasatch and San Andreas fault zones. *J. geophys. Res.* 89, 5681-5698.
- Schwartz, D. P. & Coppersmith, K. J. 1986. Seismic hazards: New trends in analysis using geological data. In: *Active Tectonics, Studies in Geophysics* (edited by Wallace, R. E.). National Academy Press, Washington, DC, 215-230.
- Schwartz, D. P. & Crone, A. J. 1985. The 1983 Borah Peak earthquake: a calibration event for quantifying earthquake recurrence and fault behavior on Great Basin normal faults. *U.S. geol. Surv. Open-file Rep.* 85-290, 153-160.
- Schwartz, D. P. & Crone, A. J. 1988. Paleoseismicity of the Lost River fault zone, Idaho: earthquake recurrence and segmentation. *Geol. Soc. Am. Abs. w. Prog.* 20, 228.
- Scott, W. E., Pierce, K. L. & Hait, M. H., Jr. 1985. Quaternary tectonic setting of the 1983 Borah Peak earthquake, central Idaho. *Bull. seism. Soc. Am.* 75, 1053-1066.
- Sibson, R. H. 1989. Earthquake faulting as a structural process. *J. Struct. Geol.* 11, 1-14.
- Slemmons, D. B. 1957. Geological effects of the Dixie Valley-Fairview Peak, Nevada, earthquakes of December 16, 1954. *Bull. seism. Soc. Am.* 47, 353-375.
- Slemmons, D. B. 1982. Determination of design earthquake magnitudes for microzonation. In: *Proc. 3rd Int. Earthquake Microzonation Conf.* (Seattle, Washington, June 28-July 1), Vol. 1, 119-130.
- Slemmons, D. B. & dePolo, C. M. 1986. Evaluation of active faulting and associated hazards. In: *Active Tectonics, Studies in Geophysics* (edited by Wallace, R. E.). National Academy Press, Washington, DC, 45-62.
- Slemmons, D. B., Steinbrugge, K. V., Tocher, D., Oakeshott, G. B. & Gianella, V. P. 1959. Wonder, Nevada, earthquake of 1903. *Bull. seism. Soc. Am.* 49, 251-265.
- Speed, R. C. 1976. Geologic Map of the Humboldt lopolith and surrounding terrane, Nevada. *Geol. Soc. Am. Map MC-14*.
- Stewart, J. H. 1980. Regional tilt patterns of late Cenozoic basin-range fault blocks in the Great Basin. *Bull. geol. Soc. Am.* 91, 460-464.
- Stewart, J. H. 1983. Cenozoic structure and tectonics of the northern Basin and Range province, California, Nevada, and Utah. In: *The Role of Heat in the Development of Energy and Mineral Resources in the Northern Basin and Range province*. Geothermal Resources Council, 25-40.
- Stewart, J. H. & Carlson, J. E. 1978. Geologic map of Nevada. 1/500,000 scale map. *U.S. geol. Surv. and Nevada Bur. Mines & Geol.*
- Stover, C. W. 1985. Isoseismal map and intensity distribution for the Borah Peak, Idaho, earthquake of October 28, 1983. *U.S. geol. Surv. Open-file Rep.* 85-290, 401-408.
- Streitz, R. & Stinson, M. C. 1974. Geologic map of California, Death Valley Sheet. 1/250,000 scale map. *Calif. Div. Mines & Geol.*
- Strand, R. G. 1967. Geological map of California, Mariposa Sheet. 1/250,000 scale map. *Calif. Div. Mines & Geol.*
- Sumner, J. R. 1977. The Sonora earthquake of 1887. *Bull. seism. Soc. Am.* 67, 1219-1223.
- Susong, D. D., Janecke, S. V. & Bruhn, R. L. 1990. Structure of a fault segment boundary in the Lost River fault zone, Idaho, and possible effect on the 1983 Borah Peak earthquake rupture. *Bull. seism. Soc. Am.* 80, 57-68.
- Thenhaus, P. C. & Barnhard, T. P. 1989. Regional termination and segmentation of Quaternary fault belts in the Great Basin, Nevada and Utah. *Bull. seism. Soc. Am.* 79, 1426-1438.
- Tocher, D. 1956. Movement on the Rainbow Mountain fault. *Bull. seism. Soc. Am.* 46, 10-14.
- U.S. Geological Survey. 1964. The Hebgen Lake, Montana, earthquake of August 17, 1959. *Prof. Pap. U.S. geol. Surv.* 435.
- Vincent, K. R. & Bull, W. B. 1989. New Evidence of surface faulting from Borah peak earthquake and project summary. *U.S. geol. Surv. Summ. Tech. Repts.* XXVIII, 149-160.
- Wallace, R. E. 1979. Earthquakes and the prefractured state of the western part of the North American continent. *Proc. Int. Res. Conf. Intra-Continental Earthquakes*, Ohrid, Yugoslavia.
- Wallace, R. E. 1984a. Notes on surface faulting in Dixie Valley, Nevada. In: 1984 *Geol. Soc. Am. Ann. Meet., West. Geol. Excurs. Guidebook 4* (edited by Lintz, J.), 402-407.
- Wallace, R. E. 1984b. Fault scarps formed during the earthquakes of October 2, 1915, Pleasant Valley, Nevada and some tectonic implications. *Prof. Pap. U.S. geol. Surv.* 1274-A.
- Wallace, R. E. 1987. Grouping and migration of surface faulting and variations in slip rates on faults in the Great Basin province. *Bull. seism. Soc. Am.* 77, 868-876.
- Wallace, R. E. 1989. Fault-plane segmentation in brittle crust and anisotropy in loading system. *U.S. geol. Surv. Open-file Rep.* 89-315, 400-408.
- Wheeler, R. L. 1987. Boundaries between segments of normal faults: Criteria for recognition and interpretation. *U.S. geol. Surv. Open-file Rep.* 87-673, 385-398.
- Wheeler, R. L. & Krystinik, K. B. 1988. Segmentation of the Wasatch fault zone, Utah: Summaries, analyses, and interpretations of geological and geophysical data. *Bull. U.S. geol. Surv.* 1827.
- Willden, R. & Speed, R. C. 1974. Geology and mineral deposits of Churchill County, Nevada. *Bull. Nevada Bur. Mines & Geol.* 83.
- Witkind, I. J., Myers, W. B., Hadley, J. B., Hamilton, W. & Fraser, G. D. 1962. Geologic features of the earthquake at Hebgen Lake, Montana, August 17, 1959. *Bull. seism. Soc. Am.* 52, 163-180.

APPENDIX D

**AN EXPLANATION TO ACCOMPANY THE GEOLOGIC MAP OF CRATER
FLAT, NEVADA**

(First Draft)

**James E. Faulds
Department of Geology
University of Iowa
Iowa City, Iowa**

**Dan Feuerbach
Center for Volcanic and Tectonic Studies
Department of Geoscience
University of Nevada, Las Vegas
Las Vegas, Nevada 89154**

**A. Ramelli and J. Bell
Nevada Bureau of Mines and Geology
University of Nevada, Reno
Reno, Nevada**

MAP LEGEND

Quaternary Surficial Units

Qfcf Crater Flat unit Active and recently active washes, inset fans, and fan skirts; shallowly incised (<2m) distributive drainage pattern; preserved to slightly subdued bar and swale topography; unvarnished to slight rock varnish; may have proto-pavement. No significant formation of genetic soil horizons; may have slight carbonate dustings or filaments on pebble bottoms (Stage I). Late Holocene age; <<6.6 ka.

Qflc Little Cones unit Fan-skirt and low basin-floor remnants; fully-smoothed surfaces; slightly varnished desert pavement. Clear pedogenic soil (torriorthents) consisting of 5 cm thick Av, cambic (Bw), and Stage I-II Bk horizons. Late Pleistocene to early Holocene age; rock varnish age of 6.6-11.1 ka.

Qflb Late Black Cone unit Fan-piedmont remnants; fully-smoothed surfaces; deeply solution etched limestone and darkly varnished volcanic clasts in well-sorted and tightly packed pavements. Soils are haplargids and locally haplic durargids with 20-30 cm thick Bt and Stage II-III Bk horizons. Late Pleistocene age; rock varnish age of 17.3-30.3 ka.

Qfeb Early Black Cone unit Fan-piedmont remnants; fully smoothed surfaces; similar surficial characteristics as late Black Cone. Soils are durargids with 30 cm thick Bt and ~1 m Stage III-IV Bk horizons. Mid- to late Pleistocene age; rock varnish age of 130-190 ka.

Qfy Yucca unit Deeply dissected fan-piedmont remnants; darkly varnished, well-sorted and tightly packed pavement. Soils are durargids with 40-60 cm thick Bt and >1 m thick Stage IV Bqkm horizons. Mid-Pleistocene age; rock varnish age of 360-370 ka.

Qfs Solitario unit Fully-rounded ridge-line remnants (ballenas); irregularly shaped, well-sorted, tightly packed pavements with darkly varnished volcanic clasts and littered with chips of duripan lamina. Original A and Bt horizons have been stripped; remnantal Bt and Stage IV Bqkm horizons are present. Contains Bishop ash (~730 ka). Mid- Pleistocene age; rock varnish age of 450 to >740 ka.

MAP LEGEND

The map "Geological Map of Crater Flat, Nevada" is included in the pocket of this annual report.

- Qal Alluvium-poorly sorted gravel, sand, and silt.
- Qc Colluvium-unconsolidated angular blocks.
- QTs Late Miocene to Quaternary, flat-lying pebble to cobble conglomerate, weakly indurated, primarily of fanglomerate origin.

Geology of the Pliocene Volcanoes

- Qab Locally derived alluvium; Non-consolidated, poorly sorted angular fragments ranging from gravel to boulders. Clasts consist of basalt with subordinant pyroclastic material shed from the local basalt flows and scoria mounds and cones.
- Qts Scoria colluvium; Non-consolidated fragments of pyroclastic material shed from cinder cones and scoria mounds.
- Qb Undifferentiated Quaternary basalt flows and pyroclastic material.
- Qs Primary pyroclastic deposits; Poorly-to-moderately welded scoria, ash, bombs, and agglutiated scoria deposited by Strombolian to Hawaiian type eruptions. Deposits range from bedded to non-bedded and form the major cinder cones. Scoria mounds at Black Cone and Red Cone are comprised primarily of non-bedded poorly-to-moderately welded scoria and volcanic bombs.
- Qbn Northern basalt flows at Black Cone; Aa and block flows of alkali-basalt that erupted from scoria mounds north of Black Cone. Basalt is porphyritic with euhedral to subhedral phenocrysts of olivine in a matrix of plagioclase, diopsidic augite and olivine.
- Qbsm Scoria mound basalt flows; Aa and block flows of alkali-basalt that erupted from scoria mounds south and southeast of Black Cone. The basalt is porphyritic with euhedral to subhedral phenocrysts of olivine in a matrix of plagioclase, diopsidic augite and olivine.
- Qbl Lava lake on Black Cone; Alkali-basalt flows that probably erupted by lava fountaining at the summit of Black Cone. Basalt locally grades into

agglutinate. Sparce inclusions of Timber Mountain tuff are present.

- Qbsw Southwestern basalt flows; Aa and block flows of alkali-basalt southwest of Black Cone. The basalt is porphyritic with euhedral to subhedral phenocrysts of olivine in a matrix of plagioclase, diopsidic augite and olivine.
- Qb3 Basalt erupted from the base of Red Cone; Aa and block flows of alkali-basalt east and west of Red Cone. The basalt is porphyritic with euhedral to subhedral phenocrysts of olivine in a matrix of plagioclase, diopsidic augite and olivine.
- Qb2 Basalt flows erupted from scoria mounds southeast of Red Cone. Aa and block flows of alkali-basalt. Basalt is porphyritic with euhedral to subhedral phenocrysts of olivine in a matrix of plagioclase, diopsidic augite and olivine.
- Qb1 Basalt flows erupted from scoria mounds south and southwest of Red Cone. Aa and block flows of alkali-basalt. Basalt is porphyritic with euhedral to subhedral phenocrysts of olivine in a matrix of plagioclase, diopsidic augite and olivine.

Pliocene Units

- Tb Pliocene alkali-basalt flows erupted from a north-south fissure in southeastern Crater Flat. Olivine is the dominant phenocryst. Olivine, plagioclase and clinopyroxene phenocrysts are set in a matrix of plagioclase, olivine, and clinopyroxene. Glomeroporphyritic clots of olivine, clinopyroxene, and plagioclase are common.
- Tbs Pliocene-aged pyroclastic deposits; Poorly-to-moderately welded scoria, ash, bombs, and agglutiated scoria deposited by Strombolian to Hawaiian eruptions.

Quaternary and Pliocene Alkali-basalt dikes; Dikes intrude scoria and range in thickness from 0.5 to 3 m wide.

- Tbc Alkali basalt flows of Crater Flat; K/Ar ages cluster at 3.7 Ma.

Miocene Volcanic Units

- Tmr** Timber Mountain Tuff, Rainier Mesa Member undifferentiated.
- Tmrw** Timber Mountain Tuff, Rainier Mesa Member: Light gray welded ash-flow tuff containing 20-25% phenocrysts of sanidine, quartz, lesser plagioclase and biotite, and rare clinopyroxene.
- Tmrn** Timber Mountain Tuff, Rainier Mesa Member: White to light gray, thinly bedded to massive nonwelded tuff, air-fall, and surge deposits. Thickness increases across some faults. Contains 10% phenocrysts of sanidine, quartz, lesser plagioclase and biotite, and accessory clinopyroxene.
- Tpc** Paintbrush Tuff, Tiva Canyon Member: Light purplish-gray to brown generally densely welded ash-flow tuff, with thin (< 5 m) basal nonwelded unit. Contains 5 to 15% phenocrysts of sanidine, lesser plagioclase and biotite, and rare clinopyroxene and quartz. Abundance of phenocrysts increases upward in section. Lenticular *fiamme* common.
- Tr** Rhyolite flows: Light gray, coarse-grained, crystal-rich rhyolite containing phenocrysts of plagioclase, quartz, alkali feldspar, and biotite.
- Tpy** Paintbrush Tuff, Yucca Mountain Member: Light gray to brownish-gray ash-flow tuff containing sparse (2%) phenocrysts of sanidine and plagioclase.
- Tpt** Paintbrush Tuff, Topopah Spring Member: Light purplish gray to light brownish-gray welded ash-flow tuff containing 10% phenocrysts of sanidine, biotite, and minor plagioclase.

Tptn Paintbrush Tuff, Topopah Spring Member: Pale orange to light brown nonwelded basal part of Tpt. Contains sparse phenocrysts of sanidine, plagioclase, and biotite.

Tcp Crater Flat Tuff, Prow Pass Member: Light gray to brownish-gray ash-flow tuff containing approximately 8% phenocrysts of plagioclase, sanidine, quartz, orthopyroxene, biotite, and magnetite.

Tcb Crater Flat Tuff, Bullfrog Member: Light gray to light brownish-gray, moderate to densely welded ash-flow tuff containing phenocrysts of quartz, plagioclase, sanidine, biotite, hornblende, and magnetite.

APPENDIX E

Late Quaternary faulting at Crater Flat, Yucca Mountain, southern Nevada

Alan R. Ramelli, John W. Bell, and Craig M. dePolo Nevada Bureau of Mines and Geology and Center for Neotectonic Studies, University of Nevada, Reno, Nevada 89557

ABSTRACT

Yucca Mountain, the sole candidate site for a commercial high-level nuclear waste repository, has a significant local seismic hazard. Recurrent Quaternary faulting has occurred on several interconnected, north- to north-northeast-trending faults. Delineation of these faults has been previously hampered by their subdued, subtle expression and small scarp heights. The Quaternary fault data base is enhanced by large-scale, low-sun-angle aerial photography which reveals: 1) the existence of additional active fault traces, 2) extensions and connections of previously mapped traces, and 3) offsets of Quaternary surfaces previously thought to be unfaulted. Several faults immediately adjacent to the repository site in eastern Crater Flat displace late Quaternary piedmont surfaces. Quaternary slip rates on these faults have been relatively low, but at least three of these faults are believed to vertically offset Holocene or latest Pleistocene deposits by up to a few tens of centimeters each. Similarities in ages and amounts of offset, and the high degree of mapped fault interconnection, strongly suggest that the recent surface faulting has occurred in a distributive manner during individual seismic events or sequences. Basaltic ash occurs in vertical fractures along at least four faults, further supporting this interpretation and suggesting that such events have occurred concurrently with local basaltic eruptions. Seismic hazards from such events could be underestimated if independent fault behavior were assumed.

INTRODUCTION

Yucca Mountain, located in southern Nevada (fig. 1), is currently the sole site under consideration for permanent storage of the nation's commercial high-level nuclear waste. One important factor bearing on the suitability of the site is the potential for disruption due to tectonic activity. Numerous Quaternary faults are present at and around Yucca Mountain, posing a significant local seismic hazard. Site suitability issues, including the significance of local seismic events, are distinctly different for "preclosure" (the period over which waste will be handled at the surface facilities and/or monitored for possible retrieval - about 100 years) and "postclosure" (the 10,000-year period following closure of the repository). Local seismic events may have a low probability of occurrence over the preclosure period, but can be considered likely over the 10,000-year postclosure period.

Local seismic events at Yucca Mountain could affect stability of the site in a number of ways, including the impact of surface rupturing and strong ground motion on surface facilities, rupture of waste packages, and possible effects on geohydrologic conditions. The presence of active faults at the site does not necessarily render the site unsuitable, but does complicate predictions of future processes and of site stability. The uncertainties involved in predicting both fault behavior and the potential impacts of local seismic events are likely to be quite large.

GEOLOGIC SETTING

Yucca Mountain is a block-faulted plateau underlain by a thick sequence of Miocene ash-flow tuffs erupted from the nearby Timber Mountain - Oasis Valley caldera complex (Byers et al., 1976; U.S. Geological Survey, 1984). A series of interconnected north- to north-northeast-trending faults offset these tuffs with dominantly down-to-the-west throw, and the fault-bounded blocks tilted to the east (Scott and Bonk, 1984). The tuffs are displaced vertically by up to about 400 m, with much of this offset occurring prior to the eruption of the Rainer Mesa member of the Timber Mountain tuff (Carr, 1984). Paleomagnetic data suggest that the tuffs are rotated clockwise, with tilts and rotations increasing to the south (Scott and Rosenbaum, 1986). The principal faults are subparallel, with interstrike distances averaging about 2 km at the surface.

Yucca Mountain lies within the southwest part of the Basin and Range structural province, a tectonically active region. Some of the highest tectonic rates in the Basin and Range occur about 50 km west of Yucca Mountain, between Death Valley and the eastern front of the Sierra Nevada in Owens Valley. Although considerably less active than the Death Valley/Owens Valley region, numerous Quaternary faults are present at and around Yucca Mountain (Swadley et al., 1984; U. S. Geological Survey, 1984).

Active tectonics at Yucca Mountain are largely extensional in style, but may be affected by strike-slip deformation as well. This area lies within the Walker Lane belt, a regional northwest-trending zone of strike-slip faulting that disrupts typical Basin and Range style faulting (Stewart, 1988). Yucca Mountain is located within the Goldfield segment of the Walker Lane belt (Stewart, 1988), which is characterized by lower rates of Quaternary deformation than much of the Walker Lane belt. No major northwest-trending late Quaternary faults have been recognized around Yucca Mountain, although a limited amount of strike-slip faulting trends into southern Amargosa Valley from Pahrump Valley (Donovan, 1991), and the Paintbrush Canyon fault on the east side of Yucca Mountain merges with northwest-trending faults of unknown activity at Timber Mountain to the north.

Much of the data on Quaternary faulting at Yucca Mountain have come from Crater Flat (Hoover et al., 1981; Swadley et al., 1984; Whitney et al., 1986; Reheis, 1986; Swadley and Carr, 1987; Swadley and Parrish, 1988; Peterson, 1988; Ramelli et al., 1988; Ramelli et al., 1989; Shroba et al., 1990). Crater Flat is an asymmetric structural depression located immediately west of the repository site (fig. 2). Relative to the eastern side of Yucca Mountain, faulting in Crater Flat is more extensive, scarps are better preserved, and there is a more complete Quaternary stratigraphic record.

In eastern Crater Flat, several fault scarps cross fan piedmont surfaces (Swadley et al., 1984). Delineation of these scarps has been previously hampered by their subdued morphology and small scarp heights. To facilitate Quaternary fault mapping, low-sun-angle aerial photography (LSAP), taken under both morning and afternoon lighting conditions, was flown over Yucca Mountain and surrounding areas. LSAP is commonly used in active fault evaluation because oblique lighting greatly enhances incongruent topographic features, such as fault scarps, through shadowing and highlighting. Scarps apparent on LSAP often can not be recognized on standard aerial mapping photography or easily detected on the ground. The LSAP of Crater Flat reveals the existence of unmapped fault scarps, extensions and connections of mapped scarps, and small scarps on Quaternary surfaces previously thought to be unfaulted.

QUATERNARY STRATIGRAPHIC RELATIONS

Six allostratigraphic units ranging in age from mid-Pleistocene to late Holocene are differentiated in the Crater Flat area on the basis of distinctive soil-geomorphic relations (Table 1 and Fig. 3; Peterson, 1988; Bell et al., 1991). These stratigraphic relations provide control for bracketing recency of faulting. Geomorphic relations are dominated by a sequence of fan piedmont remnants, fan skirts, inset fans, and ballenas originating from several of the major drainages on the western flank of Yucca Mountain. Surficial characteristics, such as microtopography, desert pavement, soil morphology, and rock varnish development, progressively change with increasing age. The differentiation of stratigraphic units allows us to approximately bracket recency of surface faulting events. Of the six allostratigraphic units, the three youngest (late Black Cone, Little Cones, and Crater Flat units) provide important maximum limits for timing of faulting during the latest Quaternary.

Rock-varnish and uranium-series ages verify and scale the mapped allostratigraphic relations, and provide minimum limiting ages for the geomorphic surfaces. Twenty-four rock varnish cation-leaching and ^{14}C AMS radiocarbon ages determined on the six allostratigraphic units (Dorn, 1988; Bell et al., 1989) have allowed the construction of a cation-leaching curve for Crater Flat (Dorn et al., 1988), which differs significantly from the one developed by Harrington and Whitney (1987). Due to relatively large uncertainties involved in cation-ratio dating, this study uses numerical age relations provided by the more definitive ^{14}C AMS data.

Eleven finite AMS radiocarbon ages were obtained on late Black Cone (Qflb) and younger surfaces. Six ages ranging between 17.3-30.3 ka were obtained from separately mapped Qflb surfaces. These ages are consistent with ^{230}Th - ^{234}U ages of 17.1 and 38.7 ka determined for pedogenic carbonate (Bk horizon) underlying the late Black Cone surface at trench CF-3 (Ku, 1989; Luo and Ku, 1991) and with one of the uranium-trend ages (40 ka) from the late Black Cone deposit in the same trench (Swadley et al., 1984). These data indicate that the late Black Cone unit is of late Wisconsin age, approximately 20-30 ka.

Little Cones surfaces have yielded four AMS radiocarbon rock varnish ages ranging between 8.4-11.1 ka, which are consistent with the regional soil-geomorphic relations. The surfaces are only slightly topographically muted, and they are inset slightly below those of late Black Cone age. They contain Camborthid soils (cambic B and stage I carbonate horizons) typical of Holocene-age aridisols (e.g., Gile et al., 1966; Machette, 1985).

A single ^{14}C AMS date of 1.3 ka on incipient rock varnish of the Crater Flat surface is consistent with the absence of genetic soil horizons in this unit and with its raw surficial characteristics. The Crater Flat unit, however, probably contains several undifferentiated subdivisions and is simply regarded here as mid- to late Holocene in age.

QUATERNARY FAULTING

Five principal, north-northeast-trending faults are present within a few kilometers of the proposed repository site (Scott and Bonk, 1984), all of which offset Quaternary deposits. The Solitario Canyon, Fatigue Wash, and Windy Wash faults in eastern Crater Flat are located west of the site, whereas the Paintbrush Canyon and Bow Ridge faults are located to the east (fig. 2). A sixth fault, the Ghostdance fault, transects the repository site and may have Quaternary movement. These principal faults are interspersed with numerous smaller, subparallel or interconnecting faults, forming a complex, anastomosing fault pattern. The distribution of fault scarps indicates that Quaternary surface faulting is also highly interconnected, similar to the fault pattern described from bedrock offsets (Scott, 1986).

The Solitario Canyon fault forms the western boundary of the subsurface repository (fig. 2). A prominent compound Quaternary fault scarp 1-3 m high extends along this fault for about 13 km. To the north, the Quaternary scarp dies out along the fault adjacent to the repository site, whereas the southern end of the scarp is obliterated by late Holocene alluviation.

A previously unrecognized scarp is present along the Fatigue Wash fault, located west of the repository site (fig. 2). At its northern end, this scarp dies out at a bend in the Fatigue Wash fault, where a zone of splay faults connect the Fatigue Wash and Windy Wash faults. North of this bend, the Fatigue Wash fault has only minor vertical displacement and no obvious recent displacement, whereas to the south it has a throw comparable to the other principal faults of the area. Where it intersects a northeast-trending, secondary fault, the Fatigue Wash scarp trends away from Jet Ridge and connects with a scarp along a fault trace previously thought to connect with the Windy Wash fault (fault "M" of Swadley et al., 1984).

The Windy Wash fault system, as originally mapped by Scott and Bonk (1984), has been extended to include one of the principal fault traces south of the site area (Whitney et al., 1986). Two exploratory trenches (CF/2 and CF/3) across this southern trace (fig. 4) have yielded some of the most detailed information on the history of late Quaternary faulting in the area (Whitney et al., 1986). In this paper, this fault trace is referred to as the southern Windy Wash fault.

The southern Windy Wash fault and a previously unrecognized late Quaternary fault, here called the "west lava fault," offset a series of Pliocene basalts in southern Crater Flat, providing one of the best sites to estimate fault offsets spanning the entire Quaternary period. These Pliocene basalts (2.5-3.7 Ma) consist of deeply dissected cinder cones and dikes aligned along a north-northwest-trending vent area and discontinuous flow outcrops lying between the vent area and the southern Windy Wash fault about 3 km to the east (fig. 3). Vaniman and Crowe (1981) suggest that these flows are not continuous in the subsurface and inferred that the eastern outcrops probably had separate sources, now buried by alluvium. Alternatively, these flows may have been erupted from a single vent area and have been subsequently isolated by faulting and alluvial activity. Surficial relations support the latter alternative.

The west lava fault bounds the west side of the largest outcrop of Pliocene basalt. This down-to-the-west fault is exposed in one location as the vertical contact between the Pliocene basalt and cemented Quaternary colluvium. A subdued scarp (<1 m high), apparent on the LSAP, is present on a late Black Cone surface north of the basalt outcrop.

The easternmost exposed Pliocene basalt is a linear outcrop stranded on the upthrown side of the southern Windy Wash fault (fig. 3). This stranded outcrop is bounded on the west by a scarp about 30 m high and sits about 40 meters higher than the main flows to the west. This topographic separation likely represents a minimum post-basalt displacement for Pliocene-Recent vertical offset along the southern Windy Wash fault. The basalts may be vertically offset by more than 40 m, if the flows are tilted eastward. Tilt of the basalts has not been precisely determined, but it appears to be considerably less than the tilt of Miocene tuffs exposed on the upthrown side of the southern Windy Wash fault.

As much as several tens of meters of post-3.7 Ma offset along the southern Windy Wash and west lava faults indicates that there has been substantially more Quaternary tectonic activity than originally interpreted from offsets of Miocene tuffs (Carr, 1984). In some places, nearly all of the post-12-13 Ma (Paintbrush Tuff) deformation appears to have occurred prior to deposition of the Rainier Mesa member of the Timber Mountain tuff (~10 m.y.) (Carr, 1984; Swadley et al., 1984). However, the displaced Pliocene basalts

indicate that greater post-Miocene displacements may have occurred along some faults. The amount of post-tuff throw varies substantially along strike of all of the principal faults in the area, ranging from 0 to >400 m. Spatial and temporal variations in fault displacement thus appear to be substantial.

EVIDENCE OF HOLOCENE FAULTING IN CRATER FLAT

Holocene surface rupture is believed to have occurred on at least three faults in Crater Flat. Two of these faults, the Solitario Canyon and "Black Cone" faults (fig. 2), display sharp lineations crossing Little Cones-age surfaces that are believed to be small scarps. A third fault, the southern Windy Wash fault, offsets an eolian silt horizon of probable Holocene age exposed in trenches CF/2 and CF/3. This eolian (cumulate Av) silt has an estimated age of 3-6 ka, based on thermoluminescence dating, and is offset vertically by about ten centimeters (Whitney et al., 1986).

Most of the lineations crossing Little Cones surfaces along the Solitario Canyon and Black Cone faults are evident only under certain LSAP conditions (i.e., with either morning or evening lighting, depending on the relative displacement), and are therefore considered to be small, shadow-enhanced scarps only a few tens of cms high. These features suggest that the most recent offsets along the Solitario Canyon and Black Cone faults are similar in both amount and age to that along the southern Windy Wash fault. Field inspection neither definitively confirms nor disproves a Holocene surface-rupture origin for these features, but recent surface faulting appears to be their most plausible origin. This uncertainty may be resolved in the future through exploratory trenching, however, small offsets are often extremely difficult to distinguish in trench exposures (Bonilla and Leinkaemper, 19??).

The young surface apparently offset by the Solitario Canyon fault is a small fan, believed to be of Little Cones-age, located approximately midway along the length of the late Quaternary trace of the Solitario Canyon fault. There is little question that this fan is of Holocene or latest Pleistocene age; it was mapped as a young (Q1) deposit by Swadley et al. (1984) and has surface morphology (e.g., bar and swale topography, weakly developed pavement) and soil development (i.e., cambic B horizon and Stage I carbonate) indicating youthfulness. A Holocene age for this fan surface is further indicated by accelerator mass spectrometer (AMS) radiocarbon dating of rock varnish ($8,425 \pm 70$ yrs; Dorn, 1988). Rock varnish radiocarbon age estimates are minimums, because they approximate the onset of varnish development, but are believed to closely approximate the actual age of surface stabilization.

Constraints on late Pleistocene offsets along the Solitario Canyon fault are provided by scarps on late Black Cone and Solitario surfaces. At trench 8, located about 2 km north of the young faulted fan, and in other locations between these two sites, late Black Cone surfaces are displaced vertically by up to 1 m. Bedrock scarps about 3 m high along the Solitario Canyon fault appear to represent post-Solitario surface displacement.

The Black Cone fault, located about 6 km west of the Solitario Canyon fault, is characterized by a zone of north-northwest-trending scarps that are mostly down-to-the-east, with some being down-to-the-west. Like the Solitario Canyon fault, vertical displacements along the Black Cone fault appear to be similar in both age and amount to the recent offset on the southern Windy Wash fault. A late Pleistocene to early Holocene age (Little Cones) for the apparently faulted surface is likewise indicated by soil development, rock varnish ^{14}C dating ($11,135 \pm 105$ yrs), and regional mapping (Swadley and Parrish, 1988; Bell et al., 1991).

The Black Cone fault is located on trend of a northwest-trending drainage extending up the Bare Mountain piedmont that may be structurally controlled. Several vegetation lineaments extend across a Yucca-age surface located between the Black Cone scarps and the Bare Mountain piedmont, but there are no obvious fault scarps on this surface. This may indicate that the recent activity of the Black Cone fault reactivated a small portion of a more extensive northwest-trending structure.

EVIDENCE FOR DISTRIBUTIVE FAULTING

The distribution of Quaternary fault scarps in Crater Flat indicates that faulting is highly interconnected, forming a complex, anastomosing pattern. Considering the close interstrike spacing and interconnection of these faults in plan view, they are likely interconnected at shallow crustal depths as well. Rather than a system of individual fault segments, each with its own rupture behavior, these faults can probably be better characterized as a system of faults responding synchronously to deformation within the mid- to lower crust.

Multiple lines of evidence suggest that recent surface faulting has involved concurrent rupture of multiple faults, and that surface faulting may accompany local basaltic volcanism. Evidence supporting this hypothesis include the high degree of fault interconnection, similarities in scarp morphology, similarities in ages and amounts of recent offset along multiple faults, and presence of basaltic ash within vertical fractures formed in fault-filling carbonate exposed in trenches across four faults.

The presence of basaltic ash within fault zone fractures is one of the stronger lines of evidence of concurrent rupture of multiple faults (Swadley et al., 1984; Fox and Carr, 1989; Shroba et al., 1990). It is unlikely that a thin blanket of ash would have remained on the fan surface for an extended period of time (e.g., Shipley, 1983). It is a reasonable inference that basaltic volcanism most likely occurred very close in time to the faulting and is geologically synchronous. Chemical correlation of the four ashes is not definitive (John Whitney, 1991, personal communication) and an alternative model would involve multiple ash eruption and faulting episodes. Geochemical analyses and stratigraphic relations of the basaltic ash suggest that it must have been derived from the Lathrop Wells Cone (Fox and Carr, 1989), the youngest cinder cone in the area, and is therefore probably late Quaternary in age.

DISCUSSION

Our study suggests that late Quaternary surface faulting at Yucca Mountain has occurred in a distributive manner, with synchronous movement on several faults, and that at least one such event may have occurred during the Holocene. The presence of active faults around the site has long been recognized, but surface rupture is now recognized to be more extensive and to have occurred more recently than was originally estimated. Other faults surely remain unrecognized, whether they failed to reach the surface, have been eroded, or are now buried by young alluvium.

Quaternary surface faulting at Yucca Mountain does not occur along a single throughgoing fault zone and can more appropriately be characterized as a broad, highly interconnected fault system. At a minimum, this fault system extends from Yucca Wash to the southern end of Crater Flat, over an area about 30 km long by 15 km wide. Throughout this area, faulting is densely spaced and highly interconnected.

With a high degree of fault interconnection, it is unlikely that the faults at Yucca

Mountain rupture independently of one another, so they should not be treated as independent structures for seismic hazard analyses. Seismic events causing rupture of multiple faults are likely associated with greater energy release, and hence larger magnitudes, than those rupturing individual fault traces. Through historical analogues (the 1932 Cedar Mountain earthquake, in particular), such complex events can conservatively be expected to have large magnitudes ($M \geq 7$). Additionally, fault traces that are part of such an interconnected system, but have not been recently active, can be considered as having a higher probability of rupture than would otherwise be estimated. Hazard estimates directed toward independent fault behavior will likely underestimate the actual seismic potential.

Evidence of possible Holocene faulting is currently limited to the three locations discussed earlier, but offsets of similar age along other faults in the area are possible. Shadowing of scarps on the LSAP reflects oversteepening from the most recent displacement along these faults, while continuity of the oversteepening strongly suggests that this occurred fairly recently, based on comparisons with the expressions of other active faults. Several faults in Crater Flat display scarp oversteepening similar to that on the faults evidently displacing Holocene deposits; it is likely that this reflects similar-aged offsets. This is difficult to substantiate, because few faults cross Holocene-age surfaces and small offsets are often difficult to recognize in coarse-grained, poorly stratified deposits. In one location, a small inset surface crossing the Fatigue Wash fault is of probable Holocene age, based on surface morphology, and appears to be offset and subsequently modified. Evidence of Holocene or latest Pleistocene faulting along faults on the east side of Yucca Mountain has not been found, but the presence of basaltic ash in a fracture along the Bow Ridge fault suggests that recent activity has likewise involved this fault.

The faulted Pliocene basalts in southern Crater Flat provide the best known constraints on the rate of deformation averaged over the Quaternary period. Topographic separation of the stranded basalt outcrop and the main flows to the west suggest a Quaternary vertical slip rate on the order of 0.01 mm/yr for the southern Windy Wash fault. If the topographic separation of these basalts is due to the stranded basalts being erupted from a separate, now buried vent area, a barrier that has been subsequently removed by erosion is required, which appears unlikely.

The best preliminary estimates of long-term Quaternary slip rates for the principal faults in Crater Flat are taken from the southern Windy Wash fault. Based on vertical offsets of 40 cm in 270 ka deposits and 10 cm in 3-6 ka deposits at trenches CF-2 and CF-3 (Whitney et al., 1986), average vertical slip rates appear to be 0.001-0.03 mm/yr. Based on estimates of vertical offset of the Pliocene basalts, ranging from 25-100 m, the long-term slip rate along this fault appears to be 0.01-0.04 mm/yr, with a best estimate of about 0.02 mm/yr.

Not all of the Quaternary faults in the Yucca Mountain/Crater Flat area have been recently active. Many of the northwest-trending traces connecting the principal faults do not appear to have ruptured during the most recent events, whereas several of the northeast-trending connecting traces have. The rupture pattern during recent events has probably resulted from reactivation of a preexisting fault system under a somewhat different stress regime than existed when the system was formed. Stress rotations over the past 10 m.y. or so have been proposed for this region (e.g., Ander, 1984) and may account for the observed relations. In the case of the Pliocene basalts, Quaternary deformation may have involved less tilting than the Miocene deformation that dominantly accounts for the present tuff configuration. The tuffs are also warped along strike of the southern Windy Wash fault (N-S), while the basalts are more uniformly uplifted. These differences in deformation may

likewise result from fault reactivation under a different stress regime and/or differing thermal properties of the crust than existed during the earlier deformation. Fault reactivation coincident with the onset of basaltic volcanism at about 3 m.y. was postulated by Fox and Carr (1989).

Immediately around the repository site, late Quaternary faulting has occurred predominantly along north- to north-northeast-trending, down-to-the-west faults, which is the manner in which faulting at Yucca Mountain is normally described. To the south (in the area just north of Lathrop Wells Cone), the pattern of faulting is similar, although the principal faults trend more northeasterly. In between these areas, a broad northwest-trending zone extending from near the Stagecoach Road fault to northeast of Black Cone has lower relief and contains several down-to-the-east fault traces (fig. 2). This zone is diffuse and contains both down-to-the-east and down-to-the-west faults, but deformation is markedly different than to the northeast and southwest. The observed deformation may result from right-lateral translation across this zone, either in response to differentially extending areas to the north and south or to strike-slip displacement along a buried northwest-trending fault.

REFERENCES CITED

- Ander, H.D., 1984, Rotation of Late Cenozoic extensional stresses, Yucca Flat region, Nevada Test Site, Nevada: unpublished Ph.D. thesis, Rice University, Houston, TX, 72 p., 1 plate.
- Bell, J.W., Peterson, F.F., Dorn, R.I., Ramelli, A.R., and Ku, T.L., 1991, Late Quaternary surficial geology in Crater Flat, Yucca Mountain, southern Nevada: Geological Society of America, Abstracts with Programs (in press).
- Bell, J.W., Ramelli, A.R., dePolo, C.M., and Bonham, H.F., 1989, Progress report for the period 1 July 1988 to 30 September 1989, Task 1 Quaternary tectonics: Report to the Nevada Nuclear Waste Project Office, Carson City, NV, 53 p.
- Byers, F. M., Jr., Carr, W. J., Orkild, P. P., Quinlivan, W. D., and Sargent, K. A., 1976, Volcanic suites and related cauldrons of Timber Mountain Oasis Valley caldera complex, southern Nevada; U. S. Geological Survey, Professional Paper 919, 70 p.
- Carr, W. J., 1984, Regional structural setting of Yucca Mountain, southwestern Nevada, and late Cenozoic rates of tectonic activity in part of the southwestern Great Basin, Nevada and California; U. S. Geological Survey, Open-file Report 84-854.
- dePolo, C. M., Bell, J. W., and Ramelli, A. R., 1989, Estimating earthquake sizes in the Basin and Range province, western North America: perspectives gained from historical earthquakes: American Nuclear Society, Proceedings of the First International High Level Radioactive Waste Management Conference, Las Vegas, Nevada.
- dePolo, C. M., Clark, D. G., Slemmons, D. B., and Ramelli, A. R., in press, Historical surface faulting in the Basin and Range province, western North America: implications for fault segmentation; *Journal of Structural Geology*.
- Donovan, D., 1991, Late Quaternary faulting in the Ash Meadows area, southern Nevada: unpublished M.S. thesis, University of Nevada, Reno, Nevada.
- Dorn, R.I., 1988, A critical evaluation of cation-ratio dating of rock varnish, and an evaluation of its application to the Yucca Mountain repository by the Department of Energy and its subcontractors: in, *Evaluation of the geologic relations and seismotectonic stability of the Yucca Mountain area (NNWSI), Quaternary geology and active faulting at and near Yucca Mountain, Appendix A, Final Report to the Nevada Nuclear Waste Project Office, 73 p.*
- Dorn, R.I., Bell, J.W., and Peterson, F.F., 1988, Implications of rock varnish dating at Crater Flat, near Yucca Mountain, Nevada: Geological Society of America, Abstracts with Programs, v. 20, p. A54.
- Fox, K. F., Jr. and Carr, M. D., 1989, Neotectonics and volcanism at Yucca Mountain and vicinity, Nevada; *Radioactive Waste Management and the Nuclear Fuel Cycle*, v. 13, p. 37-50.
- Gile, L.H., Peterson, F.F., and Grossman, R.B., 1966, Morphological and genetic sequences of carbonate accumulation in desert soils: *Soil Science*, v. 101, p. 347-360.
- Harrington, C.D., and Whitney, J.W., 1987, Scanning electron microscope method for rock varnish dating: *Geology*, v. 15, p. 967-970.
- Hoover, D. L., Swadley, W. C., and Gordon, A. J., 1981, Correlation characteristics of surficial deposits with a description of surficial stratigraphy in the Nevada Test Site region: U. S. Geological Survey, Open-file Report 81-512.
- Ku, T.L., 1989, Uranium-series age dating of pedogenic calcium carbonate samples from the Yucca Mountain area, in Bell et al., 1989, Progress report for the period 1 July 1988 to 30 September 1989, Task 1 Quaternary tectonics: Report to Nevada Nuclear Waste Project Office, Carson City, NV, 14 p.

- Luo, S. and Ku, T.L., 1991, U-series isochron dating: a generalized method employing total-sample dissolution: *Geochemica et Cosmochemica Acta*, v. 25, p. 555-564.
- Machette, M.N., 1985, Calcic soils of the southwestern United States: Geological Society of America Special Paper 203, p. 1-21.
- Peterson, F.F., 1988, Soil geomorphology studies in the Crater Flat, Nevada, area: *in*, Evaluation of the geologic relations and seismotectonic stability of the Yucca Mountain area (NNWSI), Quaternary geology and active faulting at and near Yucca Mountain, Appendix B, Final Report to the Nevada Nuclear Waste Project Office, 45 p.
- Ramelli, A. R., Bell, J. W., and dePolo, C. M., 1988, Evidence of distributive faulting at Yucca Mountain: Geological Society of America, Abstracts with Programs, v. 20, p. 383.
- Ramelli, A. R., Sawyer, T. L., Bell, J. W., Peterson, F. F., Dorn, R. I., and dePolo, C. M., 1989, Preliminary analysis of fault and fracture patterns at Yucca Mountain, southern Nevada; American Nuclear Society, Proceedings FOCUS '89 - Nuclear Waste Isolation in the Unsaturated Zone, Las Vegas, NV, September 18-20, 1989.
- Reheis, M. C., 1986, Preliminary study of Quaternary faulting on the east side of Bare Mountain, Nye County, Nevada; U. S. Geological Survey, Open-file Report 86-576.
- Scott, R. B., 1986, Extensional tectonics at Yucca Mountain, southern Nevada; Geological Society of America, Abstracts with Programs, v. 18, p. 411.
- Scott, Robert B. and Bonk, Jerry, 1984, Preliminary geologic map of Yucca Mountain, Nye County, Nevada, with geologic sections: U. S. Geological Survey, Open-file Report 84-494.
- Scott, R. B. and Rosenbaum, J. G., 1986, Structural and paleomagnetic evidence of rotation about a vertical axis during extension at Yucca Mountain; EOS, American Geophysical Union, v. 67, no. 16, p. 358.
- Scott, R. B. and Whitney, J. W., 1986, The upper crustal detachment system at Yucca Mountain, SW Nevada; Geological Society of America, Abstracts with Programs, v. 19, p. 332.
- Shipley, S., 1983, Erosional modification of the downwind tephra lobe of the 18 May 1980 eruption of Mt. St. Helens, Washington: unpublished M.S. thesis, University of Washington, 72 p.
- Stewart, J. H., 1988, Tectonics of the Walker Lane belt, western Great Basin: Mesozoic and Cenozoic deformation in a zone of shear: *in* Metamorphism and crustal evolution of the western United States, Ernst, W. G. ed., Rubey Volume VII, Prentice Hall, p. 683-713.
- Swadley, W. C., 1983, Map showing surficial geology of the Lathrop Wells quadrangle, Nye County, Nevada: U.S. Geological Survey Miscellaneous Investigations Series Map I-1361.
- Swadley, W. C., and Carr, W. J., 1987, Geologic map of the Quaternary and Tertiary deposits of the Big Dune Quadrangle, Nye County, Nevada, and Inyo County, California: U.S. Geological Survey Map I-1767.
- Swadley, W. C., and Parrish, L. D., 1988, Surficial geologic map of the Bare Mountain quadrangle, Nye County, Nevada: U.S. Geological Survey Map I-1826.
- Swadley, W. C., Hoover, D. L., and Rosholt, J. N., 1984, Preliminary report on late Cenozoic faulting and stratigraphy in the vicinity of Yucca Mountain, Nye County, Nevada: U.S. Geological Survey Open-file Report 84-788, 42 p.
- U. S. Geological Survey, 1984, A summary of geologic studies through January 1, 1983, of a potential high-level radioactive waste repository site at Yucca Mountain, southern Nye County, Nevada: U.S. Geological Survey Open-file Report 84-792, 103 p.

Vaniman, D. T. and Crowe, B. M., 1981, Geology and petrology of basalts of Crater Flat: Los Alamos LA-8845-MS UC-70-81.

Vaniman, D. T., Crowe, B. M., and Gladney, E. S., 1988, Petrology and geochemistry of Hawaiiite lavas from Crater Flat, Nevada; Contributions to Mineralogy and Petrology, v. 80, p. 341.

Whitney, J. W., Shroba, R. R., Simonds, F. W., and Harding, S. T., 1986, Recurrent Quaternary movement on the Windy Wash fault, Nye County, Nevada; Geological Society of America, Abstracts with Programs, v. 18, no. 67, p. 787.

Table 1: Quaternary stratigraphy, Crater Flat, Nevada

Unit	Distinguishing characteristics	Minimum age
Qfcf Crater Flat surface	Active/recently active washes, inset fans, and fan skirts; shallowly incised (<2m), distributive drainage pattern; preserved to slightly subdued bar and swale topography; unvarnished to slightly varnished; may have proto-pavement. No significant formation of genetic soil horizons; may have slight carbonate dustings or filaments on pebble bottoms (Stage I).	<<6.6 ka; late Holocene.
Qflc Little Cones surface	Fan-skirt and low basin-floor remnants; fully-smoothed surfaces; slightly varnished pavement. Clear pedogenic soil (torriorthents) consisting of 5 cm thick Av and Stage I Bk horizon with relatively thick carbonate coatings.	6.6-11.1 ka; early to mid-Holocene.
Qflb Late Black Cone surface	Fan-piedmont remnants; fully-smoothed surfaces; deeply solution etched limestone and darkly varnished volcanic clasts in well-sorted and tightly packed pavements. Soils are calciorthids and locally haplic durargids.	17.3-30.3 ka; late Pleistocene.
Qfeb Early Black Cone surface	Fan-piedmont remnants; fully smoothed surfaces; similar surficial characteristics as late Black Cone. Soils are durargids.	130-190 ka; mid- Pleistocene.
Qfy Yucca surface	Deeply dissected fan-piedmont remnants; darkly varnished, well-sorted and tightly packed pavement. Soils are durargids with 40-60 cm thick Bt and 30-60 cm thick Bqkm horizons.	360-370 ka; mid- Pleistocene.
Qfs Solitario surface	Fully-rounded ridge-line remnants (ballenas); irregularly shaped, well-sorted, tightly packed pavements with darkly varnished volcanic clasts and littered with chips of duripan lamina. Original A and Bt horizons have been stripped; remnantal Bt and Bkqm horizons are present.	450 to >740 ka; mid-Pleistocene.

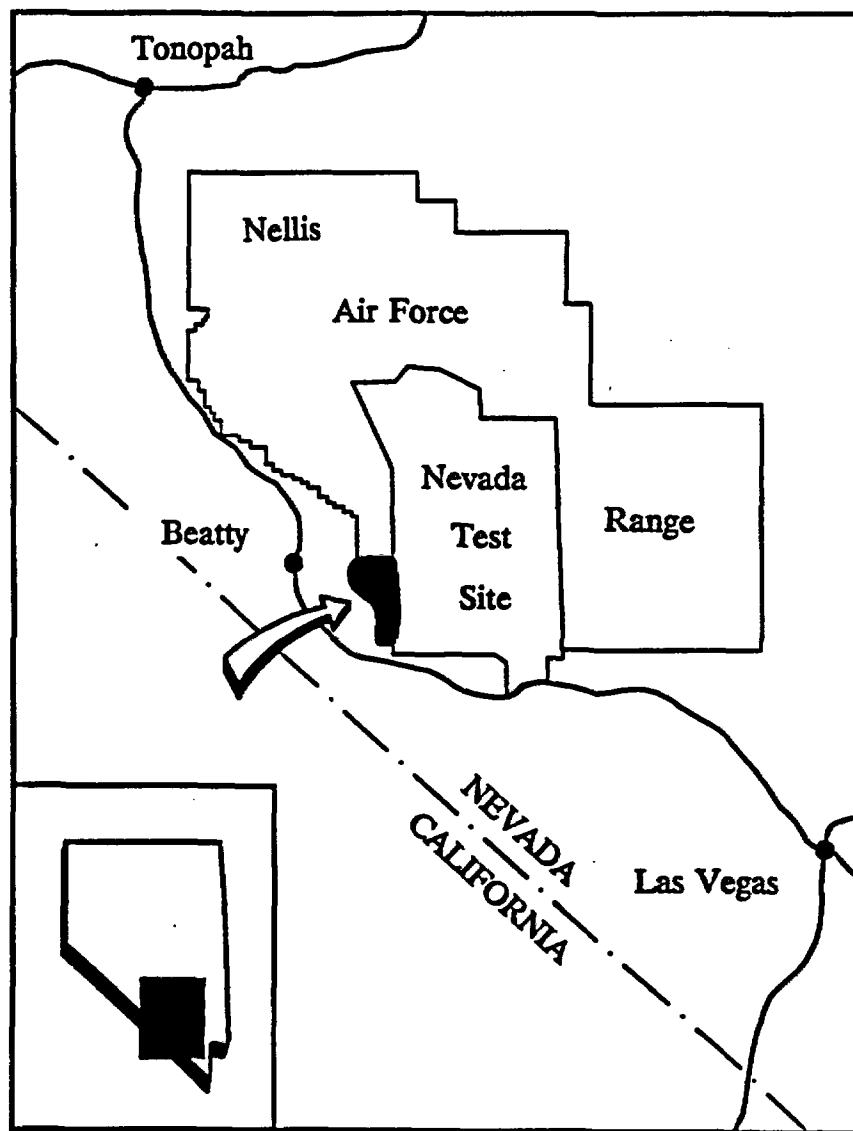


FIGURE 1: Map showing the location of Yucca Mountain and outlines of the Nevada Test Site and Nellis Air Force Range.

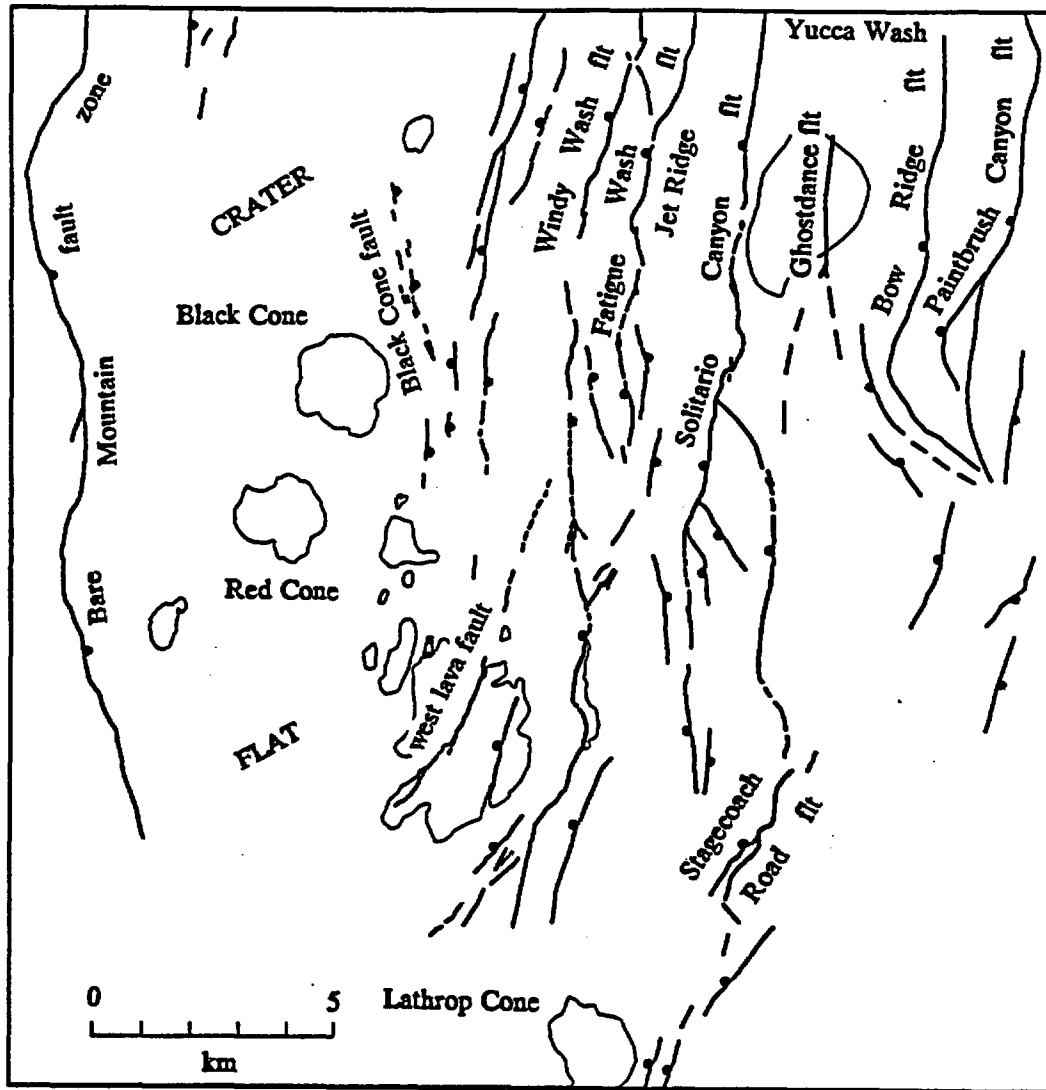


FIGURE 2: Generalized map showing Quaternary faults and Pliocene/Quaternary basalts in the Yucca Mountain/Crater Flat area, and the location of the proposed repository.

Draft: to be revised



-  Qcf Crater Flat surface
-  Qflc Little Cones surface
-  Qflbc Late Black Cone surface
-  Qfebc Early Black Cone surface
-  Qfy Yucca surface
-  Qfs Solitario surface
-  Qb Quaternary basalt
-  Tb Pliocene basalt
-  Tv Miocene tuff
-  Fault scarp

Scale
1 km

FIGURE 3: Map showing surficial geology and late Quaternary fault scarps in east Crater Flat. Quaternary surfaces are commonly complex, with gradational contacts; the surfaces as shown are therefore delineated by dominant surface characteristics. See Table 1 for characteristics of mapped Quaternary surfaces.

1-76

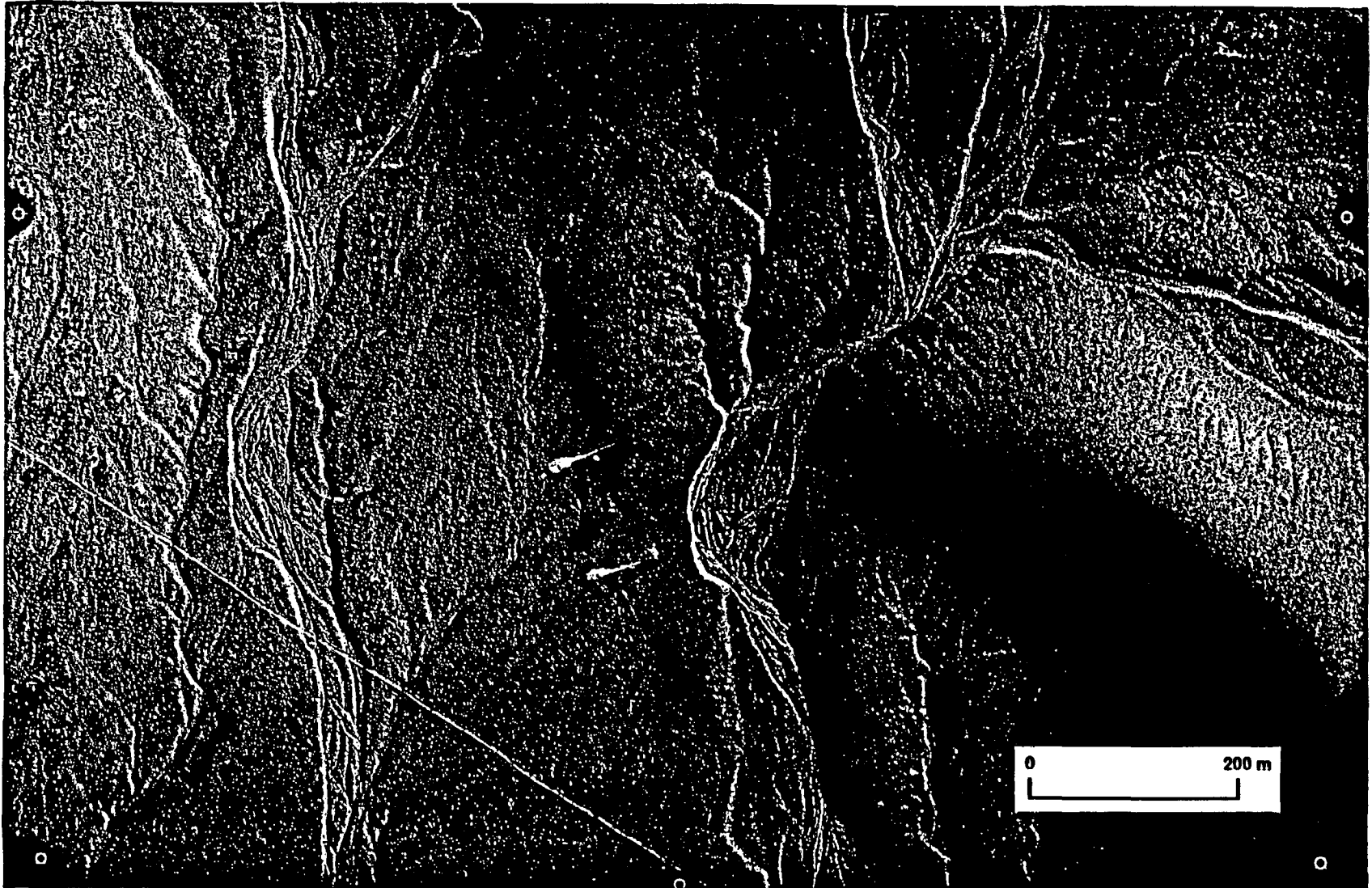


FIGURE 4: Low-sun-angle photograph of the southern Windy Wash fault at the site of Trenches CF-2 and CF-3.

**TASK 3: EVALUATION OF MINERAL RESOURCE POTENTIAL, CALDERA
GEOLOGY, AND VOLCANO-TECTONIC FRAMEWORK AT AND NEAR
YUCCA MOUNTAIN**

REPORT FOR OCTOBER, 1990 - SEPTEMBER, 1991

Steven I. Weiss,¹ Donald C. Noble,² and Lawrence T. Larson²

*Department of Geological Sciences, Mackay School of Mines,
University of Nevada, Reno*

¹ Research Associate

² Co-principal Investigators and Professors of Geology

INTRODUCTION

This report summarizes the results of Task 3 work initially discussed in our monthly reports for the period October 1, 1990 through September 30, 1991, and contained in our various papers and abstracts, both published and currently in press or review (see appendices). Although requests for samples of Yucca Mountain drill core were being considered by DOE as early as December, 1990, we did not become aware of the potential availability of specimens and necessary request procedures until June of 1991. Consequently, investigations conducted by Task 3 between October, 1990 and September, 1991 have mainly been continuations of studies begun prior to October, 1990. We have continued to focus mostly on aspects of the caldera geology, volcanic stratigraphy, magmatic activity, and extensional tectonics of the western and northwestern parts of the southwestern Nevada volcanic field (SWNVF).

PROGRESS IN RADIOMETRIC DATING STUDIES

Prolonged young silicic volcanism: the Mount Jackson domes field

As discussed in our annual report for 1989-1990, radiometric age determinations that we obtained last year on sanidine, biotite and hornblende phenocrysts from Mount Jackson lavas demonstrate a late Pliocene age for the Mount Jackson dome. This age is much younger than the Miocene age inferred by previously workers (cf. Albers and Stewart, 1972) and provides evidence for explosive silicic volcanism in southwestern Nevada well after the late magmatic stage of the SWNVF (Noble et al., 1991a; Appendix A). At least 10 other individual and locally overlapping rhyolitic domes compose the Mount Jackson dome field (Figure 1). Based on our reconnaissance field observations and thin section petrographic work, lavas of the Mount Jackson domes are very similar in petrography, lithology and degree of erosion, suggesting that all of the domes of the field were emplaced from a single magmatic system, presumably over a relatively short period of time. To test this possibility we prepared and submitted (in 1990) sanidine phenocryst concentrates separated from lavas of 3 of these domes. Sample numbers and locations are shown in Figure 1. $^{40}\text{Ar}/^{39}\text{Ar}$ age determinations were carried out using multi-grain resistance furnace fusion methods (E. H. McKee, D. C. Noble and S. I. Weiss, unpublished data, 1991). Sample numbers and age determinations, including the Mount Jackson ages discussed in our report of 1989 - 1990 (Weiss, Noble and Larson, 1990) are as follows:

DWLJ-1	2.9 \pm 0.16 Ma
DWLJ-2	3.7 \pm 0.2 Ma (biotite) 2.8 \pm 1.1 Ma (hornblende)
3SW-383b	5.8 \pm 0.18 Ma
3SW-385	6.8 \pm 0.20 Ma
3SW-387	4.4 \pm 0.13 Ma

These data indicate that some domes of the field are significantly older than Mount Jackson, and imply a remarkably long-lived magmatic feeder system for the dome field. The two oldest ages are from domes in the central and northern parts of the field, while the 4.4 Ma dome and the Mount Jackson dome (about 2.9 Ma) are located in the southern part of the field. Based on the present radiometric age data, explosive silicic volcanism of the Mount Jackson dome field appears to have migrated southward over nearly 4 Ma! A brief manuscript for journal publication is presently being prepared to document and discuss these observations.

Ash-flow sheets of the Gold Mountain - Slate Ridge area

During the past year we have continued studies of the poorly known Cenozoic stratigraphy and structure of the Gold Mountain - Slate Ridge area (GMSR) begun in 1990. We have obtained 2 additional conventional K-Ar age determinations on whole rock and hornblende concentrates from previously undated ash-flow sheets of the GMSR. Preliminary stratigraphic and age relations of the GMSR have recently been presented by Noble et al. (1991b; Appendix B) and are summarized in Table 1 (see below). These data, together with structural relations recognized by Noble et al. (1990a) and Worthington et al. (1991; Appendix C), provide evidence for a 10 Ma history of deformation and volcanism in the northwestern part of the SWNVF that is, in part, either not recorded or not exposed in the NTS-Yucca Mountain area.

Multiple episodes of hydrothermal activity and mineralization in the Bullfrog Hills

Considerable progress was made in efforts to understand the ages and stratigraphic and structural settings of Au-Ag mineralization in the Bullfrog Hills. $^{40}\text{Ar}/^{39}\text{Ar}$ age determinations were obtained from adularia separated from vein and recrystallized wallrock samples from the Original Bullfrog mine, Bond Gold Bullfrog mine, Mayflower mine and the Yellowjacket mine. These data, together with previous K-Ar adularia ages (Morton et al., 1977; Jackson, 1988) and our observations of stratigraphic, textural and structural relations of Au-Ag mineralization of the district are summarized and discussed in an abstract recently presented to the 1991 national meeting of the Geological Society of America (Weiss et al., 1991; Appendix D). Our most important observations and conclusions are as follows:

- 1) All of the currently known Au-Ag deposits in the Bullfrog Hills are of the low base-metal, adularia-sericite type of epithermal mineralization. All of the deposits were structurally controlled by the presently low-angle Original Bullfrog - Fluorspar Canyon detachment fault and/or associated moderate to steeply dipping upper plate faults, some of which penetrate and offset the Original Bullfrog - Fluorspar Canyon fault.
- 2) The $^{40}\text{Ar}/^{39}\text{Ar}$ age determinations obtained on adularia by Task 3 during the past year corroborate and supplement previous K-Ar adularia ages from the Bullfrog district given by Morton et al. (1977) and Jackson (1988). The radiometric ages of adularia indicate that hydrothermal activity and Au-Ag mineralization in the Bullfrog Hills took place during a period of about 2 - 2.5 Ma.
- 3) In the southern Bullfrog Hills Au-Ag mineralization took place at about 9.5 - 10 Ma and persisted until about 9 Ma. Mineralization may have continued until about 8.5 Ma. Hydrothermal activity coincided closely with, and followed by as much as 1 - 1.5 Ma, the end of volcanism that produced the post-Ammonia Tanks tuffs and lavas of the Bullfrog Hills.
- 4) Two periods of hydrothermal activity are evident in the northern Bullfrog Hills. Au-Ag mineralization at the Mayflower mine is of effectively the same age as mineralization at the Bond Gold Bullfrog mine (see above) in the southern Bullfrog Hills. An earlier period of mineralization (*ca.* 11-11.3 Ma) is represented by the Yellowjacket mine area where veins cutting units of the Crater Flat Tuff were deposited coeval with, or within a few tenths of a million years after, deposition of the Timber Mountain Tuff.
- 5) Breccia textures in the veins indicate that mineralization in the southern Bullfrog Hills was synchronous with displacements along the Original Bullfrog - Fluorspar Canyon fault and steeper, upper plate faults.

- 6) Textural and structural evidence for syn- and post-mineral faulting at the Bond Gold Bullfrog mine indicates that upper plate faults were active at and after *ca.* 9.8 Ma.
- 7) Breccia textures and truncation of the vein at the Original Bullfrog mine show that movement of the Original Bullfrog -Fluorspar Canyon fault took place at and continued after about 9 Ma, consistent with the post-9.8 Ma movement of upper plate faults.

A recent summary of the style of mineralization, stratigraphic settings, ore and alteration mineralogy and geochemical characteristics of the Bullfrog district is given by Castor and Weiss (in press; Appendix E).

SUMMARY OF TIMING, STYLES AND STRATIGRAPHIC AND STRUCTURAL SETTINGS OF HYDROTHERMAL MINERALIZATION IN THE SOUTHWESTERN NEVADA VOLCANIC FIELD

Most of our accumulated knowledge of the hydrothermal activity and mineralization in the Yucca Mountain area of the SWNVF is derived from field and laboratory observations carried out by Task 3 during the past 4 years. We have been primarily concerned with understanding the timing, styles, stratigraphic and structural settings, and basic geochemical nature of mineralization in the SWNVF. This work has led us to propose that hydrothermal activity and mineralization were associated with the evolution of the SWNVF and directly related to specific volcanic centers and periods of magmatic and volcanic activity (e.g. Jackson et al., 1988; Noble et al., 1990b; 1991a). We have recognized major differences in the types, styles and timing of precious metal mineralization within the southern part of the SWNVF (e.g., Noble et al., 1991a).

During the past year we have pooled our accumulated geologic knowledge and limited geochemical data from mineralized areas of the SWNVF with complimentary geochemical and ore and vein petrographic data obtained by S. B. Castor of the Nevada Bureau of Mines and Geology under contracts from the Department of Energy and Science Applications International (Castor et al., 1989; 1990). Our collaboration has resulted in the preparation of a descriptive paper summarizing contrasts in the stratigraphic and structural settings, styles and types of mineralization and associated wallrock alteration, and geochemical characteristics of areas of precious metals mineralization in the southern part of the SWNVF (Castor and Weiss, in press). Preparation of this paper entitled *Contrasting styles of epithermal precious-metal mineralization in the southwestern Nevada volcanic field* involved a significant proportion of Weiss' time during the period of this report. A copy of the manuscript, which has been accepted for publication (pending minor revisions) in the journal *Ore Geology Reviews* is included as Appendix E.

NATURE AND DISTRIBUTION OF SUBSURFACE ALTERATION IN YUCCA MOUNTAIN

A number of previous workers have implicitly and explicitly described mineralogic and petrographic evidence for at least one episode of hydrothermal activity deep within Yucca Mountain (e.g., Bish, 1987; Broxton et al., 1982; Caporuscio et al., 1982; Carr et al., 1986; Maldonado and Koether, 1983; Warren et al., 1984) that is believed to have taken place at about 10 - 11 Ma based on K-Ar age determinations on illite recovered from USW G-2 (Aronson and Bish, 1987). As discussed in our report for 1989-1990 (Weiss, Noble and Larson, 1990), our preliminary visual inspection of selected intervals of core convinced us that there is unequivocal and abundant mineralogic and textural evidence (ie. replacements,

veins, cavity infillings, authigenic pyrite, etc.) for the passage of hydrothermal fluids within the tuffs and carbonate rocks beneath Yucca Mountain. Knowledge of the nature and distribution of this hydrothermal activity is critical to the assessment of possible undiscovered mineral resources that could conceivably be present between existing deep drill holes or beneath shallow drill holes in Yucca Mountain.

During the past year we have undertaken two approaches to the problem of obtaining additional knowledge of the subsurface alteration of Yucca Mountain. First, the subsurface distribution of geologic features characteristic of hydrothermal alteration that we observed in our visual inspection last year were plotted on a fence diagram showing the deeper drill holes and stratigraphy in Yucca Mountain. Next, available USGS and Los Alamos National Laboratory reports on the subsurface stratigraphy and petrography of Yucca Mountain were systematically examined for descriptions and reports of mineralogic and petrographic features indicative of hydrothermal alteration. Information on subsurface alteration gleaned from the published drill hole reports was compiled with information from our visual observations on the fence diagram and is shown in Figure 2. This graphical compilation clearly shows that hydrothermal features, though generally not present above the top of the Bullfrog Member of the Crater Flat Tuff, are not confined to one particular stratigraphic horizon. Obvious silicification is mostly confined to the lavas underlying the Lithic Ridge Tuff in drill hole USW G-2. However, a propylitic assemblage consisting of replacement of plagioclase and mafic phenocrysts by calcite-illite/smectite \pm albite \pm adularia \pm chlorite \pm sericite(?) is widespread and not uncommonly includes pyrite (Figure 2).

Pyrite in the tuffs is present as disseminated authigenic grains in the groundmass and locally is more abundant in lithic fragments, where it is present in veinlets and as disseminated grains. These pyritic lithic fragments are particularly common in the Lithic Ridge Tuff and in the lower, lithic-rich subunit of the Tram Member of the Crater Flat Tuff.

The pyrite in ash-flow tuff at Yucca Mountain may not be reasonably attributed to biogenic sulfate reduction because of the extremely low or non-existent content of organic matter within the tuffs. It is most simply explained by the introduction of reduced sulfur species transported by hydrothermal fluids. The greater abundance of pyrite, including veinlets, in lithic fragments of the Lithic Ridge Tuff and the lower part of the Tram Member provides strong evidence for one or more periods of hydrothermal activity in the general vent area of these ash-flow units prior to their eruption.

Pyrite of hydrothermal origin is also present in the pre-Cenozoic carbonate rocks penetrated by drill hole UE25p-1 (Figure 2; Carr et al., 1986). Rotary cuttings from this drill hole contain fragments of vein pyrite, which is not likely to be of diagenetic origin. Fragments of drusy quartz and fluorite veins are associated with these pyritic intervals.

Fluorite and much less common barite are present as open-space intergrowths with calcite that infill fractures and cavities in the deeper parts of Yucca Mountain. With the exception of the barite in USW G-2, these infillings coincide with propylitic alteration in the tuffs and with zones of pyritic alteration. We interpret these relations to be consistent with a hydrothermal origin for most of the fluorite and barite. The origin of the fluorite veins in densely welded, devitrified tuff of the Topopah Spring Member in the upper part of drill hole USW G-3 is not clear. Obvious epigenetic rock alteration does not accompany these veins. Although such veins are rarely reported in descriptions of fresh ash-flow sheets, fluorite has been found in fumarolic mounds of vapor-phase origin in the ash-flow sheet of the Valley of Ten Thousand Smokes (Papike et al., 1991). A vapor-phase origin for the high-level fluorite in USW G-3, related to primary cooling of the Topopah Spring Member, is not unreasonable in the absence of associated hydrothermal alteration. Further work is required to evaluate this possibility.

The apparent gaps in alteration of the Lithic Ridge Tuff and upper lavas in USW G-1, the pre-Lithic Ridge tuffs in USW G-3, and the lower part of the volcanic section in

UE25p-1 may be real or may be due to a lack of adequate published descriptive information. During the next funding period we intend to examine additional core from these intervals to better constrain the vertical extent of hydrothermal alteration in USW G-1, USW G-3 and UE25p-1. At present the data are insufficient to provide more than a minimal understanding of the mineralogical character and spatial distribution of subsurface alteration in Yucca Mountain.

Our second approach to investigating the nature of hydrothermal activity in Yucca Mountain has been directed toward obtaining samples of core from the drill holes for direct petrographic and chemical analyses. Based on our reconnaissance inspection of core and cuttings in 1990 and published reports, a Request for Sample Removal was prepared and submitted to the Sample Overview Committee of the U.S. DOE. A total of 122 sample intervals of splits of core and cuttings were requested. These samples were specified to include intervals containing veins, cavity infillings and examples of altered rocks. During the process of physically identifying and marking the requested samples, some samples were found to be unavailable, mainly due to the recent removal of certain *entire sections of core* by J. Stuckless of the USGS. The USGS has nevertheless, at the insistence of J. Stuckless, effectively limited our group to splits of vein and cavity infillings, so as to preserve materials for possible future studies by the USGS. A result is that some requested specimens of fluoride-bearing rocks are now very small and suitable only for potential fluid inclusion work.

A few intervals requested by Task 3 overlapped with intervals specified in a Sample Removal Request of S. B. Castor that was under consideration by the Sample Overview Committee concurrent with our request. Due to the small amounts of materials available from these intervals, we have agreed to share 2 samples with Castor.

Our Sample Removal Request was approved by the Sample Overview Committee on October 23, 1991. Of the initial 122 samples requested, we expect to receive 114 samples. The DOE personnel of the Sample Management Facility and most of the members of the Sample Overview Committee have cooperated fully and provided the necessary assistance for the largely successful resolution of our Sample Removal Request. We intend to begin petrographic and chemical studies of these samples late in 1991 or early in 1992.

PRIMARY LOW-LEVEL GOLD CONTENTS OF SILICIC VOLCANIC ROCKS: APPLICATIONS TO STUDIES OF YUCCA MOUNTAIN

During this period we continued to support studies of the low-level primary gold contents of silicic volcanic rocks. These studies, carried out mainly by K. A. Connors, provide baseline information for evaluating and interpreting chemical data from rocks of Yucca Mountain. In addition, the results give significant insight into the behavior of gold in silicate melts, and bear on the possible sources of gold in ore deposits found in volcanic terranes. Connors presented the results of this work to the 15th International Symposium of the Association of Exploration Geochemists (Connors et al., 1991a; Appendix F).

Gold contents of fresh, subalkaline rhyolitic volcanic rocks of the SWNVF are listed in Table 2 (Connors et al., 1991a; Connors, in preparation). Almost all of these rocks contain <0.1 ppb to 0.4 ppb gold (Figure 3a). If only the glassy rocks are considered, higher gold contents are limited to the upper vitrophere of the Topopah Spring Member of the Paintbrush Tuff (0.8ppb) and the vitrophere near the base of the Bullfrog Member of the Crater Flat Tuff (0.5ppb) (Table 2, Figure 3b). These higher gold contents are consistent with the higher Fe/Ca ratios (more tholeiitic character) of these samples (Connors, 1991a). The glassy rocks have suffered the least post-depositional chemical exchange with meteoric fluids and most closely approximate magmatic gold contents at the time of solidification. The devitrified rocks are from densely welded portions of the Tiva Canyon Member and care was taken during preparation of these samples to avoid including material from litho-

physal cavities. They contain slightly higher amounts of gold than the glassy rocks (Figure 3c), reflecting the sum of all post-emplacement losses and additions of gold. These would include possible changes associated with degassing during primary cooling (devitrification) and possible gains or losses associated with epigenetic processes such as hydrothermal or weathering reactions, including adsorption from and/or leaching by groundwater. Although caliche is present in lithophysal cavities, obvious mineralogic or textural evidence for hydrothermal alteration of these rocks is absent, suggesting that the slight elevation of gold contents is more likely related to chemical exchange associated with primary cooling and/or weathering. Overall, these data provide a frame of reference for comparison of altered rocks and fault materials from Yucca Mountain (see below).

TRACE-METAL CHEMISTRY OF FAULT ROCKS AND DENSE TUFF FROM THE SURFACE OF YUCCA MOUNTAIN

We have continued efforts to characterize and evaluate the trace-metal chemical signature of surface exposures of fault rocks in Yucca Mountain. Our efforts can be divided into two stages: 1) acquiring reliable low-level mercury (Hg) data to test the possibility that dilute, distal fluids associated with deep hydrothermal activity may have ascended along faults and fracture zones in Yucca Mountain, and 2) determining the trace-metal concentrations of rocks with elevated mercury contents. The volatile nature of mercury and its common association with hydrothermal activity and mineralization makes mercury an important pathfinder element. Due to concerns about the volatility and possible migration of mercury in and/or out of samples over periods of months to years, and problems of reproducibility in previous analyses (cf. Weiss, Noble and Larson, 1990), a new suite of large (2-10 kg) rock samples was collected from fault materials and fresh devitrified tuff. These samples were selected for the purpose of comparing Hg contents of fresh, but weathered country rocks of densely welded, devitrified tuff to those of fault rocks that may have reacted with or precipitated from aqueous solutions of possible distal hydrothermal origin. The locations of these samples, along with certain samples analysed during 1989-1990, are shown in Figure 4.

Mercury results

Powders were prepared from the interior portions of samples soon after collection and were immediately sealed in plastic vials to prevent potential loss or gain of mercury or other volatile elements. Mercury concentrations were determined at the Nevada Bureau of Mines Analytical Laboratory by replicate analyses using atomic absorption methods with an estimated detection limit of 10 ppb (M. Desilets, unpublished data, 1991). Results are listed in Table 3. There is no consistent correlation between the atomic absorption data and Hg data from splits of the same samples analysed by inductively coupled plasma-emission spectroscopic (ICP-ES) methods (Table 4, see below). Based on our past experience (e.g, Weiss, Noble and Larson, 1990), we believe that the atomic absorption analyses are more reliable at low concentrations of Hg and give lower, and hence more conservative, Hg values.

Weathered (but otherwise fresh) devitrified, densely welded lithophysal rocks of the Tiva Canyon Member contain <10 ppb to about 35.5 ppb mercury. There is considerably more uncertainty in the higher mercury contents of 3SW-583 and 3SW-597 than in the other fresh tuff samples (Table 3). This variation could perhaps best be explained by inhomogeneous distribution of vapor-phase or hydrothermally added Hg. Consequently, we suspect that values of <10 ppb to about 15 ppb probably more closely approximate the primary mercury content of fresh, devitrified, rhyolitic ash-flow tuff. We would expect the initial Hg contents of such rocks to be in this range, or lower, owing to the volatile nature of Hg and the high temperatures of emplacement and devitrification.

Rocks that have clearly been strongly altered by hydrothermal activity are present not far north of Yucca Mountain in the lower part of Claim Canyon. Atomic absorption analyses show that a sample of silicified and partly adularized rock from Claim Canyon is strongly enriched in Hg compared to fresh tuff (Table 3).

Fault breccia and gouge from faults exposed northwest of Busted Butte and at the west side of Bow Ridge (Figure 4) do not contain elevated mercury contents relative to fresh tuff (Table 3). Hg concentrations of rocks associated with splays of the Solitario Canyon fault are slightly but significantly elevated compared to the fresh tuff samples that gave the more precise results. The elevated Hg contents of samples 3SW-599A and 3SW-599B are associated with elevated Bi, Au, Mo and Pb as well (see below).

Mercury concentrations of samples from the Bow Ridge fault at Trench 14 are variable, but in three samples Hg is very slightly elevated with respect to the more precise of the fresh tuff values (Table 3). Three other samples may contain marginally elevated Hg concentrations as well. These results are consistent with and support the atomic absorption data given in our report for 1989-1990 and, because of the relatively short time between collection, preparation and analysis, argue strongly against potential loss of Hg to explain the much lower concentrations than were measured initially with IPC-ES methods (Weiss, Noble and Larson, 1990). The fault rocks we have analysed locally contain only marginally to slightly elevated Hg concentrations relative to fresh tuff; Hg enrichments are not comparable to that found in hydrothermally altered rock of Claim Canyon.

Gold and other trace metals

Trace metal concentrations were obtained for the Trench 14 samples and other selected samples for comparison to fresh tuff samples (Table 4). Concentrations were measured using low detection limit ICP-ES methods. Gold (Au) values measured for fresh tuff by ICP-ES methods were slightly lower than those of similar samples measured by INAA methods (Table 4), suggesting that the ICP-ES measurements are not too high. The ICP-ES measurements are therefore considered useful.

Except for slight enrichments of Au and arsenic (As) (see below), our new analyses from Trench 14 do not corroborate the elevated metal concentrations measured in our initial sample set (Weiss, Noble and Larson, 1990) and discussed in our ACNW and NWTRB presentations in 1989. Silver is depleted in fault rocks relative to fresh tuff. Molybdenum (Mo), bismuth (Bi) and lead (Pb) are slightly elevated in iron-oxide reddened tuff from Solitario Canyon and northwest of Busted Butte. Our data from 3SW-599A in Solitario Canyon are similar to analyses from the same outcrop reported by Castor et al. (1989); our atomic absorption data shows that this enrichment includes Hg as well.

Relative to fresh devitrified tuff, Au and As are slightly to moderately enriched in samples from Trench 14 and one sample from Solitario Canyon, and are more strongly enriched compared to samples from the west side of Boomerang Point. The data of Castor et al. (1989) suggest a mean As content of about 1.6 ppm for fresh tuff at Yucca Mountain. The higher Au and, locally, As concentrations of our samples appear to correspond to caliche-bearing rocks. A similar correspondence is evident in the Au and As data of Castor et al. (1989). On the basis of isotopic evidence, Stuckless et al. (1991) and Zartman and Kwak (1991) have recently argued that caliche and carbonate-silica deposits at Trench 14 and Busted Butte are related to surficial processes and are genetically unrelated to present ground waters in the subsurface. The possibility that the slight elevations of Au and As concentrations are related to alkaline surficial waters, arid weathering and biogenic processes can not be ruled out. However, these enrichments are difficult to attribute solely to such surficial processes because molybdenum, another incompatible element that is highly soluble in alkaline oxygenated waters, is not similarly elevated. Surficial weathering and fluid movement would need to transport Mo out of the currently exposed parts of the system.

STRATIGRAPHY OF THE OASIS VALLEY-FLEUR DE LIS RANCH AREA: CONSTRAINTS ON THE LOCATION AND NATURE OF THE WESTERN MARGIN OF THE TIMBER MOUNTAIN I CALDERA

Mapping by Connors at the 1:24,000 scale in the Oasis Valley area, partly supported by funds from Task 3, was completed during the period of this report. This work, along with supporting thin section petrographic studies (Connors, in preparation), has resulted in a significantly improved understanding of the stratigraphic and structural relations of the western part of the Timber Mountain caldera complex. These relations are summarized by Connors et al. (1991b) in an American Geophysical Union abstract entitled *Ash-flow volcanism of Ammonia Tanks age in the Oasis Valley area, SW Nevada: Bearing on the evolution of the Timber Mountain calderas and the timing of formation of the Timber Mountain II resurgent dome* (Appendix G).

The Coffey #1 oil well, located in Oasis Valley to the southeast of Fleur de Lis Ranch, was completed at a depth of 3880 feet early in 1991. The location and depth of this well provide an opportunity to obtain exclusive subsurface data on the geometry and stratigraphy of the western part of the Timber Mountain caldera complex. The official geologist's log of the Coffey #1 (P. Hand, unpublished data 1991) reports the bottom of the well to be situated in Paintbrush Tuff. Preliminary examination by Connors of recovered drill cuttings, however, indicates that quartz phenocrysts are abundant in the welded tuff at the bottom of the drill hole, ruling out the possibility that the bottom consists of Paintbrush Tuff. Rather, Connors' examination suggests that the well penetrates and terminates within a stratigraphic succession consistent with the nearby, east-dipping units that compose the Tuffs of Fleur de Lis Ranch (Connors et al., 1991b). Detailed petrographic work on chips recovered from this well (from the Nevada Bureau of Mines and Geology cuttings collection) is presently being carried out by R. Warren of Los Alamos National Laboratory and D. Sawyer of the USGS in Denver, CO.

MIOCENE VOLCANIC STRATIGRAPHY AND STRUCTURAL GEOLOGY OF THE GOLD MOUNTAIN - SLATE RIDGE AREA

Field mapping, petrographic and radiometric dating studies of the ash-flow sheets of the Gold Mountain - Slate Ridge area (GMSR) were continued during the period of this report by J. E. Worthington and D. C. Noble. Angular unconformities, growth faults, wedges of coarse conglomerates between ash-flow sheets, and rapid lateral variations in thicknesses of units were documented by Worthington's mapping. These features demonstrate a history of normal faulting and tilting spanning from at least the late Early Miocene to after about 7.6 Ma. This record of prolonged Miocene extensional deformation is incomplete or is obscured in other parts of the SWNVF by volcanic units of middle to late Miocene age. In the GMSR area the Miocene volcanic and sedimentary section has not been observed to be structurally detached from underlying pre-Cenozoic rocks as is the case in areas of major extension to the north (Mineral Ridge - Weepah Hills), east (Trappman Hills), south (Bullfrog Hills) and southwest (Death Valley area).

The presently known ages and stratigraphic and structural relations of the Miocene section in the GMSR area are summarized in Table 1 and are discussed in two abstracts presented at the 1991 national meeting of the Geological Society of America (Noble et al., 1991b, Appendix B; Worthington et al., 1991, Appendix C). A preliminary summary of phenocryst assemblages of the pre-Timber Mountain ash-flow sheets is given in Table 5. Worthington's masters thesis, containing a 1:24,000 scale geologic map and more detailed description and discussion of the volcanic stratigraphy, petrography and Neogene deformation of the GMSR area, is currently in preparation.

UPDATE ON MINING AND MINERAL EXPLORATION

A number of significant changes took place during the period of this report in the mining and exploration industries in the Beatty area. The Mother Lode gold mine in northern Bare Mountain was closed after depletion of the upper, oxidized portion of the Au-Ag resource. Considerable refractory ore-grade mineralization remains, but is subeconomic at current gold prices. N. A. Deggerstrom, the operator, is currently pursuing permits to mine nearby oxide ore in Joshua Hollow, and U. S. Precious Metals continues to evaluate this past year's drilling results to the northeast of the Mother Lode mine. Further south in Bare Mountain gold production continues at the Sterling mine, which is situated adjacent to Crater Flat.

The name of the Bond Gold Bullfrog mine has been changed to the Lac Minerals Bullfrog mine. Annual Au production is estimated to be >200,000 oz in 1991. Underground production has recently commenced from a decline exploiting higher-grade vein mineralization extending north from the open pit. Underground production is expected to reach 1000 tons per day at an average grade of 0.23 oz/t Au by the end of 1991. Lac Minerals Ltd continued exploratory drilling in the Rhyolite area of the district.

Exploration for precious metals continued in the northern Bullfrog Hills. Sunshine Mining continued exploratory drilling west of the Yellow Jacket mine area. Pathfinder Resources has reportedly leased the Pioneer mine area and is currently conducting surface sampling and mapping in preparation for a drilling program planned for early 1992.

HG Mining Inc. of Beatty, NV. continues production of cut stone products from ash-flow tuffs quarried in the Transvaal Hills and upper Oasis Valley area. Production is reportedly up 40% from 1990 levels (D. Spicer, personal communication, 1991).

In Oasis Valley the Coffey #1 wildcat oil well was drilled to a depth of 3880 feet. This well, situated within the western part of the Timber Mountain caldera complex, is important as it demonstrates that in fact deep drilling takes place in locations where conventional models predict little or no resource potential. A nearby deep test well is presently being planned for sometime in 1992 (P. Hand, personal communication, 1991).

REVIEWS, PRESENTATIONS AND PUBLICATIONS

Reviews

Noble provided a technical review to the journal *Science* of a Turrin et al. manuscript entitled *⁴⁰Ar/³⁹Ar laser-fusion ages from the Lathrop Wells volcanic center: implications for volcanic hazards in the Yucca Mountain repository site, southwestern Nevada* (*Science*, v. 253, p. 654-657).

Publications

The following abstracts and articles resulting from Task 3 studies were produced and(or) published during the period covered by this report, and are contained in the appendices as follows:

Appendix A:

Noble, D. C., Weiss, S. I., and McKee, E. H., 1991a, Caldera geology, magmatic and hydrothermal activity and regional extension in the western part of the southwestern Nevada volcanic field: in Raines, G. L., Lisle, R. E., Shafer, R. W., and Wilkinson, W. W., eds., *Geology and ore deposits of the Great Basin: Symposium Proceedings*, Geol. Soc. of Nevada, p. 913-934, 1991.

Appendix B:

Noble, D. C., Worthington, J. E., and McKee, E. H., 1991b, Geologic and tectonic setting and Miocene volcanic stratigraphy of the Gold Mountain-Slate Ridge area, southwestern Nevada: *Geol. Soc. America Abstr. with Prog.*, v. 23, p. A247.

Appendix C:

Worthington, J. E., Noble, D. C., and Weiss, S. I., 1991, Structural geology and Neogene extensional tectonics of the Gold Mountain-Slate Ridge area, southwestern Nevada: *Geol. Soc. America Abstr. with Prog.*, v. 23, p. A247.

Appendix D:

Weiss, S. I., McKee, E. H., Noble, D. C., Connors, K. A., and Jackson, M. R., 1991, Multiple episodes of Au-Ag mineralization in the Bullfrog Hills, SW Nevada, and their relation to coeval extension and volcanism: *Geol. Soc. America Abstr. with Prog.*, v. 23, p. A246.

Appendix E:

Castor, S. B., and Weiss, S. I., Contrasting styles of epithermal precious-metal mineralization in the southwestern Nevada volcanic field: *Ore Geology Reviews (in press)*.

Appendix F:

Connors, K.A., Noble, D.C., Weiss, S.I., and Bussey, S.D., 1991a, Compositional controls on the gold contents of silicic volcanic rocks: *15th International Geochemical Exploration Symposium, Abstracts with Program*, p. 43, Association of Exploration Geochemists, Reno, NV.

Appendix G:

Connors, K. A., McKee, E. H., Noble, D. C., and Weiss, S. I., 1991b, Ash-flow volcanism of Ammonia Tanks age in the Oasis Valley area, SW Nevada: Bearing on the evolution of the Timber Mountain calderas and the timing of formation of the Timber Mountain II resurgent dome: *EOS, Trans. Am. Geophys. Union.*, v.72, p.570.

SUMMARY OF CONCLUSIONS AND RECOMMENDATIONS

Radiometric dating studies show that explosive silicic volcanism of the Mount Jackson dome field took place in southwestern Nevada over a remarkably long period of nearly 4 Ma that continued into the late Pliocene. This work, along with the results of our work on the Neogene volcanic-stratigraphic and structural evolution of the Gold Mountain area, continue to provide fundamental information on the volcanic and tectonic evolution of the southwest Nevada volcanic field.

Current subsurface information confirms the widespread extent of hydrothermal alteration in Yucca Mountain and shows that alteration is not confined to any particular stratigraphic unit. Also, the depth to alteration first decreases southward between USW G-2 and UE25b-1H and then increases southward between UE25a-1 and USW G-3. The alteration is mainly propylitic in character but silicification is present locally. Further inspection of core and cuttings is planned for the coming year. Pending receipt of drill hole samples, direct petrographic and chemical analyses will soon be possible as well. We must emphasize that a credible, realistic assessment of alteration and possible mineralization that may, or may not, lie between the existing holes will remain in the realm of wishful thinking due to the small number of deep drill holes and the large distances between them.

The chemical data we have obtained during the past year from surface samples of fault rocks and weathered are more conclusive than that of past reports. Strong enrichments of Hg and/or other trace-metals that may be clearly associated with hydrothermal alteration

were not found. However, we must emphasize that the analysis of altered rock of Claim Canyon differs very little, except for Hg, from analyses of fault rocks at Trench 14 and elsewhere in Yucca Mountain. In some fault materials Au and As show very slight, but probably real enrichment relative to both glassy and devitrified fresh tuff. The elements Bi, Mo, and Pb, \pm Hg are found to be elevated in tuff from Solitario Canyon and northwest of Busted Butte. The origin of these enrichments remains questionable; processes of surficial nature alone do not provide adequate explanations.

Even though precious metals prices have been relatively weak during the past year, strong exploration and mining efforts continued in the Beatty area of the SWNVF.

REFERENCES CITED AND OTHER PERTINENT LITERATURE

The following references were selected because of their direct bearing on the Cenozoic volcanic stratigraphy and caldera geology, hydrothermal activity, and mineral potential of the Site Vicinity. Additional pertinent references on mineral potential, and particularly unpublished data in files of the Nevada Bureau of Mines and Geology, are given by Bell and Larson [1982b].

- Ahern, R., and Corn, R.M., 1981, Mineralization related to the volcanic center at Beatty, Nevada: *Arizona Geological Society Digest*, v. XIV, p. 283-286.
- Albers, J. P., and Stewart, J. H., 1972, Geology and mineral deposits of Esmeralda County, Nevada, Nevada Bur. Mines and Geol. Bull. 78, 80 p.
- Ander, H.D., and Byers, F.M., 1984, Nevada Test Site field trip guidebook; Reno, Nevada, University of Nevada-Reno, Department of Geological Sciences, v. 2, 1984, 35 p.
- Anderson, R.E., Ekren, E.B., and Healey, D.L., 1965, Possible buried mineralized areas in Nye and Esmeraldo Counties, Nevada: U.S. Geological Survey Professional Paper 525-D, p. D144-D150.
- Anonymous, 1928, One strike of real importance made at Nevada's new camp: *Engineering and Mining Journal*, v. 125, no. 1, p. 457.
- Aronson, J.L., and Bish, D.L., 1987, Distribution, K/Ar dates, and origin of illite/smectite in tuffs from cores USW G-1 and G-2, Yucca Mountain, Nevada, a potential high-level radioactive waste repository: Abstract of presentation at Clay Minerals Society Meeting, Socorro, NM, 1987.
- Armstrong, R. L., Ekren, E. B., McKee, E. H., and Noble, D. C., 1969, Space-time relations of Cenozoic silicic volcanism in the Great Basin of the western United States: *Am. Jour. Sci.*, v. 267, p. 478-490.
- Bailey, E.H., and Phoenix, D.A., 1944, Quicksilver deposits in Nevada: Nevada Bureau of Mines and Geology Bulletin 41.
- Barton, C.C., Tectonic significance of fractures in welded tuff, Yucca Mountain, Southwest Nevada: *Geological Society of America, Abstracts with Programs*, v. 16, 1984, p. 437.
- Bath, G.D., and Jahren, C.E., 1984, Interpretations of magnetic anomalies at repository site proposed for Yucca Mountain area, Nevada Test Site: U.S. Geological Survey Open-File Report 84-120, 40 p.
- Bath, G.D., and Jahren, C.E., 1985, Investigation of an aeromagnetic anomaly on west side of Yucca Mountain, Nye County, Nevada: U.S. Geological Survey Open-File Report 85-459, 24 p.

- Beck, B. A., 1984, Geologic and gravity studies of the structures of the northern Bullfrog Hills, Nye County, Nevada: California State University at Long Beach, unpublished MSc Thesis, 86 p.
- Bedinger, M.S., Sargent, K.A., and Langer, W.H., 1984, Studies of geology and hydrology in the Basin and Range Province, Southwestern United States, for isolation of high-level radioactive waste; characterization of the Death Valley region, Nevada and California: U.S. Geological Survey Open-File Report 84-743, 173 p.
- Bedinger, M.S., Sargent, K.A., and Langer, W.H., 1984, Studies of geology and hydrology in the Basin and Range Province, Southwestern United States, for isolation of high-level radioactive waste; evaluation of the regions: U.S. Geological Survey Open-File Report 84-745, 195 p.
- Bell, E.J., and Larson, L.T., 1982a, Overview of energy and mineral resources of the Nevada Nuclear Waste Storage Investigations, Nevada Test Site, Nye County, Nevada: U.S. Department of Energy Report NVO-250 (DE83001418), 64 p. plus maps.
- Bell, E.J., and Larson, L.T., 1982b, Annotated bibliography, Overview of energy and mineral resources for the Nevada Nuclear Waste Storage Investigations, Nevada Test Site, Nye County, Nevada: U.S. Department of Energy Report NVO-251 (DE83001263), 30 p.
- Benson, L.V. and McKinley, P.W., 1985, Chemical composition of the ground water in the Yucca Mountain area, Nevada: U.S. Geological Survey Open-File Report 85-484, 10 p.
- Bentley, C.B., 1984, Geohydrologic data for test well USW G-4, Yucca Mountain area, Nye County, Nevada: U.S. Geological Survey Open-File Report 84-63, 67 p.
- Bish, D.L., 1987, Evaluation of past and future alteration in tuff at Yucca Mountain, Nevada based on clay mineralogy of drill cores USW G-1, G-2, and G-3: Los Alamos, New Mexico, Los Alamos National Laboratory Report LA-10667-MS, 42 p.
- Booth, M., 1988, Dallhold finalizes plans for huge Nevada mine: The Denver Business Journal, April 4, 1988, p. 10.
- Boyle, R. W., 1979, The geochemistry of gold and its deposits: Geological Survey of Canada Bulletin 280, 584 p.
- Boyle, R.W., and Jonasson, I.R., 1973, The geochemistry of arsenic and its use as an indicator element in geochemical prospecting: Journal of Geochemical Exploration, v. 2, p. 251-296.
- Broxton, D. E., Vaniman, D., Caporuscio, F., Arney, B., and Heiken, G., 1982, Detailed petrographic descriptions and microprobe data fro drill holes USW-G2 and UE25b-1H, Yucca Mountain, Nevada: Los Alamos, New Mexico, Los Alamos National Laboratory Report LA-10802-MS, 168 p.
- Broxton, D.E., Byers, F.M., Warren, R.G. and Scott, R.B., 1985, Trends in phenocryst chemistry in the Timber Mountain-Oasis Valley volcanic field, SW Nevada; evidence for isotopic injection of primitive magma into an evolving magma system: Geological Society of America, Abstracts with Programs, v. 17, p. 345.
- Broxton, D. E., Warren, R. G., and Byers, F. M., Jr., 1989, Chemical and mineralogic trends within the Timber Mountain-Oasis Valley caldera complex, Nevada: Evidence for multiple cycles of chemical evolution in a long-lived silicic magma system: Jour. Geophys. Res., v. 94, p. 5961-5985.

- Broxton, D.E., Warren, R.G., Byers, F.M., Jr., Scott, R.B., and Farner, G.L., 1986, Petrochemical trends in the Timber Mountain-Oasis Valley caldera complex, SW Nevada: EOS (American Geophysical Union Transactions), v. 67, p. 1260.
- Broxton, D.E., Warren, R.G., Hagan, R.C. and Luedemann, G., 1986, Chemistry of diagenetically altered tuffs at a potential nuclear waste repository, Yucca Mountain, Nye County, Nevada: Los Alamos, New Mexico, Los Alamos National Laboratory Report LA-10802-MS, 160 p.
- Byers, F. M., Jr., Carr, W. J., and Orkild, P. P., 1989, Volcanic centers of southwestern Nevada: evolution of understanding, 1960-1988: Jour. Geophys. Res., v.94, p. 5908-5924.
- Byers, F.M., Jr., Carr, W.J., and Orkild, P.P., 1986, Calderas of southwestern Nevada-Evolution of understanding, 1960-1986: EOS (American Geophysical Union Transactions), v. 67, p. 1260.
- Byers, F.M., Jr., Carr, W.J., Orkild, P.P., Quinlivan, W.D. and Sargent, K.A., 1976a, Volcanic Suites and related cauldrons of Timber Mountain-Oasis Valley caldera complex: U.S. Geological Survey Professional Paper 919, 70 p.
- Byers, F.M., Jr., Carr, W.J., Christiansen, R.L., Lipman, P.W., Orkild, P.P., and Quinlivan, W.D., 1976b, Geologic map of the Timber Mountain Caldera area, Nye County, Nevada: U.S. Geological Survey Miscellaneous Investigations Series, I-891, sections, 1:48,000 scale.
- Byers, F.M., Jr., Orkild, P.P., Carr, W. J., and Quinlivan, W.D., 1968, Timber Mountain Tuff, southern Nevada, and its relation to cauldron subsidence: Geological Society of America Memoir 110, p. 87-97.
- Caporuscio, F., Vaniman, D.T., Bish, D.L., Broxton, D.E., Arney, D., Heiken, G., Byers, F.M., and Gooley, R., 1982, Petrologic studies of drill cores USW-G2 and UE25b-1H, Yucca Mountain, Nevada: Los Alamos, New Mexico, Los Alamos National Laboratory Report LA-9255-MS, 114 p.
- Carr, M.D., and Mosen, S.E., 1988, A field trip guide to the geology of Bare Mountain: Geological Society of America Field Trip Guidebook, Cordilleran Section Meeting, Las Vegas, Nevada, p. 50-57.
- Carr, M.D., Waddell, S.J., Vick, G.S., Stock, J.M., and Mosen, S.A., Harris, A.G., Cork, B.W., and Byers, F.M., Jr., 1986, Geology of drill hole UE25p-1: A test hole into pre-Tertiary rocks near Yucca Mountain, southern Nevada: U.S. Geological Survey Open File Report 86-175.
- Carr, W.J., 1964, Structure of part of the Timber Mountain dome and caldera, Nye County, Nevada: U.S. Geological Survey Professional Paper 501-B, p. B16-B20.
- Carr, W.J., 1974, Summary of tectonic and structural evidence for stress orientation at the NTS: U.S. Geological Survey Open-File Report 74-176, 53 p.
- Carr, W.J., 1982, Volcano-tectonic history of Crater Flat, southwestern Nevada, as suggested by new evidence from drill hole USW-VH-1 and vicinity: U.S. Geological Survey Open-File Report 82-457, 23 p.
- Carr, W.J., 1984a, Regional structural setting of Yucca Mountain, southwestern Nevada, and late Cenozoic rates of tectonic activity in part of the southwestern Great Basin, Nevada and California: U.S. Geological Survey Open-File Report 84-0854, 114 p.
- Carr, W.J., 1984b, Timing and style of tectonism and localization of volcanism in the Walker Lane belt of southwestern Nevada: Geological Society of America, Abstracts with Programs, v. 16, p. 464.

- Carr, W.J., 1988a, Styles of extension in the Nevada Test Site region, southern Walker Lane Belt: an integration of volcano-tectonic and detachment fault models: Geological Society of America, Abstracts with Programs, v. 20, p. 148.
- Carr, W. J., 1988b, Volcano-tectonic setting of Yucca Mountain and Crater Flat, *in* Carr, M. D., and Yount, J. C., eds., Geologic and hydrologic investigations of a potential nuclear waste disposal site at Yucca Mountain, southern Nevada: U.S. Geol. Survey Bull. 1790, p. 35-49.
- Carr, W.J., and Quinlivan, W.D., 1966, Geologic map of the Timber Mountain quadrangle, Nye County, Nevada: U.S. Geological Survey Geologic Quadrangle Map GQ-503, 1:24,000 scale, sections.
- Carr, W.J., and Quinlivan, W.D., 1968, Structure of Timber Mountain resurgent dome, Nevada Test Site: Geological Society of America Memoir 110, p. 99-108.
- Carr, W.J. and Parrish, L.D., 1985, Geology of drill hole USW VH-2, and structure of Crater Flat, southwestern Nevada: U.S. Geological Survey Open-File Report 85-475, 41 p.
- Carr, W.J., Byers, F.M., and Orkild, P.P., 1984, Stratigraphic and volcano-tectonic relations of Crater Flat Tuff and some older volcanic units, Nye County, Nevada: U.S. Geological Survey Open-File Report 84-114, 97 p.
- Carr, W.J., Byers, F.M., and Orkild, P.P., 1986, Stratigraphic and volcano-tectonic relations of Crater Flat Tuff and some older volcanic units, Nye County, Nevada: U.S. Geological Survey Professional Paper 1323, 28p.
- Castor, Feldman and Tingley, 1989, Mineral evaluation of the Yucca Mountain Addition, Nye County, Nevada: Nevada Bureau of Mines and Geology, Open-file Report 90-4, 80 pp.
- Castor, Feldman and Tingley, 1990, Mineral potential report for the U.S. Department of Energy, Serial No. N-50250: Nevada Bureau of Mines and Geology, University of Nevada, Reno, 24 pp.
- Christiansen, R.L., and Lipman, P.W., 1965, Geologic map of the Topopah Spring NW quadrangle, Nye County, Nevada: U.S. Geological Survey Geologic Quadrangle Map GQ-444, 1:24,000 scale, sections.
- Christiansen, R.L., Lipman, P.W., Carr, W.J., Byers, F.M., Jr., Orkild, P.P., and Sargent, K.A., 1977: Timber Mountain-Oasis Valley caldera complex of southern Nevada: Geological Society of America Bulletin, v. 88, p. 943-959.
- Christiansen, R.L., Lipman, P.W., Orkild, P.P., and Byers, F.M., Jr., 1965, Structure of the Timber Mountain caldera, southern Nevada, and its relation to basin-range structure: U.S. Geological Survey Professional Paper 525-B, p. B43-B48.
- Connors, K. A., Studies in silicic volcanic geology: Part I: Compositional controls on the initial gold contents of silicic volcanic rocks; Part II: Geology of the western margin of the Timber Mountain caldera complex and post-Timber Mountain volcanism in the Bullfrog Hills: unpublished PhD dissertation, University of Nevada, Reno, (in preparation).
- Connors, K.A., Weiss, S.I., Noble, D.C., and Bussey, S.D., 1990, Primary gold contents of some silicic and intermediate tuffs and lavas: evaluation of possible igneous sources of gold: Geological Society of America Abst. with Programs, v. 22, p. A135.
- Connors, K.A., Noble, D.C., Weiss, S.I., and Bussey, S.D., 1991a, Compositional controls on the gold contents of silicic volcanic rocks: 15th International Geochemical Exploration Symposium Program with Abstracts, p. 43.

- Connors, K. A., McKee, E. H., Noble, D. C., and Weiss, S. I., 1991, Ash-flow volcanism of Ammonia Tanks age in the Oasis Valley area, SW Nevada: Bearing on the evolution of the Timber Mountain calderas and the timing of formation of the Timber Mountain II resurgent dome: EOS, Trans. Am. Geophys. Union., v. 72, p. 570.
- Cornwall, H.R., 1962, Calderas and associated volcanic rocks near Beatty, Nye County, Nevada: Geological Society of America, Petrologic Studies, A.F. Buddington Volume, p. 357-371.
- Cornwall, H.R., 1972, Geology and mineral deposits of southern Nye County, Nevada: Nevada Bureau of Mines and Geology Bulletin 77, p. 49.
- Cornwall, H.R., and Kleinhampl, F.J., 1961, Geology of the Bare Mountain quadrangle, Nevada: U.S. Geological Survey Geologic Quadrangle Map GQ-157, 1:62,500 scale.
- Cornwall, H.R., and Kleinhampl, F.J., 1964, Geology of the Bullfrog quadrangle and ore deposits related to the Bullfrog Hills caldera, Nye County, Nevada, and Inyo County, California: U.S. Geological Survey Professional Paper 454-J, 25 p.
- Cornwall, H.R., and Norberg, J.R., 1978, Mineral Resources of the Nellis Air Force Base and the Nellis Bombing and Gunnery Range, Clark, Lincoln, and Nye Counties, Nevada: U.S. Bureau of Mines Unpublished Administrative Report, 118 p.
- Craig, R.W. and Robinson, J.H., 1984, Geohydrology of rocks penetrated by test well UE-25p#1, Yucca Mountain area, Nye County, Nevada, U.S. Geological Survey Water-Resources Investigations 84-4248, 57 p.
- Craig, R.W., Reed, R.L., and Spengler, R.W., 1983, Geohydrologic data for test well USW H-6, Yucca Mountain area, Nye County, Nevada: U.S. Geological Survey Open-File Report 83-856, 52 p.
- Crowe, B.M., 1980, Disruptive event analysis: Volcanism and igneous intrusion: Batelle Pacific Northwest Laboratory Report PNL-2822, 28 p.
- Crowe, B.M., and Carr, W.J., 1980, Preliminary assessment of the risk of volcanism at a proposed nuclear waste repository in the southern Great Basin: U.S. Geological Survey Open-File Report 80-357, 15 p.
- Crowe, B.M., Johnson, M.E., and Beckman, R.J., 1982, Calculation of probability of volcanic disruption of a high-level radioactive waste repository within southern Nevada, USA: Radioactive Waste Management and the Nuclear Fuel Cycle, v. 3, p. 167-190.
- Crowe, B.M., Vaniman, D.J., and Carr, W.J., 1983b, status of volcanic hazard studies for the Nevada nuclear waste storage investigations: Los Alamos, New Mexico, Los Alamos National Laboratory Report LA-9325-MS.
- Deino, A.L., Hausback, B.P., Turrin, B.T., and McKee, E.H., 1989, New $^{40}\text{Ar}/^{39}\text{Ar}$ ages for the Spearhead and Civet Cat Canyon Members of the of Stonewall Flat Tuff, Nye County, Nevada: EOS, Trans. American Geophysical Union, v. 70, p. 1409.
- Eckel, E.B., ed., 1968, Nevada Test Site: Geological Society of America Memoir 110, 290 p.
- Ekren, E.B., and Sargent, K.A., 1965, Geologic map of Skull Mountain quadrangle at the Nevada Test Site, Nye County, Nevada: U.S. Geological Survey Geologic Quadrangle Map GQ-387.
- Ekren, E.B., Anderson, R.E., Rodgers, C.L., and Noble, D.C., 1971, Geology of northern Nellis Air Force Base Bombing and Gunnery Range, Nye County, Nevada: U.S. Geological Survey Professional Paper 651, 91 p.
- Feitler, S., 1940, Welded tuff resembling vitrophyre and pitchstone at Bare Mountain, Nevada: Geological Society of America Bulletin, v. 51, p. 1957.

- Flood, T.P., and Schuraytz, B.C., 1986, Evolution of a magmatic system. Part II: Geochemistry and mineralogy of glassy pumices from the Pah Canyon, Yucca Mountain, and Tiva Canyon Members of the Paintbrush Tuff, southern Nevada: EOS Trans. American Geophysical Union, v. 67, p. 1261.
- Foley, D., 1978, The geology of the Stonewall Mountain volcanic center, Nye County, Nevada: Ohio State University, Columbus Ohio, unpublished PhD Dissertation, 139 p.
- Fouty, S.C., 1984, Index to published geologic maps in the region around the potential Yucca Mountain Nuclear Waste Repository site, southern Nye County, Nevada: U.S. Geological Survey Open-File Report 84-524, 31 p.
- Frischknecht, F.C. and Raab, P.V., 1984, Time-domain electromagnetic soundings at the Nevada Test Site, Nevada, Geophysics, v. 49, p. 981-992.
- Frizzell, Virgil, and Shulters, Jacqueline, 1986, Geologic map of the Nevada Test Site: EOS Trans. American Geophysical Union, v. 67, p. 1260.
- Frizzell, Virgil, and Shulters, Jacqueline, 1990, Geologic map of the Nevada Test Site: U.S. Geological Survey Misc. Invest. Map I-2046, 1:100,000.
- Gans, P. B., Mahood, G. A., and Schermer, E., 1989, Synextensional magmatism in the Basin and Range province; A case study from the eastern Great Basin: Geological Society of America Spec. Paper 233, 53 p.
- Garside L.J. and Schilling, J.H., 1979, Thermal waters of Nevada: Nevada Bureau of Mines and Geology, Bulletin 91, 163 p.
- Geehan, R.W., 1946, Exploration of the Crowell fluorspar mine, Nye County, Nevada: U.S. Bureau of Mines Report of Investigations 3954, 9 p.
- Greybeck, J. D., and Wallace, A. B., 1991, Gold mineralization at Fluorspar Canyon near Beatty, Nye County, Nevada, *in* Shafer, R. W., Wilkinson, W. H., and Raines, G., eds., Geology and ore deposits of the Great Basin: Geol. Soc. of Nevada, Symposium Proceedings Volume.
- Hagstrum, J.T., Daniels, J.J., and Scott, J.H., 1980, Interpretation of geophysical well-log measurements in drill hole UE 25a-1, NTS, Radioactive Waste Program: U.S. Geological Survey Open-File Report 80-941, 32 p.
- Hall, R.B., 1978, World nonbauxite aluminum resources--Alunite: U.S. Geological Survey Professional Paper 1076-A, 35 p.
- Hamilton, W. B., 1988, Detachment faulting in the Death Valley region, California and Nevada, *in* Carr, M. D., and Yount, J. C., eds., Geologic and hydrologic investigations of a potential nuclear waste disposal site at Yucca Mountain, southern Nevada: U.S. Geol. Survey Bull. 1790, p. 51-86.
- Hausback, B. P., and Frizzell, V. A. Jr., 1987, Late Miocene syntectonic volcanism of the Stonewall Flat Tuff, Nye County, Nevada [abs.]: Geological Society of America Abst. with Programs, v. 19, p. 696.
- Hausback, B.P., Deino, A.L., Turrin, B.T., McKee, E.H., Frizzell, V.A., Noble, D.C., and Weiss, S.I., 1990, New $^{40}\text{Ar}/^{39}\text{Ar}$ ages for the Spearhead and Civet Cat Canyon Members of the Stonewall Flat Tuff, Nye County, Nevada: Evidence for systematic errors in standard K-Ar age determinations on sanidine: Isochron/West, No. 56, p. 3-7.
- Harris, R.N., and Oliver, H.W., 1986, Structural implications of an isostatic residual gravity map of the Nevada Test Site, Nevada: EOS (American Geophysical Union Transactions), v. 67, p. 1262.

- Heald, P., Foley, N.K., and Hayba, D.O., 1987, Comparative anatomy of volcanic-hosted epithermal deposits: acid-sulfate and adularia-sericite types: *Economic Geology*, v. 82, no. 1, p. 1-26.
- Heikes, V.C., 1931, Gold, silver, copper, lead and zinc in Nevada--Mine report, in *Mineral Resources of the U.S., 1928*: U.S. Department of commerce, Bureau of Mines, pt. 1, p. 441-478.
- Hill, J.M., 1912, The mining districts of the western U.S.: U.S. Geological Survey Bulletin 507, 309 p.
- Holmes, G.H., Jr., 1965, Mercury in Nevada, in *Mercury potential of the United States*: U.S. Bureau of Mines I.C., 8252, p. 215-300.
- Hoover, D.L., Eckel, E.B., and Ohl, J.P., 1978, Potential sites for a spent unprocessed fuel facility (SUREF), southwest part of the NTS: U.S. Geological Survey Open-File Report 78-269, 18 p.
- Hoover, D. B., Chornack, M. P., Nervick, K. H., and Broker, M. M., 1982, Electrical studies at the proposed Wahmonie and Calico Hills Nuclear Waste Sites, Nye County, Nevada: U.S. Geol. Survey Open-File Rept. 82-466, 45 p.
- Jackson, M. J., 1988, The Timber Mountain magmato-thermal event: an intense widespread culmination of magmatic and hydrothermal activity at the southwestern Nevada volcanic field: University of Nevada, Reno - Mackay School of Mines, Reno, Nevada, unpublished MSc Thesis.
- Jackson, M.R., Noble, D.C., Weiss, S.I., Larson, L.T., and McKee, E.H., 1988, Timber Mountain magmato-thermal event: an intense widespread culmination of magmatic and hydrothermal activity at the SW Nevada volcanic field, *Geol. Soc. Am. Abstr. Programs*, v. 20, p. 171.
- Jorgensen, D. K., Rankin, J. W., and Wilkins, J., Jr., 1989, The geology, alteration and mineralogy of the Bullfrog gold deposit, Nye County, Nevada: *Soc. Mining Eng. Preprint* 89-135, 13 p.
- Kane, M.F., and Bracken, R.E., 1983, Aeromagnetic map of Yucca Mountain and surrounding regions, southwest Nevada: U.S. Geological Survey Open-File Report 83-616, 19 p.
- Kane, M.F., Webring, M.W., and Bhattacharyya, B.K., 1981, A preliminary analysis of gravity and aeromagnetic surveys of the Timber Mountain areas, southern Nevada: U.S. Geological Survey Open-File Report 81-189, 40 p.
- Kistler, R.W., 1968, Potassium-argon ages of volcanic rocks on Nye and Esmeralda Counties, Nevada: *Geological Society of America Memoir* 110, P. 251-263.
- Knopf, A., 1915, Some cinnabar deposits in western Nevada: U.S. Geological Survey Bulletin 620-D, p. 59-68.
- Kral, V.E., 1951, Mineral resources of Nye County, Nevada: *University of Nevada Bulletin*, v. 45, no. 3, *Geological and Mining Series* 50, 223 p..
- Lahoud, R.G., Lobmeyer, D.H. and Whitfield, M.S., 1984, Geohydrology of volcanic tuff penetrated by test well UE-25b#1, Yucca Mountain, Nye County, Nevada: U.S. Geological Survey Water-Resources Investigations 84-4253, 49 p.
- Larson, L. T., Noble, D. C., and Weiss, S. I., 1988, Task 3 report for January, 1987 - June, 1988: Volcanic geology and evaluation of potential mineral and hydrocarbon resources of the Yucca Mountain area: unpublished report to the Nevada Nuclear Waste Project Office, Carson City, Nevada.

- Lincoln, F.C., 1923, Mining districts and mineral resources of Nevada: Reno, Nevada, Nevada Newsletter Publishing Co., Reno, 295 p.
- Lipman, P.W., Christiansen, R.L., and O'Connor, J.T., 1966, A compositionally zoned ash-flow sheet in southern Nevada: U.S. Geological Survey Professional Paper 524-F, p. F1-F47.
- Lipman, P.W., and McKay, E.J., 1965, Geologic map of the Topopah Spring SW quadrangle, Nevada: U.S. Geological Survey Geologic Quadrangle Map GQ-439, 1:24,000 scale.
- Lipman, P.W., Quinlivan, W.D., Carr, W.J., and Anderson, R.E., 1966, Geologic map of the Thirsty Canyon SE quadrangle, Nye County, Nevada: U.S. Geological Survey Geologic Quadrangle Map GQ-489, 1:24,000 scale.
- Lobmeyer, D.H., Whitfield, M.S., Lahoud, R.G., and Bruckheimer, L., 1983, Geohydrologic data for test well UE-25bH, Nevada Test Site, Nye County, Nevada: U.S. Geological Survey Open-File Report 83-855, 54 p.
- Luedke, R.G., and Smith, R.L., 1981, Map showing distribution, composition, and age of late Cenozoic volcanic centers in California and Nevada: U.S. Geological Survey Miscellaneous Investigation Series, I-1091-C, 2 sheets.
- Maldonado, F., 1985, Late Tertiary detachment faults in the Bullfrog Hills, southwestern Nevada: *Geol. Soc. Am. Abstr. Programs*, 17, p. 651.
- Maldonado, F., 1988, Geometry of normal faults in the upper plate of a detachment fault zone, Bullfrog Hills, southern Nevada: *Geological Society of America, Abstracts with Programs*, v. 20, P. 178.
- Maldonado, F., 1990, Structural geology of the upper plate of the Bullfrog Hills detachment fault system, southern Nevada: *Geological Society of America Bulletin*, v. 102, p. 992-1006.
- Maldonado, F. and Hausback, B.P., 1990, Geologic map of the northeastern quarter of the Bullfrog 15-minute quadrangle, Nye County, Nevada: U.S. Geological Survey Misc. Investigations Series Map I-2049, 1:24,000.
- Maldonado, F. and Koether, S.L., 1983, Stratigraphy, structure, and some petrographic features of Tertiary volcanic rocks at the USW G-2 drill hole, Yucca Mountain, Nye County, Nevada: U.S. Geological Survey Open-File Report 83-732, 83 p.
- Maldonado, F., Muller, D.C., and Morrison, J.N., 1979, Preliminary geologic and geophysical data of the UE25a-3 exploratory drill hole, Nevada Test Site, Nevada: U.S. Geological Survey Report, USGS-1543-6, 47 p.; available only from U.S. Department of Commerce, National Technical Information Service, Springfield, VA 22161.
- Maldonado, Florian, Muller, D.C., and Morrison, J.N., 1979, Preliminary geologic and geophysical data of the UE25a-3 exploratory drill hole, Nevada Test Site, Nevada: U.S. Geological Survey Open-File Report 81-522.
- Mapa, M.R., 1990 Geology and mineralization of the Mother Lode mine, Nye County, Nevada, in Hillmeyer, F., Wolverson, N., and Drobeck, P., 1990 spring fieldtrip guidebook, Volcanic-hosted gold deposits and structural setting of the Mohave region: Reno, Geol. Soc. Nevada, 4 p.
- Marvin, R.F., Byers, F.M., Mehnert, H.H., Orkild, P.P., and Stern, T.W., 1970, Radiometric ages and stratigraphic sequence of volcanic and plutonic rocks, southern Nye and western Lincoln Counties, Nevada: *Geological Society of America, Bulletin*, v. 81, p. 2657-2676.

- Marvin, R. F., and Cole, J. C., 1978, Radiometric ages: Compilation A, U.S. Geological Survey: Isochron/West, no. 22, p. 3-14.
- Marvin, R. F., Mehnert, H. H., and Naeser, C. W., 1989, U.S. Geologic Survey radiometric ages - compilation "C", part 3: California and Nevada: Isochron/West, no. 52, p. 3-11.
- McKague, H.L. and Orkild, P.P., 1984, Geologic Framework of the Nevada Test Site: Geological Society of America, Abstracts with Programs, v. 16, p. 589.
- McKay, E.J., 1963, Hydrothermal alteration in the Calico Hills, Jackass Flats quadrangle, Nevada Test Site: U.S. Geological Survey Technical Letter NTS-43, 6 p.
- McKay, E.J., and Sargent, K.A., 1970, Geologic map of the Lathrop Wells quadrangle, Nye County, Nevada: U.S. Geological Survey Geologic Quadrangle Map GQ-883, 1:24,000 scale.
- McKay, E.J., and Williams, W.P., 1964, Geology of Jackass Flats quadrangle, Nevada Test Site, Nevada: U.S. Geological Survey Geologic Quadrangle Map GQ-368, 1:24,000 scale.
- McKee, E.H., 1983, Reset K-Ar ages: evidence for three metamorphic core complexes, western Nevada: Isochron/West, no.38, p 17-20.
- McKee, E. H., Noble, D. C., and Weiss, S. I., 1989, Very young silicic volcanism in the southwestern Great Basin: The late Pliocene Mount Jackson dome field, SE Esmeralda County, Nevada: EOS, Trans. Am. Geophys. Union., v. 70, p. 1420.
- McKee, E. H., Noble, D. C., and Weiss, S. I., 1990, Late Neogene volcanism and tectonism in the Goldfield segment of the Walker Lane belt: Geological Society of America Abstracts with Programs, v. 22, p. 66.
- Miller, D.C. and Kibler, J.E., 1984, Preliminary analysis of geological logs from drill hole UE-25p#1, Yucca Mountain, Nye County, Nevada: U.S. Geological Survey Open-File Report 84-649, 17 p.
- Mills, J.G., Jr., and Rose, T.P., 1986, Geochemistry of glassy pumices from the Timber Mountain Tuff, southwestern Nevada: EOS (American Geophysical Union Transactions), v. 67, p. 1262.
- Monsen, S.A., Carr, M.D., Reheis, M.C., and Orkild, P.P., Geologic map of Bare Mountain, Nye County Nevada: U.S. Geological Survey Open-file Report 90-25, 1:24,000.
- Morton, J. L., Silberman, M. L., Bonham, H. F., Garside, L. J., and Noble, D. C., 1977, K-Ar ages of volcanic rocks, plutonic rocks, and ore deposits in Nevada and eastern California - Determinations run under the USGS-NBMG cooperative program: Isochron/West, n. 20, p. 19-29.
- Noble, D. C., and Christiansen, R. L., 1974, Black Mountain volcanic center, in Guidebook to the geology of four Tertiary volcanic centers in central Nevada: Nevada Bur. Mines Geol. Rept. 19, p. 22-26.
- Noble, D.C., McKee, E.H., and Weiss, S.I., 1988, Nature and timing of pyroclastic and hydrothermal activity and mineralization at the Stonewall Mountain volcanic center, southwestern Nevada: Isochron/West, in press.
- Noble, D. C., Weiss, S. I., and Green, S. M., 1989, High-salinity fluid inclusions suggest that Miocene gold deposits of the Bare Mtn. district, NV, are related to a large buried rare-metal rich magmatic system: Geological Society of America Abs. with Programs, v. 21, p. 123.

- Noble, D. C., Weiss, S. I., and McKee, E. H., 1990a, Style, timing, distribution, and direction of Neogene extension within and adjacent to the Goldfield section of the Walker Lane structural belt: EOS, Trans. American Geophysical Union, v. 71, p. 618-619.
- Noble, D. C., Weiss, S. I., and McKee, E. H., 1990b, Magmatic and hydrothermal activity, caldera geology and regional extension in the western part of the southwestern Nevada volcanic field: Great Basin Symposium, Program with Abstracts, Geology and ore deposits of the Great Basin, Geol. Soc. of Nevada, Reno, p. 77.
- Noble, D. C., Weiss, S. I., and McKee, E. H., 1991a, Caldera geology, magmatic and hydrothermal activity and regional extension in the western part of the southwestern Nevada volcanic field: *in* Raines, G. L., Lisle, R. E., Shafer, R. W., and Wilkinson, W. W., eds., Geology and ore deposits of the Great Basin: Symposium Proceedings, Geol. Soc. of Nevada, p. 913-934.
- Noble, D. C., Worthington, J. E., and McKee, E. H., 1991b, Geologic and tectonic setting and Miocene volcanic stratigraphy of the Gold Mountain-Slate Ridge area, southwestern Nevada: Geol. Soc. America Abstr. with Prog., v. 23, p. A247.
- Noble, D. C., Sargent, K. A., Ekren, E. B., Mehnert, H. H., and Byers, F. M., Jr., 1968, Silent Canyon volcanic center, Nye County, Nevada: Geological Society of America Spec. Paper 101, p. 412-413.
- Noble, D.C., Vogel, T. A., Weiss, S.I., Erwin, J.W., McKee, E.H., and Younker, L.W., 1984, Stratigraphic relations and source areas of ash-flow sheets of the Black Mountain and Stonewall Mountain volcanic centers, Nevada: Journal of Geophysical Research, v. 89, p. 8593-8602.
- Norberg, J.R., 1977, Mineral Resources in the vicinity of the Nellis Air Force Base and the Nellis Bombing and Gunnery Range, Clark, Lincoln, and Nye Counties, Nevada: U.S. Bureau of Mines Unpublished Report, 112 p.
- Orkild, P.P., 1968, Geologic map of the Mine Mountain quadrangle, Nye County, Nevada: U.S. Geological Survey Geologic Quadrangle Map GQ-746, 1:24,000 scale.
- Orkild, P.P., and O'Connor, J.T., 1970, Geologic map of the Topopah Springs quadrangle, Nye County, Nevada: U.S. Geological Geologic Quadrangle Map GQ-849, 1:24,000 scale.
- Odt, D. A., 1983, Geology and geochemistry of the Sterling gold deposit, Nye County, Nevada: Unpub. M.S. thesis, Univ. Nevada-Reno, 91 p.
- Papike, J. J., Keith, T. E. C., Spilde, M. N., Galbreath, K. C., Shearer, C. K., and Laul, J. C., 1991, Geochemistry and mineralogy of fumarolic deposits, Valley of Ten Thousand Smokes, Alaska: bulk chemical and mineralogical evolution of dacite-rich protolith: American Mineralogist, v. 76, p. 1662-1673.
- Papke, K.G., 1979, Fluorspar in Nevada: Nevada Bureau of Mines and Geology, Bulletin 93, 77 p.
- Ponce, D.A., 1981, Preliminary gravity investigations of the Wahmonie site, Nevada Test Site, Nye County, Nevada: U.S. Geological Survey Open-File Report 81-522, 64 p.
- Ponce, D.A., 1984, Gravity and magnetic evidence for a granitic intrusion near Wahmonie site, Nevada Test Site, Nevada, JGR, Journal of Geophysical Research, B, v. 89, p. 9401-9413.
- Ponce, D.A., Wu, S.S. and Speilman, J.B., 1985, Comparison of survey and photogrammetry methods to positive gravity data, Yucca Mountain, Nevada: U.S. Geological Survey Open-File Report 85-36, 11 p.

- Poole, F.G., 1965, Geologic map of the Frenchman Flat quadrangle, Nye, Lincoln, and Clark Counties, Nevada: U.S. Geological Survey Geological Quadrangle Map GQ-456, 1:24,000 scale.
- Poole, F.G., Carr, W.J., and Elston, D.P., 1965, Salyer and Wahmonie Formations of southeastern Nye County, Nevada: U.S. Geological Survey Bulletin 1224-A, p. A44-A51.
- Poole, F.G., Elston, D.P., and Carr, W.J., 1965, Geologic map of the Cane Spring quadrangle, Nye County, Nevada: U.S. Geological Survey Geological Quadrangle Map GQ-455, 1:24,000 scale.
- Powers, P.S. and Healey, D.L., 1985, Free-air gradient observations in Yucca Flat, Nye County, Nevada: U.S. Geological Survey Open-File Report 85-530, 18 p.
- Quade, J., and Tingley, J.V., 1983, A mineral inventory of the Nevada Test Site and portions of the Nellis Bombing and Gunnery Range, southern Nye County, Nevada: DOE/NV/10295-1, U.S. Department of Energy, Las Vegas.
- Quade, J., and Tingley, J.V., 1984, A mineral inventory of the Nevada Test Site, and portions of Nellis Bombing and Gunnery Range southern Nye County, Nevada: Nevada Bureau of Mines and Geology Open File Report 82-2, 40 p. plus sample descriptions and chemical analyses.
- Quade, J., and Tingley, J.V., 1986a, Mineral inventory and geochemical survey Groom Mountain Range Lincoln County, Nevada: Nevada Bureau of Mines and Geology Open File Report 86-9, 66 p. plus sample descriptions and chemical analyses.
- Quade, J., and Tingley, J.V., 1986b, Mineral inventory and geochemical survey appendices F., G., & H Groom Mountain Range, Lincoln County, Nevada: Nevada Bureau of Mines and Geology Open File Report 86-10.
- Quinlivan, W.D., and Byers, F.M., Jr., 1977, Chemical data and variation diagrams of igneous rock from the Timber Mountain-Oasis Valley caldera complex, southern Nevada: U.S. Geological Survey Open-File Report 77-724, 9 p.
- Ramelli, A. R., Bell, J. W., and dePolo, C. M., Late Quaternary faulting at Crater Flat and Yucca Mountain, southern Nevada: Nevada Bureau of Mines and Geology (in review).
- Raney, R. G., and Wetzel, N., Natural resource assessment methodologies for the proposed high-level nuclear waste repository at Yucca Mountain, Nye County, Nevada: U.S. Bureau of Mines report NRC FIN D1018, prepared for the Office of Nuclear Safety and Safeguards, U.S. Nuclear Regulatory Commission, 353 p.
- Ransome, F.L., 1907, Preliminary account of Goldfield, Bullfrog, and other mining districts in southern Nevada: U.S. Geological Survey Bulletin 303, 98 p.
- Ransome, F.L., Emmons, W.H., and Garrey, G.H., 1910, Geology and ore deposits of the Bullfrog district, Nevada: U.S. Geological Survey Bulletin 407, 130 p.
- Reno Gazette-Journal, June 19, 1988, Gold report is favorable: Business page, Gold, J., Business editor.
- Robinson, G.D., 1985, Structure of pre-Cenozoic rocks in the vicinity of Yucca Mountain, Nye County, Nevada; a potential nuclear-waste disposal site: U.S. Geological Survey Bulletin 1647, 22 p.
- Rowe, J. J., and Simon, F. O., 1968, The determination of gold in geologic materials by neutron-activation analysis using fire assay for the radiochemical separations: U. S. Geological Survey Circular 559, 4 p.

- Rush, F.E., Thordason, William, and Bruckheimer, Laura, 1983, Geohydrologic and drill-hole data for test well USW-H1, adjacent to Nevada Test Site, Nye County, Nevada: U.S. Geological Survey Open-File Report 83-141, 38 p.
- Sawyer, D. A., and Sargent, K. A., 1989, Petrologic evolution of divergent peralkaline magmas from the Silent Canyon caldera complex, southwestern Nevada volcanic field: *Jour. Geophys. Res.*, v. 94, p. 6021-6040.
- Sawyer, D. A., Fleck, R. J., Lanphere, M. A., Warren, R. G., and Broxton, D. E., 1990, Episodic volcanism in the southwest Nevada volcanic field: new $^{40}\text{Ar}/^{39}\text{Ar}$ geochronologic results: EOS, *Transactions of the American Geophysical Union*, v. 71, p. 1296.
- Schoen, R., White, D.E., and Hemley, J.J., 1974, Argillization by decending acid at Steamboat Springs, Nevada: *Clays and Clay Minerals*, v. 22, p. 1-22.
- Schneider, R. and Trask, N.J., 1984, U.S. Geological Survey research in radioactive waste disposal; fiscal year 1982: U.S. Geological Survey Water-Resource Investigation 84-4205, 116 p.
- Schuraytz, B.C., Vogel, T.A., and Younker, L.W., 1986, Evolution of a magmatic system. Part I: Geochemistry and mineralogy of the Topopah Spring Member of the Paintbrush Tuff, southern Nevada: EOS, *Transactions of the American Geophysical Union*, v. 67, p. 1261.
- Scott, R.B., 1984, Internal deformation of blocks bounded by basin-and-range-style faults: *Geological Society of America, Abstracts with Programs*, v. 16, p. 649.
- Scott, R.B., 1986a, Rare-earth element evidence for changes in chemical evolution of silicic magmas, southwest Nevada: *Transactions of the American Geophysical Union*, v. 67, p. 1261.
- Scott, R. B., 1986b, Extensional tectonics at Yucca Mountain, southern Nevada [abs.]: *Geological Society of America Abs. with Programs*, v. 18, p. 411.
- Scott, R.B., 1988, Tectonic setting of Yucca Mountain, southwest Nevada: *Geological Society of America, Abstracts with Programs*, v. 20, p. 229.
- Scott, R.B. and Bonk, J., 1984, Preliminary geologic map of Yucca Mountain, Nye County, Nevada, with geologic sections: U.S. Geological Survey Open-File Report 84-494, scale 1:12,000, plus 10 p.
- Scott, R.B. and Castellanos, Mayra, 1984, Stratigraphic and structural relations of volcanic rocks in drill holes USW GU-3 and USW G3, Yucca Mountain, Nye County, Nevada: U.S. Geological Survey Open-File Report 84-491, 121 p.
- Scott, R. B., and Whitney, J. W., 1987, The upper crustal detachment system at Yucca Mountain, SW Nevada [abs.]: *Geological Society of America Abs. with Programs*, v. 19, p. 332-333.
- Scott, R.B., Byers, F.M. and Warren, R.G., 1984, Evolution of magma below clustered calderas, Southwest Nevada volcanic field [abstr.], EOS, *Transactions of the American Geophysical Union*, v.65, p. 1126-1127.
- Scott, R.B., Spengler, R.W., Lappin, A.R., and Chornack, M.P., 1982, Structure and intra-cooling unit zonation in welded tuffs of the unsaturated zone, Yucca Mountain, Nevada, a potential nuclear waste repository: EOS, *Transactions of the American Geophysical Union*, v. 63, no. 18, p. 330.

- Scott, R.B., Spengler, R.W., Diehl, S., Lappin, A.R., and Chornack, M.P., 1983, Geologic character of tuffs in the unsaturated zone at Yucca Mountain, southern Nevada: in Mercer, J.M., Rao, P.C. and Marine, W., eds., Role of the unsaturated zone in radioactive and hazardous waste disposal: Ann Arbor press, Ann Arbor, Michigan, p. 289-335.
- Scott, R.B., Bath, G.D., Flanigan, V.J., Hoover, D.B., Rosenbaum, J.G., and Spengler, R.W., 1984, Geological and geophysical evidence of structures in northwest-trending washes, Yucca Mountain, southern Nevada, and their possible significance to a nuclear waste repository in the unsaturated zone: U.S. Geological Survey Open-File Report 84-567, 25 p.
- Selner, G.I. and Taylor, R.B., 1988, GSDRAW and GSMAP version 5.0: prototype programs, level 5, for the IBM PC and compatible microcomputers, to assist compilation and publication of geologic maps and illustrations: U.S. Geological Survey Open File Report #88-295A (documentation), 130 p. and #88-295B (executable program disks).
- Selner, G.I., Smith, C.L., and Taylor, R.B., 1988, GSDIG: a program to determine latitude/longitude locations using a microcomputer (IBM PC or compatible) and digitizer: U.S. Geological Survey Open File Report #88-014A (documentation) 16 p. and #88-014B (executable program disk).
- Smith, C., Ross, H.P., and Edquist, R., 1981, Interpreted resistivity and IP section line W1 Wahmonie area, Nevada Test Site, Nevada: U.S. Geological Survey Open-File Report 81-1350, 14 p.
- Smith, R.C., and Bailey, R.A., 1968, Resurgent Cauldrons: Geological Society of America Memoir 116, p. 613-662.
- Smith, R.M., 1977, Map showing mineral exploration potential in the Death Valley quadrangle, California and Nevada: U.S. Geological Survey Miscellaneous Field Investigation Map MF-873, 1:250,000 scale.
- Snyder, D.B., and Oliver, H.W., 1981, Preliminary results of gravity investigations of the Calico Hills, Nevada Test Site, Nye County, Nevada: U.S. Geological Survey Open-File Report 81-101, 42 p.
- Snyder, D.B., and Carr, W.J., 1982, Preliminary results of gravity investigations at Yucca Mountain and vicinity, southern Nye County, Nevada: U.S. Geological Survey Open-File Report 82-701, 36 p.
- Snyder, D.B. and Carr, W.J., 1984, Interpretation of gravity data in a complex volcano-tectonic setting, southwestern Nevada: Journal of Geophysical Research. B, v. 89, p. 10,193-10,206.
- Spengler, R.W., Byers, F.M., Jr., and Warner, J.B., 1981, Stratigraphy and structure of volcanic rocks in drill hole USW-G1, Yucca Mountain, Nye County, Nevada: U.S. Geological Survey Open-File Report 82-1338, 264 p.
- Spengler, R.W. and Chornack, M.P., 1984, Stratigraphic and structural characteristics of volcanic rocks in core hole USW G-4, Yucca Mountain, Nye County, Nevada: U.S. Geological Survey Open-File Report 84-789, 82 p.
- Spengler, R.W., Muller, D.C., and Livermore, R.B., 1979, Preliminary report on the geology of drill hole UE25a-1, Yucca Mountain, Nevada Test Site: U.S. Geological Survey Open-File Report 79-1244, 43 p.
- Spengler, R.W., and Rosenblum, J.G., 1980, Preliminary interpretations of geologic results obtained from boreholes UE25a-4, -5, -6, and -7, Yucca Mountain, Nevada Test Site: U.S. Geological Survey Open-File Report 80-929, 35 p.

- Stewart, J. H., 1988, Tectonics of the Walker Lane belt, western Great Basin-Mesozoic and Cenozoic deformation in a zone of shear, *in* Ernst, W. G., ed., *Metamorphism and crustal evolution of the western United States*, Rubey Vol. VII: Englewood Cliffs, New Jersey, Prentice Hall, p. 683-713.
- Stuckless, J. S., Peterman, Z. E. and Muhs, D. R., 1991, U and Sr isotopes in groundwater and calcite, Yucca Mountain, Nevada: evidence against upwelling water: *Science*, v. 254, p. 551-554.
- Sutton, V.D., 1984, Data report for the 1983 seismic-refraction experiment at Yucca Mountain, Beatty, and vicinity, southwestern Nevada: U.S. Geological Survey Open-File Report 84-661, 62 p.
- Swadley, W.C., Hoover, D.L. and Rosholt, J.N., 1984, Preliminary report on late Cenozoic faulting and stratigraphy in the vicinity of Yucca Mountain, Nye County, Nevada: U.S. Geological Survey Open-File Report 84-788, 44 p.
- Swolfs, H.S. and Savage, W.Z., 1985, Topography, stresses and stability at Yucca Mountain, Nevada, *Proceedings - Symposium on Rock Mechanics: Research and engineering applications in rock masses*, 26, p. 1121-1129.
- Szabo, B.J. and Kyser, T.K., 1985, Uranium, thorium isotopic analyses and uranium-series ages of calcite and opal, and stable isotopic compositions of calcite from drill cores UE25a 1, USW G-2 and USW G-3/GU-3, Yucca Mountain, Nevada: U.S. Geological Survey Open-File 85-224, 30 p.
- Szabo, B. J., and Kyser, T. K., 1990, Ages and stable-isotope compositions of secondary calcite and opal in drill cores from Tertiary volcanic rocks of the Yucca Mountain area, Nevada: v. 102, p. 1714-1719.
- Szabo, B.J. and O'Malley, P.A., 1985, Uranium-series dating of secondary carbonate and silica precipitates relating to fault movements in the Nevada Test Site region and of caliche and travertine samples from the Amargosa Desert: U.S. Geological Survey Open-File Report 85-0047, 17 p.
- Taylor, E.M., and Huckins, H.E., 1986, Carbonate and opaline silica fault-filling in the Bow Ridge Fault, Yucca Mountain, Nevada -- deposition from pedogenic processes of upwelling ground water: *Geological Society of America, Abstracts with Programs*, v. 18, no. 5, p. 418.
- Thordarson, William, Rush, F.E. , Spengler, R.W. and Waddell, S.J., 1984, Geohydrologic and drill-hole data for test well USW H-3, Yucca Mountain, Nye County, Nevada: U.S. Geological Survey Open-File Report 84-0149, 54 p.
- Tingley, J.V., 1984, Trace element associations in mineral deposits, Bare Mountain (Fluorine) mining district, southern Nye County, Nevada: *Nevada Bureau of Mines and Geology Report* 39, 28 p.
- Turrin, B. D., Champion, D., and Fleck, R. J., 1991, $^{40}\text{Ar}/^{39}\text{Ar}$ age of the Lathrop Wells volcanic center, Yucca Mountain Nevada: *Science*, v. 253, p. 654-657.
- U.S. Department of Energy, 1986, *Environmental Assessment Yucca Mountain Site, Nevada Research and Development Area, Nevada*, v. 1: Washington, DC, Office of Civilian Radioactive Waste Management.
- U.S. Department of Energy, 1988a, *Consultation Draft Site Characterization Plan, Yucca Mountain Site, Nevada Research and Development Area, Nevada*: Washington, DC, Office of Civilian Radioactive Waste Management, 347 p.

- U.S. Department of Energy, 1988b, Site Characterization Plan, Yucca Mountain Site, Nevada Research and Development Area, Nevada: Washington, DC, Office of Civilian Radioactive Waste Management.
- U.S. Geologic Survey, 1984, A summary of geologic studies through January 1, 1983 of a potential high-level radioactive waste repository site at Yucca Mountain, southern Nye County, Nevada: U.S. Geological Survey Open-File Report 84-792, 164 p.
- Vaniman, D. T., 1991, Calcite, opal, sepiolite, ooids, pellets, and plant/fungal traces in laminar-fabric fault fillings at Yucca Mountain Nevada: Geological Society of America, Abstracts with Programs, v. 23, p. 117.
- Vaniman, D.T., and Crowe, B.M., 1981, Geology and petrology of the basalts of Crater Flat: Applications to volcanic risk assessment for the Nevada nuclear waste storage investigations: Los Alamos, New Mexico, Los Alamos National Laboratory Report, LA-8845-MS, 67 p.
- Vaniman, D.T., Crowe, B.M., and Gladney, E.S., 1982, Petrology and geochemistry of Hawaiite lavas from Crater Flat, Nevada: Contributions to Mineralogy and Petrology, v. 80, p. 341-357.
- Vaniman, D.T., Bish, D.L., and Chipera, S., 1988, A preliminary comparison of mineral deposits in faults near Yucca Mountain, Nevada, with possible analogs: Los Alamos, New Mexico, Los Alamos National Laboratory Report LA-11298-MS, UC-70, 54 p.
- Vaniman, D.T., Bish, D., Broxton, D., Byers, F., Heiken, G., Carlos, B., Semarge, E., Caporuscio, F., and Gooley, R., 1984, Variations in authigenic mineralogy and sorptive zeolite abundance at Yucca Mountain, Nevada, based on studies of drill cores USW GU-3 and G-3.
- Vogel, T. A., Noble, D. C., and Younker, L. W., 1989, Evolution of a chemically zoned magma body: Black Mountain volcanic center, southwestern Nevada: Jour. Geophys. Res., v. 94, p. 6041-6058.
- Vogel, T.A., Ryerson, R.A., Noble, D.C., and Younker, L.W., 1987, Constraints on magma mixing in a silicic magma body: disequilibrium phenocrysts in pumices from a chemically zoned ash-flow sheet: Journal of Geology, v. 95, in press.
- Waddell, R.J., 1984, Geohydrologic and drill-hole data for test wells UE-29a#1 and UE-29a#2, Fortymile Canyon, Nevada Test Site: U.S. Geological Survey Open-File Report 84-0142, 25 p.
- Wang, J.S.Y., and Narasimhan, T.N., 1985, Hydrologic mechanisms governing fluid flow in partially saturated, fractured, porous tuff at Yucca Mountain: University of California Lawrence Berkeley Laboratory Report SAND84-7202 (LBL-18473), 46 p.
- Warren, R.G., and Broxton, D.E., 1986, Mixing of silicic and basaltic magmas in the Wahmonie Formation, southwestern Nevada volcanic field, Nevada: EOS (American Geophysical Union Transactions), v. 67, p. 1261.
- Warren, R.G., Byers, F.M., and Caporuscio, F.A., 1984, Petrography and mineral chemistry of units of the Topopah Springs, Calico Hills and Crater Flat Tuffs, and some older volcanic units, with emphasis on samples from drill hole USW G-1, Yucca Mountain, Nevada Test site: Los Alamos, New Mexico, Los Alamos National Laboratory Report LA-10003-MS.
- Warren, R.G., Nealey, L.D., Byers, F.M., Jr., and Freeman, S.H., 1986, Magmatic components of the Rainier Mesa Member of the Timber Mountain Tuff, Timber Mountain-Oasis Valley Caldera Complex: EOS (American Geophysical Union Transactions), v. 67, p. 1260.

- Warren, R. G., Byers, F. M., Jr., Broxton, D. E., Freeman, S. H., and Hagan, R. C., 1989, Phenocryst abundances and glass and phenocryst compositions as indicators of magmatic environments of large-volume ash flow sheets in southwestern Nevada: *Jour. Geophys. Res.*, v. 94, p. 5987-6020.
- Warren, R.G., McDowell, F.W., Byers, F.M., Broxton, D.E., Carr, W.J., and Orkild, P.P., 1988, Eposodic leaks from Timber Mountain caldera: new evidence from rhyolite lavas of Fortymile Canyon, southwestern Nevada Volcanic Field: *Geological Society of America, Abstracts with Programs*, v. 20, p. 241.
- Weiss, S.I., 1987, Geologic and Paleomagnetic studies of the Stonewall and Black Mountain volcanic centers, southern Nevada: University of Nevada, Reno-Mackay School of Mines, Reno, Nevada, unpublished MSc Thesis, 67 p.
- Weiss, S.I., and Noble, D.C., 1989, Stonewall Mountain volcanic center, southern Nevada: stratigraphic, structural and facies relations of outflow sheets, near-vent tuffs, and intracaldera units: *Journal of Geophysical Research*, v. 94, 6059-6074.
- Weiss, S.I., Noble, D.C., and Mckee, E.H., 1984, Inclusions of basaltic magma in near-vent facies of the Stonewall Flat Tuff: product of explosive magma mixing: *Geological Society of America, Abstracts with Programs*, v. 16, p. 689.
- Weiss, S. I., Noble, D. C., and McKee, E. H., 1988, Volcanic and tectonic significance of the presence of late Miocene Stonewall Flat Tuff in the vicinity of Beatty, Nevada: *Geological Society of America Abs. with Programs*, v. 20, p. A399.
- Weiss, S. I., Noble, D. C., and McKee, E. H., 1989, Paleomagnetic and cooling constraints on the duration of the Pahute Mesa-Trail Ridge eruptive event and associated magmatic evolution, Black Mountain volcanic center, southwestern Nevada: *Jour. Geophys. Res.*, v. 94, p. 6075-6084.
- Weiss, S. I., Noble, D. C., and Larson, L. T., 1989, Task 3: Evaluation of mineral resource potential, caldera geology and volcano-tectonic framework at and near Yucca Mountain; report for July, 1988 - September, 1989: Center for Neotectonic Studies, University of Nevad-Reno, 38 p. plus appendices.
- Weiss, S. I., Noble, D. C., and Larson, L. T., 1990, Task 3: Evaluation of mineral resource potential, caldera geology and volcano-tectonic framework at and near Yucca Mountain; report for October, 1989 - September, 1990: Center for Neotectonic Studies, University of Nevad-Reno, 29 p. plus appendices.
- Weiss, S. I., Connors, K. A., Noble, D. C., and McKee, E. H., 1990, Coeval crustal extension and magmatic activity in the Bullfrog Hills during the latter phases of Timber Mountain volcanism: *Geological Society of America Abstracts with Programs*, v. 22, p. 92-93.
- Weiss, S. I., McKee, E. H., Noble, D. C., Connors, K. A., and Jackson, M. R., 1991, Multiple episodes of Au-Ag mineralization in the Bullfrog Hills, SW Nevada, and their relation to coeval extension and volcanism: *Geological Society of America Abstracts with Programs*, v. 23, p. A246.
- Wernicke, B. P., Christiansen, R. L., England, P. C., and Sonder, L. J., 1987, Tectonomagmatic evolution of Cenozoic extension of the North America Cordillera, *in* Coward, M. P., Dewey, J. F., and Hancock, P. L., eds., *Continental extensional tectonics*: *Geol. Soc. London Spec. Pub.* 28, p. 203-222.
- White, A.F., 1979, Geochemistry of ground water associated with tuffaceous rocks, Oasis valley, Nevada: U.S. Geological Survey Professional Paper 712-E.

- Whitfield, M.S., Eshom, E.P., Thordarson, W., and Schaefer, D.H., 1985, Geohydrology of rocks penetrated in test well USW H-4, Yucca Mountain, Nye County, Nevada: U.S. Geological Survey Water-Resources Investigations Reports, 1985, 33 p.
- Whitfield, M.S., Thordarson, W. and Eshom, E.P., 1984, Geohydrologic and drill-hole data for test well USW H-4, Yucca Mountain, Nye County, Nevada: U.S. Geological ts
- Worthington, J. E., Noble, D. C., and Weiss, S. I., 1991, Structural geology and Neogene extensional tectonics of the Gold Mountain-Slate Ridge area, southwestern Nevada: Geol. Soc. America Abstr. with Prog., v. 23, p. A247.
- Wu, S.S., 1985, Topographic Maps of Yucca Mountain area, Nye County, Nevada, 6 over-size sheets, scale 1:5,000: U.S. Geological Survey Open-File Report 85-0620.
- Zartman, R. E., and Kwak, L. M., 1991, Lead isotopes in the carbonate-silica veins of Trench 14, Yucca Mountain, Nevada: Geological Society of America, Abstracts with Programs, v. 23, p. 117.

Table 1. SUMMARY OF STRATIGRAPHIC, AGE AND STRUCTURAL RELATIONS OF NEOGENE ROCKS OF THE GOLD MOUNTAIN - SLATE RIDGE AREA, SOUTHERN ESMERALDA COUNTY, NEVADA

Spearhead Member of the Stonewall Flat Tuff (7.6 Ma)

Basalt of Hanging Mesa

angular unconformity and conglomerate/fanglomerate

Ammonia Tanks Member of the Timber Mountain Tuff (11.4 Ma)

local angular unconformity

Rainier Mesa Member of the Timber Mountain Tuff (11.6 Ma)

conglomerate/fanglomerate

Tuff of Sphinx Canyon (age determination in progress)

conglomerate/fanglomerate

Tuff of Tolicha Peak (13.9 ± 0.4 Ma^{*})

local angular unconformity

Pumice and lithic-rich tuff

Tuff of Gold Coin Mine (age determination in progress)

Tuff of Oriental Wash (14.2 ± 0.4^{})**

conglomerate/fanglomerate

Tuff of Mount Dunfee (16.7 ± 0.4^{*})**

Olivine basalt (age determination in progress)

Hornblende ± biotite andesite lava

----- *(major unconformity)* -----

Sylvania Pluton (Middle Jurassic, Albers and Stewart, 1972)

Precambrian and Cambrian sedimentary and metamorphic rocks

- * Whole-rock K-Ar age determination on devitrified groundmass (E. H. McKee, D. C. Noble and J. E. Worthington, unpublished data, 1991).
- ** K-Ar age determination on hornblende (E. H. McKee, D. C. Noble and J. E. Worthington, unpublished data, 1991).
- *** K-Ar age determination on biotite (E. H. McKee, D. C. Noble and J. E. Worthington, unpublished data, 1991).

Table 2. GOLD CONTENTS OF SUBALKALINE RHYOLITIC ROCKS OF THE SOUTHWESTERN NEVADA VOLCANIC FIELD

(values given in parts per billion)

Sample #	Au	Sample type	Unit and location
3SW-171A	0.2	vitrophere	Red Rock Valley Tuff; east side of Eleana Range
K-190	0.5	vitrophere	Bullfrog Member, Crater Flat Tuff; south end of Yucca Mountain
K-192	0.7	devitrified	Bullfrog Member, Crater Flat Tuff; south end of Yucca Mountain
CP4-2OB	0.4	vitrophere	Topopah Spring Member, Paintbrush Tuff; Yucca Mountain
BB9-15	0.8	vitrophere	Topopah Spring Member, Paintbrush Tuff; Yucca Mountain
BB8-45	0.4	vitrophere	Topopah Spring Member, Paintbrush Tuff; Yucca Mountain
3SW-519G	0.1	vitrophere	Tiva Canyon Member, Paintbrush Tuff; Yucca Mountain
3SW-519GU	0.2	vitrophere	Tiva Canyon Member, Paintbrush Tuff; Yucca Mountain
3SW-521	0.1	devitrified	Tiva Canyon Member, Paintbrush Tuff; Yucca Mountain
3SW-433NA	0.5	devitrified	Tiva Canyon Member, Paintbrush Tuff; Yucca Mountain (Exile Hill)
3SW-435NA	0.6	devitrified	Tiva Canyon Member, Paintbrush Tuff; Yucca Mountain (Exile Hill)
3SW-437NA	0.6	devitrified	Tiva Canyon Member, Paintbrush Tuff; Yucca Mountain (Exile Hill)
3DCN8-82	0.2	vitrophere	Rainier Mesa Member, Timber Mountain Tuff; SE of Sleeping Butte
3SW-523GL	0.1	vitrophere	Rainier Mesa Member, Timber Mountain Tuff; NW of Scotty's Junction
3SW-525	0.1	devitrified	Rainier Mesa Member, Timber Mountain Tuff; NW of Scotty's Junction
SJW-81-ATV	0.3	vitrophere	Ammonia Tanks Member, Timber Mountain Tuff; NW of Scotty's Junction
3DN8-21	0.2	vitrophere	Ammonia Tanks Member, Timber Mountain Tuff; SE of Sleeping Butte
THR-1	0.3	vitrophere	post-Ammonia Tanks rhyolite lava #1, Bullfrog Hills
THR-2	<0.1	vitrophere	post-Ammonia Tanks rhyolite lava #2, Bullfrog Hills
3DN9-24	0.1	vitrophere	post-Ammonia Tanks rhyolite lava #1, Bullfrog Hills
3DN8-20	0.2	vitrophere	"tracking station" rhyolite, northern Bullfrog Hills
FCT-1	0.1	vitrophere	post-Ammonia Tanks tuff; between Fluorspar Canyon and Beatty Wash
OBS-B	0.2	obsidian	Rhyolite lavas of Obsidian Butte
3SW-173TR	0.4	obsidian	Rhyolite lavas of Shoshone Mountain

Analyses by XRAL Activation Services Inc., using instrumental neutron activation prior to fire assay concentration and radiochemical analyses (Rowe and Simon, 1968; Connors et al., 1990; 1991).

Table 3. MERCURY CONTENTS OF ROCK-CHIP SAMPLES FROM YUCCA MOUNTAIN
(values given in parts per billion as the means of replicate analyses)

Sample#	Hg	2 sigma	n	Description/location
<i>Bow Ridge fault at Trench 14</i>				
3SW-569	22.0	0.0	2	Rainier Mesa Member, N wall; caliche impregnated, weak argillic alteration, adjacent to main carbonate-silica vein.
3SW-571	40.5	3.0	2	brecciated Tiva Canyon Member, N wall, ~30° E of main vein; drusy quartz, silica ± caliche veins xcut drusy quartz.
3SW-573	40.5	3.0	2	brecciated Tiva Canyon Member, N wall, E of 3SW-571; w/ drusy quartz.
3SW-575	26.5	1.0	2	brecciated Tiva Canyon Member, N wall, E of 3SW-573; w/ lng drusy quartz ± caliche in lithophysae.
3SW-577	22.0	4.0	2	brecciated Tiva Canyon Member, S wall, ~18° E of main vein; w/ drusy quartz + caliche.
3SW-579	45.5	3.0	2	breccia of Tiva Canyon Member fragments in carbonate-silica matrix, S wall, adjacent to E edge of main vein.
3SW-581	<10		4	partially opalized Tiva Canyon Member, S wall, between splays of main vein.
<i>Solitario Canyon fault</i>				
3SW-599A	63.0	10.5	4	reddish, FeOx-rich opalized? bedded tuff w/caliche coating, ~100' W of Solitario Canyon fault splay ^a .
3SW-599B	67.7	7.5	3	dark rusty brown, porous bedded tuff ~12' WNW from 3SW-599A.
3SW-603	35.5	3.0	2	caliche vein, N wall of Trench 8, Solitario Canyon fault splay.
3SW-605	58.0	6.0	2	fault breccia of dark purplish brown fragments of Topopah Spring Member, minor opal in fractures; E end Trench 8.
3SW-607	33.3	10.3	4	siliceous, strain-hardened? fault breccia of Topopah Spring Member adjacent to caliche vein at E end Trench 8
<i>Bow Ridge fault near Bow Ridge</i>				
3SW-593A	19.5	5.0	2	opal? cemented fault breccia of dense Tiva Canyon Member, Bow Ridge below saddle W of Bow Ridge
3SW-593B	13.0	0.0	2	opal-veined fault breccia/gouge, ~2' E of 3SW-593A; fragments of dark Topopah Spring Member? in siliceous matrix.
<i>Fault system NW of Busted Butte</i>				
3SW-595A	11.0	0.0	2	siliceous fault gouge or vein?, fault in saddle S of Dune Wash, ~2050' SW of hill 3834.
3SW-595B	10.0	2.0	2	FeOx-rich Topopah Spring Member? in footwall of fault in saddle S of Dune Wash, adjacent to 3SW-595A.
<i>"Fresh" Tiva Canyon Member</i>				
3SW-583	31.2	14.0	6	Tiva Canyon Member, densely welded, devitrified, caliche in lithophysal cavities; E side Exile Hill.
3SW-585	<10		2	Tiva Canyon Member, densely welded, devitrified, caliche in lithophysal cavities; E side Yucca Mtn., NW of Exile Hill.
3SW-589	12.0	2.0	2	Tiva Canyon Member, densely welded, devitrified, w/caliche in lithophysal cavities; ridge E of Bow Ridge.
3SW-591	16.5	2.0	2	Tiva Canyon Member, densely welded, devitrified, w/caliche in lithophysal cavities; just W of Bow Ridge.
3SW-597	35.5	9.6	4	Tiva Canyon Member, densely welded, devitrified, w/caliche in lithophysal cavities; ~2000' SE of 3SW-595A/595B.
<i>Hydrothermally altered rock in Claim Canyon</i>				
3SW-587A	827.5	65.4	4	silicified and partially adularized rhyolite lava between units of the Paintbrush Tuff; ~3600' N35°E from Prow Pass.

Analyses carried out by M. Desilets, analyst, Nevada Bureau of Mines Analytical Laboratory on 10 gram digestions using atomic absorption spectrometry with hydride generation methods.

Uncertainty expressed in parts per billion Hg at 2 Sigma level; n = number of replicate analyses.

Detection limit is estimated to be 10 parts per billion based on the results of standard addition analysis and intrarun comparison to synthetic control samples.

^a sample is from same outcrop as SC-52 of Castor et al. (1989).

Table 4. PRECIOUS METALS AND INDICATOR-ELEMENT ABUNDANCES IN ROCK-CHIP SAMPLES FROM YUCCA MOUNTAIN

(Ag and Au expressed in parts per billion, all other elements given in parts per million)

Sample #	Ag	Au	As	Bi	Cd	Hg	Sb	Sc	Cu	Mo	Pb	Zn	Ga
<i>Bow Ridge fault at Trench 14</i>													
3SW-569	12	7.3	4.22	0.132	0.030	0.026	0.227	<0.244	0.977	0.280	4.15	11.3	1.29
3SW-571	11	0.5	9.88	0.086	0.031	0.050	0.317	<0.249	0.799	0.555	8.41	32.0	0.595
3SW-573	14	1.2	11.8	0.093	0.032	0.038	0.267	<0.246	0.931	0.604	9.20	32.5	0.431
3SW-579	6	1.1	6.65	<0.050	0.036	0.048	0.169	0.412	1.64	0.232	4.10	17.8	0.282
3SW-581	4	0.9	3.83	0.057	0.020	0.025	0.139	0.323	0.673	0.483	0.790	41.2	0.540
<i>Solitario Canyon fault</i>													
3SW-599A [*]	<9	1.1	1.68	3.99	0.077	<0.058	0.300	<0.723	1.72	1.86	70.5	43.0	1.69
3SW-599B [*]	<9	<0.6	<0.750	1.35	0.065	<0.060	0.160	<0.750	1.15	0.570	3.32	12.7	0.989
3SW-605	4	0.4	1.67	0.335	0.034	0.024	0.089	<0.247	0.263	0.389	1.59	27.4	0.812
X-15 ^f	5	<0.2	2.26	0.334	0.037	0.022	0.132	<0.247	0.255	0.383	1.49	26.2	0.760
<i>Fault system NW of Busted Bunte</i>													
3SW-595B	5	0.5	1.87	1.77	0.047	0.038	0.388	0.377	0.268	2.27	17.3	8.11	2.10
X-16 ^h	6	0.5	2.32	1.81	0.045	0.024	0.410	<0.246	0.313	2.34	18.0	9.48	2.27
<i>Densely welded, lithophysal "fresh" tuff</i>													
3SW-585	25	<0.2	6.00	0.094	0.073	<0.019	0.183	<0.242	0.597	1.2	9.98	52.9	0.608
58991 [#]	14	0.3	2.41	0.066	0.040	0.030	0.126	0.326	0.832	0.591	3.58	47.4	0.543
3SW-433NA ^v		0.5											
3SW-435NA ^v		0.6											
3SW-437NA ^v		0.6											
<i>Fault system west side of Boomerang Point</i>													
3SW-519G ^x		0.1											
3SW-519GU ^y		0.2											
3SW-521 ^z		0.1											
<i>Claim Canyon</i>													
3SW-587A	13	0.5	7.78	0.073	0.047	0.515	0.849	<0.246	0.580	0.308	3.80	26.3	0.618

Analyses by Geochemical Services Inc., using inductively-coupled plasma emission spectrography for all elements except Au which was carried out by graphite furnace - atomic absorption spectrometry; * = 5 gram digestion, all other analyses used 15 gram digestion. Values as reported by G.S.I. except Ag rounded to nearest ppb and Au rounded to nearest 0.1 ppb; number of significant figures does not indicate precision or accuracy of analyses.

Measured tellurium contents were <0.25 ppm in all samples. Measured thallium contents were <0.50 ppm in all samples except 3SW-599A and 3SW-599B which were <1.50 ppm.

^f denotes blind duplicate sample of 3SW-605.

^h denotes blind duplicate sample of 3SW-595B.

^v analyses by XRAL Activation Services, Inc., using instrumental neutron activation (INAA) methods.

^x middle part of vitrophere of Tiva Canyon Member; INAA analysis by XRAL Activation Services, Inc.

^y upper part of vitrophere of Tiva Canyon Member; INAA analysis by XRAL Activation Services, Inc.

^z devitrified Tiva Canyon Member just above vitrophere; INAA analysis by XRAL Activation Services, Inc.

58991 is composite sample of equal parts 3SW-589 and 3SW-591.

Detection limits quoted by G.S.I. based on intrarun standards and blanks as follows:

Ag	3.00 ppb	Hg	0.020 ppm	Mo	0.020 ppm
Au	0.20 ppb	Sb	0.050 ppm	Pb	0.050 ppm
As	0.250 ppm	Sc	0.250 ppm	Zn	0.250 ppm
Bi	0.050 ppm	Te	0.050 ppm	Ga	0.100 ppm
Cd	0.020 ppm	Cu	0.010 ppm	Tl	0.500 ppm

Table 5. Summary of Phenocryst Assemblages of Pre-Timber Mountain Ash-Flow Sheets in the Gold Mountain - Slate Ridge Area

Unit	quartz	plag	san	bio	hbl	cpx	sphene
Tuff of Sphinx Canyon		X	X	X	X	X	
Tolicha Peak Tuff	X	X			tr		
Tuff of Gold Coin mine	X	X	X	X	X		X
Tuff of Oriental Wash	X	X	X	X	X		X
Tuff of Mount Dunfee	X	X	X	X	X	X	

X's denote minerals present as phenocrysts.

plag = plagioclase, san = sanidine, bio = biotite, hbl = hornblende, cpx = clinopyroxene; tr = trace.

EXPLANATION

- Radiometric age date sample locations
- Quaternary alluvial and colluvial deposits
- ▨ Rhyolite of Mount Jackson, stipple shows associated near-vent pyroclastic deposits
- ▩ Rhyolite of the Montezuma Range
- Miocene and Pliocene(?) volcanic and sedimentary rocks. In the Montezuma Range unit probably includes pyroclastic deposits related to the Rhyolite of the Montezuma Range
- ▨ Paleozoic sedimentary rocks and Mesozoic granitic intrusive rocks, undivided

3-34

0 km 5

37°30'
117°30'

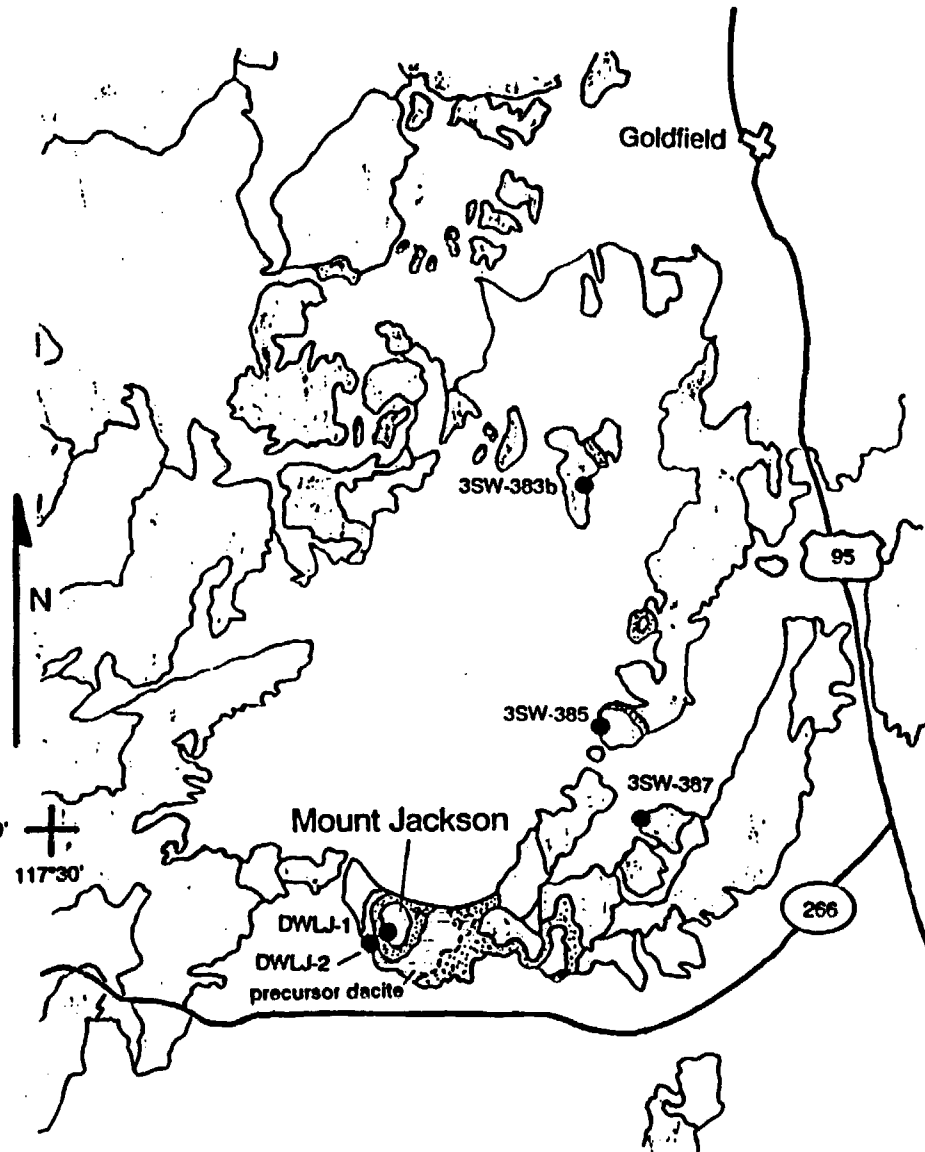


Figure 1. Simplified geologic map of the Mount Jackson dome field. Modified from Albers and Stewart, 1972.

SOUTH

DISTRIBUTION OF HYDROTHERMAL ALTERATION IN YUCCA MOUNTAIN DRILL HOLES

NORTH

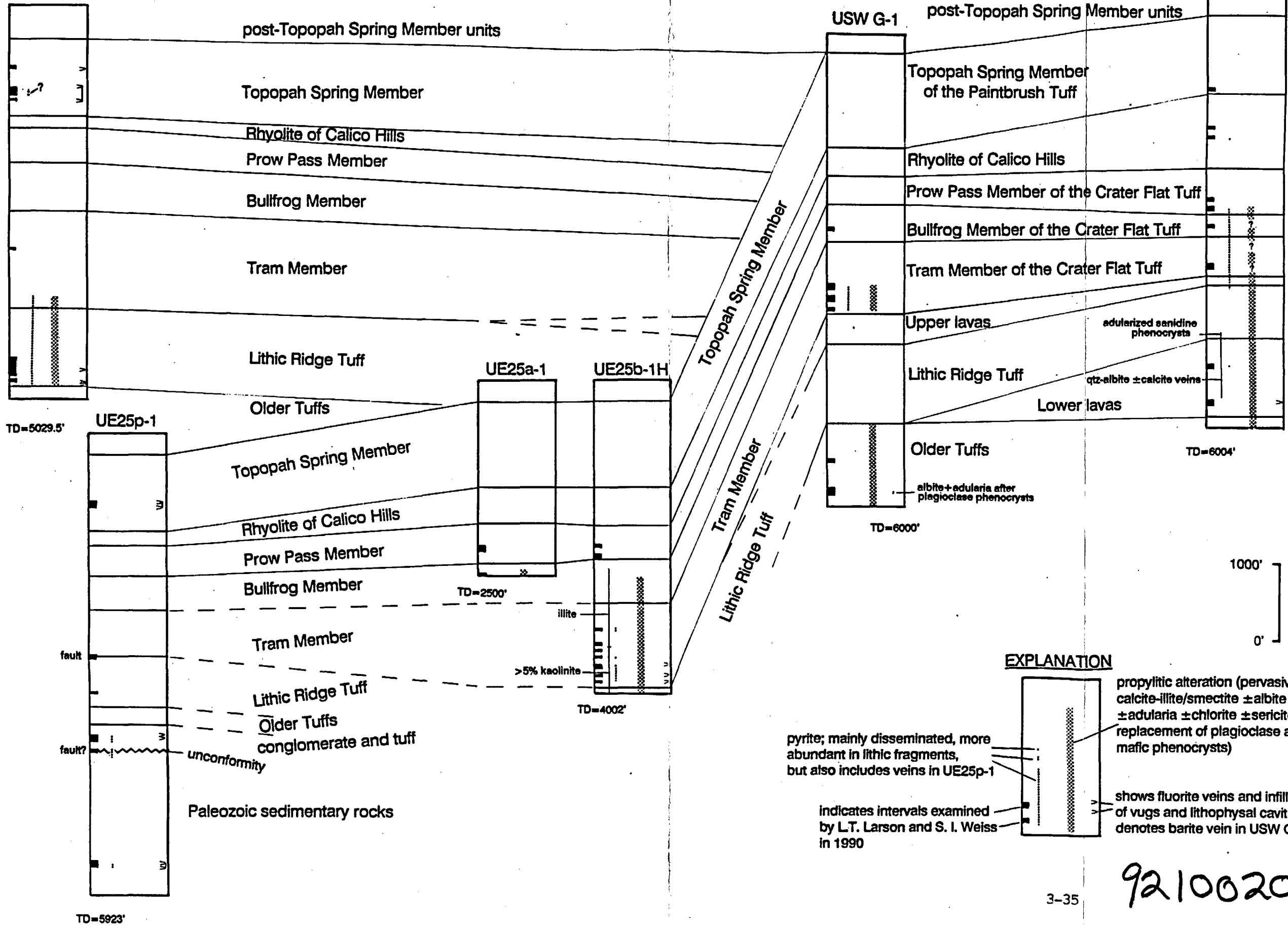
USW G-3/GU-3

USW G-2

ST APERTURE CARD

Also Available On Aperture Card

Figure 2. Subsurface stratigraphy and hydrothermal alteration features of deep drill holes in Yucca Mountain. Data from direct visual inspection by Task 3 and numerous published reports of the U.S. Geological Survey and the Los Alamos National Laboratory.

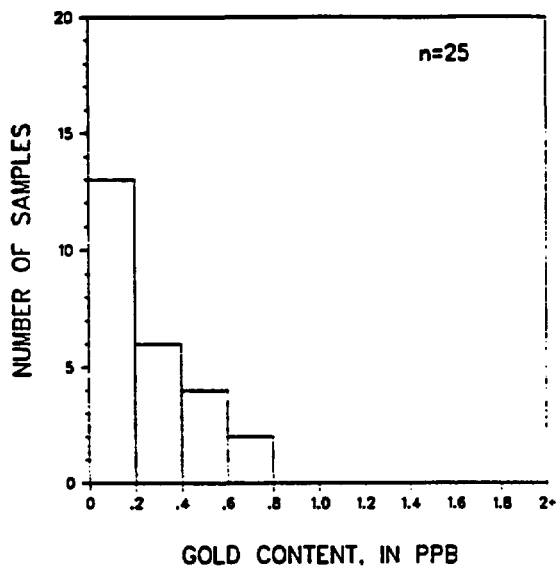


EXPLANATION

- propylitic alteration (pervasive calcite-illite/smectite ± albite ± adularia ± chlorite ± sericite? replacement of plagioclase and mafic phenocrysts)
- pyrite; mainly disseminated, more abundant in lithic fragments, but also includes veins in UE25p-1
- indicates intervals examined by L.T. Larson and S. I. Weiss in 1990
- shows fluorite veins and infillings of vugs and lithophysal cavities; denotes barite vein in USW G-2

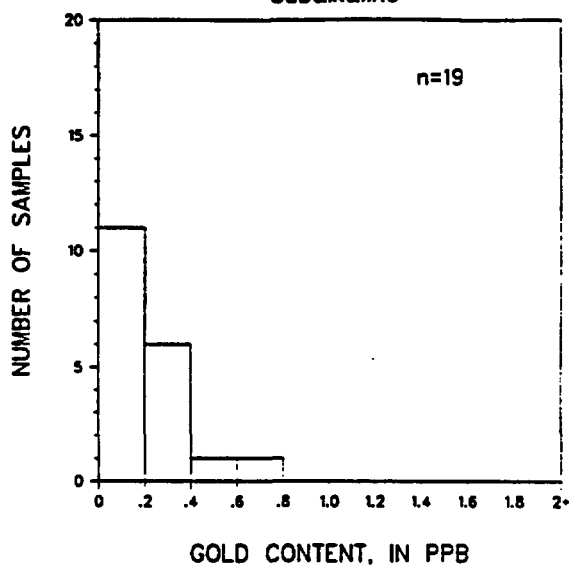
9210020067-02

Subalkaline Rhyolitic Rocks



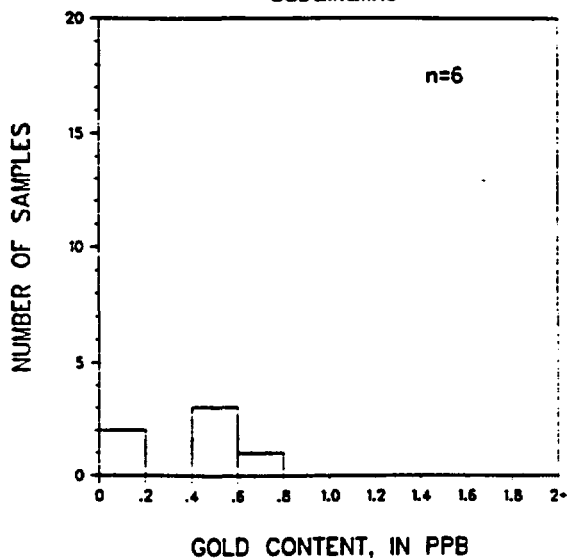
a

Glassy Rocks Subalkaline



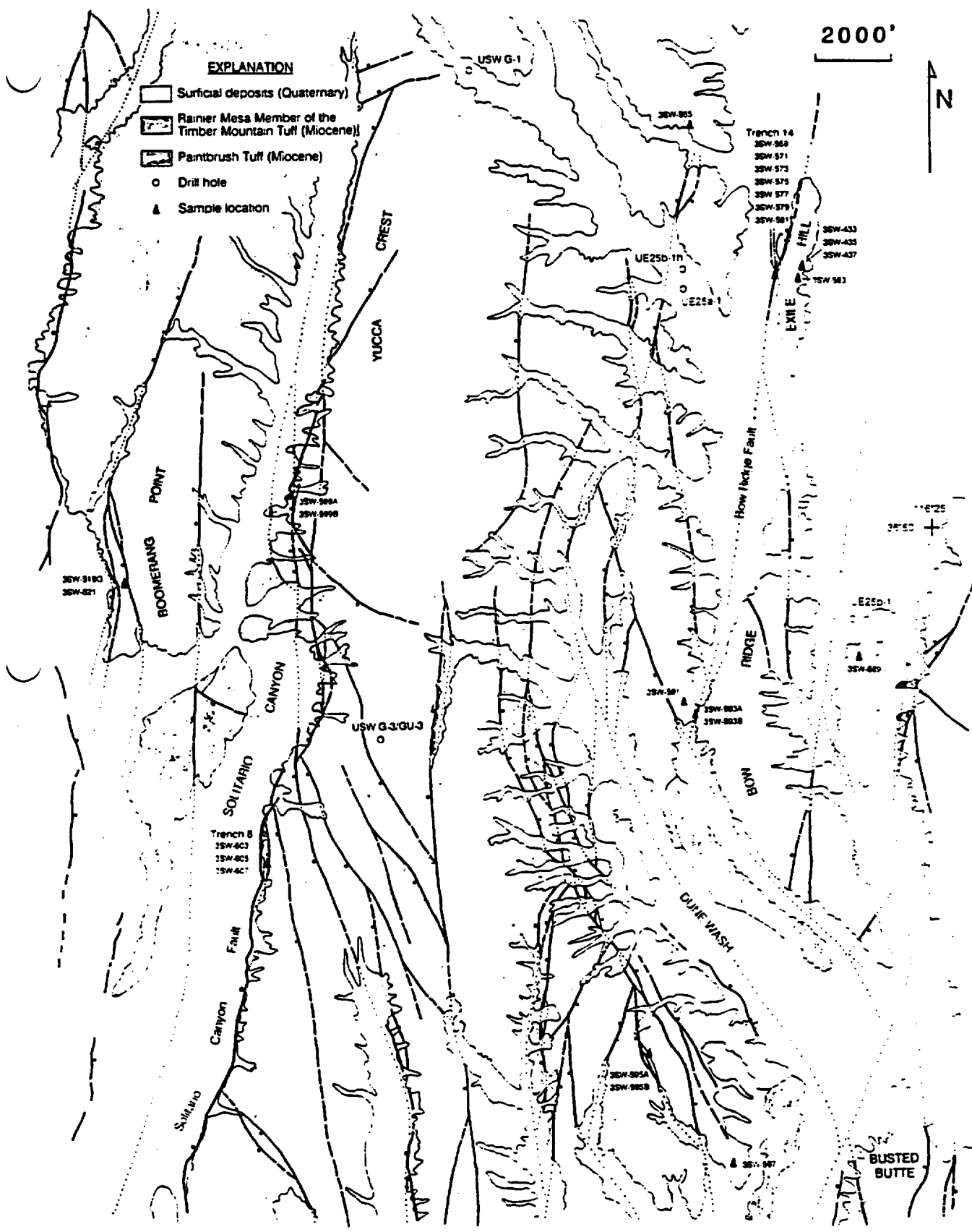
b

Devitrified Rocks Subalkaline



c

Figure 3. Frequency diagrams showing gold contents of volcanic rocks of the southwest Nevada volcanic field as determined by instrumental neutron activation methods. 3a includes one sample of vitrophere from one of the domes of the Brougher dacite in the Tonopah area.



APPENDIX A

Magmatic and Hydrothermal Activity, Caldera Geology, and Regional Extension in the Western Part of the Southwestern Nevada Volcanic Field

Donald C. Noble¹, Steven I. Weiss¹, and Edwin H. McKee²

¹*MacKay School of Mines, University of Nevada, Reno, NV 89557*

²*U.S. Geological Survey, 345 Middlefield Road, Menlo Park, CA 94025*

Abstract

Igneous activity of the southwestern Nevada volcanic field can be divided into three magmatic stages. The *main magmatic stage*, which began about 15.2 Ma and ended with eruption of the Tiva Canyon Member of the Paintbrush Tuff about 12.8 Ma, was characterized by the caldera-forming eruption of a number of voluminous silicic ash-flow sheets, mostly of subalkaline character, and small volumes of silicic and intermediate lavas. A thick, west-dipping section of intracaldera(?) ash-flow tuff exposed on Sleeping Butte appears to mark a newly recognized collapse caldera that predates the Belted Range Tuff. The onset of the *Timber Mountain magmatic stage* followed a lull in volcanic activity of about 1 to 1.5 million years. The lithologically distinctive rocks of the Timber Mountain magmatic stage include: 1) precursor rhyolite lavas and surge deposits, 2) two major compositionally zoned ash-flow sheets, the Rainier Mesa and overlying Ammonia Tanks Members of the 11.4-Ma Timber Mountain Tuff, and several overlying small-volume ash-flow units, and 3) an assemblage of late rhyolitic tuffs and lavas and associated mafic and intermediate lavas that were erupted prior to about 10 Ma. A *late magmatic stage* is represented by alkaline, peralkaline, and subalkaline rocks of the Black Mountain and Stonewall Mountain volcanic centers and rocks of other centers to the northwest that were erupted between about 7 and 9 Ma.

During the Timber Mountain magmatic stage, volcanic activity evolved from caldera-forming eruptions of major ash-flow sheets to eruption of local units of tuff and lava from vents located mainly in the western part of the southwestern Nevada volcanic field. Field relations and geochronologic constraints show that the Rainier Mesa Member of the Timber Mountain Tuff was erupted from vents within the *Timber Mountain I* caldera, which encompasses the formerly recognized Oasis Valley and Sleeping Butte caldera segments. Eruption of the Ammonia Tanks Member resulted in the formation of a smaller *Timber Mountain II* caldera nested within the Timber Mountain I caldera. Sphene-bearing ash-flow cooling units of the tuff of Fleur-de-Lis Ranch exposed locally inside the western margin of the Timber Mountain caldera, on which radiometric ages of 11.3 ± 0.3 and 11.4 ± 0.1 Ma have been obtained, are of the same age as the Ammonia Tanks Member; these tuffs may reflect pulses of pyroclastic activity related to the Ammonia Tanks Member, as do the tuff of Burrohook Wash and tuffs of Crooked Canyon exposed on and around Timber Mountain. High-Si rhyolite tuffs that lack sphene overlying the Ammonia Tanks Member in the Bullfrog Hills west of the Timber Mountain caldera represent a renewal of Rainier Mesa-type magmatism. These tuffs and associated silicic and intermediate lavas may in part have been erupted from fissure vents formed during crustal extension.

Hydrothermal activity and mineralization took place during both the main and Timber Mountain magmatic stages. Epithermal gold and fluorite mineralization at the Sterling, Goldspar, Mother Lode, Secret Pass, Daisy, and other properties along the northern and eastern margins of Bare Mountain, and probably also at the Wahmonie district, is related to subjacent porphyry-type magmatic systems about 13 to 14 million years old. The most intense and widespread hydrothermal activity and epithermal Au-Ag mineralization related to the Timber Mountain magmatic stage is found in the Bullfrog Hills in the western part of the volcanic field. Mineralization at the Bond Gold Bullfrog and Gold Bar mines as well as at a number of previously producing properties and prospects is structurally controlled by normal faults and appears to be related to magmatic activity of the later part of the Timber Mountain stage.

Crustal extension in the western part of the southwestern Nevada volcanic field involved movement along both a regional low-angle fault (the "Original Bullfrog-Fluorspar Canyon detachment fault") and higher-angle normal faults that in part postdate and cut the low-angle structure. Rotation of fault blocks in the Bullfrog Hills took place mostly after eruption of the Timber Mountain Tuff and was complete by the time the subhorizontal, 7.6-Ma Spearhead Member of the Stonewall Flat Tuff was deposited. Very similar relations are present in the Gold Mountain-Slate Ridge area west of Stonewall Mountain. A younger episode of normal faulting that postdates the Stonewall Flat Tuff produced most of the present topography in areas between longitude 117° W, and the Death Valley-Furnace Creek fault zone.

The southwestern Nevada volcanic field (herein abbreviated SWNVF) (Figs. 1 and 2) was the focus of large-scale pyroclastic volcanism for about 8 million years during middle and late Miocene time. Geologic investigations conducted over the past three decades, most carried out in connection with weapons testing and nuclear waste disposal programs of the U.S. Atomic Energy Commission and the U.S. Department of Energy, have made the SWNVF one of the most intensely studied volcanic fields in the world. A recent review by Byers et al. (1989) summarizes the wide range of geological and other studies that have been carried out by a large number of workers.

Most work in the past has focused on the many silicic ash-flow sheets and associated units of lava and on the calderas that formed as a result of large-scale pyroclastic eruption. The eastern part of the SWNVF, which lies within the Nevada Test Site, has long been better known than the western part of the field, where many aspects of the geology remained equivocal or incompletely understood. This reflects both the lesser amount of study that has been devoted to the area west of the Nevada Test Site and the combined effects of widespread and locally intense hydrothermal activity and complicated Miocene faulting. This paper is both a review and a progress report on our ongoing efforts to resolve fundamental geologic problems of the western part of the SWNVF and adjacent areas to the west and north, with an emphasis on magmatic and hydrothermal activity and caldera geology and their interrelation with the late Cenozoic faulting and extensional tectonism of the region.

Magmatic Events of the Southwestern Nevada Volcanic Field

The middle and late Miocene ash-flow sheets and lavas of the SWNVF (Table 1) were deposited on a complexly deformed and locally metamorphosed basement of Precambrian and Paleozoic sedimentary rocks of the North American miogeocline (e.g., Cornwall, 1972; Stewart, 1980; Carr, 1984a). Radiometric ages on rocks of the SWNVF (e.g., Kistler, 1968; Marvin et al., 1970; 1989; Jackson, 1988; Table 2, this paper; E. H. McKee, D. C. Noble, and S. I. Weiss, unpub. data) in conjunction with stratigraphic, petrologic, and other geologic data (e.g., Byers et al., 1976a; Noble et al., 1984; Carr et al., 1986; Broxton et al., 1989) suggest that magmatic activity of the SWNVF can be divided into three temporally well defined and genetically significant stages. These are designated the *main magmatic stage*, with major activity from about 15.2 to 12.8 Ma, the *Timber Mountain magmatic stage*, from about 11.5 to about 10.5-10.0 Ma, and the *late magmatic stage*, from about 9 to 7 Ma.

During the main magmatic stage, a complex of overlapping and nested collapse calderas (Fig. 2) developed with the eruption of at least nine voluminous sheets of silicic ash-flow tuff, as well as many smaller units of lava and tuff of silicic to intermediate composition. The oldest well-characterized ash-flow sheet attributed to volcanism of the SWNVF is the Redrock Valley Tuff, which has been radiometrically dated at about 15.2 Ma (Table 2, Specimens 9 and 10); this age is younger than the radiometric age of about 16.1 Ma reported by Marvin et al. (1970) and older than the age of about 14.0 Ma obtained on this unit by Kistler (1968). (Appreciably younger ages were obtained by standard K-Ar methods on sanidine from this and other units of the SWNVF; these ages provided the first conclusive evidence for systematic analytical errors apparently resulting from the sequestering of argon by Mo films on the argon extraction bottle (Hausback et al., 1990)). Other major ash-flow sheets erupted during this period are included within the tuff of Yucca Flat, the Lithic Ridge Tuff, the Crater Flat Tuff, the Paintbrush Tuff, and other, less well known, units (Byers et al., 1976a; 1989; Carr et al., 1986). Units of the Paintbrush Tuff are related to the Claim Canyon Cauldron (Byers et al., 1976a), and Carr et al. (1986) have proposed that the Crater Flat Tuff was erupted from the inferred Crater Flat-Prospector Pass caldera complex (Fig. 2). In addition, facies relations, distribution patterns, and subsurface information led Carr et al. (1986) to propose that one or more older calderas, buried by younger rocks, may be present beneath northern Yucca Mountain. The Belted Range Tuff and associated peralkaline lavas of the Silent Canyon caldera (Noble et al., 1968; Sawyer and Sargent, 1989) were also erupted during this period, although the different chemical character of these rocks suggests derivation from a different magma system.

Another caldera may exist in the area of Sleeping Butte (Fig. 3). There a thick sequence of densely welded and slightly to moderately hydrothermally altered tuff dips from 25° to 50° to the west-northwest and is unconformably overlain by the Grouse Canyon Member of the Belted Range Tuff. It is not known if this sequence correlates with older tuffs recognized elsewhere in the SWNVF (cf. Carr et al., 1986). If unbroken, this section is at least 1 km thick. The thickness and dip of these tuffs, combined with the local presence of lithic blocks of Mesozoic(?) granite as much as 0.5 m in diameter suggest that the section exposed at Sleeping Butte represents part of the intracaldera tuff prism, perhaps resurged, of an early caldera of the main magmatic stage. (It is emphasized that this proposed caldera is in no way related to the Sleeping Butte caldera segment as proposed by Byers et al., 1976a.) An exposure of densely welded, locally rheomorphically deformed and hydrothermally altered, quartz and sanidine bearing rhyolite tuff about 5 km southeast of sleeping Butte strikes about N30°E and dips very steeply to both the east and west. One

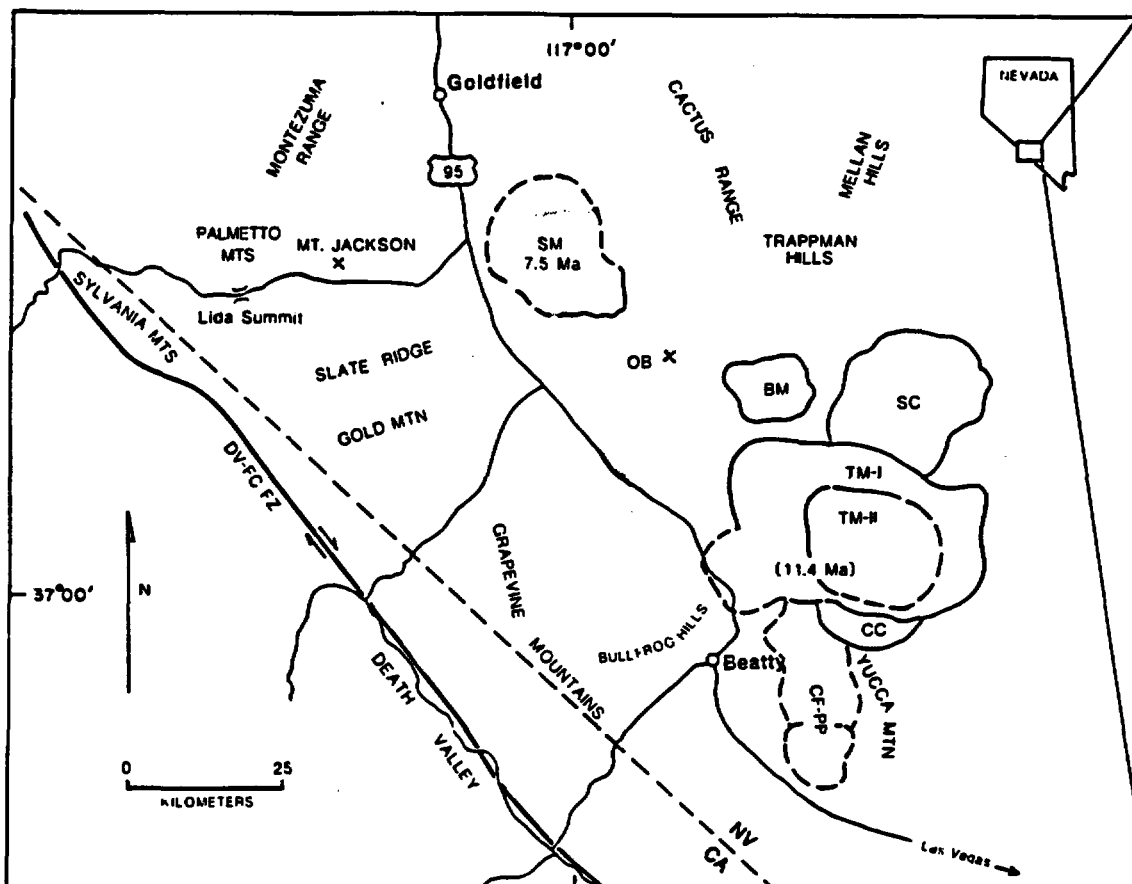


Fig. 1. Map showing volcanic centers and geographic features of the southwestern Nevada volcanic field and adjacent areas. SM = Stonewall Mountain volcanic center; OB = Obsidian Butte; BM = Black Mountain volcanic center; TM-I = Timber Mountain I caldera formed upon eruption of the Rainier Mesa Member of the Timber Mountain Tuff; TM-II = Timber Mountain II caldera formed on eruption of the Ammonia Tanks Member of the Timber Mountain Tuff; CC = Claim Canyon cauldron segment; CF-PP = Crater Flat-Prospector Pass caldera complex of Carr et al. (1986); SC = Silent Canyon caldera; DV-FC FZ = Death Valley-Furnace Creek fault zone. Stipple outlines approximate eastern limit of post-7.5-Ma normal faulting.

possibility is that this unit, which is unconformably overlain by the thick unit of tuff exposed at Sleeping Butte and by flat-lying tuff of the Rainier Mesa Member of the Timber Mountain Tuff (see below), is a large slide block within the possible caldera.

The tuff of Tolicha Peak, a unit of petrographically distinctive rhyolite ash-flow tuff that underlies the Belted Range Tuff, is exposed over an area that extends from Sleeping Butte north to areas east and west of Stonewall Mountain (Noble and Christiansen, 1968; Ekren et al., 1971; S. I. Weiss, unpub. mapping, 1989). A caldera reflecting the source for this unit probably exists somewhere within its area of known distribution.

Stocks and dikes of silicic to intermediate composition with porphyritic to hypidiomorphic granular textures were emplaced during the latter part of the main magmatic stage at Bare Mountain, Wahmonie, and possibly in the Calico Hills (Cornwall and Kleinhampl, 1961; Ekren and Sargent, 1965; Hoover et al., 1982; Ponce, 1984). Both the north-south trending dikes exposed on the eastern part of Bare Mountain, which have classic porphyry textures, and the granitic rocks at Wahmonie contain high-salinity fluid inclusions with

halite and other daughter minerals, suggesting the presence of porphyry system(s) at depth (Noble et al., 1989). K-Ar ages of 13.9 ± 0.5 , 13.9 ± 0.3 , and 13.8 ± 0.2 Ma have been reported on partly altered dikes at Tarantula Canyon and Joshua Hollow (Marvin et al., 1989; Monsen et al., 1990). We have obtained an age of 14.9 ± 0.5 Ma (Table 2, Specimen 8) on biotite from another slightly altered dike of this group exposed just north of Bare Mountain. Ages of about 12.9 Ma have been obtained on adularia from hydrothermally altered dike rock at the Goldspar Mine (see below). Although the exact age of the Bare Mountain magmatic system is uncertain, emplacement of the dikes during the main magmatic stage of the SWNVF is well demonstrated.

There was a marked decrease in magmatic activity between deposition of the 12.8-Ma Tiva Canyon Member of the Paintbrush Tuff and deposition of the 11.4-Ma Rainier Mesa Member of the Timber Mountain Tuff. This lull lasted about 1 to 1.5 m.y., an interval about half as long as the period of time during which the many centers of the main magmatic stage were active. A petrochemical transition during this interval is suggested by the differences in phenocryst mineralogy,

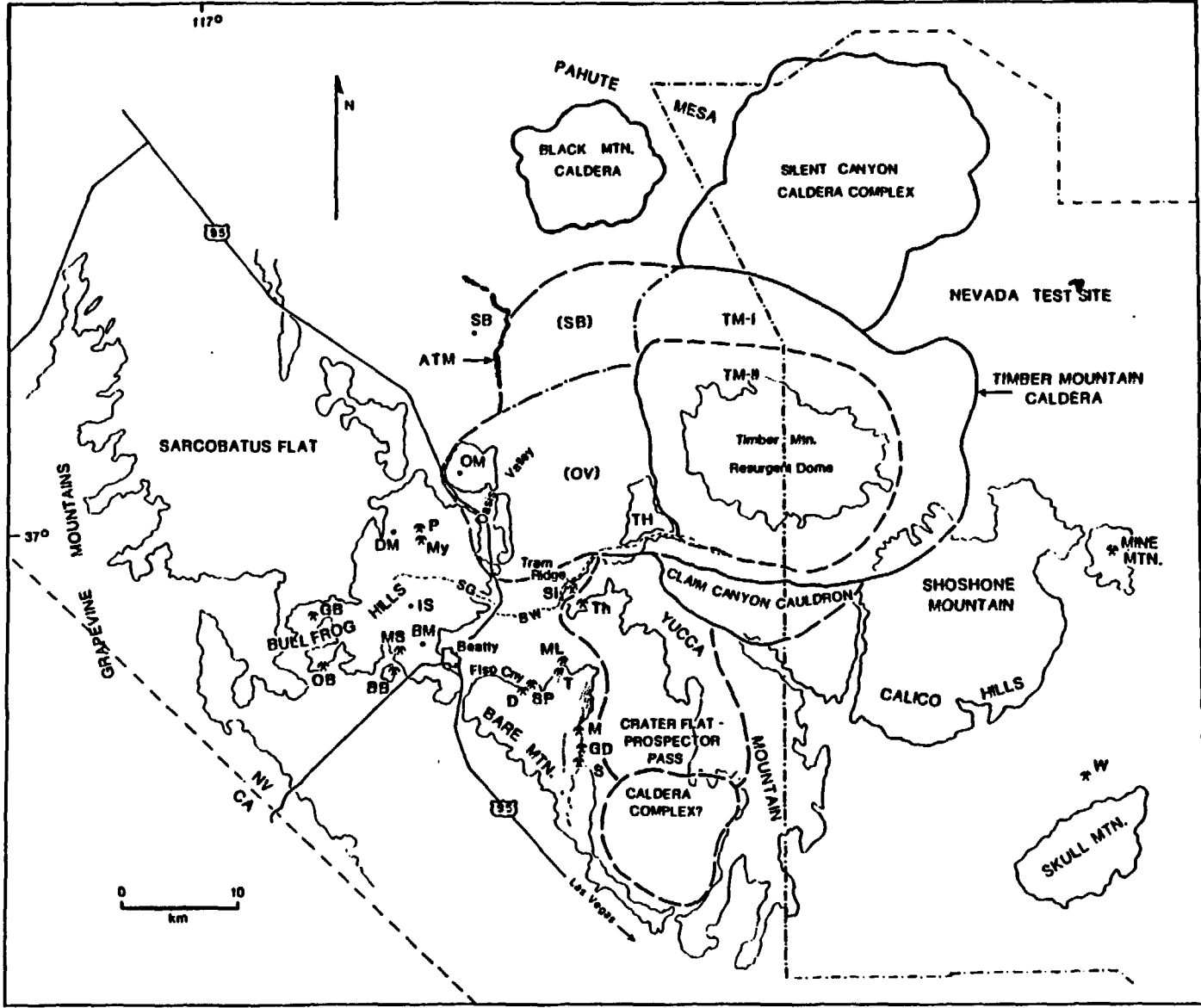


Fig. 2. Map showing major geographic features and collapse calderas of the southwestern Nevada volcanic field and other geologic features referred to in text. Dash-dot line shows boundary of the Nevada Test Site. ATM = outcrops of the Ammonia Tanks Member of the Timber Mountain Tuff near Sleeping Butte that mantle the east-facing wall of the Timber Mountain I caldera and beyond the caldera overlie tuffs of the Rainier Mesa Member. BB = Bond Bullfrog mine; BM = Burton Mountain; BW = Beatty Wash; D = Daisy mine; DM = Donovan Mountain; GB = Gold Bar mine; GD = Goldspar (Diamond Queen) mine; IS = Indian Springs; M = Mary mine; ML = Mother Lode(Gexa) mine; MS = Montgomery-Shoshone mine; My = Mayflower mine; OB = Original Bullfrog mine; OM = Oasis Mountain; P = Pioneer mine; S = Sterling mine; SB = Sleeping Butte; Si = Silicon mine; SG = Sober-up-Gulch; SP = Secret Pass Au deposit; T = Telluride mine; Th = Thompson mine; TH = Transvaal Hills; W = Wahmonie; Flsp Cny = Fluorspar Canyon; TM-I = Timber Mountain I caldera; TM-II = Timber Mountain II caldera; (SB) = Sleeping Butte caldera segment of Byers et al (1976a), herein abandoned; (OV) = Oasis Valley caldera segment of Byers et al. (1976a), herein abandoned. Dotted lines show porphyry dikes in Bare Mountain.

chemistry, and general appearance between the Paintbrush and Timber Mountain Tuffs (Byers et al., 1976a; Broxton et al., 1989; Warren et al., 1989). This change is but one example of the marked variability in the petrochemical nature of the magmas of the SWNVF (Noble et al., 1965).

Timber Mountain magmatic stage (11.5-10+ Ma)

The Timber Mountain magmatic system was superposed upon the waning magmatic system responsible for rocks of the Paintbrush Tuff of the main magmatic stage. The interval of time between the Paintbrush and Timber Mountain episodes was, however, shorter than, for example, that between the Huckleberry Ridge Tuff and the Lava Creek Tuff of the Yellowstone volcanic field, Wyoming (Christiansen, 1979), and between the Sunshine Peak Tuff and associated Lake City caldera and the earlier caldera-forming volcanism of the western part of the San Juan volcanic field, Colorado (Steven and Lipman, 1976). A number of volumetrically minor units of lava were emplaced between the Tiva Canyon and Rainier Mesa Members. Some of these lavas appear to have petrographic characteristics intermediate between the Paintbrush and Timber Mountain Tuffs (Broxton et al., 1989), and may reflect mixing of Timber Mountain magma with residual magma of the Paintbrush system.

The first major volcanic event of the Timber Mountain magmatic stage was the eruption of the Rainier Mesa Member of the Timber Mountain Tuff about 11.4 Ma (Table 1). The Rainier Mesa Member was preceded a few tenths of a million years or less by petrographically and chemically similar lavas erupted east and northwest of Beatty (Byers et al., 1976a; Broxton et al., 1989; S. I. Weiss and D. C. Noble, unpub. mapping, 1989). Rejuvenation of the Timber Mountain magmatic system led to the eruption of the Ammonia Tanks Member of the Timber Mountain Tuff about 11.4 Ma. The source area of the Ammonia Tanks Member was largely or entirely within the Timber Mountain caldera, which formed concurrently with eruption, and is now marked by a well developed and preserved resurgent dome. Two relatively small-volume units of ash-flow tuff that overlie the Ammonia Tanks Member, the tuff of Burtonhook Wash and the tuffs of Crooked Canyon, are also included within the Timber Mountain Tuff by Byers et al. (1976a).

Location of the western margin of the Timber

Mountain caldera: The geometry of the vent area and caldera associated with the Rainier Mesa Member has been a subject of debate. During the early stages of study of the SWNVF, it was believed that the Rainier Mesa Member was erupted from essentially the same vent area as that now accepted for the Ammonia Tanks Member. Noble, however, argued in 1966 that the caldera related to eruption of the Rainier Mesa Member extended west of the Timber Mountain caldera, encompassing what were subsequently termed by Byers et al. (1976a) the Oasis Valley and Sleeping Butte segments of the Timber Mountain-Oasis Valley caldera complex (D. C. Noble, unpub. manuscript, 1966, quoted in Byers et al., 1976a). Critical evidence for this interpretation was the presence of a distinctive unit of fresh, sphene-bearing ash-flow tuff containing a bimodal population of high-silica and low-silica rhyolite pumice, identified by Noble as the Ammonia Tanks Member, that mantles the east-facing scarp of the Sleeping Butte caldera segment as defined by Byers et al. (1976a, 1976b)(Fig. 2).

R. L. Christiansen, W. C. Carr, and K. A. Sargent studied parts of the area between Beatty and Sleeping Butte in 1971 (Byers et al, 1976a). They considered the sphene-bearing unit to be older than the Timber Mountain Tuff, and reinterpreted this part of the Timber Mountain caldera, which they named the Sleeping Butte caldera segment, as being the oldest segment of their Timber Mountain-Oasis Valley caldera complex (Byers et al., 1976a).

Field relations and new radiometric ages strongly support the original interpretation of Noble. The east-facing scarp of the Sleeping Butte segment of Byers et al. (1976a) is developed on a thick unit of ash-flow tuff that underlies the Grouse Canyon Member of the Belted Range Tuff (see Main Magmatic Stage, above; Table 1). The sphene-bearing cooling unit that mantles this east-facing scarp can be traced continuously to the north and northwest (Fig. 2; outcrop indicated by irregular solid black pattern), where it overlies thick outflow-facies tuffs of the Rainier Mesa Member of the Timber Mountain Tuff. In addition, a K-Ar age of 11.5 ± 0.4 Ma and a $^{40}\text{Ar}/^{39}\text{Ar}$ age of 10.7 ± 0.2 Ma (Table 2, Specimen 6) have been obtained on biotite from the sphene-bearing tuff. Phenocryst mineralogy, stratigraphic position above the Rainier Mesa Member, and radiometric age are all consistent with the original assignment of the unit to the Ammonia Tanks Member. The interpretation that the scarp is part of the topographic wall of the caldera that

**Table 1. Ash-Flow Sheets and Other Important Volcanic Units
of the Southwestern Nevada Volcanic Field**

Late magmatic stage

Stonewall Flat Tuff (Stonewall Mountain volcanic center)

Civet Cat Canyon Member
Spearhead Member (7.6 Ma)

Thirsty Canyon Tuff (Black Mountain volcanic center)

Gold Flat Member
Trail Ridge Member
Pahute Mesa Member
Rocket Wash Member

Timber Mountain magmatic stage

Rhyolite of Shoshone Mountain and rhyolite of Beatty Wash

Tuffs and lavas of the Bullfrog Hills

Timber Mountain Tuff (Timber Mountain I and II calderas)

Tuff of Buttonhook Wash and tuffs of Crooked Canyon
Tuffs of Fleur-de-Lis Ranch
Ammonia Tanks Member (11.4 Ma)
Rainier Mesa Member (11.4 Ma)

Pre-Rainier Mesa lavas (rhyolite and local basalt)

Main magmatic stage

Rhyolite of Windy Wash and rhyolite lavas of Fortymile Canyon

Paintbrush Tuff

Tiva Canyon Member (12.8 Ma)
Yucca Mountain Member
Pah Canyon Member
Topopah Spring Member

Tuffs and lavas of Calico Hills

Wahmonie and Salyer Formations

Crater Flat Tuff

Prow Pass Member
Tuff of Stockade Wash (not a member of the Crater Flat Tuff)
Bullfrog Member
Tram Member

Belted Range Tuff (Silent Canyon volcanic center; associated and intercalated with peralkaline silicic lavas)

Grouse Canyon Member
Tub Spring Member

Lavas of intermediate composition

Lithic Ridge Tuff

"Older" tuffs

Unit "A"
Unit "B"
Unit "C"

Sanidine-rich tuff

Tuff of Yucca Flat

Redrock Valley Tuff (15.2 Ma)

Modified from Byers et al. (1989), Broxton et al. (1989) and other sources. Bold type indicates individual ash-flow sheets. Ages of certain stratigraphically, tectonically, and/or volcanogenetically important ash-flow sheets are given in brackets.

Table 2.
New Radiometric Ages on Rocks of the
Southwestern Nevada Volcanic Field

Sample Number	Material	Conventional K-Ar Age Determinations				Age (Ma ± 1σ)
		K ₂ O (wt. %)	⁴⁰ Ar* (moles/gm)	⁴⁰ Ar* (percent)		
1	OBO-12A	nonhyd. glass	5.14	6.493 × 10 ⁻¹¹	72	8.8 ± 0.3
2	3DN9-20	biotite	9.28	1.377 × 10 ⁻¹⁰	42	10.1 ± 0.3
3	SMR-TOB	nonhyd. glass	5.71	8.477 × 10 ⁻¹¹	50	10.3 ± 0.3
4	Ter	sanidine	10.40	1.558 × 10 ⁻¹⁰	88	10.4 ± 0.3
5	3DN9-1	biotite	8.89	1.445 × 10 ⁻¹⁰	39	11.3 ± 0.3
6	3DN8-21	biotite	7.52	1.251 × 10 ⁻¹⁰	47	11.5 ± 0.4
7	87-2-11-4	adularia	7.68	1.434 × 10 ⁻¹⁰	59	12.9 ± 0.4
8	TWDK-BIO	biotite	8.63	1.863 × 10 ⁻¹⁰	48	14.9 ± 0.5
9	RR-BIO-2	biotite	8.62	1.875 × 10 ⁻¹⁰	49	15.1 ± 0.4

Sample Number	Material	⁴⁰ Ar/ ³⁹ Ar Multi-Grain Resistance Furnace (Total) Fusion Determinations				J	Age	
		40/39	37/39	36/39	⁴⁰ Ar*(%)			
6	3DN8-21	biotite	2.4669	0.0502	0.0047	44	0.007	10.7 ± 0.2
10	171-B	sanidine	2.1189	0.0149	2.1573	70	0.006	15.2 ± 0.2

Sample Number	Material	⁴⁰ Ar/ ³⁹ Ar Single Grain Laser Fusion Determinations		Age
		Number of Analyses		
7	87-2-11-4	adularia	3 analyses	12.9 ± 0.8
11	DN8-75	sanidine	6 analyses	11.4 ± 0.1
12	3SW-247	sanidine	6 analyses	11.7 ± 0.3
13	SW-269	sanidine	6 analyses	11.9 ± 0.7

1. Nonhydrated aphyric rhyolite obsidian from the south flank of Obsidian Butte; 37°18.3'N, 116°52.3'W.
2. Vapor-phase crystallized rhyolite ash-flow tuff of the tuffs and lavas of the Bullfrog Hills; north end of Burton Mountain; 36°55.9'N, 116°46.4'W.
3. Rhyolite lava, central Shoshone Mountain; 36°57.0'N, 116°16.7'W. Specimen is from the basal part of the uppermost flow of the rhyolite of Shoshone Mountain.
4. Partly welded, vapor-phase crystallized rhyolite ash-flow tuff of the tuff of Cutoff Road; 37°00.4'N, 116°35.6'W.
5. Densely welded glassy rhyolite ash-flow tuff from the basal vitrophyre of the lowermost cooling unit of the tuffs of Fleur-de-Lis Ranch; 37°00.6'N, 116°43.2'W.
6. Densely welded glassy rhyolite ash-flow tuff from the basal vitrophyre of the Ammonia Tanks Member of the Timber Mountain Tuff; 37°07.9'N, 116°43.1'W.
7. Hydrothermally altered quartz porphyry dike from the north pit of the Goldspar (Diamond Queen) mine, east flank of Bare Mountain; 36°50.7'N, 116°38.0'W.
8. Slightly hydrothermally altered quartz porphyry dike north of Bare Mountain; 36°54.3'N, 116°40.0'W.
9. Densely welded glassy rhyolite ash-flow tuff from the Redrock Valley Tuff; 37°06.6'N, 116°10.4'W.
10. Densely welded glassy rhyolite ash-flow tuff from the Redrock Valley Tuff; 37°06.6'N, 116°10.4'W.
11. Densely welded devitrified rhyolite ash-flow tuff from the upper cooling unit of the tuffs of Fleur-de-Lis Ranch; 37°02.8'N, 116°43.5'W.
12. Densely welded rhyolite ash-flow tuff from the Rainier Mesa Member of the Timber Mountain Tuff, north slope of Sober-Up Gulch; 36°58.5'N, 116°46.5'W.
13. Densely welded devitrified rhyolite ash-flow tuff from the west face of Oasis Mountain; 37°02.7'N, 116°45.4'W.

Constants: $\lambda_a = 0.581 \times 10^{-10} \text{ yr}^{-1}$, $\lambda_b = 4.962 \times 10^{-10} \text{ yr}^{-1}$, $^{40}\text{K}/\text{K}(\text{total}) = 1.167 \cdot 10^{-4} \text{ kmol/kmol}$. Precision of standard K-Ar age determinations in the Menlo Park laboratories is based on replicate analyses of Ar tracers, K₂O analyses, and calibration analyses. The plus and minus value of the ⁴⁰Ar/³⁹Ar laser fusion analyses is based on small population statistics of multiple analyses of individual grains.



Fig. 3. South side of Sleeping Butte composed of west-dipping rhyolitic ash-flow tuff probably belonging to the intracaldera tuff prism of a previously unrecognized collapse caldera.

formed as the result of eruption of the Rainier Mesa Member, and is not an older caldera wall, is supported by the absence of tuffs of the Rainier Mesa Member, or of older units, mantling the scarp beneath the dated exposures of the Ammonia Tanks Member.

Several lines of evidence, in part presented by Byers et al. (1976a), indicate that the Oasis Valley caldera segment was formed and subsided as a result of eruption of the Rainier Mesa Member of the Timber Mountain Tuff. These include caldera margin breccias, restudied by our group, similar to those described by Byers et al. (1976a) in the eastern and southern part of the Timber Mountain caldera. Additional evidence supporting the eruption of tuffs of the Rainier Mesa Member from vents within the Oasis Valley caldera segment are: 1) the presence of thick, large-scale and commonly lithic-rich surge deposits with phenocryst mineralogy typical of the Rainier Mesa Member lying beneath tuffs of the Rainier Mesa Member in the lower part of Beatty Wash and north of Beatty in the vicinity of Sober-up-Gulch, 2) the presence of tuffs of the Rainier Mesa Member in the Sober-up Gulch area north of Beatty (identification corroborated by radiometric dating; Table 2, Specimen 12) with secondary flowage, disruption, and crystallization features suggestive of near-vent deposition, and 3) the presence of lavas and associated surge deposits with

Rainier Mesa phenocryst mineralogy beneath the Rainier Mesa Member between Fluorspar Canyon and Beatty Wash and in the Sober-up Gulch area (Fig. 2).

The evidence presented above demonstrates that the Sleeping Butte and Oasis Valley caldera segments of Byers et al. (1976a, 1976b) should not be considered as separate, older structures of the Timber Mountain-Oasis Valley caldera complex. Instead, these areas comprise the western part of the area that subsided upon eruption of the Rainier Mesa Member of the Timber Mountain Tuff and are part of the Timber Mountain caldera (Timber Mountain I caldera, *see below*; Fig. 2). A later period of caldera collapse took place within the Timber Mountain caldera upon eruption of the Ammonia Tanks Member (Fig. 2); the well-preserved Timber Mountain resurgent dome is related to this inner caldera (Byers et al., 1976a). The term *Timber Mountain caldera* has long been attached to both the larger caldera related to eruption of the Rainier Mesa Member and the smaller, nested caldera that formed on eruption of the Ammonia Tanks Member. We suggest that the older caldera be referred to simply as the *Timber Mountain I caldera* and the younger as the *Timber Mountain II caldera*; collectively they may be termed the *Timber Mountain caldera complex*. The terms *Oasis Valley caldera segment* and *Sleeping Butte caldera segment* should be abandoned, as

perhaps should the term *Timber Mountain-Oasis Valley caldera complex*.

Tuffs of the Oasis Valley area: A sequence of cooling units of ash-flow tuff is exposed in the vicinity of Oasis Valley (Byers et al., 1976a). In outcrop and hand specimen these tuffs have the general appearance of the Timber Mountain Tuff.

The lowest unit, exposed on Oasis Mountain, has an exposed minimum thickness of 500 m and in its upper part has undergone strong secondary (reomorphic) flowage. Byers et al. (1976a) identified this tuff as the Ammonia Tanks Member of the Timber Mountain Tuff and proposed that its thickness reflected deposition within the westernmost part of the caldera that formed upon eruption of the Rainier Mesa Member. Christiansen et al. (1977), however, considered Oasis Mountain to lie outside of the Oasis Valley caldera segment (western part of Timber Mountain I caldera of this paper). The general phenocryst mineralogy of the unit is consistent with the unit belonging to the Timber Mountain Tuff, and the presence of sphene rules out the possibility that the unit is the Rainier Mesa Member. A $^{40}\text{Ar}/^{39}\text{Ar}$ age of 11.9 ± 0.7 Ma (Table 2, Specimen 13) obtained on sanidine from this unit is indistinguishable within the limits of analytical uncertainty from the age of the Ammonia Tanks Member.

The cooling units overlying the thick section of tuff exposed on Oasis Mountain provisionally assigned to the Ammonia Tanks Member have been termed the tuffs of Fleur-de-Lis Ranch by Byers et al. (1976a). Petrographically, these tuffs range from low-silica rhyolite containing moderately abundant phenocrysts of plagioclase, biotite, and clinopyroxene accompanied by little or no quartz and sanidine to tuffs containing abundant large phenocrysts of sanidine and quartz. Sphene has been identified in all units. Locally the first and second cooling units are separated by a flow of rhyolite lava. The stratigraphically highest cooling unit of the tuffs of Fleur de Lis Ranch is composed of sphene-bearing high-silica rhyolite megascopically and microscopically similar to high-silica rhyolite tuffs of the Ammonia Tanks Member whereas the other cooling units exhibit significant vertical compositional variations.

Several features of the tuffs of Fleur de Lis Ranch suggest contemporaneous movement along nearby faults. A unit of probable talus or debris flow origin composed of blocks of tuff and lava, in part of Rainier Mesa lithology, is present at the base of the first cooling unit. Large (as much as 0.25 m) lithic fragments locally present within the various cooling units, a zone of opal-impregnated tuff blocks present beneath the upper cooling unit, and brecciation locally present within the upper cooling unit are provisionally interpreted as having resulted from gravity sliding shortly after deposition (K. A. Connors, unpub. mapping, 1990). Coarse lithic-rich horizons are also present in the upper part of the Ammonia Tanks(?) Member exposed on Oasis Mountain.

A K-Ar age of 11.3 ± 0.3 Ma has been obtained on the stratigraphically lowest cooling unit and a $^{40}\text{Ar}/^{39}\text{Ar}$ age

of 11.4 ± 0.1 Ma has been obtained on the upper cooling unit (Table 2, Specimens 5 and 11). The tuffs of Fleur-de-Lis Ranch are therefore coeval, within the limits of analytical uncertainty, with the Ammonia Tanks Member of the Timber Mountain Tuff.

It is unclear whether most or all of the tuffs of Fleur-de-Lis Ranch were erupted from the same magma chamber from which the Ammonia Tanks Member was erupted or whether they are partly or entirely local units erupted at the same time as the Ammonia Tanks Member from an independent or semi-independent magma chamber of the Timber Mountain system in a manner similar to that described for tuffs related to the Yellowstone caldera (Christiansen, 1979) and the Uncompahgre and San Juan calderas (Steven and Lipman, 1976). The Ammonia Tanks Member has been recognized elsewhere as a composite sheet (Broxton et al., 1989). Based on petrography, stratigraphic position, and radiometric age, the thick unit of tuff exposed on Oasis Mountain and/or the upper cooling unit of the tuffs of Fleur-de-Lis Ranch may perhaps correlate with the Ammonia Tanks Member of the Timber Mountain Tuff as defined by Byers et al. (1976a).

Tuffs and lavas of the Bullfrog Hills: West and northwest of Beatty, Nevada (Fig. 2), outflow-facies tuffs of the Ammonia Tanks Member of the Timber Mountain Tuff are overlain by a locally complex, generally east-dipping sequence of lavas and tuffs here informally termed the tuffs and lavas of the Bullfrog Hills. These units generally dip less steeply than the Ammonia Tanks Member, and in places appear to be separated by an angular unconformity from underlying volcanic rocks. In many areas the Ammonia Tanks Member is overlain by flows of dark olivine-bearing basalt or basaltic andesite. These flows are in turn overlain by a sequence of slightly to moderately welded silicic tuffs that are very similar in phenocryst mineralogy and content to the more silicic parts of the Rainier Mesa Member (Fig. 4a). In some places these high-silica rhyolite tuffs exhibit poor sorting and lack of structure characteristic of pyroclastic flow origin; in other horizons and/or localities they possess large-scale sand-wave and cross bedding produced by surge transport and deposition. Lithic fragments, mainly of rhyolite lava, are very abundant in many horizons and locally form lenses with relatively little tuffaceous matrix. These lithic-rich zones, which locally contain blocks as large as 0.5 m in diameter, probably represent a combination of coarse surge deposits, debris flows, and lag deposits. The common surge deposits and typically abundant lithic fragments together indicate proximity to their vent areas. In most localities flows of rhyolite lava are intercalated within and overlie the tuffs (Figs. 4a, 4b), suggesting eruption of devolatilized silicic magma from high-level chambers alternating with the explosive eruption of more deeply situated volatile-rich high-silica rhyolite magma. This sequence of rhyolitic tuffs and lavas has been termed the "rhyolite lavas flows and tuffs of Rainbow Mountain" by Maldonado (1990).



Fig. 4. Tuffs and lavas of the Bullfrog Hills exposed on Rainbow Mountain, southeastern Bullfrog Hills. A sequence of alternating high-silica rhyolite ash-flow tuff (T) and rhyolite lava (R) are capped by flows of latite (L). 4a, view from southwest; 4b, view from south.

The sequence of silicic tuffs and lavas postdating the Ammonia Tanks Member is overlain by a number of flows of biotite-bearing latite and quartz latite (Fig. 4b). Some flows, for example the "quartz basalt" of Ransome et al. (1910), contain abundant large phenocrysts of quartz. These phenocrysts, which exhibit reaction relations with the groundmass, suggest the coexistence and mixing of rhyolite and latite magmas.

K-Ar ages on the silicic and intermediate lavas of about 10 to 11 Ma (Morton et al., 1977; Marvin and Cole, 1978; Marvin et al., 1989; Monsen et al., 1990) and a new age of 10.1 ± 0.3 Ma (Table 2, Specimen 2) for one of the ash-flow units together indicate that these rocks were deposited prior to about 10 Ma.

Tuffs are exposed east of Beatty that are petrographically very similar to and probably correlative with the rhyolitic tuffs of the tuffs and lavas of the Bullfrog Hills. Between Fluorspar Canyon and Beatty Wash (Fig. 2), the Ammonia Tanks Member is overlain by several flows of dark olivine-bearing lava that contain an intercalated unit of densely welded rhyolitic ash-flow tuff (ash-flow tuff Taf of Monsen et al., 1990) with a phenocryst mineralogy indistinguishable from that of the ash-flow tuffs belonging to the tuffs and lavas of the Bullfrog Hills. A cooling unit of rhyolitic ash-flow tuff exposed on the western flank of the Transvaal Hills was mapped by Lipman et al. (1966; Byers et al., 1976b) as the tuff of Cutoff Road. We have obtained a K-Ar age of 10.4 ± 0.3 Ma (Table 2, Specimen 4) on this unit, and believe that it may be a distal facies of the tuffs and lavas of the Bullfrog Hills. Domes and flows of silicic and intermediate lava, including large volumes of low-silica rhyolite generally poor in quartz phenocrysts, are also exposed over large areas in the western part of the Bullfrog Hills (Cornwall and Kleinhampl, 1964) and the eastern part of the Grapevine Mountains (Cornwall, 1972; Fig. 2).

Rocks of similar age and lithology are present, although in lesser volume, east of Bare Mountain. An age of 9.3 ± 0.3 Ma has been obtained on a specimen from the basal part of the rhyolite of Shoshone Mountain southeast of the Timber Mountain caldera (Marvin et al., 1989) and rhyolite lava that forms the uppermost part of Shoshone Mountain have been dated at 10.3 ± 0.3 Ma (Table 2, Specimen 3). We believe that the older age, obtained on nonhydrated glass, more closely approximates the true age of the sequence of flows. The rhyolite of Beatty Wash, present in the moat of the Timber Mountain caldera, is of similar age (Byers et al., 1976a; 1976b; Broxton et al., 1989).

We consider the silicic rocks of the tuffs and lavas of the Bullfrog Hills, the rhyolite of Shoshone Mountain, and the other lithologically similar rhyolitic lavas and tuffs of comparable age, and probably also the latite lavas, are an integral part of the Timber Mountain volcanic suite, although they are about 1 m.y. younger than the Ammonia Tanks Member (Jackson et al., 1988). The lines of evidence supporting this interpretation are: 1) the close lithologic and petrographic similar-

ity between the post-Ammonia Tanks Member tuffs of the tuffs and lavas of the Bullfrog Hills and the lower, rhyolitic tuffs of the Rainier Mesa Member and 2) the distribution of these rocks around and within the Timber Mountain I caldera. The Timber Mountain magmatic stage lasted for 1 to 1.5 million years, a period comparable to the lifetimes of other major caldera-forming silicic systems such as Valles, New Mexico, Long Valley, California, and Yellowstone, Wyoming. The stage evolved from major caldera-forming pyroclastic volcanism to the eruption of silicic and intermediate lavas and local units of rhyolitic tuff. This latter phase of volcanic activity, which was most intense west of the Timber Mountain I caldera, probably took place over a significant interval of time and did not result in the formation of collapse calderas or cauldron subsidence structures. Although the western margin of the Timber Mountain I caldera is located on the eastern edge of the Bullfrog Hills, it is emphasized that there is no evidence for a caldera within or encompassing the Bullfrog Hills, as was proposed by Cornwall (1962) and Cornwall and Kleinhampl, (1964).

Late magmatic stage (9-7 Ma)

Rocks of the late magmatic stage are mostly related to the Black Mountain and Stonewall Mountain volcanic centers (Figs. 1 and 2; Table 1) and include subalkaline and peralkaline ash-flow tuffs and highly potassic silicic and intermediate lavas of alkaline to peralkaline character (Noble and Christiansen, 1974; Noble et al., 1984; Weiss and Noble, 1989; Vogel et al., 1989).

These centers, located in the northwestern part of the SWNVF, were active between about 9 and 7 Ma. New $^{40}\text{Ar}/^{39}\text{Ar}$ ages on the Spearhead and Civer Car Canyon Members of the Stonewall Flat Tuff (Deino et al., 1989; Hausback et al., 1990) show that earlier K-Ar ages of 6.3 Ma are in error and that the units were erupted about 7.6 and 7.4 Ma, respectively. The Thirsty Canyon Tuff is older than the Stonewall Flat Tuff, and new radiometric ages (E. H. McKee and D. C. Noble, unpublished data) suggest that activity at the Black Mountain volcanic center began about 8.5 to 9.0 Ma. Also included in the late magmatic stage are voluminous aphyric to phenocryst-poor rhyolite lavas of Obsidian Butte (Fig. 1), on which an age of 8.8 ± 0.3 Ma have been obtained (Table 2, Specimen 1).

Mafic and silicic lavas were also erupted during this period in various places within the SWNVF and in areas to the west and north (Noble et al., 1990; unpub. data, 1987-1989). Indeed, the very significant period of time between the Timber Mountain and late magmatic stages, the distribution of silicic rocks younger than about 9 Ma to the northwest of the vent areas of the main and Timber Mountain magmatic stages, and evidence for a major period of faulting and extension between the two stages (see below) suggests that the rocks of the late magmatic stage should perhaps not be considered as part of the SWNVF.



Figure 5. View of southwest side of Mount Jackson, the largest endogeneous dome of the Mount Jackson dome field. Flow-foliated rhyolite lavas, dated at 2.9 Ma, overlie light-colored crossbedded surge deposits of the associated tuff ring, which in turn overlie older dacite lavas of the field.

Late Pliocene silicic volcanism of the Mount Jackson Dome field southwest of Goldfield (Figs. 1, 5) (McKee et al., 1989; Noble et al., 1990) appears to reflect a distinct later pulse of magmatic activity more closely related to late Pliocene and Quaternary silicic, intermediate, and mafic volcanism along the western margin of the northern Basin and Range province. Magmatic activity of this belt includes that of the Long Valley caldera (Bailey 1989), the Coso volcanic field (Bacon et al., 1982; Novak and Bacon, 1986), and Saline Range volcanic field in northern Death Valley (Elliott et al., 1984)

Hydrothermal Activity

A number of centers of Neogene hydrothermal activity and mineralization, including major producing mines such as the Sterling, Bond Gold Bullfrog, and Gold Bar, are found within the SWNVF. Various workers have reported on the mines and prospects within the SWNVF (e.g., Ransome et al., 1910; Cornwall and Kleinhampl, 1964; Ahern and Corn, 1981; Bell and Larson, 1982; Odt, 1983; Tingley, 1984; Quade and Tingley, 1984; Jorgensen et al., 1989; Greybeck and Wallace, 1990; Mapa, 1990). Until recently, however, there has been little information on the time-stratigraphic or structural

settings of mineralization in the field, and too few data to associate hydrothermal activity and mineralization with magmatic activity.

Two general periods of hydrothermal activity can be recognized in the SWNVF: An early period related to the main magmatic stage and a later period related to the Timber Mountain magmatic stage (Jackson et al., 1988; Jackson, 1988). Hydrothermal activity was more widely distributed and more intense, and economic and potentially economic mineral deposits are more abundant, in the western part of the volcanic field.

Hydrothermal activity related to main stage magmatism

Evidence for hydrothermal activity early in the evolution of the SWNVF is found in the Sleeping Butte area, where altered welded tuffs exposed east of Sleeping Butte are overlain by unaltered ash-flow tuff of the 14-Ma Grouse Canyon Member of the Belted Range Tuff. In the Bullfrog Hills between the Mayflower mine and Sober-up-Gulch (Fig. 2) unaltered rocks predating the 11.4-Ma Timber Mountain Tuff overlie hydrothermally altered ash-flow tuffs. At Wahmonie, southeast of the Timber Mountain caldera complex (Fig. 2), hydrother-



Figure 6. North wall of the open pit of the Bond Gold Bullfrog mine, December, 1989. Welded ash-flow tuffs of the Rainier Mesa Member of the Timber Mountain Tuff and other units dip to the east (right); Light-colored sheared, silicified and otherwise hydrothermally altered zone containing most of the ore of the deposit dips to the west (left).

mal activity dated at about 12.5 to 13.0 Ma was coeval with, or slightly younger than, the lavas and intrusive bodies of the Wahmonie center and with the Paintbrush Tuff (Jackson, 1988). A similar age has been obtained for fine-grained hypogene alunite from the Thompson Mine, which is hosted by the Paintbrush Tuff, adjacent to the southwestern margin of the Claim Canyon cauldron segment (Jackson, 1988).

Similar age relationships have been established for the hydrothermal activity that produced the various sedimentary- and volcanic-rock hosted gold and fluorite deposits along the eastern and northern flanks of Bare Mountain. At the Sterling, Goldspar, Telluride, and GEXA properties on the east and north sides of Bare Mountain, hydrothermal activity postdated the emplacement of the previously mentioned porphyry dikes, which are closely associated spatially with mineralization. K-Ar and $^{40}\text{Ar}/^{39}\text{Ar}$ ages of 12.9 ± 0.4 and 12.9 ± 0.8 Ma, respectively, (Table 2, Specimen 7) have been obtained on hydrothermal potassium feldspar that pseudomorphs phenocrysts of igneous potassium feldspar in the dike at the Goldspar mine. In the upper part of Fluorspar Canyon, hydrothermal alteration and mineralization has strongly affected the Crater Flat Tuff as well as pre-Cenozoic rocks in the vicinity of the Daisy (Crowell) mine (Greybeck and Wallace, 1990; J. D.

Greybeck, personal commun., 1989). Ages of 11.2 ± 0.3 and 12.2 ± 0.4 Ma have been obtained on fine-grained hypogene alunite from the Telluride mine (Jackson, 1988).

The gold and fluorite mineralization, accompanied by anomalous concentrations of Mo, As, Sb, Hg, and Tl (Tingley, 1984; Greybeck and Wallace, 1990), in these areas was probably deposited from relatively dilute hydrothermal fluids developed late in the evolution of the magmatic system beneath Bare Mountain (Noble et al., 1989). High-salinity fluids, as demonstrated by fluid inclusions containing halite and other daughter minerals, were evolved earlier by the system, which may perhaps have petrochemical similarities to the Late Cretaceous lithophile-element rich systems of the Great Basin (Barton and Trim, 1990). Possible analogues are provided by the carbonate-hosted gold deposits at Tennessee Pass, Colorado (Beatty et al., 1987), Rico, Colorado (Larson, 1987), the Kidston deposit, Australia (Baker et al., 1987) and the Au-Ag veins of the Shila district, southern Peru (J. Benavides A., D. C. Noble and K. A. Swanson, unpub. data, 1989). A similar origin for the epithermal precious-metal veins of the Wahmonie district seems likely.

Evidence for hydrothermal activity and mineralization that postdate eruption of the Timber Mountain Tuff is found in a number of areas. The prospects and mineral deposits of this age are adularia-sericite type systems characterized by very low base metal contents and relatively low Ag/Au ratios. Intense potassium metasomatism and adularization is present in many places, for example in the Mayflower-Pioneer and Montgomery-Shoshone and Bond Gold Bullfrog areas in the Bullfrog Hills (Fig. 2).

In some places hydrothermal activity followed eruption of units of the Timber Mountain Tuff by 0.5 m.y or less, and elsewhere took place as much as 2 to 2.5 m.y. later. Major hydrothermal activity of this period occurred in the Calico Hills (Fig. 2) southeast of the Timber Mountain caldera complex (Jackson et al., 1988; Jackson, 1988) and at Mine Mountain farther to the east (E. H. McKee and S. I. Weiss, unpub. data). K-Ar ages and borehole data on alteration minerals in tuffs of the main magmatic stage beneath Yucca Mountain (Aronson and Bish, 1987; Bish, 1988) indicate that a hydrothermal system of large lateral extent existed near the southern margins of the Timber Mountain caldera complex during this period.

Areas of hydrothermal alteration and mineralization are generally more abundant in the western part of the volcanic field (Fig. 2). The presently producing precious-metal deposits of this age, including the Gold Bar mine and the recently opened 7,500 ton/day Bond Gold Bullfrog mine (Fig. 6), and virtually all of the previously producing precious-metal deposits of this age, including the Original Bullfrog, Montgomery-Shoshone, Mayflower, and Pioneer, are located in the Bullfrog Hills. Areas outside the Bullfrog Hills include the Transvaal Hills, Silicon Mine-Tram Ridge, and Oasis Mountain areas east of U.S. Highway 95 (Jackson et al., 1988; Jackson, 1988). Stratigraphic and radiometric data available for these areas indicate that most of the hydrothermal activity of this period postdates the 11.4-Ma Timber Mountain Tuff. Farther to the west, in the western part of the Bullfrog Hills and the eastern part of the Grapevine Mountains, hydrothermal alteration affects the Paintbrush and Timber Mountain Tuffs, suggesting a similar age for development of these systems.

Hydrothermal activity during the late magmatic stage

Although no hydrothermal activity occurred at the Black Mountain volcanic center, hydrothermal activity and the deposition of presently subeconomic quantities of precious metals took place at the Stonewall Mountain center (Noble et al., 1988).

The later stages of development of the SWNVF have most likely involved a complex interplay between deformation associated with: 1) the rise, accumulation and eruption of the magma bodies that produced the tremendous volumes of silicic ash-flow tuff, 2) deep structures of the Walker Lane structural belt, and 3) shallower structures that have accommodated major upper crustal extension in the region. The SWNVF is situated within a part of the Walker Lane belt for which active, throughgoing strike-slip faults characteristic of other parts of the Walker Lane belt are poorly developed and, where present, have experienced very little movement since middle Miocene time (Stewart, 1988). Extension in southwestern Nevada has long been recognized, with normal faulting beginning prior to inception of the SWNVF and in places postdating eruption of the late Miocene Stonewall Flat Tuff (Ekren et al., 1968; Weiss, 1987; Hausback and Frizzell, 1987). Doming and faulting related to various stages of caldera development have been important in the area of the Timber Mountain caldera complex and the Claim Canyon cauldron segment (e.g., Christiansen et al., 1965; 1977).

Pronounced late Paleogene uplift, faulting, and erosion are demonstrated by coarse conglomerates and interfingering megabreccia deposits in the Oligocene Titus Canyon Formation exposed in the Grapevine Mountains and locally in the Bullfrog Hills (Stock and Bode, 1935; Cornwall and Kleinhampfle, 1964; Reynolds, 1969). Post-depositional compression is indicated by rounded cobbles within the Titus Canyon Formation that have been fractured, deformed, and reheated subsequent to deposition. Normal faulting of early to middle Miocene age, in part low-angle and perhaps locally associated with the exposure of a metamorphic core complex, is documented in the Mellan Hills-Trappman Hills area and the Cactus, Kawich, and Belted Ranges within the Northern Nellis Bombing and Gunnery Range (Ekren et al., 1968, 1971; McKee, 1983) and within the Goldfield district (Ashley, 1974). Evidence for the onset of rotational faulting and related uplift and erosion by early middle Miocene time is present in the Gold Mountain-Slate Ridge area (J. E. Worthington, D. C. Noble, and S. I. Weiss, unpub. mapping, 1989-1990). Conglomerate of possible early Miocene age is present at Joshua Hollow on the northeast flank of Bare Mountain (Carr and Monsen, 1988; Monsen et al., 1990). Schweickert and Caskey (1990) have suggested that some faults mapped in pre-Cenozoic rock to the south may be of Cenozoic, and perhaps in part of Neogene, age. Northwest- (e.g., Yucca-Frenchman) and northeast-trending strike-slip faults have been recognized east of Timber Mountain in the Nevada Test Site (Yucca Flat-Frenchman Flat and Mine Mountain-Spotted Range structural zones of Carr, 1974, 1984a), and right-lateral offset along a north- to northwest-trending strike slip fault or fault zone between Yucca Mountain and Bare Mountain has been proposed by

Schweickert (1989; see also Carr et al., 1986; 1988). Right-lateral movement along this fault may explain the clockwise rotation of exposures of the Paintbrush Tuff in the southern part of Yucca Mountain (Scott and Rosenbaum, 1986).

Most of the movement along these Walker Lane structures in the SWNVF, however, appears to have taken place prior to onset of volcanic activity of the SWNVF about 15 Ma, although appreciable movement appears to have taken place on the southern part of the Walker Lane belt between about 12 and 9 Ma (Duebendorfer et al., 1990). Volcanic rocks of the main magmatic stage are in places offset, but only very locally, as at Mine Mountain, has the Timber Mountain Tuff been affected by these deep-seated strike-slip structures (Carr, 1984a). It has been suggested that major volcanic centers of the field developed above deep-seated pull apart structures at right steps between shear zone segments (Carr, 1984b; 1988b; Carr et al., 1986); however, there is little direct evidence to support this model.

Regional topography during Timber Mountain time

The Timber Mountain Tuff is, in general, thicker and more widely distributed west and northwest of the Timber Mountain caldera complex than to the east and south (Albers and Stewart, 1972; Byers et al., 1976a; Carr, 1984a; S. I. Weiss and D. C. Noble, unpub. mapping). The northwesternmost known exposure of the Timber Mountain Tuff is in the western Sylvania Mountains (37°19'N, 117°38'W), where an east-dipping section composed of the Rainier Mesa and Ammonia Tanks Members is faulted against granitic rocks of the Sylvania pluton (McKee, 1985; D. C. Noble and S. I. Weiss, unpub. data, 1989). This suggests that the area to the west-northwest of the complex lay at a significantly lower average elevation than the area to the east and south.

Neogene faulting and block rotation in the Bullfrog Hills

Volcanic rocks exposed along the northern margin of Bare Mountain, in the Bullfrog Hills, and in the Oasis Valley area dip moderately to steeply to the east and are cut by numerous, generally west-dipping normal faults, a style of deformation long considered indicative of crustal extension (e.g., Emmons and Garrey, Fig. 15, p. 84, in Ransome et al., 1910; Stewart, 1978). In the southern Bullfrog Hills and along the northern margin of Bare Mountain the faulted and tilted Neogene section is separated by one or more low-angle structures (the "Original Bullfrog-Fluorspar Canyon detachment fault") from Late Precambrian and Paleozoic sedimentary rocks and, locally, from gneisses and other metamorphic rocks (Ransome et al., 1910; Cornwall and Kleinhampl, 1964; Maldonado, 1985). Reset ages of 16.3 ± 0.4 Ma (muscovite), 14.6 ± 0.9 Ma (hornblende), and 11.2 ± 1.1 Ma (muscovite) have been

obtained on the metamorphosed rocks (McKee, 1983; Marvin et al., 1989), and McKee (1983) pointed out the similarity of the structural picture to that of various metamorphic core complexes in the Basin and Range Province. Since then, much attention has been focused on the nature and amount of cumulative movement on the Original Bullfrog-Fluorspar Canyon fault system and on possible eastward and westward extensions of this structure (Maldonado, 1985; 1988; Scott, 1986, 1988; Scott and Whitney, 1987; Carr, 1988a, 1988b; Carr and Monsen, 1988; Hamilton, 1988).

Timing of extension and volcanic activity in the western SWNVF

In contrast to Yucca Mountain and much of the Nevada Test Site region, where extensional faulting more strongly affects units of the Paintbrush Tuff and older rocks (Carr, 1984a; 1988), extension above the Original Bullfrog-Fluorspar Canyon fault in the Bullfrog Hills began after deposition of the Ammonia Tanks Member of the Timber Mountain Tuff about 11.4 Ma, but prior to deposition of the tuffs and lavas of the Bullfrog Hills. This is shown by the conformable relationships between units of the Timber Mountain Tuff and the underlying older ash-flow sheets in the southern Bullfrog Hills, and by the fact that the Timber Mountain Tuff is in many places more steeply dipping than nearby rocks of the tuffs and lavas of the Bullfrog Hills (Cornwall and Kleinhampl, 1964; Weiss et al., 1990; S. I. Weiss and K. A. Connors, unpub. mapping, 1989).

Extension began earlier in the northern part of Bare Mountain. Here stratigraphic and structural relations suggest that faulting and local tilting of the Paintbrush Tuff and older rocks occurred prior to eruption of the Timber Mountain Tuff (Carr, 1988; Carr and Monson, 1988; J. D. Greybeck, unpub. mapping, 1989; Monsen et al., 1990). In the Oasis Valley area, faulting appears to have taken place during the time the Ammonia Tanks Member was deposited (see above).

Several lines of evidence indicate that normal faulting and block rotation in the western part of the SWNVF took place both during and after eruption of the several units that compose the tuffs and lavas of the Bullfrog Hills. Dips decrease upwards within the tuffs and lavas of the Bullfrog Hills in several areas, particularly between rhyolitic ash-flow tuffs and lavas and overlying latite flows southwest of Donovan Mountain (Cornwall and Kleinhampl, 1964) and locally between flows of latite southwest of Indian Springs (S. I. Weiss and K. A. Connors, unpub. mapping, 1989). In the vicinity of the Mayflower mine and north and east of the Pioneer mine extensive layers of breccia containing abundant clasts, some many meters in diameter, of both pre-Cenozoic rock and Cenozoic welded tuff, including blocks of both the Rainier Mesa and Ammonia Tanks Members, are overlain by rhyolitic ash-flow tuffs of the tuffs and lavas of the Bullfrog Hills. These are interpreted as debris flows and slide masses shed off nearby fault scarps prior



Fig. 7. Spearhead Member of the Stonewall Flat Tuff at an elevation of 6,789 feet between Slate Ridge and Gold Mountain. Horizontal ash-flow tuff unconformably overlies south-dipping gravels that in turn overlie more steeply dipping rocks of the Timber Mountain Tuff.

to eruption of some or all of the tuffs and lavas of the Bullfrog Hills.

Locally silicic domes and lavas are closely associated with generally north-south trending faults: several small domes are aligned in a north-south trend at the west base of Donovan Mountain, and in some areas steeply-dipping flow banding preferentially strikes north-south. A feeder dike that widens upward into a flow directly south of Sober-up-Gulch intrudes a north-south fault. These features suggest that the magmatic activity and volcanism that produced the tuffs and lavas of the Bullfrog Hills took place under the same direction of least principal stress as did extensional faulting, and support the interpretation of coeval volcanism and extension in the western part of the SWNVF (Weiss et al., 1990).

The latest generation of normal faults cuts and rotates complete sections of the tuffs and lavas of the Bullfrog Hills, indicating that extension continued after their eruption. An upper limit on the time of this period of extension is provided by the 7.6-Ma age of the Spearhead Member of the Stonewall Flat Tuff. As emphasized by Weiss et al. (1988), the Spearhead Member was not, as previously believed by Maldonado (1985, 1988), affected by the pervasive tilting that affected older rocks within the Bullfrog Hills. Flat-lying distal

flows of the Spearhead Member were deposited in low areas of the Bullfrog Hills and Oasis Valley unconformably over the older, highly extended and tilted rocks of the area. (The last sentence of the Weiss et al. 1988 abstract was insisted upon by Florian Maldonado who withdrew his name after submittal because he then firmly believed that the Spearhead Member was involved in the rotational faulting of the Bullfrog Hills.) In the lower part of Oasis Valley and near the mouth of Beatty Wash, the Spearhead Member was deposited within and overlain by an extensive, flat-lying sequence of coarse gravel and conglomerate deposits that lap directly upon the faulted and rotated rocks above the Fluorspar Canyon fault to the south and southeast and the highly extended rocks of the Bullfrog Hills to the west and southwest.

Faulting very similar in style and age to that in the Bullfrog Hills is present in the Gold Mountain-Slate Ridge area of southern Esmeralda County (McKee et al., 1990; Noble et al., 1990), where north-northwest dipping listric(?) faults cut the Timber Mountain Tuff. The resultant rotated and eroded tuffs and underlying rocks are overlain unconformably by coarse gravels that in turn are overlain by the Stonewall Flat Tuff (Fig. 7).

Syntectonic volcanism and geometry of extensional faults in the western part of the SWNVF

Features of the silicic domes and feeder dikes of the tuffs and lavas of the Bullfrog Hills and other geologic relations provide evidence for the interaction of post-collapse magma of Timber Mountain type with high-level normal faults accommodating extension (Weiss et al., 1990). An inference drawn from this is that the ash-flow tuffs and surge deposits of the tuffs and lavas of the Bullfrog Hills, within which the rhyolite lava flows are intercalated, were also erupted from linear fissure vents controlled by extensional faults, perhaps as these faults intersected, or were invaded by, bodies of volatile-charged silicic magma.

Similar evidence suggests that the tuffs of Fleur-de-Lis Ranch (coeval with the Ammonia Tanks Member), and possibly the underlying unit of ash-flow tuff exposed on Oasis Mountain provisionally assigned to the Ammonia Tanks Member, were also erupted from fissure vents produced by extensional faulting. The units are of small areal extent and locally contain large lithic fragments and lenses of microbreccia, which suggest nearness to vent areas and/or to steep, unstable topography. The great thickness of the unit of tuff exposed on Oasis Mountain, the presence of rheomorphically deformed tuff and angular discordance in compaction foliation, and lenses of coarse lithic blocks within the unit are consistent with deposition upon an unstable slope and possibly within an actively forming tectonic depression.

The Original Bullfrog-Fluorspar Canyon detachment system probably accommodated extension only in the upper few kilometers of the crust in the western part of the SWNVF. It is the consensus of recent workers that west-northwest directed movement of the upper plate is indicated by the generally eastward rotation of fault blocks (e.g., Maldonado, 1985; 1988; Carr and Monson, 1988; Hamilton, 1988). The "breakaway zone" or eastern limit of this faulting is inferred to lie north of Bare Mountain and west of Tram Ridge, and from lower Fluorspar Canyon through the southern Bullfrog Hills, the fault generally dips about 20° to 30° northward (Ransome et al., 1910; Cornwall and Kleinhampl, 1964; Carr and Monson, 1988).

The Cenozoic volcanic section in the Bare Mountain-Bullfrog Hills area was about 3 km or less in thickness prior to eruption of the tuffs and lavas of the Bullfrog Hills (Maldonado, 1990; Monson et al., 1990). The magma bodies that fed the tuffs and lavas of the Bullfrog Hills and the tuffs of the Oasis Valley area were, therefore, situated at appreciably deeper levels than the detachment, even if during extension the fault dipped more steeply westward than at present. It is inferred that the normal faults that fed eruptions of the tuffs and lavas of the Bullfrog Hills and the tuffs of the Oasis Valley area must have penetrated considerable distances beneath the Original Bullfrog-Fluorspar Canyon low-angle fault system and that these and perhaps other deeper structures, presumably also of extensional origin, facilitated the

upward movement of magma (Weiss et al., 1990). Either case requires extension well *below* the Original Bullfrog-Fluorspar Canyon fault system, which has been considered as the major extensional structure in the region. This line of reasoning supports the concept that in some regions brittle extensional strain is not entirely accommodated by high-level detachment-style faulting.

The silicic tuffs and lavas of the Bullfrog Hills, tuffs and lava of the Oasis Valley area, and the thick sequence of silicic domes, flows and tuffs in the western Bullfrog Hills and northern Grapevine Mountains represent a large volume of silicic magma erupted during and after formation of the Timber Mountain caldera. The rhyolitic tuffs are best developed in the eastern part of the Bullfrog Hills, and probably were erupted from vents located relatively close to the western topographic margin of the Timber Mountain I caldera. The striking petrographic similarity of the high-silica rhyolite tuffs of the tuffs and lavas of the Bullfrog Hills to the lower part of the Rainier Mesa Member suggests that they were derived from the same caldera-related magma suite as were the various ash-flow sheets of the Timber Mountain Tuff. The silicic lavas are more widely distributed, extending westward into the Grapevine Mountains, and show a much greater range in phenocryst abundance and mineralogy and, presumably, chemical composition.

We hypothesize that rapid syn- and post-Ammonia Tanks extension in the western part of the SWNVF not only provided numerous, closely spaced feeder structures and frequent eruption triggers, but may also have promoted the generation of relatively small bodies of chemically diverse magma from which some of the silicic to intermediate lavas were erupted. The basalt flows commonly present at the base of the tuffs and lavas of the Bullfrog Hills may be the surface manifestation of the major input of mafic magma into the crust required to produce the more silicic magmas. Thus, extension may have led to the shift to widespread eruption of silicic and intermediate lava and precluded the accumulation of volumes of magma of sufficient size and instability necessary for further large-scale caldera-producing volcanism in the region west of the Timber Mountain caldera.

Relation of Hydrothermal Mineralization to Extension and Volcanism

Based on past and current production and on recent discoveries, it appears that more productive hydrothermal activity of the Timber Mountain stage took place in the Bullfrog Hills, concurrent with and slightly after syntectonic volcanism there, than in other parts of the volcanic field. Numerous, closely spaced extension-related faults in the Bullfrog Hills probably provided better ground preparation and channelways for hydrothermal fluids. Another factor may have been the presence of intermediate magma at high levels in the crust beneath the Bullfrog Hills. Calc-alkalic lavas of intermediate composition magmas are closely associated

with epithermal mineralization in many districts, for example, Bodie, California, Paradise Peak, Nevada, and Arcata, Peru, (Silberman et al., 1972; John et al., 1989; Candiotti et al., 1990). With the exception of the Wahmonie center of the main magmatic stage, only small volumes of intermediate rocks are known elsewhere in the central and eastern parts of the SWNVF. Studies of the pumice fragments and cognate inclusions in the Timber Mountain Tuff have demonstrated the presence, presumably within the lower parts of the magma chambers, of intermediate magmas, some having SiO₂ contents of less than 60 wt. percent (Byers et al., 1968; Broxton et al., 1989; Warren et al., 1989). These intermediate magmas did not reach the surface within the Timber Mountain caldera complex, and may not have ascended into the upper crust if the geochemical evidence for a deep silicic magma chamber for the Timber Mountain Tuff and other units (Warren et al., 1989; Stormer and Whitney, 1985) is correct. In the Bullfrog Hills, however, the presence of such magmas near the surface is shown by the areally extensive sequence of latite lava flows that cap Donovan Mountain and are present in much of the Bullfrog Hills and to the west in the Grapevine Mountains.

Regional Relations and Volcano-Tectonic Constraints

The ash-flow sheets and cogenetic lavas and intrusions of the SWNVF provide important time-stratigraphic, compositional, and paleotopographic information spanning about 8 million years of middle and late Miocene time in southwestern Nevada and record the interaction between large-scale volcanic activity and regional extension. It has long been recognized (e.g., Armstrong et al., 1969) that large-scale silicic and intermediate magmatic activity in regions such as the Great Basin must reflect major input from the asthenosphere. Magmatic activity in the SWNVF can be subdivided into three stages that may involve major injection of basalt into the lithosphere. Although the formation of peralkaline silicic magmas at the Silent Canyon volcanic center indicates the presence of mafic magma during the main magmatic stage, the amount of mantle-derived material visible in the geologic record appears to increase with the evolution of the SWNVF. Pumice fragments and cognate inclusions with less than 60 wt. % SiO₂ are present in the Timber Mountain Tuff, and mafic and low-silica intermediate lavas were erupted within the Timber Mountain caldera (e.g., Dome Mountain) and in the Bullfrog Hills after eruption of the Ammonia Tanks Member. Major mafic input is clearly involved in the alkaline and peralkaline volcanism of the late magmatic stage (e.g., Vogel et al., 1989; Weiss et al., 1984; Weiss and Noble, 1989).

The general increase in involvement of mafic magma with time appears to correlate with the changes in style of eruption and the onset and/or increase in intensity of extensional faulting, particularly in the western part of

the volcanic field. These observations provide information on the nature of crustal extension and tend to support models that relate lithospheric extension to upwelling and partial melting of mantle material and large influxes of mantle-derived basalt into the lower crust, with eventual failure localized in areas of more intense thermal weakening (e.g., Gans et al., 1989), rather than "passive" spreading models such as that of Wernicke et al. (1987). An episode of major extension began in southwestern Nevada synchronous with or shortly following peak magmatic and volcanic activity, as shown by faulting in the Yucca Mountain area soon after the eruption of the Paintbrush Tuff (culmination of main magmatic stage) and, with greater intensity, in the Bullfrog Hills following the eruption of the Timber Mountain Tuff and subsequent post-collapse volcanism.

The region of greatest extension was offset to the west from the area of large-volume, caldera-related volcanism of the main and Timber Mountain magmatic stages. The reason for this is unclear, but processes in addition to magmatic heating probably contributed to localizing extension. One such factor may have been that pre-middle Miocene extension in the region (Hamilton, 1988) had already attenuated the upper crust and penetratively thinned the lower lithosphere. Magmatic uplift of the area of the Timber Mountain caldera complex and the presence of very large bodies of magma unable to support directed stresses may have influenced local and possibly regional stress patterns. Synextensional volcanism in the strict sense was not spatially related to large cauldron structures, which implies a reasonably coherent crust (e.g., Gans et al., 1989; but see Lipman, 1983; 1988), but rather was related to extensional faults west of the calderas of the SWNVF.

Stylistically, kinematically, and chronologically distinct domains of coeval and younger extensional faulting are present in other areas of southwestern Nevada and adjacent California. In the Gold Mountain-Slate Ridge block west of Stonewall Mountain (Fig. 1), the Timber Mountain Tuff was rotated by movement along NNW-dipping listric(?) faults prior to deposition of the 7.6-Ma Stonewall Flat Tuff. Similar northwest-directed extension may have taken place throughout most of the Goldfield section between 11.4 and 7.6 Ma (Noble et al., 1990). Much of the present topography north of the Bullfrog Hills and west of longitude 117°W was, however, formed after 7.6 Ma. This is shown by differences in elevation of from 1,500 to 3,000+ feet between outcrops of the Stonewall Flat Tuff on the top of Slate Ridge and Gold Mountain and at and above Lida Summit on the southern flank of the Palmetto Mountains (McKee, 1968b) and outcrops at the margins of adjacent valleys (McKee et al., 1990). This faulting involved relatively little tilting, and thus appears to have taken place along relatively steep normal faults. Late Pliocene silicic volcanism of the Mount Jackson dome field south of Goldfield (Fig. 6; McKee et al., 1989) was localized along northeast-trending structures that may have formed during this period of faulting. Stratigraphic

relations within the Esmeralda Formation to the north (Stewart and Diamond, 1988; Stewart, 1989), indicating multiple stages of late Cenozoic extension, appear consistent with the patterns that we have recognized.

South of Gold Mountain, in Sarcobatus Flat and in the northern Grapevine Mountains, the Timber Mountain Tuff has been cut and rotated, generally to northwest dips, by at least eight major NE-striking normal faults (Albers and Stewart, 1972; S. I. Weiss, unpub. mapping, 1989). It is not clear whether movement within this zone of *south-eastward directed* extension took place concurrent with the major northwest directed extension recognized to the south and north, or whether most, or all, of this faulting postdates the Stonewall Flat Tuff.

Major faulting of Pliocene and Quaternary age is largely restricted to areas west of the Death Valley-Furnace Creek fault zone (McKee et al., 1990). Miocene volcanic rocks are offset (McKee, 1968a; Fleck, 1970), late Pliocene and younger basalts in the Saline Range are cut by normal faults (Elliott et al., 1984), and detachment faults in Death Valley are inferred to cut Pliocene, Pleistocene, and Holocene(?) alluvial deposits (Wernicke et al., 1988). Local young mafic and intermediate volcanism and neotectonic activity in the Lunar Crater-Reveille Range belt (Scott and Trask, 1972; Naumann et al., 1990) and in the area of Bare Mountain, Crater Flat, and Yucca Mountain (Vaniman et al., 1982; Crowe et al., 1983; Swadley et al., 1984; Whitney et al., 1986; Swadley and Parrish, 1988; Ramelli et al., 1988; Reheis, 1988) appear to reflect relatively minor extension and strike-slip movement well east of the zone of major late Pliocene and Quaternary volcanism and faulting.

Hydrothermal activity and mineralization coeval with or postdating the Timber Mountain magmatic stage is better developed in the western than in the eastern part of the SWNVF. This may reflect the greater extensional fault dissection and structural involvement of the western part of the field, which may have both provided better ground preparation and allowed the ascent of bodies of "productive" intermediate magma to high crustal levels.

A final, but important, matter involves the interrelation between late, high-level extensional faulting, magmatic and hydrothermal activity, and low-angle extensional faulting. The reset potassium-argon ages of rocks beneath the Original Bullfrog-Fluorspar Canyon detachment fault are within the range of activity of the main and Timber Mountain magmatic stages of the SWNVF, and are provisionally interpreted as mainly a result of magmatic heating (e.g., Jackson et al., 1988). As discussed above, the Timber Mountain Tuff and older volcanic units in the Bullfrog Hills in general dip more steeply than do the tuffs and lavas of the Bullfrog Hills. Moreover, the magmas that erupted to form the tuffs and lavas of the Bullfrog Hills must have been derived from beneath the detachment fault (Weiss et al., 1990). Perhaps movement on the Original Bullfrog-Fluorspar Canyon detachment mostly took place prior to eruption of the tuffs and lavas of the Bullfrog Hills.

Subsequent extension and rotation along more steeply dipping faults cut the detachment structures and, at least in part, provided channelways for the magmas that erupted to form the tuffs and lavas of the Bullfrog Hills.

Acknowledgments

Work by Noble in 1964, 1965, and 1966 was done as an employee of the U.S. Geological Survey. Studies by Noble and Weiss at various times between 1987 and 1990 were supported by contracts with the Nevada Nuclear Waste Project Office and Cordex Exploration Company, Inc. We thank GEXA Gold Corporation, Cordex Exploration, and H. G. Mining for access to their properties and B. W. Claybourn, S. M. Green, J. D. Greybeck and especially A. B. Wallace for sharing their knowledge and insights on local geologic relations and mineralization. J. R. Bergquist, K. A. Connors, J. J. Rytuba, and Eric Seedorf provided constructive reviews of the manuscript. Finally, we are indebted to F. M. Byers, Jr., W. J. Carr, E. B. Ekren, and the many other geologists whose years of work established the foundation upon which the contributions of this paper are based.

References

- Ahern, R., and Corn, R. M., 1981, Mineralization related to the volcanic center at Beatty, Nevada: Arizona Geol. Soc. Digest, v. XIV, p. 283-286.
- Albers, J. P., and Stewart, J. H., 1972, Geology and mineral deposits of Esmeralda County, Nevada, Nevada Bur. Mines and Geol. Bull. 78, 80 p.
- Armstrong, R. L., Ekren, E. B., McKee, E. H., and Noble, D. C., 1969, Space-time relations of Cenozoic silicic volcanism in the Great Basin of the western United States: Am. Jour. Sci., v. 267, p. 478-490.
- Aronson, J. L., and Bish, D. L., 1987, Distribution, K/Ar dates, and origin of illite/smectite in tuffs from cores USW G-1 and G-2, Yucca Mountain, Nevada, a potential high-level radioactive waste repository: Abstract of presentation at Clay Minerals Society Meeting, Socorro, NM, 1987.
- Ashley, R. P., 1974, Goldfield mining district, in Guidebook to the geology of four Tertiary volcanic centers in central Nevada: Nev. Bur. Mines Geol. Rept. 19, p. 49-66.
- Bacon, C. R., Giovannetti, D. M., Duffield, W. A., Dalrymple, G. B., and Drake, R. E., 1982, Age of the Coso Formation, Inyo County, California: U.S. Geol. Survey Bull. 1527, 18 p.
- Bailey, R. A., 1989, Geologic map of the Long Valley caldera. Mono-Inyo craters volcanic chain, and vicinity, eastern California: U.S. Geol. Survey Misc. Invest. Series Map I-1933, scale 1:62,500.
- Baker, E. M., 1987, Brecciation, mineralization and alteration of the Kidston gold deposit: Pacific Rim Congress 87, Proceedings, p. 29-33.
- Barton, M. D., and Trim, H. E., 1990, Late Cretaceous two-mica granites and lithophile-element mineralization in the Great Basin [abs.]: Geology and Ore Deposits of the Great Basin, Reno/Sparks, Nevada, 1990, Program with Abstracts, p. 76.
- Beatty, D. W., Naeser, C. W., and Lynch, W. C., 1987, The origin and significance of the strata-bound, carbonate-hosted gold deposits at Tennessee Pass, Colorado: Econ. Geol., v. 82, p. 2158-2178.
- Bell, E. J., and Larson, L. T., 1982, Overview of energy and mineral resources for the Nevada Nuclear Waste Storage Investigations, Nevada Test Site, Nye County, Nevada: NVO-250, Nevada Operations Office, USDOE, Las Vegas, 67 p.
- Bish, D. L., 1988, Evaluation of past and future alterations in tuff at

- Yucca Mountain, Nevada based on the clay minerals of drill cores USW G-1, G-2, and G-3: Los Alamos National Laboratory Rept. LA-10667-MS, 42 p.
- Broxton, D. E., Warren, R. G., and Byers, F. M., Jr., 1989, Chemical and mineralogic trends within the Timber Mountain-Oasis Valley caldera complex, Nevada: Evidence for multiple cycles of chemical evolution in a long-lived silicic magma system: *Jour. Geophys. Res.*, v. 94, p. 5961-5985.
- Byers, F. M., Jr., Carr, W. J., and Orkild, P. P., 1989, Volcanic centers of southwestern Nevada: evolution of understanding, 1960-1988: *Jour. Geophys. Res.*, v. 94, p. 5908-5924.
- Byers, F. M., Jr., Carr, W. J., Orkild, P. P., Quinlivan, W. D. and Sargent, K. A., 1976a, Volcanic Suites and related cauldrons of Timber Mountain-Oasis Valley caldera complex: U.S. Geol. Survey Prof. Paper 919, 70 p.
- Byers, F. M., Jr., Orkild, P. P., Carr, W. J., and Quinlivan, W. D., 1968, Timber Mountain Tuff, southern Nevada, and its relation to cauldron subsidence, in *Studies of Geology and Hydrology, Nevada Test Site: Geol. Soc. America Mem.* 110, p. 87-97.
- Byers, F. M., Jr., Carr, W. J., Christiansen, R. L., Lipman, P. W., Orkild, P. P., and Quinlivan, W. D., 1976b, Geologic map of the Timber Mountain Caldera area, Nye County, Nevada: U.S. Geol. Survey Misc. Inv. Ser. Map I-891.
- Candiotti de los Rios, Hugo, Noble, D. C., and McKee, E. H., 1990, Geological setting and epithermal silver veins of the Arcata district, southern Peru: *Econ. Geol.*, v. 85, in *press*.
- Carr, M. D., et al., 1986, Geology of drill hole UE25#1: A test hole into pre-Tertiary rocks near Yucca Mountain, southern Nevada: U.S. Geol. Survey Open-file Report 86-175, 87 p.
- Carr, M. D., and Monsen, S. E., 1988, A field trip guide to the geology of Bare Mountain, in Weide, D. L., and Faber, M. L., eds., This extended land: Geological journeys in the southern Basin and Range, *Geol. Soc. of America Cordilleran Section Field Trip Guidebook*, Las Vegas, Nevada, p. 50-57.
- Carr, W. J., 1974, Summary of tectonic and structural evidence for stress orientation at the Nevada Test Site: U.S. Geol. Survey Open-file Rept. 74-176, 53 p.
- Carr, W. J., 1984a, Regional structural setting of Yucca Mountain, southwestern Nevada, and late Cenozoic rates of tectonic activity in part of the southwestern Great Basin, Nevada and California: U.S. Geol. Survey Open-file Rept. 84-0854, 114 p.
- Carr, W. J., 1984b, Timing and style of tectonism and localization of volcanism in the Walker Lane belt of southwestern Nevada [abs.]: *Geol. Soc. of America, Abstracts with Programs*, v. 16, p. 464.
- Carr, W. J., 1988a, Styles of extension in the Nevada Test Site region, southern Walker Lane Belt: An integration of volcano-tectonic and detachment fault models [abs.]: *Geol. Soc. America Abs. with Programs*, v. 20, p. 148.
- Carr, W. J., 1988b, Volcano-tectonic setting of Yucca Mountain and Crater Flat, in Carr, M. D., and Yount, J. C., eds., *Geologic and hydrologic investigations of a potential nuclear waste disposal site at Yucca Mountain, southern Nevada: U.S. Geol. Survey Bull.* 1790, p. 35-49.
- Carr, W. J., Byers, F. M., and Orkild, P. P., 1986, Stratigraphic and volcano-tectonic relations of Crater Flat Tuff and some older volcanic units, Nye County, Nevada: U.S. Geol. Survey Prof. Paper 1323, 28 p.
- Christiansen, R. L., 1979, Cooling units and composite sheets in relation to caldera structure, in Chapin, C. E., and Elston, W. E., eds., *Ash-flow ruffs: Geol. Soc. America Spec. Paper* 180, p. 29-42.
- Christiansen, R. L., Lipman, P. W., Carr, W. J., Byers, F. M., Jr., Orkild, P. P., and Sargent, K. A., 1977: Timber Mountain-Oasis Valley caldera complex of southern Nevada: *Geol. Soc. America Bull.*, v. 88, p. 943-959.
- Christiansen, R. L., Lipman, P. W., Orkild, P. P., and Byers, F. M., Jr., 1965, Structure of the Timber Mountain caldera, southern Nevada, and its relation to basin-range structure, U.S. Geol. Survey Prof. Paper 525-B, p. B43-B48.
- Cornwall, H. R., 1962, Calderas and associated volcanic rocks near Beatty, Nye County, Nevada, in Engle, A. E. J., James, H. L., and Leonard, B. G., eds., *Petrologic studies: A volume in honor of A. F. Buddington: Geol. Soc. America Buddington Volume*, p. 357-371.
- Cornwall, H. R., 1972, Geology and mineral deposits of southern Nye County, Nevada: Nevada Bur. Mines Geol. Bull. 77, 49 p.
- Cornwall, H. R., and Kleinhampl, F. J., 1961, Geologic map of the Bare Mountain quadrangle, Nevada: U.S. Geol. Survey Geol. Quad. Map GQ-157, scale 1:62,500.
- Cornwall, H. R., and Kleinhampl, F. J., 1964, Geology of the Bullfrog quadrangle and ore deposits related to Bullfrog Hills caldera, Nye County, Nevada, and Inyo County, California: U.S. Geol. Survey Prof. Paper 454-J, 25 p.
- Crowe, B. M., Self, S., Vaniman, D., Amos, R., and Perry, F., 1983, Aspects of potential magmatic disruption of a high-level radioactive waste repository in southern Nevada: *Jour. Geology*, v. 91, p. 259-276.
- Deino, A. L., Hausback, B. P., Turrin, B. T., and McKee, E. H., 1989, New $40\text{Ar}/^{39}\text{Ar}$ ages for the Spearhead and Civet Cat Canyon Members of the Stonewall Flat Tuff, Nye County, Nevada [abs.]: *EOS, Trans. Am. Geophys. Union*, v. 70, p. 1409.
- Duebendorfer, E. M., Feuerbach, D. L., and Smith, E. I., 1990, Syntectonic sedimentation, volcanism, and kinematics along the inferred eastern extension of the Las Vegas Valley shear zone, Nevada [abs.]: *Geol. Soc. America Abs. with Programs*, v. 22, p. 20.
- Ekren, E. B., Anderson, R. E., Rogers, C. L., and Noble, D. C., 1971, Geology of northern Nellis Air Force Base Bombing and Gunnery Range, Nye County, Nevada: U.S. Geol. Survey Prof. Paper 651, 91 p.
- Ekren, E. B., Rogers, C. L., Anderson, R. A., and Orkild, P. P., 1968, Age of basin and range normal faults in Nevada Test Site and Nellis Air Force Range, Nevada: *Geol. Soc. America Mem.* 110, p. 247-250.
- Ekren, E. B., and Sargent, K. A., 1965, Geologic map of Skull Mountain quadrangle at the Nevada Test Site, Nye County, Nevada: U.S. Geol. Survey Geol. Quad. Map. GQ-387, scale 1:24,000.
- Elliott, G. S., Wrucke, C. T., and Nedell, S. S., 1984, K-Ar ages of late Cenozoic volcanic rocks from the northern Death Valley region, California: *Isochron/West*, no. 39, p. 3-7.
- Fleck, R. J., 1970, Age and tectonic significance of volcanic rocks, Death Valley area, California: *Geol. Soc. America Bull.*, v. 81, p. 2807-2815.
- Gans, P. B., Mahood, G. A., and Schermer, E., 1989, *Synextensional magmatism in the Basin and Range province: A case study from the eastern Great Basin: Geol. Soc. America Spec. Paper* 233, 53 p.
- Greybeck, J. D., and Wallace, A. B., 1990, Gold mineralization at Fluorspar Canyon near Beatty, Nye County, Nevada, in Schafer, R. W., Wilkinson, W. H., and Raines, G., eds., *Geology and ore deposits of the Great Basin: Geol. Soc. Nevada, Symposium Proceedings Volume*.
- Hamilton, W. B., 1988, Detachment faulting in the Death Valley region, California and Nevada, in Carr, M. D., and Yount, J. C., eds., *Geologic and hydrologic investigations of a potential nuclear waste disposal site at Yucca Mountain, southern Nevada: U.S. Geol. Survey Bull.* 1790, p. 51-86.
- Hausback, B. P., Deino, A. L., Turrin, B. T., McKee, E. H., Frizzell, V. A., Noble, D. C., and Weiss, S. I., 1990, New $^{40}\text{Ar}/^{39}\text{Ar}$ ages for the Spearhead and Civet Cat Canyon Members of the Stonewall Flat Tuff, Nye County, Nevada: Evidence for systematic errors in standard K-Ar age determinations on sanidine: *Isochron/West*, in *press*.
- Hausback, B. P., and Frizzell, V. A. Jr., 1987, Late Miocene syntectonic volcanism of the Stonewall Flat Tuff, Nye County, Nevada [abs.]: *Geol. Soc. America Abstr. with Programs*, v. 19, p. 696.
- Hoover, D. B., Chornack, M. P., Nervick, K. H., and Broker, M. M., 1982, Electrical studies at the proposed Wahmonie and Calico Hills Nuclear Waste Sites, Nye County, Nevada: U.S. Geol. Survey Open-file Rept. 82-466, 45 p.
- Jackson, M. R., 1988, The Timber Mountain magmato-thermal event: an intense widespread culmination of magmatic and hydrothermal activity at the southwestern Nevada volcanic field: Unpub. M.S. thesis, Univ. Nevada-Reno, 46 p.
- Jackson, M. R., Noble, D. C., Weiss, S. I., Larson, L. T., and McKee, E. H., 1988, The Timber Mountain magmato-thermal event: an

- intense widespread culmination of magmatic and hydrothermal activity at the southwestern Nevada volcanic field [abs.]: *Geol. Soc. America Abs. with Programs*, v. 20, p. 171.
- John, D. A., Thomason, R. E., and McKee, E. H., 1989, Geology and K-Ar geochronology of the Paradise Peak mine and the relationship of pre-basin and range extension to early Miocene precious metal mineralization in west-central Nevada: *Econ. Geol.*, v. 84, p. 631-650.
- Jorgensen, D. K., Rankin, J. W., and Wilkins, J., Jr., 1989, The geology, alteration and mineralogy of the Bullfrog gold deposit, Nye County, Nevada: *Soc. Mining Eng. Preprint* 89-135, 13 p.
- Kistler, R. W., 1968, Potassium-argon ages of volcanic rocks on Nye and Esmeralda Counties, Nevada: *Geol. Soc. America Mem.* 110, p. 251-263.
- Larson, P. B., 1987, Stable isotope and fluid inclusion investigations of epithermal vein and porphyry molybdenum mineralization in the Rico mining district, Colorado: *Econ. Geol.*, v. 82, p. 2141-2157.
- Lipman, P. W., 1983, The Miocene Questa caldera, northern New Mexico: Relation to batholith emplacement and associated molybdenum mineralization: in *The genesis of Rocky Mountain ore deposits: changes with time and tectonics*, Proc., Denver Region Exploration Geologists Society Symposium, Nov. 4-5, 1982, Denver, Colorado, p. 133-147.
- Lipman, P. W., 1988, Evolution of silicic magma in the upper crust: the mid-Tertiary Latir volcanic field and its cogenetic granite batholith, northern New Mexico, U.S.A.: *Trans. Royal Soc. Edinburgh: Earth Sciences*, v. 79, p. 265-288.
- Lipman, P. W., Quinlivan, W. D., Carr, W. J., and Anderson, R. E., 1966, Geologic map of the Thirsty Canyon S.E. quadrangle, Nye County, Nevada: U.S. Geol. Survey Geol. Quad. Map GQ-489, Scale 1:24,000.
- McKee, E. H., 1968a, Age and rate of movement of the northern part of the Death Valley-Furnace Creek fault zone, California: *Geol. Soc. America Bull.*, v. 79, p. 509-512.
- McKee, E. H., 1968b, Geology of the Magruder Mountain area, Nevada-California: U.S. Geol. Survey Bull. 1251-H, 40 p.
- McKee, E. H., 1983, Reset K-Ar ages - Evidence for three metamorphic core complexes, western Nevada: *Ischron/West*, v. 38, p. 17-20.
- McKee, E. H., 1985, Geologic map of the Magruder Mountain quadrangle, Esmeralda County, Nevada, and Inyo County, California: U.S. Geol. Survey Geol. Quad. Map GQ-1587, scale 1:62,500.
- McKee, E. H., Noble, D. C., and Weiss, S. I., 1989, Very young silicic volcanism in the southwestern Great Basin: The late Pliocene Mount Jackson dome field, southeast Esmeralda County, Nevada [abs.]: *EOS, Trans. Am. Geophys. Union*, v. 70, p. 1420.
- McKee, E. H., Noble, D. C., and Weiss, S. I., 1990, Late Neogene volcanism and tectonism in the Goldfield segment of the Walker Lane belt [abs.]: *Geol. Soc. America Abs. with Programs*, v. 22, p. 66.
- Maldonado, F., 1985, Late Tertiary detachment faults in the Bullfrog Hills, southwestern Nevada [abs.]: *Geol. Soc. America Abs. with Programs*, v. 17, p. 651.
- Maldonado, F., 1988, Geometry of normal faults in the upper plate of a detachment fault zone, Bullfrog Hills, southern Nevada [abs.]: *Geol. Soc. America Abs. with Programs*, v. 20, p. 178.
- Maldonado, F., 1990, Structure, stratigraphy, and mineralization of the upper plate of the Bullfrog Hills detachment fault system, Bullfrog Hills area, with emphasis on the geology of Bullfrog Mountain, Nye County, southern Nevada, in Hillemeier, Frank, Wolverson, Nancy, and Drobeck, Peter, 1990 spring field trip guide book, Volcanic-hosted gold deposits and structural setting of the Mohave region: Reno, Geol. Soc. Nevada, 18 p.
- Mapa, M. R., 1990, Geology and mineralization of the Mocher Lode mine, Nye County, Nevada, in Hillemeier, Frank, Wolverson, Nancy, and Drobeck, Peter, 1990 spring field trip guide book, Volcanic-hosted gold deposits and structural setting of the Mohave region: Reno, Geol. Soc. Nevada, 4 p.
- Marvin, R. F., Byers, F. M., Mehnert, H. H., Orkild, P. P., and Stern, T. W., 1970, Radiometric ages and stratigraphic sequence of volcanic and plutonic rocks, southern Nye and western Lincoln Counties, Nevada: *Geol. Soc. America Bull.*, v. 81, p. 2657-2676.
- Marvin, R. F., and Cole, J. C., 1978, Radiometric ages: Compilation A, U.S. Geological Survey: *Ischron/West*, no. 22, p. 3-14.
- Marvin, R. F., Mehnert, H. H., and Naeser, C. W., 1989, U.S. Geologic Survey radiometric ages - compilation "C", part 3: California and Nevada: *Ischron/West*, no. 52, p. 3-11.
- Monsen, S. A., Carr, M. D., Reheis, M. C., and Orkild, P. P., 1990, Geologic map of Bare Mountain, Nye County, Nevada: U.S. Geol. Survey Open-file Report 90-25, 17 p.
- Morton, J. L., Silberman, M. L., Bonham, H. F., Garside, L. J., and Noble, D. C., 1977, K-Ar ages of volcanic rocks, plutonic rocks, and ore deposits in Nevada and eastern California - Determinations run under the USGS-NBMG cooperative program: *Ischron/West*, n. 20, p. 19-29.
- Naumann, T. R., Smith, E. I., and Shafiquillah, M., 1990, Post-6 Ma intermediate (trachytic) volcanism in the Reveille Range, central Great Basin, Nevada [abs.]: *Geol. Soc. America Abs. with Programs*, v. 22, p. 72.
- Noble, D. C., and Christiansen, R. L., 1968, Geologic map of the southwest quarter of the Black Mountain quadrangle, Nye County, Nevada: U.S. Geol. Survey Misc. Geol. Invest. Map I-562.
- Noble, D. C., and Christiansen, R. L., 1974, Black Mountain volcanic center, in *Guidebook to the geology of four Tertiary volcanic centers in central Nevada*: Nevada Bur. Mines Geol. Rept. 19, p. 22-26.
- Noble, D. C., Kistler, R. W., Christiansen, R. L., Lipman, P. W., and Poole, F. G., 1965, Close association in space and time of alkalic, calc-alkalic, and calcic volcanism in southern Nevada [abs.]: *Geol. Soc. America Spec. Paper* 82, p. 143.
- Noble, D. C., McKee, E. H., and Weiss, S. I., 1988, Nature and timing of pyroclastic and hydrothermal activity and mineralization at the Stonewall Mountain volcanic center, southwestern Nevada: *Ischron/West*, No. 51, p. 25-28.
- Noble, D. C., Sargent, K. A., Ekren, E. B., Mehnert, H. H., and Byers, F. M., Jr., 1968, Silent Canyon volcanic center, Nye County, Nevada: *Geol. Soc. America Spec. Paper* 101, p. 412-413.
- Noble, D. C., Vogel, T. A., Weiss, S. I., Erwin, J. W., McKee, E. H., and Younker, L. W., 1984, Stratigraphic relations and source areas of ash-flow sheets of the Black Mountain and Stonewall Mountain volcanic centers, Nevada: *Jour. Geophys. Res.*, v. 89, p. 8593-8602.
- Noble, D. C., Weiss, S. I., and Green, S. M., 1989, High-salinity fluid inclusions suggest that Miocene gold deposits of the Bare Mtn. district, NV, are related to a large buried rare-metal rich magmatic system [abs.]: *Geol. Soc. America Abs. with Programs*, v. 21, p. 123.
- Noble, D. C., Weiss, S. I., and McKee, E. H., 1990, Style, timing, distribution, and direction of Neogene extension within and adjacent to the Goldfield Section of the Walker Lane structural belt [abs.]: *EOS (Trans. Am. Geophys. Union)*, v. 71, p. 618-619.
- Novak, S. W., and Bacon, C. R., 1986, Pliocene volcanic rocks of the Coso Range, Inyo County, California: U.S. Geol. Survey Prof. Paper 1383, 44 p.
- Odt, D. A., 1983, Geology and geochemistry of the Sterling gold deposit, Nye County, Nevada: Unpub. M.S. thesis, Univ. Nevada-Reno, 91 p.
- Ponce, D. A., 1984, Gravity and magnetic evidence for a granitic intrusion near Wahmonie site, Nevada Test Site, Nevada, *Jour. Geophys. Res.*, v. 89, p. 9401-9413.
- Quade, J., and Tingley, J. V., 1984, A mineral inventory of the Nevada Test Site, and portions of Nellis Bombing and Gunnery Range southern Nye County, Nevada: Nevada Bur. Mines Geol. Open-file Rept. 82-2, 40 p.
- Ramelli, A. R., Bell, J. W., and de Polo, C. M., 1988, Evidence for distributive faulting at Yucca Mountain, Nevada [abs.]: *Geol. Soc. America Abs. with Programs*, v. 20, p. A383.
- Ransome, F. L., Emmons, W. H., and Garrey, G. H., 1910, Geology and ore deposits of the Bullfrog district, Nevada: U.S. Geol. Survey Bull. 407, 130 p.
- Reheis, M. C., 1988, Preliminary study of Quaternary faulting on the east side of Bare Mountain, Nye County, Nevada, in Carr, M. D.,

- and Yount, J. C., eds., Geologic and hydrologic investigations of a potential nuclear waste disposal site at Yucca Mountain, southern Nevada: U.S. Geol. Survey Bull. 1790, p. 103-111.
- Reynolds, M. W., 1969, Stratigraphy and structural geology of the Titus and Titanothera Canyons area, Death Valley, California: Unpub. Ph.D. dissertation, Univ. California, Berkeley, 310 p.
- Sawyer, D. A., and Sargent, K. A., 1989, Petrologic evolution of divergent peralkaline magmas from the Silent Canyon caldera complex, southwestern Nevada volcanic field: *Jour. Geophys. Res.*, v. 94, p. 6021-6040.
- Schweickert, R. A., 1989, Evidence for a concealed dextral strike-slip fault beneath Crater Flat, Nevada [abs.]: *Geol. Soc. America Abs. with Programs*, v. 22, p. 81.
- Schweickert, R. A., and Caskey, S. J., 1990, Pre-middle Miocene extensional history of the Nevada Test Site region, southern Nevada [abs.]: *Geol. Soc. America Abs. with Programs*, v. 21, p. A90.
- Scott, D. D., and Trask, N. J., 1972, Geology of the Lunar Crater volcanic field, Nye County, Nevada: U.S. Geol. Survey Prof. Paper 5991, p. 11-122.
- Scott, R. B., 1986, Extensional tectonics at Yucca Mountain, southern Nevada [abs.]: *Geol. Soc. America Abs. with Programs*, v. 18, p. 411.
- Scott, R. B., 1988, Tectonic setting of Yucca Mountain, southwest Nevada [abs.]: *Geol. Soc. America Abs. with Programs*, v. 20, p. 229.
- Scott, R. B., and Rosenbaum, J. G., 1986, Evidence for rotation about a vertical axis during extension at Yucca Mountain, southern Nevada [abs.]: *EOS (Trans. American Geophys. Union)*, v. 67, p. 358.
- Scott, R. B., and Whitney, J. W., 1987, The upper crustal detachment system at Yucca Mountain, SW Nevada [abs.]: *Geol. Soc. America Abs. with Programs*, v. 19, p. 332-333.
- Silberman, M. L., Chesterman, C. W., Kleinhampl, F. J., and Gray, C. H., Jr., 1972, K-Ar ages of volcanic rocks and gold-bearing quartz-adularia veins in the Bodie mining district, Mono County, California: *Econ. Geol.*, v. 67, p. 597-604.
- Steven, T. A., and Lipman, P. W., 1976, Calderas of the San Juan volcanic field, southwestern Colorado: U.S. Geol. Survey Prof. Paper 958, 35 p.
- Stewart, J. H., 1978, Basin-range structure in western North America: A review: *Geol. Soc. America Mem.* 152, p. 1-31.
- Stewart, J. H., 1980, Geology of Nevada: Nevada Bur. Mines Geol. Spec. Pub. 4, 136 p.
- Stewart, J. H., 1988, Tectonics of the Walker Lane belt, western Great Basin-Mesozoic and Cenozoic deformation in a zone of shear, in Ernst, W. G., ed., *Metamorphism and crustal evolution of the western United States*, Rubey Vol. VII: Englewood Cliffs, New Jersey, Prentice Hall, p. 683-713.
- Stewart, J. H., 1989, Description, stratigraphic sections, and maps of middle and upper Miocene Esmeralda Formation in Alum, Blanco Mine, and Coaldale areas, Esmeralda County, NV: U.S. Geol. Survey Open-file Rept. 89-0324, 31 p.
- Stewart, J. H., and Diamond, D. S., 1988, Changing late Cenozoic tectonic patterns in western Nevada: A middle and upper Miocene extensional basin unrelated to present-day basin-range structure: *Geol. Soc. America Abs. with Programs*, v. 20, p. 235.
- Stock, Chester, and Bode, F. D., 1935, Occurrence of lower Oligocene mammal-bearing beds near Death Valley, California: *Natl. Acad. Sci. Proc.*, v. 21, no. 10, p. 571-579.
- Stormer, J. C., Jr., and Whitney, J. A., 1985, Two feldspar and iron-titanium oxide equilibria in silicic magmas and the depth of origin of large volume ashflow tuffs: *Am. Mineral.*, v. 70, p. 52-64.
- Swadley, W. C., Hoover, D. L., and Rosholt, J. W., 1984, Preliminary report on late Cenozoic faulting and stratigraphy in the vicinity of Yucca Mountain, Nye County, Nevada: U.S. Geol. Survey Open-file Rept. 84-788.
- Swadley, W. C., and Parrish, L. D., 1988, Surficial geologic map of the Bare Mountain quadrangle, Nye County, Nevada: U.S. Geol. Survey Map 1-1826, scale 1:48,000.
- Tingley, J. V., 1984, Trace element associations in mineral deposits, Bare Mountain (Fluorine) mining district, southern Nye County, Nevada: Nevada Bur. Mines Geol. Rept. 39, 28 p.
- Vaniman, D. T., Crowe, B. M., and Gladney, E. S., 1982, Petrology and geochemistry of Hawaiiite lavas from Crater Flat, Nevada: *Contrib. Mineral. Petrol.*, v. 80, p. 341-357.
- Vogel, T. A., Noble, D. C., and Younker, L. W., 1989, Evolution of a chemically zoned magma body: Black Mountain volcanic center, southwestern Nevada: *Jour. Geophys. Res.*, v. 94, p. 6041-6058.
- Warren, R. G., Byers, F. M., Jr., Broxton, D. E., Freeman, S. H., and Hagan, R. C., 1989, Phenocryst abundances and glass and phenocryst compositions as indicators of magmatic environments of large-volume ash flow sheets in southwestern Nevada: *Jour. Geophys. Res.*, v. 94, p. 5987-6020.
- Weiss, S. I., 1987, Geologic and paleomagnetic studies of the Stonewall Mountain and Black Mountain volcanic centers, southern Nevada: Unpub. M.S. thesis, Univ. of Nevada-Reno, 67 p.
- Weiss, S. I., Connors, K. A., Noble, D. C., and McKee, E. H., 1990, Coeval crustal extension and magmatic activity in the Bullfrog Hills during the latter phases of Timber Mountain volcanism [abs.]: *Geol. Soc. America Abs. with Programs*, v. 22, p. 92-93.
- Weiss, S. I., and Noble, D. C., 1989, Stonewall Mountain volcanic center, southern Nevada: Stratigraphic, structural and facies relations of outflow sheets, near-vent tuffs, and intracaldera units: *Jour. Geophys. Res.*, v. 94, p. 6039-6074.
- Weiss, S. I., Noble, D. C., and McKee, E. H., 1984, Inclusions of basaltic magma in near-vent facies of the Stonewall Flat Tuff: Product of explosive magma mixing [abs.]: *Geol. Soc. America Abs. with Programs*, v. 16, p. 6890.
- Weiss, S. I., Noble, D. C., and McKee, E. H., 1988, Volcanic and tectonic significance of the presence of Late Miocene Stonewall Flat tuff in the vicinity of Beatty, Nevada [abs.]: *Geol. Soc. America Abs. with Programs*, v. 20, p. A399.
- Wernicke, B. P., Christiansen, R. L., England, P. C., and Sonder, L. J., 1987, Tectonomagmatic evolution of Cenozoic extension of the North America Cordillera, in Coward, M. P., Dewey, J. F., and Hancock, P. L., eds., *Continental extensional tectonics*: *Geol. Soc. London Spec. Pub.* 28, p. 203-222.
- Wernicke, B. P., Walker, J. D., and Hodges, K. V., 1988, Field guide to the northern part of the Tucki Mountain fault system, Death Valley region, California, in Weide, D. L., and Faber, M. L., eds., *This extended land: Geological journeys in the southern Basin and Range*, *Geol. Soc. of America Cordilleran Section Field Trip Guidebook*, Las Vegas, Nevada, p. 58-63.
- Whitney, J. W., Shroba, R. R., and Harding, S. T., 1986, Recurrent Quaternary movement on the Windy Wash fault, Nye County, Nevada: *Geol. Soc. America Abs. with Programs*, v. 18, p. 787.

APPENDIX B

ABSTRACT FORM FOR ALL GSA MEETINGS IN 1991

Complete all sections ① through ⑤ below

① TYPE ABSTRACT COMPLETELY WITHIN THE BLUE LINES BELOW.

Geol. Soc. America Abstr. with Program
v. 23, p. A247

No 25893

② CHECK ONE DISCIPLINE (category) below in which reviewers will be best qualified to evaluate your abstract. Check "Other" if you want the program chairs to choose for you.

GEOLOGIC AND TECTONIC SETTING AND MIOCENE VOLCANIC STRATIGRAPHY OF THE GOLD MOUNTAIN - SLATE RIDGE AREA, SOUTHWESTERN NEVADA

NOBLE, Donald C. and WORTHINGTON, Joseph E., IV, Mackay School of Mines, University of Nevada, Reno, NV 89557; McKEE, Edwin H., U.S. Geological Survey, 345 Middlefield Road, Menlo Park, CA 94025

Early to late Miocene ash-flow sheets and lavas, in part older than rocks of the southwestern Nevada volcanic field, are exposed in southern Esmeralda County, NV, directly northeast of the Death Valley-Furnace Creek fault zone. Rock units of this field exhibit major lateral changes in thickness, distribution, and attitude attributed mostly to slightly earlier and coeval normal faulting.

The oldest ash-flow sheet is a distinctive, previously unrecognized unit of commonly platy-weathering, phenocryst-rich low-silica rhyolite ash-flow tuff containing abundant biotite, hornblende, and clinopyroxene. This compositionally zoned unit, well exposed on the southwestern flank of Mount Dunfee, has been dated at 16.7 ± 0.4 Ma. Above this ash-flow sheet are two, or possibly more, previously unrecognized rhyolitic ash-flow sheets containing phenocrysts of plagioclase, sanidine, biotite, hornblende, sphene, low or moderate quartz, and no clinopyroxene. The lower sheet, well developed in vicinity of the upper part of Oriental Wash, is characterized by very abundant sphene. The upper unit, well developed east of the Gold Coin mine and along the south flank of Gold Mountain, is thick, compositionally variable, shows strong compound cooling, and contains less sphene. It has been traced from northwest of Oriental Wash to northeast of Slate Ridge. These units are overlain by the Tuff of Tolicha Peak, a distinctive unit of very phenocryst-poor high-silica rhyolite dated at 13.9 ± 0.4 Ma, and by a local overlying ash-flow unit. The tuff of Tolicha Peak, mapped on the Nellis Air Force Range perhaps as far east as the Belted Range, has been identified northwest of Oriental Wash. This sequence of ash-flow sheets and intercalated sedimentary rocks is overlain by the Rainier Mesa and Ammonia Tanks Members of the ca. 11.5 Ma Timber Mountain Tuff and in turn by the 7.5 Ma Stonewall Flat Tuff and mafic lavas of similar age. A very thin, but distinctive and possibly genetically related layer of dark mafic to intermediate air-fall pumice is present at the base of the Rainier Mesa Member.

The restriction of the lowermost ash-flow sheet to the northeastern part of Slate Ridge suggests a source to the north of Slate Ridge. The overlying sphene-bearing units were probably erupted from sources located south of Gold Mountain based on distribution, thickness variations and size of lithic fragments in the upper of the two units. Distribution of the tuff of Tolicha Peak suggests that its source may be located at far west as the northern part of Sarcobatus Flat.

The ash-flow sequence overlies potassium- and olivine-rich basalt that in turn overlies hornblende- and biotite-bearing intermediate lavas. The intermediate lavas belong to a suite of calc-alkalic rocks present throughout west-central Nevada and northeastern California and extending eastward into the Nellis Air Force Range. The basalts, older than 16.7 ± 0.4 Ma, are the oldest mafic lavas yet recognized in the southern Great Basin and are perhaps tectonically equivalent to coeval K-rich mafic rocks present along the southeastern and western margins of the Great Basin.

- 1 archaeological geology
- 2 coal geology
- 3 computers
- 4 economic geology
- 5 engineering geology
- 6 environmental geology
- 7 geochemistry, aqueous
- 8 geochemistry, other
- 9 geology education
- 10 geomorphology
- 11 geophysics/
tectonogeophysics
- 12 geoscience information
- 13 global geoscience
- 14 history of geology
- 15 hydrogeology
- 16 marine geology
- 17 micropaleontology
- 18 mineralogy/
crystallography
- 19 paleoceanography/
paleoclimatology
- 20 paleontology/
paleobotany
- 21 petroleum geology
- 22 petrology, experimental
- 23 petrology, igneous
- 24 petrology, metamorphic
- 25 petrology, sedimentary
- 26 planetary geology
- 27 Precambrian geology
- 28 Quaternary geology
- 29 remote sensing
- 30 sedimentology
- 31 stratigraphy
- 32 structural geology
- 33 tectonics
- 34 volcanology
- 35 OTHER

PLEASE NOTE: This is one of a pair of related papers: The other is by Worthington, Noble & Weiss. If at all possible, this paper should be scheduled directly before Worthington et al.

③ SELECT ONE FORMAT

- INVITED FOR SYMPOSIUM NUMBER: _____
(first five words of symposium title)
- VOLUNTEERED FOR DISCIPLINE SESSION
- VOLUNTEERED FOR THEME SESSION NUMBER: T25
Cenozoic Extension in the Cordillera
(first five words of Theme Session title)

④ SELECT ONE MODE (Be aware that some sessions may have been designated specifically as either "poster" or "oral.")

- ORAL— Verbal presentation before a seated audience.
- POSTER— Graphic display on poster boards supplemented by speaker comments.
- EITHER— Either mode is acceptable.

⑤ CHECK IF THIS APPLIES

- WITHDRAW— If the abstract cannot be accepted in the mode I have indicated, please withdraw it.

⑥ INDICATE % OF THIS PAPER PREVIOUSLY PRESENTED 10%

Where? GSA
When? Cord. Meeting, 1990

⑦ CHECK IF YOU ARE WILLING TO BE A SESSION CHAIR _____

Your Name Donald C. Noble
Office Phone 702/784-6928 Home Phone 702/972-7911

⑧ SPEAKER'S IDENTITY AND MAILING ADDRESS

Name Donald C. Noble
Address Mackay School of Mines
Univ. Nevada, Reno
City/State/ZIP Reno, NV 89557
Country _____
Office Phone 702/784-6928 Home Phone 702/972-7911

If the speaker will be unavailable at these numbers during the 45 days following the abstract deadline, list phone numbers to be used instead.
Office Phone 702/784-1104 Home Phone 702-747-5921
(S.I. Weiss)

⑨ MAILING INSTRUCTIONS

INVITED ABSTRACTS: Mail original + 5 copies DIRECTLY TO THE CONVENER.
VOLUNTEERED ABSTRACTS: Mail original + 8 copies to the appropriate address to arrive on or before the deadline. Abstracts may NOT be sent by fax.

APPENDIX C

ABSTRACT FORM FOR ALL GSA MEETINGS IN 1991

Complete all sections 1 through 9 below

1 TYPE ABSTRACT COMPLETELY WITHIN THE BLUE LINES BELOW.

Geol. Soc. America Abstr. with Programs
v. 23, p. A247

No 25892

2 CHECK ONE DISCIPLINE (category) below in which reviewers will be best qualified to evaluate your abstract. Check "Other" if you want the program chairs to choose for you.

STRUCTURAL GEOLOGY AND NEOGENE EXTENSIONAL TECTONICS OF THE GOLD MOUNTAIN-SLATE RIDGE AREA, SOUTHWESTERN NEVADA

WORTHINGTON, Joseph E., IV, NOBLE, Donald C., and WEISS, Steven I., Mackay School of Mines, University of Nevada, Reno, Reno, NV 89557

Geological relations of Neogene volcanic and sedimentary rocks and style and orientation of several ages of normal faults reveal a complicated history of early to late Miocene crustal extension and uplift in the Gold Mountain-Slate Ridge (GM-SR) area, southern Esmeralda County, NV. The preservation of early Miocene and early middle Miocene rocks permits documentation of an appreciably earlier period of Neogene history than is available in the Bullfrog Hills to the south and the Mineral Ridge-Weepah Hills region to the north. Available data nevertheless suggests a continuity of regional extension over a large part of the southern Walker Lane belt.

Faulting and extension in the GM-SR area prior to deposition of the oldest (16.7 ± 0.4 Ma) ash-flow sheet is shown by 1) the rugged topography upon which the unit was deposited, 2) its irregular distribution, 3) the absence of older ash-flow units exposed NE of the region and 4) the presence of basalt beneath the ash-flow sequence. These relations are consistent with the observations of Albers and Stewart (1972), who recognized pre-volcanic E-W trending normal faults, one of which along the northern margin of Slate Ridge had 4,000 feet of offset before volcanism.

Normal faulting, block rotation, and differential uplift and subsidence took place throughout the period of ash-flow deposition. This is demonstrated by 1) the common presence of rapidly thickening and thinning wedges of conglomerate and fanglomerate between virtually all of the ash-flow sheets, 2) angular unconformities between volcanic and/or sedimentary units, 3) erosion and/or nondeposition of one or more ash-flow units in many localities, 4) presence of growth faults, and 5) very irregular thickness relations of successive ash-flow sheets. Cenozoic rocks are everywhere in depositional contact with older units; no detachments or low-angle structures in which volcanic or associated sedimentary rocks dip into older rock are seen.

Most faults older than the 7.5 Ma Stonewall Flat Tuff trend E-W, changing to ENE to NE to the east. Offsets are down to the north over most of the area, but between Gold Mountain and Sarcobatus Flat are down to the SE; it is unclear whether the latter group of faults pre- or postdate the Stonewall Flat Tuff. Neogene normal faults generally parallel folds and dips mapped by Albers and Stewart (1972) in Cambrian and Precambrian strata. Amount of tilt, inferred from the angle of dip of early and middle Miocene volcanic units, generally ranges from about 15° to 40°, with a general up-section decrease in dip. The eastern part of the Sylvania pluton was tilted about 15° to 40° to the south by Neogene faulting. Much fault movement and rotation and deposition of conglomerate and fanglomerate appears to have taken place after deposition of the 11.5 Ma Timber Mtn. Tuff.

After deposition of the Stonewall Flat Tuff, normal faulting with little tilting created many of the present-day mountain ranges in the region west of 117°W, as discussed by McKee and others (1990) and Noble and others (1990, 1991). Most fault movement and uplift took place prior to emplacement of 3 to 7 Ma silicic domes along similar structures to the north.

- 1 archaeological geology
- 2 coal geology
- 3 computers
- 4 economic geology
- 5 engineering geology
- 6 environmental geology
- 7 geochemistry, aqueous
- 8 geochemistry, other
- 9 geology education
- 10 geomorphology
- 11 geophysics/
tectonogeophysics
- 12 geoscience information
- 13 global geoscience
- 14 history of geology
- 15 hydrogeology
- 16 marine geology
- 17 micropaleontology
- 18 mineralogy/
crystallography
- 19 paleoceanography/
paleoclimatology
- 20 paleontology/
paleobotany
- 21 petroleum geology
- 22 petrology, experimental
- 23 petrology, igneous
- 24 petrology, metamorphic
- 25 petrology, sedimentary
- 26 planetary geology
- 27 Precambrian geology
- 28 Quaternary geology
- 29 remote sensing
- 30 sedimentology
- 31 stratigraphy
- 32 structural geology
- 33 tectonics
- 34 volcanology
- 35 OTHER

PLEASE NOTE: This is one of a pair of closely related papers: The other is by Noble, Worthington & McKee. If at all possible, this paper should be scheduled directly after Noble et al.

3 SELECT ONE FORMAT

- INVITED FOR SYMPOSIUM NUMBER: _____
(first five words of symposium title)
- VOLUNTEERED FOR DISCIPLINE SESSION
- VOLUNTEERED FOR THEME SESSION NUMBER: T25
Cenozoic Extension in the Cordillera
(first five words of Theme Session title)

4 SELECT ONE MODE (Be aware that some sessions may have been designated specifically as either "poster" or "oral.")

- ORAL—Verbal presentation before a seated audience.
- POSTER—Graphic display on poster boards supplemented by speaker comments.
- EITHER—Either mode is acceptable.

5 CHECK IF THIS APPLIES

- WITHDRAW—If the abstract cannot be accepted in the mode I have indicated, please withdraw it.

6 INDICATE % OF THIS PAPER PREVIOUSLY PRESENTED 10%

Where? GSA
When? Cord. Meeting, 1990

7 CHECK IF YOU ARE WILLING TO BE A SESSION CHAIR _____

Your Name S. I. Weiss
Office Phone 702/784-1104 Home Phone 702/747-5921

8 SPEAKER'S IDENTITY AND MAILING ADDRESS

Name Joseph E. Worthington
Address Mackay School of Mines
Address Univ. of Nevada, Reno
City/ST/ZIP Reno, NV 89557
Country _____
Office Phone 702/784-6050 Home Phone _____
If the speaker will be unavailable at these numbers during the 45 days following the abstract deadline, list phone numbers to be used instead.
Office Phone 702/784-1104 Home Phone 702/747-5921
(S. I. Weiss)

9 MAILING INSTRUCTIONS

INVITED ABSTRACTS: Mail original + 5 copies DIRECTLY TO THE CONVENER.
VOLUNTEERED ABSTRACTS: Mail original + 8 copies to the appropriate address to arrive on or before the deadline. Abstracts may NOT be sent by fax.

APPENDIX D

ABSTRACT FORM FOR ALL GSA MEETINGS IN 1991

Complete all sections ① through ⑤ below

① TYPE ABSTRACT COMPLETELY WITHIN THE BLUE LINES BELOW.

Geological Society of America Abstracts, v. 23, p.A246.

No 6442

MULTIPLE EPISODES OF Au-Ag MINERALIZATION IN THE BULLFROG HILLS, SW NEVADA, AND THEIR RELATION TO COEVAL EXTENSION AND VOLCANISM

WEISS, Steven I., Mackay School of Mines, Univ. Nevada, Reno, NV 89557; McKEE, E. H., U.S. Geol. Survey, 345 Middlefield Road, Menlo Park, CA 94025; NOBLE, D. C., CONNORS, K. A., Mackay School of Mines, Univ. Nevada, Reno, NV 89557; JACKSON, M. R., Western States Minerals, Box 3094, Elko, NV, 89801.

In the southern Bullfrog Hills, epithermal Au-Ag vein deposits at the Original Bullfrog, Gold Bar, Bond Gold Bullfrog, Montgomery-Shoshone and Rhyolite mines are localized along low-, moderate- and high-angle faults and fractures that formed during a pulse of regional extension accommodated by imbricate normal faulting and movement along the low-angle Original Bullfrog - Fluorspar Canyon (OB-FC) detachment fault system. The timing of this deformation has previously been bracketed between 11.4 Ma and 7.6 Ma based on stratigraphic and structural relations, with some movement occurring before deposition of the ca. 10-10.5 Ma tuffs and lavas overlying the Timber Mountain Tuff. $^{40}\text{Ar}/^{39}\text{Ar}$ age determinations on adularia (hydrothermal K-spar) are consistent with previous K-Ar ages, and together show that hydrothermal activity and precious-metal mineralization in the Bullfrog Hills took place over a period of about 2 Ma. These ages, together with structural and textural relations, also bear on the absolute age of faulting associated with the OB-FC detachment system. Adularia age determinations from the Bullfrog Hills are:

Original Bullfrog mine	$^{40}\text{Ar}/^{39}\text{Ar}$: 9.2 ± 0.3 Ma	K-Ar: 8.7 ± 0.3 Ma
Bond Gold Bullfrog mine	$^{40}\text{Ar}/^{39}\text{Ar}$: 9.8 ± 0.3 Ma	
Montgomery-Shoshone mine (Morton et al., 1977)		K-Ar: 9.5 ± 0.2 Ma
Mayflower mine	$^{40}\text{Ar}/^{39}\text{Ar}$: 9.9 ± 0.3 Ma	K-Ar: 10.0 ± 0.3 Ma
North of Pioneer mine		K-Ar: 11.0 ± 0.4 Ma
Yellowjacket mine	$^{40}\text{Ar}/^{39}\text{Ar}$: 11.3 ± 0.3 Ma	

Repeated episodes of brecciation and vein deposition at the Original Bullfrog and Bond Gold Bullfrog mines provide evidence for syndepositional movements of the host faults at about 9.0 Ma and 9.8 Ma, respectively. The Original Bullfrog vein is shattered and truncated by the OB-FC fault, indicating that movement on this structure continued after about 9 Ma. Well-developed, subparallel fault surfaces bounding the main vein of the Bond Gold Bullfrog deposit post-date vein deposition, showing that movement of the upper plate continued after about 9.8 Ma. These relations are consistent with the fact that ca. 10-10.5 Ma tuffs and lavas in the Bullfrog Hills are cut and tilted by imbricate normal faults. Mineralization in the southern Bullfrog Hills closely coincided with and followed by as much as 1 Ma the end of the 10-10.5 Ma volcanism. Mineralization was penecontemporaneous with extensional faulting, which continued after mineralization.

In the northern Bullfrog Hills, Au-Ag mineralization at the Mayflower mine was of effectively the same age as the deposits to the south. However, a few kilometers to the north, veins cutting the Crater Flat Tuff in the Pioneer-Yellowjacket area were formed at most a few tenths of a million years after deposition of the Timber Mountain Tuff and Tuffs of Fleur de Lis Ranch.

② CHECK ONE DISCIPLINE (category) below in which reviewers will be best qualified to evaluate your abstract. Check "Other" if you want the program chairs to choose for you.

- 1 archaeological geology
- 2 coal geology
- 3 computers
- 4 economic geology
- 5 engineering geology
- 6 environmental geology
- 7 geochemistry, aqueous
- 8 geochemistry, other
- 9 geology education
- 10 geomorphology
- 11 geophysics/ tectonogeophysics
- 12 geoscience information
- 13 global geoscience
- 14 history of geology
- 15 hydrogeology
- 16 marine geology
- 17 micropaleontology
- 18 mineralogy/ crystallography
- 19 paleoceanography/ paleoclimatology
- 20 paleontology/ paleobotany
- 21 petroleum geology
- 22 petrology, experimental
- 23 petrology, igneous
- 24 petrology, metamorphic
- 25 petrology, sedimentary
- 26 planetary geology
- 27 Precambrian geology
- 28 Quaternary geology
- 29 remote sensing
- 30 sedimentology
- 31 stratigraphy
- 32 structural geology
- 33 tectonics
- 34 volcanology
- 35 OTHER

③ SELECT ONE FORMAT

INVITED FOR SYMPOSIUM NUMBER: _____

(first five words of symposium title)

VOLUNTEERED FOR DISCIPLINE SESSION (#4)

VOLUNTEERED FOR THEME SESSION NUMBER: T25
Cenozoic Extension in the Cordillera

(first five words of Theme Session title)

I would prefer T25 but an Econ Geolo. session would be acceptable too.

④ SELECT ONE MODE (Be aware that some sessions may have been designated specifically as either "poster" or "oral.")

ORAL—Verbal presentation before a seated audience.

POSTER—Graphic display on poster boards supplemented by speaker comments.

EITHER—Either mode is acceptable.

⑤ CHECK IF THIS APPLIES

WITHDRAW—If the abstract cannot be accepted in the mode I have indicated, please withdraw it.

⑥ INDICATE % OF THIS PAPER PREVIOUSLY PRESENTED 0

Where? _____

When? _____

⑦ CHECK IF YOU ARE WILLING TO BE A SESSION CHAIR yes

Your Name Steven I. Weiss

Office Phone 702-784-1104 Home Phone 702-747-5921

⑧ SPEAKER'S IDENTITY AND MAILING ADDRESS

Name Steven I. Weiss

Address Dept. Geological Sciences

Address University of Nevada, Reno

City/S/ZIP Reno, NV 89557

Country USA

Office Phone 702-784-1104 Home Phone 702-747-5921

If the speaker will be unavailable at these numbers during the 45 days following the abstract deadline, list phone numbers to be used instead.

Office Phone _____

Home Phone _____

⑨ MAILING INSTRUCTIONS

INVITED ABSTRACTS: Mail original + 5 copies DIRECTLY TO THE CONVENER.

VOLUNTEERED ABSTRACTS: Mail original + 8 copies to the appropriate address to arrive on or before the deadline. Abstracts may NOT be sent by fax.

APPENDIX E

CONTRASTING STYLES OF EPITHERMAL PRECIOUS-METAL MINERALIZATION IN THE SOUTHWESTERN NEVADA VOLCANIC FIELD.

Stephen B. Castor, Nevada Bureau of Mines and Geology, Mackay School of Mines,
University of Nevada, Reno NV 89557.

Steven I. Weiss, Department of Geological Sciences, Mackay School of Mines,
University of Nevada, Reno NV 89557.

ABSTRACT

The southwestern Nevada volcanic field contains epithermal precious-metal deposits hosted by Miocene volcanic rocks and pre-Tertiary sedimentary rocks with production + reserves greater than 60 t of gold and 150 t of silver. The volcanic rocks consist predominantly of ash-flow tuffs erupted between 15 Ma and 7 Ma during three major magmatic stages. Hydrothermal activity and precious-metal mineralization in the southern part of the field took place between ca. 13 and 8.5 Ma, coinciding with portions of all three magmatic stages. Regional extension during this period produced imbricate normal and detachment faulting that provided structural control for some of the mineralization.

Contrasts in the style and geochemistry of mineralization, together with stratigraphic and radiometric age data and differences in geologic setting reflect the variable nature of hydrothermal activity during development of the southwestern Nevada volcanic field. During the main magmatic stage at Wahmonie, silver-rich vein mineralization of the adularia-sericite type occurred in an intermediate volcanic center. Secondary high-salinity fluid inclusions in felsic subvolcanic intrusions, a trace element suite that includes bismuth and tellurium, and geophysical data support the presence of a buried porphyry-type magmatic system at Wahmonie.

Hydrothermal activity at Bare Mountain took place during the main magmatic stage, and may have continued into the Timber Mountain magmatic stage. Bare Mountain contains gold-rich, disseminated Carlin-type deposits with high arsenic, antimony, mercury, and fluorine in sedimentary and igneous rocks. In northern and eastern Bare Mountain mineralization is associated with felsic porphyry dikes that contain secondary high-salinity fluid inclusions. A genetic relationship

between porphyry magmatism and shallow Carlin-type gold deposits seems likely at Bare Mountain.

Sedimentary rock-hosted mineralization at Mine Mountain is spatially associated with a thrust fault and was apparently deposited, in part, by a hydrothermal system active during the Timber Mountain magmatic stage. The silver:gold ratio is high and base-metal, arsenic, antimony, mercury, and selenium contents are very high. Mine Mountain mineralization shares features with vein and disseminated silver deposits at Candelaria, Nevada.

Gold-silver deposits in the areally extensive Bullfrog district comprise the largest known precious metal resource in the volcanic field. They are mainly quartz-carbonate \pm adularia veins with alteration and mineralization styles similar to other adularia-sericite type deposits in the Great Basin. Deposits in the Rhyolite area and at the Gold Bar mine have very low contents of arsenic and mercury compared to other epithermal deposits in the Great Basin, although copper and antimony are locally elevated. Similarities in mineralization style and assemblages, which include two occurrences of the rare gold-silver sulfide uytenbogaardtite, indicate deposition under similar conditions in different parts of the district. Hydrothermal activity in the Bullfrog district was coeval with extensional tectonism and may have continued from the Timber Mountain stage into the late magmatic stage. Mineralization at some deposits in the Bullfrog and Bare Mountain districts is spatially associated with and, in part, structurally controlled by a regional detachment fault system. However, significant differences in age, mineralization style, and geochemistry indicate that mineralization in the two districts is unrelated.

INTRODUCTION

The southwestern Nevada volcanic field (SWNVF) consists of Middle to Late Miocene volcanic rocks that once covered an area of more than 10,000 km² (Byers et al., 1989) centered about 150 km northwest of Las Vegas (Fig. 1). The southern part of the SWNVF contains precious-metal deposits that have been exploited intermittently from the mid 19th century to the present. These deposits are hosted by volcanic rocks of the SWNVF and underlying pre-Tertiary sedimentary rocks.

In the course of more than three decades of geologic investigations, conducted mainly in support of nuclear weapons testing and proposed nuclear waste storage programs, the SWNVF has become one of the most well-studied intracontinental

volcanic fields in the world. Considerable efforts have been directed toward understanding the intense, long-lived history of magmatic and volcanic activity, caldera geology, volcano-tectonic evolution, and Neogene structural setting of the SWNVF. Investigations of hydrothermal activity and mineralization in the SWNVF have mostly been limited to reports on individual ore deposits and mineralized districts (e.g., Ransome et al., 1910; Cornwall and Kleinhampl, 1964; Tingley, 1984; Jorgensen et al., 1989) or to mineral inventories of large areas that include parts of the SWNVF (e.g., Cornwall, 1972; Quade et al., 1984;). Jackson (1988) summarized time-space patterns of hydrothermal activity and mineralization, and proposed that hydrothermal activity and epithermal mineralization in the southern part of the SWNVF were related to magmatic and volcanic activity at major volcanic centers. More recently, Noble et al. (1991) proposed that hydrothermal activity and mineralization were associated with specific magmatic stages in the development of the SWNVF. However, comparisons of geologic and geochemical features of precious-metal deposits for the SWNVF as a whole are lacking.

In this paper we compare geologic settings, geochemical characteristics, mineralization and alteration assemblages, and general styles of mineralization of four selected areas in the southern part of the SWNVF: the Bullfrog district; northern and eastern Bare Mountain; the Wahmonie district; and Mine Mountain. Contrasts between these four mineralized areas illustrate the diverse nature of hydrothermal systems associated with the development of the SWNVF.

GEOLOGY OF THE SWNVF

The SWNVF is composed predominantly of silicic ash-flow tuff, including 12 sheets of regional extent, along with related surge and air-fall deposits and subordinate silicic to mafic lavas and intrusions. These rocks overlie complexly deformed and locally metamorphosed Late Precambrian and Paleozoic miogeoclinal sedimentary rocks. Rocks of the SWNVF are distinctly younger than Late Oligocene to Early Miocene volcanic rocks exposed to the north (such as the volcanic rocks of the Goldfield district). Most rocks of the SWNVF were erupted between 15 Ma and 10 Ma during the development of a large central complex of nested and overlapping volcanic centers of the collapse caldera type (Fig. 1). From about 9 to 7 Ma volcanism in the SWNVF shifted to volcanic centers in the northwestern part of the field. Table 1 summarizes the stratigraphy and geochronology of the three major magmatic

stages of the SWNVF proposed by Noble et al. (1991): the 15.2- to 12.7-Ma main stage; the 11.6- to 9-Ma Timber Mountain stage; and the 9- to 7-Ma late stage.

Although the SWNVF is located within the Walker Lane structural belt, northwest-trending right-lateral faults and shear zones that characterize other parts of the belt are poorly developed in the SWNVF (Stewart, 1988). Instead, the majority of structural features within the SWNVF are attributed to magmatic and volcanic processes, including magmatic tumescence, caldera collapse, and resurgent doming (Christiansen et al., 1977) and to Middle to Late Miocene regional extension that resulted in imbricate normal faulting and detachment faulting. In the southwestern part of the SWNVF, much extension appears to have been accommodated along the Original Bullfrog - Fluorspar Canyon (OB-FC) detachment fault system (Fig. 2), which is part of a regional fault system that continues southwest into Death Valley (Carr and Mosen, 1988; Hamilton, 1988).

ANALYTICAL METHODS

Chemical analyses were performed by Geochemical Services Inc., Rocklin, California, using inductively-coupled plasma emission spectroscopy (ICP-ES). Blind repeat analyses of sample pulps showed good reproducibility of results for all elements; but analyses on duplicate rock specimens show some differences (particularly for moderate to high-level gold analyses) that are probably due to the "nugget effect." Comparative analyses done at the Nevada Bureau of Mines and Geology (NBMG) using atomic absorption for arsenic, bismuth, mercury, and antimony showed excellent agreement for background-level samples collected from the SWNVF (Castor et al., 1990). Comparative analyses for gold, silver, arsenic, and antimony performed by Bondar-Clegg, Inc. by instrumental neutron activation methods showed good agreement with the ICP-ES values for samples that ranged from background to highly mineralized. In addition, a comparison of Geochemical Services Inc. gold and silver values for NBMG standards (Lechler and Desilets, 1991) showed good agreement at high levels with recommended values obtained by averaging analyses by a number of commercial laboratories.

Mineral identifications were made using standard petrographic techniques, X-ray diffraction, and scanning electron microscope (SEM) analyses. Mineral compositions were obtained during SEM examination by energy dispersive X-ray (EDX) techniques using pure metal standards at the U. S. Bureau of Mines Western

Research Center, Reno, Nevada. Mineral compositions reported are as molecular contents (rather than by weight percent). Descriptions of vein textures are based on a formal classification of the textures of vein quartz developed by Dowling and Morrison (1989).

MINERALIZED AREAS

Although records are sparse, we estimate that early gold production from the southern part of the SWNVF was about 3 t (100,000 oz) until significant operations ceased in the 1940s; silver production was of about the same magnitude. However, extensive exploration and development has taken place since the mid-1970s, and production and reserves for the SWNVF now total over 60 t (2 million oz) of gold and 150 t (5 million oz) of silver.

In connection with studies of mineral potential at the proposed nuclear waste site at Yucca Mountain, we obtained multi-element analyses of 150 vein and(or) altered wall rock samples from areas with precious-metal mineralization in the SWNVF. Our results (Table 2) together with data from the literature show significant variations in trace element suites for different mineralized areas in the SWNVF. For comparative purposes, analyses of unaltered volcanic rocks from the SWNVF are also reported (Table 3). Correlation coefficients between trace element contents for each area represented by 13 or more samples are shown in Figure 3.

WAHMONIE DISTRICT

The earliest mining activity in rocks of the SWNVF took place in the Wahmonie mining district (Figs. 2 and 4) where near-surface ores are thought to have been worked as early as 1853 (Quade et al., 1984). Discoveries of high-grade silver-gold ore in 1928 resulted in considerable development, including the 150-m-deep Wingfield shaft, but little ore was shipped. In 1940, the Wahmonie district was withdrawn from mineral entry when it was included within the Tonopah Bombing and Gunnery Range. This area later became part of the Nevada Test Site of the U. S. Department of Energy and remains excluded from civilian development.

Precious-metal mineralization in the Wahmonie district lies in a northeast-trending 8 km by 4 km elliptical area underlain by intensely altered andesitic to latitic lavas, tuffs, and breccias of the Wahmonie Formation (Ekren and Sargent,

1965). The altered area includes a central northeast-trending 3 km by 1 km horst containing weakly to strongly altered rhyodacitic volcanic rocks that are cut by intermediate to silicic subvolcanic intrusions (Fig. 4). The intermediate to felsic igneous rocks at Wahmonie probably comprise the eroded remnants of a central volcano or dome and flow field. K-Ar ages (recalculated to current constants) indicate that these rocks were emplaced between about 13.2 and 12.8 Ma (Kistler, 1968). They are overlain by units of the Paintbrush Tuff (Ekren and Sargent, 1965), which have similar to slightly younger ages of about 13.0 to 12.7 Ma (Sawyer et al., 1990).

The area of the most intense prospecting and development, which includes the Wingfield shaft (Fig. 4), is a northeast-trending zone of abundant quartz veins about 1 km long in strongly altered rock along the southeastern side of the central horst. Near-vein alteration in this area is dominated by silicification and adularization with some argillic minerals. Feldspar phenocrysts are replaced by granular adularia with illite + sericite \pm kaolinite or by single crystals of secondary potash feldspar with mottled extinction. According to Jackson (1988), near-vein adularia + sericite + silica alteration grades outward to kaolinite-bearing rock. Alunite was reported to occur in strongly altered rock and in quartz veins (Ekren and Sargent, 1965; Quade et al., 1984), but no alunite was found during petrographic and X-ray diffraction analyses by the writers. Sulfide-rich silicified rock on mine dumps in the Wingfield shaft area, and widespread limonite indicate that significant amounts of pyrite were previously present in altered wall rock. Propylitic alteration consisting of chlorite \pm albite \pm calcite \pm pyrite is widespread in the central horst. Argillic alteration, potassic alteration (with secondary biotite), and tourmaline veinlets are locally present in, or adjacent to, central horst intrusions.

Precious-metal-bearing veins consist mainly of fine comb quartz \pm calcite with minor adularia. They carry free gold, cerargyrite, hessite, iron and manganese oxides, acanthite, and other sulfides (Quade et al., 1984). Very finely granular quartz veins with anomalously high precious-metal contents (up to 0.4 ppm gold and 3.5 ppm silver) are exposed in the vicinity of the Wingfield shaft. Stockworks of fine comb to granular quartz veinlets with adularia rhombs are also present.

SEM/EDX studies of highly mineralized rock from Wahmonie disclosed electrum ($\text{Au}_{77}\text{Ag}_{23}$) occurring as irregular threads or flakes in cerargyrite (Fig. 5a) and hessite (Ag_2Te) occurring as colloform bands in cerargyrite (Fig. 5b). Iron tellurite containing minor gold and manganese (possibly mackayite, $\text{Fe}_2\{\text{TeO}\}_3 \cdot x\text{H}_2\text{O}$) was found in cerargyrite. Frobergite (FeTe_2) and hedleyite (BiTe_2) were also tentatively

identified, and cinnabar was found in cavities as micron-size granules on cerargyrite (J. Sjöberg and J. Quade, personal communication, 1991).

Vein samples analyzed during this study contain up to 109 oz silver and 11 oz gold per ton, but samples carrying up to 1130 oz silver and 50 oz gold per ton have been reported previously (Quade et al., 1984). Mineralized and(or) altered samples from the Wahmonie district have relatively high silver:gold ratios (Table 2) and bismuth, mercury, and tellurium correlate well with gold (Figs. 3 and 6). Copper, lead, and antimony are locally high, but do not correlate with gold. Base-metal contents are low in mineralized samples from Wahmonie, with the exception of a single vein sample with secondary copper minerals that is enriched in copper and lead but poor in silver and gold. Arsenic content is generally low (Table 2), but pyrite-rich silicified rock with 360 ppm arsenic was collected from a dump near the Wingfield shaft.

Rock with high precious-metal and tellurium contents in the Wahmonie district is not restricted to the Wingfield shaft area, and may occur widely in the district. Hessite-bearing comb quartz from a small dump in the central horst 1 km northeast of the Wingfield shaft contains 748 ppm silver 11 ppm gold and 90 ppm tellurium. Granodiorite altered to a mixture of quartz and illite 4 km northeast of the Wingfield shaft also has elevated gold and tellurium contents (Quade et al., 1984).

Adularia from altered rocks with abundant silica-adularia veins in the Wahmonie district gave K-Ar ages of 12.6 ± 0.4 and 12.9 ± 0.4 Ma (Jackson, 1988). These ages indicate that hydrothermal activity and mineralization closely followed magmatic and volcanic activity of the main magmatic stage of the SWNVF at Wahmonie.

On the basis of a positive residual gravity anomaly centered about 1 km southwest of the mineralized area at Wahmonie and associated magnetic highs, Ponce (1981) inferred the presence of a large buried felsic intrusive mass similar to and contiguous with granodiorite exposures in the central horst. The highest portions of this intrusive body appear to be along the east side of the central horst, coincident with the area of precious-metal mineralization. As pointed out by Hoover et al. (1982), the edges of the inferred intrusion correspond approximately with alteration in the Wahmonie district. Relatively high resistivity in the inferred intrusion indicates high porosity due to fracturing, faulting, alteration, and(or) mineralization. Induced polarization data indicate that 2% or more sulfides are present below the water table at Wahmonie (Hoover et al., 1982).

Alteration and veining in granodioritic porphyry intrusions in the central horst, along with high bismuth and tellurium support the presence of a porphyry magmatic-hydrothermal system at Wahmonie. In addition, quartz phenocrysts containing hypersaline secondary fluid inclusions, which are indicative of magmatic hydrothermal fluids, occur in samples with secondary biotite (D. C. Noble, personal communication, 1990).

BARE MOUNTAIN AREA

Between initial discovery in 1905 and the late 1970s small amounts of gold and mercury were produced intermittently from deposits in northern and eastern Bare Mountain, including the Panama-Sterling gold mine and the Telluride gold-mercury camp (Fig. 2). Fluorspar was produced more-or-less continuously from the same area between 1918 and 1989 from the Daisy, Goldspar and Mary mines. Approximately 2.5 t (80,000 oz) of gold were produced from disseminated deposits at the Sterling and Mother Lode mines between 1983 and 1990 (Bonham and Hess, in review). Additional, currently subeconomic disseminated gold deposits are present at the Daisy mine, Secret Pass, Goldspar mine, and near the Mother Lode mine (J. Marr, personal communication, 1987; Greybeck and Wallace, 1991).

Bare Mountain consists predominantly of weakly metamorphosed Late Proterozoic through Late Paleozoic sedimentary rocks of the Cordilleran miogeocline that underwent Mesozoic folding and thrust-faulting and Tertiary low- to high-angle normal and strike-slip faulting (Cornwall and Kleinhampl, 1961; Monsen et al., 1990). In northern Bare Mountain these rocks are separated from overlying, imbricately faulted volcanic rocks of the SWNVF by the north-dipping, low- to moderate-angle Fluorspar Canyon fault (Cornwall and Kleinhampl, 1961) which is considered by recent workers to be the eastern continuation of the Original Bullfrog fault (e.g., Carr and Monsen, 1988). In contrast to the Bullfrog Hills, where major faulting and tilting post-dated deposition of the 11.4 Ma Ammonia Tanks Member, deformation in northeastern Bare Mountain had mostly ceased by 11.6 Ma, as indicated by strong angular discordance between the flat-lying, 11.6-Ma Rainier Mesa Member of the Timber Mountain Tuff and underlying tilted units of the SWNVF (Carr, 1984; Carr and Monsen, 1988; Monsen et al., 1990; Weiss et al., 1990).

A swarm of north-trending felsic porphyry dikes intrudes the pre-Cenozoic rocks in eastern and northern Bare Mountain. The dike rocks typically have coarsely granophyric groundmass and have been affected by variable degrees of

potassium-feldspar, sericitic, and argillic alteration. Hypersaline fluid inclusions that are present in quartz phenocrysts reflect the passage of an early high-salinity hydrothermal fluid (Noble et al., 1989). The dikes were emplaced during the main magmatic stage of the SWNVF, as demonstrated by radiometric age determinations ranging between 14.9 ± 0.5 Ma and 13.8 ± 0.2 Ma (Marvin et al., 1989; Monsen et al., 1990; Noble et al., 1991). Most mineral deposits along the east flank of Bare Mountain are spatially associated with, and post-date or are nearly contemporaneous with the emplacement of, these dikes.

Several base-metal \pm gold occurrences, generally associated with quartz veins in Precambrian and Cambrian rocks, have been reported along the west flank of Bare Mountain (Cornwall, 1972; Tingley, 1984). However, most of the mineral deposits in Bare Mountain are located in its northern and eastern flanks.

At the Sterling mine (Fig. 2), sediment-hosted disseminated gold-silver mineralization is controlled by the intersection of normal faults with a thrust fault that juxtaposes clastic rocks of the Late Proterozoic to Early Cambrian Wood Canyon Formation over carbonate rocks of the Middle Cambrian Bonanza King Formation (Odt, 1983). This mineralization is associated with alteration assemblages that include kaolinite, illite, sericite, jarosite, and alunite, and with very little introduction or removal of silica and iron (Odt, 1983). Stibnite, cinnabar and fluorite are present in ore and in nearby exposures of hydrothermal breccia (Tingley, 1984). Hydrothermally altered porphyry dikes are abundant in the Sterling Mine area, and locally have elevated gold contents (Odt, 1983; Tingley, 1984; Jackson, 1988).

North of the Sterling mine, a zone of argillic alteration and bleaching accompanies the porphyry dikes and locally contains fluorite and disseminated gold mineralization in Paleozoic carbonate rocks (Tingley, 1984; D. Odt, personal communication, 1987). At the Goldspar mine (Fig. 2), fluorite replaces brecciated and sheared carbonate rocks of the Nopah Formation and fills fractures in altered dike rock (Papke, 1979; Tingley, 1984; Jackson, 1988). Similar fluorite mineralization and alteration is present in Silurian dolomite at the Mary mine.

The Goldspar deposit has been interpreted as a high-level breccia pipe (e.g. Tingley, 1984). Altered clasts of Tertiary volcanic rocks in the breccia (Jackson, 1988) are unlikely to have been transported from below the Cambrian host rocks. This suggests that the breccia was open to much higher stratigraphic levels at the time of hydrothermal activity.

In the Telluride mine area (Fig. 2), gold mineralization is present with quartz, opal, alunite, and pyrite along the Fluorspar Canyon fault (Jackson, 1988) and occurs

in altered porphyry dikes that intrude carbonate rocks in the foot wall of the fault. Mercury was mined from pipelike breccia bodies and also occurs as disseminated cinnabar with fluorite, calcite, opal, and alunite at the Telluride mine (Tingley, 1984).

The Mother Lode gold mine is situated immediately to the north of the Telluride mine area, near the northeasternmost exposure of the Fluorspar Canyon fault segment of the OB-FC fault system (Fig. 2). Disseminated gold mineralization is present in felsic porphyry dikes, sills and extrusive(?) rocks and in adjacent interbedded sandstone, siltstone, and limestone. Mapa (1990) considered the sedimentary host rocks to be part of the Mississippian Eleana Formation, whereas others (e.g., S. Ristorcelli, personal communication, 1990) interpret them as belonging to the Silurian Roberts Mountain Formation and to the Early(?) to Middle Miocene rocks of Joshua Hollow of Monsen et al. (1990). Alteration is primarily argillic, with pyrite in unoxidized rocks and jarosite in oxidized rocks. Altered rock is mostly composed of quartz and illite, and feldspar phenocrysts are generally completely replaced by illite \pm calcite, but some samples contain sanidine that is apparently unaltered. Mafic minerals are replaced by sericite \pm illite \pm calcite \pm rutile. Sooty remobilized carbon is abundant locally in the sedimentary rocks. Very sparse, irregular veins containing fine to medium drusy quartz + manganese oxide \pm opal occur in oxidized ore, and calcite veins cut limestone. About 150 m west of the mine, glassy bedded tuff that is considered to lie stratigraphically between the Paintbrush and Timber Mountain Tuffs (Monsen et al., 1990) contains very fine-grained alunite. In addition, chalcedony replaces conglomerate and opal replaces bedded tuff in the same unit about 600 m northwest of the mine.

Three mineralized zones containing a total of 12.3 Mt that average 0.81 g/t of gold (13.5 Mst @ 0.026 oz/st) have been delineated in Fluorspar Canyon 3 to 5 km southwest of the Mother Lode mine (Greybeck and Wallace, 1991). In this area, two disseminated gold deposits associated with fluorite mineralization are present within Cambrian rocks of the Nopah, Bonanza King and Carrara Formations in and near the Daisy fluorite mine (Papke, 1979; Tingley, 1984; Greybeck and Wallace, 1991). These deposits, which are situated beneath the Fluorspar Canyon fault (Fig. 2), are associated with alteration that ranges from subtle decalcification to intense silicification (Greybeck and Wallace, 1991). Cinnabar commonly accompanies fluorite in the Daisy mine.

The nearby volcanic-hosted Secret Pass deposit contains disseminated gold in altered ash-flow tuff of the Bullfrog Member of the Crater Flat Tuff. The deposit is bounded by the underlying Fluorspar Canyon fault (Greybeck and Wallace, 1991). An

alteration assemblage including quartz, adularia, calcite, and pyrite, with generally weak silicification, is associated with gold mineralization (Greybeck and Wallace, 1991). Although precious-metal mineralization is confined to the Crater Flat Tuff, adularia- and illite(?) -bearing alteration assemblages continue up into the overlying ca. 13-Ma Topopah Spring Member of the Paintbrush Tuff. In addition, chalcedonic veins that may be related to this mineralization are present in the 12.7-Ma Tiva Canyon Member.

Altered and(or) mineralized samples from the Bare Mountain area collected during this study include 20 samples from the Mother Lode orebody and 16 samples from workings and outcrops within 1 km south and west of the mine. The average silver:gold ratio for all samples is 10:1, but samples from the Mother Lode mine average about 2:1. The samples have high arsenic and antimony contents, and gold correlates strongly with these two elements (Figs. 3 and 6). Gold is also correlative with copper, lead, mercury, tellurium, and thallium, although the contents of these metals are not highly anomalous. In general, Mother Lode mine samples with the highest gold contents contain drusy quartz and(or) opal along with manganese oxide. Pyritic ore contains gold contents similar to adjacent oxidized ore (W. Hickinbotham, personal communication, 1990). Gold-bearing phases could not be found using reflected light and scanning electron microscopy in samples containing up to 7 ppm gold.

The mineralized areas in Fluorspar Canyon southwest of the Mother Lode mine have similar correlations between gold and other trace elements, particularly antimony, thallium, and molybdenum (Greybeck and Wallace, 1991). Arsenic, mercury, and base metals are also correlative with gold, but not in all three deposits. Silver:gold ratios are generally low.

Gold-rich samples from the Sterling mine area have high arsenic, antimony, mercury, and thallium contents (Odt, 1983; Hill et al., 1986). Tingley (1984) reports high arsenic, antimony, and molybdenum contents in samples from the Telluride, Sterling, and Daisy mine areas, and high lead and zinc from the latter two areas.

The presence of hydrothermal alteration, fluorite, and locally elevated gold concentrations in porphyry dikes indicates that much, or all, of the mineralization in Bare Mountain postdates emplacement of the dikes. Radiometric ages of about 12.9 Ma were obtained on hydrothermal potassium feldspar that replaces groundmass and phenocrysts of igneous potassium feldspar in altered dike rock at the Goldspar mine, indicating that hydrothermal activity took place there during the main magmatic stage of the SWNVF (Noble et al., 1991). Close similarities in mineralization style and

trace element signatures support a similar timing for gold mineralization in pre-Cenozoic rocks in the vicinity of the Daisy mine. At the nearby Secret Pass deposit, hydrothermal alteration extends into the ca. 13-Ma Topopah Spring Member of the Paintbrush Tuff, but not into adjacent exposures of the 11.6-Ma Rainier Mesa Member of the Timber Mountain Tuff. In the Telluride mine area, alunite occurs in altered gravel in the hanging wall of the Fluorspar Canyon fault and in hydrothermal breccia in the foot wall of the fault. Samples of this alunite were dated at 12.2 ± 0.4 Ma and 11.2 ± 0.3 Ma, respectively, by K-Ar methods (Jackson, 1988). Alunitic alteration is also found near the Mother Lode mine in bedded tuff between the Paintbrush Tuff and Rainier Mesa Member of the Timber Mountain Tuff.

The dated alunite is fine-grained, suggesting either a supergene origin or a vapor-dominated depositional environment (e.g., Thompson, 1991), and the dates therefore represent minimum ages for mineralization. If the alunite was deposited by hypogene fluids, the ages suggest the possibility of more than one period of activity or that hydrothermal activity in the Telluride-Mother Lode area was of long duration.

A number of lines of evidence suggest a shallow or high-level environment for mineralization in Bare Mountain. Hydrothermal breccia in the Sterling, Goldspar, and Telluride mine areas indicates a high-level environment. The altered Tertiary volcanic rocks present in fluoritized breccia at the Goldspar mine include clasts of the Paintbrush Tuff. The most reasonable interpretation is that the volcanic rock fragments fell into the breccia prior to, or during, hydrothermal activity. Because the age of hydrothermal activity is essentially the same as the age of the Paintbrush Tuff, the deposit was probably open to the paleosurface. Cinnabar and(or) high mercury concentrations are widespread in northern and eastern Bare Mountain and alunite \pm opal is present in several mineralized areas. Such mineral associations are considered indicative of a shallow hydrothermal environment, although it is possible that the alunite is not entirely hypogene.

Noble et al. (1989) inferred the presence of a buried, granite-type porphyry molybdenum system in Bare Mountain from the presence of porphyry-style crystallization textures and hypersaline fluid inclusions in the felsic dikes, the spatial association of mineralization with the dikes, and the fluorite-molybdenum component of the trace element assemblage of the mineralization in Bare Mountain. Gold-silver-mercury-fluorite mineralization in Bare Mountain may represent the distal, near-surface expression of hydrothermal activity related to a deeper porphyry molybdenum system (Noble et al., 1989).

MINE MOUNTAIN

Mine Mountain, in the southeast part of the SWNVF (Fig. 1), was the site of mercury, base-metal, and precious-metal prospecting in the 1920s, but was subsequently included in the Nevada Test Site and withdrawn from mineral entry. A 2-km-long northeast-trending area along the crest of Mine Mountain contains quartz \pm calcite \pm barite \pm sulfides in veins, hydrothermal breccia, and silicified areas (Quade et al., 1984; L. T. Larson and S. I. Weiss, unpub. mapping, 1989). Mineralization is closely associated with the flat-lying Mine Mountain thrust fault, which separates underlying Mississippian clastic rocks from Devonian carbonate rocks in the upper plate (Orkild, 1968). The mineralization occurs both above and below the thrust fault, but appears to be most strongly developed within a few tens of meters above the fault in highly brecciated rock (L. T. Larson and S. I. Weiss, unpublished mapping, 1989).

Above the Mine Mountain thrust, mineralization is closely associated with moderate- to high-angle northeasterly-striking faults and fractures, and north- to northwest-striking high-angle fractures. Subhorizontal slickensides on these structures indicate lateral slip probably related to movements along the nearby, northeast-trending, left-slip Mine Mountain fault zone of Carr (1984). Locally, quartz-barite veins both crosscut and are offset by faults with subhorizontal slickensides, indicating that mineralization was coeval with strike-slip movement.

In the lower plate of the Mine Mountain thrust, quartz- and calcite-cemented fault and hydrothermal breccia comprise narrow veins that trend NW to nearly E-W and can be traced for as much as 1 km in clastic rocks of the Eleana Formation. Samples of these veins, which yielded the highest gold analyses of any rocks from Mine Mountain, contain very finely granular to chalcedonic quartz along with alunite and cinnabar. SEM/EDX examination of a breccia-vein sample with 0.6 ppm gold and very high arsenic and lead contents shows an arsenate, iodide, and selenide assemblage including mimetite ($3\text{Pb}_3(\text{AsO}_4)_2 \cdot \text{PbCl}_2$), conichalcite ($8\{\text{Cu,Ca}\}\text{As}_2\text{O}_3 \cdot 3\text{H}_2\text{O}$), tocomalite (HgAgI), and tiemannite (HgSe). Trace amounts of pyrite and arsenopyrite are also present.

Alteration mineralogy at Mine Mountain is dominated by fine-grained silicification. In massive carbonate rocks in the upper plate, silicification includes variable amounts of chalcedonic replacement (jasperoid) and millimeter- to centimeter-width sheeted or stockwork quartz veins. White calcite veins are abundant in carbonate rocks surrounding the area of silicification. Vein quartz has fine- to medium-granular or fine comb textures, and clear drusy quartz is also

present. Barite, calcite, galena, sphalerite, and anglesite have been identified in veins and silicified rocks. Cinnabar is present in veins and is also disseminated in leached, decalcified, and silicified carbonate rocks. Small amounts of gossan are associated with massive white calcite and barite-rich hydrothermal breccia.

Samples from Mine Mountain have high base-metal contents, along with an epithermal precious-metal suite that includes arsenic, antimony, and mercury (Table 2). Lead, zinc, selenium, cadmium, antimony, and mercury contents are very high relative to other mineralized areas in the SWNVF. The gold and silver correlation with base metals is strong at Mine Mountain (Fig. 3). The correlation between gold and selenium is particularly striking, but silver correlates much more strongly with cadmium, mercury, and base metals than does gold. The gold-silver correlation is weaker at Mine Mountain than it is in other mineralized areas in the SWNVF (Fig. 3).

The timing of hydrothermal activity at Mine Mountain is constrained by indirect stratigraphic and structural relations. Based on the presence of argillic and alunitic alteration in tuffs as young as the Ammonia Tanks Member of the Timber Mountain Tuff on the south flank of Mine Mountain, Jackson (1988) inferred the mineralization to be approximately contemporaneous with Timber Mountain magmatic activity. Alunite from an outcrop of the altered Ammonia Tanks Member has given a K-Ar age of 11.1 ± 0.3 Ma (E.H. McKee, S.I. Weiss and L.T. Larson, unpub. data, 1989), consistent with alteration shortly after deposition of the 11.4 Ma Ammonia Tanks Member. Alteration has not been traced from the dated outcrop directly into the main mineralized area. However, if syn-mineralization lateral slip movements on fault surfaces along the crest of Mine Mountain were associated with deformation along the Mine Mountain strike-slip fault system, which offsets both units of the Timber Mountain Tuff (Orkild, 1968; Carr, 1984), then mineralization occurred after 11.4 Ma as well, consistent with the K-Ar age of the alunitic alteration.

The geochemical data at Mine Mountain are consistent with mineralization from more than one hydrothermal system. Base-metal and silver vein or replacement mineralization in Paleozoic sedimentary rocks may have been remobilized and overprinted by later epithermal metallization during magmatic activity of the Timber Mountain stage of the SWNVF.

BULLFROG DISTRICT

The Bullfrog district in the Bullfrog Hills west of the town of Beatty (Fig. 1), has been the most important source of precious metals in the SWNVF. The district

contains gold-silver vein deposits that are scattered within large areas underlain by hydrothermally altered rock, particularly in the southern part of the Bullfrog Hills (Fig. 2).

The Original Bullfrog mine in the southwest corner of the Bullfrog district was discovered in 1904, but most early production came from the Montgomery-Shoshone mine 6.5 km to the east (Fig. 2). By 1940, the Bullfrog district had recorded precious metals production totalling about 3 million dollars (Couch and Carpenter, 1943). Minor precious-metal production came from the Gold Bar mine and from several mines near the town of Rhyolite. The Mayflower and Pioneer mines, about 12 km north of Rhyolite, also had minor early production. Renewed exploration in the district since the mid-1970s resulted in open-pit mining for three years at the Gold Bar mine, the delineation of open-pit mineable reserves at the Montgomery-Shoshone mine, and the discovery and development of the Bond Gold Bullfrog mine (Fig. 2), an entirely new deposit on the east side of Ladd Mountain that is expected to produce about 7.5 t (240,000 oz) of gold annually for 5 to 7 years (Jones, 1990).

The Bullfrog Hills consist of an upper, imbricately normal-faulted, extensional allocthon composed mostly of Miocene volcanic rocks that is separated from underlying Paleozoic and Proterozoic sedimentary and metamorphic rocks by a low-angle fault first recognized by Ransome et al. (1910). This structure is the Original Bullfrog segment of the regional OB-FC detachment fault system (Fig. 2) (Carr and Monsen, 1988; Maldonado, 1990a). Upper-plate rocks consist chiefly of silicic ash-flow sheets including units of the Crater Flat, Paintbrush and Timber Mountain Tuffs that were erupted from the central caldera complex of the SWNVF between about 15 and 11.4 Ma. Lesser volumes of lava flows, domes and local tuffs of silicic composition, and relatively minor amounts of mafic and intermediate composition lava flows are intercalated with the regional ash-flow sheets. Units of tuffaceous sandstone, conglomerate, shale and lacustrine limestone are present mainly in the lower part of the volcanic section. Lying with angular discordance upon the Timber Mountain Tuff and older ash-flow sheets is a local sequence of interbedded rhyolitic flows, domes and associated pyroclastic deposits which are capped by latite flows. These post-Timber Mountain Tuff rocks were erupted prior to about 10 Ma (Marvin et al., 1989; Noble et al., 1991).

Throughout much of the Bullfrog Hills, upper-plate rocks are cut by numerous west-dipping normal faults, many of listric geometry, that mostly strike north to northeast. This deformation has long been recognized as the result of WNW-ESE directed upper crustal extension, and estimates of the amount of extension range

from about 25% (Ransome et al., 1910) to more than 100% (Maldonado, 1990a). Most of the faulting and tilting began after about 11.4 Ma as demonstrated by conformable and paraconformable relations between the Ammonia Tanks Member of the Timber Mountain Tuff and underlying ash-flow sheets. Major tilting and faulting ceased before deposition of the flat-lying, 7.6 Ma Spearhead Member of the Stonewall Flat Tuff and local, Late Miocene conglomeratic deposits (Weiss et al., 1990).

Original Bullfrog Mine

The Original Bullfrog mine was developed in a complex, shallowly north-dipping vein that is approximately 10 m thick. The vein is a shattered mass of banded crustiform quartz, calcite, and silicified breccia that lies along the Original Bullfrog fault (Ransome et al., 1910). This fault, which appears to truncate the vein material against underlying, strongly sheared Paleozoic clastic and carbonate rocks that contain only minor veining, is part of the Bullfrog detachment fault system of Maldonado (1990a; 1990b). The main vein grades upwards into sheeted veins within moderately east-dipping silicified ash-flow tuff of the 13.85 Ma Lithic Ridge Tuff (Carr et al., 1986; Sawyer et al., 1990). Adularia and albite replace feldspar phenocrysts and groundmass potash-feldspar and locally, between closely spaced veins, the tuff has been pervasively adularized. This alteration grades laterally and up-section into quartz-illite and sericite-albite-calcite assemblages, and at greater distances, into weak illite-calcite ± albite alteration.

Vein quartz ranges from white, yellow and grey banded fine granular or chalcedonic material to white, clear or amethystine fine to medium comb quartz. Calcite occurs as coarsely crystalline masses intergrown with comb quartz, as inwardly-growing crystals along the walls of veins that were subsequently filled with comb quartz, or as irregular drusy veins with little or no quartz.

In addition to quartz and calcite, the main vein carries visible gold that is associated with limonite, malachite, chrysocolla, and sulfide. SEM/EDX examinations of high-grade ore show that gold occurs in irregular electrum grains up to 1 mm in diameter (Fig. 7) with compositions that range between Au₅₂Ag₄₈ and Au₄₂Ag₅₈. Gold also occurs in mixed grains of native metal (Au₈₀Ag₂₀) and uytenbogaardtite (Ag₃AuS₂). Silver is also present as acanthite, which occurs as irregular grains in quartz, and as mixed grains with uytenbogaardtite and gold. Textural relations indicate a complex paragenetic sequence. In ore containing visible gold, early calcite was followed by white comb quartz with sulfide and electrum, and lastly by vein-filling grey to amethystine quartz. The calcite is locally replaced by malachite

and chrysocolla, which also occur in irregular masses surrounding gold and sulfide, and in late veinlets with sulfide and limonite. Textural relationships indicate that electrum and acanthite are the earliest ore minerals, followed by uytenbogaardtite and gold.

Samples from the Original Bullfrog Mine have relatively high average silver:gold when compared to other mineralized areas in the Bullfrog district (Table 2). In addition, Original Bullfrog samples have strong arsenic, copper, antimony, and bismuth correlations with gold (Figs. 3 and 6).

Adularia from altered Lithic Ridge Tuff adjacent to the main vein has given a K-Ar age of 8.7 ± 0.3 Ma (Jackson, 1988) indicating that hydrothermal activity took place about 1 to 1.5 Ma after the end of volcanic activity in the Bullfrog Hills. This age, along with shattering of the vein and apparent truncation of the vein by the underlying Original Bullfrog fault, is consistent with mineralization during the major period of detachment-style faulting in the region between 11.4 and 7.6 Ma.

Gold Bar Mine

At the Gold Bar mine in the northwest corner of the Bullfrog district (Fig. 2), silver-gold mineralization is present in quartz-calcite veins and quartz-calcite cemented breccia along a northeast-trending, west-dipping normal fault system cutting units of the Crater Flat and Paintbrush Tuff and minor basaltic rocks. The main area of mineralization lies about 2 km from the surface trace of the Bullfrog detachment fault system (Maldonado, 1990a). Veins consist of banded crustiform intergrowths of calcite and fine granular and comb quartz commonly with drusy quartz and calcite and minor amethystine comb quartz. Late calcite veins are also present. Pyrite is the only sulfide mineral reported in vein material at the Gold Bar mine (Ransome et al., 1910). Wall-rock alteration appears to be similar to that at the Original Bullfrog mine. Variable albitization and adularization of feldspar phenocrysts and groundmass, along with illite/sericite alteration, are associated with silicification adjacent to veins. Disseminated pyrite is also present in unoxidized altered wall rock.

Samples collected from the Gold Bar mine have a moderate average silver:gold ratio and show only a weak gold-copper association (Figs. 3 and 6). Arsenic, antimony, mercury, and the base metals are extremely low (Table 2). The highest gold and silver contents are in veins of finely crystalline quartz with intergrown thinly bladed calcite (Fig. 8a).

Alteration and mineralization at the Gold Bar mine postdate deposition of the ca. 13- to 12.7-Ma Paintbrush Tuff but have not been dated directly. Vein and alteration styles, textures, and mineral assemblages are similar to those of other deposits in the Bullfrog district, suggesting that mineralization at the Gold Bar mine is genetically related to mineralization elsewhere in the district. In addition, veins at the Gold Bar mine were localized by upper-plate faults that were probably active during detachment-related extensional deformation between 11.4 and 7.6 Ma, indicating vein emplacement at approximately the same time as mineralization in the other deposits (see below).

Rhyolite Area

The Rhyolite area contains the largest and highest grade known gold-silver ore reserves in the SWNVF. It includes vein systems at the Montgomery-Shoshone mine, the Bond Gold Bullfrog mine and several small mines near the town of Rhyolite (Fig. 2). Most of the reserves are in the Bond Gold Bullfrog deposit where 13.0 Mt of ore averaging 3.77 g/t (14.3 Mst @ 0.110 oz/st) were reported to be present prior to the start of production in 1989 (Jorgensen et al., 1989). Most of the historic gold and silver production in the Bullfrog district came from the Montgomery-Shoshone mine, about 1.5 km northeast of Rhyolite (Couch and Carpenter, 1943), which has current reserves of 2.8 Mt of gold ore at an average grade of 2.5 g/t (3.1 Mst @ 0.072 oz/st) (Jorgensen et al., 1989). Host rocks for veins in the Rhyolite area are predominantly densely welded, devitrified portions of ash-flow sheets of the Paintbrush and Timber Mountain Tuffs.

At the Bond Gold Bullfrog mine gold-silver ore is mined from a moderately west-dipping vein system that lies along a normal fault ("middle-plate fault" of Jorgensen et al., 1989) at the eastern foot of Ladd Mountain. Ore comprises a central zone, as much as 70 m thick, of complexly cross-cutting veins, hydrothermal breccia and silicified volcanic rock, that lies within the vein system. Closely-spaced veins in the ore zone form stockworks and/or sheeted swarms. More widely-spaced veins also form stockworks above and below the ore zone (Jorgensen et al., 1989). Well developed faults that have been the locus of significant displacement bound the ore zone in most places and are accompanied by gold-rich hydrothermal breccia (B. Claybourne, personal commun., 1991). The hanging wall rocks are well exposed on Ladd Mountain, an east-tilted fault-block that is composed mainly of a pervasively altered section of the Timber Mountain Tuff, a thin basaltic flow or sill, and underlying units of the Paintbrush Tuff and Crater Flat Tuff (Maldonado and

Hausback, 1990). Exposed foot wall rocks include strongly altered rocks probably belonging to the Crater Flat Tuff and an underlying unit of dacitic to rhyodacitic lava that is widely exposed beneath the Crater Flat and Lithic Ridge Tuffs elsewhere in the Bullfrog Hills (c.f., Maldonado and Hausback, 1990).

Vein material consists mostly of crustiform fine granular and comb quartz (locally amethystine) \pm intergrown calcite of anhedral to finely bladed habit (Fig. 8b). Bands and veins of very finely granular to chalcedonic quartz and moderately coarse comb quartz are also present, and bands of fine adularia occur in minor amounts. Fluorite and barite have also been reported (Jorgensen et al., 1989). Fragments of wallrock are included in the veins and have been partly to nearly completely replaced by fine-grained quartz and potash feldspar.

Multiple generations of cross-cutting quartz \pm calcite veins, open space infillings, and fragments of vein material surrounded by later stages of quartz \pm calcite provide evidence for a multi-stage paragenesis and for fracturing and brecciation concurrent with vein deposition. Much of the vein material is highly fractured, and faults generally form the margins of the main ore zone. These features suggest that the latest movements on the host fault post-date the last stages of vein deposition.

The style of mineralization at the Montgomery-Shoshone mine is similar to that at the Bond Gold Bullfrog deposit (Jorgensen et al., 1989). Most of the gold-silver ore came from veins and breccia along a major, northeast-trending high-angle fault that juxtaposes unmineralized and unaltered, to very weakly altered, post-Timber Mountain rhyolitic to latitic rocks on the north against strongly altered rocks, mainly of the Ammonia Tanks Member of the Timber Mountain Tuff, to the south.

Mineralization extends southward for as much as 0.5 km in and along several north-trending quartz-calcite veins that occupy fractures and minor faults (Jorgensen et al., 1989; Maldonado and Hausback, 1990). Faults and fractures that control mineralization are part of the imbricate fault system associated with extension above the OB-FC fault (Maldonado, 1990a).

A number of smaller gold-silver bearing quartz and quartz-calcite veins similar to those of the Bond Gold Bullfrog and Montgomery-Shoshone deposits were mined in the immediate vicinity of Rhyolite. The most notable workings include those of the National Bank mine, where sheeted and stockwork veins of fine granular quartz cut silicified and adularized tuffs of the Paintbrush Tuff and the Rainier Mesa Member of the Timber Mountain Tuff. At the Denver-Tramp mine these units host a system of subparallel steeply-dipping north-south-trending quartz-carbonate veins up to 8 m wide that carry visible gold. The Denver-Tramp veins contain banded very

finely granular to fine comb quartz that is locally amethystine, and pockets of calcite that has been partially leached, leaving dark earthy manganese and iron oxides.

In addition to local silicification, mineralization in the Rhyolite area is associated with local potash feldspar flooding and widespread adularization and albitization of feldspar phenocrysts. Thin veins within the Rainier Mesa Member on Ladd Mountain west of the Bond Gold Bullfrog mine have potash feldspar envelopes up to 1 cm thick, and sheeted veins at the National Bank mine occur in hard rock composed almost completely of secondary potash feldspar. In the Bond Gold Bullfrog, Montgomery-Shoshone, National Bank, and Denver-Tramp mines, near-vein alteration consists of replacement of feldspar phenocrysts with adularia (Fig. 9a) and(or) albite (Fig. 9b) and probable adularization of groundmass feldspar. Small amounts of illite are present, generally intergrown with secondary K-feldspar and quartz. Strong phyllosilicate alteration is uncommon in the Rhyolite area, except locally at the Montgomery-Shoshone mine. Primary biotite is commonly preserved, even in strongly altered rocks, reflecting the high activity of K⁺ needed to produce adularia. At the Bold Gold Bullfrog mine pseudomorphs of limonite after pyrite are present in oxidized rock, and unoxidized rocks contain 1-2% disseminated pyrite.

Near-vein alteration described above grades outward from mineralized structures to much more subtle, but nevertheless pervasive and widespread illite-calcite ± quartz ± albite assemblages that could be considered propylitic in character (e.g., Sander and Einaudi, 1990). Chlorite-and carbonate-bearing assemblages have been reported only from sedimentary and metamorphic rocks beneath the Original Bullfrog - Fluorspar Canyon fault (Jorgensen et al., 1989).

All of the gold identified visually in samples from the Rhyolite area was found in fine granular and comb quartz. Very fine granular vein quartz is generally present in gold ore, but was not seen to contain gold. Finely bladed calcite intergrown with quartz in vein material from the Bond Gold Bullfrog mine is similar to that observed in vein material from the Gold Bar mine. Acanthite is a major silver-bearing phase in some ore at the Bond Gold Bullfrog mine and minor amounts of chalcopyrite, galena, and sphalerite have also been reported (Jorgenson et al., 1989). Cerargyrite was reported at the Montgomery-Shoshone mine by Ransome et al. (1910). Secondary copper minerals are locally associated with gold at depth in the Bond-Bullfrog mine (B. W. Claybourn, personal communication, 1991) and tetrahedrite has also been identified (D. Brosnahan, personal communication, 1991). This mineral association is similar to that at the Original Bullfrog mine.

Ransome et al. (1910) reported that gold in the Bullfrog district characteristically occurs as electrum in limonitic specks that represent oxidized pyrite crystals. Electrum of this type is present at the Bond Gold Bullfrog mine as well (Fig. 10a). We found other types of gold in the district. Electrum occurs as contorted flakes between quartz grains (Fig. 10b) at the Bond Gold Bullfrog and Denver-Tramp mines. SEM/EDX analysis shows that electrum in this form from the Bond Gold Bullfrog mine has a composition of Au₄₄Ag₅₆. In addition, electrum and gold are present in irregular lenses composed of quartz, limonite, chrysocolla, acanthite, and uytenbogaardtite that are similar to mineralization described above at the Original Bullfrog mine. The electrum (Au₅₇Ag₄₃ to Au₅₁Ag₄₉) is in irregular grains up to 1 mm in maximum dimension, and gold (Au₇₂Ag₂₈) is present as narrow borders on electrum. The uytenbogaardtite is intergrown with gold (Au₇₂Ag₂₈ to Au₇₇Ag₂₃) and acanthite, and appears to replace electrum (Fig. 10c).

Most samples of veins and(or) altered volcanic rocks from the Rhyolite area contain elevated gold and silver contents relative to unaltered silicic volcanic rocks, but have low contents of other trace elements (Table 2). A sample of unusually rich ore containing 9223 ppm gold and 2.1% silver from the Bond Gold Bullfrog mine is an exception, containing high copper, lead, antimony, zinc, selenium, and tellurium. A few samples contain anomalous Mo or Te, but copper is the only trace element that correlates well with precious metals (Fig. 3). Copper reportedly increases in abundance with depth at the Bond Gold Bullfrog mine (Jorgenson et al., 1989). Arsenic is remarkably low; maximum arsenic content in samples that we obtained from the Rhyolite area is 88 ppm, and arsenic values are not correlative with gold (Figs. 3 and 6).

Alteration and mineralization in the Rhyolite area post-date deposition of the 11.4-Ma Ammonia Tanks Member of the Timber Mountain Tuff and are structurally controlled by faults and fractures that formed in the upper plate of the Bullfrog detachment system during the period of regional extensional faulting between 11.4 and 7.6 Ma. A K-Ar age of 9.5 ± 0.2 Ma on adularia from the Montgomery-Shoshone mine (Morton et al., 1977) indicates that mineralization took place there during this period. Fault relationships and quartz-healed brecciation in the Bond Gold Bullfrog vein suggest that mineralization took place during faulting and prior to the last movements along the controlling structure. The similarities in structural control, mineralogy, style of veins, and alteration lead us to infer that mineralization throughout the Rhyolite area took place at about the same time as that at the Montgomery-Shoshone mine.

Mayflower-Pioneer area

The Mayflower and Pioneer mines, about 12 km north of Rhyolite, were developed between 1905 and the early 1920s, but little production was recorded (Ransome et al., 1910; Cornwall, 1972). The original gold strike at the Pioneer mine consisted of mineralized gouge and breccia along a steeply southwest-dipping shear zone (unpublished information, NBMG mining district files). At the Mayflower mine, gold ore was found in a southwest-dipping fracture zone with sheeted to irregular quartz-calcite veins (Ransome et al., 1910). Both mines are in rocks containing adularia-albite-illite alteration and quartz-calcite veining similar to that in the Rhyolite area. Host rocks include the Crater Flat Tuff as well as overlying coarse volcanoclastic and megabreccia deposits consisting of debris that includes pre-Tertiary rock and ash-flow units as young as the 11.4-Ma Tuffs of Fleur de Lis Ranch (S. Weiss and K. Connors, unpublished mapping, 1990). The coarse clastic rocks are overlain by rhyolitic tuffs and lavas erupted by about 10 Ma (Marvin et al., 1989; Noble et al., 1991).

Analyses of a small number of mineralized and altered samples reported gold values up to 15.3 ppm along with high mercury and antimony, but relatively low arsenic. A vein sample from the Mayflower mine was found to contain contorted electrum flakes in fine grey comb quartz with finely bladed calcite (Fig. 8c) similar to that found in gold-rich veins in the Rhyolite area and at the Gold Bar mine.

Adularia from mineralized rock at the Mayflower mine has given a K-Ar age of 10.0 ± 0.3 Ma (Jackson, 1988), consistent with stratigraphic constraints. This date overlaps, within analytical uncertainty, the adularia age-date for the Montgomery-Shoshone mine, but is appreciably older than the date reported for adularia from the Original Bullfrog mine.

DISCUSSION

Hydrothermal activity and precious-metal mineralization in the southern part of the SWNVF took place over a period of approximately 4.5 million years that overlapped with episodes of magmatic activity. Although all of the mineralization is epithermal in nature, its style and geochemistry varies significantly from area to area.

Silver-gold mineralization in the Wahmonie district differs from mineralization in other parts of the SWNVF in that it is situated in the eroded

remnants of a volcanic center dominated by rocks of intermediate composition. K-Ar ages indicate that hydrothermal activity at Wahmonie occurred during the main magmatic stage of the SWNVF, and coincided with, or closely followed, the end of magmatic and volcanic activity at the Wahmonie-Salyer volcanic center. Based on mineral assemblages in ore, vein, and wallrock alteration, type of host rocks, and available geochemical data, mineralization at Wahmonie comprises an epithermal precious-metal system of the adularia-sericite type of Heald et al. (1987) or the low sulfur type of Bonham (1989).

Available data show that base metals, arsenic, antimony and mercury at Wahmonie are relatively low compared to high base-metal, adularia-sericite type deposits (e.g., Creede, Colorado, Heald et al., 1987), and suggest kinship with high silver:gold ratio, relatively base-metal-poor deposits such as Tonopah, Nevada (e.g., Bonham, 1989). However, the high bismuth and tellurium concentrations of the Wahmonie district are not typical of adularia-sericite type precious-metal deposits: these elements are more commonly associated with porphyry-related gold deposits such as the Top deposit at Bald Mountain and the Fortitude and McCoy deposits in Nevada (e.g., Bonham, 1989; Brooks et al., 1991). Two other characteristics of the Wahmonie area suggest that exposed and near-surface mineralization may be associated with an underlying porphyry system. First, subvolcanic stocks and rhyolite dikes exposed in the central horst as well as geophysical evidence for a pluton beneath the district are consistent with the presence of a buried, perhaps composite, porphyry intrusion. Secondly, the presence of hypersaline fluid inclusions in quartz phenocrysts, secondary biotite, and tourmaline veinlets within the porphyritic granodiorite argue strongly for at least some porphyry-type magmatic-hydrothermal activity.

Although it is apparently similar in age to Wahmonie, precious-metal mineralization in the Bare Mountain district occupies an entirely different geologic setting. Mineral assemblages, chemistry, and style of Bare Mountain mineralization and alteration are also markedly different from the Wahmonie district. Stratigraphic, structural and radiometric age relations indicate that gold-silver \pm mercury \pm fluorite mineralization in Bare Mountain took place during the main magmatic stage of the SWNVF subsequent to the emplacement of the felsic dike swarm. With the exception of the Secret Pass deposit, areas of gold-silver mineralization in northern and eastern Bare Mountain have geochemical and geologic characteristics of Carlin-type, sedimentary rock-hosted disseminated deposits (e.g., Radtke, 1985; Bagby and Berger, 1985). Gold deposits in Bare Mountain

consist of disseminated mineralization in sedimentary, hypabyssal, and extrusive rocks with only minor quartz veining, little or no silicification, and common fluorite and cinnabar. Alteration is mainly illitic to kaolinitic with decalcification \pm silica replacement of sedimentary rocks. Remobilized carbon is conspicuous at the Mother Lode deposit. High contents of arsenic, antimony, mercury, and molybdenum as well as anomalous thallium are associated with mineralization in the north and east parts of Bare Mountain, and base metals are locally high. Silver contents, however, are generally low, and silver:gold ratios are distinctly lower than in other areas of precious-metal mineralization in the southern part of the SWNVF.

The Secret Pass deposit differs from the sediment-hosted deposits in host-rock lithology, alteration assemblage, and in having lower thallium contents. Although significant veining and(or) silicification have not been reported at Secret Pass, the alteration assemblage, perhaps strongly influenced by host lithology, best fits that of the adularia-sericite type of epithermal precious metal system.

Gold-silver mineralization in Bare Mountain is clearly epithermal in nature, and has features strongly suggestive of a shallow level of emplacement; nevertheless, it is similar in several respects to Carlin-type disseminated deposits. As Noble et al. (1989) proposed, the presence of a buried, granite-type porphyry molybdenum system in Bare Mountain is likely on the basis of geologic, geochemical, and fluid inclusion data. ^{Following Noble et al (1989),} we propose that most of the gold-silver deposits in Bare Mountain provide examples of distal disseminated sediment-hosted deposits genetically related to magmatic-hydrothermal systems (e.g., Sillitoe and Bonham, 1990) such as deposits in the Bau District, Sarawak (Percival et al., 1990), Purisima Concepcion, Peru (Alvarez and Noble, 1988) and Barney's Canyon, Utah (Sillitoe and Bonham, 1990).

Sediment-hosted precious-metal mineralization is also present within the SWNVF at Mine Mountain. Structural relations and the K-Ar age of alunitic alteration at Mine Mountain indicate that hydrothermal activity and mineralization were, at least in part, concurrent with magmatic and volcanic activity of the Timber Mountain magmatic stage of the SWNVF as first proposed by Jackson (1988). The hydrothermal breccia veins, cinnabar, and chalcedonic quartz at Mine Mountain, along with abundant mercury, arsenic and antimony (Table 2), are indicative of epithermal mineralization. Mine Mountain also possesses characteristics common to Carlin-type disseminated gold deposits, including association with a thrust fault, occurrence in sedimentary rocks that are variably decalcified, veined, silicified (including jasperoid) and cut by hydrothermal breccia, and the presence of barite

veins. However, the high lead and zinc contents, low thallium contents, high silver:gold ratio, and abundance of quartz in veins at Mine Mountain are not typical of Carlin-type deposits (e.g., Radtke, 1985).

On the basis of geology and trace element chemistry, Mine Mountain is similar to the Candelaria silver district approximately 150 km northwest of Mine Mountain. At Candelaria, disseminated silver ore is associated with thrust faults and intrusions cutting Mesozoic sedimentary and igneous rocks (Moeller, 1988). Carbonate-quartz veins mined for silver, gold, lead, zinc, and antimony are present as well (Page, 1959). Candelaria veins have lead, zinc, arsenic, antimony, and cadmium contents similar to the Mine Mountain veins and also carry anomalously high mercury (Hill et al., 1986), though not as high as at Mine Mountain. Alternatively, geochemical and geologic data at Mine Mountain are consistent with more than one period of hydrothermal activity that may, in part, have preceded development of the SWNVF.

A distinctly younger episode of mineralization is present in the Bullfrog district. Hydrothermal activity in the district, at ca. 9 to 11 Ma, occurred during the latter part of the Timber Mountain magmatic stage and may have extended into the late magmatic stage of the SWNVF as proposed by Jackson (1988). The age of mineralization in the Bullfrog district overlaps with a period of intense extensional tectonism in the Bullfrog Hills that provided structural preparation for mineralization, and may also have displaced mineralized rock.

Vein and alteration mineral assemblages, along with mineralization style and host-rock lithology, show that mineralization in the Bullfrog district was the result of adularia-sericite (low sulfur) type hydrothermal activity. Wall rock alteration in the Bullfrog district, which includes large volumes of rock with subtle potash feldspar and albite replacement of feldspar phenocrysts, is similar to alteration described at Round Mountain, Nevada (e.g., Sander and Einaudi, 1990). Precious-metal mineralization in the Bullfrog district is mainly restricted to several quartz-carbonate vein deposits that are similar to each other in texture and mineralogy.

The low content of precious-metal-related trace elements serves to distinguish the Rhyolite area from other areas that contain economic gold and silver mineralization in adularia-sericite systems. In comparison with such systems elsewhere in the Great Basin (e.g., Round Mountain, Tingley and Berger, 1985; Sleeper, Nash et al., 1990; Hollister, Bartlet et al., 1991; Rawhide, Black et al., 1991; and Hart Mountain, Capps and Moore, 1991), altered and mineralized rock from the Rhyolite area has the lowest overall contents of precious-metal pathfinder elements, particularly arsenic, antimony, and mercury. Most, but not all, of the samples

collected during this study came from the oxidized zone, and low metal contents might be the result of supergene leaching; however, most of the data from the other systems listed above are also from analyses of oxidized material. Rhyolite area mineralization took place in an areally extensive hydrothermal system from which typical epithermal and base-metal elements may have been flushed by late-stage fluids. The uytendogaardtite that appears to replace electrum in the Bond Gold Bullfrog mine in association with acanthite may be evidence of such a process, because uytendogaardtite can only occur in equilibrium with acanthite at temperatures below 113° C (Barton et al., 1978). Alternatively, Rhyolite area mineralization may simply have been introduced by fluids with lower base-metal and pathfinder element budgets than those responsible for other volcanic-hosted precious-metal deposits.

The Gold Bar mine in the northwest part of the Bullfrog district has a similar lack of trace elements to mineralized rock at Rhyolite. In comparison, available trace element data show that the Original Bullfrog and Mayflower mines have higher trace element contents. The style of veining and occurrence of uytendogaardtite in both the Original Bullfrog and Bond Gold Bullfrog deposits indicates that physical conditions were similar during precious-metal mineralization in widely separated parts of the Bullfrog district, despite differences in trace element geochemistry.

Precious-metal deposits in the Gold Bar mine, Original Bullfrog mine, Rhyolite area, Fluorspar Canyon, and Mother Lode mine are located within 2 km of the trace of the OB-FC detachment fault (Fig. 2). Jorgensen et al. (1989) implied that deposits in the Bullfrog district and Fluorspar Canyon resulted from the same hydrothermal system. We believe that this is not the case. Mineralized rock in the Bare Mountain district contains a consistent suite of trace elements that contrasts with the trace element suite in the Bullfrog district, and the age of hydrothermal activity is significantly younger in the Bullfrog district than in the Bare Mountain area. Moreover, the quartz-carbonate ± adularia veins and style of wall rock alteration that are typical of the Bullfrog district are uncommon in the Bare Mountain area, and large areas of unaltered rock separate the two districts.

CONCLUSIONS

Strong differences in ore and gangue mineralogy, style of mineralization, wall-rock alteration assemblages, and trace element chemistry between areas of precious-metal mineralization reflect the variable geologic settings and chemical diversity of hydrothermal systems active during the development of the SWNVF. These systems were active over a period of about 4.5 million years that spanned portions of the three magmatic stages of the field and gave rise to a broad spectrum of deposit types. The presence of intrusive porphyry, trace element suites associated with porphyry-related mineralization, and evidence for the passage of high-salinity fluids suggest that mineralization during the main magmatic stage of the SWNVF at Bare Mountain and Wahmonie was associated with porphyry-type magmatic systems. At Wahmonie silver-rich vein mineralization of the adularia-sericite type is hosted by an intermediate volcanic center, and is temporally and spatially associated with subvolcanic intrusions. At Bare Mountain, a genetic relationship between porphyry magmatism and shallow Carlin-type gold deposits seems likely.

The relatively base-metal- and silver-rich system at Mine Mountain was apparently active during the Timber Mountain stage of SWNVF volcanism. It shares features with vein and disseminated silver mineralization at Candelaria, Nevada, and may be the result of mineralization from more than one hydrothermal system.

The style of mineralization and alteration in the Bullfrog district is similar to other quartz-adularia precious-metal deposits in the Great Basin. The district contains gold-rich deposits that are largely devoid of epithermal elements and base-metals. Hydrothermal activity was coeval with strong extensional tectonism and may have continued into the late magmatic stage of the SWNVF. Mineralization in the Bullfrog district and some deposits in the Bare Mountain district were structurally controlled by the OB-FC detachment fault system. However, differences in age, mineralization style, and geochemistry indicate that mineralization in the two districts is unrelated.

ACKNOWLEDGEMENTS

Our studies have been partially supported by funds provided by the Nevada Nuclear Waste Project Office through the Center for Neotectonic Studies (to Weiss) and by the U. S. Department of Energy and Science Applications International

Corporation (to Castor). J. J. Sjoberg, U. S. Bureau of Mines Western Research Center, Reno, Nevada, is gratefully acknowledged for providing SEM/EDX analyses. We thank M. O. Desilets of the NBMG for calculation of correlation coefficients for the chemical analyses. J. V. Tingley and H. F. Bonham of the NBMG, and L. T. Larson and D. C. Noble of the Mackay School of Mines, University of Nevada, Reno, contributed useful comments and discussion on data and ideas reported herein. J. Quade kindly provided unpublished data on the Wahmonie mining district. We are grateful to the staff of Bond Gold Bullfrog, Inc., GEXA Gold Corp., U. S. Precious Metals, Ltd., and Angst, Inc. for allowing access to their properties, as well as discussions on the geology of their deposits.

REFERENCES CITED

- Alvarez, A. A., and Noble, D. C., 1988. Sedimentary rock-hosted disseminated precious metal mineralization at Purisima Concepcion, Yauricocha district, central Peru: *Economic Geology*, 83, 1368-1378.
- Bartlett, M. W., Enders, M. S., and Hruska, D. C., 1991. Geology of the Hollister gold deposit, Ivanhoe district, Elko County, Nevada. In: Raines, G. L., Lisle, R. E., Schafer, R. W., and Wilkinson, W. H. (Editors) *Geology and Ore Deposits of the Great Basin, Vol. II*. Geological Society of Nevada, Reno, Nevada, pp. 957-978.
- Barton, M. D., Kieft, C., Burke, E. A. J., and Oen, I. S., 1978. Uyttenbogaardtite, a new silver-gold sulfide: *Canadian Mineralogist*, 16, 651-657.
- Black, J. E., Mancuso, T. K., and Gant, J. L., 1991. Geology and mineralization at the Rawhide Au-Ag deposit, Elko County, Nevada. In: Raines, G. L., Lisle, R. E., Schafer, R. W., and Wilkinson, W. H. (Editors) *Geology and Ore Deposits of the Great Basin, Vol. II*, Geological Society of Nevada, Reno, Nevada, pp. 1123-1144.
- Bonham, H. F., Jr., 1989. Bulk mineable gold deposits of the western United States. in Keays, R. R., Ramsay, R. H., and Groves, D. L., eds., *The geology of gold deposits: the perspective in 1988*. *Economic Geology Monograph* 6, pp. 193-207.
- Bonham, H. F., Jr., and Hess, R. H., 1991. Bulk-mineable precious-metal deposits. in *The Nevada mineral industry - 1990*. Nevada Bureau of Mines and Geology Special Publication MI-1990, pp. 19-26.
- Brooks, J. W., Meinert, L. D., Kuyper, B. A., and Lane, M. L., 1991. Petrology and geochemistry of the McCoy gold skarn, Lander County, Nevada. In: Raines, G. L., Lisle, R. E., Schafer, R. W., and Wilkinson, W. H. (Editors) *Geology and Ore Deposits of the Great Basin, Vol. II*, Geological Society of Nevada, Reno, Nevada, pp. 419-442.
- Byers, F. M., Jr., Carr, W. J., Orkild, P.P., 1976. Volcanic suites and cauldrons of Timber Mountain-Oasis Valley Caldera Complex, Southern Nevada. U. S. Geological Survey Professional Paper 919, 70 pp.

Byers, F. M. Jr., Carr, W. J., and Orkild, P. P., 1989. Volcanic centers of southwestern Nevada: evolution of understanding, 1960-1988. *Journal of Geophysical Research*, 94, B5, p.5908-5924.

Capps, R. C., and Moore, J. A., 1991. Geologic setting of mid-Miocene gold deposits in the Castle Mountains, San Bernardino County, California and Clark County, Nevada. In: Raines, G. L., Lisle, R. E., Schafer, R. W., and Wilkinson, W. H. (Editors) *Geology and Ore Deposits of the Great Basin, Vol. II*. Geological Society of Nevada, Reno, Nevada, pp. 1195-1219.

Carr, M. D., and Monsen, S.A., 1988. A field trip guide to the geology of Bare Mountain. In: Weide, D. L., and Faber, M. L. (Editors), *This extended land - Geological journeys in the southern Basin and Range*. Geological Society of America, Cordilleran Section, Field Trip Guidebook, pp. 50-57.

Carr, W. J., 1984. Regional structural setting of Yucca Mountain, southwestern Nevada, and late Cenozoic rates of tectonic activity in part of the southwestern Great Basin, Nevada and California. U. S. Geological Survey Open-File Report 84-854, 114 pp.

Carr, W.J., Byers, F.M., and Orkild, P.P., 1986. Stratigraphic and volcano-tectonic relations of Crater Flat Tuff and some older volcanic units, Nye County, Nevada. U. S. Geological Survey Professional Paper 1323, 23 pp.

Castor, S.B., Feldman, S.C. Tingley, J.V., 1990. Mineral evaluation of the Yucca Mountain Addition, Nye County, Nevada. Nevada Bureau of Mines and Geology Open-File Report 90-4, 107 pp.

Christiansen, R. L., Lipman, P. W., Carr, W. J., Byers, F. M., Jr., Orkild, P. P., and Sargent, K. A., 1977. Timber Mountain-Oasis Valley caldera complex of southern Nevada. *Geological Society of America Bulletin*, 88, p.943-959.

Cornwall, H. R., 1972. Geology and mineral deposits of southern Nye County, Nevada. Nevada Bureau of Mines and Geology Bulletin 77, 49 pp.

Cornwall, H. R., and Kleinhampl, F. J., 1961. Geology of the Bare Mountain quadrangle. U. S. Geological Survey Map GQ-157, 1:62,500 scale.

Cornwall, H. R., and Kleinhampl, F. J., 1964. Geology of the Bullfrog quadrangle and ore deposits related to the Bullfrog Hills caldera, Nye County, Nevada, and Inyo County, California. U. S. Geological Survey Professional Paper 454-J, 25 pp.

Couch, B. F., and Carpenter, J. A., 1943. Nevada's metal and mineral production. Nevada Bureau of Mines and Geology Bulletin 38, 159 pp.

Dowling, K., and Morrison, G., 1989. Application of quartz textures to the classification of gold deposits using North Queensland examples. In: Keays, R. R., Ramsay, R. H., and Groves, D. I., eds., *The geology of gold deposits: the perspective in 1988*. Economic Geology Monograph 6, pp. 342-355.

Ekren, E. B., and Sargent, K. A., 1965. Geologic map of the Skull Mountain quadrangle, Nye County, Nevada. U. S. Geological Survey Map GQ-387, 1:24,000 scale.

Greybeck, J. D., and Wallace, A. B., 1991. Gold mineralization at Fluorspar Canyon near Beatty, Nye County, Nevada. In: Raines, G. L., Lisle, R. E., Schafer, R. W., and Wilkinson, W. H. (Editors) *Geology and Ore Deposits of the Great Basin, Vol. II*, Geological Society of Nevada. Reno, Nevada, pp. 935-946

Hamilton, W. B., 1988. Detachment faulting in the Death Valley region, California and Nevada. *U. S. Geological Survey Bulletin* 1790, 51-85.

Herald, P., Foley, J. K., and Hayba, D. O., 1987. Comparative anatomy of volcanic-hosted epithermal deposits: acid-sulfate and adularia-sericite types. *Economic Geology*, 82, 1, 1-26.

Hill, R. H., Adrian, B. M., Bagby, W. C., Bailey, E. A., Goldfarb, R. J., and Pickthorn, W. J., 1986. Geochemical data for rock samples collected from selected sediment-hosted disseminated precious-metal deposits in Nevada. *U. S. Geological Survey Open-File Report* 86-107, 30 pp.

Hoover, D. B., Chornack, M. P., Nervick, K. H., and Broker, M. M., 1982. Electrical studies at the proposed Wahmonie and Calico Hills nuclear waste sites, Nevada Test Site, Nye County, Nevada. *U. S. Geological Survey Open-file Report* 82-466, 45 pp.

Jackson, M. R., Jr., 1988. The Timber Mountain magmato-thermal event: an intense widespread culmination of magmatic and hydrothermal activity at the southwestern Nevada volcanic field. unpublished MSc Thesis, University of Nevada, Reno, Nevada, 46 pp.

Jones, R. B., 1990. Metals. In: *The Nevada mineral industry - 1989*. Nevada Bureau of Mines and Geology Special Publication MI-1989, pp. 10-18.

Jorgensen, D. K., Rankin, J. W., and Wilkins, J., Jr., 1989. The geology, alteration, and mineralogy of the Bullfrog gold deposit, Nye County, Nevada. *Society of Mining Engineers Preprint* 89-135, 13 pp.

Kistler, R. W., 1968. Potassium-argon ages of volcanic rocks in Nye and Esmeralda Counties, Nevada. *Geological Society of America Memoir*, 110, 251-263.

Lechler, P. L., and Desilets, M. O., 1991. The NBMG standard reference material project: *Nevada Geology*, 10, 1-2.

Maldonado, F., 1990a. Structural geology of the upper plate of the Bullfrog Hills detachment fault system, southern Nevada. *Geological Society of America Bulletin*, 102, 992-1006.

Maldonado, F., 1990b. Geologic map of the northwest quarter of the Bullfrog 15-minute quadrangle, Nye County, Nevada. *U.S. Geological Survey Map* I-1985, 1:24,000 scale.

Maldonado, F., and Hausback, B. P., 1990. Geologic map of the northeast quarter of the Bullfrog 15-minute quadrangle, Nye County, Nevada. *U.S. Geological Survey Map* I-2049, 1:24,000 scale.

Mapa, M. R., 1991. Geology and mineralization of the Mother Lode mine, Nye County, Nevada. In: Buffa, R. H., and Coyner, A. R. (Editors), Geology and Ore Deposits of the Great Basin Symposium, April, 1990; Field Trip Guidebook Compendium. Geological Society of Nevada, Reno, Nevada, pp. 1076-1077.

Marvin, R. F., Mehnert, H. H., and Naeser, C. W., 1989. U. S. Geological Survey radiometric ages - compilation "C", part 3: California and Nevada. *Isochron/West*, 52, 3-11.

Moeller, S. A., 1988. Geology and mineralization in the Candelaria district, Mineral County, Nevada. In: Schafer, R. W., Cooper, J. J., and Vikre, P. G. (Editors) Bulk Mineable Precious Metal Deposits of the Western United States, Symposium Proceedings. Geological Society of Nevada, Reno, Nevada, pp. 135-158.

Monsen, S. A., Carr, M. D., Reheis, M. C., and Orkild, P. P., 1990. Geologic map of Bare Mountain, Nye County, Nevada. U. S. Geological Survey Open-file Report 90-25, 17 pp.

Morton, J. L., Silberman, M. L., Bonham, H. F., Garside, L. J., and Noble, D. C., 1977. K-Ar ages of volcanic rocks, plutonic rocks, and ore deposits in Nevada and eastern California. *Isochron/West*, 20, 19-29.

Nash, J. T., Fey, D. L., Motooka, J. M., and Siems, D. F., 1990. Geochemical analyses of ore and host rocks, Sleeper gold-silver deposit, Humboldt County, Nevada. U. S. Geological Survey Open-File Report 90-702A, 69 pp.

Noble, D. C., Weiss, S. I., and Green, S. M., 1989. High-salinity fluid inclusions suggest that Miocene gold deposits of the Bare Mtn. district, NV, are related to a large buried rare-metal rich magmatic system (abstract). *Geological Society of America Abstracts with Programs*, 20, 3, 123.

Noble, D. C., Weiss, S. I., and McKee, E. H., 1991. Magmatic and hydrothermal activity, caldera geology, and regional extension in the western part of the southwestern Nevada volcanic field. In: Raines, G. L., Lisle, R. E., Schafer, R. W., and Wilkinson, W. H. (Editors) Geology and Ore Deposits of the Great Basin, Vol. II. Geological Society of Nevada, Reno, Nevada, pp. 913-934.

Odt, D. A., 1983. Geology and geochemistry of the Sterling gold deposit, Nye County, Nevada. unpublished MSc Thesis, University of Nevada, Reno - Mackay School of Mines, Reno, Nevada, 100 pp.

Orkild, P. P., 1968. Geologic map of the Mine Mountain Quadrangle, Nye County, Nevada. U. S. Geological Survey Map GQ-746, 1:24,000 scale.

Page, B. M., 1959. Geology of the Candelaria mining district, Mineral County, Nevada. Nevada Bureau of Mines and Geology Bulletin 56, 67 pp.

Papke, K. G., 1979. Fluorspar in Nevada. Nevada Bureau of Mines and Geology Bulletin 93, 40-47.

Percival, T. J., Radtke, A. S., and Bagby, W. C., 1990. Relationships among carbonate-replacement gold deposits, gold skarns and intrusive rocks, Bau mining district, Sarawak, Malaysia. *Mining Geology*, 40, 1-16.

- Ponce, D. A., 1981. Preliminary gravity investigations of the Wahmonie site, Nevada Test Site, Nye County, Nevada. U. S. Geological Survey Open-file Report 81-522, 64 pp.
- Quade, J., Tingley, J. V., Bentz, J. L., and Smith, P. L., 1984. A mineral inventory of the Nevada Test Site and portions of Nellis Bombing and Gunnery Range southern Nye County, Nevada. Nevada Bureau of Mines and Geology Open-File Report 84-2, 68 pp.
- Radtke, A. S., 1985. Geology of the Carlin gold deposit, Nevada. U. S. Geological Survey Professional Paper 1262, 124 pp.
- Ransome, F. L., Emmons, W. H., and Garrey, G. H., 1910. Geology and ore deposits of the Bullfrog District, Nevada. U. S. Geological Survey Bulletin 407, 129 pp.
- Sander, M. V., and Einaudi, M. T., 1990. Epithermal deposition of gold during transition from propylitic to potassic alteration at Round Mountain, Nevada. *Economic Geology*, 85, 285-311.
- Sawyer, D. A., Fleck, R. J., Lanphere, M.A., Warren, R. G., and Broxton, D. E., 1990. Episodic volcanism in the southwestern Nevada volcanic field: new $^{40}\text{Ar}/^{39}\text{Ar}$ geochronologic results.
- Sillitoe, R. H., and Bonham, H. F., Jr., 1990. Sediment-hosted gold deposits: distal products of magmatic-hydrothermal systems. *Geology*, 18, 157-161.
- Stewart, J. H., 1988. Tectonics of the Walker Lane belt, western Great Basin - Mesozoic and Cenozoic deformation in a zone of shear. In: Ernst, W. G. (Editor) *Metamorphism and Crustal Evolution of the Western United States: Rubey Volume VII*, Prentice-Hall, Inc., Englewood Cliffs, New Jersey, pp. 683-713.
- Tingley, J. V., 1984. Trace element associations in mineral deposits, Bare Mountain (fluorine) mining district, Southern Nye County, Nevada. Nevada Bureau of Mines and Geology Report 39, 28 pp.
- Tingley, J. V., and Berger, B. R., 1985. Lode gold deposits of Round Mountain, Nevada. Nevada Bureau of Mines and Geology Bulletin 100, 62 pp.
- Weiss, S. I., Connors, K. A., Noble, D. C., and McKee, E. H., 1990. Coeval crustal extension and magmatic activity in the Bullfrog Hills during the latter phases of Timber Mountain volcanism (abstract). *Geological Society of America Abstracts with Programs*, 22, 92-93.

FIGURES

Figure 1. Map of the southwestern Nevada volcanic field showing major volcanic centers and mineralized areas. BM = Black Mountain caldera, CF-PP= Inferred Crater Flat-Prospector Pass caldera complex, CC = Claim Canyon cauldron, SC = Silent Canyon caldera, SM = Stonewall Mountain volcanic center, TM-I = Timber Mountain caldera complex I, TM-II = Timber Mountain caldera complex II. Heavy dashed line is approximate limit of SWNVF. Modified from Noble et al.(1991) and Byers et al. (1989).

Figure 2. Map of the south part of the southwestern Nevada volcanic field showing caldera margins, mineral deposits, and other features cited. BB = Bond Gold Bullfrog mine, D = Daisy mine, GB = Gold Bar mine, GD = Goldspar mine, M = Mary mine, ML = Mother Lode mine, MS = Montgomery-Shoshone mine, My = Mayflower mine, P = Pioneer mine, S = Sterling mine, SP = Secret Pass deposit, T = Telluride mines. Heavy dashed line shows approximate surface trace of the OB-FC detachment fault system.

Figure 3. Spearman correlation coefficients for trace element analyses in samples from mineralized areas in the southwestern Nevada volcanic field.

Figure 4. Map showing mine workings and generalized geology for part of the Wahmonie district. Modified from Ekren and Sargent (1965).

Figure 5. Backscattered SEM images showing precious-metal minerals in high-grade ore from the Wingfield shaft, Wahmonie district: (a) threads or flakes of native gold (bright) in cerargyrite (gray); (b) colloform layers of hessite (light gray) in cerargyrite (grey).

Figure 6. Plots of Ag, As, Hg, and Cu against Au in samples from mineralized areas in the southwestern Nevada volcanic field. Plots on the left represent samples from Wahmonie (■) Bare Mountain (×), and Mine Mountain (Δ). Plots on the right are of samples from the Bullfrog mining district: Original Bullfrog mine (○); Gold Bar mine (□); and Rhyolite area (●).

Figure 7. Backscattered SEM image of electrum (e) in a veinlet with border of Sb-Bi-Cu silicate (x) and inner zones of chrysocolla (c), acanthite (a), and uytenbogaardtite (u). Sample is quartz + carbonate vein from the Original Bullfrog mine with 117 ppm gold and 1100 ppm silver.

Figure 8. Reflected light photomicrographs of finely bladed calcite (dark) in quartz from (a) Gold Bar, (b) Bond-Bullfrog, and (c) Mayflower mines.

Figure 9. Photomicrograph in cross-polarized transmitted light of (a) adularized and (b) albitized feldspar phenocrysts from near-vein altered rhyolite in the Bullfrog mining district.

Figure 10. Backscattered SEM photomicrographs of electrum in ore from the Bond-Bullfrog mine: (a) electrum replacing a limonitized pyrite cube; (b) an irregular flake of electrum; (c) electrum that is partially replaced by uytenbogaardtite.

TABLES

Table 1. Generalized stratigraphy and geochronology of the southwestern Nevada volcanic field.

Table 2. Median, maximum and minimum trace element contents of mineralized and altered samples from areas of precious-metal mineralization in the southwest Nevada volcanic field, based on analyses by Geochemical Services, Inc. All values are in ppm.

Table 3. Trace element analyses of background samples from the southwestern Nevada volcanic field. Analyses by Geochemical Services, Inc. All values are in ppm.

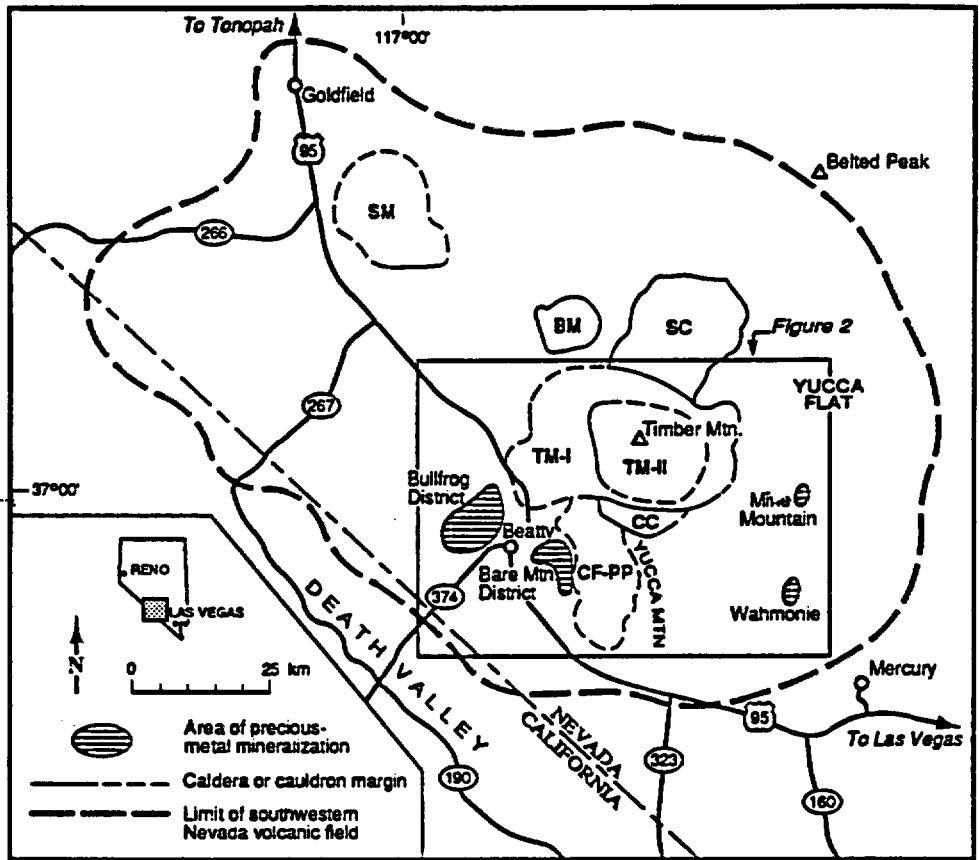


Fig. 1

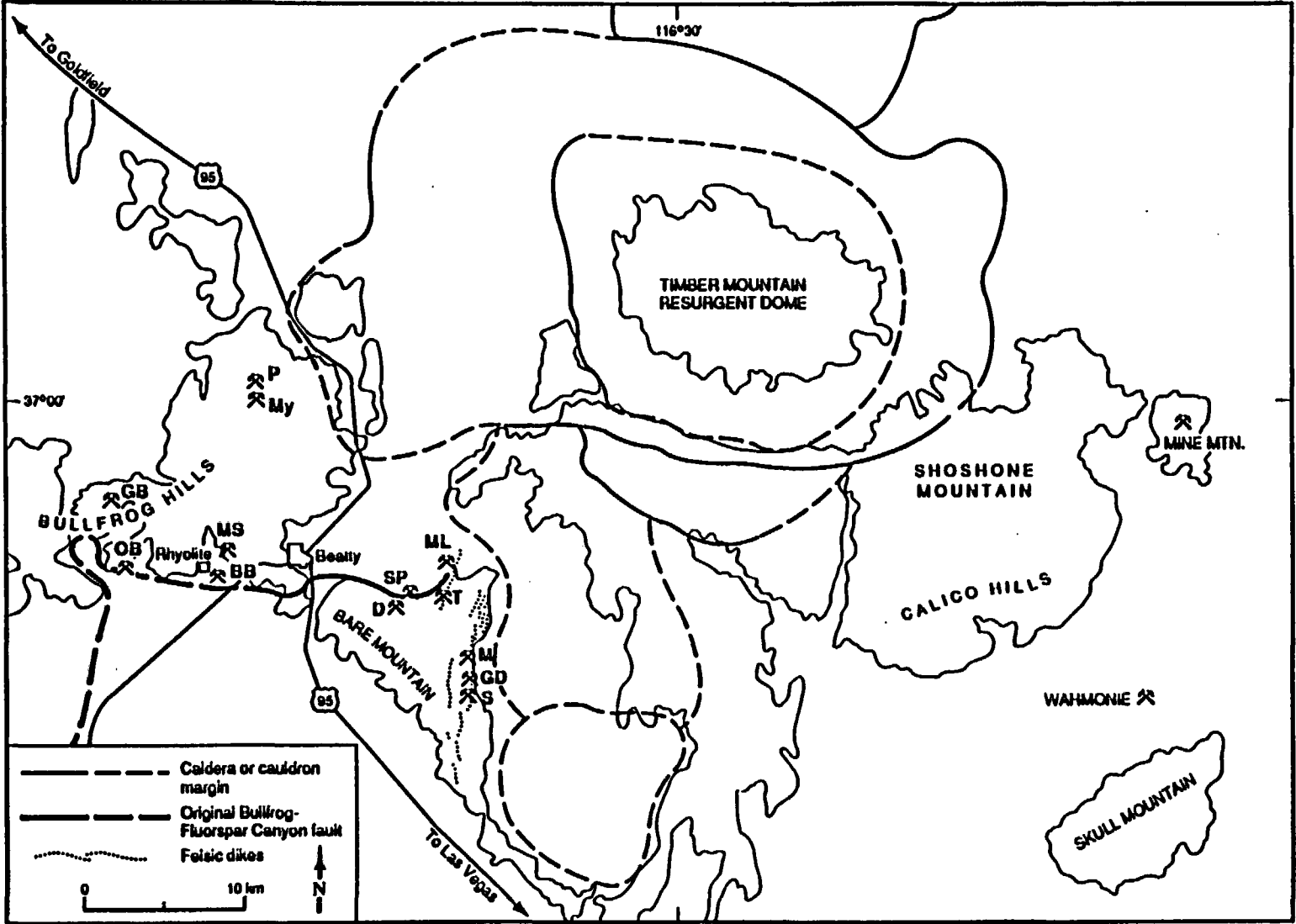


Fig. 2

Ag	1.00														
As	0.62	1.00													
Au	0.72	0.62	1.00												
Bi	-0.29	-0.04	-0.01	1.00											
Cd	0.46	0.43	0.27	-0.14	1.00										
Cu	0.49	0.67	0.52	-0.13	0.37	1.00									
Ge	-0.18	0.17	-0.07	0.17	-0.16	0.12	1.00								
Hg	0.29	0.43	0.34	0.18	0.39	0.40	-0.22	1.00							
Mo	-0.08	0.04	-0.14	0.14	0.27	0.30	-0.09	0.27	1.00						
Pb	0.59	0.67	0.50	0.17	0.24	0.47	0.20	0.29	0.05	1.00					
Sb	0.63	0.88	0.65	0.00	0.52	0.61	0.06	0.51	0.10	0.71	1.00				
Se	0.22	0.64	0.25	0.23	0.42	0.48	0.25	0.26	0.35	0.47	0.43	1.00			
Te	0.62	0.54	0.58	-0.10	0.40	0.33	0.18	0.34	0.07	0.54	0.66	0.22	1.00		
Tl	0.61	0.61	0.56	-0.08	0.31	0.35	0.18	0.39	-0.02	0.51	0.62	0.05	0.80	1.00	
Zn	0.44	0.65	0.29	-0.28	0.69	0.64	-0.04	0.46	0.30	0.37	0.64	0.41	0.33	0.40	1.00
	Ag	As	Au	Bi	Cd	Cu	Ge	Hg	Mo	Pb	Sb	Se	Te	Tl	Zn

MOTHER LODE MNE

Ag	1.00														
As	0.53	1.00													
Au	0.89	0.28	1.00												
Bi	0.59	0.51	0.42	1.00											
Cd	0.61	0.89	0.53	0.54	1.00										
Cu	0.82	0.54	0.54	0.74	0.63	1.00									
Ge	0.59	-0.02	-0.59	-0.58	-0.18	-0.86	1.00								
Hg	0.51	0.06	-0.47	-0.47	-0.11	-0.65	0.60	1.00							
Mo	0.23	0.56	0.12	0.47	0.57	0.34	-0.18	-0.05	1.00						
Pb	0.14	0.76	0.00	0.49	0.62	0.24	0.30	0.25	0.35	1.00					
Sb	0.92	0.50	0.91	0.21	0.71	0.78	-0.45	-0.50	0.21	0.24	1.00				
Se												1.00			
Te	0.08	0.00	-0.16	0.08	0.08	0.08	-0.25	-0.16	0.48	0.23	-0.16		1.00		
Tl	-0.23	0.10	-0.30	0.09	0.07	-0.13	0.08	0.22	0.76	0.02	-0.27		0.41	1.00	
Zn	-0.42	0.57	-0.44	-0.19	0.32	-0.21	0.63	0.50	0.42	0.39	-0.21		-0.08	0.39	1.00
	Ag	As	Au	Bi	Cd	Cu	Ge	Hg	Mo	Pb	Sb	Se	Te	Tl	Zn

ORIGINAL BULLFROG MNE

Ag	1.00														
As	0.11	1.00													
Au	0.84	0.28	1.00												
Bi	0.51	0.32	0.47	1.00											
Cd	0.49	0.41	0.38	0.22	1.00										
Cu	0.21	0.24	0.07	0.47	0.22	1.00									
Ge	-0.23	0.51	0.09	0.03	-0.10	0.08	1.00								
Hg	0.69	0.04	0.62	0.43	0.51	0.29	-0.14	1.00							
Mo	-0.16	0.16	-0.02	-0.02	-0.16	0.05	0.50	0.14	1.00						
Pb	0.07	0.44	0.06	0.70	0.18	0.34	0.25	0.13	0.18	1.00					
Sb	-0.01	0.74	0.15	0.12	0.24	0.23	0.25	0.18	0.17	0.30	1.00				
Se	-0.18	0.46	-0.18	0.19	-0.05	-0.06	0.32	-0.10	0.24	0.38	0.14	1.00			
Te	0.72	0.36	0.68	0.75	0.30	0.32	-0.04	0.38	-0.03	0.49	0.39	0.03	1.00		
Tl	0.33	0.31	0.33	0.28	0.41	0.28	0.30	0.35	0.33	0.29	0.31	-0.13	0.34	1.00	
Zn	0.25	0.32	0.32	0.15	0.52	0.28	-0.12	0.40	-0.08	0.25	0.43	-0.32	0.42	0.33	1.00
	Ag	As	Au	Bi	Cd	Cu	Ge	Hg	Mo	Pb	Sb	Se	Te	Tl	Zn

WASHOME DISTRICT

Ag	1.00														
As	-0.26	1.00													
Au	0.60	0.29	1.00												
Bi				1.00											
Cd	-0.37	-0.25	-0.25		1.00										
Cu	0.31	0.41	0.63		-0.25	1.00									
Ge	-0.08	0.31	0.31		0.31	0.22	1.00								
Hg	-0.09	0.77	0.48		-0.18	0.71	0.30	1.00							
Mo	0.09	0.29	0.22		-0.37	0.37	-0.31	0.40	1.00						
Pb	-0.38	0.65	0.08		-0.22	0.28	-0.17	0.86	0.73	1.00					
Sb	-0.19	0.43	0.29		0.22	0.25	0.50	0.49	0.04	0.38	1.00				
Se												1.00			
Te													1.00		
Tl														1.00	
Zn	-0.69	0.40	-0.26		0.40	-0.21	0.89	0.13	-0.24	0.13	0.35				1.00
	Ag	As	Au	Bi	Cd	Cu	Ge	Hg	Mo	Pb	Sb	Se	Te	Tl	Zn

GOLD BAR MNE

Ag	1.00														
As	0.65	1.00													
Au	0.85	0.78	1.00												
Bi	-0.13	-0.10	-0.04	1.00											
Cd	0.90	0.68	0.52	-0.20	1.00										
Cu	0.47	0.45	0.58	0.00	0.52	1.00									
Ge	-0.22	0.00	0.03	-0.03	-0.28	-0.21	1.00								
Hg	0.90	0.68	0.43	-0.20	0.55	0.44	-0.18	1.00							
Mo	0.23	0.16	0.06	-0.10	0.09	-0.22	0.17	0.23	1.00						
Pb	0.93	0.72	0.56	-0.18	0.89	0.40	-0.29	0.86	0.26	1.00					
Sb	0.83	0.69	0.54	-0.08	0.79	0.29	-0.18	0.74	0.33	0.92	1.00				
Se	0.42	0.72	0.68	0.04	0.48	0.45	0.03	0.37	0.03	0.46	0.45	1.00			
Te	0.13	0.19	-0.02	-0.10	0.13	-0.14	0.47	0.12	0.22	0.10	0.07	0.23	1.00		
Tl	-0.04	0.19	0.03	-0.18	-0.14	-0.37	0.34	-0.01	0.39	0.02	-0.18	0.06	0.33	1.00	
Zn	0.79	0.85	0.37	-0.28	0.92	0.44	-0.22	0.93	0.19	0.79	0.85	0.47	0.33	0.06	1.00
	Ag	As	Au	Bi	Cd	Cu	Ge	Hg	Mo	Pb	Sb	Se	Te	Tl	Zn

MINE MOUNTAIN

Ag	1.00														
As	0.05	1.00													
Au	0.78	0.09	1.00												
Bi	0.27	-0.01	0.22	1.00											
Cd	0.22	0.21	0.01	0.12	1.00										
Cu	0.47	0.36	0.37	0.24	0.26	1.00									
Ge	0.35	0.52	-0.29	-0.30	-0.24	-0.08	1.00								
Hg	0.20	0.09	0.21	-0.10	0.06	-0.02	0.14	1.00							
Mo	0.28	-0.07	0.02	0.17	0.34	-0.19	-0.31	-0.05	1.00						
Pb	-0.12	0.41	-0.17	0.18	0.25	0.19	0.19	-0.13	-0.06	1.00					
Sb	0.28	0.65	0.10	0.28	0.28	0.48	0.19	0.00	0.02	0.25	1.00				
Se	0.37	0.29	0.38	0.29	0.30	0.25	-0.03	0.05	0.28	0.06	0.21	1.00			
Te	0.42	-0.06	0.44	0.48	0.22	0.27	-0.21	0.17	0.01	0.29	-0.02	0.40	1.00		
Tl	0.31	-0.17	0.11	0.43	0.51	0.18	0.46	-0.15	0.34	-0.01	0.22	0.25	0.17	1.00	
Zn	-0.08	0.50	-0.18	-0.05	0.47	0.10	0.36	0.06	0.18	0.32	0.34	0.18	0.00	0.07	1.00
	Ag	As	Au	Bi	Cd	Cu	Ge	Hg	Mo	Pb	Sb	Se	Te	Tl	Zn

RHYOLITE AREA

† Correlation coefficient significant at 99% confidence level

† Correlation coefficient significant at 99% confidence level

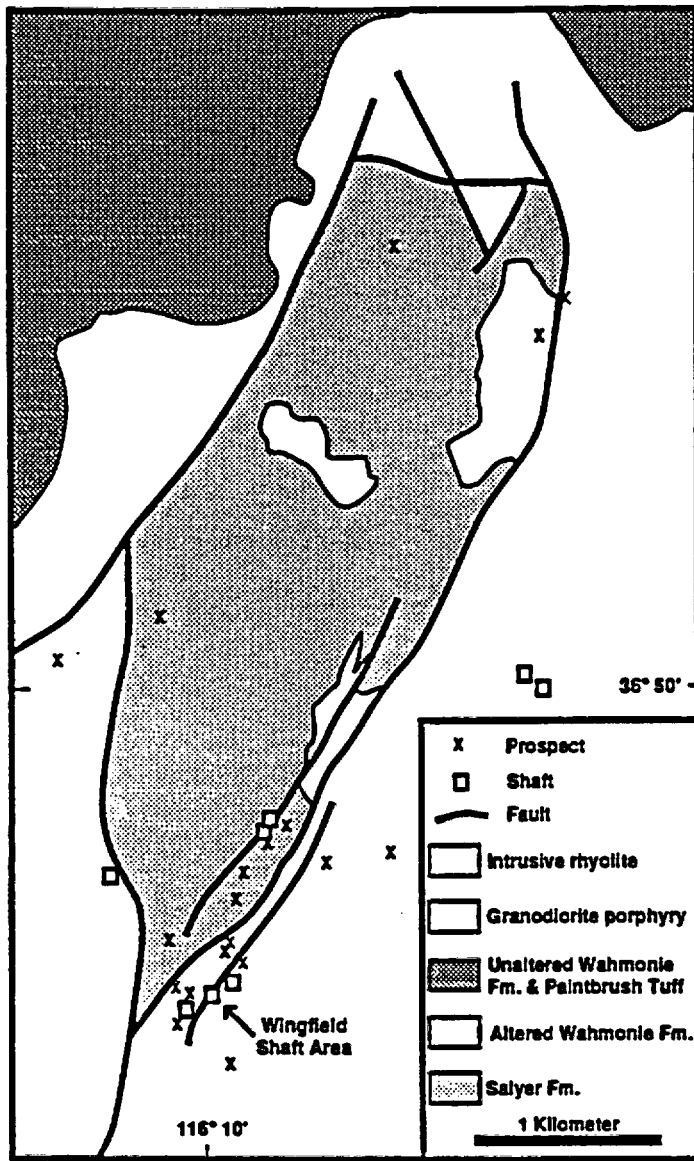
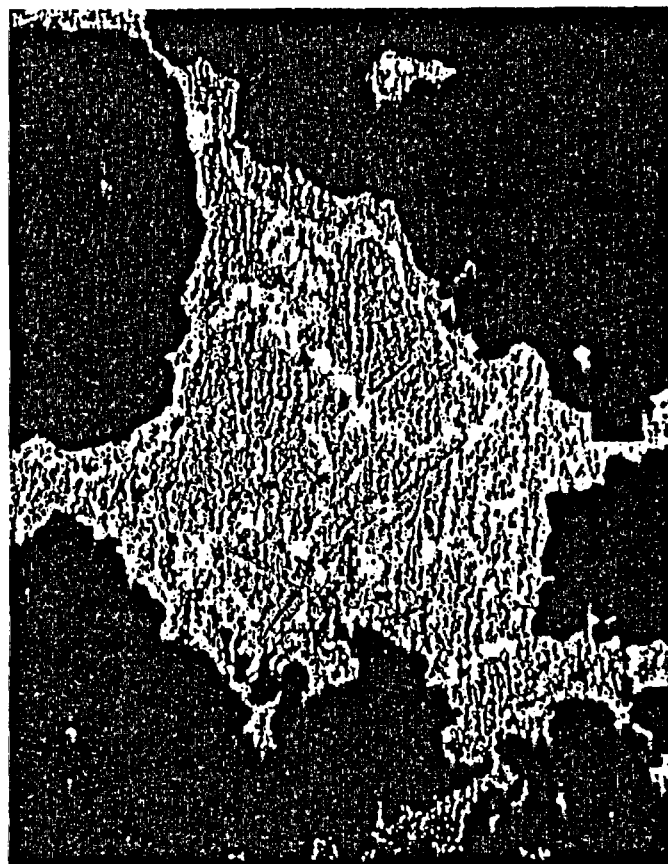


Fig. 4



W-14

Fig. 50



W-14 v.f. Ag_2Te (brt) & $AgCl$ (gray)

Fig. 51

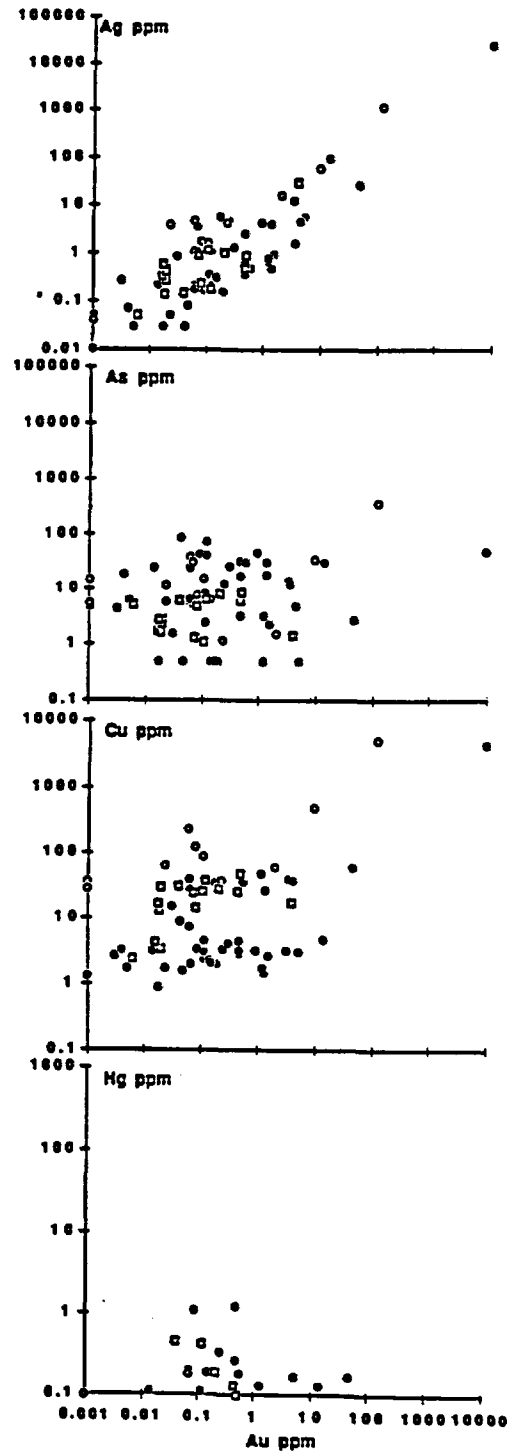
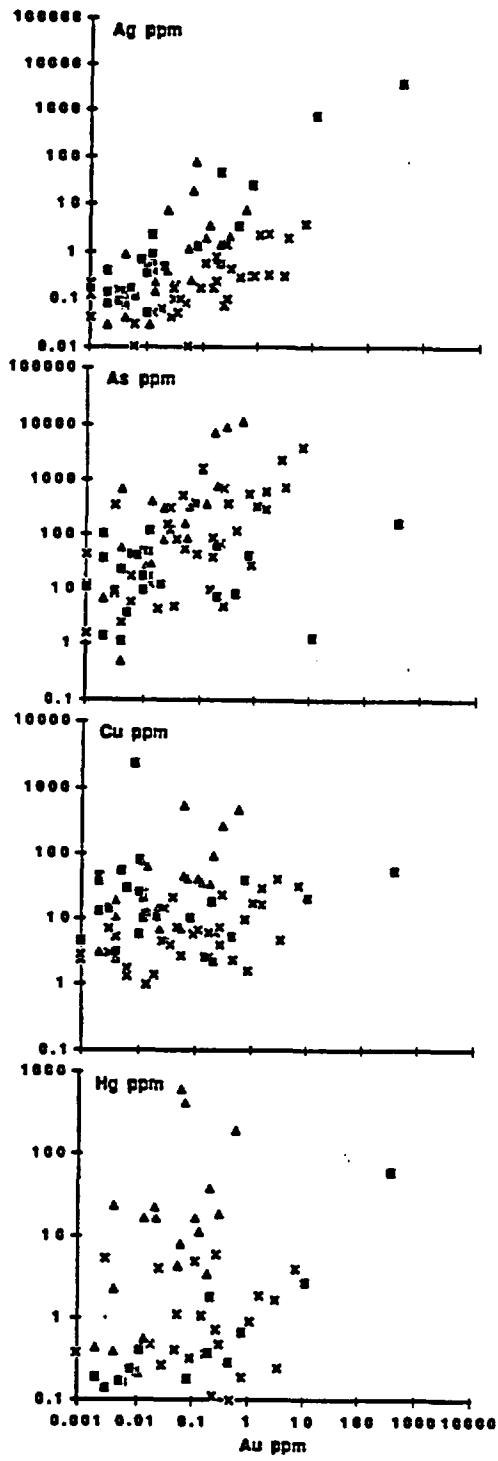


Fig 6



BA 20 v. 1

F4 7

3-102



GOU BAR KCG B3 2.5x2.5 5x5um

Fig 8a

H F V 1.75 um



3 SW 400 2.5x2.5 5x5um

Fig 8b

H F V 1.75 um



P1 Pol 2.5x2.5 300-103 Mayflower

Fig 8c

H F V 3.5 um



HFU = 1.75 mm

Fig 9a



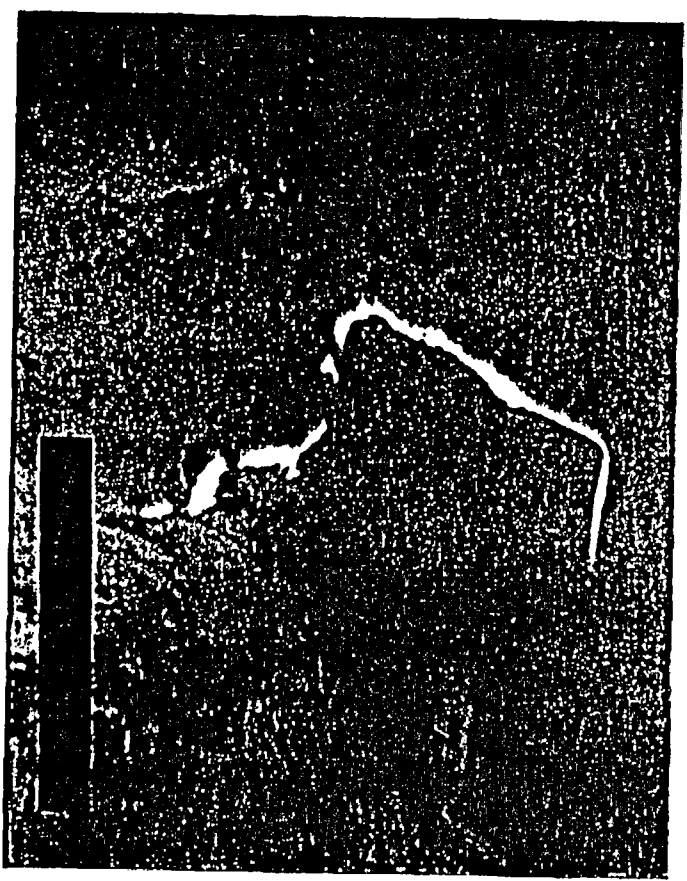
HFU 1.75 mm

Fig 9b



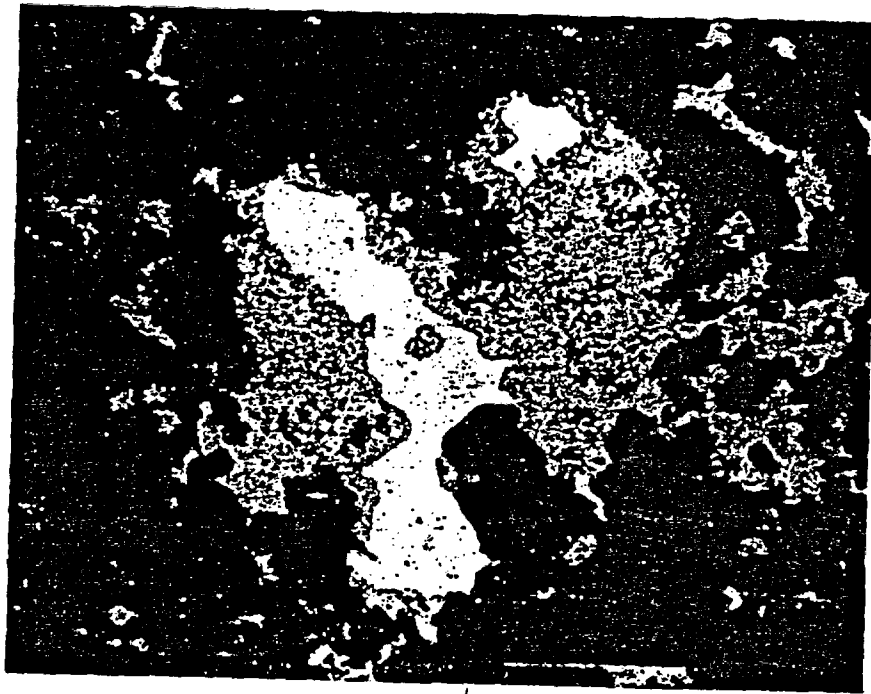
3500 449 v. 4 detail slab

Fig 105



v. 3 3500 449 slab

Fig 105



BCBH v. 1

100 μ m

Fig. 1

APPENDIX F

**PRIMARY AND SECONDARY DISPERSION PATTERNS ASSOCIATED WITH
MOTHER LODE-TYPE GOLD MINERALIZATION, HODSON DISTRICT,
CALAVERAS COUNTY, CALIFORNIA
CHAFFEE, M.A. AND KUHL, T.O.**

The Hodson district lies along the West Gold Belt, about 17 km west of the main Mother Lode Gold Belt and the town of Angels Camp. Rocks in the area consist of two major units: (1) metasedimentary rocks comprising mainly buffaceous wackes and carbonaceous slates and phyllites, and (2) metavolcanic rocks comprising flows, tuffs, and agglomerates mainly of andesitic basalt to basaltic composition. Rocks in the region have been metamorphosed to greenschist facies. The entire area has been intensely faulted; the Mother Lode-type, gold-pyrite deposits are in or near quartz veins associated with some of these faults, mainly the large Hodson fault, which trends northwest and has many splays.

The three orebodies in the district contain zones of altered rock that surround the Au-bearing mineralized structures. The extent and mineralogy of these zones varies with each host lithology and orebody. Typical alteration assemblages include quartz, sericite, pyrite, calcite, ankerite, and malenite in the metavolcanic unit, and quartz, sericite, and pyrite, plus bleaching, in the metasedimentary unit.

A total of 300 samples of core and cuttings were collected from drill holes on three sections, each of which transects an orebody. Analyses for 37 elements (Ag, Al, As, Au, Ba, Ca, Cd, Ce, Co, Cr, Cu, Fe, Ga, Hg, K, La, Li, Mg, Mn, Mo, Na, Ni, Pb, P, Sb, Se, Si, Sr, Te, Ti, Tl, V, W, Y, and Zn) and for loss-on-ignition (LOI) at 825°C were evaluated.

Pathfinder elements with positive anomalies spatially associated with anomalous Au zones include Ag, As, Hg, K, S, Sb, Sr, Tl, and W, plus LOI. Elements with negative anomalies in the same zones include Al, Ba, Cu, Fe, Ga, Li, Mn, Mo, Na, P, Sc, Te, Ti, V, and Y, and Zn. Elements with the broadest anomalies include Ag, As, K, Li, S, Sr, Sb, Tl, and W; those for As, W, and Li extend farthest (at least 60 m) from mineralized structures. These three elements thus should be especially useful in delineating the outermost manifestations of alteration associated with blind Au mineralization in this district.

Chemical abundances are useful in distinguishing rock lithologies, particularly where the rocks have been strongly altered. Elements that seem to best discriminate lithology, mainly below the weathered zone, include Cd, Ce, Co, Ni, Nd, and Pb.

Chemical weathering has overprinted and modified primary hydrothermal zoning. Samples with low concentrations of Ca, Mg, and S generally define those areas most affected by weathering. Elements locally enriched in weathered rocks include Ag, As, Au, Ce, La, Ni, Pb, Te, and W. Cadmium, Cu, and Zn are locally enriched secondarily near the base of the zone of weathering.

**PRIMARY ELEMENT DISPERSION PATTERNS IN A CARBONATE-ROSTED,
EPITHEMAL, HIGH-GRADE, Au-Ag TELLURIDE SYSTEM: MAYFLOWER
MINE, MADISON COUNTY, MONTANA, U.S.A.
COCKER, M.D.**

High-grade, Au-Ag telluride mineralization in the Mayflower mine occurs in hydrothermally altered carbonates of the Middle Cambrian Meagher Formation. Primary element dispersion patterns and hydrothermal alteration zoning suggest that the mineralization and alteration were principally guided by detrital quartz-bearing, paleo-tidal channels in the vertical to overturned Meagher Formation where this unit is cut by the Late Cretaceous to Paleocene Mayflower fault. Proximity of the Mayflower mineralization to the deep-seated, Mayflower fault and lateral geochemical zoning along strike of the Meagher Formation away from the fault suggests that the Mayflower fault acted as a source conduit for the hydrothermal fluids. With increasing distance from the Mayflower fault, Cu, Pb, Ag, Au and V decrease, Mn and MgO increase, and Hg, Tl, As, and Zn tend to remain the same or show a slight increase. Vertical zoning is evident by an increase in base-metals and Ag to the presently explored depth of 670 m. Alteration and geochemistry is zoned relative to the paleo-tidal channels with: 1) a central zone of quartz, adularia and roscoelite anomalous in Te, V, Zn, Mo, and Pb; 2) a proximal zone of quartz and adularia; and 3) a distal zone of hydrothermal dolomite with anomalous Mn. The quartz-adularia and dolomite zones show significant increases in SiO₂ and K₂O and MgO respectively relative to unaltered carbonates of the Meagher Formation. Anomalous Hg, Tl, As, and Cu overlap zones 1 and 2. High-grade, gold and silver mineralization is best developed in and adjacent to zone 1. The major controls on element dispersion are principally: 1) lithologic (permeable, paleo-tidal channels, reactive carbonates and hydrothermal alteration), 2) structural (deep-seated, Mayflower fault as a fluid conduit), and 3) distance from source (lateral along strike and vertical along paleo-tidal channels) that may also reflect changes in the chemistry, pressure and temperature of the hydrothermal fluids.

**COMPOSITIONAL CONTROLS ON THE GOLD CONTENTS OF SILICIC
VOLCANIC ROCKS**

CONNORS, K.A., NOBLE, D.C., WEISS, S.I. and BUSSEY, S.D.
79 volcanic rocks, mostly from the Western U.S., were carefully selected: 1) to sample a wide range of silicic to intermediate magma compositions and 2) to represent as closely as possible the composition of the magmas when erupted. Nonhydrated glasses or dense hydrated glassy rocks were analyzed in preference to devitrified materials. Gold contents were determined by XRAL Activation Services using neutron activation-fir assay concentration methods (Rowe and Simon, 1968) with a detection limit of 0.1 ppb.

Silicic volcanic rocks as a group contain less gold than shown in much of the geochemical literature. Most samples have less than 1.0 ppb, and many contain only 0.1 to 0.3 ppb Au. Subalkaline high-silica rhyolites and peraluminous rhyolites have the lowest Au contents (mean and median values 0.2 and 0.1 ppb, respectively). Lower silica rhyolites have only slightly higher values (mean 0.3 ppb). The highest gold contents are in peralkaline rhyolites (0.2 to 4.5 ppb, mean 1.0 ppb) and in subalkaline ferrotrochilite (0.4 to 1.0 ppb, mean 0.7 ppb). This pattern is well illustrated on a plot of FeO versus CaO (Warshaw and Smith, 1988). Intermediate rocks, in general, appear to have higher gold contents than silicic rocks, and tholeiitic andesites (icelandites) appear to be higher in gold than calc-alkaline types.

The gold in many of the specimens appears to be concentrated in the groundmass rather than the phenocryst fraction. A phenocryst-rich vitrophyre of the Soldier Meadow Tuff, NW Nevada, contains 0.6 ppb Au whereas nonhydrated glass separated from the rock contains 0.9 ppb Au. The relatively high gold contents of some aphyric peralkaline obsidian samples also support the timing of most of the gold within the groundmass.

An important control of the gold contents of silicic rocks appears to be melt structure. Network-modifying cations, particularly Fe³⁺ and Na⁺, depolymerize Fe-rich and peralkaline melts, markedly reducing the partition coefficients between the silica melt and coexisting crystal and liquid phases. Our data suggest that crystal fractionation will increase the gold contents of peralkaline rhyolites in a manner generally accepted for the elevated Fe, Zr, Nb, REE, etc., contents of such rocks. High-silica rhyolites with low iron contents are, in contrast, very highly polymerized, and a wide range of minor elements, apparently including gold, are not readily accommodated. The very low gold contents of low-iron subalkaline rhyolites may reflect separation of gold during differentiation (Tilling et al., 1973). An additional, and possibly very important control of gold contents of many rocks may perhaps be the degree and timing of separation of a sulfide melt phase.

High-silica subalkaline igneous rocks and magmas appear to be poor sources of gold for the formation of economic deposits. Although gold in iron-rich peralkaline and subalkaline rhyolites and/or magmas may have contributed to the development of certain deposits (e.g., Hog Ranch, NV), there is an overall scarcity of gold deposits in volcanic fields dominated by iron-rich rhyolites. An attractive hypothesis is that the necessarily high gold contents of magmas responsible for gold-rich porphyry systems, as well as the elevated gold contents of certain iron-rich rhyolites, may reflect mixing of small amounts of highly gold-enriched mafic magmas with intermediate to silicic magmas of "normal" gold contents.

The extremely low gold contents of many subalkaline silicic volcanic rocks imply that very low-level gold anomalies detected in silicic volcanic terranes are real. Such patterns, which may in part reflect the transport of gold by groundwater as well as ascending hydrothermal solutions, may help assist in delineating structural features and other controls of hydrologic circulation.

**A GRAPHICAL APPROACH TO MINERAL-SOLUTION EQUILIBRIA
DEFREYES, K.S.**

The familiar Eh-pH and other potential-potential diagrams need to be turned inside out. Using conserved properties as axes and contouring the potentials on the interior of the diagram emphasizes that the potentials, like Eh and pH, are usually symptoms and not causes. Following Redlich's usage, the conserved properties are called **COORDINATES** and the potentials **FORCES**.

Coordinates, in this sense, are those properties which are conserved on mixing of two solutions. They are independent of pressure and temperature. Examples of coordinates are 1) the sum of silver (in all dissolved forms) per kilogram of water, 2) alkalinity, and 3) the sum of all sulfur species per kilogram of water. On graphs using these coordinates, vector sums work and the lever rule correctly describes the mixing of solutions.

Forces are independent of the volume of solution; they can often be measured by inserting a probe into a large, and unknown, volume. Examples of forces are gas pressures, voltages across an electrode pair (Eh and pH), solid phase solubilities, and absorbance of light or sound.

These diagrams associate one force as a master variable with each coordinate. A typical choice would associate Ag⁺ activity, as a force, with the sum of all silver, as a coordinate. In addition to the two coordinates on the page, any number of additional coordinates can be held constant. In effect, the page is a two-dimensional slice through a multidimensional system. Specifying that the solution is in equilibrium with a solid always results in eliminating one force and one coordinate. The electro-neutrality requirement can be handled through an appropriate definition of alkalinity. Equilibration with a gas volume, as during boiling, results in an apparent equilibrium constant incorporating Henry's Law. A set of simultaneous nonlinear equations result, one for each coordinate. Roots of the equations are found in order to produce contours of chemical species, sums or products of species, gas pressures, or electrode voltages.

Even a relatively slow personal computer finds results fast enough to stay ahead of a pen plotter. Modern workstations can compute "what-if" diagrams rapidly on the screen. Examples of geologically interesting diagrams include the solubility of gold in the presence of iron oxide and pyrite, and mixing of a gold bisulfide solution with oxygenated water. An example from extractive metallurgy optimizes the cyanidation of silver sulfide.

APPENDIX G

Ash-Flow Volcanism of Ammonia Tanks Age in the Oasis Valley Area, SW Nevada: Bearing on the Evolution of the Timber Mountain Calderas and the Timing of Formation of the Timber Mountain II Resurgent Dome.

K A Connors (Mackay School of Mines, University of Nevada-Reno, Reno, NV 89557)

E H McKee (U.S. Geol. Survey, 345 Middlefield Rd., Menlo Park, CA 94025)
D C Noble and S I Weiss (both at: Mackay School of Mines, University of Nevada-Reno, Reno, NV 89557)

A sequence of four ash-flow sheets of nearly the same age is exposed in the Oasis Valley area north of Beatty, Nevada. The sequence begins with the Ammonia Tanks Member (ATM), the second of the two major ash-flow sheets of the Timber Mountain Tuff (TMT). More than 600 m of the ATM is exposed at Oasis Mtn., where the unit dips to the east. Our mapping has shown that the ATM composes the bottom of the sequence exposed south of Fleur-de-Lis Road (FDLR), where it was previously identified by others as the older Rainier Mesa Member (RMM) of the TMT. The ATM is compositionally variable, ranging from tuff containing abundant hornblende, biotite and plagioclase with little quartz and sanidine, to high-Si rhyolite with abundant large phenocrysts of quartz and sanidine. East of Oasis Mtn. the ATM is overlain by fine-grained lacustrine sedimentary rocks with interbeds of fresh-water limestone. These are overlain by the tuffs of Fleur-de-Lis Ranch (TFDL), which consist of two local units of quartz-poor, plagioclase- and biotite-rich tuffs that lack sphene, and are separated by a unit of rhyolite lava. The first TFDL unit, which contains abundant lithics, including granitic and metamorphic rock, can be traced only a short distance south of the FDLR where it pinches out between the ATM and overlying rhyolite lava flows. The rhyolite lava flows also pinch out just south of the FDLR. To the south the second TFDL sheet directly overlies the ATM. The second TFDL unit has smaller phenocrysts and contains clinopyroxene, which is lacking in the first. The top of the sequence is an ash-flow sheet identified as the tuff of Cutoff Road (TCR) by USGS geologists (USGS Prof. Paper 919; P. P. Orkild, oral commun., 1991). Our work supports this correlation. The TCR is poor in quartz, but contains abundant hornblende and sphene. This unit generally overlies the second TFDL unit conformably, with the contact marked by a cooling break. Directly east of Oasis Mtn., however, there may be a slight angular discordance and a thin, discontinuous debris-flow breccia is present which contains blocks of the second TFDL unit; here, the cooling break is equivocal.

The Ammonia Tanks Member has been precisely dated at 11.44 ± 0.03 Ma by Fleck et al. (1990), the age being an average of a number of $^{40}\text{Ar}/^{39}\text{Ar}$ ages determined by the USGS, Menlo Park, CA. Noble et al. (1990, 1991) published an age of 11.4 ± 0.1 on the TCR at Oasis Valley. This age was rounded from the value of 11.38 (or 11.42 weighing individual determinations according to the inverse of their uncertainty) obtained by averaging six high-precision laser fusion $^{40}\text{Ar}/^{39}\text{Ar}$ age determinations made at the Berkeley Geochronology Center. There may be differences of as much as 1.5 percent between ages reported by the two laboratories, with Berkeley ages being older. This appears to reflect both differences in monitor age value (ca. 1%), peak measurement procedures, and/or irradiation flux.

The thick sequence of tuffs of the coeval ATM, TFDL, and TCR support the Oasis Valley area as the location for the western margin of the Timber Mtn. I caldera. Secondary flowage features in the upper part of the ATM at Oasis Mtn. probably resulted from over-steepening of the very thick sequence of hot tuff as it compacted against the topographic wall of the Timber Mtn. I caldera located west of Oasis Mtn. Lithic fragments as large as 5 m in diameter present in the ATM at Oasis Mtn. may have travelled from the vent area of the Timber Mtn. II caldera, facilitated by the considerable elevation difference between the resurgent dome of the Timber Mtn. I caldera, itself further uplifted by AMT magma, and the western moat of the Timber Mtn. I caldera. The blocks may also have been derived from the nearby wall of the Timber Mtn. I caldera. The local occurrence of the ash-flow units and the absence of sphene suggest that the TFDL may not be related to the ATM magmatic system, but rather to a discrete system in the vicinity of the western margin of the Timber Mtn. I caldera.

The age of the TCR appears to be, at most, 0.2 to 0.3 Ma younger than the Ammonia Tanks Member. To the east, in the Transvaal Hills, the TCR overlies the tuff of Buttonhook Wash (TBW) (P.P. 919). As the TBW unconformably overlies the ATM along the western flank of the resurgent dome of the Timber Mtn. II caldera, the TCR must post-date resurgence, and the age of the TCR provides an upper limit on the time of resurgence. The high-precision ages and stratigraphic and structural data demonstrate that, as in the Quaternary Long Valley, Yellowstone and Valles calderas, resurgence of the Timber Mtn. II caldera took place very shortly after eruption and subsidence.

Submittal Information

1. 1991 Fall Meeting
2. 010956236
3. (a) Katherine A. Connors
Mackay School of Mines
University of Nevada-Reno 89557

(b) Tel: 702-784-4216

(c) Fax: 702-784-1766
4. V
5. (a) --
(b) 3635 Geochronology
(b) 8404 Ash Deposits
6. PO
7. 0 %
8. \$40.00 enclosed (student rate)
9. C
- 10.
11. Yes

(22) Prepared Guralp borehole instruments for Deep Springs were made ready for installation.

(22) Compared character of microearthquake records from Yucca Mtn. with those from Mammoth area.

(23) Made repairs on Nellis Boundary microearthquake station - verified gains at Black Crater station.

(23) Copied selected microearthquake records from Yucca Mtn. region.

(24) Received reviews and made small revisions in SSA microearthquake manuscript. The manuscript was accepted for publication. (See attached preprint.)

PUBLICATIONS

Microearthquakes at Yucca Mountain, Nevada, James N. Brune, Walter Nicks, and Arturo Aburto, Bull. Seismol. Soc. Am., in press, 1991.

Real Time Analog and Digital Data Acquisition through CUSP, William A. Peppin, Seis. Res. Lett., submitted 1991.

MEETINGS, WORKSHOPS

Invited to India to give lectures on seismic hazard. Gave seminar and consulted with scientists at Baba Atomic Research Center, Bombay, and University of Roorkee, on comparison of India and US plans for high level nuclear waste disposal.

Invited to Santiago, Chile, to lecture on earthquake source mechanics and earthquake hazard at international workshop.

Invited to give lecture on earthquake source mechanics at conferences at Santa Barbara, Lawrence Livermore Labs, and USGS.

MICROEARTHQUAKES AT YUCCA MOUNTAIN, NEVADA

James N. Brune, Walter Nicks, and Arturo Aburto
Seismological Laboratory and Center for Neotectonics
University of Nevada, Reno

ABSTRACT

We operated a microearthquake array in the neighborhood of the proposed high level nuclear waste repository at Yucca Mountain, Nevada. The array consists of four high-gain (up to 34 million), narrow band (25 hz) telemetered stations.

Based on approximate magnitude calibration of the array we expect during quiet periods, for distances less than 15 km, complete recording of events at Yucca Mt. for $M \geq -1$. We have operated the four stations for 12 hour periods overnight between August and October, 1990 and intermittently afterward, until April, 1991, when we began more or less continuous operation.

The pattern of microearthquake activity confirms the existence of a zone of seismic quiescence in the vicinity of proposed repository. We recorded only about 10 events with S-P times less than 3 sec. ($\Delta < 24$ km). Most events had S-P times between 3 and 6.5 sec., consistent with the higher seismic activity at distances between 24 and 52 km observed by Rogers et al., (1987), and Gomberg (1991). Oliver et al. (1966) found, contrary to what has been observed by us for Yucca Mountain, that in seismically active areas, most of the events had S-P times less than 3 sec. We confirmed this expectation for four microearthquake stations near Mammoth Lakes, where we observed microearthquake rates of over 100 per day, most with S-P times less than 3 seconds. Extrapolation of seismicity data from the Southern Great Basin Seismic Network confirms the low microearthquake activity in the immediate vicinity of Yucca Mountain.

INTRODUCTION

The proposed high level waste nuclear repository at Yucca Mountain, Nevada, would be one of the largest and most important construction projects ever undertaken by mankind. Tectonic stability is a crucial issue because the facility must be engineered to specifications for 10,000 years in the future. There are many questions that need to be answered concerning earthquakes, volcanic activity, and the response of the facility to excavation and thermal stressing from the 70,000 tons of high level radioactive material expected to be stored at the site. There are unanswered questions relating to the interaction of the tectonic stress field and the hydrologic regime of the region. Hydrofracture experiments have been interpreted to indicate possible incipient normal faulting (Stock et al., 1985). Important questions and uncertainties about the site are expected to be answered by the Site Characterization Plan, which will last at least several years and cost billions of dollars. Because of the critical importance of understanding all tectonic, geological, and geophysical aspects of the site, we undertook extended microearthquake monitoring there.

Submitted to Bulletin of the Seismological Society of America, May 1991.

PREVIOUS STUDIES

Previous seismicity studies of the region have been based primarily on data from the Southern Great Basin Seismic Network (SGBSN), currently consisting of 55 stations operated by the USGS (Rogers et al., 1987; Gomberg, 1991). The station spacing is denser (a few km spacing) in the immediate neighborhood of Yucca Mountain. Gomberg (1991) has estimated that the detection threshold of the array is about $ML = 0.1-0.3$, but there is considerable uncertainty in this because magnitudes are determined based on both the Richter ML scale and on a duration scale, and many smaller local events are recorded at only a few stations near the epicenter, while larger events may saturate the records.

Several features of the spatial seismicity pattern are discussed in the Rogers et al. (1987) and Gomberg (1991) studies. There is a concentration of seismicity in regions of previous nuclear testing, at a distance of several tens of kilometers from the Yucca Mountain site, but it is unclear how much of this is directly connected with nuclear testing. Of most importance to this study is the almost complete lack of seismicity near Yucca Mountain. It is not known whether this is simply a result of statistical temporal and spatial variations in seismicity or whether it is closely connected with some aspect of the strain field. Gomberg (1991) suggests that the "gap" in seismicity may be either a gap ready to be filled by a large event, or simply a region where shear strain is not accumulating. Parsons and Thompson (1991) suggested that volcanic magma pressure could temporarily lock up faults in a region of active volcanism. They suggested that this might be the case for the region of low seismicity at Yucca Mountain. Continued monitoring of seismicity should help to answer some of these questions, especially if coupled with accurate measurements of the strain field, which we have proposed be carried out at the site.

Microearthquake surveys have been made in several areas of Nevada and California. Oliver et al. (1966) recorded microearthquake rates in northern Nevada ranging from several per day to over two hundred per day (magnitudes mostly less than zero), with highest rates observed in areas of recent faulting. Rates at all sites were considerably higher than in aseismic areas. Molnar et al. (1969) operated high gain microearthquake seismographs for several weeks before and after the nuclear explosion Benham (at nearby sites in Nevada and California). Although a pronounced increase in seismic activity was observed in the immediate vicinity of the explosion, no significant increase in activity was observed near (<25 km) any of the microearthquake recording sites, indicating no far field triggering of microearthquakes by either the dynamic or static change in strain field associated with the explosion. An average of about 1 event per day was detected by the experiment, considerably less than observed by Oliver et al. (1966). This could in part be a result of different instrumentation, but was also probably due to the lower level of tectonic activity in southern Nevada as compared to the northern and central Nevada sites occupied in the Oliver et al. (1966) study.

Brune and Allen (1967) carried out a microearthquake study along the San Andreas Fault System in southern California and found that short term activity is not necessarily positively correlated with long term activity and seismic hazard, even though in this study and others there is a general similarity between microearthquake activity and macroseismicity. Observed microearthquake activity varied from more than 75 events per day in Imperial Valley to virtually nil along the central section of the San Andreas fault (near Palmdale and Lake

Hughes). The area of minimal microearthquake activity along the central segment of the San Andreas fault, the very segment which broke in the great 1857 earthquake, is a particularly dramatic example of a lack of correlation between microseismicity and long term fault activity. In a related study Wesnousky (1990) has suggested that seismic productivity (in terms of small earthquakes) of a fault zone is related to the maturity of the fault system. Fault systems with hundreds of kilometers of displacement tend to have low rates of small earthquake activity, whereas faults with less cumulative slip had higher rates (in each case normalized to the long term slip rate). This is consistent with the low microearthquake rates observed by Brune and Allen (1967) for the site of the 1857 earthquake.

INSTRUMENTATION

Most of the previously discussed microearthquake studies were carried out with portable seismographs. However, we felt that because of the importance of the site, microearthquakes should be monitored as close to continuously as possible. Therefore we decided to test more or less permanent sites, and transmit data continuously back to the Seismological Laboratory at the University of Nevada, Reno. This was accomplished via radio links to a nearby microwave relay station (see Figure 1). Four sites were selected, two on Yucca mountain near the Solitario Canyon fault (YNB and YYM), one about 5 kilometers to the west in Crater Flat (YCF), and one still further west on Black Cone (YBC) near the center of Crater Flat. The YBC station on Black Cone is important for monitoring any microseismicity which might be associated with the relatively young volcanic activity in Crater Flat. The instrumentation and telemetry setup is illustrated in the block diagram in Figure 2. Because we are using a full radio channel bandwidth for each station (single vertical component) we have higher dynamic range, and associated signal to noise ratio, than is possible for the usual situation of placing several channels on one radio band. The seismometers we are using are Geotech GS-13 instruments. The amplifiers and band pass filters peak the system response near 25 hz to help give high gain and relatively low noise level. Of special interest and importance to the experiment is the high dynamic range digital chart recorder, a Astro-Med Inc. DASH IV. Because true microearthquake signals are often difficult to detect in the presence of noise, we wished to have continuous recording at as high a gain as possible. The digital chart recorder format allows a high dynamic range and continuous recording, because the trace does not saturate or become faint or non-linear at high amplitudes. Since the signal is relatively narrow band, there is little need for actual storage of the bits of digital information. The four signals from the four stations are recorded continuously on four traces of the recorder paper going in one direction, and four traces in the other direction, giving two days of recording on each role of paper. In the initial part of the study in August through October we ran at approximately twice this chart speed, and only recorded at night, except for special occasions.

The response of our system with recording sensitivity set at 1 volt full scale is compared with the USGS, Yucca Mountain S13Y system as given in Rogers et al. (1987) in Figure 3. Of course the actual useful sensitivity of the system depends on the trace noise level at each setting. We found that we could operate the system as shown in figure 3 with less than 1 mm noise trace amplitude during quiet nights with little wind. We could occasionally record with twice the sensitivity for short periods of time. During windy periods we often reduced the sensitivity because the trace noise level exceeded (sometimes greatly) 1 mm. The

chart recorder automatically records the gain settings of each channel along with the approximate time. The response curve shown in figure 3 suggests that during the quietest periods of operation we should be able to detect events 1 to 2 magnitude units lower than the USGS stations.

SEISMOGRAMS

Typical records are shown in figures 4 a,b. Figure 4a shows an event arriving from the west (first at YBC) with an S-P time of about 2 sec at YBC. This event did not trigger the USGS automated system. Figure 4b shows a more distant event (about 15 sec S-P time) along with an explosive sonic which could be confused with an earthquake if four recording stations had not been available. The use of four stations is critical for identifying small events when the noise level is relatively high, because sonic events always show a slow moveout (slow sonic velocity) whereas earthquakes appear to arrive nearly simultaneously at the stations, and a trained observer quickly learns to distinguish earthquakes from sonic bursts and other noise.

Figure 5 shows typical events with short S-P times at the Yucca Mountain microearthquake array. None of these events triggered the USGS automated recording. These events are relatively rare and only a few were recorded during the first three months of operation. The magnitudes are estimated to be about 0 to -1 (see later section). This qualitative observation confirms a very low rate of microearthquake activity at Yucca Mountain, consistent with the low seismicity for higher magnitudes observed by Rogers et al. (1987) and Gomberg (1991). Of particular note is the lack of events with short S-P times, less than three seconds (see dashed curve, Fig. 7). Oliver et al. (1966) found that in seismically active areas most events had S-P times less than 3 seconds, as might be expected because of the rapid attenuation with distance of 30 hz energy. This qualitative observation of few events with short S-P times further emphasizes the relatively low microearthquake activity in the immediate vicinity of the microearthquake stations at Yucca Mountain.

Because we wished to validate the operation of our system, and the qualitative arguments given above, we temporarily transferred the recording to four stations in the Mammoth Lakes region (Red Slate Mountain, Casa Diablo Hot Springs, Deadman Pass, and Montgomery Pass), with filters applied to give approximately the same response shape as the Yucca Mountain stations. Typical seismograms from the Mammoth region are shown in Figure 6. As expected from this highly active area the great majority of events has s-p times less than three seconds (Figure 7), and microearthquake rates were orders of magnitude higher than at Yucca Mountain, over a hundred events per day.

DISTRIBUTION OF S-P TIMES

A careful count of all events with short S-P times was made from the Yucca Mountain recordings, and compared with results from the Mammoth Lakes region. Results are shown in Figure 7. The dashed line histogram indicates the results from Yucca Mountain for 600 hours (25 cumulative days) of low noise recording. Most of the events recorded have S-P times between 4 and 10 seconds, with a peak at about 6.5 seconds. The relatively few events recorded with S-P times less than three seconds confirms the relatively low microearthquake activity in the immediate vicinity of Yucca Mountain. The overall microearthquake rates with S-P times less than 10 seconds (distances less than about 80 km) was about 5 events

per day, but the number of events per day with S-P times of less than 3 seconds was less than 1 event per 5 days. In contrast the events from the Mammoth region almost all had S-P times less than 3 seconds, (solid line, Figure 7) and the overall rates were over a hundred events per day.

ATTENUATION AND MAGNITUDE DETERMINATION

In order to approximately calibrate our system with respect to SGBSN magnitudes we estimated an amplitude versus distance attenuation curve for a magnitude zero earthquake (as inferred from the SGBSN). We obtained a number of on-scale recordings of events which were given magnitudes from the SGBSN. In some cases the gain was considerably lower than shown in Figure 3 so that recordings were on scale for events large enough to trigger the SGBSN. We then plotted, as a function of distance, the following quantity:

$$\text{Log } A_0(x) = \text{Log } A(x) - M$$

where A_0 is the estimate of the amplitude of a magnitude zero event at a distance x , A is the trace amplitude (zero to peak) recorded on our system, corrected to a recorder sensitivity of 1 volt per millimeter, and M is the SGBSN magnitude.

The results are shown in Figure 8. The black dots are individual estimates of $\text{Log } A_0$. The solid curve is an approximate fit to the data based on theoretical attenuation curves forced to pass through the mean of the data near a distance of 50 km. Beyond 50 km the theoretical curve has a shape corresponding to geometrical spreading proportional to the inverse square root of distance and a Q (at 20 hz) of 800 (with a small correction for scattering and dispersion). For distances less than 50 km the theoretical curve corresponds to geometrical spreading proportional to the inverse of distance and a Q of 400, corresponding to a lower Q , and to inverse distance spreading, as might be expected at shorter distances. For the purposes of this study the derivation of the theoretical curves is not important, as they were constrained to have parameters giving an approximate fit to the data in order to define a curve to be used in the approximate definition of magnitude. As a further comparison, the curve obtained by Frankel et al. (1991) from narrow band filtering (at 30 hz) of records from the ANZA seismic array is shown (forced to go through the same point at a distance of 50 km). At short distances we would expect the attenuation at ANZA to be similar to that at Yucca Mountain since at close distances the attenuation due to differences in Q will be minimized. Because of the low microseismicity at Yucca Mountain, and consequent lack of data points at near distances, we wanted an independent estimate of the shape of the attenuation curve. This is provided by the results of Frankel et al. (1991) since they made observations with a narrow band system similar to that used by us.

If we accept the solid curve in figure 8 as our definition of magnitude, it indicates that we should be able to record events down to magnitude about -1.5 at distances of about 10 km (with amplitudes of >1 mm). If we take the Frankel et al. (1991) curve, the estimated magnitude of an event with 1mm trace amplitude is less than -2. These results are consistent with the relative magnification curves for the Yucca Mountain and SGBSN stations shown in figure 3. We conclude that if many events with magnitudes greater than -1 were occurring at Yucca Mountain, we should have easily observed them.

B-VALUES AND ESTIMATED MICROEARTHQUAKE RATES

Gomberg(1991) estimated the seismicity distribution for the SGBSN using the Gutenberg-Richter relationship(Gutenberg and Richter, 1941, 1954):

$$\log N(M) = a - bM$$

where $N(M)$ is the number of earthquakes with magnitude M , and a and b are two constants derived from the seismicity distribution. This equation can be extrapolated to estimate the number of earthquakes occurring in a magnitude range not covered by the SGBSN data. Gomberg fits two curves to the SGBSN data. The curve which predicts the lowest number of events near magnitude zero has constants $a=4.56$ and $b=1.27$ (for magnitude intervals of 0.1 magnitude units). Correcting the area covered by the SGBSN to a region of hypocentral distance equal to 24 km (s-p time equal or less than 3 sec), and correcting from the time period of the SGBSN data set (7 years) to the time of quiet operation in our data set (25 days) gives an estimate of 89 events with magnitude greater than -0.5 which should have been observed by us if the seismicity level at Yucca Mountain were the same as the average seismicity over the whole SGBSN for 7 years. If we extend the magnitude range to -1.5, (which should have been detected by us, see above), the estimated number of events would be over several hundred. Since we only observe a few events with s-p times less than 3 seconds, this calculation confirms that the current microearthquake rate in the immediate vicinity of Yucca Mountain is much lower than the average for the SGBSN region.

CONCLUSION

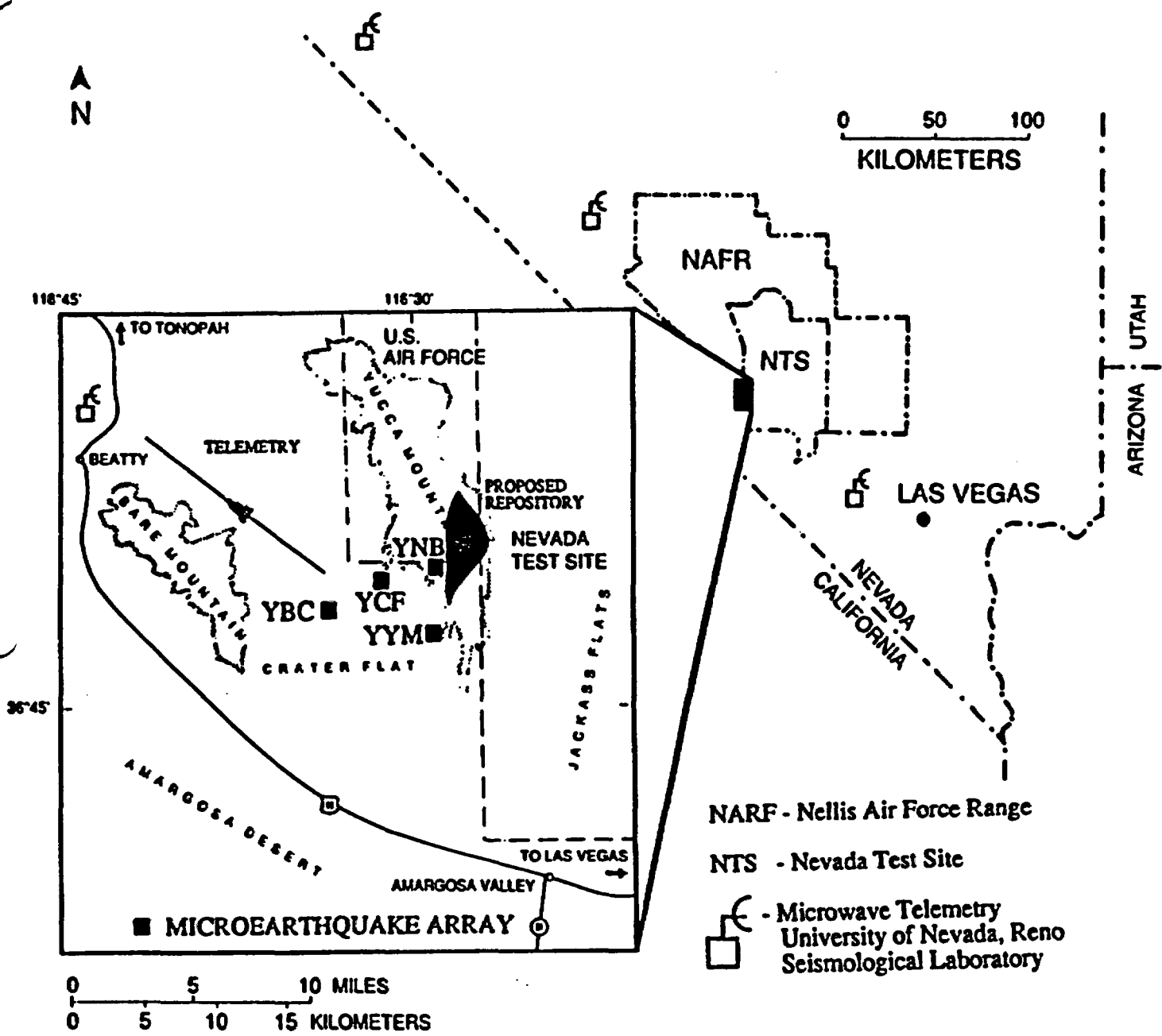
We have operated a sensitive, narrow band, 4-station telemetered microearthquake array in the immediate vicinity of the proposed high level nuclear waste repository at Yucca Mountain, Nevada. Microearthquake rates were found to be very low, lower than for tectonically active areas in northern Nevada, lower than most sites in southern California, and lower than the average microearthquake rates for the whole region of southern Nevada monitored by the Southern Great Basin Seismic Network. The existence of a region of very low microearthquake activity in the immediate vicinity of the Yucca Mountain site is consistent with the low rate of macroseismicity observed in the same region by Rogers et al. (1987) and Gomberg (1991). Explanations suggested for the low rate of activity have ranged from low shear strain accumulation, to a possible seismic gap related to a future large earthquake (Gomberg, 1991), or possible magmatic locking by a build up of magma pressure in the Crater Flat region (Parsons and Thompson, 1991). The lack of microearthquake activity has potential importance relative to the suggestion that the region is near incipient normal faulting, as suggested by some hydrofracture measurements (Stock et al., 1985). No matter what the explanation for the current low rate of microearthquake activity, it is very important to continue monitoring the site to establish a base line of activity from which to judge the effects of future mining activity and thermal loading from radioactive decay.

ACKNOWLEDGEMENTS

This experiment was funded by the Nevada Nuclear Waste Projects Office through the Center For Neotectonics of the University of Nevada, Reno.

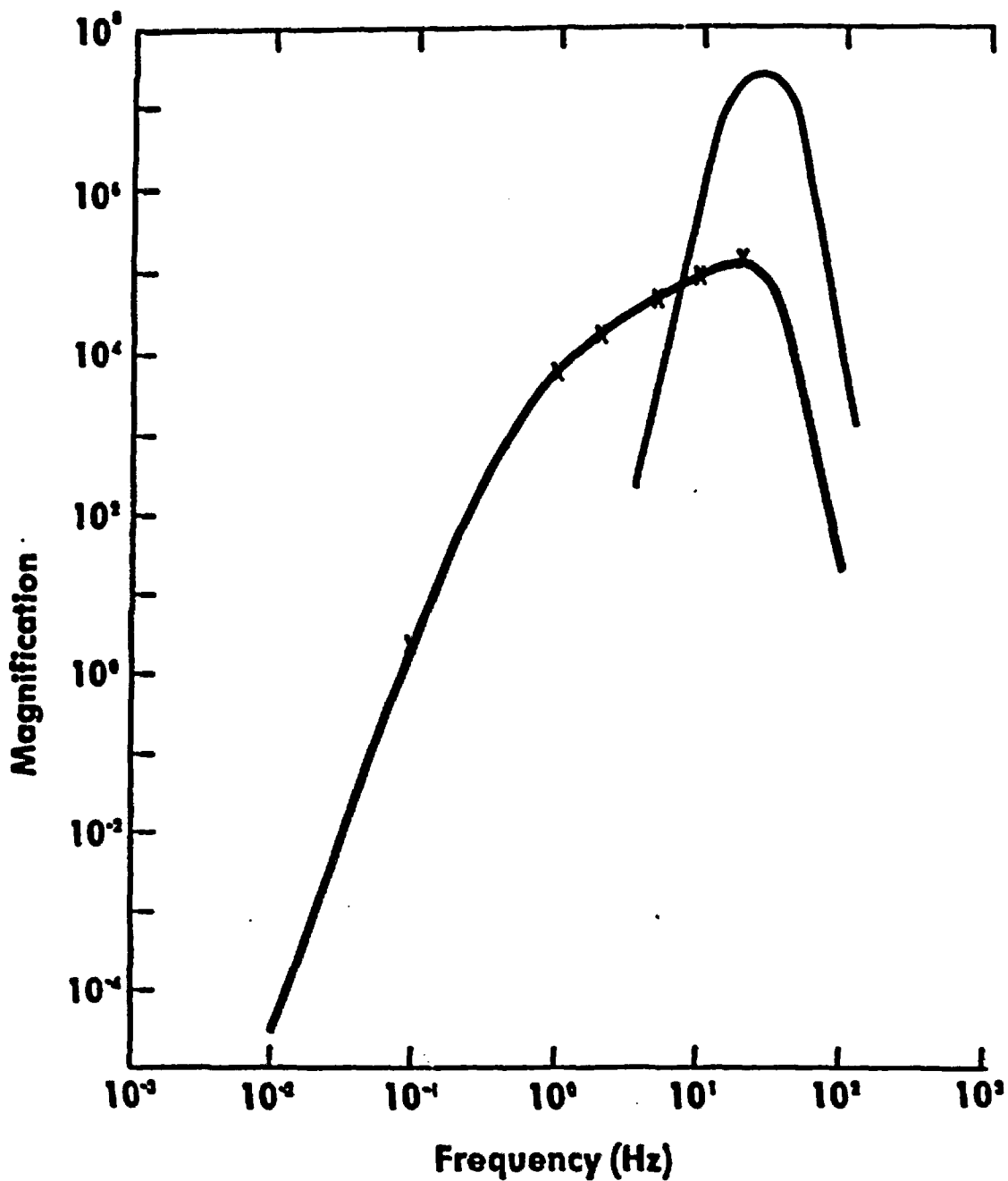
REFERENCES

- Brune, J.N. and C.R. Allen, A Micro-Earthquake Survey of the San Andreas Fault System in Southern California, Bull. Seismol. Soc. Am., v. 57, 277-296, 1967.
- Frankel, A., A. McGarr, J. Bicknell, J. Mori, L. Seeber and E. Cranswick, Attenuation of High-Frequency Shear Waves in the Crust: Measurement from New York State, South Africa, and Southern California, J. Geophys. Res., v 95, 17,441-17,458, 1990.
- Gomberg, J., Seismicity and Detection/Location Threshold in the Southern Great Basin Seismic Network, accepted to J. Geophys. Res.
- Molnar, P., K. Jacob and L.R. Sykes, Microearthquake Activity in Eastern Nevada and Death Valley California Before and After the Nuclear Explosion Benham, Bull. Seismol. Soc. Am., v. 59, 2177-2184, 1969.
- Oliver, J., A. Ryall, J.N. Brune and D.B. Slemmons, Microearthquake Activity Recorded by Portable Seismographs of High Sensitivity, Bull. Seismol. Soc. Am., v. 56, 899-924, 1966.
- Parsons, T., and G.A. Thompson, Coupled Processes of Normal Faulting and Dike Intrusion in Tectonically Extended Regions, Seismol. Res. Ltrrs., v. 62, p. 26, 1991.
- Stock, J.M., J.H. Healy, S.H. Hickman and M.D. Zoback, Hydraulic Fracturing Stress Measurements at Yucca Mountain, Nevada, and Relationship to the Regional Stress Field, J. Geophys. Res., v. 90, 8691-8706, 1985.
- Wesnousky, S.G., Seismicity as a Function of Cumulative Geologic Offset: Some Observations from Southern California, Bull. Seismol. Soc. Am., 80, 1374-1381, 1990.



YUCCA MTN. TELEMETERED MICROEARTHQUAKE ARRAY

FIGURE 1



Response of USGS, Yucca Mtn. S13Y system into a helicorder with amplifier gain of 84 dB compared with UNRSL narrow band, high frequency micro-earthquake array at Yucca Mtn., Nevada.

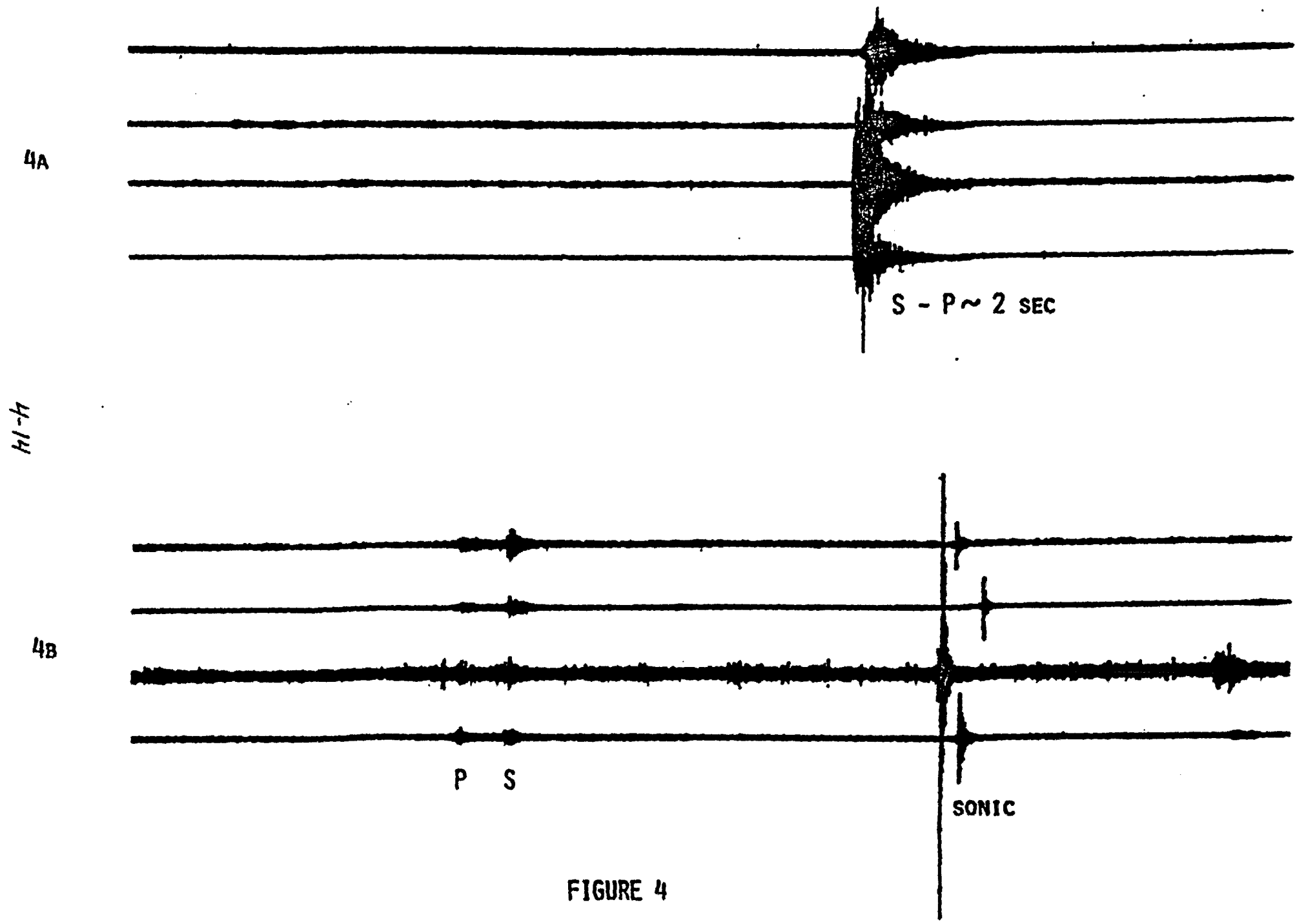


FIGURE 4

4-15

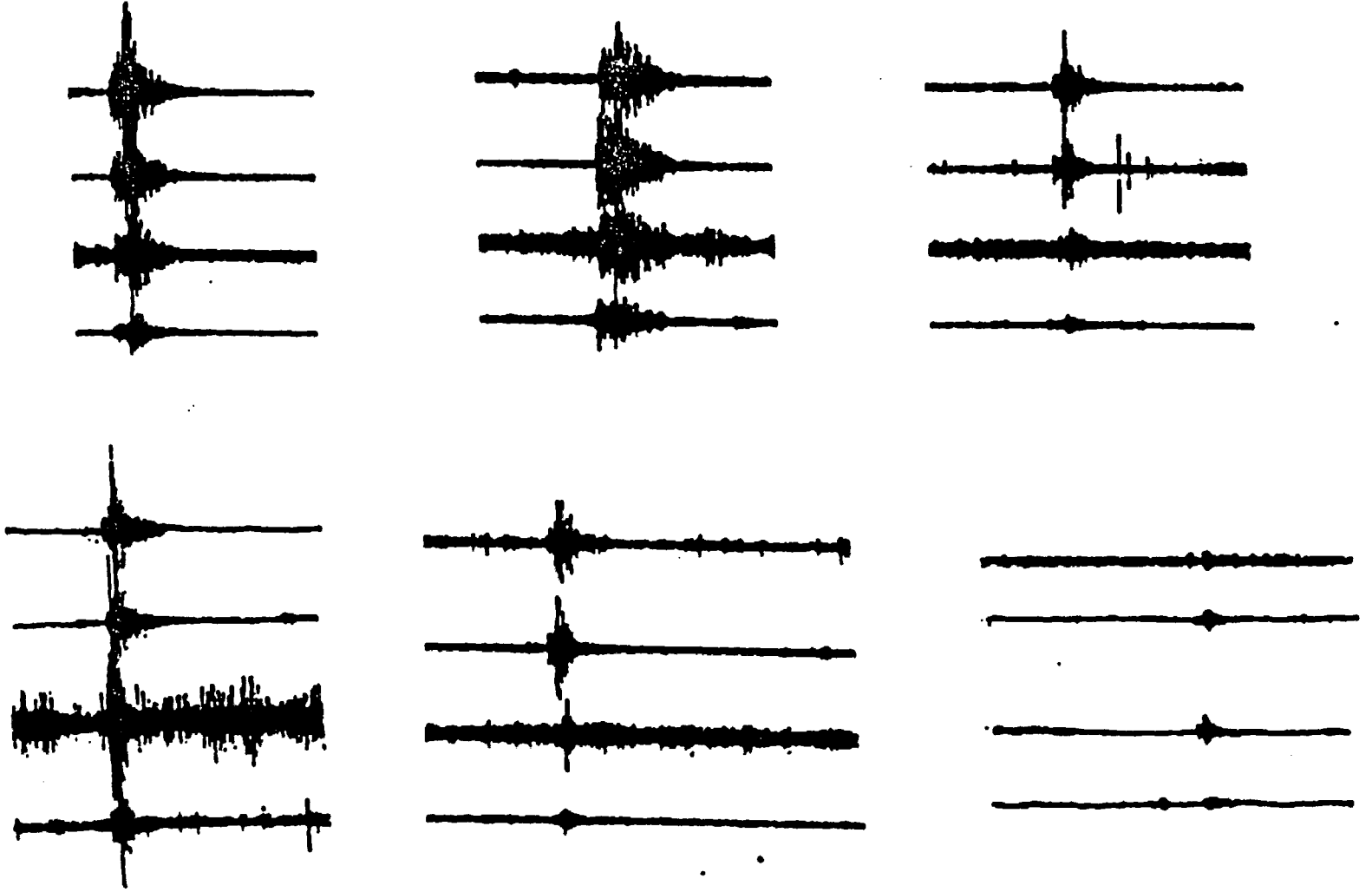


FIGURE 5

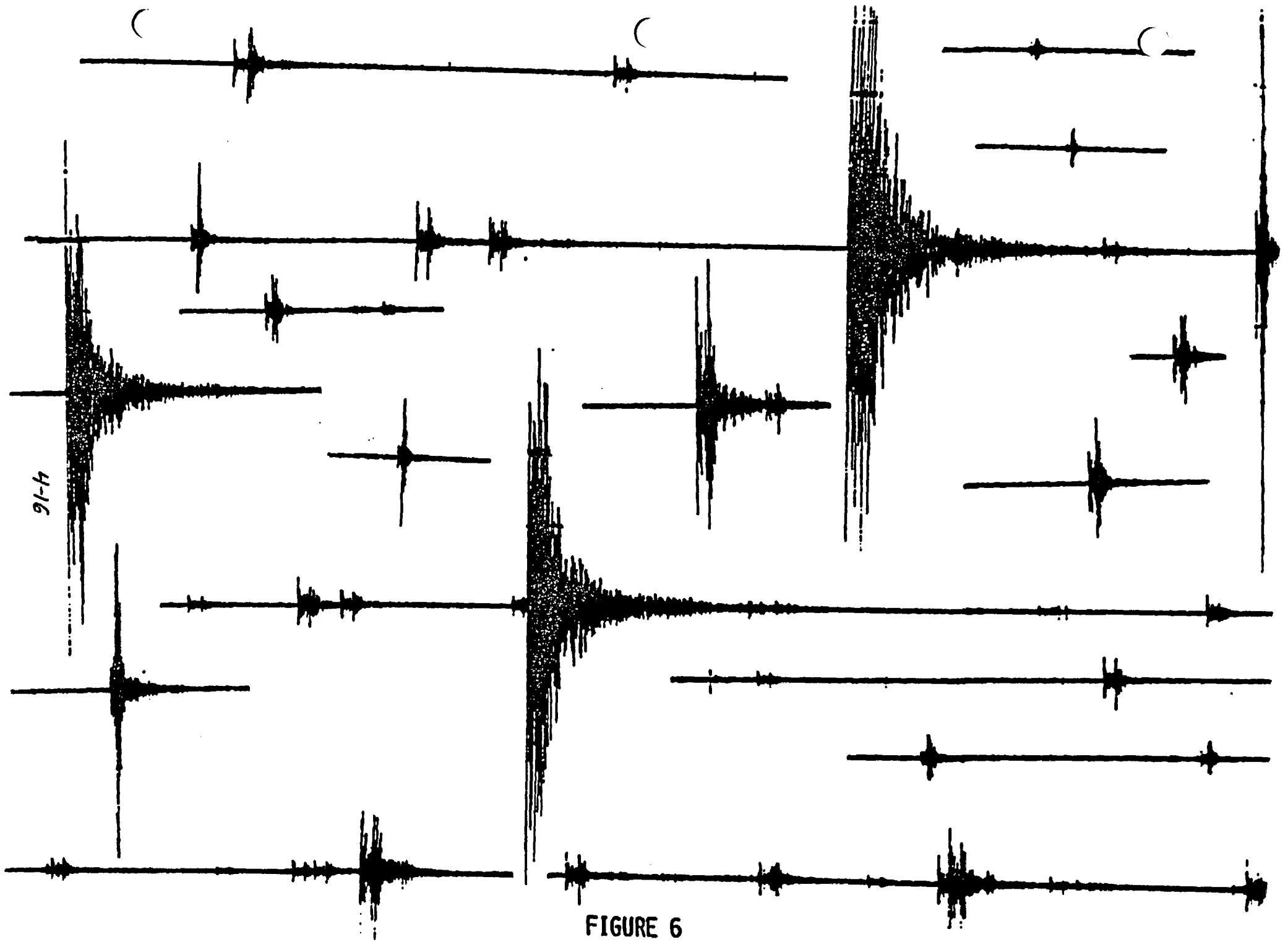


FIGURE 6

±1-h

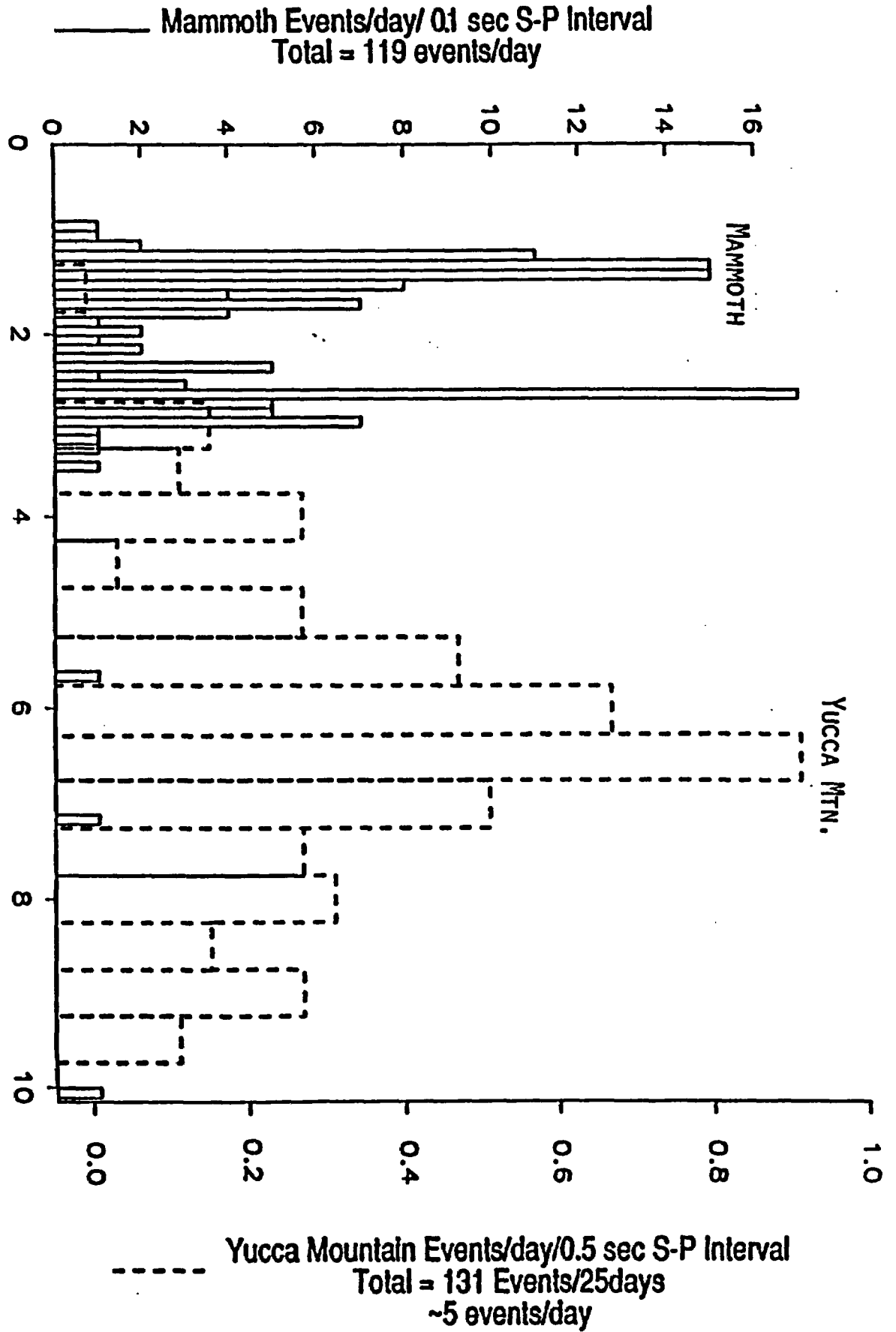


FIGURE 7

Magnitude Calibration of Yucca Mtn. Microearthquake Array

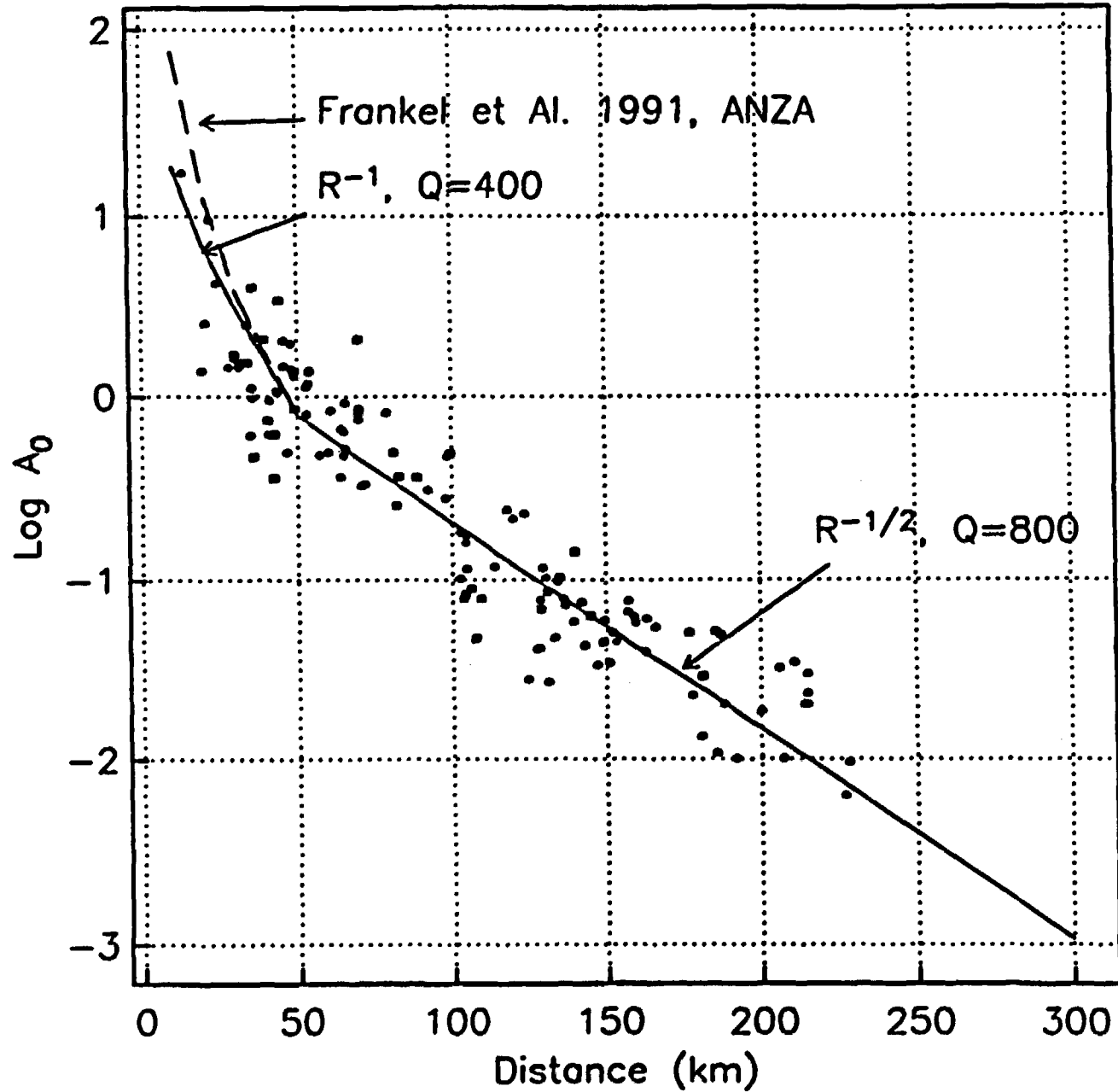


FIGURE 8

4-18

APPENDIX A

Real-Time Analogue and Digital Data Acquisition through CUSP

*William A. Peppin **

*Seismological Laboratory, MS 168

University of Nevada

Reno, NV 89557 Sept 1991

Abstract

The University of Nevada Seismological Laboratory operates an array of 60 analogue short-period and 10 three-component digital telemetered seismic stations, 90 data traces in all, in Nevada and eastern California. Formerly, the seismic data streams were recorded and processed on three separate computers running disparate software and writing incompatible data formats which made access to the digital data quite cumbersome. These systems were recently replaced by a single computer system, a Microvax II running VAX/VMS, together with *Generic CUSP* (Caltech -U.S.G.S. Seismic Processing System), a controlled software system from the U.S.G.S. in Menlo Park. Telemetered digital data is stored simultaneously in two ways, unique to this network. First, the data is brought asynchronously into the computer using a standard direct-memory access interface and recorded continuously on an Exabyte 8-mm helical-scan tapedrive. Second, the data is passed through a D to A converter and intermixed with the incoming analogue data stream used for routine network processing. In this way, calibrated digital waveforms are available in the routine data processing stream used to locate earthquakes. At the same time, this allows easy access to this data in research applications involving the processing of seismic waveforms.

Introduction

The University of Nevada, Reno (UNR) operates a seismic network covering western Nevada and eastern California (Figure 1). This network has been funded almost entirely by federal grants and contracts directed at addressing specific scientific problems involved with

the seismicity in this active region. The Defense Advanced Research Projects Agency has funded recording of Nevada Test Site explosions for basic studies of the seismic source of nuclear explosions and for regional studies aimed at improved understanding of regional waveform propagation, crustal structure, and attenuation. The U.S. Geological Survey has funded operation of this network for almost two decades under a variety of auspices, most recently the National Earthquake Hazards Reduction Program, whose recent emphasis has been the intense earthquake sequence at Mammoth Lakes - Bishop which has been underway since October of 1978 and continues to this writing. The Department of Energy has funded work aimed at delineating shallow-crustal magma bodies in the western Great Basin, especially near Mammoth Lakes. The Nevada Nuclear Waste Project Office has recently funded a major systems upgrade in connection with the Yucca Mountain site characterization study in progress by the Department of Energy. This paper discusses some unique aspects of this system upgrade, which may be of interest to other network operators.

UNR has been acquiring seismic data and recording it via digital computers since 1981. In 1981, using support from the Air Force Office of Scientific Research, an array of three 3-component digital stations was installed in Nevada. The data from this system were brought into the Lab via telephone lines and radio links and recorded on a PDP 11/23 computer running RT-11. Digital recording of the standard telemetered analogue network commenced in May of 1984, replacing the analogue recording system that had been in place since the late 1960s. Starting at this time the recording system was the U.S.G.S. - sponsored on-line, off-line processor system. The "on-line" processor, a PDP 11/34 running RSX-11M, was dedicated to event detection; software for this system was written by Carl Johnson at Caltech. Incoming analogue signals were digitized and presented to a memory buffer. A triggering algorithm, based on the ratio of short-term to long-term signal averages, was run over this memory buffer to decide if an earthquake had occurred. If the occurrence of an earthquake was declared, then the memory buffer, with pre-trigger information stored, was written to a magnetic tape. Thus, the new network system became an event-triggered digital system rather

than a system in which all of the incoming data were recorded in analogue form. Analysis of the seismic data was accomplished on the "off-line" processor, a PDP 11/70 running Berkeley UNIX. Tapes written by the 11/34 were read on the 11/70, demultiplexed, and phase timing and locations were accomplished interactively on a storage tube terminal (Tektronix 4014) using the interactive PING and PONG programs, developed at the University of Washington by Steve Malone and Don Leaver, for timing and event locations. The system of three computers was replaced in 1989 by a single computer, a Microvax II running VAX/VMS and using the *Generic CUSP* software developed by the U.S. Geological Survey at Caltech and at Menlo Park (principal authors Carl Johnson, Robert Dollar, and Peter Johnson). A seismic Bulletin covering the entire operation of this first-generation system through 1989 is nearing completion (Peppin and others, 1991); bulletins covering seismic observations on the UNR network extend back to 1969.

One major change in the UNR network since 1984 is that, through the efforts of UNR technical staff (especially Walter F. Nicks), the entire seismic data stream is brought to Reno via microwave linkups, thus eliminating the great yearly cost of bringing in signals by telephone lines. In addition, the development of this technology at UNR (e.g., using home-built microwave equipment) gives us the ability to deploy seismometers almost anywhere in Nevada and bring in signals via microwave, thus providing the possibility to cover aftershock sequences using *CUSP* directly. Recently, we deployed an array of four high-gain stations near Yucca Mountain which are brought into Reno using UNR-built microwave equipment. This is recorded by *CUSP* and on a continuously-recording analogue stripchart recorder used to scan for microearthquakes.

The Microvax - CUSP System

The *CUSP* processing system (Johnson, 1983; Dollar and Johnson, 1988; Lee and Stewart, 1989) offered several advantages to us at UNR which dictated its selection from among the several choices available. First, *CUSP* has had very extensive field testing, as it has been involved in routine data collection at two of the largest seismic data acquisition sites,

the California Institute of Technology in Pasadena and the U.S. Geological Survey in Menlo Park. Newer systems based on either PCs or UNIX-based processors take advantage of newer hardware technology, but do not have the extensive history of shakedown behind the CUSP software. Second, because of our long association with the U.S.G.S., we felt that it was wise to adopt a new network data recording strategy consistent with their operation, so that we could obtain support of systems operations from them, and so that our areas of overlapping interest and networks (e.g., the Long Valley caldera region) would be recorded in a compatible fashion.. This section describes general features of CUSP which pertain to the UNR seismic network.

The CUSP system was originally developed on Digital Equipment Corporation (DEC) computers of the PDP 11 family in 1983, and then later migrated to Vax and Microvax computers. *Generic CUSP* is a body of software which is controlled in the way that commercial software packages are controlled. When CUSP is modified, the various CUSP installations receive a copy of a directory structure containing this software. The update is accomplished simply by copying this distribution to the disc and discarding the older directory tree (once testing of the new software is complete). In this way, CUSP sites are freed from the responsibility of supporting the code, which occupies some 25 Mbytes and which contains a wealth of extremely useful software, not only to support the main purposes of CUSP, but which can give excellent support to research projects as well. A manual (Wald and Jones, 1989) provides an excellent guide for researchers interested in making use of CUSP data. An extensive on-line help facility is also provided.

The main purpose of CUSP, and the reason for its development, derives from the general task of acquiring seismic data from remote field sites. Originally, this exclusively entailed acquisition of analogue signals from outstations, usually transmitted by FM radio or microwave, to a common recording site. At this central site, these signals were recorded on either an analogue or a digital medium, which were later scanned for events of interest. With the onset of digital recording, only selected time segments were recorded digitally (discrete

event recording), with the entire frequency-modulated analogue data stream recorded continuously on analogue magnetic tape.

"Selected time segments" was a demanding requirement in the days when discs could only hold a few tens of Mbytes, and continues to be a problem today: in large networks such as ours, it is not yet practical to retain the entire incoming data stream (Gbytes/day). Streaming and/or helical scan tape and CD technology have made this choice a possibility, but for routine network analysis it continues to be cost effective to use discrete event recording. CUSP, as with most other comparable systems, is an event-detection system. The CUSP package consists of several programs which run concurrently. One of the programs (CORE) maintains a circular first in - first out buffer of the incoming data stream in memory. Another program SCARAB writes disc files from computer memory when the event detection program SPIDER declares an event and marks a piece of the data stream to save. From this point the disc files are automatically demultiplexed and "thrashed" to eliminate noise traces. Data acquisition from the incoming analogue data stream still amounts to 75 Mbytes/day on a system where the open storage ranges between 150 and 300 Mbytes. Mass-storage management is an important design feature of CUSP, permitting quick reconfiguration of the destination of data being recorded by the system, e.g., during major aftershock sequences.

A problem with the traditional data collection scheme is that it takes no account of the fact that seismology has progressed to *digital* data acquisition, in which the incoming seismic data arrives not as an analogue signal, but as a pre-digitized bit stream; mixed-mode networks, in which both analogue and digital data streams arrive at the central site, are becoming common. Up until recently, this entirely different mode of data transmission has made it necessary to record such incoming data streams on a separate computer system, with the attendant problems and headaches of merging data and system incompatibility. In our case, digital data extraction from the day tapes written by the PDP 11/23 was very laborious, which discouraged abundant use of this excellent data set.

Resolution of this problem, that is, how to record the digital data in a way which would

allow relatively easy access to it, was a main goal of our recent transition from the former system to CUSP. The University of Nevada now records both the analogue network data stream and the asynchronous digital data stream on the same Microvax II system using two separate real-time CUSP processes, but in a configuration which is unique to CUSP sites at this writing as described below. Because CUSP was designed to be general and flexible, the recording of both data streams on a single computer required changing only one variable within the entire body of CUSP code. The UNR software contribution was the development of the program PICKEM to do interactive timing and location of earthquakes. This program is intended not only for use in routine analysis, and for upward compatibility with future CUSP software, but also to support research use of the CUSP data.

In addition to the routine acquisition and analysis of the analogue and digital network data, the CUSP system is used at UNR in an entirely different environment involving laboratory measurements of motions in a foam rubber model (J.N. Brune, Principal Investigator). The application here is to record accelerations from several tens of sensors located in a system of foam blocks which is operated to produce stick-slip motions. The frequencies involved reach the kHz range. Data are recorded from this experiment on a VAXstation/GPX running the third realtime CUSP process. Data streams of up to 50,000 samples/second are easily treated using this system, which involves home-built electronics to gather the data (up to 64 channels) and present it to the computer. From there all of the existing CUSP processing software applies. It was the work of a few hours to put up this system on the GPX, a tribute to the power and generality of the CUSP system in this completely different data acquisition environment.

Digital Data Acquisition Design Considerations

A number of considerations drove our move to the CUSP system. First, the existing system was near capacity and we were planning to add quite a few new data sources in connection with studies of southern Nevada: we are bringing in 20 data components from this region today. Second, our research applications called for the ability to acquire digital data taken at

higher sampling rates, as much as 200 samples per second (SPS). The existing digital system was limited to 50 SPS and a small number of data channels. Our solution to the digital data acquisition problem depended on the ability to record *asynchronous* digital data (i.e., data which arrive independently from different outstations) at a mixture of sampling rates, with a design capacity of 64 incoming three-component digital streams. Why asynchronous? Because two-way technology in so large an area as Nevada was prohibitively expensive; anything we designed would have to involve one-way communications from digital outstations with independent A to D converters, and therefore the data would necessarily be asynchronous. Why mixed sampling rates? Research requirements at the University of Nevada involve studies both of teleseismic data (where the lower sampling rate is adequate) and special studies of the seismic source similar to the work being carried out at the ANZA network (Berger and others, 1984), and proposed by us for analysis of Mammoth Lakes, California seismic data using deep-hole instrumentation. Therefore, the mix of incoming sampling rates could reasonably be expected to range between 1 and 200 samples/second, and we wanted to record all of this on the same system.

One consideration is the combined total data capacity of the two incoming data streams (the analogue short-period data and the continuous digital data). At UNR, the combined rate from the two data streams (90 analogue channels and 30 digital channels) is under 50,000 samples/second, well within the design specifications of realtime CUSP even on the relatively slow Microvax II hardware. In addition, the same computer is used as the boot node for a Microvax cluster with three VAXstation 2000 workstations used for the off-line processing of network data. Therefore, it can be seen that the real-time part of CUSP is quite efficient, as the Microvax II is relatively slow compared to processors now being sold by the computer vendors including DEC.

Digital Data Acquisition

First Process: Direct and Continuous Digital Recording

Our solution to the problem of digital data acquisition is as follows; see Figure 2. The digital data are brought into the computer using exactly the same technology as used for the analogue system at all CUSP installations: the hardware interface is the Q-Bus parallel controller (the DRV11-W) and the software used to acquire the data is standard realtime CUSP. Exactly as with the analogue data, a second CORE process runs and acquires data, and a second SCARAB process writes the data to the disc in 30-minute records (6 Mbytes each today, with 10 three-component digital outstations). The CUSP process POUNCE is used to mark the data in overlapping segments, so that all of the incoming data is staged to disc. Finally, every two hours a process restarts which writes these disc files to an Exabyte streaming tape drive which can hold five days of continuous data at the present rate. If desired, the data can be written to a 9-track magnetic tape rather than the Exabyte, with a capacity of about 10 hours. The Exabyte tape, a VMS COPY tape, can be read either on the Microvax system or can be read directly on a SUN workstation, making this data accessible either to VMS or UNIX users with equal ease. Demultiplexing software, written in C by George Randall of the Seismological Laboratory, is available on the UNIX/SUN system. These data can also easily be brought back from the SUN to the Microvax network via TCP/IP software.

The hardware used to bring the digital data to Reno over microwave, a digital data assembler, and a digital-to-analogue (D to A) converter, were built by Walter F. Nicks of the Seismological Laboratory. The resulting designs are reliable and modular. This hardware is the only part of the system which is not commercially available; however, board layouts and other documentation are available.

Second Process: Digital Data Within the Analogue Data Stream

A frustration faced in our former data-logging system was that, because the analogue data come from uncalibrated systems, it was not possible to use this data for applications requiring estimation of ground motion; rather, this information had to come from the digital data being recorded in an entirely different format. Our aim was to permit easy access to the calibrated digital data during standard network processing of the analogue data. This was

accomplished as follows.

The incoming digital data stream is split (Figure 2); it is recorded continuously on Exabyte tape as described above, and it is also passed through a 16-bit digital to analogue converter, built by Walter F. Nicks of UNR. The resulting analogue data stream is intermixed with the other incoming analogue signals, all of which are resampled at 100 SPS on a Tustin Industries A/D converter: thus, both the digital and analogue station data are available for routine analysis through CUSP (Figures 2 and 3). Programs are now available to make use of this high-quality information for the posting of seismometric analyses in the standard event-locations data base.

Figure 3 shows a presentation of traces as seen by a network analyst doing routine timing and processing of an earthquake. The bottom five traces, each from analogue stations, are clipped. The top three traces, unclipped, come from the redigitized digital outstations. It is expected that during incorporation of the digital data with the network traces (Figure 3), redigitization causes a certain amount of distortion. To assess how much, consider a comparison of spectra on a regional seismogram computed in two ways, first, from the unaltered incoming digital data recorded on the Exabyte, and second, from the redigitized data which enters the analogue data set. The signal is above the noise from 0.05 to 25 Hz. Figure 4 compares the percent difference between the amplitude and phase spectrum for this wideband signal. Over the whole band the amplitudes agree to 1 percent for all but frequencies quite close to the Nyquist frequency (15 - 25 Hz), and for those the largest percent differences occur for spectral values which are quite small. The phase spectral differences have occasional spikes caused by phase wraparound. This shows that the redigitized data can be used interchangeably with the Exabyte data for applications in which some distortion can be tolerated.

Conclusions

The generality of generic CUSP has permitted the University of Nevada, Reno to undertake recording of both analogue and digital data. This includes combining digital data with

the analogue for immediate access during routine analysis, and recording continuous digital data on high capacity tapes. All of this is performed on a single commercially-supported computer environment involving Microvax computers and workstations sold by Digital Equipment Corporation. This recording configuration is unique among CUSP sites, and permits research applications with easy access to this excellent and valuable data set.

Acknowledgments. This work was supported by U.S.G.S. Contract 14-08-0001-G1524 and by the Nevada Nuclear Waste Project Office through the University of Nevada Center for Neotectonic Studies. Walter F. Nicks designed and built special-purpose hardware components for the UNR - CUSP system. John Anderson and Peggy Johnson provided critical reviews of the manuscript. **Disclaimer:** computer hardware is named in this article for identification purposes only, and constitutes no endorsement by UNR or the U.S.G.S of this equipment.

References Cited

- Berger, J., L.M. Baker, J.N. Brune, J.B. Fletcher, T.C. Hanks, and F.L. Vernon, 1984. The Anza array: a high-dynamic-range, broadband digitally radio-telemetered seismic array, *Bull. Seism. Soc. Am.*, **74**, 1469 - 1481.
- Dollar, R.S. and P.J. Johnson, 1988. The Parkfield digital seismic experiment: realtime high frequency data acquisition and analysis system, *Seis. Res. Letters*, **59**, 22.
- Johnson, C.E., 1983. CUSP - automated processing and management for large, regional seismic networks, *Earthquake Notes, Seismological Soc. Am. Eastern Section*, **54**, 13.
- Lee, W.H.K. and Stewart, S.W., 1989. Large-Scale Processing and Analysis of Digital Waveform Data from the USGS Central California Microearthquake Network in *Observational Seismology*, J. J. Litehiser, ed, University of California Press, 86 - 98.
- Peppin and others, 1990. Bulletin of the Seismological Laboratory for the Period May 1984 to December 1989, Mackay School of Mines, University of Nevada, Reno, in preparation.

Wald, Lisa A. and Lucile M. Jones, 1989. LEAPing Into CUSP: Local Earthquake Analysis Programs for CUSP Data, *U.S.G.S. Open-File Report 89-479*.

Figure Captions

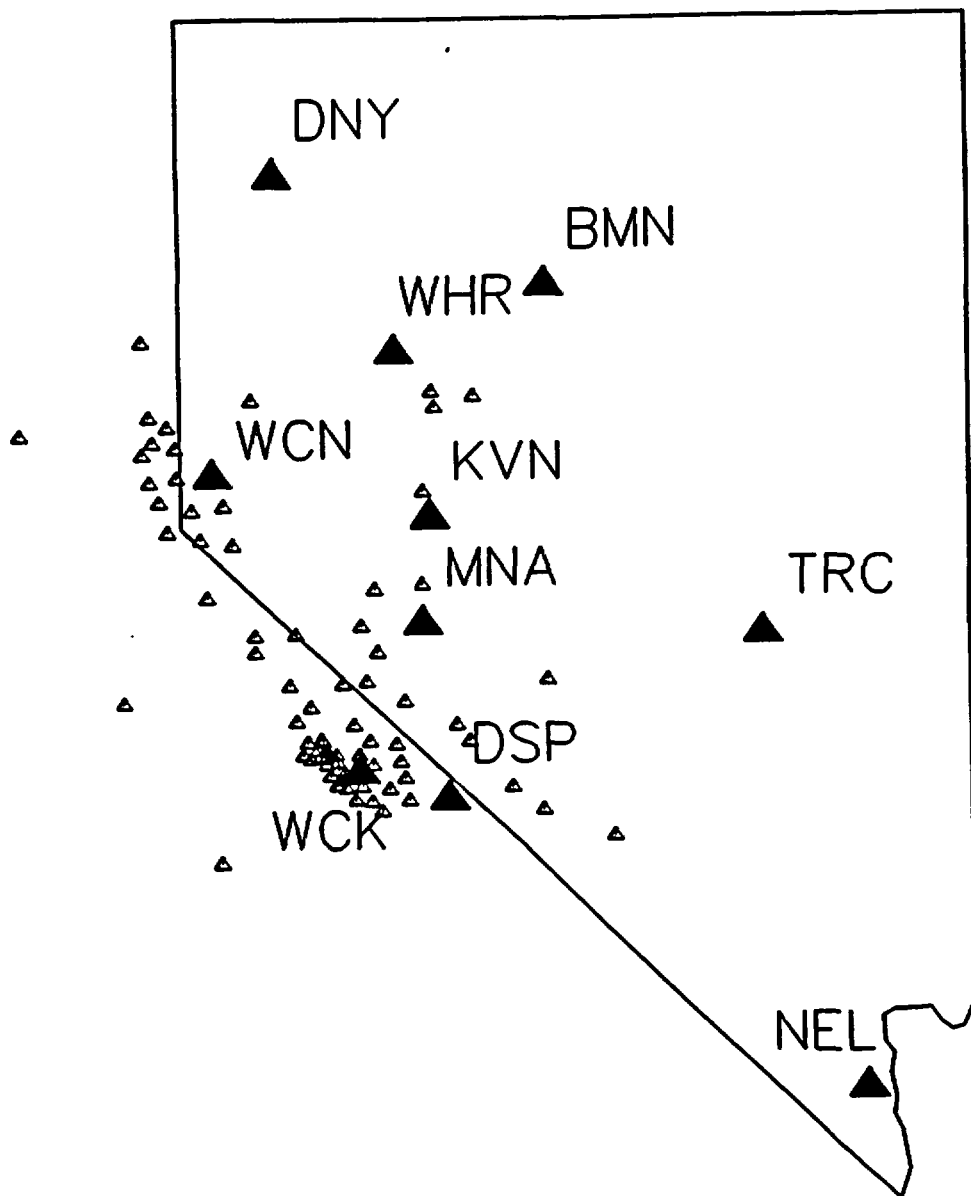
Figure 1. Seismic stations presently being recorded by the University of Nevada Seismological Laboratory, with the three-component digitals as solid triangles.

Figure 2. Block diagram showing the way in which incoming data streams (analogue left, digital right) are recorded on the Microvax II computer, enclosed by the dashed box. Other than the two elements at the upper right, all this equipment is available commercially.

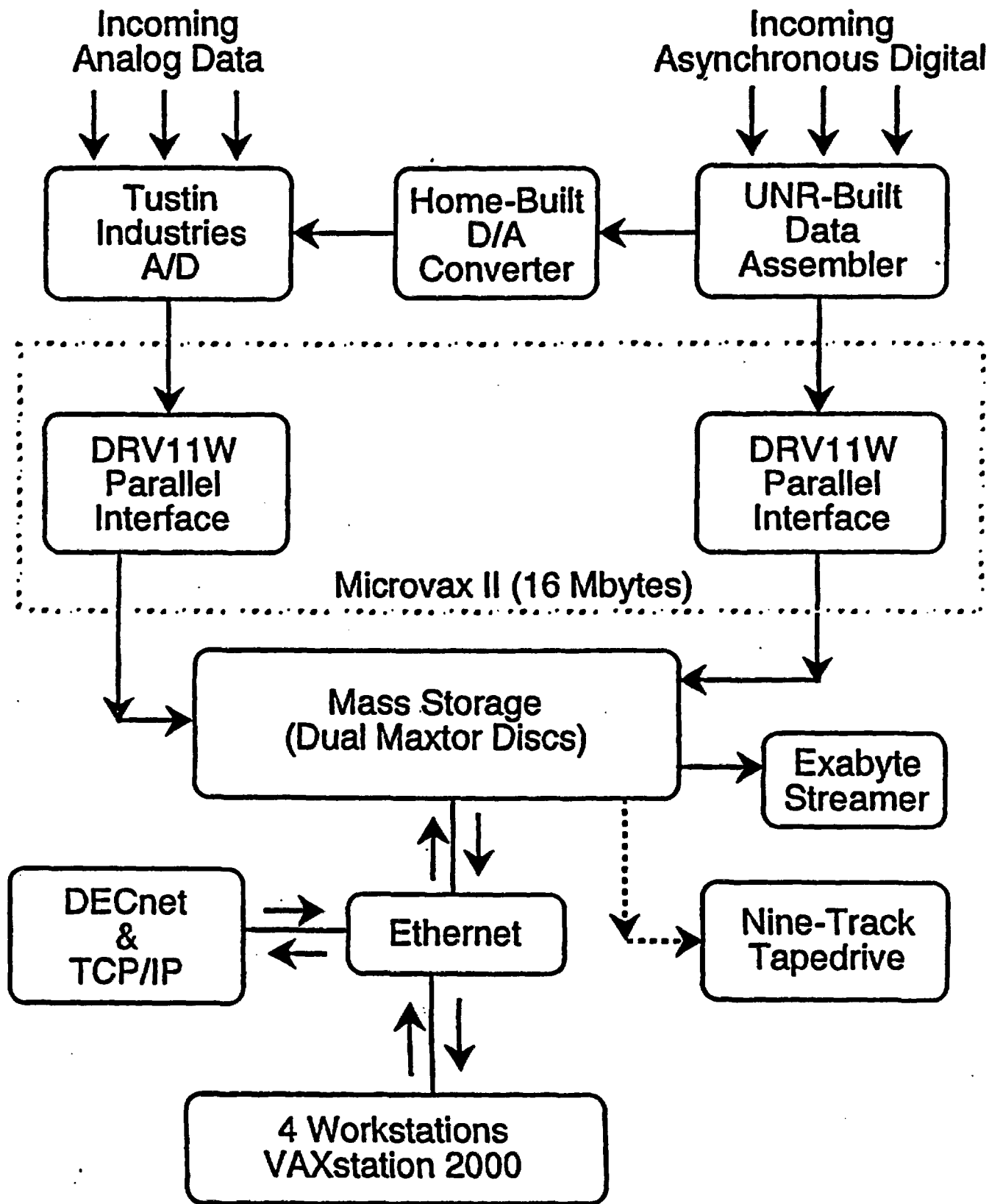
Figure 3. This image shows what an analyst sees when timing earthquakes within the routine data processing stream using the UNR program PICKEM. Eight traces at a time are available for random selection (below); one of these is selected and can be expanded, moved, filtered, and timed in the upper picking window (topmost, largest trace labeled WCKRZ; the vertical line indicates the selected P onset. Top three of the eight traces: three-component data from the broad-band WCK. Lower five traces: signals from analogue stations. Note that these five are clipped, while the digitals are on scale except for minor clipping of the north component (third trace, maximum amplitude 32,767 digital counts). Data shown are for a local earthquake of magnitude 2.5, 26 February 1989 at 1548 GCT

Figure 4. Comparison of wideband spectrum for a regional seismogram recorded at BMN for the Luning earthquake of 24 March 1990 at 08:16 GCT, $M = 4.5$, as recorded directly on the Exabyte and as recorded by CUSP after the redigitization process. The processed trace is shown on the *bottom*. Above the time trace is the spectrum of the entire Pg wave group (20 seconds), with the Exabyte and redigitized network data, overplotted, visually indistinguishable. The "noise" spectrum was obtained

by identical processing of the quiet section preceding the event onset. The *top two* traces show the amplitude and phase differences in percent between the spectra of the Exabyte series and the redigitized series. Amplitude discrepancies are below 1 percent except for isolated frequencies where the signal to noise ratio is low; phase discrepancies are also mostly below 1 percent, with the spikes being caused by phase wrap-around.

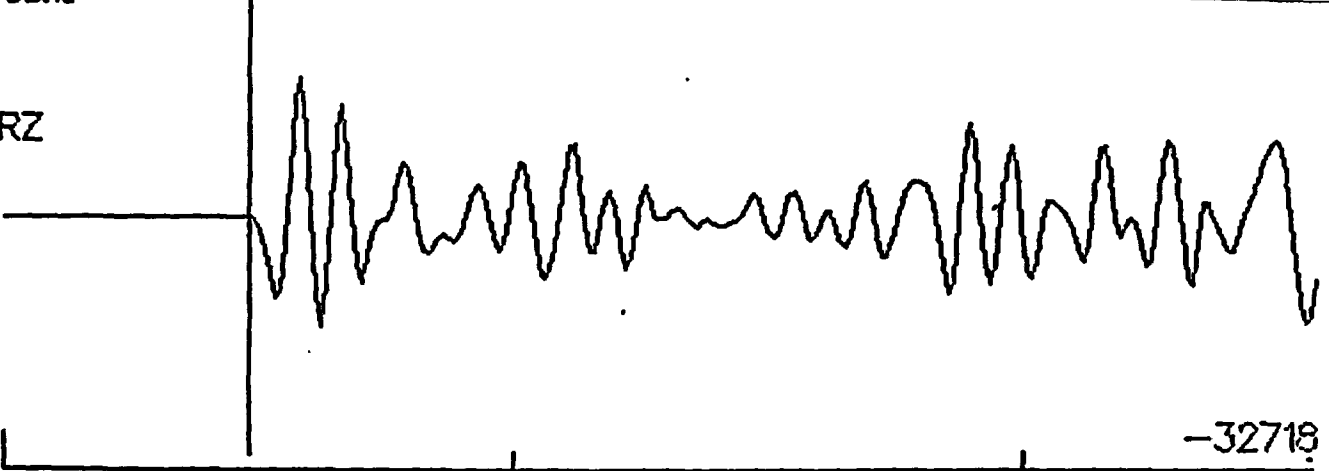


0 125 Km



IFW 02.10
S

WCKRZ



-32718

1990 Feb 26 1548 45.06

ROOT\$DUAL:000000.LNR.90FEBX124308.GRM.1

32635.
WCKRZ
-32718.

32726.
WCKRE
-32727.

32741.
WCKRN
-32768.

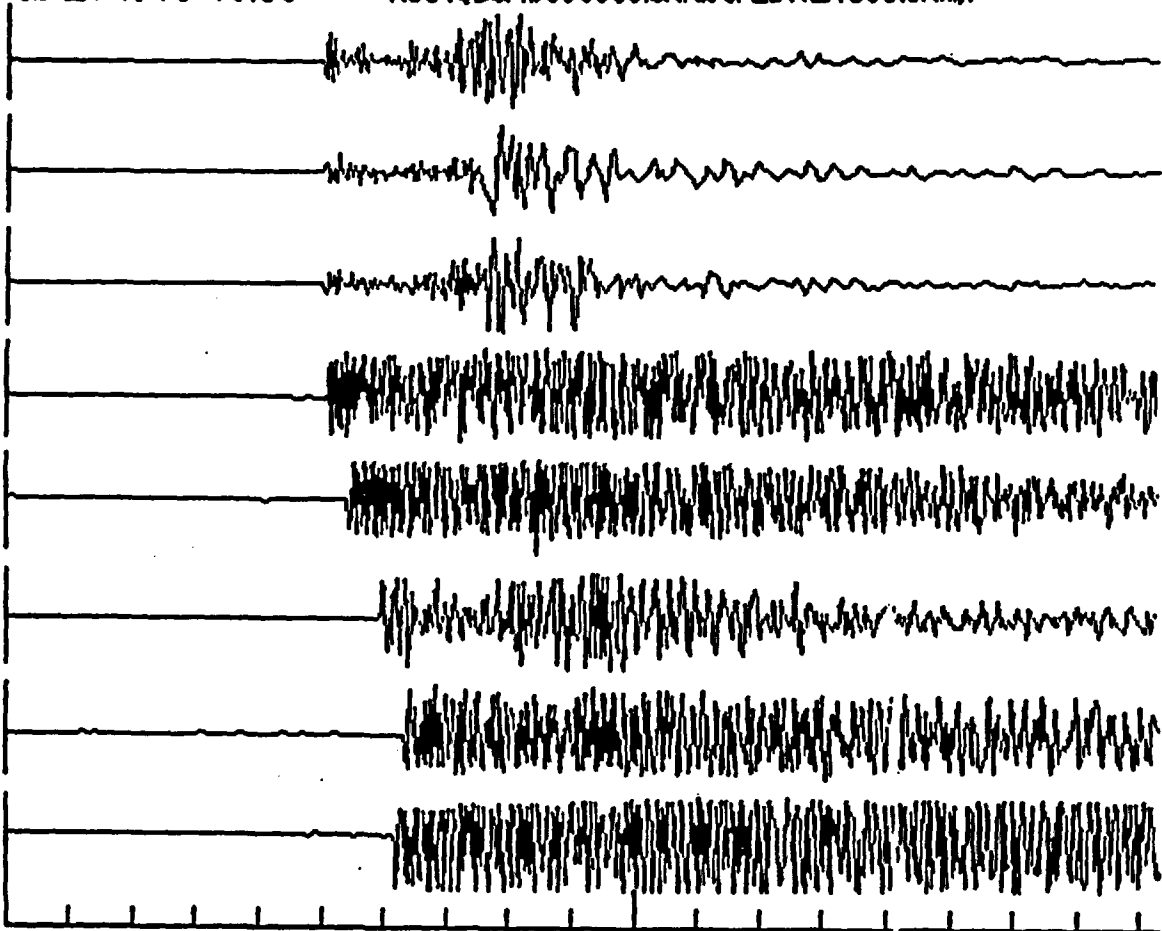
9055.
RSMZ
-8701

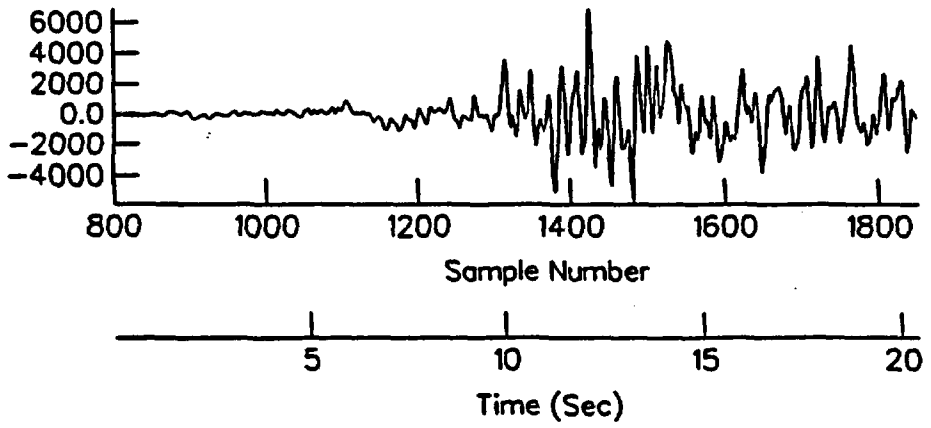
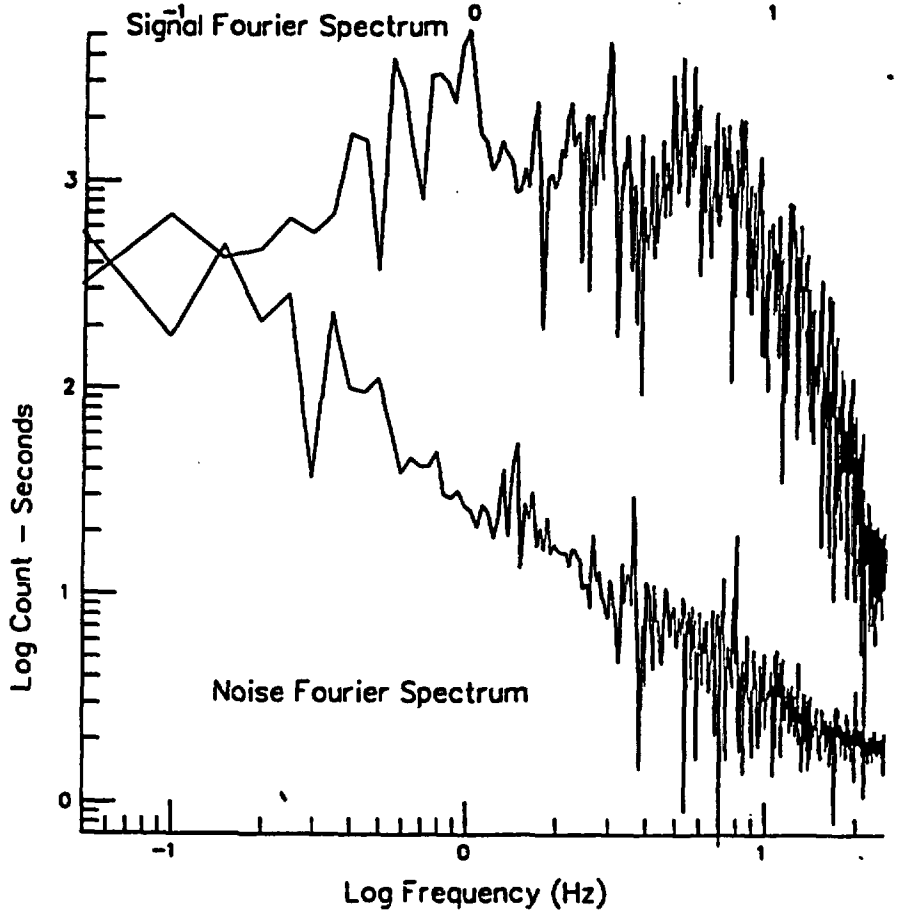
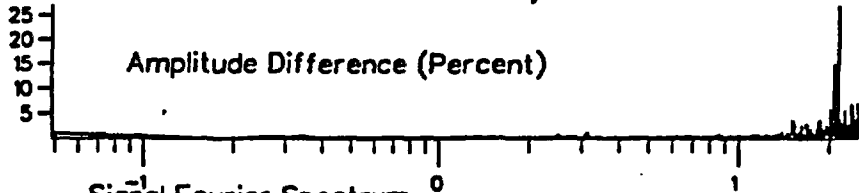
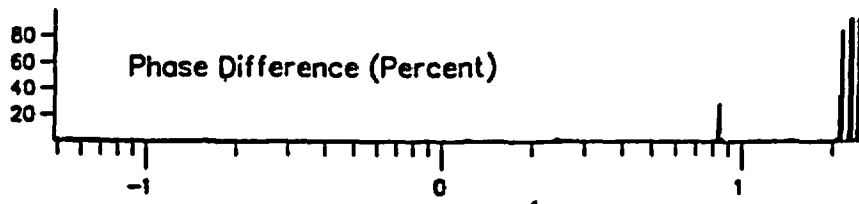
10737.
LKMZ
-13350.

12495.
TUNMZ
-13507.

5193.
DOEMZ
-4135.

10341.
ORCRZ
-13650.





PROGRESS REPORT--OCTOBER 1, 1990 TO SEPTEMBER 30, 1991

TASK 5 Tectonic and Neotectonic framework of the Yucca Mountain Region

Personnel

Principal Investigator: Richard A. Schweickert

Research Associate: Mary M. Lahren July 1, 1991 to September 30, 1991

Graduate Research Assistants:

- a. Caskey, S. J.--October, 1990-July, 1991
- b. Elwood, R.--October, 1990-January, 1991
- c. Donovan, D.--October, 1990; March-April, 1991
- d. Hoffard, J.--October, 1990; January-February, 1991
- e. Zhang, Y.--October, 1990-July, 1991

Funding levels during 1990-1991 were insufficient to provide adequate support to all GRA's and allowed only a minimal amount of fieldwork. Several of the accomplishments below were made by GRA's with only partial funding from this project.

Part I. Highlights of major research accomplishments

- a. Completion of M.S. theses of S. J. Caskey, D. Donovan, and J. Hoffard
- b. Final revision of manuscript submitted to GSA Bulletin on Mesozoic thrust belt by S.J. Caskey and R. A. Schweickert
- c. Publication of two abstracts based upon research funded under Task 5: Elwood (1991), and Zhang and Schweickert (1991).
- d. Publication of an article on extensional faulting by M.A. Ellis (Nature, v. 348, p. 689-693) (Ellis's work was supported in 1989-1990 by Task 5).
- e. Completion of mapping of late Quaternary to Holocene(?) strike-slip and normal faults in southern Amargosa Valley and Stewart-Pahrump Valleys (DD and JH).
- f. Completion of detailed structural mapping of Paleozoic and

- Cenozoic deposits in CP Hills, Nevada Test Site (SJC).
- g. Completion of regional cross-section from Eleana Range to Sheep Range (SJC)
 - h. Recognition of significance of pre-Middle Miocene normal and strike-slip faulting at Bare Mountain (YZ)
 - i. Completion of mapping and stratigraphic analysis of Miocene ash flow tuffs along western part of Pahranaगत shear zone (RE).
 - j. Paleomagnetic sampling of Paleozoic and Cenozoic units at Bare Mountain and Jurassic granitic rocks at Slate Ridge (RS, in conjunction with Y. Zhang, S. Gillette, and R. Karlin).

Part II. Research projects

This section highlights the research projects conducted by Task 5 personnel.

1. *Tectonics and Neotectonics of the Pahranaगत shear zone, Lincoln County, Nevada;* R. Elwood (T. Reynolds, formerly supported here, has left UNR but still plans to complete his study).

The rationale for this study has been that the Pahranaगत shear zone lies on trend with the Spotted Range - Mine Mountain structural zone, which is composed of seismically active, ENE - striking, sinistral faults, and which lies immediately south of Yucca Mountain. Studies of the Pahranaगत shear zone have been undertaken to evaluate whether the two zones are parts of a related zone of crustal weakness that may be active.

In addition, the Pahranaगत shear zone shows clear evidence that shortening occurs within the Basin and Range province. Such shortening may be manifest as thrust earthquakes and (or) as shortening through aseismic folding. Elwood's part of this project was completed in 1991, and her thesis report is in progress.

2. *Structure and geometry of the Mine Mountain and CP Hills thrust complex, NTS, Nye County, Nevada;* S. J. Caskey.

The rationale for this study has been to develop an understanding of kinematics and geometry of Mesozoic thrusts east of Yucca Mountain to

enable more confident modeling of the deep structural geometry of pre-Tertiary units beneath Yucca Mountain and correlation of deep structures through the region. In addition, this study has placed better constraints on the magnitude and direction of extension in the southern Great Basin. A by-product of this study is a better understanding of pre-, syn, and post-volcanic normal faulting in the Yucca Mountain region. This project was completed in 1991.

3. *Active tectonics of the central and northwest parts of Pahrump and Stewart Valleys, Nevada and California.* J. Hoffard.

Pahrump and Stewart Valleys are host to the strike-slip Pahrump Valley fault system, considered to represent the youngest tectonic feature to the south of the Yucca Mountain area. This NW-trending fault system is at least 60 km in length and is composed of three important fault zones that cut deposits of late Quaternary to Holocene age. Most evidence suggests the zone has been characterized by dextral strike-slip displacements. The Pahrump Valley fault system trends northward into the southern Amargosa Valley near Ash Meadows. This project was completed in 1991.

4. *Active tectonics of the eastern half of the Death Valley 2-degree sheet, with emphasis on the southern half of Amargosa Valley;* D. Donovan.

This work has involved a detailed analysis of low-sun angle photography and other images to develop a compilation of all Quaternary and active faults. The project concentrated on southern Amargosa Valley, which is the location of multiple short, variably oriented fault scarps. These have been investigated in the field and several trenches have also been excavated and logged. The results suggest that several Quaternary fault systems extend northward from Stewart Valley and the Resting Spring Range into southern Amargosa Valley. One or more of these may be kinematically linked to the Pahrump fault system and may have dextral strike-slip displacement. One northeast-trending fault zone may be the SW continuation of the Rock Valley fault of the southern NTS area. This project was completed in 1991.

5. *Regional overview of structure and geometry of Mesozoic thrust*

faults and folds in the area around Yucca Mountain; R. A. Schweickert.

Together with 2 above, this study aims to provide information about the deep geometry of Paleozoic units and their bounding faults, which is necessary both for understanding of Tertiary faults and for the correct formulation of regional hydrologic models. It has also provided evidence for a previously unknown strike-slip fault beneath Crater Flat, and for the existence of major pre-Middle Miocene extension in the NTS region.

6. Kinematic analysis of low and high angle normal faults in the Bare Mountain area, and comparison of structures with the Grapevine Mountains Y. Zhang.

The purpose of this study is to determine the timing and slip directions of high and low-angle normal faults exposed at Bare Mountain, which is a direct analogue of the deep structure beneath Yucca Mountain. This will provide better constraints on the displacement histories of the faults. In addition, metamorphic fabrics will be characterized in the deeper northern parts of the mountain and traced to the lower grade, shallower part of the mountain. Finally, the development of these structures will be compared with possible analogues in the Grapevine Mountains and the CP Hills to develop firm constraints on the deep structure beneath the Yucca Mountain area.

7. Evaluation of pre-Middle Miocene structure of Grapevine Mountains and its relation to Bare Mountain. R. Schweickert and M.M. Lahren

This project is intended to establish the Mesozoic and Cenozoic structural geometry and timing of deformation in the Grapevine Mountains, which presumably developed in close proximity to the Bullfrog Hills and Bare Mountain prior to post-10 Ma displacement on the Bullfrog Hills-Boundary Canyon detachment fault. This will lead to a deeper understanding of the significance of pre-Middle Miocene and possibly pre-Tertiary extension and detachment faulting on crustal structure in the area between the NTS and Death Valley.

8. Evaluation of paleomagnetic character of Tertiary and pre-

Tertiary units in the Yucca Mountain region, as tests of the Crater Flat shear zone hypothesis and the concept of oroclinal bending. S. Gillett, R. Karlin, Y. Zhang, and R. A. Schweickert.

Paleomagnetic data from various volcanic units at Yucca Mountain show that up to 30° of progressive north-to-south clockwise rotation has occurred since mid-Miocene. These studies are geographically relatively limited; one of the goals of this study is to expand the data base to various Paleozoic and Mesozoic units to understand the regional variations of magnitude and timing of rotations. In addition, since the timing of rotation is poorly known, this study will expand the data base through the Tertiary section as far as possible.

Part III.

Brief summaries of research results

This section presents a summary of progress to date. Because these projects are long-term and field-intensive, the results are still preliminary, and should not be quoted without permission. Many of our interpretations are speculative. Low budget levels have hampered our research efforts.

1. *Structure and geometry of the Mine Mountain and CP Hills thrust complex, NTS, Nye County, Nevada;* S. J. Caskey. (see attached abstract from Caskey's thesis).
2. *Tectonics and neotectonics of the Pahrnagat shear zone, Lincoln County, Nevada.* (see attached abstract published in 1991).
3. *Quaternary fault patterns and basin history of Pahrump and Stewart Valleys, Nevada and California.* (See attached abstract from Hoffard's thesis)
4. *Active tectonics of the eastern half of the Death Valley 2-degree sheet, with emphasis on the southern half of Amargosa Valley.* (See attached abstract from Donovan's thesis).
5. *Regional overview of structure and geometry of Mesozoic thrust faults and folds in the area around Yucca Mountain.* R. A. Schweickert.

(See abstract of manuscript by Caskey and Schweickert).

6. *Kinematic analysis of low and high angle normal faults in the Bare Mountain area, and comparison of structures with the Grapevine Mountains* Y. Zhang. (see attached abstract by Zhang and Schweickert).

7. *Evaluation of pre-Middle Miocene structure of Grapevine Mountains and its relation to Bare Mountain.* R. Schweickert and M.M. Lahren.

Limited field work and map-scale structural analysis has confirmed that the Oligocene Titus Canyon Formation unconformably overlaps a major detachment fault system related to the Titus Canyon fault (as mapped by Reynolds (1969)). This detachment fault excises the upright limb of a major Mesozoic recumbent fold, the Titus Canyon anticline, and has a structural relation similar to that of the Wildcat Peak normal fault at the southern end of Bare Mountain, which excises the upright limb of a large recumbent anticline in the hangingwall of the Panama thrust (as mapped by Monsen and others (1990)). The Titus Canyon fault is undated, and could even be of Late Cretaceous age. Our working hypothesis is that the Late Miocene Fluorspar Canyon-Bullfrog-Boundary Canyon detachment system pulled apart and exposed elements of a much older detachment system, which includes the Titus Canyon fault, the lower detachment in the Bullfrog Hills, and the Conejo Canyon and Wildcat Peak faults at Bare Mountain. We suspect that this older detachment system was largely responsible for the exhumation of deep metamorphic rocks at northern Bare Mountain, Bullfrog Hills, and the Funeral Mountains, and that these metamorphic rocks were already exposed at high structural levels when ash flow tuffs of the Southwest Nevada Volcanic Field were erupted.

8. *Evaluation of paleomagnetic character of Tertiary and pre-Tertiary units in the Yucca Mountain region, as tests of the Crater Flat shear zone hypothesis and the concept of oroclinal bending.* S. Gillett, R. Karlin, Y. Zhang, and R. A. Schweickert.

In January, 1991, paleomagnetic sampling of the following units was completed: Lower Cambrian Carrara Formation at Carrara Canyon and Gold Ace Canyon at Bare Mountain, and in Striped Hills; Devonian rocks of Tarantula Canyon in Tarantula Canyon, at north end of Bare Mountain; 14 Ma dacite dikes at Tarantula Canyon; Middle Jurassic Sylvania pluton at

Slate Ridge. These units were sampled to determine whether Paleozoic units in the Bare Mountain area show large clockwise rotation, as suggested by the oroclinal bending hypothesis, and to test whether any rotations in these rocks are matched by rotations of Miocene dikes in Bare Mountain. The Jurassic plutonic rocks will be tested to see whether possible oroclinal bending affected units at the north end of Sarcobatus Flat.

Part IV. Other activities of Task 5 personnel

1. Technical review of reports for the Center

None formally assigned;
reviewed new publications by Maldonado (1990), Wernicke (1990), and Carr (1991)

2. Meetings attended in relation to the Center

- a. SOBART (Southern Basin and Range Transect) Meeting, Phoenix, Arizona, October 9-12, 1990; Schweickert served on Steering Committee, and acted as Coordinator of discussions on Tectonics of southern Basin and Range province; also attended by S.J. Caskey. Schweickert subsequently wrote parts of Science Plan.
- b. Lecture given by Schweickert on Tectonic evolution of Nevada Test Site, at Lawrence Livermore Laboratory, January, 1991
- c. Geological Society of America, Cordilleran Section, San Francisco, March 25-27, 1991 (attended by Schweickert, Elwood, and Zhang; see abstract by Elwood)

3. Field work

- a. Structural mapping and paleomagnetic sampling, January, 12-16, 1991--localities in Bare Mountain, Striped Hills, and Slate Ridge-Gold Mountain; fieldwork involved S. Gillette, R. Karlin, R. Schweickert, and Y. Zhang

- b. Structural mapping in Bare Mountain, Y. Zhang, January 5-14, 1991, and May 24- 30, 1991
- c. Geologic mapping in the CP Hills, S.J. Caskey--January 6-13, 1991

4. Professional reports provided to NWPO

- a. Donovan, D., 1991, Neotectonics of the southern Amargosa Desert, Nye County, Nevada and Inyo County, California, 151p.
- b. Sawyer, T.L., 1989, Quaternary geology and neotectonic activity along the Fish Lake Valley fault zone, Nevada and California, 379 p.
- c. Hoffard, J.L., 1991, Quaternary tectonics and basin history of Pahrump and Stewart Valleys, Nevada and California, 138p.
- d. Caskey, S.J., 1991, Mesozoic and Cenozoic structural geology of the CP Hills, Nevada Test Site, Nye County, Nevada; and regional implications, 153p.

5. Abstracts published

- a. Elwood, R., 1991, Structure of the western Pahranaagat shear system (abs.): Geol. Soc. America Abs. with Programs, v. 23, p. 22.
- b. Zhang, Y., and Schweickert, R.A., 1991, Structural analysis of Bare Mountain, southern Nevada (abs.): Geol. Soc. America Abs. with Programs, v. 24, p. 185.

6. Papers published in peer-review literature

- a. G. King and M. Ellis, 1991, The origin of large local uplift in extensional regions: Nature, v. 348, p. 689-693. (Ellis's role in this research was supported by Task 5).

7. Papers submitted for publication in peer-review literature

- a. Caskey, S.J., and Schweickert, R.A., Mesozoic thrusting in the Nevada Test Site and vicinity--a new perspective from the CP

Hills, Nye County, Nevada: Geol. Soc. America Bulletin, submitted, 3/91, in final revision, 12/91.

8. Graduate theses supported by NWPO and completed during 1990-91

- a. Hoffard, J.L., 1991, Quaternary tectonics and basin history of Pahrump and Stewart Valleys, Nevada and California: M.S. Thesis, University of Nevada, Reno, 138p.
- b. Donovan, D.E., 1991, Neotectonics of the southern Amargosa Desert, Nye County, Nevada and Inyo County, California: M.S. Thesis, University of Nevada, Reno, 151p.
- c. Caskey, S.J., 1991, Mesozoic and Cenozoic structural geology of the CP Hills, Nevada Test Site, Nye County, Nevada; and regional implications: M.S. Thesis, University of Nevada, Reno, 153p.

9. Other facets of research by Task 5

a. **Neotectonics:** We are almost in a position to compile an accurate Quaternary fault map covering the eastern half of the Death Valley 1 x 2° sheet, which includes the southern half of the NTS and Yucca Mountain, based upon new work of D. Donovan, M. Ellis, J. Hoffard, and P. Zhang, and published information. This work shows that Yucca Mountain lies within a broad, northerly trending zone of diffuse Quaternary faulting, part of which demonstrably shows dextral strike-slip displacements. Detailed studies of Quaternary deposits are now needed to provide quantitative constraints on overall rates of displacement throughout this zone.

b. **Tectonic framework of Yucca Mountain:** Structural studies that offer the best hope for modeling the subsurface structure at Yucca Mountain are well advanced; S.J. Caskey's study of the CP Hills is complete, and Y. Zhang's kinematic study of Bare Mountain has made good progress. Paleomagnetic sampling of key Tertiary and Paleozoic units has been completed at Bare Mountain, and laboratory measurements await the completion of the new shielded laboratory at UNR. Yucca Mountain lies along structural strike between these two areas, and very likely contains

many of the same structural elements. In addition, these studies and our reconnaissance of the Striped Hills and the Grapevine Mountains will allow tests of the hypothesis that a major strike-slip fault extends from Pahrump Valley through and beneath Crater Flat (Schweickert, 1989).

Appendices

Abstracts and published papers

1. Elwood, R., 1991, Structure of the western Pahranaगत shear system (abs.): Geol. Soc. America Abs. with Programs, v. 23, p. 22.
2. Zhang, Y., and Schweickert, R.A., 1991, Structural analysis of Bare Mountain, Southern Nevada (abs.): Geol. Soc. America Abs. with Programs, v. 23, p. A185.
3. Caskey, S. J., 1991, Mesozoic and Cenozoic structural geology of the CP Hills, Nevada Test Site, Nye County, Nevada; and regional implications (abstract of thesis): Reno, University of Nevada.
4. Donovan, D., 1991, Neotectonics of the southern Amargosa Desert, Nye County, Nevada and Inyo County, California (abstract of thesis): Reno, University of Nevada.
5. Hoffard, J., 1991, Quaternary tectonics and basin history of Pahrump and Stewart Valleys, Nevada and California (abstract of thesis): Reno, University of Nevada.
6. Caskey, S.J., and Schweickert, R.A., 1991, Mesozoic deformation in the Nevada Test Site and vicinity: A new perspective from the CP Hills, Nye County, Nevada (abs.): In final revision, Geol. Soc. America Bulletin.
7. G. King and M. Ellis, 1991, The origin of large local uplift in extensional regions: Nature, v. 348, p. 689-693.

APPENDIX A

STRUCTURE OF THE WESTERN PAHRANAGAT SHEAR SYSTEM

ELWOOD, R., Geology Dept., Univ. of NV, Reno, Reno,
NV 89557-0072

The Pahrnagat Lake and Pahrnagat Lake NW quadrangles, Nevada, contain the western portion of the Pahrnagat Shear System, a set of three parallel, northeast striking, left-lateral faults. At the southern end of the quadrangles is the Maynard Lake strand which truncates the Sheep Range to form a steep, linear mountain front. Next to this strand, is a 1 sq. km outcrop of Tertiary volcanic rocks which are folded into a northeast plunging anticline.

About 6 km north of the Maynard Lake strand is the Buckhorn Ranch strand. Between these two strands is a north-south oriented, 4 km long sliver of Paleozoic rock of relatively high relief which dips westward and Tertiary volcanic rocks which have been faulted, tilted eastward, and gently folded. Relatively low relief but significant stratigraphic omission within the volcanic rocks suggests low-angle faulting.

Three sets of faults are recognized on the basis of similar strike: (1) a northeast set (2) a north-south set and (3) a northwest set. The northeast set is mostly topographically expressed and has horizontal and oblique slickensides associated with it. The north-south set often has minor movement but can have significant normal offset. The northwest faults are responsible for significant stratigraphic omission within the Tertiary volcanic rocks and in some cases must have a relatively shallow dip. However, this set also displays pure strike-slip movement as is demonstrated by slickensides.

APPENDIX B

STRUCTURAL ANALYSIS OF BARE MOUNTAIN, SOUTHERN NEVADA

ZHANG, Yang, and SCHWEICKERT, Ricardo A. *Center for Neotectonic studies*
Mackay School of Mines, University of Nevada, Reno, NV 89557

An understanding of the structure and tectonics of Bare Mountain is very important in evaluating the risks associated with locating a nuclear waste repository at Yucca Mountain since similar upper Proterozoic through Mississippian strata exposed at Bare Mountain also underlie Cenozoic volcanic tuffs of Yucca Mountain. Thrust faults and detachment faults have recently been recognized and mapped by several geologists (Monson, Carr, et al., 1990). Our field reconnaissance and structural analysis provide data for kinematic interpretations of faulting at Bare Mountain. Four major structural elements are: (1) The north-vergent Panama thrust emplaced older rocks (upper pC & C) northward over younger Pz rocks. A klippe of C rocks rests upon Miss strata, 6 km north of the thrust root zone in southern Bare Mountain. North-vergent recumbent folds occurred in hinge wall and foot wall of the Panama thrust. (2) The south-vergent Meiklejohn Peak thrust consists of northward dipping of Ord-Sil rocks and are resting on a south-facing footwall syncline of Dev-Miss rocks. The syncline itself rests on a klippe of the Panama thrust. This relationship suggests the Meiklejohn Peak thrust is younger than the Panama thrust. Drag folds in the upper plate imply southward movement of the upper plate. (3) Top-to-the-south detachment faults (Conejo Canyon detachment & Wildcat Peak detachment) ruptured the entire Bare Mountain range. Faults root to south, and are arched above the middle of the range. The upper plate comprises fragmented slivers of Pz strata which are generally unmetamorphosed. Lower plate rocks are locally metamorphosed. In Conejo Canyon, lower plate rocks (upper pC & C) are penetratively deformed and metamorphosed to amphibolite facies, and here are considered to be a metamorphic core complex. (4) The youngest detachment fault (Fluorspar Canyon fault) involved volcanic rocks as its upper plate, and truncated all pre-Tertiary structures at north end of the range. Bare Mountain has been domed, tilted and deeply eroded during Cenozoic extension since volcanic rocks have been stripped from the range. Large scale folding related to thrusts is compatible with N-S shortening that resulted from Mz orogenesis, probably pre-91 Ma (Monson et al., 1990). Detachment faulting and denudation are closely associated with Cenozoic extension in Basin and Range Province. Conejo Canyon fault and Wildcat Peak fault probably occurred pre-Miocene, and Fluorspar Canyon fault occurred between 10-8 Ma (Maldonado, 1990).

APPENDIX C

Caskey, 1991

ABSTRACT

Detailed mapping and structural analysis of upper Proterozoic and Paleozoic rocks in the CP Hills of the Nevada Test Site, together with analysis of published maps and cross sections and a reconnaissance of regional structural relations indicate that the CP thrust of Barnes and Poole (1968) actually comprises two separate, oppositely verging Mesozoic thrust systems: 1) the west-vergent CP thrust which is well exposed in the CP Hills and at Mine Mountain, and 2) the east-vergent Belted Range thrust located northwest of Yucca Flat. West-vergence of the CP thrust is indicated by large-scale west-vergent recumbent folds in both its hangingwall and footwall and by the fact that the CP thrust ramps up section through hangingwall strata toward the northwest. Regional structural relations indicate that the CP thrust forms part of a narrow sigmoidal belt of west-vergent folding and thrusting traceable for over 180 km along strike. The Belted Range thrust represents earlier Mesozoic deformation that was probably related to the Last Chance thrust system in southeastern California, as suggested by earlier workers. A pre-Tertiary reconstruction of the Cordilleran fold and thrust belt in the region between the NTS and the Las Vegas Range bears a close resemblance to other regions of the Cordillera and has important

implications for the development of hinterland-vergent deformation as well as for the probable magnitude of Tertiary extension north of Las Vegas Valley.

Subsequent to Mesozoic deformation, the CP Hills were disrupted by at least two episodes of Tertiary extensional deformation: 1) an earlier episode represented by pre- middle Miocene low-angle normal faults, and 2) a later, post- 11 Ma episode of high-angle normal faulting. Both episodes of extension were related to regional deformation, the latter of which has resulted in the present basin and range topography of the NTS region. There appears to be a direct correspondence between the regional structural grain of the earlier episode of low-angle faulting and that of (hinterland-vergent) Mesozoic structures. Regional structural relations indicate that both Mesozoic and pre- middle Miocene structures in the CP Hills broadly correlate with those at Bare Mountain. This has important implications for subsurface structural models beneath Yucca Mountain, the candidate high-level nuclear waste repository.

APPENDIX D

ABSTRACT

A complex pattern of active faults occurs in the southern Amargosa Desert, southern Nye County, Nevada. These faults can be grouped into three main fault systems: (1) a NE-striking zone of faults that forms the southwest extension of the left-lateral Rock Valley fault zone, in the much larger Spotted Range-Mine Mountain structural zone, (2) a N-striking fault zone coinciding with a NNW-trending alignment of springs that is either a northward continuation of a fault along the west side of the Resting Spring Range or a N-striking branch fault of the Pahrump fault system, and (3) a NW-striking fault zone which is parallel to the Pahrump fault system, but is offset approximately 5 km with a left step in southern Ash Meadows.

These three fault zones suggest extension is occurring in an E-W direction, which is compatible with the ~N10W structural grain prevalent in the Death Valley extensional region to the west.

APPENDIX E

ABSTRACT

The Pahrump fault system is an active fault system located in Pahrump and Stewart Valleys, Nevada and California, in the southern part of the Basin and Range Province. This system is 50 km long by 30 km wide and is comprised of three fault zones: the right-lateral East Nopah fault zone, the right-oblique Pahrump Valley fault zone, and the normal West Spring Mountains fault zone. All three zones have geomorphic evidence for late Quaternary activity. Analysis of active fault patterns and seismic reflection lines suggests that the Pahrump basin has had a two-stage genesis, an early history associated with a period of low-angle detachment faulting probably active 10-15 Ma, and a more recent history related to the present dextral shear system, probably active post-4 Ma.

APPENDIX F

ABSTRACT

Detailed studies in the CP Hills and Mine Mountain area of the Nevada Test Site (NTS), together with analysis of published maps and cross sections and a reconnaissance of regional structural relations, indicate that the CP thrust of Barnes and Poole (1968) actually comprises two separate, oppositely verging Mesozoic thrust systems: 1) the west-vergent CP thrust which is well exposed in the CP Hills and at Mine Mountain; and 2) the east-vergent Belted Range thrust located northwest of Yucca Flat. Regional structural relations indicate that the CP thrust forms part of a narrow sigmoidal belt of west-vergent folding and thrusting traceable for over 180 km along strike. The Belted Range thrust represents earlier Mesozoic deformation that was probably related to the Last Chance thrust system in southeastern California, as suggested by earlier workers. A pre-Tertiary reconstruction of the Cordilleran fold and thrust belt in the region between the NTS and the Las Vegas Range bears a close resemblance to other regions of the Cordillera and has important implications for the development of hinterland-vergent deformation as well as for the probable magnitude of Tertiary extension north of Las Vegas Valley.

APPENDIX G

The origin of large local uplift in extensional regions

Geoffrey King* & Michael Ellis†

* United States Geological Survey, 345 Middlefield Road, Menlo Park, California 94025, USA

† Center for Earthquake Research and Information, Memphis State University, Memphis, Tennessee 38152, USA

Large localized uplift is commonly observed in continental regions undergoing extension. These observations can be modelled by planar, high-angle normal faulting of an elastic upper crust overlying an inviscid lower crust. Isostasy provides the necessary driving force. The model quantifies the role of flexural rigidity, density variations in the crust, and erosion and deposition of sediment.

MANY authors have noted that uplift of several kilometres can occur in extensional regions. The uplift is usually local in extent, extending 10–20 kilometres perpendicular to the strike of the structures and many tens of kilometres along strike. Evidence for uplift, possibly as much as 15 km, comes from local stratigraphic relations, metamorphic mineral assemblages, and fluid-inclusion studies in rocks that must have been generated in the middle or lower crust. The origin of such large localized uplift is a subject of lively debate, centering on the geometry of the normal faults and the role of isostasy and crustal flexural rigidity.

Here we show that the observations may be explained quantitatively by simple planar high-angle faulting of an elastic upper crust overlying an inviscid lower crust that is subject to isostatic forces. The model is consistent with observed gravity profiles and earthquake source mechanisms^{1–3}, and with the observation of crustal shortening in the upper parts of footwalls. We illustrate the model with a number of examples of structures from the Basin and Range province in the United States.

The model

The approach to modelling these structures follows from that used by King *et al.*¹ and Stein *et al.*². There the mechanical behaviour of the crust was modelled as an elastic layer overlying a fluid. The vertical component of motion at the surface was calculated using the thick-plate solution described by Rundle⁴. It was shown that the main features of the geological structures associated with some dip-slip faults could be explained if the fault was assumed to be planar through an elastic-brittle layer dipping at 45° or greater and if the effects of loading due to erosion and sedimentation were considered. The most surprising feature of the model was the need to reduce the effective elastic thickness from the 10–15 km depth of the seismogenic zone to between 2 and 4 km.

Here we adopt a different computational approach using a boundary-element system modified, as described below, from that of Crouch and Starfield⁵. This allows us to extend the earlier work and calculate both vertical and horizontal displacements and strains for two-dimensional models. We use a version of the boundary-element technique that uses constant relative displacement elements. This approach is very effective. A minimum of computational steps allow many models to be run on a small computer and because the approach is easy to understand avoiding numerical errors is straightforward.

The technique consists of introducing a series of dislocation elements into an elastic medium. The location and amplitude of slip on the elements is then adjusted such that stresses and displacements at boundaries and interfaces reasonably approxi-

mate the real problem being examined.

The two-media problem we examine can be expressed as a solution of the following equations

$$\begin{aligned} b_i^i &= \sum_{j=1}^N C_{ss}^{ij} D_j^i + \sum_{j=1}^N C_{sn}^{ij} D_n^j \\ b_n^i &= \sum_{j=1}^N C_{ns}^{ij} D_s^j + \sum_{j=1}^N C_{nn}^{ij} D_n^j \end{aligned} \quad (1)$$

where $i = 1-N$. The b_x^i are displacements ($b_x^i = u_x^i$) or stresses ($b_x^i = \sigma_x^i$) on the i th boundary element. For normal components $x = n$ and for shear $x = s$. The D_x^j are normal ($x = n$) or shear ($x = s$) displacements between the faces of the j th boundary element, and the C_{xy}^{ij} are the influence coefficients between the i th and j th elements. Subscripts indicate normal (x or $y = n$) or shear (x or $y = s$) components.

The first N_1 elements are in region 1 and the remainder $N_2 = N - N_1$ are in region 2. These elements may either represent a free part of the boundary of region 1 or region 2 or a segment on the interface between the two regions. If the i th element is an interface element in region 1 then a corresponding interface element i^* must exist in region 2.

Four conditions must be satisfied at an interface and hence relate any pair of interface elements. These may be conveniently expressed as two on the region 1 element and two on the region 2 element.

Two stress conditions are imposed on the region 1 element

$$\begin{aligned} \sigma_s^{i(1)} - \sigma_s^{i^*(2)} &= 0 \\ \sigma_n^{i(1)} - \sigma_n^{i^*(2)} &= 0 \end{aligned} \quad (2)$$

where $\sigma_x^{(1)}$ corresponds to an interface stress in region 1 and $\sigma_x^{(2)}$ corresponds to an interface stress in region 2. The stress conditions are satisfied in equation (1) if

$$\begin{aligned} b_s^i &= \sigma_s^{i(1)} - \sigma_s^{i^*(2)} = 0 \\ b_n^i &= \sigma_n^{i(1)} - \sigma_n^{i^*(2)} = 0 \\ C_{ss}^{ij} &= A_{ss}^{ij} \quad j \leq N_1 \\ C_{sn}^{ij} &= -A_{sn}^{ij(2)} \quad N_1 + 1 \leq j \leq N \end{aligned} \quad (3)$$

The $A^{(1)}$ are influence coefficients relating stress to displacement for region 1 and $A^{(2)}$ are similar coefficients for region 2. C_{sn}^{ij} , C_{ns}^{ij} and C_{nn}^{ij} are defined similarly. On the region 2 element, the following displacement conditions are imposed

$$\begin{aligned} u_s^{i(2)} + u_s^{i^*(1)} &= 0 \\ u_n^{i(2)} + u_n^{i^*(1)} &= 0 \end{aligned} \quad (4)$$

which are satisfied in equation (1) if

$$\begin{aligned} b_s^i &= u_s^{i(2)} + u_s^{i^*(1)} = 0 \\ b_n^i &= u_n^{i(2)} + u_n^{i^*(1)} = 0 \\ C_{ss}^{ij} &= B_{ss}^{ij(1)} \quad j \leq N_1 \\ C_{sn}^{ij} &= B_{sn}^{ij(2)} \quad N_1 + 1 \leq j \leq N \end{aligned} \quad (5)$$

The $B^{(1)}$ are influence coefficients relating displacement to displacement in region 1 and $B^{(2)}$ are similar coefficients for region 2.

With the appropriate values for element stress, displacements

and influence coefficients, the $2N$ equations can be solved for the $2N$ values of D by the usual methods. Once the D are known it is straightforward to calculate displacements anywhere in region 1 or 2 for which valid expressions can be written in terms of D . The procedure for setting up influence coefficients in an elastic media is straightforward and is described in Crouch and Starfield⁵. The behaviour of a horizontal gravitating interface between an elastic medium (region 1) and an inviscid fluid medium (region 2), for which the pressure change with depth is H , can be expressed if the region 2 influence coefficients take the following values

$$A_{nn}^{ij(2)} = \begin{cases} H^i & \text{if } i=j \\ 0 & \text{if } i \neq j \end{cases} \quad (6)$$

$$B_{nn}^{ij(2)} = \begin{cases} 1 & \text{if } i=j \\ 0 & \text{if } i \neq j \end{cases}$$

All other $A^{(2)}$ and $B^{(2)}$ are zero.

In our models the x_1 axis is vertical and positive downwards and the x_3 axis is horizontal. Two horizontal gravitating interfaces are defined. One represents the Earth's surface ($x_1 = 0$ km) and the second, the base of the brittle layer ($x_1 = 12$ km). At $x_3 = -60$ km the horizontal displacement along a vertical boundary is fixed ($u_3 = 0$) and the shear stress is set to zero ($\sigma_{13} = 0$). At $x_3 = 48$ km both shear and normal stresses are set to zero ($\sigma_{33} = \sigma_{13} = 0$) at a second vertical boundary. These conditions produce a stress-free floating block 'tethered' at -60 km. The length of the block is sufficient that details of the way in which the boundary conditions are imposed do not affect the deformation in the region where faulting is introduced.

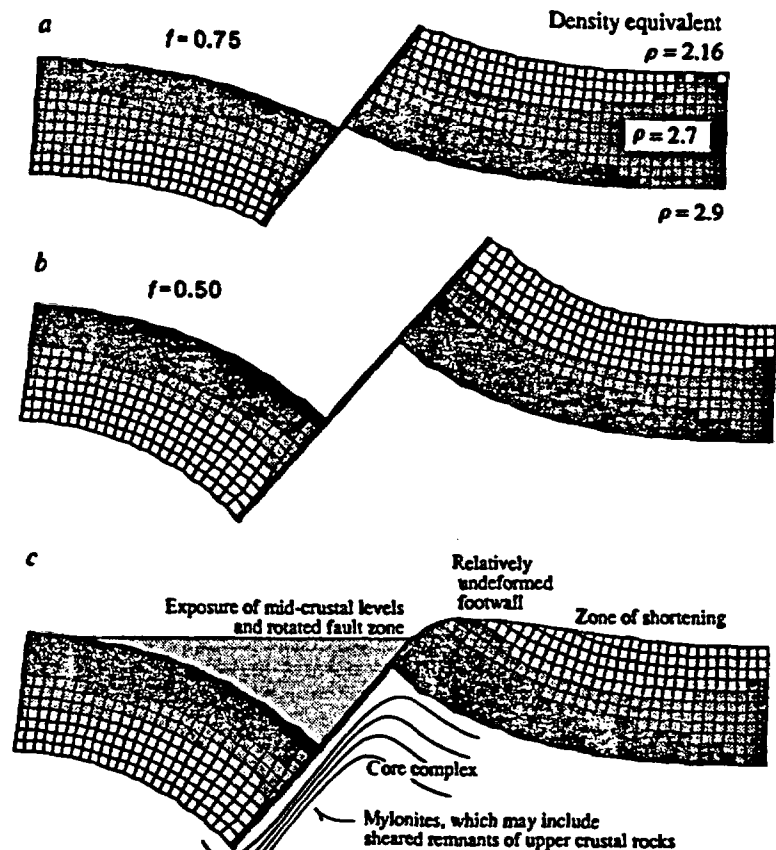
The driving force to deform the block is derived in the following manner. In the Earth we may suppose that the upper crust is able to sustain a certain magnitude of deviatoric stress over a time of millions of years. We further assume that over the

same time repeated motion on major faults in the crust is appropriately modelled by assuming that the fault is effectively of zero strength. The nature of this assumption is discussed by Rundle⁶. Because we wish to examine the stresses and strains due to the fault displacement only (rather than these combined with any initial state of stress) we effectively turn the situation around in the numerical model by allowing the initial state of stress to be zero (hence the boundary conditions above) and by driving displacement with a shear stress τ_0 applied to the fault. Thus, specifying the right-hand vertical boundary condition in our model as $\sigma_{33} = 0$ is not equivalent to assuming that σ_{33} is actually zero in the Earth. The effective σ_{33} in the real world determines our choice of shear stress across the fault. In a gravitating block with free boundaries the vertical stress at depth h is $\sigma_{11} = h\rho g$. The resolved shear stress on a plane dipping at an angle θ is given by $\tau = (\sigma_{11} - \sigma_{33}) \sin \theta \cos \theta$, and its average by $\tau_0 \approx \tau/2$. Assuming a density of upper crustal material of $2,700 \text{ kg m}^{-3}$, a fault dip of 60° gives $\tau \approx 140(1-f)$ MPa, where $f = \sigma_{33}/\sigma_{11}$. To model a fault of zero long-term strength, we therefore apply $\tau_0 \approx 70(1-f)$ MPa.

The choice of f is open to debate. If $f = 0$, this implies that the crust can reach the verge of going into tension. Even with displacement boundary conditions this is unlikely to occur. Other have proposed values between $1/3$ and 1 , based on near-surface measurements or on models much simpler than ours (for example, ref. 7). We therefore choose $f = 0.5$, which we regard as a likely maximum stress difference. For comparison, we also show the result for $f = 0.75$.

At the base of the elastic layer the fluid has a density of $\rho_3 = 2,900 \text{ kg m}^{-3}$ and in the absence of erosion and sedimentation, the density above the elastic layer would be $\rho_1 = 0.0$. A convenient way to represent the effects of erosion and sedimentation is to substitute a medium of significant density for the air. It would be most straightforward to choose a medium with a

FIG. 1 Representative boundary-element models shaded with dilational strain at a 0.02 contour interval. The grid units represent square kilometres and are for scale only. Dark areas represent extension (areal increase), light areas contraction (areal decrease). The strains are shaded from 0.5 km to a depth of 11.5 km and represent those due only to the motion across the fault and not due to any preexisting condition or body forces. These plot limits (0.5–11.5 km) avoid the large local strains associated with the singularities at the end of the boundary elements. Effective elastic thickness is ~ 3 km assuming a crustal Young's modulus of 40 GPa and a Poisson ratio of 0.25. Density below the layer is $2,900 \text{ kg m}^{-3}$. We assume 80% erosion and sedimentation, which corresponds to assuming a density above the top surface of $2,160 \text{ kg m}^{-3}$. The fault and distant shear boundaries are in 1.5-km segments in the central region, increasing to 6-km segments outside the region shown. The vertical boundary at -60 km is fixed, and at $+48$ km $\sigma_3 = 0$. *a* and *b* show a fault model driven by a shear stress that corresponds to a ratio of vertical to horizontal stress in the crust of 0.75 and 0.5, respectively. *c*, A modification of *b* illustrates the effect of erosion and sedimentation and is annotated by commonly observed features. The same calculations were carried out for element lengths of 3 and 6 km. The resulting displacements were the same to within a few per cent, but the strain patterns became ragged when fewer, longer elements were used. In both models, shortening occurs in the upper part of the footwall, and extension in the lower part. Uplift of the footwall is significant; in particular, *b* and *c* show the ease with which mid-crustal levels can be exposed at the surface with relatively minor extension.



density related to the proportion of underlying material removed by erosion or added by sedimentation. For example, choosing a medium of density $2,160 \text{ kg m}^{-3}$ is mechanically equivalent to removing 80% of the uplifted mass by erosion and replacing 80% of the mass removed by subsidence through sedimentation. Were this the case, the value for H below the elastic layer would be $g\rho_3$ and that above would be $g\rho_1$. Net forces applied to the plate that resists flexure are proportional to $(\rho_1 - \rho_3)g$, and forces proportional to $(\rho_1 + \rho_3)g$ are applied across the plate creating strains within the plate. Such a model does not allow for the reduction of modulus E to E_{eff} (where $E/E_{\text{eff}} = 60$), introduced to allow the elastic layer to possess a long-term effective elastic thickness of $\sim 3 \text{ km}$. In the absence of a correction, unreasonably large strains appear in the layer. A number of corrections are possible. The flexure is largely determined by the term $(\rho_3 - \rho_1)g$, which must remain the same. On the other hand, $(\rho_1 + \rho_3)g$ may be reduced by E_{eff}/E . This may be achieved if we replace ρ_1 by $\rho_1 E_{\text{eff}}/E$ and ρ_2 by $(\rho_2 - \rho_1)(1 - (E_{\text{eff}}/E))$.

The foregoing provides one approach to applying boundary conditions to the layer, but others are possible. For example, if displacements are infinitesimal such that points do not displace with respect to a fixed axis system, then H at the base becomes $(\rho_3 - \rho_2)g$ and at the surface $(\rho_2 - \rho_1)g$.

Within reasonable limits, details of the way these boundary conditions are applied do not affect the final result, provided that the net restoring force remains proportional to $(\rho_3 - \rho_1)g$. They may be chosen according to what is perceived to be the physical processes that cause effects such as the long-term loss of strength of the elastic layer. Unfortunately, the insensitivity to details of these boundary conditions also has the consequence that data of the sort we describe cannot be used to determine more detail about the behaviour of the plate.

Some representative models are shown in Fig. 1. In Fig. 1a-c the fault dips at $\sim 60^\circ$ and cuts through a 12-km-thick layer of density $2,700 \text{ kg m}^{-3}$. Although the elastic layer is 12 km thick we use a Young's modulus such that its equivalent flexural rigidity (10^{20} N m) is the same as an elastic layer $\sim 3 \text{ km}$ thick, assuming a crustal modulus of $\sim 40 \text{ GPa}$. Our models support the previous result^{1,2} that only models with an effective elastic layer 2-4 km thick yield sensible geological structures. Models with greater elastic thickness produce structures wider than those observed, and those with a smaller elastic thickness produce structures that are too narrow.

Figure 1a and b shows the deformation for $f=0.75$ and $f=0.5$, respectively. The results can be interpreted in several ways. For example, if $f=0.5$ is considered to be the maximum stress difference, then the deformation shown in Fig. 1b is the maximum that can be achieved by gravity alone. If this is the case, then the result for $f=0.75$ (Fig. 1a) may be interpreted as 50% of the maximum deformation, or as the maximum deformation if the fault is capable of sustaining half of the available shear stress. The significance of the model, however, is separate from these interpretations: large local uplift of the footwall driven only by gravity is an unavoidable result of a realistic dynamic model.

Figure 1c is the same as Fig. 1b but shows the effects of erosion and sedimentation and is annotated with commonly observed features. In particular, it shows the relatively undeformed but rotated footwall, the zone of shortening in the upper part of the footwall, exposure of mid-crustal level rocks, and the inferred development of mylonites in the inviscid lower crust.

The figures are shaded to indicate strain changes due to fault motion. Areal strain ($\epsilon_{11} + \epsilon_{33}$) is plotted with lighter shades representing contraction and darker shades dilation. The slight checkerboard effect at the upper and lower boundaries are associated with singularities at the ends of the elements. (See also the caption to Fig. 1.) At the surface, dilation occurs in the hanging wall and contraction occurs in the footwall. Field observations of gentle to close folds and conjugate strike-slip faults in the footwall reflect the contractional strains produced

in the upper part of the model footwall. At the base of the elastic layer the conditions are reversed with contraction in the hanging wall and extension in the footwall. We regard the dilational strains at the base of the footwall as significant, and we suggest elsewhere (ref. 8 and M.E. and G.K., manuscript in preparation) that the implied volume increase may provide a mechanism to tap locally available partial melt, which eventually ascends to produce the commonly observed flank volcanism.

Field examples of finite structures

Many examples of large localized uplift occur in the Basin and Range province, two of which are shown in Fig. 2. Examples share the characteristics that uplift and tilting is confined to a relatively narrow ($\sim 10\text{-}20 \text{ km}$) zone parallel to the associated high-angle normal fault, and minor shortening occurs in the upper part of the footwall. It is also commonly observed that volcanism and shallow intrusives occur preferentially in the footwall.

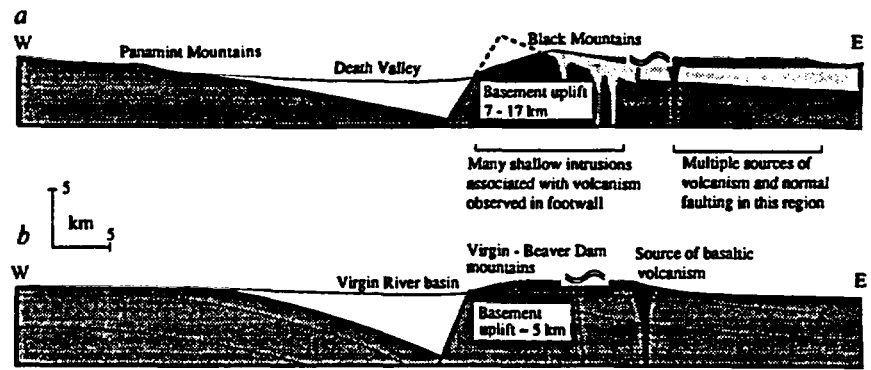
Central Death Valley (Fig. 2a) is an asymmetrical east-tilted graben, bounded to the east by an active high-angle, range-front normal fault that bounds the western side of the Black Mountains⁹. The present range-front has been active since at least 10 Myr, although most of the uplift has probably occurred in the past 6 Myr (ref. 8). Gravity measurements over the valley floor⁹ and seismic reflection¹⁰ and refraction information¹¹ suggest that the basin fill is 3-5 km thick.

Significant local uplift of between 7 and 17 km and the eastward tilt of the Black Mountain block, confined to a relatively narrow 10-20 km perpendicular to the main fault, is evidenced by exposure of middle-crust rocks near the range-front fault and lower-grade, stratigraphically higher rocks to the east^{9,11-14}, by aluminium geobarometry analysis of a local mid-Tertiary intrusion¹⁵ and by the geometry of tilted extrusive rocks¹¹. Total displacement across the main fault zone is therefore 10-22 km. Pliocene basalts exposed near their source in the footwall are gently folded along axes parallel to the main normal fault.

The active Virgin-Beaver Dam fault system (Fig. 2b) marks the eastern edge of the transition zone between the southern Great Basin and the Colorado Plateau. The system was initiated during the middle Miocene and is responsible for $\sim 6 \text{ km}$ of subsidence in the hanging wall and a minimum of 5 km of uplift in the footwall (R. E. Anderson, personal communication). The footwall exposes Precambrian basement in an eastward tilted block and preserves an older part of the normal fault (the Castle Cliff detachment) now stranded at a low angle on top of the basement culmination. The Palaeozoic and Mesozoic cover sequence is gently to closely folded within, and parallel to, the footwall of the Beaver Dam section and is shortened by conjugate strike-slip faults in the Virgin Mountain section. Significant Tertiary basalts of local origin are also observed in the footwall. The age of the folds is not precisely known, although various arguments suggest that they are associated with the development of the main normal-fault system¹⁶.

Further examples from the Basin and Range province include the Shoshone and Cortez ranges in northern Nevada^{17,18}, the Humboldt and Stillwater ranges of north central Nevada^{17,19}, the Wassuk range of central Nevada^{20,21}, and the Wasatch range in Utah. Each of these ranges, except the Humboldt, is associated with a large active range-bounding normal-fault system, which was initiated in the middle Miocene and which is associated with volcanic rocks and (or) shallow intrusions in the footwall. Folds of Pliocene units are observed in the footwalls of the Stillwater²² and Wassuk ranges²⁰. The adjacent basins are about 3-4 km thick and displacement across the normal faults is at least 4-5 km^{17,19}. The Humboldt fault system seems to be less developed (1-2 km displacement) and is probably a younger system. The presence of relatively young volcanic rocks (late Pliocene or possibly Pleistocene) confined to the footwall of the Humboldt range supports the supposed young age of the fault. The Wasatch range and its associated basin is a particularly

FIG. 2 Examples of structures from the Basin and Range province having large localized uplift along high-angle planar faults. Dark shading indicates pre-Tertiary basement. Light shading indicates middle Miocene volcanic rocks or intrusions associated with the early stages of faulting. White indicates basin-fill sedimentary units, black indicates basalts. *a*. Death Valley, data from refs 9 and 11. Uplift of footwall may be up to 17 km based on geobarometry studies²⁸, although the regional stratigraphic column probably limits displacement to <10 km. Source of Miocene volcanics lies within the footwall of the main fault. *b*. Virgin-Beaver Dam Mountains (cross-section supplied by R. E. Anderson, personal communication).



striking example of the potential importance of erosion and sedimentation. Stratigraphic arguments²³ and fluid-inclusion studies²⁴ suggest that the Wasatch range has a vertical offset of ~11 km, and seismic reflection and gravity suggest that the basin is only ~4 km deep²⁵. This type of structure may be modelled by allowing the system to be open to mass change (see also refs 1, 2), such that the rate of erosion is relatively high (promoting uplift), and the rate of sedimentation is relatively low (inhibiting subsidence). Seismic reflection, gravity models and earthquake seismology suggest that the faults described here, and in general for the Basin and Range province, are high-angle and planar^{26,27}.

The models shown in Fig. 1 are generally consistent with these examples. In particular, they produce the high uplift of individual ranges while retaining the relatively narrow dimension of each basin and range, and they correctly predict shortening in the elbow of the footwall.

Discussion

Other investigators have addressed some of the observations described here, and have recognized that a successful model must incorporate elements of the model we propose^{28,29}. The numerical modelling illustrates that a simple isostatic model incorporating only high-angle faults explains the observations very effectively.

Localized and rapid uplift in extensional regions has been attributed to the isostatic response of a previously suppressed crustal root broken by high-angle faulting³⁰. Our analysis avoids the difficulty of assuming that the crust can maintain isostatically unbalanced roots for extended periods of time before the faulting occurs (such as in ref. 31) and of assuming that each highly displaced and elevated range was underlain by a preexisting root. Our model provides a means to produce large uplift and displacements from an elastic upper crust that was originally in isostatic equilibrium.

A controversial topic in Basin and Range tectonics is the role of low-angle faults in extension of the upper crust³². Our model shows that the appropriate structural and topographic cross-sections can be produced by planar high-angle faulting of the upper crust. We do not dispute the field evidence for low-angle faulting and suggest that minor low-angle normal faulting may be produced along the higher sections of the main fault as it is rotated with the footwall. Eventually the high part of the fault will be abandoned (for example, ref. 29) and will continue to be rotated and uplifted in the footwall. The turtlebacks of central Death Valley³³ and the Castle Cliff detachment of the Beaver Dam Mountains represent examples of this abandonment process.

Low-angle faults will also be produced by imbrication of the footwall (commonly observed in extensional regions), a process in which slices of the footwall are transferred into the hanging wall and subsequently rotated to a lower angle. This process, as well as imbrication of the hanging wall, also has the effect of juxtaposing severely attenuated upper-plate rocks against highly sheared and mylonitized rocks of the lower plate. This is a fundamental characteristic of metamorphic core complexes.

The finite structure of Fig. 1b is likely to be the maximum deformation possible given a gravitational driving force, a reasonable density structure and flexural strength, and the minimum plausible ratio of horizontal to vertical stress. Large extension of the continental crust requires the development of many such structures, giving rise to a distributed basin and range structure. This distinguishes our model from the rolling footwall hinge model^{29,30}, which requires that substantially more uplift should readily occur.

Controversy centres around estimates of crustal extension in the southern Basin and Range. We have shown that significant uplift of the footwall can occur with only minor horizontal extension (Fig. 1). Wernicke *et al.*³⁴, however, suggest that crustal extension at this latitude is ~300% (~250 km), based on palinspastic reconstructions of displaced stratigraphic and structural features. It is possible that much of this displacement, which is in any case disputed³⁵, may be accomplished by a combination of strike-slip faulting (see, for example, refs 36, 37) and large volumes of intrusives, as observed in the Death Valley region of California.

Conclusions

Our numerical model resolves a number of difficulties with previous ideas about the origin of large localized uplift in extensional regions and quantitatively examines factors such as flexural rigidity, density differences, and erosion and deposition of sediment. Others have introduced these ideas but have only considered them in isolation or in qualitative terms. A striking feature of the models is that the modelled flexural rigidity of the elastic upper crust is consistent with results found by other techniques¹⁷⁻¹⁸, and the choice of high-angle planar normal faults is independently justified by results from earthquake seismology^{26,27}. □

Received 25 April; accepted 21 November 1990.

- King, G. C. P., Stein, R. S. & Rundle, J. B. *J. geophys. Res.* **83**, 13307-13318 (1988).
- Stern, R. S., King, G. C. P. & Rundle, J. B. *J. geophys. Res.* **83**, 13319-13331 (1988).
- Jackson, J. A. *Continental Extensional Tectonics*. *Spec. Publs geol. Soc.* **22**, 3-17 (1987).
- Rundle, J. B. *J. geophys. Res.* **87**, 7767-7796 (1982).
- Crouch, S. L. & Starfield, A. M. *Boundary Element Methods in Solid Mechanics* (Allen & Unwin, London, 1983).
- Rundle, J. B. *J. geophys. Res.* **83**, 6237-6254 (1988).
- McGarr, A. *J. geophys. Res.* **83**, 13609-13617 (1988).
- Ellis, M. A. & King, G. C. P. *Geol. Soc. Am. Abstr. Progr.* **22**, 273 (1990).
- Hunt, C. B. & Mabey, D. R. *Prof. Pap. U.S. geol. Surv.* 494-A (1966).
- Serpa, L. *Geol. Soc. Am. Bull.* **100**, 1437-1450 (1988).
- Geist, E. L. & Brocher, T. M. *Geology* **15**, 1159-1162 (1987).
- Wright, L. A., Troxel, B. W., Burchfiel, B. C., Chapman, R. H. & Labotka, T. C. *Geol. Soc. Am. Map and Chart Ser.* MC-25M (1981).
- Wright, L. A. *Geol. Soc. Am. Abstr. Progr.* **2**, 221 (1971).
- Camen, I., Wright, L. A., Draks, R. E. & Johnson, F. C. *Spec. Publs Soc. Econ. Paleont. Miner.* **37**, 127-141 (1985).
- Holm, D. K. & Wernicke, B. *Geology* **18**, 520-523 (1990).
- Anderson, R. E. *U.S. geol. Surv. Open-File Rep.* 83-504 (1983).
- Stewart, J. H. *Geology of Nevada*. *Spec. Publ. 4 Nevada Bureau of Mines and Geology*, Reno, 1980.
- Roberts, R. J., Montgomery, K. M. & Leitner, R. E. *Nevada Bur. Mines Geol. Bull.* **64** (1967).
- Okaya, D. A. & Thompson, G. A. *Tectonics* **4**, 107-126 (1985).
- Gilbert, C. M. & Reynolds, M. W. *Geol. Soc. Am. Bull.* **84**, 2489-2510 (1973).
- Ross, D. C. *Nevada Bur. Mines Geol. Bull.* **68** (1961).
- Willden, R. & Speed, R. C. *Nevada Bur. Mines Geol. Bull.* **63** (1974).
- King, C. *Systematic Geology*. Vol. 1 (U.S. Government Printing Office, Washington, DC, 1878).

24. Parry, W. T. & Bruhn, R. L. *Geology* **15**, 67-70 (1987).
 25. Zebach, M. L. *Geol. Soc. Am. Mem.* **187**, 3-28 (1983).
 26. Doer, D. I. *Phys. Earth planet. Inter.* **48**, 64-72 (1987).
 27. Doer, D. I. & Smith, R. B. *Bull. seismol. Soc. Am.* **79**, 1383-1409 (1989).
 28. Wernicke, B. & Axen, G. J. *Geology* **16**, 848-851 (1988).
 29. Buck, W. R. *Tectonics* **7**, 959-975 (1988).
 30. Chase, C. G. & Wallace, T. C. *J. geophys. Res.* **83**, 2795-2802 (1988).
 31. O'Connor, J. E. & Chase, C. G. *Tectonics* **8**, 833-844 (1989).
 32. Ellis, M. A., Bodin, P. A. & Anderson, J. G. *Geol. Soc. Am. Abstr. Progr.* **20**, 235-236 (1988).
33. Wright, L. A., Otton, J. K. & Troxel, B. W. *Geology* **2**, 53-54 (1974).
 34. Wernicke, B., Axen, G. J. & Snow, J. K. *Geol. Soc. Am. Bull.* **100**, 1738-1757 (1988).
 35. Corbett, K. *Geol. Soc. Am. Bull.* **102**, 267-270 (1990).
 36. Wright, L. A. *Geology* **4**, 489-494 (1976).
 37. Ellis, M. A., Zhang, P. & Stiemmons, B. *Eos* **70**, 465 (1989).
 38. Bechtel, T. D., Forsyth, D. W., Sherpton, V. L. & Grieve, R. A. F. *Nature* **343**, 636-638 (1990).

ACKNOWLEDGEMENTS. We thank R. E. Anderson for his insight and help, and B. Julian, W. Mooney and R. Schweickert, M.E. was supported by the State of Nevada Nuclear Waste Projects Office.

TASK 8 PROGRESS REPORT 10/1/90 - 9/30/91

EXECUTIVE SUMMARY

Task 8 is responsible for assessing the hydrocarbon potential of the Yucca Mountain vicinity. We continue to focus on source rock stratigraphy, both in the oil-producing region of east-central Nevada and in the NTS vicinity in southern Nevada. In addition, we are trying to understand the contractional and extensional structures at NTS, in order to reconstruct Paleozoic facies trends and better predict the nature of the Mississippian rocks under Yucca Mountain.

Our stratigraphic studies this year have concentrated on testing our reinterpretation of the Mississippian -- i.e., that rocks mapped as the "Eleana Formation" in fact comprise two different, coeval, sedimentary units. We have seen the depositional base of the western facies of the Eleana (at Bare Mountain), and suspect that we can also document the depositional base of the eastern facies (at Shoshone Mountain). So far, we have seen the top of the eastern facies only. During the course of our remapping, we have found that all of the potential source rocks we have identified (i.e., TOC > 05.%) are from the eastern facies.

Our structural studies have focussed on understanding the distribution of Mississippian units at NTS. The fault juxtaposing eastern and western facies Eleana has regional significance, but is poorly exposed. Several lines of evidence suggest that it is a low-angle east-dipping feature, probably with reverse motion. In addition, our mapping has identified both thrust-related and normal fault-related features, but much remains to be done in order to determine the nature and orientation of the significant faults offsetting the Eleana Formation. Drillhole information has added another important dimension to our understanding of both structure and stratigraphy locally; we will continue to pursue this source of structural data.

TASK 8 PROGRESS REPORT 10/1/90 - 9/30/91

INTRODUCTION

Our studies continue to focus on source rock stratigraphy, with a secondary, crucial, emphasis on structural geology. Our intent has been to establish the stratigraphic framework first (age, thickness, lateral extent and inter-relationships of the different facies), with the idea that we can then concentrate the source rock geochemistry and maturation studies where they will be the most useful. At NTS, a detailed understanding of the structural geology is needed in order to decipher the stratigraphy; ultimately, it will also be needed for evaluating the potential for maturation and trapping of hydrocarbons.

We continue to carry out two parallel studies in different parts of the Mississippian Antler basin; our work has resulted in major changes to the conventional stratigraphic interpretations in both places. One of these studies is in the proven oil-producing region of east-central Nevada (funded by a grant from NSF to Trexler), and one in the vicinity of NTS. In central Nevada, stratigraphic and sedimentologic studies by Trexler and his students have shown that basin fill is thin, the strata are not generally progradational, and uplift plays a large role in basin evolution. They have recognized three unconformity-bounded stratigraphic sequences in the Antler basin: a submarine fan system, a fluvial and delta plain system and a delta and shelf carbonate system. Unconformities between these sequences reflect deformation, uplift and erosion during the orogeny (Trexler and Nitchman, 1990; Trexler and Cashman, 1991). From the point of view of hydrocarbon source rock potential, the sequence stratigraphy interpretation implies that the proven source rocks in Railroad Valley (the type Chainman Formation, of Chesterian age) do not extend west to the central part of the state. Rocks mapped as "Chainman" in the Diamond Mountains are in fact Osagian and Meramecian in age, and Chesterian rocks in the Diamond Mountains and adjacent ranges differ in composition and depositional environment from the type Chainman. In southern Nevada, our studies have shown that rocks mapped as the Mississippian Eleana Formation in fact comprise two completely different, but probably coeval, sedimentary units (Cashman and Trexler, 1991). The western of these has affinities with the (allochthon-derived) Antler foreland of central Nevada; the eastern has affinities with the (craton-derived) shelf assemblage in

eastern Nevada. Based on our limited studies to date, it appears that only the eastern has significant source rock potential.

This report summarizes new results of our stratigraphic and structural studies in southern Nevada. Directions for future work conclude each section. These are followed by a summary of regional stratigraphy and paleogeography, based in part on new work in east-central Nevada. In a final section entitled "other considerations", we discuss several topics from the current scientific and popular literature which are relevant to evaluation of hydrocarbon potential of the Yucca Mountain vicinity.

STRATIGRAPHY OF MISSISSIPPIAN ROCKS AT NTS

The main conclusion of our stratigraphic studies -- that rocks mapped as the Mississippian Eleana Formation in fact comprise two different, but probably coeval, sedimentary units -- and the lines of evidence leading to this conclusion were published this year (Cashman and Trexler, 1991; see Appendix) and will not be repeated here. Our field work this year has attempted, first of all, to determine the distribution of each of these units on the ground. Although the informal "a - j" unit designations of Poole and others (1961) in the original description of the Eleana Formation can locally be reinterpreted in terms of our new understanding, the mapping of these units is not consistent, and virtually all outcrop areas of "Eleana Formation" must be revisited. Until we are able to correlate one or both of the "Eleana" units definitively with established stratigraphic units elsewhere in the region, we retain the informal designations "eastern facies" and "western facies" defined in our paper. New stratigraphic information since Cashman and Trexler (1991) is summarized below:

The exposures of Eleana Formation at Bare Mountain (west of NTS) all represent the western facies of the Eleana, and provide several new pieces of information about this unit. The base of the section, which we have not observed at NTS, is exposed in Tarantula Canyon and is marked at least locally by a silicified fossil hash. The Eleana depositionally overlies a carbonate unit mapped as "Dc, Devonian carbonate" (Carr and Mosen, 1988). The entire lower, siliciclastic, portion of the section is present -- from the base to the first appearance of calcareous detritus. The

siliciclastic section is 540m thick, significantly thinner than the minimum of 900m we have observed in the Eleana Range. Since our paleocurrent data indicate that the sediments are derived from a source to the NNE, it is not surprising to find a decrease in thickness between NTS and Bare Mountain. A 500m thickness of the upper, calcareous, portion of the section is present at Bare Mountain below the fault truncation of the Eleana. This is thicker than the calcareous sections observed to date at NTS, and suggests that much of the upper part of the section is missing in our measured sections from the Eleana Range. The Bare Mountain exposures suggest that there are no surprises in the upper part of the section, however -- it continues to comprise a mixture of siliciclastic and calcareous horizons.

The limited biostratigraphic data we have from Bare Mountain only generally constrain the age of the western facies: The carbonate ("Dc") that underlies the Eleana Formation was analyzed for endothyrids, palynomorphs and conodonts. The samples were barren of all traces of endothyrids, calcareous algae, and shallow water carbonate fossils. A single palynomorph suggests an age no older than Mississippian and probably no younger than Early Permian. Numerous conodont elements suggest an Upper Middle Devonian age; however, conodonts are notoriously resistant to erosion, and may be recycled into younger sediments to give an anomalously old age. Further dating (preferably not based on conodonts) is clearly needed to determine the age of the carbonate below the Eleana unequivocally. Dates were also obtained from the upper, calcareous, part of the section; two different dating techniques were used. Reworked endothyrids indicate a Visean age (i.e., Meramecian or younger); conodonts constrain the age to post- Early Kinderhook. Although inconclusive, both of these ages are compatible with the Chesterian endothyrid ages we have consistently obtained from the calcareous part of the western facies Eleana at NTS (Cashman and Trexler, 1991, and Mamet, written communication, 1991).

At NTS, our remapping to distinguish eastern facies from western facies Eleana has already led to revisions of both the published maps and the earlier work done by Nitchman for Task 8. The limestone north of Tippipah Spring (at the base of Nitchman's North Tippipah Spring measured section) is not the depositional basement of the Eleana; it is the upper, calcareous, part of the western facies and is in a different structural block than the bulk of the North Tippipah Spring measured section.

Similarly, the black shale structurally overlying this limestone is a fault-bounded slice of eastern facies Eleana rather than a part of the western facies. This is significant to evaluation of hydrocarbon potential because a TOC value of > 1 from this shale was cited in our last progress report (10/90) as evidence of source rock potential for the western facies. It now appears that all TOC values > 1 are from eastern facies rocks. In a further simplification, the remainder of the North Tippipah Spring measured section correlates with the West Gap Wash measured section, which is depositionally overlain by the upper, calcareous part of the western facies Eleana. Thus, both of these measured sections are now solidly tied to the known stratigraphy and biochronology, rather than being "floating" sections.

Drillhole information has added another important dimension to our understanding of both the structure and stratigraphy in the vicinity of Syncline Ridge. We have obtained access to well logs, wellsite geologists' reports, cuttings and cores from all of the deep holes ($> 1000'$) in the Eleana. The virtually continuous core from UE-17e gives us a much more accurate idea of the composition of the eastern facies Eleana than the limited, weathered, surface exposures. The core is dominantly competent black shale, with local dark gray, deep-water limestone and uncommon quartz arenite horizons. Biostratigraphic dates from core samples are somewhat younger than dates previously obtained from correlative surface rocks; the new dates are probably more reliable, because the core samples are less weathered than the surface samples. Several folding, veining and faulting events are apparent in the core, and can be distinguished on the basis of mesoscopic structural characteristics and of cross-cutting relationships. The presence of these structures, and the similarity of biostratigraphic dates throughout much of the core, together suggest that structural repetition is probable. Thus, estimates of original thickness of the eastern facies in this area are unreliable. Observations from several of the other drillholes are significant for regional structural interpretations; we plan to look into these in the upcoming year.

There are several obvious directions for future work on the Mississippian stratigraphy at NTS, most of which are designed to test aspects of our interpretation that rocks mapped as Eleana are in fact parts of two separate stratigraphic units. The general topics are: (1) The identity and correlation of unit "MI" at Shoshone Mountain. If, as we suspect, it represents the depositional base of the eastern facies Eleana,

it provides inescapable evidence that there are two Mississippian sedimentary units at NTS. (2) The identity, age and correlation of the carbonate rocks underlying both eastern and western facies Eleana (at Shoshone Mountain and Bare Mountain/Carbonate Wash, resp.). This could provide helpful information regarding paleogeography at the time the Eleana was deposited, and constrain the amount and possibly sense of faulting that juxtaposed the two Eleana facies. (3) The source and correlation of western facies sediments. While this is by far the most interesting stratigraphic problem resulting from our work at NTS, it does not appear to have any important implications for hydrocarbon potential and so cannot be the highest priority for Task 8. (4) Well-constrained biostratigraphic dates throughout both eastern and western facies Eleana. At present, we particularly need better age control from the lower part of the western facies and the upper part of the eastern facies. In addition, we would like to find a section through the western facies that is not structurally truncated at the top, so we could date the top of the unit and see what overlies it. (5) Thorough sampling for TOC (and possibly other of organic geochemical analyses) throughout both the eastern and western facies. To be useful, this should be done on stratigraphically complete and structurally undisrupted sections.

STRUCTURAL GEOLOGY OF MISSISSIPPIAN ROCKS AT NTS

Our most significant new structural interpretation -- that eastern and western facies Eleana are structurally juxtaposed, probably along an east-dipping fault -- is also documented in our paper published this year. Significant structural observations since the publication of Cashman and Trexler (1991) are summarized briefly below:

Map relationships in the Eleana Range require a fault between the western and eastern facies along the east edge of the range. We have tentatively interpreted this fault to be an east-dipping reverse fault, based on cryptic mesoscopic structures (Cashman and Trexler, 1991). Bioclastic carbonate is present at the bottom of drillhole UE11, on the east side of Syncline Ridge. If, this is equivalent to Eleana unit i of Poole and others (1961) (which we can usually equate with the carbonate turbidite unit of the western facies Eleana), it is strong support for a low-angle, east-dipping contact between eastern and western facies.

Near its southern end, the Eleana Range bifurcates into two ridges which diverge and then converge again southward, reaching maximum separation in the vicinity of the Pahute Mesa road. Our mapping shows that western facies rocks comprise both ridges. The internal structure of each is relatively simple. The western ridge is composed primarily of the siliciclastic turbidite unit but also contains some carbonate turbidites, while the eastern ridge contains rocks of the carbonate turbidite unit exclusively. The intervening valley is underlain by eastern facies rocks. These relationships require at least one additional fault (or fold) in addition to the fundamental structure which juxtaposes eastern and western facies. Small-scale folds in the southern Eleana Range record at least two folding events. An E-verging set characterized by NNE-trending, sub-horizontal fold axes appears to be the most recent. A very preliminary interpretation of these folds is that one set may have formed during juxtaposition of eastern and western facies Eleana, and the second, NNE-trending, set may have formed during later, east-verging, folding and thrusting.

Late, brittle, low-angle faulting is present locally, and should be considered when trying to interpret rock distributions. We have found evidence for both normal and strike-slip motion along what we interpret to be late faults; much remains to be done on this faulting.

Interpretations of which Eleana facies occur(s) under Yucca Mountain must be based on extrapolation of structures and facies trends from the two closest exposures -- Calico Hills on the east and Bare Mountain on the west. The most complete section of western facies Eleana we have found occurs at Bare Mountain; the eastern facies has not been identified there. Rocks of the western facies depositionally overlie Devonian carbonates in Tarantula Canyon at Bare Mountain; this is the only known exposure of the base of the Eleana other than the base of the type section at Carbonate Wash (Poole and others, 1961). The Tarantula Canyon section also includes the entire siliciclastic turbidite unit and a thicker section of the overlying carbonate turbidite unit than we have yet seen at NTS. Both eastern and western facies Eleana occur at the Calico Hills, but only eastern facies occurs in the 2500' drillhole UE25a-3. Nitchman's field notes from a reconnaissance trip to the Calico Hills report the presence of chert litharenites (which we would now interpret as western facies rocks) structurally overlying mudstones and quartz arenites (which we would interpret as eastern facies). This is potentially an important

relationship, and is a high priority for next year's field work.

The highest priority future work on the structural geology at NTS is designed first, to determine the present position of eastern facies Eleana and second, to reconstruct the position of eastern facies Eleana through time -- for estimates of maturation history. [Note: for the time being, we are assuming that western facies Eleana is not a potential source rock; if our sampling program shows otherwise, the same kinds of structural studies must be done for western facies.] The structural topics to be addressed are: (1) The position, orientation and nature of the contact between eastern and western facies. This is the most important, but probably also the most obscure, structural contact at NTS from our point of view. Detailed surface mapping and examination of the relevant cores and drillhole records are needed to resolve this question. (2) Determine the position and orientation of the major Mesozoic compressional structures, and the amount of shortening across them. Specific projects to accomplish this include: a) map the thrust and thrust-related fold at Red Canyon along strike to the north and south; b) map the slice of Bird Spring Limestone near the southern end of the Eleana Range; c) map the contact between eastern and western facies at the Calico Hills. (3) Determine the position and orientation of Cenozoic extensional structures (note the probability of both low-angle and high-angle faults). This, too, will involve detailed mapping, both of fault geometries and of structural styles. The approach will be to document the small-scale structures associated with faults we know to be extensional features, then look for these mesoscopic structures at poorly understood contacts elsewhere. (4) Determine what Paleozoic rocks underlie the tuffs at Yucca Mountain. This requires determining what thrust sheets project under Yucca Mountain and what units (particularly what Mississippian unit(s)) occur within these thrust sheets.

Regional Stratigraphy/Paleogeography, and Our Present Thinking on Hydrocarbon Potential at Yucca Mountain

Paleozoic strata in Utah, Nevada and southern California record a west-facing, passive margin that was stable for at least 200 million years, and locally, 300 million years. From Cambrian through Devonian

time, the craton margin was dominated by a broad, carbonate-producing shelf. This cratonal stratigraphy is characterized by thick, shallow marine dolomite and limestone sections punctuated by quartz-arenite beds comprising mature sands derived from the craton interior. In easternmost Nevada and Utah, this system continued to be stable through Permian time.

Throughout most of Nevada, the passive margin was disrupted in Late Devonian by the Antler orogeny. In northern and central Nevada, the western edge of the carbonate platform foundered in the late Devonian and Mississippian, and Late Paleozoic stratigraphy is a complex interplay of foreland basin fill derived both from the east (reworked carbonate from the shelf) and west (mainly oceanic rock eroded from newly emergent highlands) (Poole, 1974; Poole and Sandberg, 1977; Johnson and others, 1991; Poole and Sandberg, 1991; Goebel, 1991). In north-central Nevada, this evolution has been attributed to the collision-obduction of the Antler allochthon along a west-dipping subduction zone that finally sutured oceanic terrane to the craton margin at the longitude of Carlin-Eureka (Poole, 1974; Smith and Ketner, 1977, 1978; Johnson and Pendergast, 1981). The final docking of the Antler allochthon against the craton margin in central Nevada is presently thought to have been complete by the early Kinderhookian (Johnson and Pendergast, 1981; Murphy and others, 1984), based on stratigraphic arguments in the Roberts Mountains and Piñon Range.

The Mississippian stratigraphy we have identified in southern Nevada differs in several important regards from that elsewhere in the state. Stevens and others (1991) note that there is no record of terrane accretion in the Mississippian rocks at this latitude. Our studies show that western facies Eleana records a Late Devonian and/or Mississippian foundering of the margin and influx of siliciclastics from an oceanic allochthon. The abrupt change from siliciclastic turbidites to calcareous turbidites in earliest Chesterian time documents a change in the sediment source for the western facies at this time. The eastern facies Eleana does not appear to be derived from the allochthon, nor does it record an early Chester deformational event. Many questions remain about stratigraphic correlations between both eastern and western facies Eleana and known Mississippian strata elsewhere in the state.

Lateral and vertical variations in the Late Paleozoic stratigraphic record are critical to the investigation of hydrocarbon potential because

these strata comprise both proven source rocks and potential reservoir rocks. Most of the hydrocarbon produced in Nevada is sourced primarily in the Mississippian Chainman Shale (French, 1983). The Chainman and its lateral equivalents have been mapped throughout southern Nevada and adjoining California (many refs., e.g., Stevens and others, 1991). The Eleana Formation is thought to be the lateral equivalent of the Chainman on NTS (Reso, 1963); we suggest that the eastern facies of the Eleana is the most likely equivalent of the Chainman and adjacent units (Cashman and Trexler, 1991).

For Task 8, the two most important questions about the Chainman-Eleana are (1) do these strata maintain their organic content (i.e., hydrocarbon source rock potential) -- known from Railroad Valley -- as they change lithofacies to the west, and (2) can we reasonably expect the Eleana to be present under Yucca Mountain? Both these questions must have a strong "yes" answer before we can reasonably pursue the question of actual hydrocarbon reservoirs under Yucca Mountain.

(1) Hydrocarbon source-potential of the Chainman-Eleana:

The Chainman Shale is known to be the source of much of the oil being produced in Railroad Valley (French, 1983; Poole and Claypool, 1984). In the Pahranaagat Mountains (the nearest accessible outcrops of Chainman east of the Nellis/NTS reserve), the Chainman has been analyzed for organic content and shown to contain quite high TOC values locally (up to 13%, Poole and Claypool, 1984). These rocks are probably thermally immature (Poole and Claypool, 1984). We in Task 8 (and our predecessor in Task 3) have analyzed a total of about thirty samples of the Eleana for TOC content, and results to date have been marginal to low. We have not undertaken a systematic sampling program since our recognition of eastern and western Eleana facies; we intend to establish a better internal stratigraphy of each facies before undertaking such a program. Our results to date are extremely limited for the western facies, and are not encouraging. We have three analyses from the western facies and three from Devonian(?) limestone probably associated with it. All have TOC < 0.55%, and are not good potential source rocks. The majority of our results to date from the eastern facies have TOC contents between 0.5% and 1.0%, with a few higher and a few lower than this range. Although these are at the low extreme of the range usually considered to be source rocks, they are reasonable background values. A program of closely spaced sampling might locate horizons higher in TOC, but we need to identify the

most complete eastern facies sections (complete both stratigraphically and structurally) before doing detailed sampling. Although the industry rule of thumb set minimum TOC for potential source rocks at 0.5% or 1.0%, Lewan (pers. comm., 1991) has shown that rocks having less than about 2.0 - 2.5% TOC will not normally generate hydrocarbons that will be expelled and migrate to other formations (see below). Based on present knowledge, then, the Eleana is not an outstanding candidate for a hydrocarbon source in southern Nevada.

(2) Is the Eleana Fm. under Yucca Mountain, and if so, which facies?

This is a difficult question to answer, because it requires interpretation of superimposed (a) facies trends, (b) compressional structures, and (c) extensional structures ... and the limited exposures mean that none of these can be done with complete confidence. There are two general interpretations at this point, and they have different implications for the nature of the Paleozoic strata under Yucca Mountain. Each will be discussed briefly below.

Stevens and others (1991) believe that the Mississippian carbonate margin is relatively intact, and facies trends on either side of Yucca Mountain can thus be projected reliably. These workers map the southeast-to-northwest Mississippian facies transition from carbonate platform to siliciclastic basin as a belt less than 20 km wide which extends from the vicinity of Las Vegas to Owens Valley. This transition zone is offset by several throughgoing, right-lateral shear zones, but strata at NTS are not thought to be affected by lateral offset. While Mesozoic thrusts can be mapped through the area (and indeed have been correlated using facies transitions (Wernicke and others, 1988)), Stevens and others (1991) do not find that these thrusts translate or telescope the Paleozoic facies long distances.

Assuming that Stevens and others (1991) are correct about the continuity of the Paleozoic margin, our present understanding of facies trends suggests that:

- * The western facies was deposited as part of a southwestern-trending transport system. It is thinning and fining in the direction of Bare Mountain, and can be expected to comprise siliceous, generally fine-grained sediments with low TOC values in the

vicinity of Yucca Mtn.

* The eastern facies is structurally adjacent to the western facies in the Eleana Range and Calico Hills, but is not present at Bare Mountain. Without local thrusting, the eastern facies equivalent should be expected well to the south of Yucca Mountain -- Stevens and others (1991) identified strata similar to the eastern facies at Indian Springs (south of Mercury) and in the Montgomery Mountains (near Pahrump).

Since the only potential source rocks we have yet analyzed are in the eastern facies, this interpretation suggests that the Yucca Mountain vicinity is a poor candidate for potential hydrocarbon reserves.

The other interpretation is that a more rigorous structural reconstruction from the Eleana Range (or preferably, the Pahranaगत Range) to Bare Mountain is needed before predicting Mississippian facies trends. Stevens and others (1991) were unaware of the existence of the western facies of the Eleana when they made their reconstructions, and so did not consider the fault that has juxtaposed the two Eleana facies. They were also unaware of recent reinterpretations of the geometry, movement sense and magnitude of Mesozoic thrusting (e.g., Caskey and Schweickert, in press) or of Cenozoic extension (e.g., Cole and others, in press). Although the extent and total offset of these structures are not well enough understood to allow a palinspastic reconstruction at present, we feel that a thorough structural analysis is mandatory for understanding current distributions of Mississippian facies.

OTHER CONSIDERATIONS

A small but vocal group of petroleum geologists is currently promoting a "thrust belt play" exploration model for use in Nevada. These workers suggest that a situation analogous to the Wyoming overthrust belt exists in the east-central and southern parts of the state. This model implies a different type of hydrocarbon trap, and a different (generally larger) reservoir volume, than the "fault block play" exploration model commonly used in Nevada to date. Task 8 will direct some future mapping toward evaluating the applicability of the thrust belt model at NTS. Detailed mapping of thrust faults to determine their regional extent, sense of motion and magnitude of slip will provide the data base to test

this model.

A new approach to source rock geochemical analysis suggests some modifications to the currently accepted criteria for evaluating source rock potential and possibly also hydrocarbon maturation. We became aware of this approach in a lecture shortly before the preparation of this report, and so have not yet researched the published literature on the subject. The following summary is based on a lecture delivered by Michael Lewan, USGS, to the Nevada Petroleum Society in November, 1991.

Lewan's approach has been to understand generation and expulsion of hydrocarbons through experiments. Traditional (anhydrous) pyrolysis techniques (e.g., Rock-Eval) use mechanisms that are very different from those in nature. Lewan has developed a hydrous pyrolysis technique which has produced hydrocarbons from known source rocks that closely resemble the naturally occurring hydrocarbons thought to be from the same source rock. Advantages of the experimental approach include the opportunity to (1) compare kerogen (the solid organic component), bitumen and oil all known to be from the same rock, and (2) examine different stages in the experimental process. Two of his most significant conclusions and their implications are:

- * During hydrocarbon generation, kerogen breaks down into bitumen, then (at higher temperatures) bitumen breaks down into oil. This is important because most models have looked for the peak breakdown of kerogen ... but in fact it is bitumen breakdown which results in the generation of oil.

- * A continuous bitumen network through the rock is necessary for the liquid oil to be expelled -- i.e., for an effective source rock. A continuous network won't exist until the rock is 2 or 2.5 wt.% TOC ... considerably higher than the 0.5 or 1% TOC commonly used as a lower limit for hydrocarbon source rocks.

REFERENCES CITED

- Carr, M.D. and Monsen, S.A., 1988, A field guide to the geology of Bare Mountain: *in* Weide, D.L. and Faber, M.L. (eds.), This Extended Land, Geological Journeys in the Southern Basin and Range, Geological Society of America, Cordilleran Section, Field Trip Guidebook, p. 50-57.
- Cashman, P.H. and Trexler, J.H., Jr., 1991, The Mississippian Antler foreland and continental margin in southern Nevada: the Eleana Formation reinterpreted: *in* Cooper, J.D. and Stevens, C.H. (eds.), Paleozoic Paleogeography of the Western United States II, Pacific Section SEPM, vol. 67, p. 271-280.
- Caskey, S.J. and Schweickert, R.A., *in press*, Mesozoic thrusting in the Nevada Test Site and vicinity -- a new perspective from the CP Hills, Nye County, Nevada: *Tectonics*
- Cole, J.C., Wahl, R.R., and Hudson, M.R., *in press*, Structural relations within the Paleozoic basement of the Mine Mountain block; implications for interpretation of gravity data in Yucca Flat, Nevada Test Site: *in* Olsen, C.L. (ed.), Proceedings of the Fifth Symposium on the Containment of Underground Nuclear Detonations: Lawrence Livermore National Laboratory Report, Conf. 89-09163, p. 431-455.
- French, D.E., 1983, Origin of oil in Railroad Valley, Nye County, Nevada: Wyoming Geological Association Earth Science Bulletin, v. 16, p. 9-21.
- Goebel, K.A., 1991, Paleogeographic setting of Late Devonian to Early Mississippian transition from passive to collisional margin, eastern Nevada and western Utah: *in* Cooper, J.D. and Stevens, C.H. (eds.), Paleozoic Paleogeography of the Western United States II, Pacific Section SEPM, vol. 67, p. 401-418.
- Johnson, J.G. and Pendergast, A., 1981, Timing and mode of emplacement of the Roberts Mountain allochthon, Antler orogeny: *Geol. Soc. America Bull.*, part I, v. 92, p. 648-658.

- Johnson, J.G., Sandberg, C.A. and Poole, F.G., 1991, Devonian lithofacies in the western United States: *in* Cooper, J.D. and Stevens, C.H. (eds.), Paleozoic Paleogeography of the Western United States II, Pacific Section SEPM, vol. 67, p. 83-106.
- Murphy, M.A., Power, J.D. and Johnson, J.G., 1984, Evidence for Late Devonian movement within the Roberts Mountain allochthon, Roberts Mountain, Nevada: *Geology*, v. 12, p.20-23.
- Poole, F.G., 1974, Flysch deposits of the Antler foreland basin, western United States: *in* Dickinson, W.R. (ed.), Tectonics and Sedimentation: SEPM Spec. Pub. no. 22, p. 58-82.
- Poole, F.G., Houser, F.N. and Orkild, P.P., 1961, Eleana Formation of the Nevada Test Site and vicinity, Nevada: USGS Professional Paper 242D, p. D104-D111.
- Poole, F.G. and Claypool, G.E., 1984, Petroleum source-rock potential and crude oil correlation in the Great Basin: *in* Woodward, J., Meissner, F.F. and Clayton, J.L. (eds.), Hydrocarbon Source Rocks of the Greater Rocky Mountain Region: Rocky Mountain Association of Geologists, Denver, CO, p. 179-229.
- Poole, F.G., and Sandberg, C.A., 1977, Mississippian paleogeography and tectonics of the western United States: *in* Stewart, J.H., Stevens, C.H., and Fritsche, A.E. (eds.), Paleozoic Paleogeography of the Western United States: Pacific Section SEPM Symposium, p. 36-65.
- Poole, F. G. and Sandberg, C.A., 1991, Mississippian paleogeography and conodont biostratigraphy of the western United States: *in* Cooper, J.D. and Stevens, C.H. (eds.), Paleozoic Paleogeography of the Western United States II, Pacific Section SEPM, vol. 67, p. 107-136.
- Reso, A., 1963, Composite columnar section of exposed Paleozoic and Cenozoic rocks in the Pahrnagat Range, Lincoln County, Nevada: Geological Society of America Bulletin, v. 74, p. 901-918.
- Smith, J.F., Jr. and Ketner, K.B., 1977, Tectonic events since the early Paleozoic in the Carlin-Pinyon Range area, Nevada: USGS Professional Paper 876-C, 18 p.

Smith, J.F. and Ketner, K.A., 1978, Geologic Map of the Carlin-Piñon Range Area, Elko and Eureka Counties, Nevada: USGS Misc. Inv. Series Map I-1028, 1:62,500.

Stevens, C.H., 1991, Summary of Paleozoic paleogeography of the western United States; *in* Cooper, J.D. and Stevens, C.H. (eds.), Paleozoic Paleogeography of the Western United States II, Pacific Section SEPM, vol. 67, p. 1-12.

Stevens, C.H., Stone, P. and Belasky, P., 1991, Paleogeographic and structural significance of an Upper Mississippian facies boundary in southern Nevada and east-central California: *Geol. Soc. America Bull.*, v. 103(7), p. 876-885.

Trexler, J.H. and Nitchman, S.P., 1990, Sequence stratigraphy and evolution of the Antler foreland basin, east-central Nevada: *Geology*, v. 18, p. 422-425.

Trexler, J.H., Jr. and Cashman, P.H., 1991, Mississippian stratigraphy and tectonics of east-central Nevada: post-Antler orogenesis; *in* Cooper, J.D. and Stevens, C.H. (eds.), Paleozoic Paleogeography of the Western United States II, Pacific Section SEPM, vol. 67, p. 331-342.

Wernicke, B., Snow, J.K. and Walker, J.D., 1988, Correlations of early Mesozoic thrusts in the southern Great Basin and their possible indication of 250 - 300 km of Neogene crustal extension: *in* Weide, D.L. and Faber, M.L. (eds.), This Extended Land: Geological Journeys in the Southern Basin and Range, GSA Cordilleran Section Field Trip Guidebook, p. 255-267.

APPENDIX: TASK 8 PUBLICATIONS 10/1/90 - 9/30/91

Publications

Cashman, P.H. and Trexler, J.H., Jr., 1991, The Mississippian Antler foreland and continental margin in southern Nevada: the Eleana Formation reinterpreted: *in* Cooper, J.D. and Stevens, C.H. (eds.), Paleozoic Paleogeography of the Western United States II, Pacific Section SEPM, vol. 67, p. 271-280.

Trexler, J.H., Jr. and Cashman, P.H., 1991, Mississippian stratigraphy and tectonics of east-central Nevada: post-Antler orogenesis; *in* Cooper, J.D. and Stevens, C.H. (eds.), Paleozoic Paleogeography of the Western United States II, Pacific Section SEPM, vol. 67, p. 331-342.

Trexler, J.H., Jr., Snyder, W.S., Cashman, P.H., Gallegos, D.M. and Spinoso, C., 1991, Mississippian through Permian orogenesis in eastern Nevada: post-Antler, pre-Sonoma tectonics of the western Cordillera: post-Antler orogenesis; *in* Cooper, J.D. and Stevens, C.H. (eds.), Paleozoic Paleogeography of the Western United States II, Pacific Section SEPM, vol. 67, p. 317-330.

Invited Abstracts and Presentations

Cashman, P.H. and Trexler, J.H., Jr., 1991, The Mississippian Antler foreland and continental margin in southern Nevada: the Eleana Formation reinterpreted (abs.): SEPM Pacific Section Program and Abstracts, p. 26.

Trexler, J.H., Jr., 1991, Unexplained deformation implied by foreland basin - craton margin stratigraphy: Early Mississippian craton margin (Stansbury Mountains) and Late Mississippian foreland basin (Diamond Mountains): invited poster presented at the Foreland Basin Penrose Conference, Can Boix, Spain

Trexler, J.H., Jr. and Cashman, P.H., 1991, Mississippian stratigraphy and tectonics of east-central Nevada: post-Antler orogenesis (abs.): SEPM Pacific Section Program and Abstracts, p. 51.

Trexler, J.H., Jr., Snyder, W.S., Cashman, P.H., Gallegos, D.M. and Spinosa, C., 1991, Mississippian through Permian orogenesis in eastern Nevada: post-Antler, pre-Sonoma tectonics of the western Cordillera: post-Antler orogenesis (abs.): SEPM Pacific Section Program and Abstracts, p. 51.

APPENDIX A

The Mississippian Antler Foreland and Continental Margin
in Southern Nevada: the Eleana Formation Reinterpreted

Patricia E. Cashman and James H. Trexler, Jr.

Department of Geological Sciences, and
Center for Neotectonic Studies,
Mackay School of Mines,
University of Nevada, Reno, NV 89557-0138

ABSTRACT

Rocks mapped as the Mississippian Eleana Formation at the type locality on the Nevada Test Site appear to comprise two completely different, but coeval, sedimentary units. In the Eleana Range ("western Eleana Formation"), the strata are siliciclastic and carbonate turbidites of Mississippian age. From immediately east of the Eleana Range to Syncline Ridge ("eastern Eleana Formation"), the strata are Devonian-Mississippian mudstone and quartzite conformably overlying Devonian limestone and underlying Pennsylvanian limestones. Although the contact between the two sedimentary packages is not exposed, small-scale structures suggest an east-dipping fault contact with reverse motion.

Sandstone petrography and stratigraphic considerations support the age data in distinguishing two separate Mississippian units. Sandstones from the western Eleana are chert litharenites with significant amounts of feldspar and both sedimentary and volcanic lithic grains. These rocks are interpreted to be a submarine fan deposit; southwest-directed paleocurrent indicators suggest that they were deposited in an elongate trough, filled axially from the northeast. The source of the sediment was the Antler allochthon and foreland basin. We tentatively correlate this section with the Dale Canyon - Chainman - Diamond Peak section near Eureka, Nevada. Sandstones from the eastern Eleana are quartz arenites with rare chert and detrital heavy minerals. These strata are tentatively interpreted to be a shelf deposit, with sediment derived from the continent to the east. We tentatively correlate this section with the Guilmette - Pilot - Chainman - Scotty Wash section of eastern Nevada. These sedimentary systems were initially separated an unknown distance across the late Paleozoic continental margin.

INTRODUCTION

Mississippian clastic rocks of the Antler foreland basin crop out in the western U.S. in a belt that extends from Idaho to southern Nevada (Fig. 1). They document emplacement of the Antler allochthon onto the carbonate-dominated western margin of North America (e.g., Nilsen and Stewart, 1980), and subsequent deformation of the foreland basin itself (Trexler and Cashman, 1990, this volume). The record of the Antler orogeny has been obscured by later deformation; late Paleozoic and Mesozoic compression, and Tertiary extension and volcanism have all overprinted any Antler structures. Detailed studies of Mississippian stratigraphy can improve our understanding of the Antler orogeny and later deformations by: documenting the compositions of the sediments, establishing the positions of the continental margin and allochthon, and constraining the timing and number of deformation events.

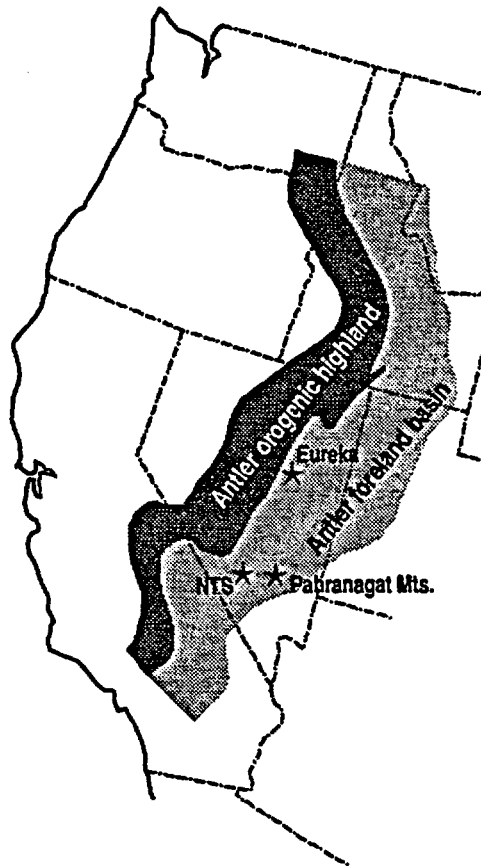


Figure 1. Location map of the western United States, showing the Antler foreland basin and localities mentioned in the text.

The name "Eleana Formation" originally was used by Johnson and Hibbard (1957) for sedimentary rocks of inferred Mississippian age at the Nevada Proving Grounds (now the Nevada Test Site, "NTS") (Fig. 2). The Eleana Formation is confined to NTS and vicinity. It crops out in the Eleana Range and its northern continuation, Quartzite Ridge, and in scattered exposures to the south and west at least as far as Bare Mountain. Equivalent-age rocks in the ranges to the north and northeast are dominantly siliciclastic, and are mapped as Joana Limestone and Chainman Shale (Quinlivan and others, 1974; Poole and Sandberg, 1977). Coeval rocks in the ranges to the south and east are dominantly carbonates, (e.g., Monte Cristo Group and Battleship Wash Formation of the Arrow Canyon Range, or Narrow Canyon Limestone, Mercury Limestone, limestone of Timpi Canyon and Chainman Shale of the Spotted Range (Poole and Sandberg, 1977)). The Eleana is lithologically diverse, and includes argillite, sandstone and distinctive chert-pebble

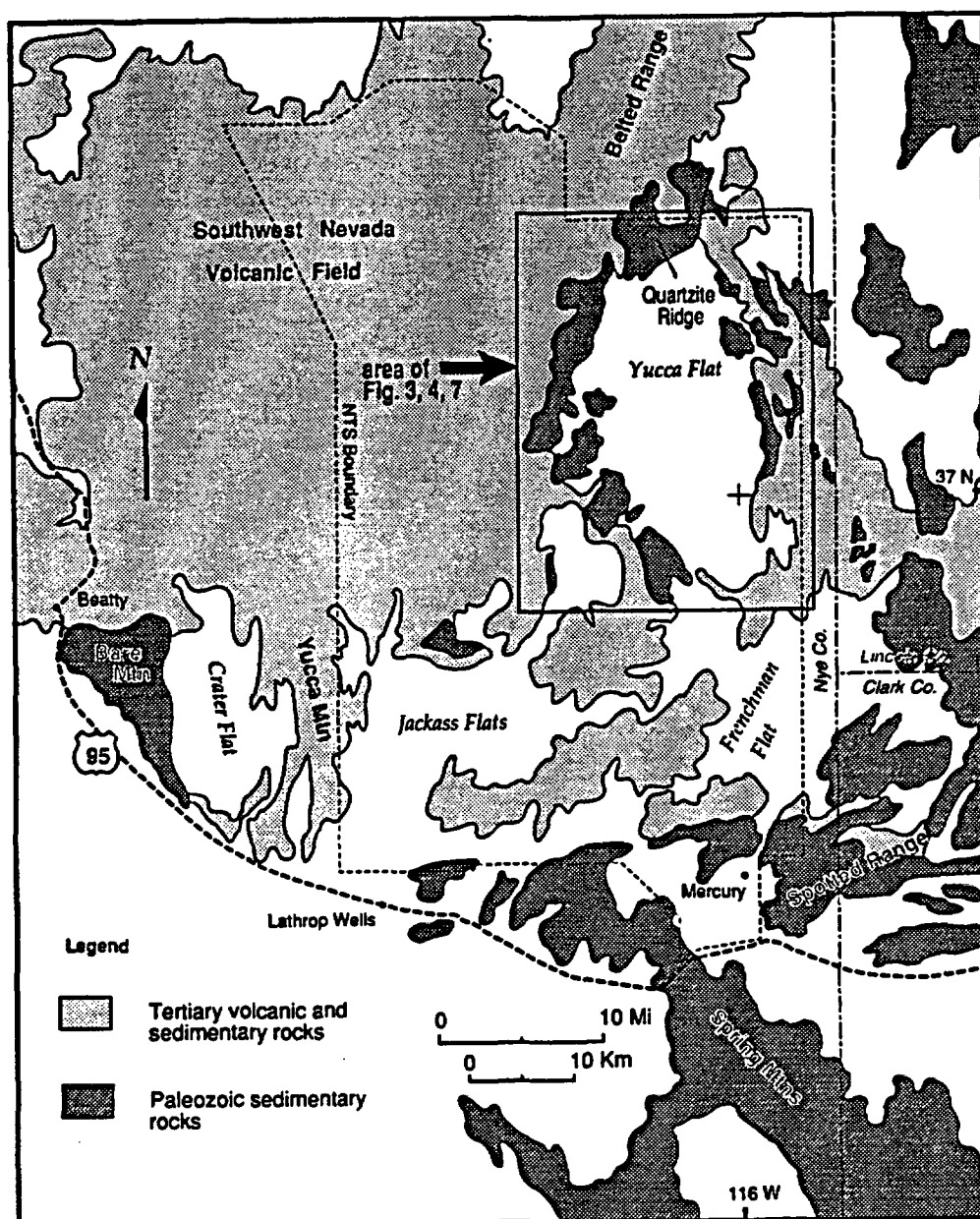


Figure 2. Generalized geologic map of the Nevada Test Site (NTS) and vicinity, southern Nevada. Area of the maps in Figures 3, 4, and 7 is shown.

conglomerate (Johnson and Hibbard, 1957). No fossils were collected in the initial study, but a Mississippian age was inferred from similarities in both lithologic characteristics and stratigraphic position to the Mississippian Chairman Shale and Diamond Peak Formation of the Eureka area to the north (Johnson and Hibbard, 1957). A stratigraphic study of the Eleana Formation by Poole and others (1961) confirmed a Mississippian age, by bracketing the Eleana between Devonian limestones below and Pennsylvanian limestones above.

The new work presented here has been aided by two factors: new biostratigraphic dating, and access to rocks that have been off-limits to most geologists for the past several decades. Our stratigraphic studies have been aided by age dates from foraminifera (Mamet and Skipp, 1970; Mamet, 1976; B. Mamet, written commun., 1989, 1990) and palynomorphs (T. Hutter, written commun., 1990)

that were not available to previous workers. These have supplemented the dates from conodonts (e.g. Sandberg and Poole, 1970) and microfossils (e.g. Reso, 1963; Gordon and Poole, 1968), and made it possible to date a wider variety of rock types. Geologic studies at NTS were possible because of renewed interest in understanding the bedrock geology near the proposed Nuclear Waste Repository at Yucca Mountain.

Our preliminary studies indicate that rocks mapped as the Eleana Formation comprise two separate, but coeval, sedimentary units. Although the interpretations are preliminary and undoubtedly will be modified by more detailed study, we present them here in the hope that they will both: (1) stimulate a more critical examination of Mississippian clastic rocks by other workers in the region, and (2) suggest a somewhat different approach to interpreting late Paleozoic paleogeography in southern Nevada.

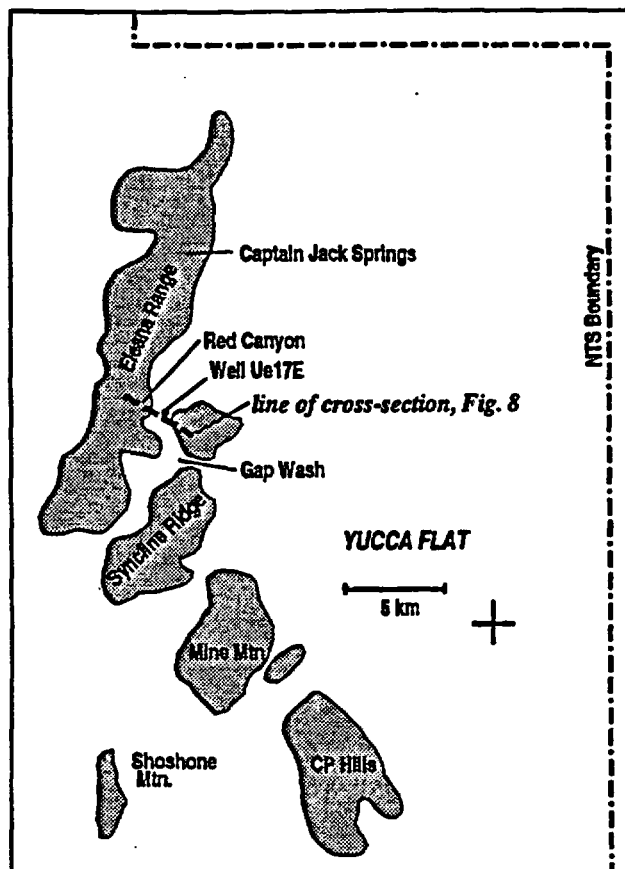


Figure 3. Map of the study area, showing localities discussed in text. Shaded areas are Paleozoic bedrock.

STRATIGRAPHY

The Eleana Formation has not been studied in detail. The original report, which included all aspects of the geology at NTS (Johnson and Hibbard, 1957), was followed by a more detailed description of the Eleana Formation by Poole and others (1961). Poole and others (1961) present a ~ 2350m- (7700'-) thick composite section through the Eleana at NTS, divided into ten lithologic units. These members are each highly variable, however, and it is not possible to map or correlate them into adjacent areas. These workers noted that their correlation between parts of the section was tentative because of structural complexities and partial cover. Subsequent work on the Paleozoic stratigraphy has been hindered by the inaccessibility of NTS and adjacent areas; newer studies have relied on remotely sensed data, and on earlier interpretations. Recent publications on the Eleana are limited to summary articles (e.g., Poole and Sandberg, 1977), geophysical studies which infer the presence of Paleozoic strata under the Tertiary tuffs (Snyder and Carr, 1982, summarized in Carr and others, 1986; Bath and Jahren, 1984), and geochemical analyses included in a study of hydrocarbon source rock potential (Poole and Claypool, 1984).

New measured sections with preliminary biostratigraphic control in the vicinity of the Eleana Range and Syncline Ridge (Fig. 3) indicate that the Eleana Formation actually consists of two lithologically dissimilar yet coeval sedimentary

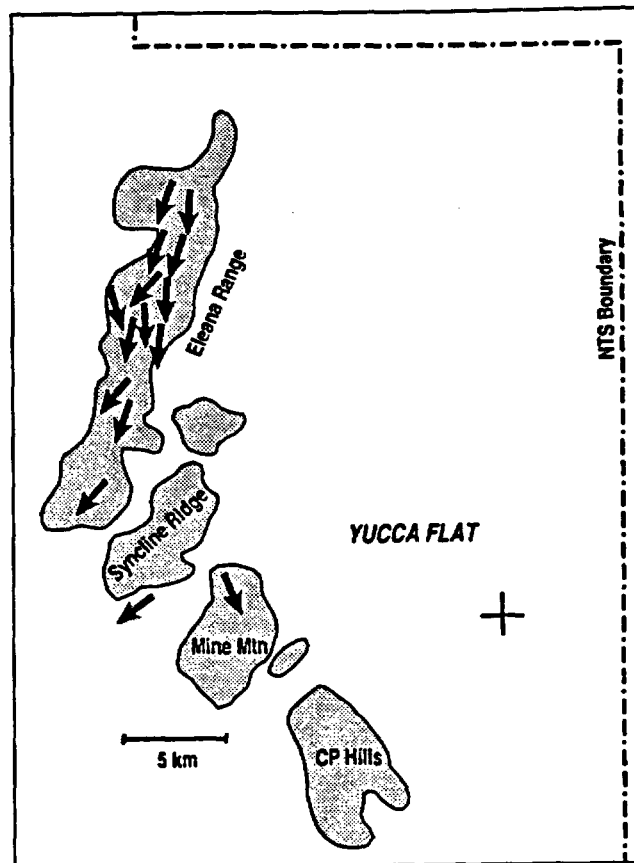


Figure 4. Paleocurrent directions from the western Eleana Formation. Paleocurrent indicators are primarily flute and tool marks, but also include planar cross-strata, channel axes or walls, and rare parting lamination. Number of measurements = 82. Note: We suspect that there are structural complications between rocks at Mine Mountain and the Eleana Range. Therefore, paleocurrent directions shown at Mine Mountain and at the southern end of Syncline Ridge may not be valid.

sections structurally juxtaposed along a previously-unrecognized fault of unknown displacement. We informally designate these two units as the "western Eleana Formation" and the "eastern Eleana Formation". As discussed below, the eastern Eleana probably should be assigned to other stratigraphic units.

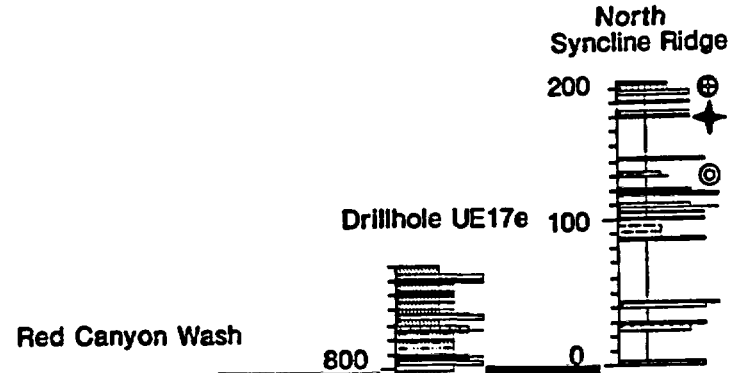
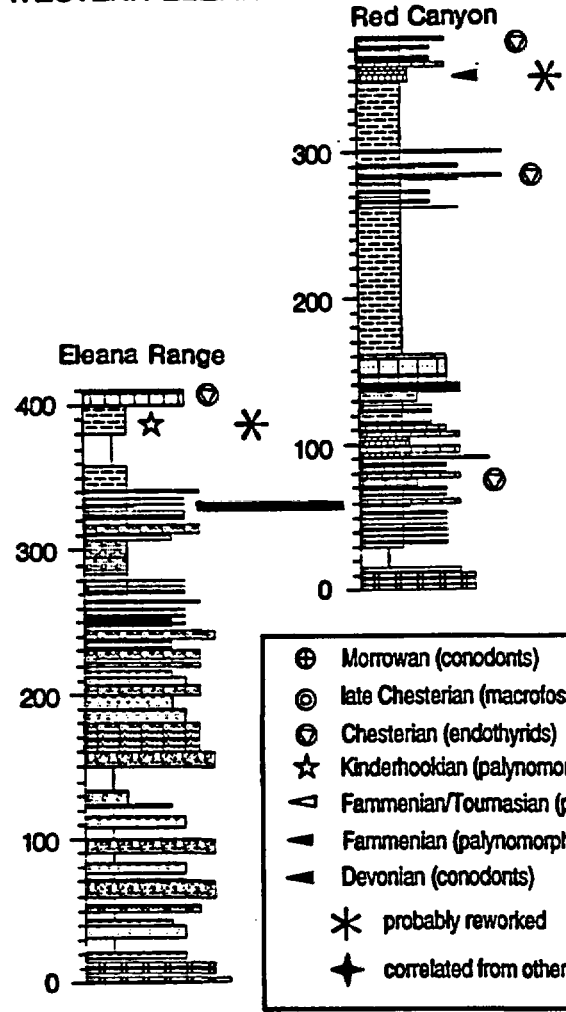
Western Eleana Formation

In the southern Eleana Range, rocks mapped as the Eleana Formation (herein referred to as western Eleana Formation) are siliciclastic and limestone turbidites of Mississippian age. Grain size ranges from siltstone to conglomerate. Siliciclastic detritus occurs throughout the section; limestone clasts and fossil debris appear abruptly in the upper part of the section. The siliciclastic turbidite interval is at least 900 m thick, and the limestone turbidite section above it is at least 300 m thick. Neither the base nor the top of this section is exposed in the southern Eleana Range.

The internal stratigraphy of the western Eleana is characterized by vertical and lateral variability. Conglomerate beds throughout the

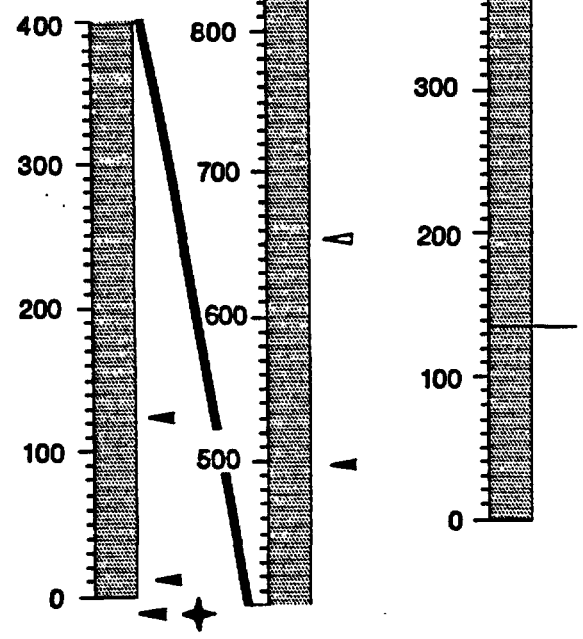
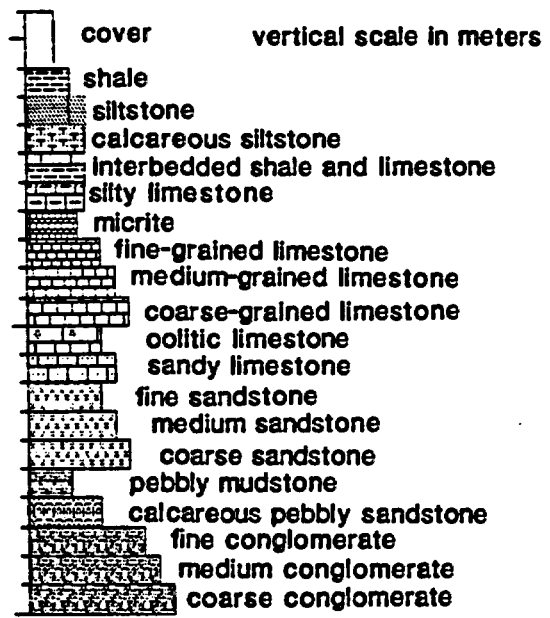
WESTERN ELEANA FORMATION

EASTERN ELEANA FORMATION



- ⊕ Morrowan (conodonts)
- ⊙ late Chesterian (macrofossils)
- ⊖ Chesterian (endothyrids)
- ★ Kinderhookian (palynomorphs)
- △ Fammenian/Tourmasian (palynomorphs)
- ▲ Fammenian (palynomorphs)
- ▲ Devonian (conodonts)
- * probably reworked
- ◆ correlated from other sections

KEY TO LITHOLOGIC SYMBOLS



8-22

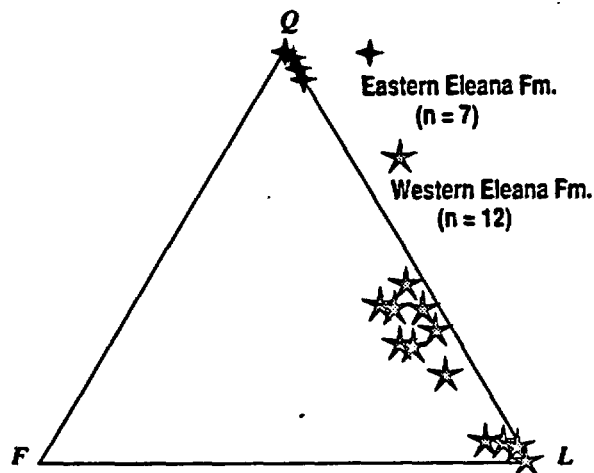
Figure 5 (opposite). Measured stratigraphic sections of the western and eastern Eleana Formation. The tie line between western Eleana sections is the first appearance of carbonate detritus in the turbidites. The tie line between the eastern Eleana sections is the lowest resistant quartz arenite bed. Locations of measured sections are on Figure 8, and the drill-hole is also shown on Figure 3.

section are laterally limited channel-fill deposits and lobes which pinch out along strikes. Litharenite beds are thin and laterally persistent. Sedimentary structures in litharenite beds include graded bedding, flute and scour structures, convolute laminae, and other features associated with turbidites. These strata have been interpreted as representing a submarine fan depositional environment (Poole and others, 1961; Nitchman, 1990). Paleocurrent indicators occur throughout both siliciclastic and carbonate turbidites; they consist primarily of flute and tool marks but also include planar cross-strata, channel axes or walls, and rare parting lineations. Paleocurrent measurements document SSW-directed transport (Fig. 4), suggesting that the submarine fan was deposited in an elongate trough which filled axially from the northeast (Nitchman, 1990).

We have attempted to date both siliciclastic and carbonate samples from the western Eleana, and have obtained several new age dates (Fig. 5). Palynomorphs from the siliciclastic rocks are not particularly diagnostic, and yield "Late Devonian - Early Mississippian" ages (T. Hutter, written commun., 1990). Endothyrids from the carbonate turbidites, however, yield consistent Chesterian (most commonly zone 16) ages (B. Mamet, written commun., 1990). Conodonts from rocks currently interpreted to be western Eleana at Mine Mountain were dated as Early Mississippian, probably Kinderhookian (unpub. report from MicroStrat, 1989). All fossils in the western Eleana section have the potential of being reworked by turbidity currents, so we place the most confidence on the youngest (Chesterian) dates.

Litharenites from the western Eleana Formation have a distinctive provenance, supporting a correlation between these rocks and the Mississippian section in central Nevada (Trexler and Cashman, this volume). The sandstone from the

Figure 6. Ternary composition plot of sandstone samples from the eastern and western Eleana.



siliciclastic turbidites is chert litharenite. These rocks contain lithic grains and significant amounts of detrital feldspar (Fig. 6). Lithic clasts include mafic and intermediate volcanic rocks, chert, argillite, and rare phyllite, schist and tectonized quartzite. These compositions, particularly when combined with the paleocurrent information, suggest that the source of the sediment was the Antler allochthon and uplifted foreland basin to the north and northwest. Therefore, we tentatively correlate the western Eleana Formation with the Dale Canyon - Chairman - Diamond Peak section (Diamond Range sequence of Trexler and Nitchman, 1990; Trexler and Cashman, 1990, and this volume) near Eureka, Nevada.

Eastern Eleana Formation

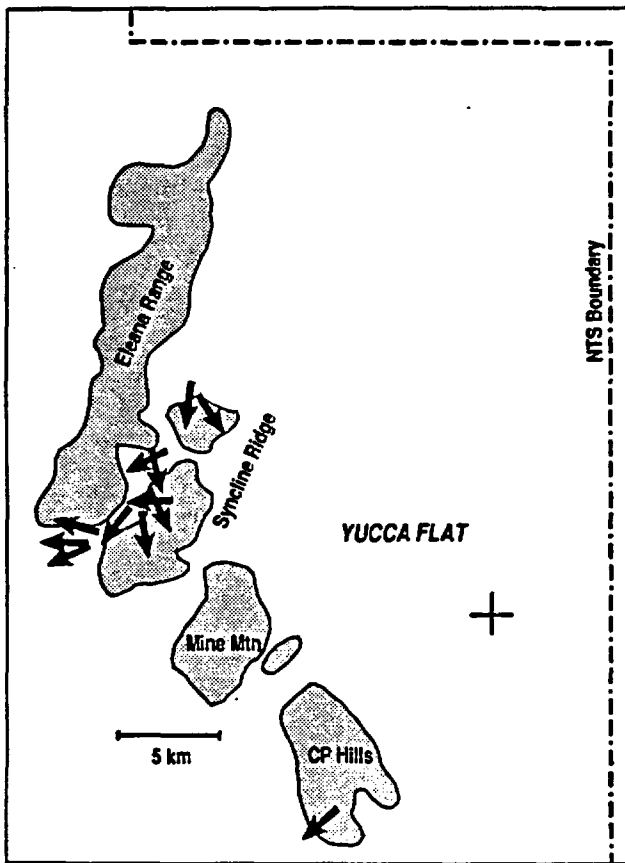
Immediately east of the Eleana Range, underlying Gap Wash and Red Canyon Wash, rocks mapped as the Eleana Formation (herein referred to as eastern Eleana Formation) are mudstone and quartz arenite. No complete section is exposed, but this unit is at least 1450 m thick (Fig. 5). Rocks tentatively interpreted to be the eastern Eleana depositionally overlie limestone mapped as Devonian Devils Gate Formation at Shoshone Mountain (Orkild, 1968). The upper contact of the eastern Eleana is gradational into the Pennsylvanian Tippipah Limestone.

Poorly exposed, dark greenish to brown mudstone dominates the eastern Eleana section. Thin quartz arenite layers occur throughout the section; these become much more common in the upper 200 m. Primary sedimentary structures are not preserved in the mudstone. Sandstone beds, particularly the thicker quartz-arenites higher in the section, have small-scale trough and planar cross-stratification, hummocky cross-stratification in places, and preserve wood debris on bedding planes. Paleocurrent indicators consist of planar and trough cross-stratification. Paleocurrent measurements show a wide range of directions, from southeast to due west (Fig. 7).

These strata are tentatively interpreted to have been deposited on a shelf. Sedimentary structures in the quartz-arenite beds suggest that deposition occurred above storm wave-base. Inter-calated marine limestone (grading upward into the Tippipah Limestone) is tentatively interpreted to have been deposited in moderately deep water (C.H. Stevens, written commun., 1990).

The eastern Eleana Formation appears to span the entire Mississippian (Fig. 5). Carbonates mapped as depositionally underlying the eastern Eleana Formation are Devonian in age (Orkild, 1968). Palynomorph dates throughout a section in Red Canyon Wash indicate a progression from Upper Devonian (Famennian) to Lower Mississippian (Kinderhookian) (T. Hutter, pers. commun., 1990). Limestones in the uppermost part of the section have been dated as Late Mississippian (latest Chesterian) and Early Pennsylvanian (Morrowan). The Mississippian dates are based on macrofossils (Gordon and Poole, 1968), and the Pennsylvanian ages on conodonts (unpub. report from MicroStrat, 1989).

The composition of sandstone from the eastern Eleana Formation is very different from that of the western Eleana Formation, indicating a separate provenance for this unit. Throughout the section,



The Figure 7. Paleocurrent directions from the eastern Eleana Formation. Paleocurrent indicators are primarily planar cross-strata, but also include trough cross-stratification. Total number of measurements = 35.

the sandstone is pure quartz arenite (Fig. 6). The only clasts other than quartz are chert and heavy minerals such as epidote and amphibole; neither of these makes up more than 2% of any sandstone. Matrix makes up much less of these rocks than it does of the western Eleana -- generally <10%. These compositional characteristics resemble those of the Scotty Wash Formation (Westgate and Knopf, 1932), exposed in the Pahranaagat Range to the northeast of NTS (Reso, 1963). The Scotty Wash is interpreted to have been deposited in a shallow, near-shore environment (Reso, 1963). We tentatively correlate the eastern Eleana Formation with the craton-derived Guilmette - Pilot - Chainman - Scotty Wash section of eastern Nevada.

In summary, the sediments of the western Eleana Formation and the eastern Eleana Formation were derived from different sources and deposited in different environments, and the available dating indicates that they were, at least in part, being deposited at the same time (i.e., Late Mississippian). Rocks previously mapped as the "Eleana Formation" therefore represent two different sedimentary systems. At the time of their formation, these sedimentary systems were separated by an unknown distance across the late Paleozoic continental margin; since that time, they have been structurally juxtaposed.

Based on our tentative correlations, it is probably desirable to retain the name "Eleana Formation" for the rocks called the western Eleana Formation in this paper. These rocks make up most of the Eleana Range, their type locality, and they have no known correlatives in the immediate vicinity. In contrast, the rocks of the eastern Eleana Formation appear to be correlative with the Scotty Wash and adjacent formations in the ranges to the east of the NTS. Contingent on mapping of units between the area we describe at NTS and the well documented stratigraphy of the Pahranaagat Range, the eastern Eleana rocks would more accurately be remapped as the Guilmette, Pilot, Chainman and/or Scotty Wash formations. Interestingly, Reso (1963, p. 912) stated that the Peers Spring, Chainman and Scotty Wash formations he mapped in the Pahranaagat Range "are probably represented in" the Eleana Formation of NTS.

STRUCTURE

Post-Mississippian deformation at NTS includes Mesozoic thrusting, Cenozoic extensional faulting, and possibly other deformational events. The Cenozoic faulting did not cause penetrative deformation or interleaving of the Mississippian section, and will not be discussed further here. The Mesozoic thrusting, however, has resulted in truncation and out-of-sequence juxtaposition of units of the Eleana Formation, so an understanding of thrust geometry is crucial to unravelling the internal stratigraphy of the Eleana. Johnson and Hibbard (1957) reported several thrust relationships in the Paleozoic strata of NTS. They estimated offset and suggested possible correlations between some of these thrusts, but did not have evidence for sense of motion on them. More recent maps (Orkild, 1963; Gibbons and others, 1963; Orkild, 1968; McKeoun and others, 1976) confirmed the thrust relationships with local revisions, but did not include discussions of thrust sense or displacement. Barnes and Poole (1968) and Hinrichs (1968) interpreted several mapped thrust faults to be parts of a single, east-vergent thrust system, the CP thrust. Current workers believe that the "CP thrust" actually includes two separate, oppositely verging thrust systems (Caskey and Schweickert, 1989; Caskey and Schweickert, in review). Mississippian rocks occur in the common footwall of these thrusts.

Our preliminary mapping of a thrust in the southern Eleana Range allows us to expand on the interpretations of Johnson and Hibbard (1957) and Orkild (1963). This thrust is a relatively small-scale feature, containing siliciclastic and carbonate turbidites of the western Eleana in both upper and lower plates. Several lines of evidence confirm eastward vergence: the thrust clearly cuts up-section to the east, and bedding orientations in the upper plate document an east-verging anticline which we interpret to be the hanging-wall portion of a faulted fault-propagation fold (Fig. 8). Bedding orientations in the lower plate are consistent with a footwall syncline, but other structural complications obscure the details of the structure of the footwall. Displacement along the thrust is approximately 1 km, based on matching of a distinctive stratigraphic horizon across the fault. At the regional scale, this is a minor feature which occurs in the footwall of the east-vergent Belted Range thrust of Caskey and Schweickert (in review).

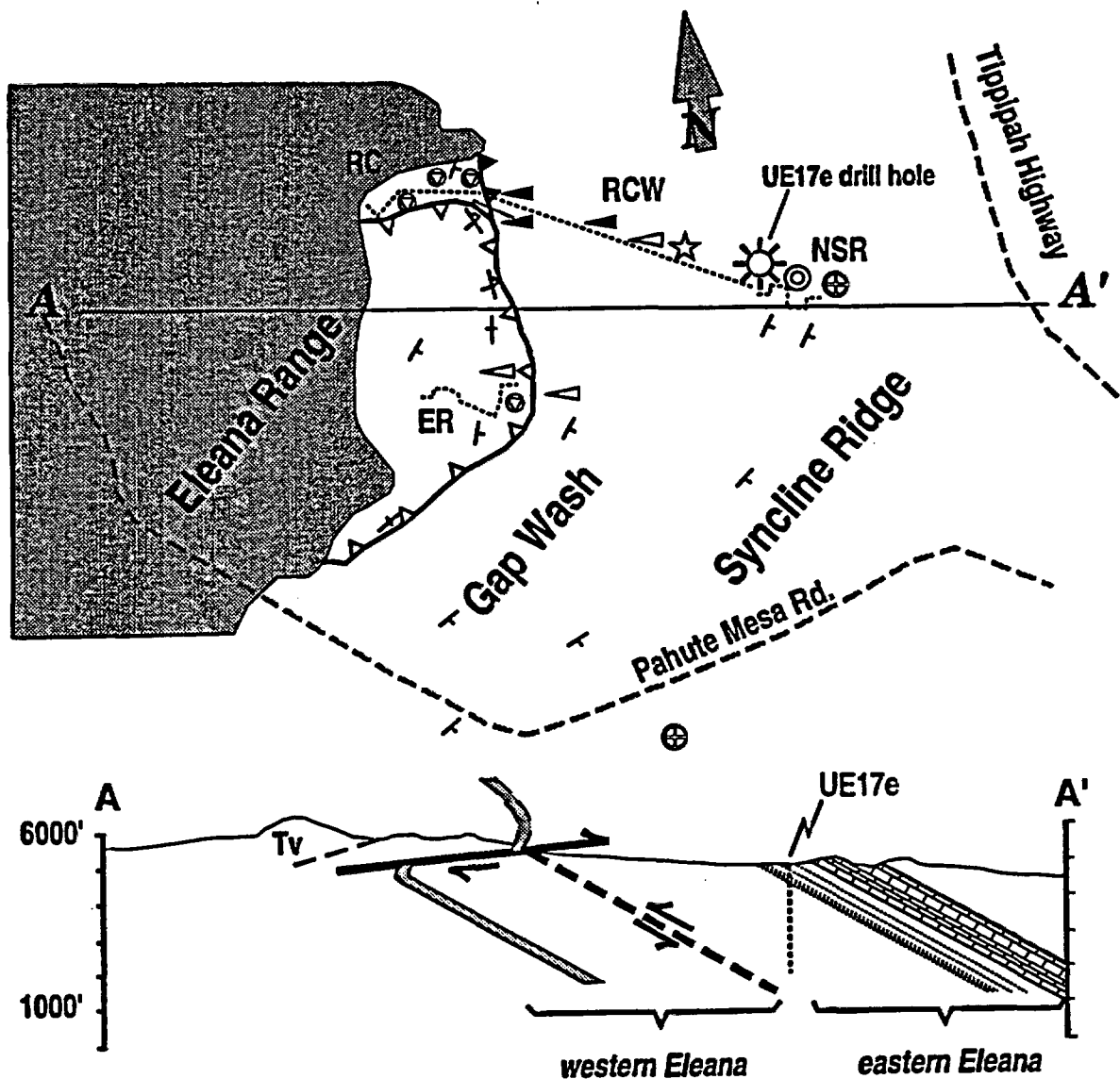


Figure 8. Diagrammatic geologic map and cross section of the southern Eleana Range and northern Syncline Ridge. Gray = Tertiary volcanic rocks. East-verging thrust is shown with open teeth, west-verging thrust with solid teeth. Dotted lines are measured section traverses, with labels: ER = Eleana Range section, RC = Red Canyon section, RCW = Red Canyon Wash section, NSR = north Syncline Ridge section. Symbols for age dates are the same as on Figure 5. Representative strikes and dip symbols are from our mapping, and from Orkild (1963). Vertical scale in the cross-section is not exaggerated.

The contact between the eastern Eleana Formation and western Eleana Formation is not exposed, but small-scale structures near the contact suggest reverse motion along an east-dipping fault (Fig. 8). The strike ridges of the Eleana Range (western Eleana) and Syncline Ridge (eastern Eleana) clearly converge southward, requiring that part of the lower eastern Eleana be cut out; the proposed fault explains this observation in addition to explaining the stratigraphic juxtaposition described above. The clastic rocks on both sides of the fault are east-dipping and generally conformable, so they were previously interpreted to be a continuous (presumed Mississippian) section (Johnson and Hibbard, 1957; Poole and others, 1961; Nitchman, 1990). The mudstones of the eastern Eleana Formation are not penetratively deformed, either in

the scattered exposures in Red Canyon Wash, or in a core obtained from drillhole UE-17e (Fig. 5) that includes the upper 870m of the ~ 1450 m section. A penetrative cleavage is developed, however, in the closest outcrop to the contact with the western Eleana Formation, near the mouth of Red Canyon. This outcrop is characterized by boudinage and disrupted west-vergent folds in thin sandstone beds, steeply east-dipping slaty cleavage that is axial planar to the folds in the mudstone beds, and planar jointing perpendicular to the fold hingelines (Fig. 9). All of these structures document shortening in the plane of the foliation and extension in the direction of the fold hingelines. The asymmetry of the folds suggests a component of east-over-west simple shear (i.e., reverse motion) along an east-dipping surface. We have done very

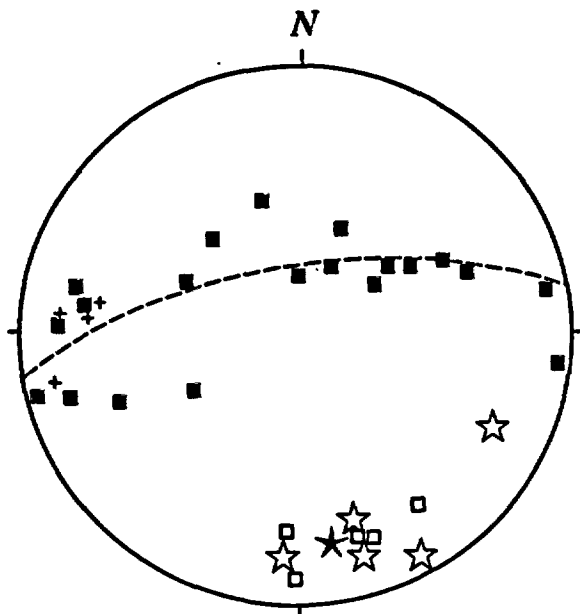


Figure 9. Stereogram (equal area) of small-scale structures near the western Eleana/eastern Eleana contact. Computed fold axis (solid star) plunges 20° toward 171° . Filled squares = poles to bedding; pluses = poles to foliation; open squares = poles to joints in sandstone; open stars = measured hingelines.

little structural work to date, and therefore have little evidence for the age of this deformation or for its occurrence elsewhere at NTS. Our map relations (Fig. 8) suggest that the juxtaposition of eastern and western Eleana pre-dates the east-vergent thrust in the western Eleana. (Note that present evidence for the timing of deformation precludes correlation of this west-verging thrust with the west-verging CP thrust system described by Caskey and Schweickert (in review).) We have no other evidence for the timing, and Paleozoic deformation cannot be ruled out. Nilsen (1977) described a very similar facies juxtaposition in Idaho, and interpreted the contact to be an east-verging thrust. In this Idaho example, sediments derived from the thrust plate are thought to be Late Mississippian in age; the thrusting is therefore thought to have occurred in early Late Mississippian time (Nilsen, 1977).

DISCUSSION

The western Eleana Formation apparently records both Early Mississippian (Roberts Mountains phase) and Late Mississippian (Christina Peak phase) deformation (Trexler and Cashman, this volume). The Antler peripheral foreland basin, caused by obduction of the Antler allochthon, may be represented here by the siliciclastic turbidite section of the western Eleana. These rocks are thought to occupy a narrow, axial trough filled by turbidity currents forming a southern lobe of the submarine fan system to the north (the Diamond Range sequence of Trexler and Nitchman, 1990) (Trexler and Cashman, 1990). Alternatively, these siliciclastic sediments may have been reworked from the Diamond Range sequence in central Nevada as it was uplifted in late Meramecian time. Resolution of these alternatives requires better age control of the western Eleana strata.

In late Meramecian (Late Mississippian) time, the Antler foreland basin was uplifted and deformed in central Nevada (the Christina Peak phase) followed by erosion and gradual subsidence (Trexler and Cashman, this volume). In central Nevada, deposition of the siliciclastic Newark Valley sequence accompanied post-deformation subsidence. This consisted of fluvial and deltaic sedimentation, gradually succeeded by carbonate sedimentation on a shallow marine platform. The first appearance of carbonate turbidites in the western Eleana Formation correlates well with the deposition of the basal Newark Valley sequence - both are early Chesterian in age (B. Mamet, written commun., 1990). The SSW-directed paleocurrents in the western Eleana Formation also support the conclusion that central Nevada was the source of carbonate as well as siliciclastic western Eleana Formation sediment. Interestingly, the eastern Eleana Formation does not contain sedimentological evidence of the Christina Peak phase of deformation and basin subsidence.

Re-examination of all rocks mapped as Eleana Formation will be necessary, in order to determine which have cratonic affinities (i.e., are part of the eastern Eleana Formation) and which have affinities to the allochthon and foreland basin (i.e., are part of the western Eleana Formation). Such a re-examination will result in a better understanding of the Mississippian continental margin, and of the geometry and extent of deformation related to (1) the Antler orogeny, and (2) other late Paleozoic deformational events.

A better understanding of Mississippian stratigraphy in southern Nevada also will aid in structural interpretations: at present, very little is known about the fault that juxtaposes the eastern Eleana and western Eleana, but mapping of these as different units will reveal the position and orientation of this fault, and may constrain its displacement and timing. In addition, a detailed internal stratigraphy of the western Eleana Formation, in particular, may provide markers which can be used to reconstruct both Mesozoic (compressional) and Cenozoic (extensional) deformation.

In conclusion, a reinterpretation of the Eleana Formation, dividing it into two partially coeval units with different provenances and depositional environments, has resulted in: (1) a better explanation of the geologic relationships in the vicinity of the Eleana Range, (2) testable predictions about Mississippian stratigraphy in southern Nevada, and (3) a new framework for evaluating other aspects of both structure and late Paleozoic stratigraphy in southern Nevada. We suggest that the name "Eleana Formation" be restricted to the rocks containing chert litharenites (i.e., to the unit we have termed the western Eleana Formation, and have interpreted to be derived from the Antler allochthon and foreland basin). We suggest that the rocks characterized by quartz arenites (i.e., the unit we have termed the eastern Eleana Formation and interpreted to be derived from the craton) be mapped as Guilmette, Pilot, Chainman and/or Scotty Wash, depending on detailed correlations with the well described Paleozoic section to the east of NTS.

ACKNOWLEDGMENTS

This work was funded by a grant to the Center for Neotectonic Studies, University of Nevada, from the Nuclear Waste Project Office, State of Nevada. The stratigraphic sections on which our interpretation is based were measured by S.P. Nitchman, a student research assistant funded by this NWPO grant. Access to the log and core from drillhole #UZ-17a was aided by Jerry Wagner of the U.S. Geological Survey Core Library and Data Center at Mercury, Nevada. Sample locations and conodont age and CAI data were provided by Anita Harris, U.S. Geological Survey, Reston, Virginia. Our understanding of Paleozoic stratigraphy and Mesozoic structure in southern Nevada was substantially improved by discussions with M.J. Silberling, K.M. Nichols, R.A. Schweickert, S.J. Caskey, and A.S. Jayko. A draft of this manuscript was improved by reviews from M.J. Silberling and C.H. Stevens.

REFERENCES CITED

- Bath, G.D., and Jahren, C.E., 1984, Interpretations of magnetic anomalies at a potential repository site located in the Yucca Mountain area, Nevada Test Site: U.S. Geological Survey Open-File Report OFR-84-120.
- Barnes, H., and Poole, F.G., 1968, Regional thrust-fault system in Nevada Test Site and vicinity, in Eckel, E.G., ed., Nevada Test Site: Geological Society of America Memoir 110, p. 233-238.
- Carr, M.D., Waddell, S.J., Vick, G.S., Stock, J.M., Monsen, S.A., Harris, A.G., Cork, B.W., and Byers, F.M., Jr., 1986, Geology of drill hole UE25p#1: a test hole into pre-Tertiary rocks near Yucca Mountain, southern Nevada: U.S. Geological Survey Open-File Report OF-86-175, 87 p.
- Caskey, S.J., and Schweickert, R.A., 1989, Mesozoic west-vergent thrust in the CP Hills, Nevada Test Site, Nye County, Nevada: Geological Society of America Abstracts with Programs, v. 21, p. 64.
- _____, in review, Mesozoic thrusting in the Nevada Test Site and vicinity - a new perspective from the CP Hills, Nye County, Nevada: submitted to Tectonics.
- Gibbons, A.B., Hinrichs, E.M., Hansen, W.R., and Lemke, R.W., 1963, Geology of the Rainier Mesa quadrangle, Nye County, Nevada: U.S. Geological Survey Map GQ-215, scale 1:24,000.
- Gordon, M., Jr., and Poole, F.G., 1968, Mississippian - Pennsylvanian boundary in southwestern Nevada and southeastern California: Geological Society of America Memoir 110, 157 p.
- Hinrichs, E.M., 1968, Geologic structure of Yucca Flat area, Nevada, in Eckel, E.G., ed., Nevada Test Site: Geological Society of America Memoir 110, p. 239-246.
- Johnson, M.S., and Hibbard, D.E., 1957, Geology of the Atomic Energy Commission Nevada proving grounds area, Nevada: U.S. Geological Survey Bulletin 1021K, 333p.
- McKeown, F.A., Healey, D.L., and Miller, C.H., 1976, Geologic map of the Yucca Lake quadrangle, Nye County, Nevada: U.S. Geological Survey Map GQ-1327, scale 1:24,000.
- Mamet, B.L., 1976, An atlas of microfacies in Carboniferous carbonates of the Canadian Cordillera: Geological Survey of Canada Bulletin 255, 131 p.
- Mamet, B.L., and Skipp, B., 1970 Lower Carboniferous calcareous foraminifera: preliminary zonation and stratigraphic implications for the Mississippian of North America, in Compte Rendu Sixième Congrès International de Stratigraphie et de Géologie du Carbonifère, Sheffield, v. 3, p. 1129-1146.
- Nilsen, T.H., 1977, Paleogeography of Mississippian turbidites in south-central Idaho: in Stewart, J.H., Stevens, C.H., and Fritsche, A.E. eds., Paleozoic paleogeography of the western United States: Los Angeles, Pacific Section, Society of Economic Paleontologists and Mineralogists Pacific Coast Paleogeography Symposium I, p. 275-299.
- Nilsen, T.H., and Stewart, J.H., 1980, The Antler Orogeny - mid-Paleozoic tectonism in western North America: Geology, v.8, p. 298-302.
- Nitchman, S.P., 1990, Depositional environments of the Mississippian Eleana Formation, Nevada Test Site, Nye County, Nevada: Geological Society of America Abstracts with Programs, v. 22, p. 73.
- Orkild, P.F., 1963, Geologic map of the Tippipah Spring quadrangle, Nye County, Nevada: U.S. Geological Survey Map GQ-213, scale 1:24,000.
- _____, 1968, Geologic map of the Mine Mountain quadrangle, Nye County, Nevada: U.S. Geological Survey Map GQ-746, scale 1:24,000.
- Poole, F.G., and Claypool, G.E., 1984, Petroleum source-rock potential and crude oil correlation in the Great Basin, in Woodward, J., Meissner, F.F. and Clayton, J.L., eds., Hydrocarbon source rocks of the greater Rocky Mountain Region: Denver, Rocky Mountain Association of Geologists, p. 179-229.
- Poole, F.G., Houser, F.N., and Orkild, P.F., 1961, Eleana Formation of Nevada Test Site and vicinity, Nevada: U.S. Geological Survey Professional Paper 424-D, p. D104 - D111.
- Poole, F.G., and Sandberg, C.A., 1977, Mississippian paleogeography and tectonics of the western United States, in Stewart, J.H., Stevens, C.H., and Fritsche, A.E. eds., Paleozoic paleogeography of the western United States: Los Angeles, Pacific Section, Society of Economic Paleontologists and Mineralogists Pacific Coast Paleogeography Symposium I, p. 67-85.
- Quinlivan, W.D., Rogers, C.L., and Dodge, H.W., Jr., 1974, Geologic map of the Portuguese Mountain quadrangle, Nye County, Nevada: U.S. Geological Survey Miscellaneous Investigations Map I-804, scale 1:48,000.
- Reso, A., 1963, Composite columnar section of exposed Paleozoic and Cenozoic rocks in the Fahrangat Range, Lincoln County, Nevada: Geological Society of America Bulletin, v. 74, p. 901-918.
- Sandberg, C.A., and Poole, F.G., 1970, Conodont biostratigraphy and age of West Range Limestone and Pilot Shale at Bactrian Mountain, Fahrangat Range, Nevada: Geological Society of America Abstracts with Programs, v. 2, p.139.

- Snyder, D.B., and Carr, W.J., 1982, Preliminary results of gravity investigations at Yucca Mountain and vicinity, southern Nye County, Nevada: U.S. Geological Survey Open File Report OF-82-701, 36p.
- Trexler, J.H., Jr., and Nitchman, S.P., 1990, Sequence stratigraphy of the Antler foreland basin, east-central Nevada: *Geology*, v. 18, p. 422-425.
- Trexler, J.H., Jr., and Cashman, P.H., 1990, The Diamond Mountain phase of the Antler orogeny: Late Mississippian compressional deformation in east-central Nevada: *Geological Society of America Abstracts with Programs*, v.22, p. A274.
- Wernicke, B., Snow, J.K., and Walker, J.D., 1988, Correlations of early Mesozoic thrusts in the southern Great Basin and their possible indication of 250 - 300 km of Neogene crustal extension: in Weide, D.L., and Faber, M.L., eds., *This Extended Land: Geological Society of America Cordilleran Section Field Trip Guidebook, Geological Journeys in the Southern Basin and Range*, p. 255-267.
- Westgate, L.G., and Knopf, A., 1932, *Geology and mineral deposits of the Pioche District, Nevada*: U.S. Geological Survey Professional Paper 171, 79 p.

APPENDIX B

MISSISSIPPIAN STRATIGRAPHY AND TECTONICS OF EAST-CENTRAL NEVADA:
POST-ANTLER OROGENESIS

James H. Trexler, Jr. and Patricia M. Cashman

Department of Geological Sciences, and
Center for Neotectonic Studies
Mackay School of Mines
University of Nevada, Reno
Reno, NV 89557-0138

ABSTRACT

Mississippian strata in central Nevada record two tectonic phases: the Roberts Mountains phase which is the latest part of the larger-scale Antler orogeny, and the Christina Peak phase which we interpret as a post-Antler episode of folding, uplift, erosion, and basin subsidence. The Roberts Mountains phase involved obduction of allochthonous strata from the west onto the continental margin, accompanied by down-flexing of the craton margin due to loading. The Antler foreland basin subsided rapidly, and received submarine fan sediments (Diamond Range sequence) from the Antler highlands to the west. The Christina Peak phase deformed Diamond Range sequence strata. It documents eastward migration of deformation, involving broad folding and uplift in the vicinity of the Diamond Mountains. Subsidence of the successor basin was slow and probably isostatic. The resulting strata (Newark Valley sequence) represent a marine transgression over a fluvial and deltaic environment, and establishment of a shallow-marine, carbonate-dominated seaway between the low-lying Antler highlands and the craton. Siliciclastic sediments in this successor basin were derived both from the craton to the east, and from locally uplifted and eroded Antler foreland strata to the west.

INTRODUCTION

The late Paleozoic continent margin of the western Cordillera is often characterized as having a long history of terrane-accretion. West-dipping subduction (Speed and Sleep, 1982) of the early and middle Paleozoic passive margin resulted in structural juxtaposition of oceanic and cratonal rocks (Dickinson, 1977). Major episodes of allochthon obduction occurred at the beginning and end of this collisional history: the Devonian-Mississippian Antler orogeny, and the Permo-Triassic Sonoma orogeny. Deformation continued between these two obduction events. The detailed tectonic history of the Mississippian through Permian craton margin is only beginning to be understood, but can be viewed as a series of tectonic phases (Trexler and others, 1990; this volume).

Mississippian stratigraphy in the Diamond Mountains records two distinct tectonic episodes: the Roberts Mountains phase, which represents the final emplacement of the Antler allochthon in the Early Mississippian, and the Christina Peak phase, which was a folding and uplift episode in the Late Mississippian. Each tectonic pulse resulted in formation of a sedimentary basin with distinctive characteristics related to the setting in which it formed. The detailed stratigraphy of these two basins is the key to understanding the timing and style of this tectonism.

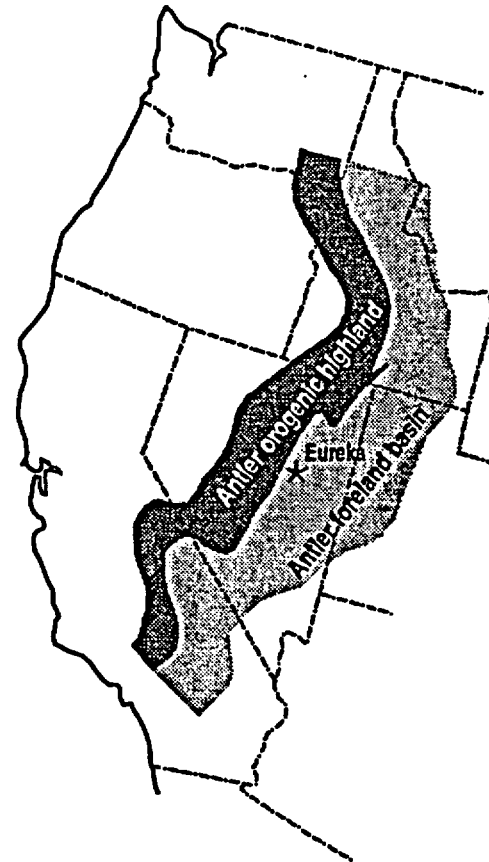


Figure 1. The Antler orogenic belt in the western United States.

THE ROBERTS MOUNTAINS PHASE

The Antler orogeny was originally designated as comprising all Devonian-Mississippian orogenic activity (Roberts and others, 1958; Johnson, 1971). However, many workers now restrict the definition to the obduction of allochthonous oceanic strata onto the North American craton margin in Late Devonian to Early Mississippian time (Nilson and Stewart, 1980). Obduction probably was complete by early Kinderhookian time (Johnson and Fendergast, 1981; Murphy and others, 1984), although many workers suggest later reactivation along the fault contact (i.e., Roberts Mountains thrust and related structures; Ketner and Smith, 1982; Stahl, 1989). Following the scheme of Trexler and others (1990), we refer to the actual emplacement of the allochthon as the Roberts Mountains phase.

The Diamond Range Sequence

The most obvious stratigraphic result of Early Mississippian thrusting was thrust-induced subsidence which created a peripheral foreland basin (Fig. 1). In central Nevada, this was a marine basin that received sediments shed from highlands in the allochthonous terranes to the west (Sadlick, 1960; Poole, 1974; Poole and Sandburg, 1977). In the vicinity of Eureka, Nevada (Fig. 2, 3), basin fill comprising strata of the Dale Canyon Formation, the Chainman Shale, and in some places part of the Diamond Peak Formation is interpreted as a submarine fan sequence (Fig. 4). This, the original foreland-basin fill, is the Diamond Range sequence (Trexler and Nitchman, 1990).

Stratigraphy and Age Control

The Diamond Range sequence is defined as the west-derived submarine fan systems tract within the Antler foreland basin in central Nevada (following the definition of "sequence" by Mitchum and others,

Figure 2. Location map of the Diamond Mountains and vicinity, east-central Nevada. Measured sections (Fig. 6) are in boxes. Major stratigraphic boundaries are shown; see geologic map (Fig. 5).

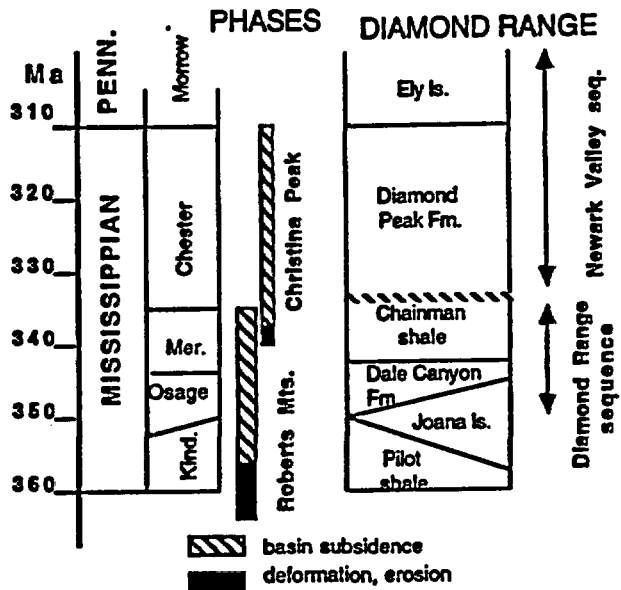
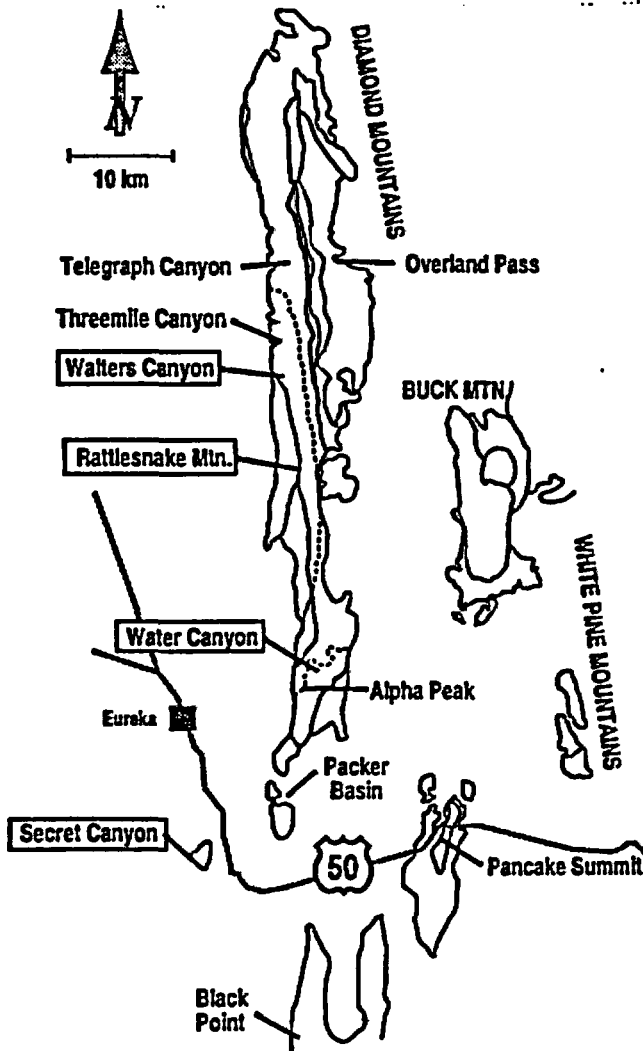


Figure 3. Schematic Mississippian stratigraphy along the Antler foreland-basin belt. Tectonic phases from Trexler and others (1990; this volume). Stratigraphy after Poole (1974, 1976); and Trexler and Nitchman, 1990.

1977). The base of the Diamond Range sequence is the base of the Chainman Shale, or the Dale Canyon Formation where it occurs (Fig. 3, 4). The lower Chainman Shale in the Diamond Range has been dated as early Osagean based on palynomorphs (T. Hutter, written commun., 1989). The Dale Canyon Formation, which has been identified in the southern Diamond Range and in the southern Pinon Range to the northwest of the study area, but does not occur in the central and northern Diamond Range, is Kinderhookian to Osagean in age (Visconti, 1983). In the Diamond Mountains the basal contact of the sequence is conformable on the Joana Limestone or the Pilot Shale.

Strata below the Diamond Range sequence are related to the craton to the east. The Joana Limestone in the Diamond Mountains is Kinderhookian in age (K. Goebel, pers. commun., 1990) and consists of bioclastic limestone turbidites which have been correlated with the Tripson Pass Limestone (Poole and Claypool, 1984). The Joana Limestone was shed from a carbonate platform, westernmost outcrops of which occur in the Pancake Range, where the platform rocks also are mapped as Joana (K. Goebel, pers. commun., 1990). The Pilot Shale was derived from the craton, and may represent sedimentation down a westward-steepening off-shore slope (Poole, 1974, 1977).

The Diamond Range sequence in the Diamond Range comprises a minimum of 1000 and not more than 1800 m of mudrock and siltstone, punctuated by intervals of litharenite and conglomerate (Fig. 6). With the exception of Dale Canyon litharenite, coarse intervals are traceable for a few kilometers at most along strike, and are not persistent enough to be useful for correlation.

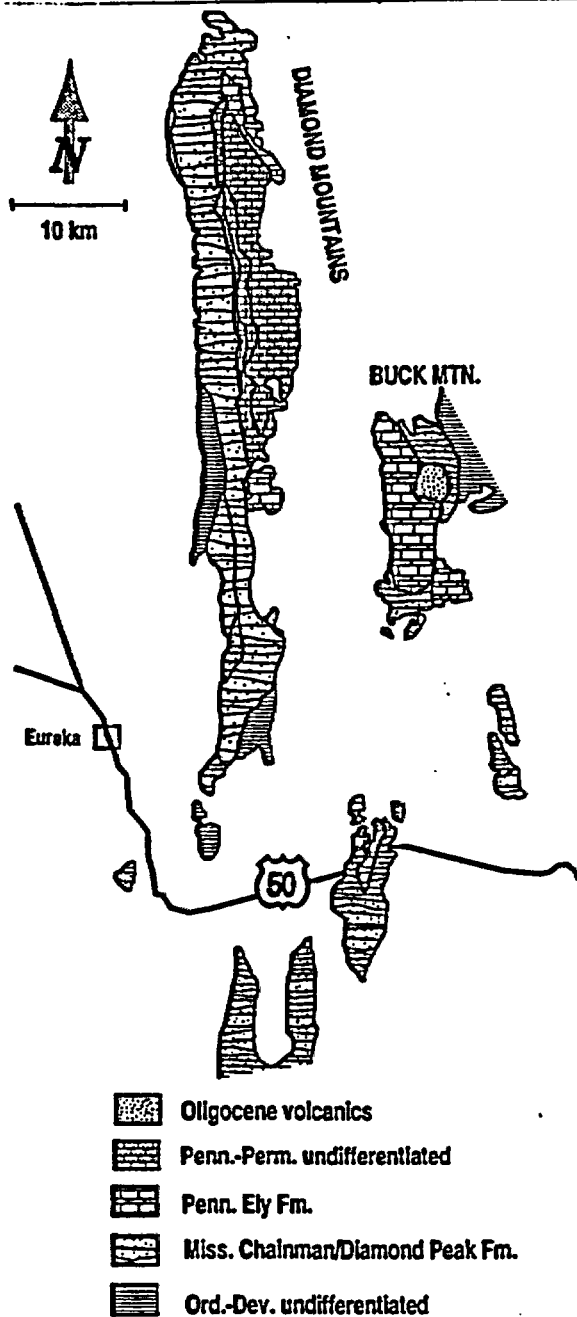


Figure 4. Generalized geologic map of the Diamond Mountains and vicinity (after Roberts and others, 1967; Hoss and Blake, 1976).

The Diamond Range sequence, which is folded and erosionally truncated, is overlain unconformably by the Newark Valley sequence (Fig. 5). The youngest ages obtained from the Diamond Range sequence are middle-upper Osagean (T. Hutter, written commun., 1989). Because of the angular nature of the upper unconformity, it is impossible to determine the age of the top of the Diamond Range sequence here.

Most of the Diamond Range sequence in the Diamond Mountains is mapped as Chainman Shale (Fig. 4, 5), but locally the upper part of the sequence

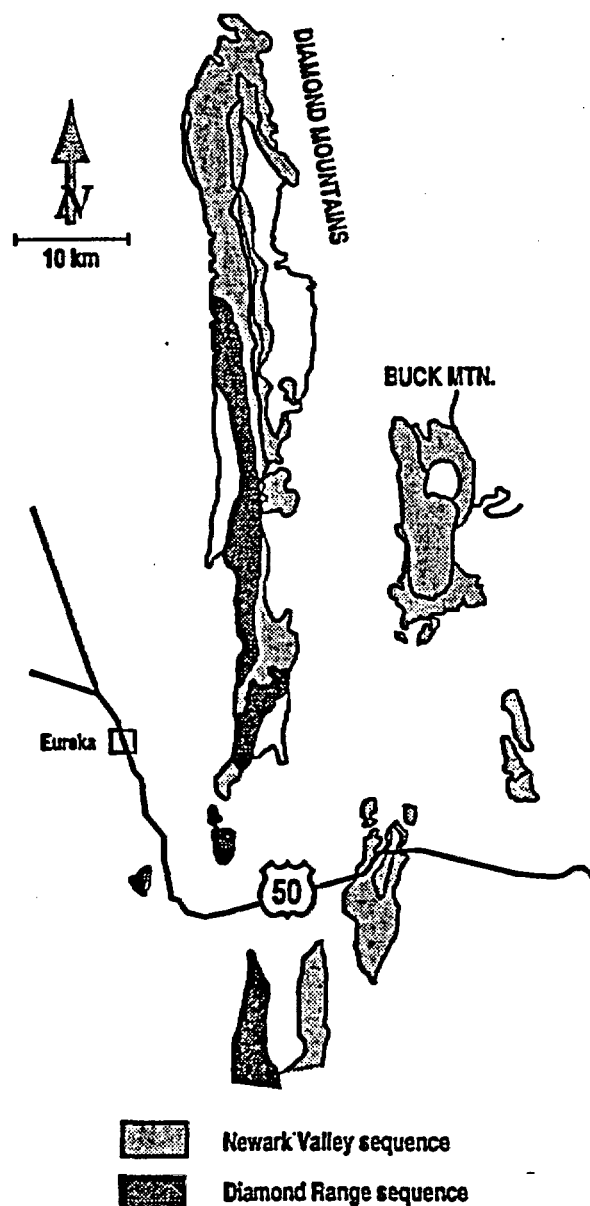
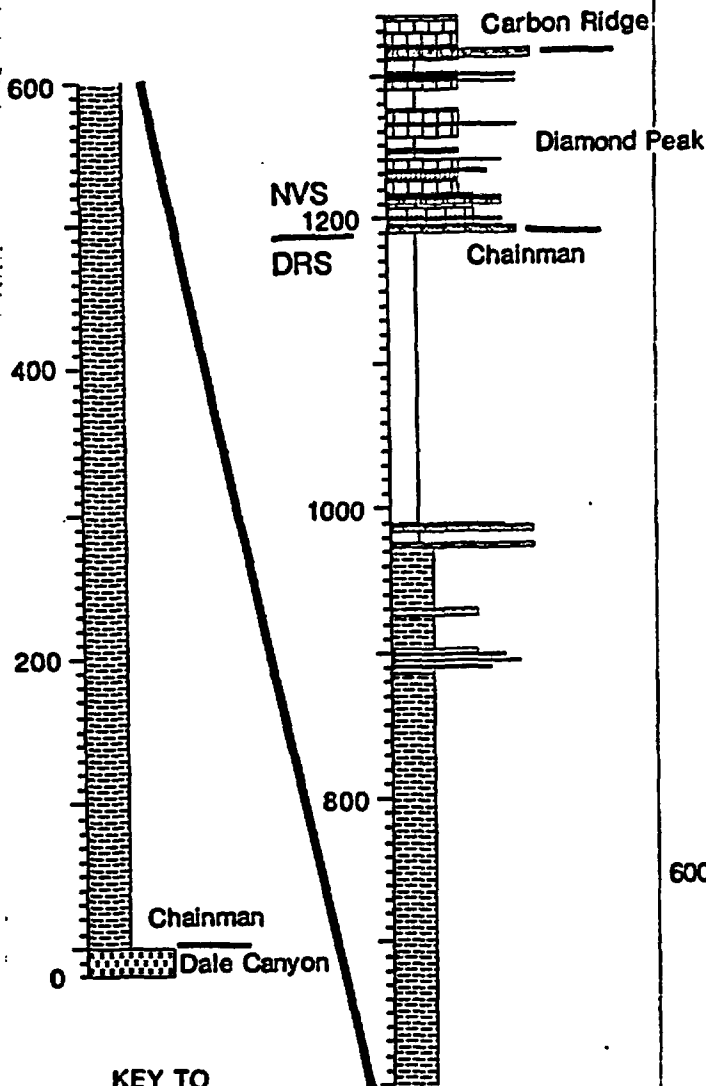


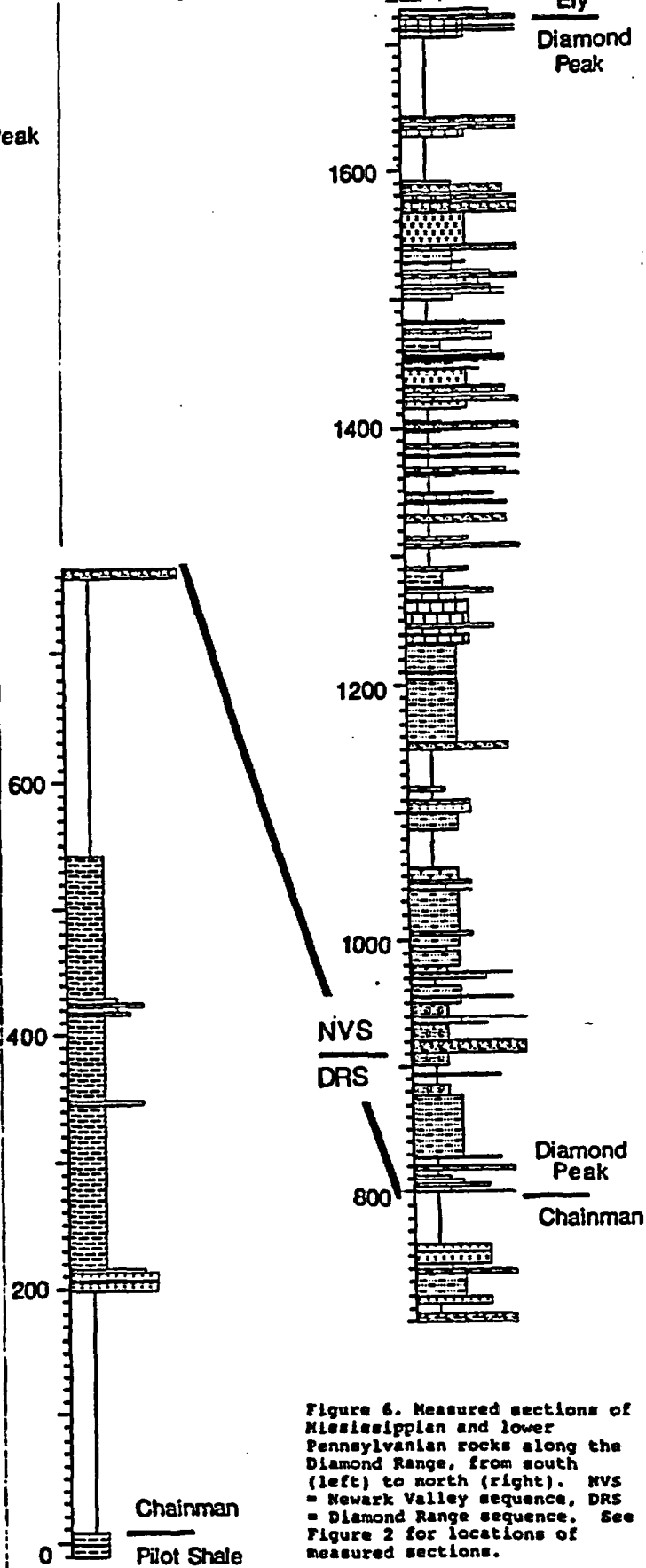
Figure 5. Geologic map of the Diamond Mountains, showing the Dale Canyon Formation, Chainman Shale, Diamond Peak Formation, and Ely Limestone, here remapped as the Diamond Range sequence and the Newark Valley sequence.

includes the Diamond Peak Formation. The base of the Diamond Peak Formation commonly is placed at the base of the lowest prominent conglomerate. This contact rarely coincides with the unconformity at the top of the sequence, which may occur either above or below the lowest conglomerate. In places where coarse clastic rocks first appear low in the section, such as at Walters Canyon (Fig. 6), the base of the Diamond Peak Formation is mapped below the sequence boundary. At Rattlesnake Mountain, the sequence boundary occurs in a mostly fine-grained interval and the lowest conglomerate occurs well within the overlying Newark Valley sequence

Secret Canyon



Water Canyon

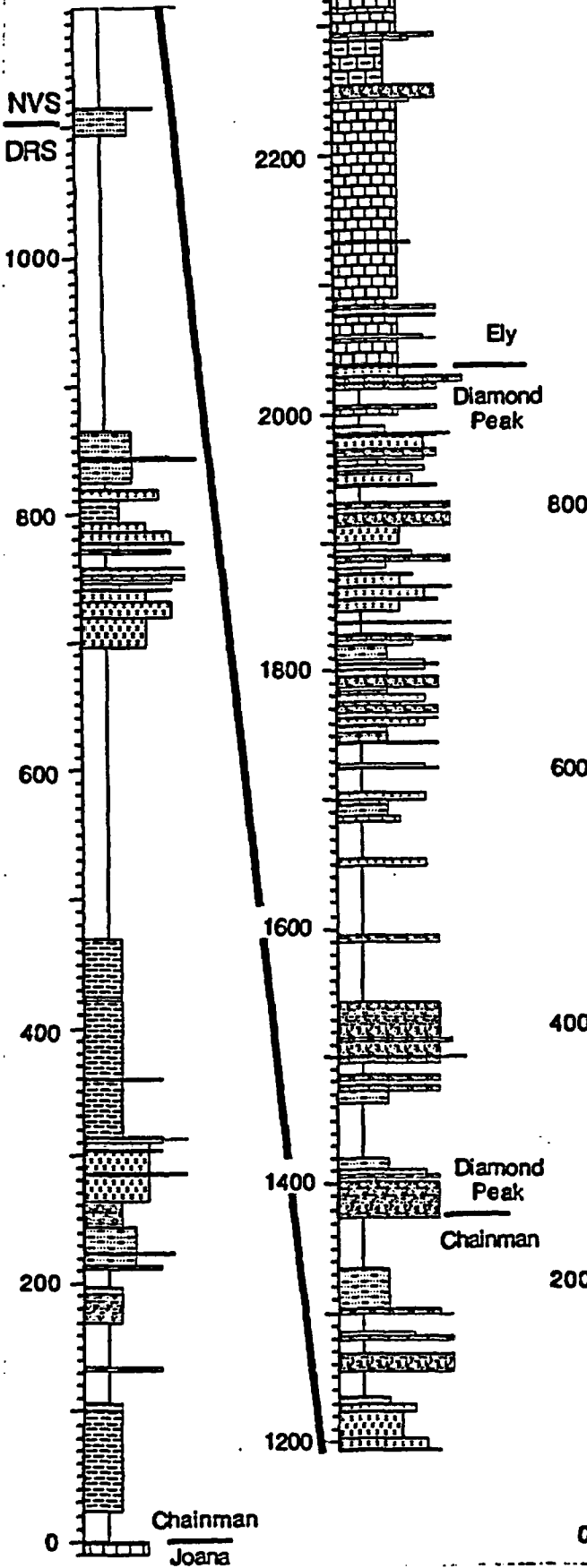


KEY TO LITHOLOGIC SYMBOLS

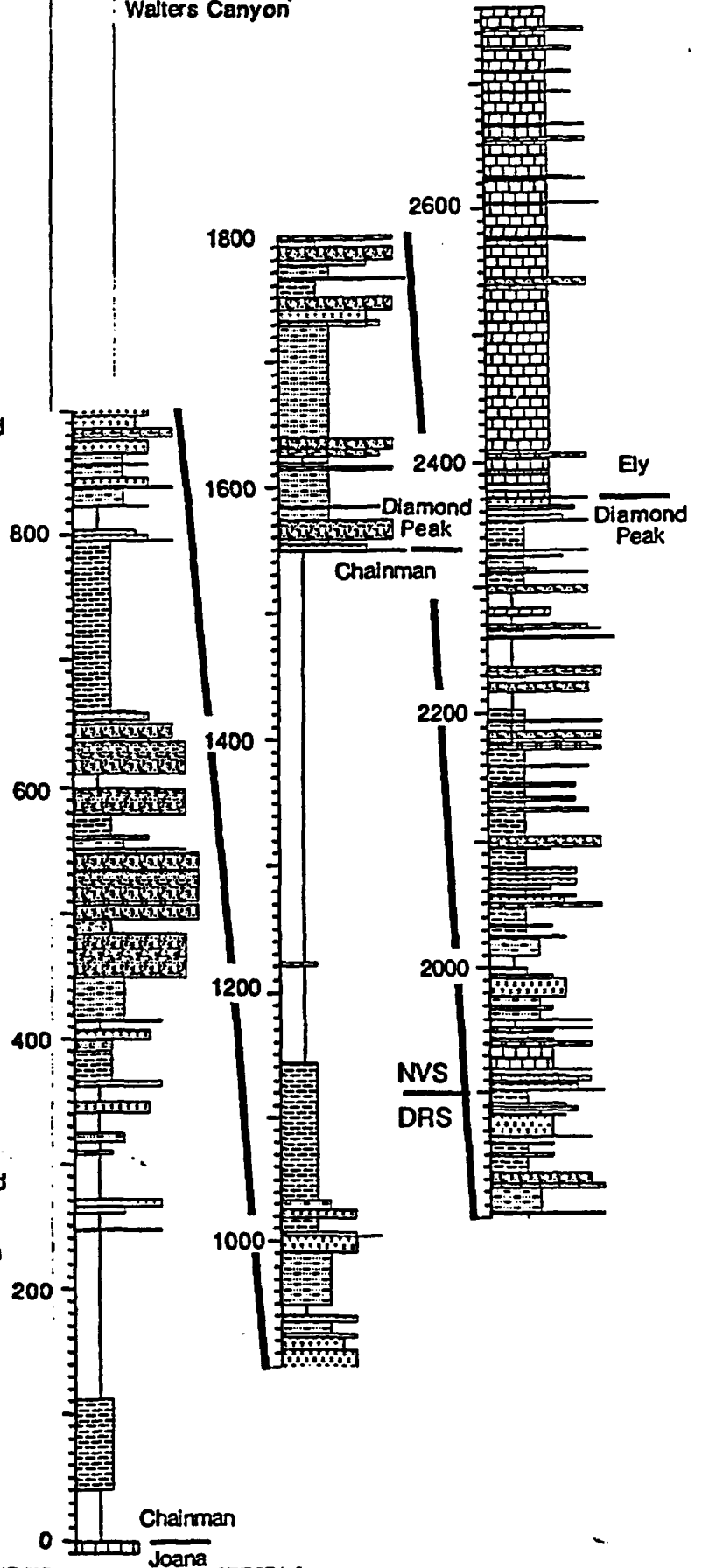
- vertical scale in meters
- cover
 - shale
 - siltstone
 - calcareous siltstone
 - interbedded shale and limestone
 - silty limestone
 - micrite
 - fine-grained limestone
 - medium-grained limestone
 - coarse-grained limestone
 - oolitic limestone
 - sandy limestone
 - fine sandstone
 - medium sandstone
 - coarse sandstone
 - pebbly mudstone
 - calcareous pebbly sandstone
 - fine conglomerate
 - medium conglomerate
 - coarse conglomerate

Figure 6. Measured sections of Mississippian and lower Pennsylvanian rocks along the Diamond Range, from south (left) to north (right). NVS = Newark Valley sequence, DRS = Diamond Range sequence. See Figure 2 for locations of measured sections.

Rattlesnake Mountain



Walters Canyon



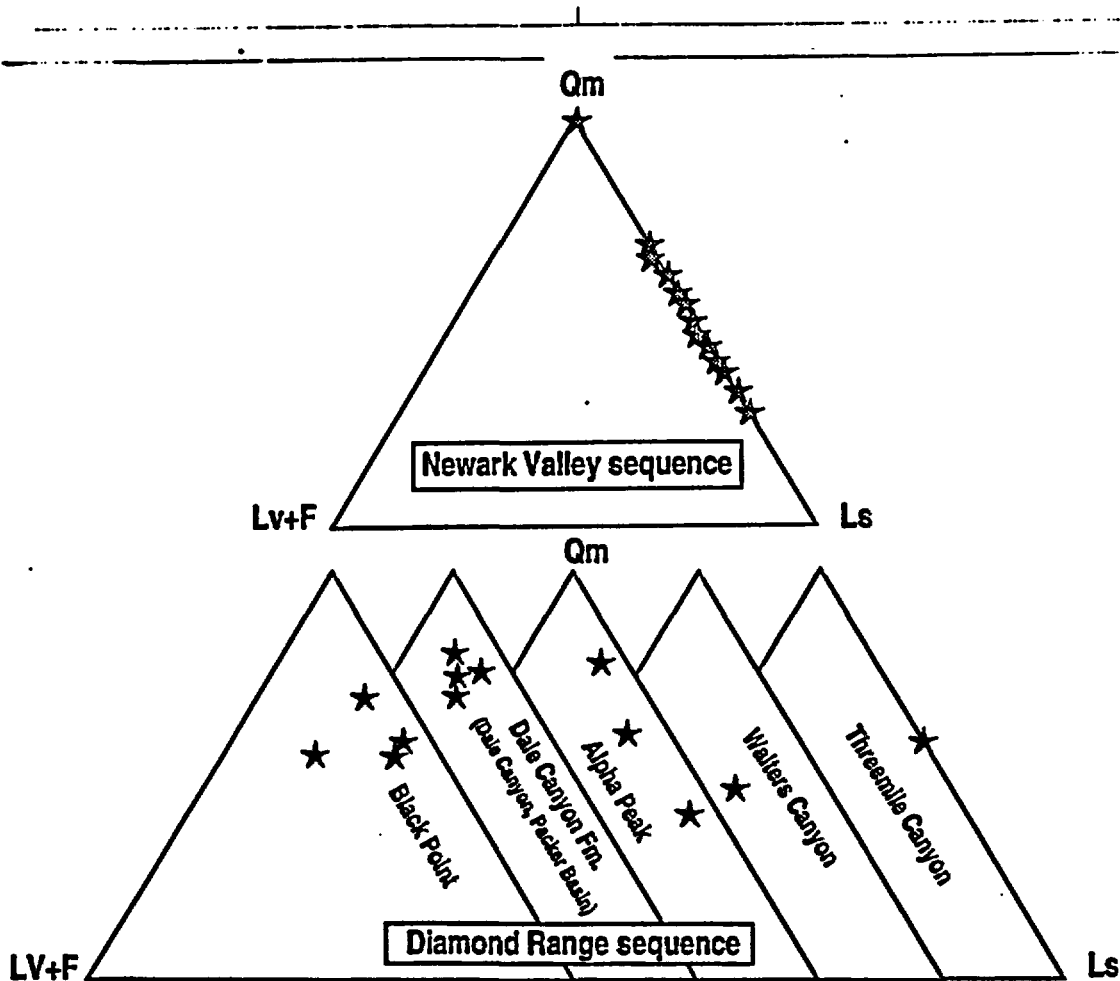


Figure 7. Ternary plots of sandstone detrital modes for samples from the Diamond Range and Newark Valley sequences. Qm = monocrystalline quartz, Lv = volcanic lithic grains, F = plagioclase + orthoclase feldspar, Ls = all non-volcanic lithic grains including chert (excluding carbonate allochems). Each sample represents a minimum of 300 grains counted. See Figure 2 for locations of sample suites.

Sedimentology

The Diamond Range sequence consists of thick intervals of mudrock and fine litharenite, and thinner intervals of lithic conglomerate. Finer parts of the section tend to be covered, whereas coarser parts form well-exposed ribs. The sedimentology of these rocks has been documented by Brew (1971), Poole (1974, 1976), Harbaugh (1980), Harbaugh and Dickinson (1981), and Visconti (1982). The following description, drawn from the authors' observations, agrees substantially with previous work, and is intended here only as a review.

Mudrock intervals of the Diamond Range sequence are finely laminated siltstone and shale with wisps of fine sand and local starved-ripple laminae. The most striking aspect of the fine-grained rocks is the abundance of *Horitza*, a bedding plane trace-fossil that indicates quiet, but well-oxygenated, marine conditions.

Litharenite intervals are typically thin-bedded and laterally persistent, with many of the features associated with "Bouma sequence" turbidites: scoured and fluted bases, graded bedding, and convolute laminae. Litharenite bed-sets commonly form both coarsening- and thickening-upward and

fining- and thinning-upward intervals from 5 to 10 meters thick.

Conglomerate beds in this sequence are matrix-supported and mud-rich; they range from pebbly mudstone to muddy conglomerate. Clast size ranges from grit to cobble, and clasts are typically well-rounded. The coarsest clasts are intraformational mudstone rip-ups up to 1 m across. Conglomerate beds display channelized and eroded bases, and in many places are 15 to 20 m thick. Conglomerate units are not traceable laterally for more than a few hundred meters, and in many places occur in laterally stacked sets.

Petrology

Sandstone point-count data for this study of the Diamond Range sequence shows most sandstones to be litharenites and quartz-arenites (Fig. 7). The most abundant lithic clast type is chert, and most samples have significant feldspar and volcanic clasts. Volcanic clasts are highly altered, in many cases to pseudomatrix, but they appear to reflect an intermediate volcanic composition. Preliminary clast data from conglomerates in this sequence shows that there are numerous different clast types, including (in approximate order of

abundance) quartzite, chert, argillite, litharenite, lithic wacke, recrystallized limestones, and siltstone.

The siliciclastic sediments of the Diamond Range sequence reflect a provenance in the Antler allochthon to the west. Most of the sediment appears to be derived from the Vinini chert, as pointed out by many workers (Poole, 1974, 1977; Harbaugh, 1980; Harbaugh and Dickinson, 1981; Dickinson and others, 1983). The relative abundance of feldspar and volcanic fragments in these rocks has not been previously recognized. The abundance of feldspars and volcanic fragments is wide-ranging (Fig. 7); it is not presently understood what controls the distribution of these grains, but the volcanic signature reflects influence of an arc that was only sporadically available as a sediment source.

Depositional Environment

Rocks of the Diamond Range sequence have been identified by several workers as a submarine fan sequence (Poole, 1974, 1977; Harbaugh, 1980; Harbaugh and Dickinson, 1981; Visconti, 1982), and our study confirms this interpretation. Mudrock intervals have the characteristics of distal and interlobe deposits. Sections with litharenite and conglomerate represent fan lobes and channel deposits.

Measured sections suggest several eastward lobe-building episodes. The section at Rattlesnake Mountain (Fig. 6) contains at least two of these intervals, at 300 and 700 m respectively. South of Eureka at Secret Canyon and at Packer Basin (Fig. 2), the Dale Canyon Formation forms a single fan-lobe interval at the base of the section, and the remainder of the sequence has only thin beds of coarser material near the top of the section. A similar fan lobe mapped as Dale Canyon Formation occurs in the southern Pinon Range northwest of Eureka (Visconti, 1982), but the two lobes are not laterally connected. At Walters Canyon (Fig. 2, 6) the bottom of the section is dominated by mudrock, but three fan-lobe intervals occur in the middle of this section. Fan-lobe intervals are not correlatable from section to section, consistent with an interpretation of east-building, laterally limited facies.

Measured sections in the Diamond Range sequence do not suggest any systematic vertical or lateral trends. The upper sections at Water and Walters Canyons (Fig. 2, 6) are coarse at the top, but the sections at Secret Canyon and Rattlesnake Mountain are fine at the top. The Dale Canyon Formation fan lobes occur only in sections at the south end of the Diamond Mountains and to the northwest in the Pinon Range; elsewhere the base of the section is fine grained. Dramatic differences in the thickness of the section at different localities is attributed to deformation and erosional truncation at the upper sequence boundary.

THE CHRISTINA PEAK PHASE

Introduction

In late Meramecian time, the Diamond Range sequence and subjacent strata were deformed, uplifted, and erosionally beveled in a tectonic episode we have called the Christina Peak phase. (This was previously called the Diamond Mountain phase by Trexler and Cashman, 1990; we rename it here to avoid confusion with the similarly named

Diamond Peak Formation and Diamond Range sequence.) This tectonic phase is a regional event. In southern Idaho, Nilsen (1977) documented an unconformity of this age, and proposed an orogenic origin. Dorobek (1990) has documented renewed subsidence at this time in Montana. In southern Nevada, a pronounced shift in sedimentary provenance occurs in strata of this age (Cashman and Trexler, this volume). In central Nevada, Johnson and Pendergast (1981) have suggested isostatic uplift in the late Mississippian and reworking of submarine-fan sediment.

In the Diamond Mountains, the local tectonic effects of the Christina Peak phase are referred to here as the Overland Pass event. An angular unconformity separates middle-upper Meramecian submarine fan strata of the Diamond Range sequence from early Chesterian deltaic and shallow marine sediments of the Newark Valley sequence. This relationship documents deformation and uplift of the Diamond Range sequence, and establishment of a successor basin overlying the Antler peripheral foreland basin.

The Newark Valley Sequence

The Newark Valley sequence is defined as the systems tract of fluvial, deltaic, and shallow marine sediment that filled the successor basin formed by subsidence after Christina Peak phase deformation. The base of the Newark Valley sequence is early Chesterian everywhere it has been dated; this includes sections not only in the Diamond Range, but also at Buck Mountain and the Pancake Range to the east. The sequence ranges in age into the Pennsylvanian, but the upper limit is unknown due to erosion during the Permian. In the Diamond Range, the sequence is overlain unconformably by the Permian Carbon Ridge Formation.

Stratigraphy

Strata of the Newark Valley sequence include the Diamond Peak and parts of the Ely Formations. The lower boundary of the sequence only rarely coincides exactly with the base of the Diamond Peak Formation (Fig. 5, 6), because submarine-fan conglomerates of the Diamond Range sequence commonly are included in the Diamond Peak Formation (see discussion above). The Diamond Peak Formation grades upward into the Ely Limestone, and thus at least the lower Ely is considered to be part of this systems tract.

The Newark Valley sequence is at least 1000 m thick, based on measured sections throughout the Diamond Range (Fig. 6). In all sections measured to date, the top of the sequence is truncated by a Permian unconformity; in Secret Canyon only about 100 m of the Newark Valley sequence is preserved.

The lower 400 to 700 m of the Newark Valley sequence is dominated by siliciclastic conglomerate and sandstone, and generally is mapped as Diamond Peak Formation. The base of the Ely Limestone is taken as the level at which limestone first dominates the section. At Rattlesnake Mountain (Fig. 5) the Diamond Peak Formation is over 1000 meters thick, but at Walters Canyon to the north, the Diamond Peak only accounts for 400 meters of section. Basal limestone of the Ely invariably carries latest Mississippian or very early Pennsylvanian microfossils (B. Mamet, written commun., 1988, 1989).

Sedimentology

The Newark Valley sequence comprises interbedded intervals of conglomerate and sandstone, mudstone, lithic-pebble limestone, calcarenite, and micrite. The sedimentology of these rocks has been studied by many workers (Brew, 1971; Poole, 1974, 1976; Harbaugh, 1980; Harbaugh and Dickinson, 1981). The following descriptions taken from data obtained for this study are in agreement with previous work; this discussion is intended only as a review.

Conglomerate and sandstone in the Newark Valley sequence is clean, clast-supported, and the clasts are well-rounded. Coarse clastic rocks are most common in the lower part of measured sections (Fig. 6). Bedform fabric, well developed in most places, generally consists of foresets at many scales, nested channels, and trough or planar cross-lamination. Large-scale foreset fabric is up to 10 m thick, with foreset angles between 12° and 20°. Conglomerate and sandstone beds are lenticular in cross-section, and persist laterally from tens to hundreds of meters. They commonly are interbedded with mudstone.

Mudstone intervals are volumetrically significant low in the Newark Valley sequence. Typically, mudstone beds are dark maroon or olive green in color, and show evidence of diagenetic migration of the minerals that give the rock its color. Silty laminations and thin sandy beds are common. The upper part of the Newark Valley sequence (and entire sections measured in ranges to the east of the Diamond Mountains) are mud-free.

Lithic-pebble limestone consists of rounded chert and quartzite pebbles in a calcarenite matrix, with variable amounts of interstratified, clean litharenite. Sedimentary fabric consists of low-angle planar stratification, trough cross-lamination, and imbrication. Lithic-pebble limestone beds commonly are interbedded with calcarenite or micrite intervals.

Limestone beds occur throughout the Newark Valley sequence, and are more abundant in the upper part of all sections. Grainstone and wackestone predominate, but intervals of micrite are common. Calcarenite beds show current-reworking structures such as cross-lamination and grain-orientation fabric in most cases. They are commonly fossiliferous, and contain a wide variety of taxa including crinoid fragments, brachiopods, pelecypods, corals, bryozoans, and foraminifera. The latter allow high-resolution dating of many sections (B. Mamet, written commun., 1988). Limestone intervals commonly contain lithic-pebble and litharenite beds, especially near the Diamond Peak/Ely contact. Micrite beds in many places have a nodular fabric termed "phenoplastic", which has been associated with shallow-marine, wave-reworked deposits (Carozzi, 1986).

Petrology

Sand grains and conglomerate clasts of the Newark Valley sequence consists almost entirely of quartz and stable lithic grains (Fig. 7). Conglomerate clasts are chert and quartzite. Sand grains are chert, monocrystalline and polycrystalline quartz, and intrabasinal carbonate grains. Newark Valley sequence sediments inspected to date are virtually free of volcanic lithic clasts and

feldspar. Some sections contain ortho-quartzites, and the quartz grains are highly rounded both in these beds and in nearby litharenite beds. In general, quartz grains appear texturally more mature than the chert and quartzite grains with which they are mixed, indicating recycling, and possibly a different source, for the quartz.

We suggest two sources for the Newark Valley sequence sediment: eroded and reworked Diamond Range sequence, and the craton. Because these sediments are in most cases free of volcanic-derived material, the allochthon no longer seems to be a direct sediment source. The overmature and clearly reworked quartz grains apparently are derived from the craton. Paleocurrent studies corroborate both local and eastern sources for much of this sediment (see below). Previous work on the Mississippian clastic section in the region has not made a petrographic distinction between the two sequences, although Poole (1977) postulated that there is an upward trend toward greater maturity, due to reworking. Dickinson and others (1983) pointed out the occurrence of volcanic fragments and feldspars in the Chainman Shale, and lack of them in the Diamond Peak Formation, but they did not draw any conclusions from these data.

Depositional Environment

We interpret the Newark Valley sequence as being a fluvial-deltaic to shallow marine transgressive sequence. Lower parts of the sequence in all measured sections are either deltaic, fluvial, or lagoonal marine. Higher in the section, deltaic siliciclastic beds are interbedded with shallow marine limestone, and finally marine limestone dominates. This paleoenvironmental interpretation is largely in agreement with that of Brew (1971) and Harbaugh (1980).

Some workers have proposed that the coarser clastic section is a progradational molasse sequence derived from the Antler allochthon (Poole, 1974, 1977; Harbaugh, 1980). Harbaugh and Dickinson (1981) demonstrated that the Diamond Peak Formation was transgressive rather than progradational. Our interpretation provides the additional insight that the coarse clastic section (lower Newark Valley sequence, Diamond Peak Formation) is not a clastic wedge that represents the proximal equivalent of the Diamond Range sequence submarine fan system. Rather, it is a transgressive successor basin with sediment derived both from the east and locally.

Thick conglomerate and sandstone intervals at the base of some sections (Fig. 6) contain large-scale foreset fabric and nested channel geometries typical of a braid-delta setting. Foreset progradation direction in the Alpha Peak area is north-northwest (Fig. 8), along the foreland axis and possibly back toward the allochthon. Other correlative sections from ranges to the east show many examples of west-directed paleoflow. Maroon and green mudrock intervals associated with these conglomerates are probably delta-plain muds (Brew, 1971). Phenoplastic limestones in this part of the section are interpreted to be lagoonal, tidal flat, or near-shore deposits.

Limestone interbedded with litharenite and lithic-pebble limestone are characteristic of upper parts of the sequence, and are interpreted to have been deposited on a relatively high-energy

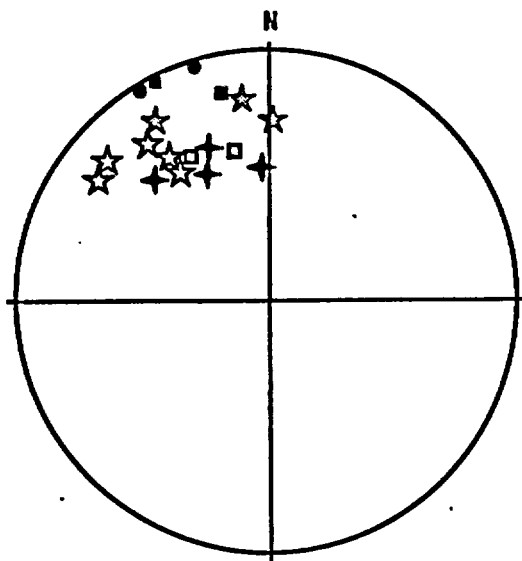


Figure 8. Foreset attitudes (topsets restored to horizontal) for six, stacked deltaic lobes near Alpha Peak. Each symbol type refers to a separate lobe. See Figure 2 for location.

carbonate platform. Litharenites represent beach and shoal deposits, and some appear to be derived from siliciclastic shelf sands to the east, such as the Scotty Wash Quartzite. Lithic-pebble limestones are off-shore bar deposits of deltaic conglomerate reworked onto the carbonate platform.

The Newark Valley sequence documents a waning clastic source and a subsiding basin. Siliciclastic sediment was distributed throughout the basin by large fluvial and deltaic systems early in the successor basin history, but no systematic distributary organization is yet apparent. Lowest fluvial and deltaic strata in the Newark Valley sequence preserve paleoflow indicators (Fig. 9) that show a variety of directions. In the Diamond Mountains, these distributaries appear to have flowed north and west. At Buck Mountain and at Pancake Summit, east of the Diamond Mountains, the flow was south and west. In several cases, especially in the northern Diamond Mountains, the bi-directional flow suggests estuarine deposition. By middle Chesterian time, the major fluvial systems were drowned and siliciclastic sediment was being reworked around the basin by tides or waves. The mud associated with the lower deltaic deposits was no longer present, so calcium carbonate production was no longer inhibited. Limestone dominates the upper section, and calcium carbonate production kept pace with subsidence.

THE MISSISSIPPIAN "ANTLER FORELAND": TWO SUPERIMPOSED BASINS

Mississippian stratigraphy of the Diamond Mountains records two orogenic phases and two post-tectonic basins. In early Mississippian time, allochthon obduction and margin down-warp (Roberts Mountains phase) produced the initial peripheral foreland basin, as documented by the Diamond Range sequence. This phase fits present concepts of the Antler orogeny (e.g., Dickinson and others, 1983), and Poole's (1974, 1977) "flysch trough" reconstruction.

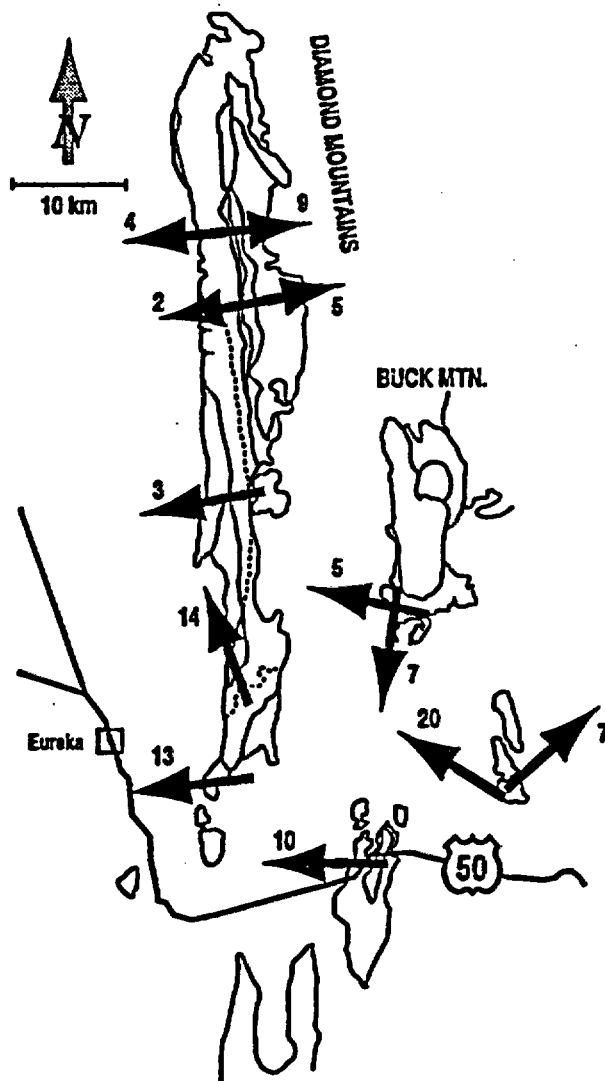


Figure 9. Paleocurrent data from the lower part of the Newark Valley sequence. Numbers with arrows are the number of measurements (each group from a bedding coset), and arrow azimuths are vector means.

The subsidence history of the Diamond Range sequence is poorly understood; age control is mostly of low resolution, and the paleobathymetry is virtually unconstrained. The Pilot Shale and Joana Limestone slope deposits, however, indicate that the basin subsided quickly, early in its history (Poole, 1977). Initial Diamond Range sequence rocks (Chainman Shale and/or Dale Canyon Formation) appear to be relatively "deep" marine, that is, at least below storm wave-base. When the Newark Valley sequence (Diamond Peak Formation) is recognized as being a separate stratigraphic sequences, the "progradational" (albeit transgressive) trends proposed by Poole (1974, 1977), Harbaugh (1980), Harbaugh and Dickinson (1981), and Dickinson and others (1983) disappear. The Diamond Range sequence alone shows no obvious trends such as deepening, shallowing, prograding, or regressing.

Unfortunately, the critical upper and proximal parts of this foreland basin history are mostly missing due to latest Meramecian erosion. The Antelope Range Formation in the Fish Creek Mountains south of Eureka may be a relict of the proximal foreland. These strata comprise a thick section of litharenite and conglomerate of early Mississippian age that has been interpreted as deltaic or estuarine (Sans, 1986).

In late Meramecian time, the peripheral foreland was deformed and uplifted (the Christina Peak phase) and a successor basin was created, resulting in deposition of the Newark Valley sequence. This basin was filled with eroded and reworked Antler foreland basin sediment, plus intrabasinal limestone and cratonal sediment, in a transgressive sequence. Paleocurrent data (Fig. 9) indicate topographic highs within the Antler foreland and to the east of the present position of the Diamond Mountains.

The timing of the Christina Peak phase is well constrained by dated strata above and below the unconformity. The youngest pre-deformation strata dated so far are middle-late Meramecian. The oldest post-uplift strata are early Chesterian. This restricts the uplift and deformation event to latest Meramecian time.

The style of deformation at this time is less well understood. Mapping of the unconformity in the Diamond Range demonstrates a considerable range of sub-unconformity attitudes. When the unconformity is restored to a flat surface (Fig. 10), the Diamond Range sequence strata appear to be folded around a north-northwest trending axis; this trend is roughly coaxial with Mesozoic folding in the area. The position of this folding (e.g. in the Diamond Mountains) indicates a shift in the locus of deformation from the Roberts Mountains (Roberts Mountains phase, above) eastward toward the craton.

Whereas the reasons for renewed subsidence in Chesterian time are a subject of speculation at this point in our investigation, some constraints are known. The upper Mississippian transgression in central Nevada has been attributed to isostatic subsidence of the craton margin subsequent to the Antler orogeny (Johnson and Fendergast, 1981). However, at least 25 million years elapsed between the Roberts Mountains phase and deposition of the transgressive Newark Valley sequence. Deformation of the Christina Peak phase was apparently centered in the area of the Diamond Mountains, so thrust-forced crustal thickening could account for local uplift. Subsidence subsequent to this later episode could have played a role in the transgression. In any case, siliciclastic sedimentation did not keep pace with subsidence in the Newark Valley sequence, and therefore was not a factor in driving the basin down.

Eustatic controls seem to play a minimal role in basin sea-level during deposition of the upper Newark Valley sequence. Eustatic sea-level fluctuation has often been invoked as a control on sedimentation in the Carboniferous, a time of known, large-scale, eustatic changes. Certainly, eustasy must have affected Mississippian strata in Nevada (e.g. Johnson, 1971). Early and middle Chesterian time was a period of worldwide transgression (Ross and Ross, 1987), perhaps accounting

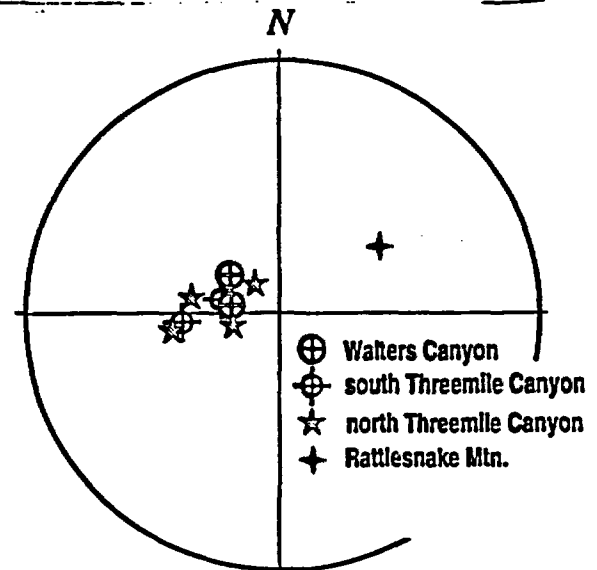


Figure 10. Sub-unconformity attitudes on the Diamond Range sequence, with overlying Newark Valley sequence strata restored to horizontal. See Figure 2 for localities.

for the early transgression of the Newark Valley sequence basin. By contrast, late Chesterian time marks a major regressive cycle world-wide, but at that time the Newark Valley basin was drowning its deltas and becoming a subsiding, carbonate-dominated system.

Several themes are apparent in the development of the foreland and successor basins. Deformational episodes seem to have been relatively short-lived pulses. This is less clear for the Roberts Mountains phase, although that obduction event seems to cease abruptly sometime in Kinderhookian time. The Christina Peak phase deformation is constrained to a short period in latest Meramecian time. In both phases, the basins that resulted were persistent features that lasted for tens of millions of years.

Compressional deformation thickened the crust during both the Roberts Mountains and Christina Peak phases. In the former case this created both a highland sediment source and an asymmetric peripheral foreland basin. In the latter, local highlands were uplifted but a deep basin never formed, and subsidence seems to have accommodated isostatic loading at a much slower rate. We speculate that this change in tectonic style reflects a change in accommodation of plate-margin compression: oceanic-terrane obduction at the craton edge was replaced by deformation of the continental crust inboard of the craton margin.

Acknowledgements

This research was supported by a grant to the authors by the Nevada Nuclear Waste Projects Office through the Center for Neotectonic Studies, University of Nevada, Reno, and by N.S.F. grant EAR-8916525 to Trexler. Our present understanding of the region was substantially enhanced by conversations with many workers, including N. Silberling, K. Nichols, R.A. Schweickert, T. Nilsen, F.G. Poole, W.R. Dickinson, K. Goebel, W.S. Snyder, and C. Guthrie. The manuscript was greatly improved from reviews by C. Stevens and N. Silberling.

REFERENCES CITED

- Brew, D.A., 1971, Mississippian stratigraphy of the Diamond Peak area, Eureka County, Nevada, U.S. Geological Survey Professional Paper 661, 79p.
- Carozzi, Albert, 1956, An intraformational conglomerate by mixed sedimentation in the upper Cretaceous of the Roc-De-Chere, Autochthonous chains of High Savoy, France: *Journal of Sedimentary Petrology*, v. 26, no. 3, p. 253-257.
- Dickinson, W.R., 1977, Paleozoic plate tectonics and the evolution of the Cordilleran margin, in Stewart, J.H., Stevens, C.H., and Fritsche, A.E., eds., *Paleozoic paleogeography of the western United States*, Pacific Section, Society of Economic Paleontologists and Mineralogists, Pacific Coast Paleogeography Symposium 1, p. 363-369.
- Dickinson, W.R., Harbaugh, D.W., Saller, A.H., Heller, P.L., and Snyder, W.S., 1983, Detrital modes of upper Paleozoic sandstones from Antler orogen in Nevada: Implications for nature of Antler orogeny: *American Journal of Science*, v. 283, p. 481-509.
- Dorobek, S.L. and Reid, S.K., 1990, Timing and scale of foreland response to episodic Antler convergence events, Devonian-Mississippian stratigraphy of Montana and Idaho: Effects of horizontal and vertical loading: *Geological Society of America, Abstracts with Programs*, v. 22, p. 283.
- Harbaugh, D.W., 1980, Depositional facies and provenance of the Mississippian Chainman shale and Diamond Peak Formation, central Diamond Mountains, Nevada, [M.S. thesis]: Stanford, California, Stanford University, 81p.
- Harbaugh, D.W., and Dickinson, W.R., 1981, Depositional facies of Mississippian Clastics, Antler foreland basin, central Diamond Mountains, Nevada: *Journal of Sedimentary Petrology*, v. 51, p. 1223-1234.
- Hose, R.K. and Blake, M.C., Jr., 1976, Geology and mineral resources of White Pine County, Nevada, Part 1: Geology: Nevada Bureau of Mines and Geology Bulletin no. 85, p. 1-32
- Johnson, J.C., 1971, Timing and coordination of orogenic, epirogenic, and eustatic events: *Geological Society of America Bulletin*, v. 82, p. 3263-3298.
- Johnson, J.C. and Pendergast, A., 1981, Timing and mode of emplacement of the Roberts Mountain allochthon, Antler orogeny: *Geological Society of America Bulletin*, part 1, v. 92, p. 648-658.
- Ketner, K.E., and Smith, J.F., Jr., 1982, Mid-Paleozoic age of the Roberts thrust unsettled by new data from northern Nevada: *Geology*, v. 10, p. 298-302.
- Mitchum, C.W., Vall, F.R., and Thompson, S., III, 1977, The depositional sequence as a basic unit for stratigraphic analysis, in Payton, C.E., ed., *Seismic Stratigraphy - Applications to Hydrocarbon Exploration*, American Association of Petroleum Geologists Memoir 26, p. 53-62.
- Murphy, M.A., Power, J.D., and Johnson, J.C., 1984, Evidence for Late Devonian movement within the Roberts Mountain allochthon, Roberts Mountains, Nevada: *Geology*, v. 12, p. 20-23.
- Nilsen, T.H., 1977, Paleogeography of Mississippian turbidites in south-central Nevada, in Stewart, J.H., Stevens, C.H., and Fritsche, A.E., eds., *Paleozoic paleogeography of the western United States: Pacific Section, Society of Economic Paleontologists and Mineralogists, Pacific Coast Paleogeography Symposium 1*, p. 275-300
- Nilsen, T.H. and Stewart, J.H., 1980, The Antler orogeny - mid-Paleozoic tectonism in western North America: *Geology*, v. 8, p. 298-302.
- Poole, F.G., 1974, Flysch deposits of Antler foreland basin, western United States, in Dickinson, W.R., ed., *Tectonics and Sedimentation*, Society of Economic Paleontologists and Mineralogists Special Publication 22, p. 58-82.
- Poole, F.G. and Sandburg, C.A., 1977, Mississippian paleogeography and tectonics of the western United States, in Stewart, J.H., Stevens, C.H., and Fritsche, A.E., eds., *Paleozoic paleogeography of the western United States*, Pacific Section, Society of Economic Paleontologists and Mineralogists, Pacific Coast Paleogeography Symposium 1, p. 67-86.
- Poole, F.G. and Claypool, G.E., 1984, Petroleum source-rock potential and crude-oil correlation in the Great Basin, in Woodward, J., Malsner, F.F., and Clayton, J.L., eds., *Hydrocarbon Source Rocks of the Greater Rocky Mountain Region*: Denver, Rocky Mountain Assoc. of Geologists, p. 179-229.
- Roberts, R.J., Hots, P.E., Gillyuly, J., and Ferguson, E.J., 1958, Paleozoic rocks of north-central Nevada: *American Association of Petroleum Geologists Bulletin*, v. 42, no. 12, p. 2813-2857.
- Roberts, R.J., Montgomery, K.H., and Lehner, R.E., 1967, Geology and mineral resources of Eureka County, Nevada: Nevada Bureau of Mines Bulletin no. 64, 152 pp.
- Ross, C.A. and Ross, R.P., 1987, Late Paleozoic sea levels and depositional sequences, in Ross C.A. and Haman, D., eds., *Timing and Depositional History of Eustatic Sequences: Constraints on Seismic Stratigraphy*: Cushman Foundation for Foraminiferal Research, Special Publication 24, p. 137-150.
- Sadlick, W. 1960, Some preliminary aspects of Chainman stratigraphy, in Boettcher, J.W. and Sloan, W.W., eds., *Guidebook to the geology of east-central Nevada*: Intermountain Association of Petroleum Geologists 11th Annual Field Conference Guidebook, Salt Lake City, p. 81-90.
- Sans, R.S., 1986, Origin of Devonian rock units in the southern Fish Creek Range, Nye County, Nevada [M.S. thesis]: Corvallis, Oregon State University, 68p.
- Speed, R.C. and Sleep, N.H., 1982, Antler orogeny and foreland basin: a model: *Geological Society of America Bulletin*, v. 93, p. 815-823.
- Stahl, S.D., 1989, Recognition of Jurassic transport of rocks of the Roberts Mountain allochthon: evidence from the Sonoma Range, north central Nevada: *Geology*, v. 17, p. 645-648.
- Trexler, J.H., Jr. and Cashman, P.H., 1990, The Diamond Mountain phase of the Antler orogeny: Late Mississippian compressional deformation in east-central Nevada: *Geological Society of America, Abstracts with Programs*, v. 22, p. 274.

Trexler, J.H., Jr. and Mitchman, S.P., 1990, Sequence stratigraphy and evolution of the Antler foreland basin, east-central Nevada: *Geology*, v. 18, p. 422-425.

Trexler, J.H., Jr., Snyder, W.S., Cashman, P.H., Callegos, D.M., and Spinosa, C., 1990, An orogenic hierarchy: Examples from western North America: *Geological Society of America, Abstracts with Programs*, v. 22, p. A328.

Visconti, R.V., 1982, Paleozoic stratigraphy and structure of the Dry Creek area, Elko and Eureka Counties, Nevada [M.S. thesis]: Corvallis, Oregon State University, 67p.

APPENDIX C

MISSISSIPPIAN THROUGH PERMIAN OROGENESIS IN EASTERN NEVADA:
POST-ANTLER, PRE-SONOMA TECTONICS OF THE WESTERN CORDILLERA

James H. Trexler, Jr.
Department of Geological Sciences,
and Center for Neotectonic Studies
University of Nevada, Reno
Reno, Nevada 89557

Walter S. Snyder
Department of Geology and Geophysics
Boise State University
Boise, Idaho 83725

Patricia H. Cashman
Department of Geological Sciences
and Center for Neotectonic Studies
University of Nevada, Reno
Reno, Nevada 89557

Dora M. Gallegos
Department of Geology and Geophysics
Boise State University
Boise, Idaho 83725

Claude Spinosa
Department of Geology and Geophysics
Boise State University
Boise, Idaho 83725

ABSTRACT

Mississippian through Permian strata in eastern Nevada, and related strata in southern Nevada and southern Idaho, document a series of tectonic episodes that are either generally unrecognized, or assigned to the Antler or Sonoma orogenies. Some of these were local and others were regional in scale, and none fit either the Antler or Sonoma orogenies as normally defined. They are listed below, along with the last phase of the Antler and the first phase of the Sonoma orogenies:

- > **Antler orogeny:** Roberts Mountains phase (Early Mississippian) - emplacement of Antler accretionary wedge on the passive margin;
- > Wendover phase: (early Mississippian) - regional uplift, erosion;
- > Christina Peak phase: (middle Mississippian) - uplift, folding, and erosion;
- > Oquirrh phase: (Early-Middle Pennsylvanian) - basin segmentation and subsidence;
- > Humboldt phase: (Middle-Late Pennsylvanian) - uplift, tilting and erosion;
- > Dry Mountain phase: (latest Pennsylvanian-Early Permian) - uplift, tilting, erosion, and basin segmentation;
- > Ishbel phase: (late Early - early Late Permian) - uplift, tilting, and erosion;
- > **Sonoma orogeny:** Golconda phase (early Triassic) - obduction of the Golconda allochthon.

The tectonic episodes between the Antler and Sonoma orogenies have mostly escaped notice until now for two reasons: (1) established cratonal stratigraphy, when applied to highly variable craton-edge sequences, tends to obscure important local perturbations; and, (2) the commonly held assumption that there were only two late Paleozoic - early Mesozoic orogenies with a quiet interlude between leaves little room for more complexity, and inevitably leads to unresolvable arguments about timing and style. Little used, older terminology (e.g. "Wendover phase") is available to describe these events in some cases; refinement or abandonment of existing terminology may be necessary in others. Careful, objective stratigraphic studies will result in a more accurate, and complex, regional history.

INTRODUCTION

The upper Paleozoic tectonic history of the western craton margin in the United States is generally thought of as a long and complex story bracketed by two collision episodes: the Late Devonian-Early Mississippian Antler orogeny, and the Permo-Triassic Sonoma orogeny. Several authors have noted aspects of tectonic unrest between the Antler and Sonoma orogenies. For example, Speed (1977) noted continued, but unexplained, differential uplift within the Antler orogenic belt. Ketner (1977) coined the term "Humboldt orogeny" for Late Pennsylvanian reactivation of the Antler orogenic belt and dispersal of clastic debris eastward into a stable "epicontinental sea". Dickinson (1981), Oldow and others (1989) and Smith and Miller (1990) mentioned the formation of several late Paleozoic basins within the Antler belt and along its eastern edge, and suggested a period of possible regional extension. Stewart (1980) summarized much of the Pennsylvanian-Permian tectonism that affected Nevada. Nevertheless, most review papers describe a quiet tectonic setting from middle Mississippian through early Late Permian time (e.g., Dickinson, 1977; Burchfiel, 1979; Speed and others, 1988; Coney, 1989). A large-scale, low-resolution tectonic scenario for the Mississippian through Triassic is generally agreed upon: the western edge of the craton was a collisional margin along which various oceanic terranes were accreted. The specific details of how the margin and nearby craton interior accommodated this orogenesis are not well understood. Arguments about timing and style of tectonic episodes are ongoing (e.g. Ketner and Smith, 1982; Jansma and Speed, 1990).

The result of this tectonic history is a very complicated upper Paleozoic stratigraphy, not only in parautochthonous and allochthonous strata in accreted terranes to the west, but also in craton-margin and overlap strata. Devonian through Permian craton strata, when traced east to west, undergo dramatic facies changes in areas where tectonism affected sedimentation, and some are locally missing due to uplift and erosion. Clastic sediment shed from syntectonic highlands along the margin formed strata that are difficult to correlate with units to the east. Many workers have

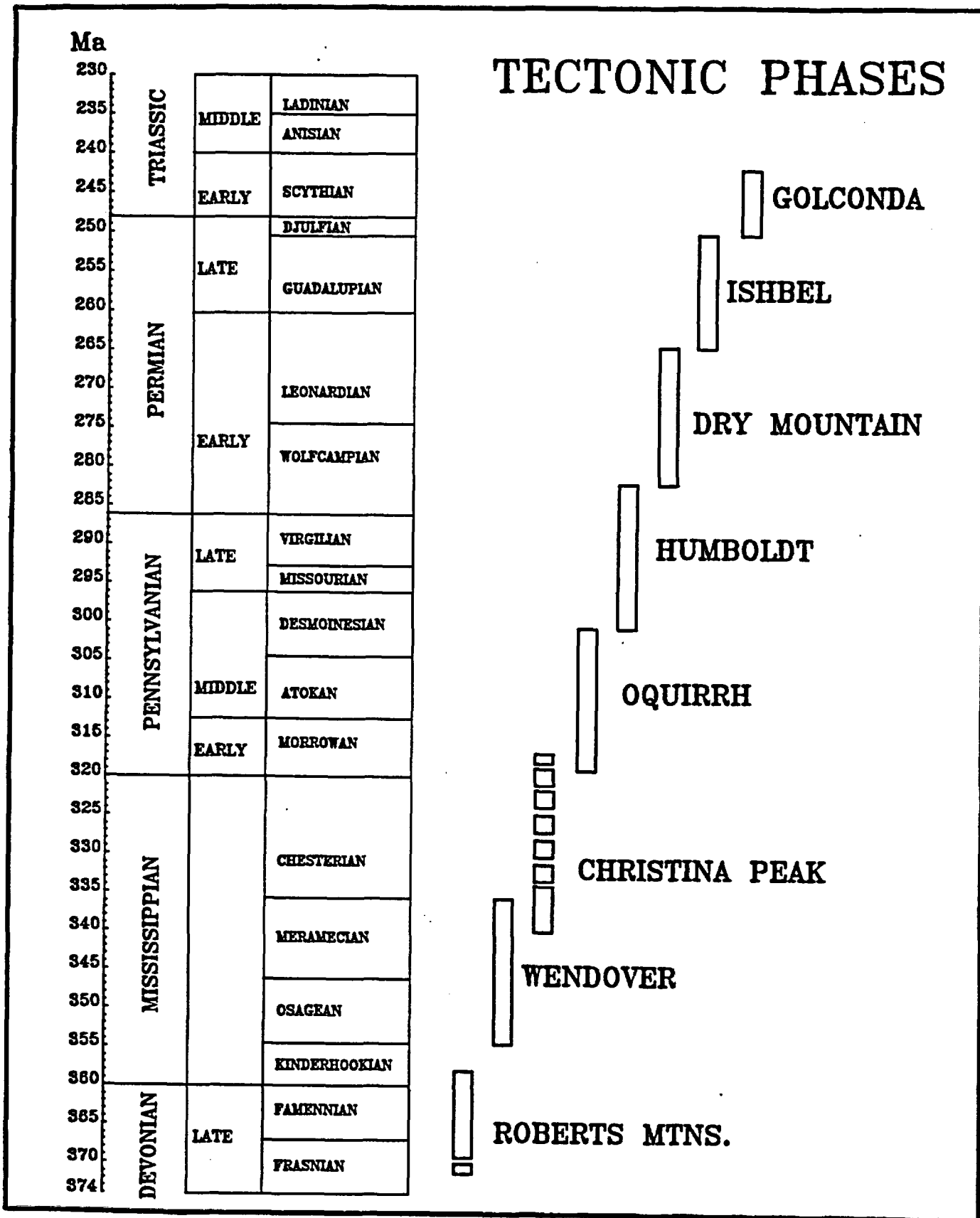


Figure 1 (opposite). Tectonic phases presently known from latest Devonian through earliest Triassic time in the North American miogeocline.

recognized this lateral variability (e.g., Poole and Sandberg, 1977), but new work in the region suggests that the situation is even more complex than was thought. Detailed knowledge of this stratigraphic record is the key to unravelling the details of the tectonic history of the margin.

We propose that a somewhat different stratigraphic approach to resolving the details of the tectonic evolution of this continental margin is to identify tectonic "events" and "phases" in the sense of Trexler and others (1990). Events are tectonic episodes with effects visible at outcrop scale, such as angular unconformities, pervasive deformation, and stratigraphic evidence for basin formation. These events should be defined in terms of local evidence. Phases are episodes with regional effects, but of short duration, and reflect a characteristic tectonic style. Ideally, events should be established first, based directly on field evidence. These events can then be linked together to define phases. This approach has the advantage of establishing the local evidence first, and then building the regional picture.

There are various ways of assembling events into phases and orogenies, but this is not the problem we address here. Our approach is not to redefine the Antler and Sonoma orogenies, but rather to identify and describe as many specific phases of orogenesis as possible. This can provide a framework for a fresh look at the detailed tectonic history of the craton margin.

Mississippian through Permian orogenesis can therefore be viewed as a series of phases of relatively short duration (Fig. 1). Each of these phases comprises local events that document its style and extent. Some, such as the Roberts Mountains phase, are well known. Some, such as the Christina Peak, Dry Mountain, and Ishbel phases, are newly documented. Others, like the Humboldt phase, are controversial. Each can be thought of as a discrete episode in the evolution of the craton margin.

In the following discussion, the Mississippian history was primarily reviewed by Trexler and Cashman, and the Pennsylvanian-Permian history by Snyder, Gallegos, and Spinosa. All of the authors do not necessarily agree on all points, and Trexler and Snyder take responsibility for the approach and synthesis.

MISSISSIPPIAN TECTONIC PHASES

The Roberts Mountains Phase

Tectonic activity in the Devonian and Mississippian has been generally attributed to the Antler orogeny (Johnson, 1971; Poole, 1974). Currently, this orogeny is widely understood to include the obduction of an accretionary prism onto the craton margin, and the subsequent filling of a peripheral foreland basin (Poole and Sandberg, 1977; Speed and Sleep, 1982). Defined in this way, the last deformation event of the Antler orogeny is the emplacement of allochthonous western assemblage rocks over autochthonous cratonal strata. We refer

to this as the Roberts Mountains phase, arguably the last part of the larger-scale and longer-lived Antler orogeny.

Whereas a full description of what is known of the timing and style of the Antler orogeny is beyond the scope of this paper, a brief discussion of the Roberts Mountains phase of this orogeny is a starting point for a review of the evolution of late Paleozoic, post-Antler tectonics in the Great Basin region.

Central Nevada

Evidence for the Roberts Mountains phase in central Nevada includes both the thrust fault along which obduction is thought to have occurred (Roberts Mountains thrust), and sedimentary strata deposited both in the hinterland and in the subsequent foreland basin. There are four main lines of evidence that, taken together, suggest a Late Devonian to Early Mississippian age for Antler compression, and an Early Mississippian age for the episode that we call the Roberts Mountains phase:

(1) Motion on the Roberts Mountains thrust:

The Roberts Mountains thrust is commonly believed to be the thrust along which the Antler allochthon was emplaced over the craton margin (Merriam and Anderson, 1942; Roberts and others, 1958). Most contacts between strata of the Antler allochthon and rocks related to the craton are identified as this thrust. Evidence for the age of motion ranges from middle Paleozoic (Roberts and others, 1958) to post-Permian (Nolan and others, 1956; Ketner and Smith, 1982) to Jurassic (Stahl, 1989). Most workers agree that reactivation on this thrust is likely.

(2) Oldest strata overlapping the Roberts Mountains thrust:

Overlapping stratigraphic relationships in the Roberts Mountains have led some workers to suggest that motion on the Roberts Mountains thrust ceased in late Kinderhookian time (Johnson and Pendergast, 1981; Murphy and others, 1984).

(3) Inception of the Antler foreland basin:

The sedimentological signal for downwarping of the craton margin may be the Tripson Pass Formation and the western facies of the Pilot Shale and Joana Limestone (Poole and Sandberg, 1977) of late Devonian to early Mississippian age. Strata of the middle and upper Mississippian Diamond Peak Formation have been assigned to the Antler foreland basin (Poole, 1974; Poole and Sandberg, 1977), but are now known to be related to later and different tectonic phases (see Trexler and Cashman, this volume).

(4) Youngest strata incorporated into the allochthon:

Rocks that range up to Kinderhookian age (and are assigned to the allochthonous Vinini Formation) are clearly deformed by emplacement of the allochthon (Coles and Snyder, 1985).

The Roberts Mountains phase, then, is defined as a regional, compressional episode that placed the Antler allochthon on the craton margin. Most effects of this tectonism are limited to the early Mississippian. The resulting "Antler foreland basin" (Fig. 2) is the sedimentary fill of the

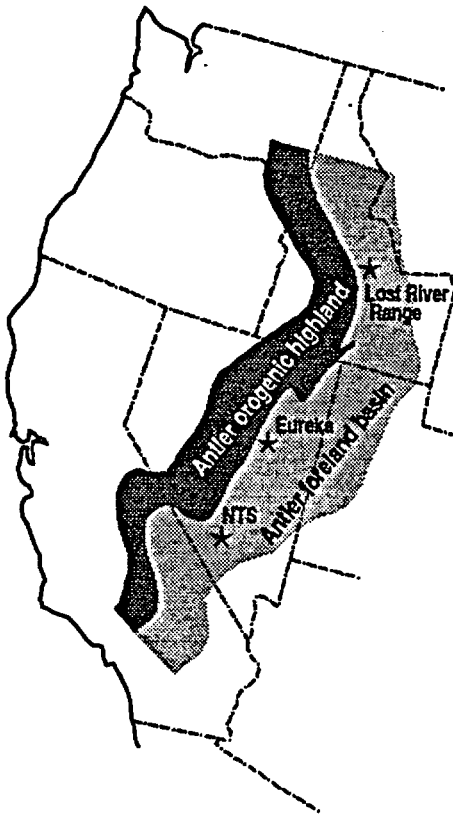


Figure 2. Schematic paleogeography during the Roberts Mountains, Wendover, and Christina Peak phases in the Mississippian.

peripheral foreland basin that formed on the down-flexed craton margin. These strata in central Nevada (Fig. 3) primarily consist of the Osagean to Meramecian Chainman Shale. Locally, some of the rocks mapped as Diamond Peak Formation also are part of this sequence. In the southern Pinon Range, southern Diamond Range, and Fish Creek Mountains, the Dale Canyon Formation is also part of this sequence. These strata are composed of submarine fan sediments shed eastward into a marine basin (Sadlick, 1960; Poole, 1974; Poole and Sandberg, 1977; Harbaugh, 1980; Harbaugh and Dickinson, 1981) from allochthonous highlands to the west. This sequence is a genetically defined facies tract called the "Diamond Range sequence" in central Nevada (Trexler and Nitchman, 1990; Trexler and Cashman, 1990). For a detailed description of this tectonic phase, see Trexler and Cashman (this volume).

Idaho and Southern Nevada

In Idaho, the Roberts Mountains phase and resulting foreland basin are represented by the Copper Basin Formation (Fig. 3) and related strata (Nilsen, 1977). The peripheral foreland basin there is of early to middle Mississippian age, and like in central Nevada, it contains both siliciclastic turbidites shed from the allochthon to the west, and limestone turbidites derived from the cratonal carbonate shelf to the east. Whereas facies relationships strongly suggest a structural setting similar to that of central Nevada (Nilsen, 1977), there is no known obduction-related thrust relationship analogous to the Roberts Mountains

thrust in southwestern Idaho, and some workers have suggested that none exists (Paull, 1970, 1976).

The Antler foreland basin is represented in the vicinity of the Nevada Test Site (NTS) in southern Nevada by part of the Eleana Formation (Johnson and Hibbard, 1957; Poole and others, 1961). Coarse, siliciclastic turbidites of Meramecian age are preserved in a narrow, southwest-trending belt. These strata have been interpreted as a remnant-ocean basin receiving sediment along a southwest-trending trough axis, based on paleocurrent studies. The sediment may have been derived from the large submarine fan systems in the Eureka area (Nitchman, 1990). This southern portion of the Antler foreland basin did not have a sediment source in the allochthon directly to the west. The eastern part of the marginal succession in southern Nevada is represented by a section of mudstone and thin quartzite beds, suggesting that east-derived sediment prograded completely across the basin here, and there was no cratonal carbonate shelf nearby; these craton-derived pelagic muds and deltaic sands are coeval with the siliciclastic turbidites (Cashman and Trexler, this volume).

Wendover Phase

In the Silver Island Range northeast of Wendover, Nevada, Chainman Shale of middle Mississippian age unconformably overlies older folded strata (Sadlick and Schaeffer, 1959). The unconformity places Chainman on strata as young as Osagean (Joana Limestone) to as old as Late Devonian (Fammenian Pilot Shale). Rocks mapped as Chainman here include eastward-thickening limestones and westward-thickening siliciclastic rocks correlated with the Diamond Peak Formation. These coarse clastic rocks apparently are concentrated locally in the vicinity of the Silver Island Range.

The age of folding is constrained to early Valmeyer (middle Mississippian) time, based on fossils occurring both above and below the unconformity (Sadlick and Schaeffer, 1959). Stratigraphic trimming on the unconformity is low-angle, and the folding event is thought to be mild. It is not presently known whether the coarse clastic section in the Silver Island Range is recycled material derived from uplifted foreland strata, or first-cycle sediment from rejuvenation of the allochthonous highlands to the west. The age of the unconformity corresponds to a period of apparently continuous deposition in central Nevada, where slightly older (Kinderhookian) Joana Limestone is conformably overlain by lower Osagean Chainman Shale and deposition was continuous until late Meramecian time.

The Christina Peak Phase

Central Nevada

In the Diamond Mountains in east-central Nevada, lower and middle Mississippian strata of the Diamond Range sequence (Trexler and Nitchman, 1990) were uplifted, deformed into broad folds, and erosionally truncated. This has been defined as the Overland Pass event (Trexler and Cashman, 1990; this volume). The youngest sub-unconformity strata yet identified are middle-late Meramecian. Diamond Range sequence strata are deformed into open folds with axes trending north-northwest, suggesting east-west shortening.

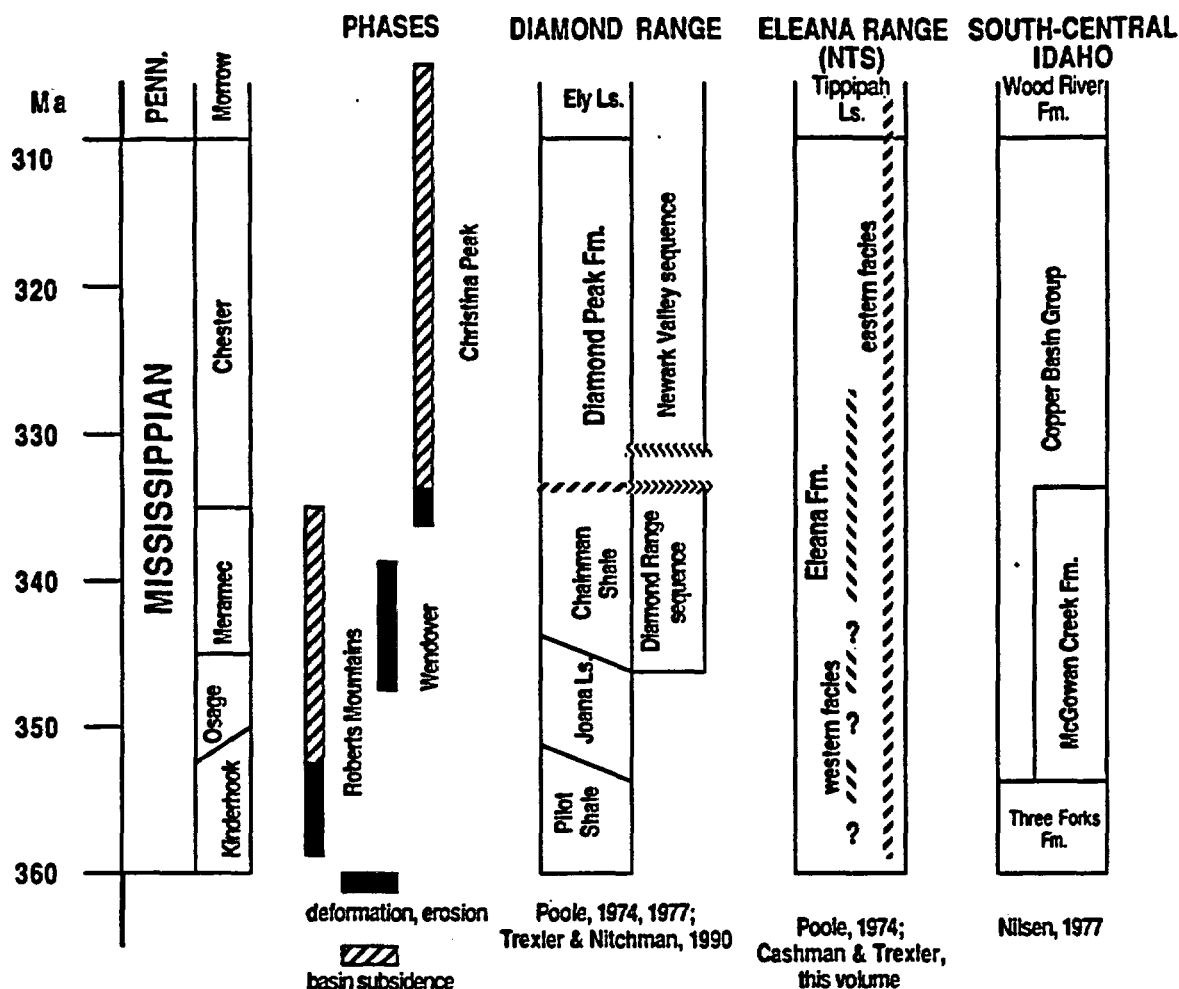


Figure 3. Mississippian stratigraphy in Nevada and Idaho related to the Roberts Mountains, Wendover, and Christina Peak tectonic phases.

Overlying strata of the Newark Valley sequence (Trexler and Nitchman, 1990) represent a successor basin with a lower age limit of early Chesterian. The Newark Valley sequence includes most of the Diamond Peak Formation and the lower Ely Limestone in a transgressive succession of recycled Antler foreland basin clastic sediment and local shelf carbonates. These strata and relationships are discussed in detail elsewhere in this volume (Trexler and Cashman).

Idaho

In Idaho, Nilsen (1977) suggested an upper Mississippian compressional event that structurally telescopes the Copper Basin submarine fan system, juxtaposing proximal and distal fan facies. Analysis of Mississippian and Pennsylvanian strata in Montana and Idaho also suggests a tectonically driven subsidence event at about this time (Dorobek and Reid, 1990). Whereas all these lines of evidence indicate a renewal of compression in the upper Mississippian, evidence from Idaho does not indicate uplift and significant erosion.

Southern Nevada

The Eleana Formation of southern Nevada includes a sequence of limestone turbidites of Chesterian age. They conformably overlie siliciclastic turbidites which are attributed to

the Roberts Mountains phase (Cashman and Trexler, this volume). The limestone turbidites were derived from a carbonate platform; we believe that this source of carbonate detritus was the Chesterian carbonate shelf in the Newark Valley sequence of central Nevada. We call this dramatic change in provenance, from allochthon-derived siliciclastics to shelf-derived carbonate clasts, the Red Canyon event. Thus, the Christina Peak phase affects the southern Nevada Antler remnant ocean basin by providing a new source of carbonate detritus, but structural deformation of this age has not been documented this far south.

Christina Peak Phase Overview

Renewed crustal shortening driven by east-directed compression in the Late Mississippian had varying effects along the craton margin in the Great Basin region. The most severe effects were folding, uplift, and erosion of foreland basin strata in central Nevada (the Overland Pass event). Related effects in Idaho and Montana included renewed subsidence and structural telescoping. In southern Nevada, the effects apparently were restricted to a dramatic change in clastic provenance (the Red Canyon event).

Lateral variation in effects of the Christina Peak phase along the Antler belt can be attributed

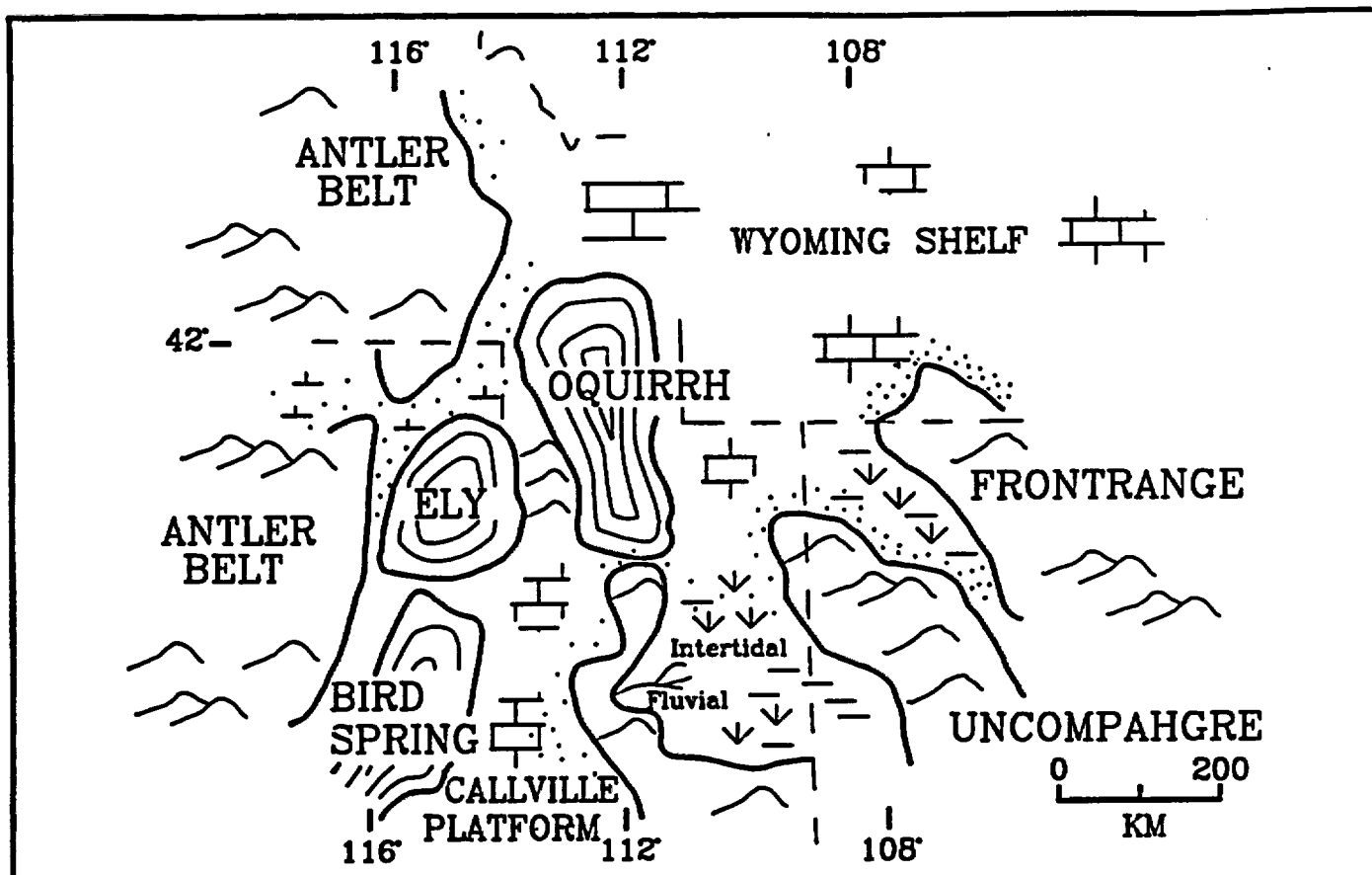


Figure 4. Middle Pennsylvanian paleogeography during the Oquirrh tectonic phase.

to unevenness in the trace of the craton margin, heterogeneity of the marginal crust, and the distribution of the Antler accretionary prism and volcanic arc. Uplift and structural telescoping of the Overland Pass event suggests that central Nevada was a salient in the margin. The Red Canyon event is recorded in sediment deposited in a persistent ocean basin that probably occupied a reentrant in the margin.

PENNSYLVANIAN-PERMIAN TECTONIC PHASES

Tectonic activity continued to disrupt the "miogeocline" during Pennsylvanian and Permian time. Regional and local uplifts, folding, tilting, and basin formation document this tectonism. Recognition of these Pennsylvanian and Permian tectonic phases helps to clarify some aspects of the intraplate deformation associated with the Ouachita-Marathon orogeny (e.g., Snyder and others, 1989; Smith and Miller, 1990) and the nature and age of the Sonoma orogeny (Stewart and others, 1977; Dickinson, 1977; Gabrielse and others, 1983; Snyder and Brueckner, 1983).

Oquirrh Phase

The Morrowan through medial Desmoinesian Oquirrh tectonic phase (Fig. 1) is marked by the appearance of the Ely and Oquirrh basins. Ancestral Rocky Mountain uplifts were well developed at this time and may reflect the same tectonic drive that produced the Ely and Oquirrh basins. In Canada, Oquirrh phase tectonism may be recorded

within the youngest strata of the Prophet trough, a Late Devonian to Early Pennsylvanian, fault-generated basin that extended along most of the Canadian continental margin (Richards, 1989).

Evidence for the Oquirrh phase in the Great Basin includes early tectonic subsidence within the Oquirrh basin. The Oquirrh basin formed to the west and northwest of the synchronously developing Ancestral Rocky Mountain uplifts and basins. Initial subsidence within the Oquirrh basin produced a distinct, although still shallow-marine, basin (e.g., Roberts and others, 1965; Armstrong, 1968; Bissell, 1974; Jordan and Douglas, 1980; Stevens and Armin, 1983).

In east-central Nevada, the Oquirrh phase is marked by the development of the Ely basin, a deeper-water shelf basin similar to the Oquirrh basin (Bissell, 1964, 1967; Rich, 1971; Wardlaw, 1980) (Fig. 4). Ely basin sediments were deposited from Morrowan through Desmoinesian and possibly into Missourian time. The Ely basin encompassed much of the region occupied by the earlier Antler foreland basin. The silt- and micrite-rich strata of the Ely contrast with the predominant packstone, wackestone and grainstone of the surrounding shallower-water shelf. A small area of subaerial uplift may have separated the Oquirrh and Ely basins. A regional unconformity marks the uplift of the Ely basin and the end of the Oquirrh phase in east-central Nevada.

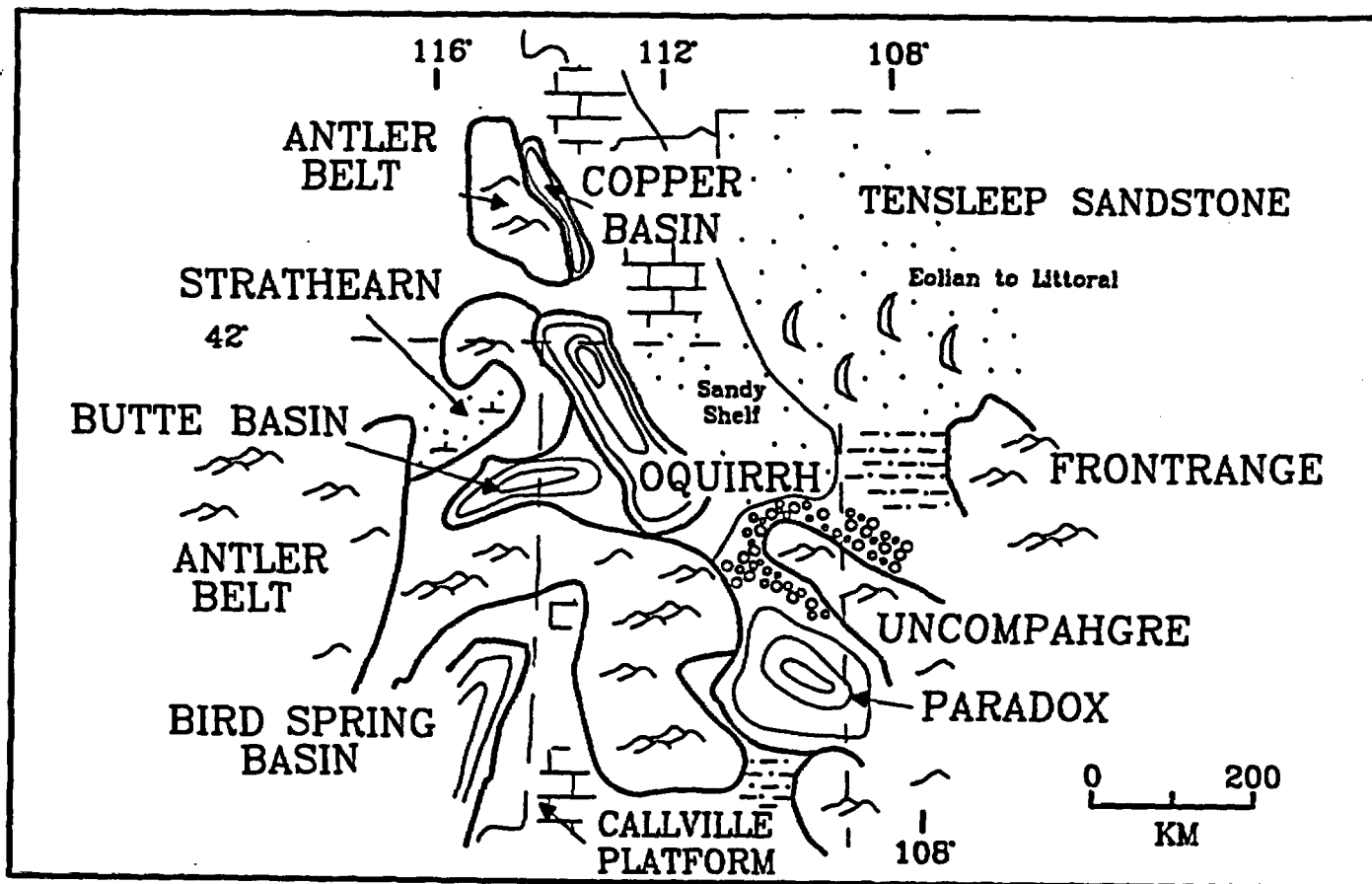


Figure 5. Late Pennsylvanian paleogeography during the Humboldt tectonic phase.

In central Nevada within and adjacent to the Antler highlands, the coarse clastic units of the Atokan and Desmoinesian Battle Conglomerate and Tomera Formation (Dott, 1955; Saller and Dickinson, 1982) suggest renewed tectonic activity. The development of the Bird Spring basin in southern Nevada may be due to Oquirrh phase tectonism. The Bird Spring basin was a deeper-water portion of the miogeocline and may reflect a basinal phase similar to that for the Ely and Oquirrh basins.

Humboldt Phase

The Late Pennsylvanian Humboldt phase tectonism is marked by localized, but regionally extensive, uplift and erosion (Fig. 5). In the Canadian Cordillera, this tectonic unrest produced a major, sub-Permian unconformity that forms the boundary between the Carboniferous Prophant trough (youngest preserved strata are earliest Desmoinesian age) and the Early Permian rocks of the Ishbel trough (Henderson, 1989).

Great Basin

During Late Pennsylvanian time the Oquirrh basin had become a discrete structural trough. A thick succession of laminated siltstone, subarkosic sandstone, pebble and cobble conglomerate, and bioclastic packstone was deposited within the basin. The siltstone is only rarely bioturbated and is interpreted to reflect hemipelagic sedimentation under low oxygen conditions. The clastic beds are interpreted as turbidites. Lack of wave-generated sedimentary structures implies

that deposition within the basin was below wave-base. Jordan and Douglass (1980) suggested that the conglomerate was deposited adjacent to basin-bounding faults. This episode of Oquirrh basin development has been linked to continued tectonic activity in the Ancestral Rocky Mountains (Jordan and Douglas, 1980).

To the west of the Oquirrh basin, a regional unconformity separates Pennsylvanian Ely Limestone from overlying Permian units. The unconformity developed only within the region encompassed by the Ely basin, and did not form in the surrounding shelf. This unconformity indicates differential uplift and erosion of the former Ely basin. In most areas Permian strata rest disconformably on Pennsylvanian rocks, but adjacent to and along the edge of the Antler highlands this contact is a marked angular unconformity (the sub-Strathearn unconformity of Dott (1955)).

Uninterrupted Late Pennsylvanian deposition occurred in a small region of northeastern Nevada, west of Wendover in the Butte basin (Marcantel, 1975). The Butte basin may be a remnant of the Ely Basin and therefore reflect differential subsidence with respect to uplift of the Ely.

The uplift of the Ely basin during a sea level highstand, the local angularity of the Pennsylvanian-Permian unconformity, and the sustained relative submergence of the Butte and Oquirrh basins, all strongly suggest structural

control for uplift and subsidence. No unconformities have been recognized within the Late Pennsylvanian strata of the Bird Spring basin. The Bird Spring basin, however, continued to be a site of somewhat deeper water shelf sedimentation relative to that of the Callville platform, and this may reflect continued differential subsidence.

Death Valley

In Death Valley, Desmoinesian through early Wolfcampian sedimentary facies suggest that tectonism disrupted the miogeocline (Stone and Stevens, 1984). In the southeastern part of the Death Valley region, deposition of a thick sequence of fossiliferous limestones reflects a shallow-water shelf. In the northwestern part of the region, however, a large volume of calcareous turbidites was deposited during the Desmoinesian to earliest Wolfcampian and are interpreted to reflect deposition in a deeper-water basin northwest of the shelf. Between shelf and basinal sequences, a disconformity between Atokan and Wolfcampian strata has been explained as a period of nondeposition or submarine erosion on a sediment by-pass slope (Stone and Stevens, 1984, 1988a,b).

Dry Mountain Phase

The Dry Mountain phase began in medial to late Wolfcampian time with the development of a series of sedimentary basins along the continental margin (Fig. 6). The phase ended in medial Leonardian time when regional uplift and low intensity compressive deformation initiated the Ishbel phase. During the Dry Mountain phase, a series of deeper water basins and associated highs (e.g., the Deep Creek-Tintic uplift) developed along the continental margin from the Mojave Desert region northward to the Yukon (Fig. 6). A shallow-marine carbonate shelf occupied the region between and east of these basins.

Canada

In Canada, Dry Mountain phase tectonism is exhibited by the formation of the Ishbel trough, an Early to early Late Permian basin that occurs along most of the western margin of the Canadian craton (Fig. 6) (Henderson, 1989). The laterally persistent sedimentary rocks of the Ishbel trough extend from 49° north latitude to the Ancestral Aklavik Arch in the northern Yukon. A regional unconformity juxtaposes the early Wolfcampian basinal rocks of the Ishbel trough with the subjacent Morrowan to Desmoinesian strata. This unconformity reflects Humboldt phase tectonism and is similar to the pre-Permian unconformity of the Dry Mountain trough in Nevada. Although not a thick sequence, the sedimentary rocks delineate a distinct basinal phase of deposition. At least locally, development of the Ishbel trough was structurally controlled (Henderson, 1989).

Great Basin

Within the Great Basin, Dry Mountain phase tectonism is recorded by a progression of Permian basins: the Wood River basin, Cassia basin, Ferguson trough and Dry Mountain trough (Fig. 6). In east-central Idaho, Late Pennsylvanian (?) - Permian basinal sedimentary rocks record subsidence within the Antler orogenic belt and formation of the Wood River basin. A thick, poorly dated sequence of turbidite and black shale reflects this subsidence. Present stratigraphic control suggests

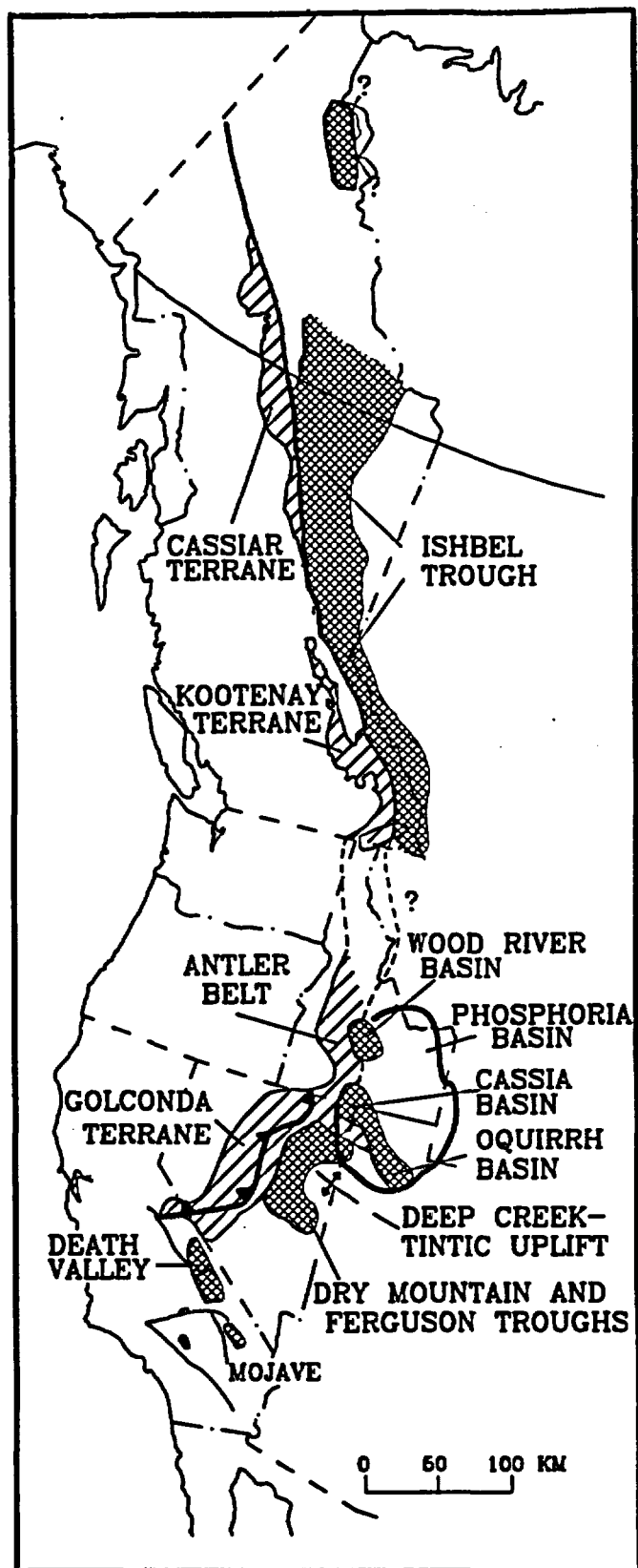


Figure 6. Permian paleogeography during the Dry Mountain and Ishbel tectonic phases.

it is part of the Dry Mountain phase (Link and others, 1989).

Basinal Wolfcampian to Leonardian units in the Cassia basin in south-central Idaho and north-eastern Nevada (Fig. 6) consist of turbidites and hemipelagic sedimentary rocks reflecting subsidence synchronous with the Wood River basin evolution. The Oquirrh basin may have been connected to the Cassia and possibly the Wood River basins (Mytton and others, 1983; Miller, S.T., and others, 1984; Link and others, 1989). However, the Oquirrh, in contrast with the Wood River and Cassia basins, ceased active subsidence and was passively filled during the late Wolfcampian (Jordan and Douglas, 1980).

The Lower Permian Dry Mountain and Ferguson troughs developed in east-central Nevada adjacent to the Antler orogenic belt (Stevens, 1977, 1979) (Fig. 6). Wolfcampian to mid-Leonardian carbonate and siliciclastic sediment was unconformably deposited on the Ely Limestone over most of east-central Nevada. However, along the eastern margin of the Antler highlands this sediment was deposited on the Mississippian Diamond Peak Formation, and locally on Late Devonian Slaven Chert. Faults bounded the Dry Mountain trough on the west (Gallegos and others, this volume), and the Ferguson trough on the north (Marcantel, 1975).

The geometry of the Dry Mountain trough is reflected by depositional facies. On the western edge of the basin, medium to thick-bedded packstone, wackestone, and conglomerate indicate marginal to shallow-marine and deltaic facies deposition (Gallegos and others, this volume). Eastward, thin-bedded, dark, organic-rich micritic siltstone and silty micrite with interbedded packstone and wackestone reflect a basinal facies characterized by deeper water hemipelagic, pelagic and turbidite deposition. Farther east, the basinal facies grades into a carbonate ramp environment (Gallegos and others, 1989). The carbonate ramp then grades eastward into a carbonate platform environment that also forms the southern boundary of the Ferguson trough. A regional unconformity, locally angular, caps the sequences of the Dry Mountain and Ferguson troughs, and marks the end of Dry Mountain phase.

Death Valley

In Death Valley, middle and late Wolfcampian folding and thrusting produced a submarine ridge that segmented the margin into two distinct basins (Stevens and Stone, 1988; Stone and Stevens, 1984, 1988a,b). The southeastern basin, formerly a shallow-water shelf, became the depositional site for large amounts of quartzose and calcareous turbidite sediment. The northwestern basin was transformed from a region of active turbidite deposition to a sediment-starved basin receiving mostly hemipelagic mudstone. Terrigenous clastic sedimentation was cut off in the northwestern basin due to a sediment dam created by the submarine ridge.

Ishbel Phase

The late Leonardian-Guadalupian Ishbel phase is defined by the development of sedimentary basins and basal unconformities typically developed on folded and tilted subjacent strata. The basins formed include the Phosphoria basin and an unnamed basin in the Mojave Desert. The Ishbel phase is

named for the discrete second stage development of the Ishbel trough in the Canadian Cordillera.

Canada

The second stage of the Ishbel trough in Canada comprises a transgressive sequence with a basal chert-pebble conglomerate that grades upward into phosphatic and spicular chert, shale and then locally to quartzose sandstone. This sequence was deposited above a regional unconformity ("intra-Permian unconformity"), forming a consistent depositional sequence from southeastern British Columbia to the southern Mackenzie Fold Belt (Henderson, 1989). The sequence ranges in age from late Leonardian to early Guadalupian and includes the Ranger Canyon, Fantasque and Mowitch Formations. Lower Triassic Spray River Group is regionally disconformable on strata of the Ishbel trough. Therefore the end of the Ishbel phase in Canada can only be bracketed as between late Guadalupian and earliest Triassic.

Great Basin

In the Great Basin, signatures of the Ishbel phase include the initiation of the Phosphoria basin and a renewed influx of siliciclastic debris from the Antler highlands. The term "sag basin" has been used by Wardlaw and Collinson (1986) to describe the origin of the Phosphoria basin. The tectonic drive for its subsidence has not been determined, and like its Canadian counterpart, structure may be at least locally important. Throughout much of the Great Basin, and south of the Phosphoria basin, shallow-marine carbonate deposition was reestablished during the Late Permian (e.g., Park City Group and equivalents). However, within the Dry Mountain trough, the lower Ishbel phase boundary is marked by an angular unconformity and the rapid progradation of Leonardian Garden Valley conglomerates eastward from the Antler highlands (Gallegos and others, this volume). In the Cassia basin, Mytton and others (1983) pointed out that a unconformity, based on missing conodont zones, separates the Early Permian strata from overlying late Leonardian and Guadalupian rocks. This unconformity correlates with the Dry Mountain-Ishbel phase boundary. A similar sequence boundary may exist in the Ferguson trough, but has not yet been documented.

Death Valley

In Death Valley, map relationships document Leonardian and early Guadalupian regional uplift via thrust faults and en echelon folds. The age of the tectonic activity is constrained by folded late Wolfcampian units below the unconformity and by the late Guadalupian (Capitanian) Conglomerate Mesa Formation above the unconformity. The Conglomerate Mesa strata are interpreted to have accumulated while uplift and erosion were taking place in other localized areas. If this deformation began during the Leonardian, it correlates with the Ishbel tectonic phase.

Golconda Phase

The "Sonoma orogeny" is a poorly defined tectonic episode. Despite attempts at clarification (Gabriels and others, 1983), an all-encompassing definition of the Sonoma orogeny has not been generally accepted. At a minimum, the Sonoma orogeny involves some deformation within the Golconda allochthon (or "Golconda terrane") and the accretion (obduction) of this terrane onto the

continental margin. We prefer to describe the emplacement of the Golconda allochthon (that is, accretion of the Golconda terrane) as part of the "Golconda phase," distinct from the earlier continental margin tectonism of the Ishbel phase and older deformational events recorded within the Golconda allochthon.

Great Basin

The Golconda phase is herein defined to include the eastward thrust emplacement of the Golconda allochthon to its pre-Jurassic position structurally above the remnants of the Antler highland and the Pennsylvanian-early Late Permian overlap sequence. The definition should include other events associated with this emplacement, although a listing of all the events that comprise this phase is not yet possible. The timing of emplacement is constrained in central Nevada by the youngest rock beneath the allochthon (the Guadalupian Edna Mountain Formation) and the overlapping Late Triassic Auld Lange Syncline Group (Snyder and Brueckner, 1983). Thus, the Golconda phase within Nevada is latest Permian to early Late Triassic in age, as presently defined, but this age range may narrow with additional data. Regardless, the definition of the Golconda phase avoids the problem of whether or not deformation recorded within the allochthon is longer lived than just the emplacement of the allochthon (compare Snyder and Brueckner (1983) and Brueckner and Snyder (1985) with Miller, E.L., and others, (1984).

Death Valley-Mojave

Continued tectonic activity in the Death Valley-Mojave region during the Late Permian Golconda phase is recorded by the development of unconformities, deformation of Leonardian and older strata, and latest Permian-earliest Triassic volcanism and plutonism. Within the Inyo Mountains-Argus Range area of the Death Valley region, an unconformity separates the late Guadalupian Conglomerate Mesa Formation from overlying Early-Middle (?) Triassic strata (Stone and Stevens, 1988a). Latest Permian-Early Triassic deformation and magmatism occurred in the Mojave Desert region. Near Victorville, the region was deformed and intruded by a 241-Ma monzonite pluton (J.E. Wright, in Walker, 1988) prior to deposition of Lower Triassic rocks. In the El Paso Mountains, Permian strata were deformed and subsequently intruded by a 249-Ma pluton (latest Permian to earliest Triassic) (Walker, 1988). Therefore, this latest Permian-Early Triassic tectonism in the Mojave Desert is broadly coeval with the emplacement of the Golconda terrane to the north (Walker, 1988). This deformation and magmatism thus may be considered as an event within the Golconda phase of tectonism.

DISCUSSION

The Roberts Mountains and Golconda phases reflect obduction of basinal to oceanic rocks, and in both cases the lower plate was little deformed. The Roberts Mountains phase resulted in a foreland basin, whereas the Golconda did not. Both orogenic phases were continent-accretion phases; that is, rocks were added to the craton margin.

The phases between these two obduction episodes, the Wendover, Christina Peak, Oquirrh, Humboldt, Dry Mountain, and Ishbel, probably are not margin-accretion episodes. This series of

phases seems to represent propagating and sometimes localized compression, accompanied by segmentation of the margin into localized sedimentary basins with separate subsidence histories.

The collision of South and North America (the Ouachita-Marathon orogeny) has been suggested as a tectonic drive for the formation of the Ancestral Rockies as well as for portions of the Pennsylvanian-Permian, western continental-margin tectonism (Schwarz, 1987; Snyder and others, 1989; Link and others, 1989; Smith and Miller, 1990; Snyder and others, in press). Although this explanation is reasonable for the scale and style of deformation observed, it does not explain the timing. The Oquirrh and Humboldt phases could have resulted from this collision of North and South America, but the Wendover and Christina Peak phases are too old and the Dry Mountain and Ishbel are too young.

Alternatively, all the phases discussed here (and others yet to be described) may simply be intraplate effects of the Antler, Ouachita, and Sonoma orogenies (Dickinson, 1977). For instance, the Wendover and Christina Peak phases can be interpreted as post-obduction, eastward-propagating compression related to continued margin collapse.

It is our view that assembly of phases into orogenies is not merely a semantic problem; phases within an orogeny should be genetically linked. It is not very productive to argue over the significance of outcrop data to something as nebulous as an orogeny, but it can be very instructive to fit those data into a scheme of tectonic phases. Until we have identified and described all the phases involved in this history, the debate about large-scale orogenies and tectonic drive may be premature.

ACKNOWLEDGEMENTS

This paper is an outgrowth of research projects in the Mississippian rocks of central and southern Nevada sponsored by N.S.F. (EAR-8916525 to Trexler) and the Nevada Nuclear Waste Project Office (Cashman and Trexler), and work in Pennsylvanian and Permian strata supported by N.S.F. grants EAR-8618450, EAR-8746085, and EAR-9004909, and Idaho State Board of Education Grant #91-090 (Snyder, Gallegos, and Spinosa).

Discussions with many workers have contributed to the ideas presented here, including especially M. Silberling, K. Nichols, J. Stewart, F.C. Poole, C. Henderson, C. Stevens, K. Ketner, B.R. Wardlaw, and visitors to our poster session at the Dallas Geological Society of America national meeting, 1990, too numerous to mention.

REFERENCES CITED

- Armstrong, R.L., 1968, The Cordilleran miogeosyncline in Nevada and Utah: Utah Geological and Mineralogical Survey Bulletin, v. 78, 58 p.
Bissell, H.J., 1964, Ely, Arcturus, and Park City Groups (Pennsylvanian-Permian) in eastern Nevada and western Utah: American Association of Petroleum Geologists Bulletin, v. 48, p. 565-636.

- _____, 1967, Pennsylvanian and Permian basins in northwestern Utah, north-eastern Nevada, and south-central Idaho: Discussion: American Association of Petroleum Geologists Bulletin, v. 51, p. 791-802.
- _____, 1974, Tectonic control of late Paleozoic and Early Mesozoic sedimentation near the hinge line of the Cordilleran miogeosynclinal belt, in Dickinson, W.R., ed., Tectonics and sedimentation: Society Economic Paleontologists and Mineralogists Special Publication 22, p. 83-97.
- Brueckner, H.K., and Snyder, W.S., 1985, Structure of the Havallah sequence, Colconda allochthon, Nevada: Evidence for prolonged evolution in an accretionary wedge: Geological Society of America Bulletin, v. 96, p. 1113-1130.
- Burchfiel, B.C., 1979, Geologic history of the central western United States, in Ridge, J.D., ed., Papers on mineral deposits of western North America: Nevada Bureau of Mines and Geology Report 33, p. 1-11.
- Carr, M.D., Poole, F.G., and Christiansen, R.L., 1984, Pre-Cenozoic geology of the El Paso Mountains, southwestern Great Basin, California - A summary, in Lintz, J., Jr., ed., Western geological excursions, v. 4: Rano, Geological Society America Field Trip Guide, p. 84-93.
- Coles, K.S. and Snyder, W.S. 1985, Significance of lower and middle Paleozoic chert in the Toquima Range, central Nevada: Geology, v. 13, p. 573-576.
- Coney, P.J., 1989, The North American Cordillera in Ben-Avraham, Z. ed., The evolution of the Pacific Ocean margins: Oxford, England, Oxford Monographs on Geology and Geophysics No.8, p. 43-52.
- Dickinson, W.R., 1977, Paleozoic plate tectonics and the evolution of the Cordilleran continental margin, in Stewart, J. H., Stevens, C. H., and Fritsche, A. E., eds., Paleozoic paleogeography of the western United States: Los Angeles, Pacific Section Society Economic Mineralogists and Mineralogists, Pacific Coast Paleogeography Symposium 1, p. 137-155.
- Dott, R. H., Jr., 1955, Pennsylvanian stratigraphy of Elko and northern Diamond Ranges, northeastern Nevada: American Association of Petroleum Geologists Bulletin, v. 39, 2211-2305.
- Dorobek, S.L. and Reid, S.K., 1990, Timing and scale of foreland response to episodic Antler convergence events, Devonian-Mississippian stratigraphy of Montana and Idaho: Effects of horizontal and vertical loading, Geological Society of America Abstracts with Programs, v. 22, p. 283.
- Gabrielsa, R., Snyder, W.S., and Stewart, J.H., 1983, Sonoma orogeny and Permian to Triassic tectonism in western North America: Geology, v. 11, p. 484-486.
- Gallegos, D.M., Snyder, W. S., Spinosa, C., 1989, Depositional environments and facies patterns along a west-east transect across the Permian Dry Mountain trough, northeastern, Nevada: Geological Society of America Abstracts with Programs, v. 21, p. 81.
- Harbaugh, D.W., 1980, Depositional facies and provenance of the Mississippian Chainman Shale and Diamond Peak Formation, central Diamond Mountains, Nevada (M.S. thesis): Stanford, California; Stanford University, 81 p.
- Harbaugh, D.W., and Dickinson, W.R., 1981, Depositional facies of Mississippian clastics, Antler foreland basin, central Diamond Mountains, Nevada, Jour. Sed. Pet., v. 51(4), p. 1223-1234.
- Henderson, C.M., 1989, Upper Carboniferous and Permian Western Canada Sedimentary Basin, in Ricketts, B.D., ed., Western Canada Sedimentary Basin, A Case History: Calgary, Canadian Society of Petroleum Geology, p. 203-217.
- Jansma, P.E., and Speed, R.C., 1990, Omissional faulting during Mesozoic regional contraction at Carlin Canyon, Nevada, G.S.A. Bulletin, v. 102, p. 417-427.
- Johnson, M.S. and Hibbard, D.E., 1957, Geology of the Atomic Energy Commission Nevada proving grounds area, Nevada, U.S.C.S. Bulletin 1021K, 333p.
- Johnson, J.G., 1971, Timing and coordination of orogenic, epeirogenic, and eustatic events, Geol. Soc. America Bulletin v. 82, p. 3263-3298.
- Johnson, J.G., and Pendergast, A., 1981, Timing and mode of emplacement of the Roberts Mountain allochthon, Antler orogeny, Geological Society of America Bulletin, part 1, v. 92, p. 648-658.
- Jordan, T. E., and Douglas, R. C., 1980, Paleogeography and structural development of the Late Pennsylvanian to Early Permian Oquirrh basin, northwestern Utah, in Fouch, T.D., ed., Paleozoic paleogeography of the west-central United States: Denver, Rocky Mountain Section, Society Economic Paleontologists and Mineralogists, Rocky Mountain Paleogeography Symposium 1, p. 217-230.
- Ketner, K.B., 1977, Late Paleozoic orogeny and sedimentation, southern California, Nevada, Idaho, and Montana, in Stewart, J.H., Stevens, C.H., and Fritsche, A.E., eds., Paleozoic Paleogeography of the Western United States: Los Angeles, Pacific Section, Society of Economic Paleontologists and Mineralogists Pacific Coast Symposium 1, p. 363-369.
- Ketner, K.B. and Smith, J.F., Jr., 1982, Mid-Paleozoic age of the Roberts thrust unsettled by new data from northern Nevada: Geology, v. 10, p. 298-302.
- Link, P.K., Mahoney, J.B., Burton, B.R., 1989, Pennsylvanian-Permian tectonics, south central Idaho: The Wood River basin and the Copper Basin highland: Geological Society America Abstracts with Programs, v. 21, p. 107-108.
- Marcantel, J. E., 1975, Late Pennsylvanian and Early Permian sedimentation in northeast Nevada: American Association of Petroleum Geologists Bulletin, v. 59, p. 2079-2098.
- Merriam, C.W. and Anderson, C.A., 1942, Reconnaissance survey of the Roberts Mountains, Nevada: Geological Society of America Bulletin, v. 53, p. 1675-1726.

- Miller, E.L., Holdsworth, B.K., Whiteford, W.B., and Rodgers, D., 1984, Stratigraphy and structure of the Schoonover sequence, northeastern Nevada: Implications for Paleozoic plate-margin tectonics: Geological Society America Bulletin, v. 95, p. 1063-1076.
- Miller, S.T., Martindale, S.G., and Fedewa, W.T., 1984, Permian stratigraphy of the Leach Mountains, Elko County, Nevada: Utah Geological Association Publication 13, Geology of northwest Utah, southern Idaho, and northeast Nevada, p. 65-78.
- Murphy, M.A., Power, J.D., and Johnson, J.G., 1984, Evidence for Late Devonian movement within the Roberts Mountain allochthon, Roberts Mountains, Nevada: Geology, v. 12, p. 20-23.
- Mytton, J. W., Morgan, W. A., and Wardlaw, E. R., 1983, Stratigraphic relations of Permian units, Cassia Mountains, Idaho, in Miller, D.M., Todd, V.R., and Howard, K.A., eds., Tectonic and stratigraphic studies in the eastern Great Basin: Geological Society America Memoir 157, p. 281-303.
- Nilsen, T.H., 1977, Paleogeography of Mississippian turbidites in south-central Nevada, in Stewart, J.H. Stevens, C.H., and Fritche, A.E., eds., Paleozoic paleogeography of the Western United States, Los Angeles, Pacific Section, Society of Economic Paleontologists and Mineralogists Pacific Coast Paleogeography Symposium 1, p. 275-300.
- Nilsen, T.H., and Stewart, J.H., 1980, The Antler orogeny - mid-Paleozoic tectonism in western North America: Geology, v. 8, p. 298-302.
- Nitchman, S.F., 1990, Depositional environments of the Mississippian Eleana Formation, Nevada Test Site, Nye County, Nevada: Geological Society of America Abstracts with Programs, v. 22, p. 73.
- Nolan, T.B., Merriam, C.W., and Williams, J.S., 1956, The stratigraphic section in the vicinity of Eureka, Nevada, U.S. Geological Survey Professional Paper 276, 26 p.
- Oldow, J.S., Bally, A.W., Ave Lallement, H.G., and Leeman, W.P., 1989, Phanerozoic evolution of the North American Cordillera, United States and Canada: in Bally, A.W., and Palmer, A.R., eds., The Geology of North America - An Overview: Geological Society of America, The Geology of North America, v. A, p. 139-232.
- Pauli, R.A., 1970, Evidence against the existence of the Antler orogenic belt in central Idaho Geological Society of America Abstracts with Programs, v. 2, p. 343.
- _____, 1976, Evidence against Antler-age thrusts in south-central Idaho, Geological Society of America Abstracts with Programs, v. 8, p. 617-618.
- Poole, F.G., Houser, F.N., and Orkild, P.P., 1961, Eleana Formation of Nevada Test Site and vicinity, Nevada: U.S. Geological Survey Research, 1961, p. D104-D111.
- Poole, F.G., 1974, Flysch deposits of Antler foreland basin, western United States, in Dickinson, W.R., ed., Tectonics and Sedimentation: Society of Economic Paleontologists and Mineralogists Special Publication 22, p. 58-82.
- _____, and Sandberg, C.A., 1977, Mississippian paleogeography and tectonics of the western United States, in Stewart, J.H., Stevens, C.H., and Fritche, A.E., eds., Paleozoic paleogeography of the Western United States: Los Angeles, Pacific Section, Society of Economic Paleontologists and Mineralogists, Pacific Coast Paleogeography Symposium 1, p. 67-86.
- Rich, M., 1971, Middle Pennsylvanian rocks of the eastern Great Basin: American Association Petroleum Geologists Bulletin, v. 55, p. 432-453.
- _____, 1977, Pennsylvanian paleogeographic patterns in the western United States, in Stewart, J.H., Stevens, C.H., and Fritche, A.E., eds., Paleozoic paleogeography of the western United States: Los Angeles, Pacific Section, Society Economic Paleontologists and Mineralogists, Pacific Coast Paleogeography Symposium 1, p. 87-112.
- Richards, B.C., 1989, Upper Kaskaskia Sequence: Uppermost Devonian and Lower Carboniferous, in Ricketts, B.D., ed., Western Canada Sedimentary Basin, A Case History: Calgary, Canadian Society of Petroleum Geology, p.165-201.
- Roberts, R.J., Hotz, P.E., Gilluly, J., and Ferguson, H.G., 1958, Paleozoic rocks of north-central Nevada: American Association of Petroleum Geologists Bulletin, v. 42, p. 2813-2857.
- Sadlick, W. 1960, Some preliminary aspects of Chainman stratigraphy: Intermountain Association of Petroleum Geologists 11th Annual Field Conference Guidebook, p. 81-90.
- Sadlick, W. and Schaeffer, F.E., 1959, Dating of an Antler orogenic phase (Middle Mississippian) in western Utah: Geological Society of America Bulletin, v. 70, part 2, p. 1786.
- Saller, A.H., and Dickinson, W.R., 1982, Alluvial to marine facies transition in the Antler overlap sequence, Pennsylvanian and Permian of north-central Nevada: Journal of Sedimentary Petrology, v. 52, p. 925-940.
- Schwarz, D.L., 1987, Geology of the Lower Permian Dry Mountain trough, Buck Mountain, Limestone Peak, and Secret Canyon areas, east-central Nevada: [MS thesis]: Boise, Idaho, Boise State University, 149 p.
- Smith, D.L., and Miller, E.L., 1990, Late Paleozoic extension in the Great Basin, western United States: Geology, v. 18, p. 712-715.
- Snyder, W.S., and Brueckner, H. K., 1983, Tectonic evolution of the Golconda allochthon, Nevada: problems and perspectives, in Stevens, C.H., ed., Pre-Jurassic rock in western North American suspect terranes: Los Angeles, Pacific Section, Society Economic Paleontologists and Mineralogists, v. 32, p. 103-123.
- Snyder, W.S., Spinosa, C., and Gallegos, D.M., 1989, Late Pennsylvanian to Permian tectonism along the western United States Continental margin: Geological Society of America, Abstracts with Programs, v. 21, p. 147.

- Stons, P., and Stevens, C. H., 1984, Stratigraphy and depositional history of Pennsylvanian and Permian rocks in the Owens Valley - Death Valley region, eastern California, in Lintz, J., Jr., ed., Western Geological Excursions, v. 4: Reno, Cordilleran Section, Geological Society of America Field Trip Guide, p. 94-119.
- _____, 1988a, An angular unconformity in the Permian section of east-central California: Geological Society America Bulletin, v. 100, p. 547-551.
- _____, 1988b, Pennsylvanian and Early Permian paleogeography of east-central California: Implications for the shape of the continental margin and the timing of continental truncation: Geology, v. 16, p. 330-333.
- Trexler, J.H., Jr. and Nitchman, S.P., 1990, Sequence stratigraphy and evolution of the Antler foreland basin, east-central Nevada, Geology, v. 18, p. 422-425.
- Trexler, J.H., Jr., and Cashman, P.H., 1990, The Diamond Mountain phase of the Antler orogeny: Late Mississippian compressional deformation in east-central Nevada: Geological Society of America Abstracts with Programs, v. 22, p. 274.
- Trexler, J.H., Jr., Snyder, W.S., Cashman, P.H., Callegos, D.M., and Spinosa, C., 1990, An orogenic hierarchy: Examples from western North America: Geological Society of America Abstracts with Programs, v. 22, p. A328.
- Walker, J. D., 1988, Permian and Triassic rocks of the Mojave Desert and their implications for timing and mechanisms of continental truncation: Tectonics, v. 7, p.685-709.
- Wardlaw, E.R., 1980, The Pennsylvanian Callville Limestone in Beaver County, southwestern Utah, in Fouch, T.D., and Magathan, E.R., eds., Paleozoic paleogeography of west-central United States: Denver, Rocky Mountain Section, Society of Economic Mineralogists and Mineralogists, Rocky Mountain Paleogeography Symposium 1, p. 175-179.
- Wardlaw, E.R., and Collinson, J.W., 1986, Paleontology and deposition of the Phosphoria Formation: Laramie, Wyoming, Contributions to Geology, v. 24, University of Wyoming, p. 107-142.

**THIS PAGE IS AN
OVERSIZED DRAWING OR
FIGURE,
THAT CAN BE VIEWED AT THE
RECORD TITLED:**

"GEOLOGIC MAP OF CRATER FLAT "

WITHIN THIS PACKAGE

NOTE: Because of these page's large file size, it may be more convenient to copy the file to a local drive and use the Imaging (Wang) viewer, which can be accessed from the Programs/Accessories menu.

D-01